frontiers | Research Topics

Salmonella spp.- transmission, pathogenesis, host-pathogen interaction, prevention and treatment

Edited by
Sébastien Holbert, George Grant and Patrick J. Naughton

Published in
Frontiers in Microbiology

ISSN 1664-8714
ISBN 978-2-8325-5725-9
DOI 10.3389/978-2-8325-5725-9

About Frontiers

Frontiers is more than just an open access publisher of scholarly articles: it is a pioneering approach to the world of academia, radically improving the way scholarly research is managed. The grand vision of Frontiers is a world where all people have an equal opportunity to seek, share and generate knowledge. Frontiers provides immediate and permanent online open access to all its publications, but this alone is not enough to realize our grand goals.

Frontiers journal series

The Frontiers journal series is a multi-tier and interdisciplinary set of open-access, online journals, promising a paradigm shift from the current review, selection and dissemination processes in academic publishing. All Frontiers journals are driven by researchers for researchers; therefore, they constitute a service to the scholarly community. At the same time, the *Frontiers journal series* operates on a revolutionary invention, the tiered publishing system, initially addressing specific communities of scholars, and gradually climbing up to broader public understanding, thus serving the interests of the lay society, too.

Dedication to quality

Each Frontiers article is a landmark of the highest quality, thanks to genuinely collaborative interactions between authors and review editors, who include some of the world's best academicians. Research must be certified by peers before entering a stream of knowledge that may eventually reach the public - and shape society; therefore, Frontiers only applies the most rigorous and unbiased reviews. Frontiers revolutionizes research publishing by freely delivering the most outstanding research, evaluated with no bias from both the academic and social point of view. By applying the most advanced information technologies, Frontiers is catapulting scholarly publishing into a new generation.

What are Frontiers Research Topics?

Frontiers Research Topics are very popular trademarks of the *Frontiers journals series*: they are collections of at least ten articles, all centered on a particular subject. With their unique mix of varied contributions from Original Research to Review Articles, Frontiers Research Topics unify the most influential researchers, the latest key findings and historical advances in a hot research area.

Find out more on how to host your own Frontiers Research Topic or contribute to one as an author by contacting the Frontiers editorial office: frontiersin.org/about/contact

Salmonella spp.- transmission, pathogenesis, host-pathogen interaction, prevention and treatment

Topic editors

Sébastien Holbert — INRA Centre Val de Loire, France

George Grant — University of Aberdeen (retired) / now independent researcher, United Kingdom

Patrick J. Naughton — Ulster University, United Kingdom

Citation

Holbert, S., Grant, G., Naughton, P. J., eds. (2024). *Salmonella spp.- transmission, pathogenesis, host-pathogen interaction, prevention and treatment*.

Lausanne: Frontiers Media SA. doi: 10.3389/978-2-8325-5725-9

Table of contents

frontiers | Frontiers in Microbiology

TYPE Original Research
PUBLISHED 06 June 2023
DOI 10.3389/fmicb.2023.1184387

OPEN ACCESS

EDITED BY
Patrick J. Naughton,
Ulster University, United Kingdom

REVIEWED BY
Peter S. Evans,
Food Safety and Inspection Service (USDA), United States
Alexey V. Rakov,
Central Research Institute of Epidemiology (CRIE), Russia

*CORRESPONDENCE
Carmen Losasso
✉ closasso@izsvenezie.it

RECEIVED 11 March 2023
ACCEPTED 15 May 2023
PUBLISHED 06 June 2023

CITATION
Petrin S, Wijnands L, Bencinà E, Mughini-Gras L, Delfgou-van Asch EHM, Villa L, Orsini M, Losasso C, Olsen JE and Barco L (2023) Assessing phenotypic virulence of *Salmonella enterica* across serovars and sources. *Front. Microbiol.* 14:1184387. doi: 10.3389/fmicb.2023.1184387

Assessing phenotypic virulence of *Salmonella enterica* across serovars and sources

Sara Petrin[1,2], Lucas Wijnands[3], Elisa Bencinà[3], Lapo Mughini-Gras[3,4], Ellen H. M. Delfgou-van Asch[3], Laura Villa[5], Massimiliano Orsini[1], Carmen Losasso[1]*, John E. Olsen[2] and Lisa Barco[6]

[1]Microbial Ecology and Microrganisms Genomics Laboratory, Istituto Zooprofilattico Sperimentale delle Venezie, Legnaro, Padova, Italy, [2]Department of Veterinary and Animal Sciences, Faculty of Health and Medical Sciences, University of Copenhagen, Frederiksberg C, Denmark, [3]Centre for Infectious Disease Control (CIb), National Institute for Public Health and the Environment (RIVM), Bilthoven, Netherlands, [4]Institute for Risk Assessment Sciences (IRAS), Utrecht University, Utrecht, Netherlands, [5]Department of Infectious Diseases, Istituto Superiore di Sanità, Rome, Italy, [6]WHOA and National Reference Laboratory for Salmonellosis, Istituto Zooprofilattico Sperimentale delle Venezie, Legnaro, Padova, Italy

Introduction: Whole genome sequencing (WGS) is increasingly used for characterizing foodborne pathogens and it has become a standard typing technique for surveillance and research purposes. WGS data can help assessing microbial risks and defining risk mitigating strategies for foodborne pathogens, including *Salmonella enterica*.

Methods: To test the hypothesis that (combinations of) different genes can predict the probability of infection [P(inf)] given exposure to a certain pathogen strain, we determined P(inf) based on invasion potential of 87 *S. enterica* strains belonging to 15 serovars isolated from animals, foodstuffs and human patients, in an *in vitro* gastrointestinal tract (GIT) model system. These genomes were sequenced with WGS and screened for genes potentially involved in virulence. A random forest (RF) model was applied to assess whether P(inf) of a strain could be predicted based on the presence/absence of those genes. Moreover, the association between P(inf) and biofilm formation in different experimental conditions was assessed.

Results and Discussion: P(inf) values ranged from 6.7E-05 to 5.2E-01, showing variability both among and within serovars. P(inf) values also varied between isolation sources, but no unambiguous pattern was observed in the tested serovars. Interestingly, serovars causing the highest number of human infections did not show better ability to invade cells in the GIT model system, with strains belonging to other serovars displaying even higher infectivity. The RF model did not identify any virulence factor as significant P(inf) predictors. Significant associations of P(inf) with biofilm formation were found in all the different conditions for a limited number of serovars, indicating that the two phenotypes are governed by different mechanisms and that the ability to form biofilm does not correlate with the ability to invade epithelial cells. Other omics techniques therefore seem more promising as alternatives to identify genes associated with P(inf), and different hypotheses, such as gene expression rather than presence/absence, could be tested to explain phenotypic virulence [P(inf)].

KEYWORDS

***Salmonella enterica*, whole genome sequencing, phenotypic virulence, Bayesian approach, gastrointestinal tract model system, probability of infection, virulence genes**

1. Introduction

Non-typhoidal *Salmonella enterica* (NTS) is the second most common causative agent among reported human zoonotic infections in the European Union (EU) (EFSA and ECDC, 2021a) and one of the major challenges facing food safety and public health nowadays. Different serovars have been implicated in foodborne outbreaks and human cases of salmonellosis, but three of them, namely *Salmonella* (hereafter *S.*) Enteritidis, *S. Typhimurium* and the monophasic variant of *S. Typhimurium* (MVST), account for over 70% of the confirmed human cases in Europe (EFSA and ECDC, 2021a,b). Other *Salmonella* serovars are also commonly implicated in human infections, but their occurrence among clinical cases is lower. For instance, *S. Infantis*, *S.* Newport and *S.* Derby altogether accounted for only 4.4% of the confirmed human cases in 2019 (EFSA and ECDC, 2021b).

NTS is mainly spread from farm animals to humans through food sources. *S. Typhimurium* and MVST are primarily associated with pigs and chickens, *S.* Derby with pigs and turkeys, and *S. Enteritidis* and *S. Infantis* with layers and chickens, respectively (EFSA and ECDC, 2021a,b). Foodstuffs are important sources for human salmonellosis, as highlighted by the number of foodborne outbreaks in which foods have been strongly implicated in recent years (EFSA and ECDC, 2017; EFSA and ECDC, 2021a,b; Chanamè-Pinedo et al., 2022b). To lower the prevalence of *Salmonella* along the food chain, from farm to fork, control measures have been implemented in the EU. In particular, national control programs to reduce the prevalence of *Salmonella* in poultry farms have been established according to EU Regulation (EC) No 2160/2003. Consequently, serovars that are relevant to public health, namely *S. Enteritidis*, *S. Typhimurium* and MVST, are considered target *Salmonella* serovars in poultry flocks. On the contrary, only few countries have implemented control programs for *Salmonella* in pigs, and these programs are not harmonized across the EU (Bonardi et al., 2021; Correia-Gomes et al., 2021). In addition, EU Regulation (EC) No 2073/2005, sets the microbiological criteria for *Salmonella* in foodstuffs, determining food safety and process hygiene criteria for both poultry and pig products, as well as other food matrices.

Despite the implementation of control plans in the poultry production chain, no significant decrease in human salmonellosis has been observed since 2012 (Koutsoumanis et al., 2019b; Chanamè-Pinedo et al., 2022a), challenging the current choice of the identified target *Salmonella* serovars. Indeed, a higher impact on public health might be expected if the selection of target serovars is amended according to their occurrence and epidemiology in each European country. Moreover, it has been proposed to select serovars considering additional criteria than those currently used, including antimicrobial resistance and virulence characteristics [Annex III from the Commission Regulation (EU) No 2160/2003; Koutsoumanis et al., 2019a; Leati et al., 2021]. The focus on serovar without consideration of the actual pathogenicity potential of the single strain for animals and humans might overlook highly pathogenic *Salmonella* strains, which do not necessarily belong to the target serovars, and such strains could spread as emerging clones, becoming potential causes of new outbreaks.

The success of *Salmonella* as a pathogen results from the ability to cause acute intestinal inflammation in many host species, including humans, differently from close relatives such as *E. coli*. The invasion of epithelial cells evokes an acute inflammatory reaction in the intestinal mucosa that ultimately involves neutrophils, which, during infection, generate reactive oxygen species (ROS) in the intestinal lumen. As a consequence, ROS produced during inflammation oxidize thiosulfate, a metabolite generated from the oxidation of hydrogen sulphide produced by the fermenting microbiota, to tetrathionate. *Salmonella* can use tetrathionate as a terminal electron acceptor in tetrathionate respiration (Hensel et al., 1999), and the induced acute intestinal inflammation provides a significant growth advantage over competing microbes, which rely only on fermentation to obtain energy for growth (Bäumler et al., 2011; Rivera-Chávez and Bäumler, 2015).

The evolution of *Salmonella* as a pathogen occurred over time also through the acquisition of genetic material by horizontal gene transfer and genome erosion through pseudogenes formation, and led to host adaptation of a number of *Salmonella* serovars and variability in terms of infection outcomes (Uzzau et al., 2000; Matthews et al., 2015; Parisi et al., 2018). Moreover, the ability of *Salmonella* to colonize and cause disease in different hosts could also depend on the allelic variations within a collection of specific virulence genes or effector proteins (Yue and Schifferli, 2014), and different studies have demonstrated how allelic variations affected *Salmonella* pathogenesis (Hopkins and Threlfall, 2004; Thornbrough and Worley, 2012; Yue et al., 2015; Rakov et al., 2019) and contributed to bacterial adaptation to preferential hosts (De Masi et al., 2017).

The potential of whole genome sequencing (WGS) in the identification and characterization of foodborne pathogens has been widely recognized to the point that it is now becoming a standard surveillance technique for epidemiological purposes (Koutsoumanis et al., 2019a), and the amount of data generated by WGS could potentially be used in defining microbial risk and to set mitigation strategies aimed at reducing the human cases caused by zoonotic *Salmonella*.

Building upon the hypothesis that different genes can predict the probability of infection (P(inf)), given exposure to a certain strain and thus help define the public health relevance of such strain, here we determined P(inf), as a proxy of infectivity, based on the invasion potential of 87 *Salmonella* strains belonging to 15 different serovars using an *in vitro* gastrointestinal tract (GIT) model system (Pielaat et al., 2016; Wijnands et al., 2017). We further applied a random forest model to assess whether the P(inf) of a strain can be predicted as a function of the presence/absence of a set of genes related to virulence or as a function of its ability to form biofilm.

2. Materials and methods

2.1. Bacterial strains

Eighty-seven *S. enterica* strains, belonging to the selection of isolates already described in Petrin et al. (2022), were included in this study. Briefly, the strains were isolated in Italy between 2009 and 2019 and belonged to the collection of the Italian National Reference Laboratory for Salmonellosis, Istituto Zooprofilattico Sperimentale delle Venezie (IZSVe) and the Istituto Superiore di Sanità (ISS). The strains belonged to 15 different serovars, representing both frequently occurring serovars in relation to human salmonellosis cases in Italy and other European countries (EFSA and ECDC, 2021a) [i.e., *S. Enteritidis*, *S. Typhimurium* and monophasic variant of

S. Typhimurium (MVST)], and more rarely occurring serovars (i.e., *S.* Derby, *S.* Dublin, *S.* Hadar, *S. Infantis*, *S.* Kentucky, *S.* Livingstone, *S.* Mbandaka, *S.* Montevideo, *S.* Newport, *S.* Rissen, *S.* Senftenberg, and *S.* Thompson). Strains were isolated from animal, food and human sources details regarding the selected strains are reported in Supplementary Table S1 (Sheet 1, Bacterial strains). The strains were maintained at −80°C on cryobank beads (Microbank, Pro-Lab Diagnostics) until use. Single bacteria colonies were cultured in BHI-broth overnight at 37°C for testing in a simulated gastro-intestinal tract (GIT) system assay, in which a *S.* Typhimurium isolate (STM 3283) was included as control, as described in detail elsewhere (Wijnands et al., 2017).

2.2. Genome sequences for *Salmonella* pangenome

A collection of 759 *Salmonella* genome sequences, including those of the 87 strains used in the GIT assay, were selected to build the *Salmonella* pangenome for this study. Of the genomic sequences, 370 genomes were newly sequenced as described in Section 2.3, while 389 genomes were downloaded from EnteroBase [Last access 03/06/2019 (Zhou et al., 2020)][1], among *Salmonella* genomic sequences using the same inclusion criteria in terms of serovar and source of isolation as for the GIT strains. The complete dataset is described in Supplementary Table S1 (Sheet 2, Genome sequences).

2.3. Whole genome sequencing

The *Salmonella* isolates were sequenced starting from pure culture on tryptose agar, grown overnight at 37°C. Genomic DNA (gDNA) was extracted using a commercial column-based kit (QIAamp DNA Mini, QIAGEN), and purified gDNA was quantified with a Qubit 3.0 Fluorometer (Life Technologies). Libraries for whole genome sequencing were prepared using the Nextera XT DNA sample preparation kit (Illumina) following the manufacturer's instructions. High-throughput sequencing was performed with MiSeq Reagent kit v3, resulting in 251 bp long paired-end reads or NextSeq High Output kit v2.5, resulting in 151 bp long paired end reads. FastQC v0.11.2 (Andrews, 2010) was used to assess the sample quality, while Trimmomatic 0.32 (Bolger et al., 2014) was used to trim both quality and length, with the following options: removal of Nextera adapters sequences; cut bases off the start of the read, if below a quality score of 20; cut bases off the end of the read, if below a quality score of 20; sliding window trimming, clipping the read once the average quality within the window (4 bp) falls below 20; finally, drop the read if it is shorter than 100 bp (Mastrorilli et al., 2020). Subsequently, reads were *de novo* assembled using Spades 3.10.1 (Bankevich et al., 2012) with default parameters for Illumina reads, and the quality of assembly was assessed using QUAST 3.1 (Gurevich et al., 2013). Details about quality and metrics of the assemblies are reported in Supplementary Table S1.

1 www.enterobase.warwick.ac.uk

2.4. Pangenome determination and database for genes prediction

Salmonella genomes were annotated using Prokka v1.14.5 with default parameters. The final pangenome was built using Roary v3.13.0, excluding singletons. At the same time, the 28,639 protein sequences collected in Virulence Factor database [VFDB, last access 08/01/2021, (Chen et al., 2005)] were downloaded and searched in the *Salmonella* pangenome. Protein sequences were preferred since proteins are usually the biological effectors and allow to not accounting for degenerate codons. The presence of a protein sequence in the pangenome was assessed with Diamond v0.9.17 (Buchfink et al., 2015), setting 90% coverage and 90% identity. Protein sequences that were found in all or none of the *Salmonella* genomes were excluded from the subsequent analyses. Moreover, a second subset of proteins (hereafter 'informative sequences'), collecting only the sequences present in at least 10% and no more than 95% of the genomes, were used in the following analyses.

2.5. Gastro-intestinal tract system assay

The gastro-intestinal tract (GIT) model system developed by Wijnands et al. (2017) was used to quantify the *in-vitro* infectivity of *Salmonella* strains by estimating their *in vitro* probability of infection or P(inf). P(inf) is calculated as the ratio invasion (INV) to overnight (ON) bacterial concentrations (see below). The system is composed of four sequential stages through which *Salmonella* isolates are transferred without intermediate culturing: simulated gastric fluid (SGF), simulated intestinal fluid (SIF), attachment (ATT) and invasion (INV) (Figure 1). The composition and preparation of simulated gastric and intestinal fluids are reported in Supplementary material S1.

2.5.1. Simulated gastrointestinal passages

One ml of overnight (ON) culture was added to 9 mL of SGF and incubated for 30 min at 37°C in a humidified atmosphere of 95% air – 5% CO_2. After the incubation, 1 mL was used for enumeration of viable cells (see 2.5.3), while 4 mL were transferred to 40 mL of SIF and incubated for 2 h at 37°C, under microaerophilic conditions (6% O_2), with shaking at 50 rpm. After that, surviving cells were used for the invasion/attachment assay (see 2.5.2) and enumerated.

2.5.2. Attachment/invasion assay with Caco-2 cells

Caco-2 (HTB-37, ATCC) cells were cultured as described in Oliveira et al. (2011) and maintained in Dulbecco's Modified Eagle's Medium (DMEM, Gibco) with 10% heat-inactivated fetal bovine serum (FBS, Gibco), 1% non-essential amino acids (Gibco), 1% 100X glutamine (Gibco) and 0,1% gentamycin (50 mg/mL, Gibco) in 75 cm^2 flasks (Corning Inc.). Caco-2 cells were grown to confluence at 37°C in a humidified atmosphere of 95% air – 5% CO_2 and differentiated into cells simulating the small intestine epithelial cells by culturing the cells in monolayers, in 12-wells tissue culture plates (Corning Inc.). To achieve the differentiation, cells were seeded at a density of 1.6×10^5 cell/ml and growth media was changed every 2 or 3 days. The cells completely differentiate in 14 days after being cultured (Pinto et al., 1983).

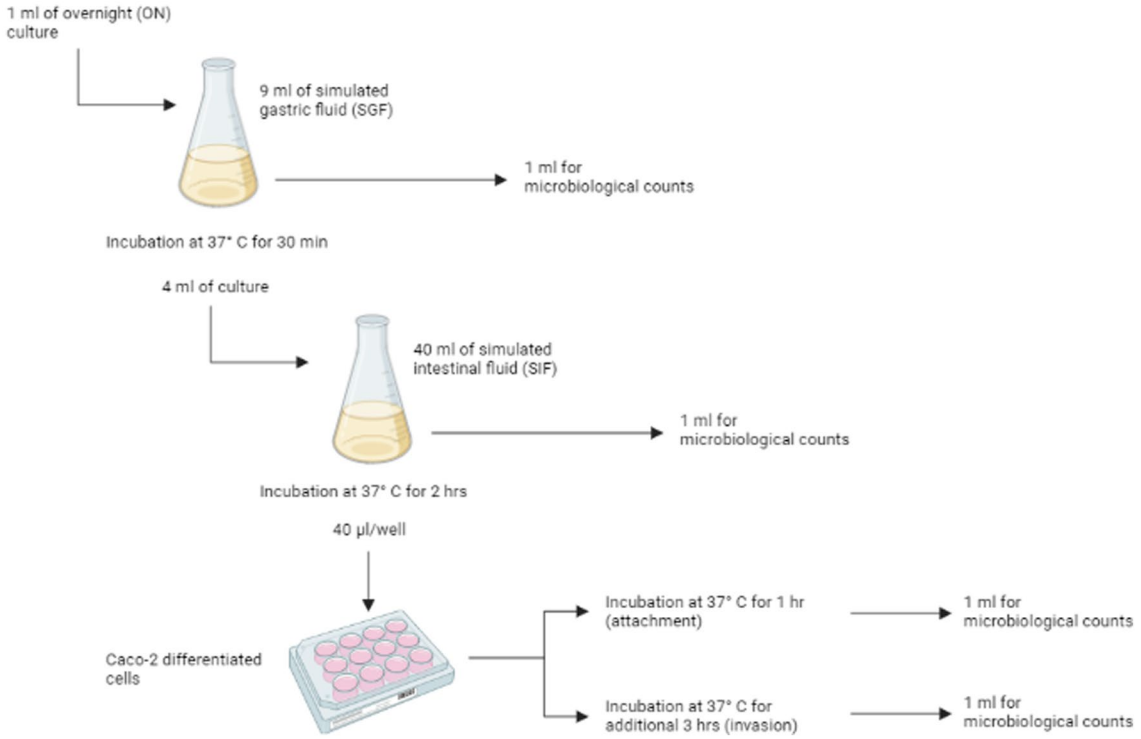

FIGURE 1
Schematic representation of the *in vitro* gastrointestinal tract (GIT) model system passages. For each of the different stages [ON, SGF, SIF, attachment (ATT) and invasion (INV)] replicate counts were prepared. Figure is created with BioRender.

Caco-2 cells were washed three times with sterile phosphate buffered solution (PBS) before the assay, in order to remove traces of gentamycin antibiotic. After that, 1 mL of experimental culture medium (ECM, i.e., prewarmed DMEM without gentamycin and FBS) was added to each of the 12 wells. 40 µL of the cell mixture from the previous steps were inoculate in each well, and the plates were incubated at 37°C in a humidified atmosphere of 95% air – 5% CO_2 for 1 h. After the incubation, the medium was discarded and monolayers were rinsed three times with sterile PBS, to remove non-attached or loosely attached bacteria. The cells were then used to determine both attached and invading bacteria and invading bacteria. For the enumeration of attached and invading bacteria, six wells of Caco-2 cells were lysed with 1% Triton-X100 (Merck) in PBS for 5 min at room temperature. The lysate from three wells was combined and named ATT1 and ATT2. The Caco-2 cells in the remaining six wells were treated with ECM supplemented with gentamycin (300 µg/mL) to inactivate attached bacteria (Berk, 2008) and incubated at 37°C in a humidified atmosphere of 95% air – 5% CO_2. After 3 h, cells were washed three times with sterile PBS to remove residual antibiotic and lysed with 1% Triton-X100. To enumerate the invading bacteria, the lysate from three wells was combined and named INV1 and INV2.

2.5.3. Enumeration of bacterial load

Single bacteria samples from overnight (ON) culture, SGF and SIF passages, and both the aliquots ATT1 and ATT2, and INV1 and INV2 were used to enumerate the bacterial load at each stage of the simulated gastrointestinal system. Appropriate 10-fold dilutions were prepared, and dilutions were plated on Tryptone soy agar (TSA) in duplicate. To estimate P(inf) (see below), duplicate counts for each appropriate dilution from the three first stages (ON, SGF and SIF), and duplicate counts for each appropriate dilution for ATT1, ATT2, INV1 and INV2 were considered.

2.6. Statistical analysis

2.6.1. GIT system data analysis

The bacterial count data obtained from the GIT system were analyzed using a Bayesian model that is able to distinguish between experimental uncertainty and biological variability in the estimates of bacterial counts, as presented in details elsewhere (Wijnands et al., 2017; Kuijpers et al., 2019). Briefly, the measured bacterial counts in the different stages of the GIT system were assumed to follow a Poisson distribution, while the bacterial concentrations were assumed to follow a log-normal distribution and the log changes at any phase of the GIT were estimated by using a Markov chain Monte Carlo (MCMC) sampling scheme. The logarithm of the probability of infection, or P(inf), which provides an estimate of the *in vitro* infectivity of the tested isolate, was then defined as the sum of all log changes in bacterial concentrations throughout the GIT system passages, from the overnight culture (ON) to invasion of Caco-2 cells (INV). The outputs of the model resulted in a posterior distribution of P(inf) values for each *Salmonella* isolate tested with the GIT system. From the estimated distribution of P(inf), the mean value and the 95% confidence intervals were then calculated.

2.6.2. Virulence difference testing

Multivariable generalized linear models (GLM) with Gamma error distribution and a log link function were used for statistical significance testing of the differences in P(inf) (dependent variable) among serovars and sources of isolation (independent variables). This GLM parameterization was chosen given the positively skewed P(inf) distribution. The same approach was used to test associations between P(inf) and biofilm formation ability under different experimental conditions, as studied by Petrin et al. (2022). Estimates were thus adjusted for differences among serovars and sources of isolations (covariates), and clustering of observation (replicates) at the isolate level using cluster-robust (Sandwich) variance estimators (Williams, 2000). Prior to GLM analysis, to limit the number of hypotheses tested and therefore minimize Type-I error, two-way ANOVA was used to screen whether there were significant differences among serovars (15 groups) and sources (3 groups) in each passage of the GIT system, i.e., survival to exposure to gastric and intestinal fluid, adhesion and invasion. Analyses were performed in STATA 17 (StataCorp, College Station, TX, USA). A $p < 0.05$ was considered statistically significant.

2.6.3. Assessing the similarity of clusters based on virulence and genetic characteristics

To investigate the potential associations between the mean value of P(inf) and the presence or absence of specific virulence genes, an unsupervised cluster algorithm was used. A distance matrix was then built for mean P(inf) values based on the pairwise Euclidean distances between the mean P(inf) of each isolate, while the distance matrix for the gene presence/absence was built based on the Jaccard distance, defined as 1-Jaccard index. The Jaccard index was computed pairwise on each pair of isolates. From the calculated matrices, a hierarchical agglomerative algorithm based on the Ward method (Ward, 1963) was applied to build cluster trees. To quantify similarities between the two cluster trees, the B_k statistics was used (Fowlkes and Mallows, 1983), which is defined as follows.

Considering two trees, each one with the same number of elements n, and partitioning each of them into $k = 2, \ldots, n-1$ sub-clusters, B_k is then defined as:

$$B_k = \frac{T_k}{\sqrt{P_k Q_k}}; \quad (1)$$

with:

$$T_k = \sum_{i=1}^{k}\sum_{j=1}^{k} {s_{i,j}}^2 - n; \quad (2)$$

$$P_k = \sum_{i=1}^{k}\left(\sum_{j=1}^{k} s_{i,j}\right)^2 - n; \quad (3)$$

$$Q_k = \sum_{j=1}^{k}\left(\sum_{i=1}^{k} s_{i,j}\right)^2 - n; \quad (4)$$

and with $s_{i,j}$ quantifying the number of elements shared between the ith cluster of the first tree and the jth cluster of the second tree. B_k values range between 0 and 1, with 1 indicating complete correspondence and 0 indicating complete non-correspondence between the sub-clusters of the two trees. B_k has been computed by using the R package "Dendextend" (Galili, 2015) for all sub-clusters k.

2.6.4. Predicting mean P(inf) from virulence genes and ability to produce biofilm

In order to assess whether the mean value of P(inf) could be predicted by the presence/absence of specific genes, a Random Forest model was applied by using the 'randomForest' package in R (RStudio Team, 2021). The same analysis was repeated using the informative sequences, ability to form biofilm and serovar as predictors (Supplementary material S1). The random forest models were applied in two ways: regression and classification mode. In the regression mode the variable of interest, P(inf), was considered as a continuous variable, while in the classification mode, P(inf) values were split in two categories: 'low' if P(inf) < median [P(inf)] and 'high' if P(inf) ≥ median [P(inf)]. The virulence genes from the presence/absence matrix, as well as informative sequences, ability to produce biofilm and serovar (Supplementary material S1), were used as model predictors after removing the non-informative records from the databases, i.e., those genes that were present or absent in all isolates. Proportion of explained variance (PEV) and out-of-bag (OOB) predictions were calculated after running the models with 10,000 trees.

3. Results

3.1. *In vitro* virulence

Box plots of the P(inf) values estimated with the Bayesian model for all tested isolates, sorted by serovars, are shown in Figure 2, while the measured P(inf) values from the GIT system are reported in Supplementary Table S2. A degree of variability existed between the tested strains, with a *S.* Kentucky isolate from an animal source having the lowest average P(inf), 6.7E-05, and an *S.* Kentucky strain from a human source having the highest average P(inf), 5.2E-01. At the serovar level, individual isolates displayed a wide range of P(inf) values, except for *S.* Hadar, for which most of the isolates (4 out of 6) showed similar *in vitro* virulence behavior, with P(inf) values being 51 to 55% lower than the P(inf) of the most virulent strain (Figure 2; Supplementary Table S2). Also *S.* Dublin showed small differences in P(inf) for the individual strains, with P(inf) values ranging from 1.93E-02 to 1.8E-01, corresponding to a variation of maximum 11% within *S.* Dublin strains, while *S.* Kentucky, *S.* Newport and *S. Typhimurium* displayed larger differences in P(inf).

Overall, there was no statistical difference in the estimated mean P(inf) values depending on the source (animal, food, human: value of $p = 0.7159$) or serovar (value of $p = 0.3760$).

Similar to the lack of statistical difference in P(inf) between serovars and sources, there were no statistically significant differences among serovars or sources in their invasiveness (value of $ps = 0.1127$ and 0.5192, respectively), intestinal survival, i.e., the fraction of bacteria surviving exposure to intestinal fluid over bacteria surviving exposure to gastric fluid (value of $ps = 0.0879$ and 0.0756, respectively) and gastric survival, i.e., the fraction of bacteria surviving exposure to gastric fluid over the original bacterial load introduced in the GIT system (value of $ps = 0.7918$ and 0.9585, respectively). The ANOVA test showed statistically significant differences in the attachment

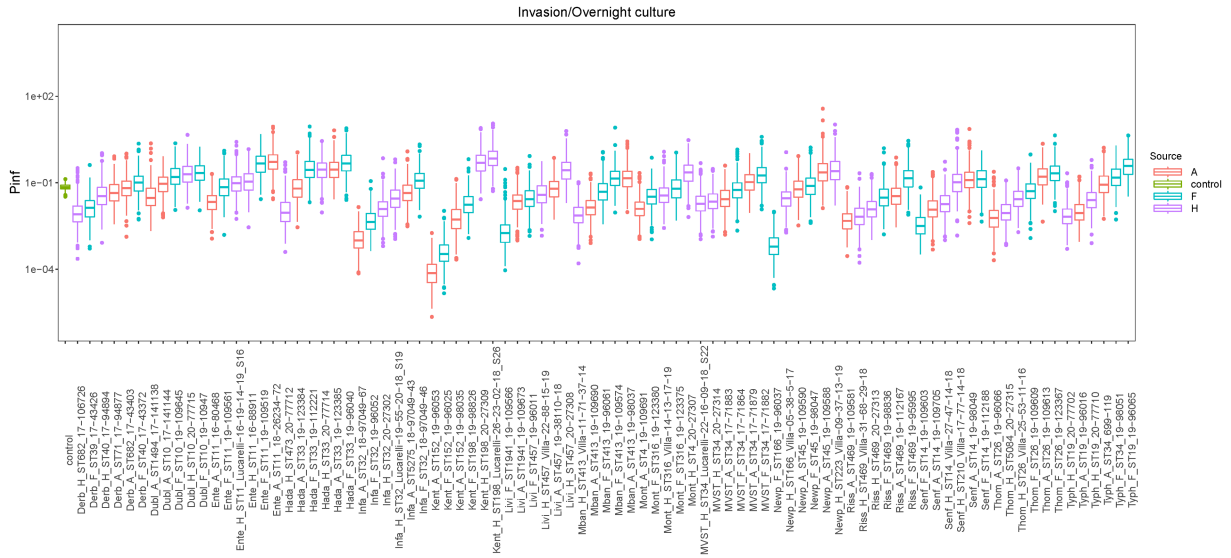

FIGURE 2
Boxplots of the estimated P(inf) values from the GIT system bacterial counts with the Bayesian model for each strain, sorted by serotype. Mean P(inf) is indicated with horizontal bold lines inside boxplots. Colors indicate the source of the isolate [red=animal sources (A in the strain name), light blue=food sources (F in the strain name), purple=human sources (H in the strain name), green=control strain (STM 3283 from Wijnands et al., 2017)]. Additional strains information can be found in Supplementary Table S2.

ability among the different serovars, i.e., the fraction of bacteria attaching to cells over bacteria surviving exposure to intestinal fluid (value of $p = 0.0002$). Thus, the Bonferroni-corrected comparisons in adhesiveness (post-hoc comparisons between serovars) showed that *S. Typhimurium* differed significantly from *S.* Livingstone (value of $p = 0.004$), MVST (value of $p = 0.005$), *S.* Mbandaka (value of $p = 0.026$), *S.* Rissen (value of $p < 0.001$) and *S.* Senftenberg (value of $p = 0.001$). Conversely, differences among sources were not statistically significant (value of $p = 0.8470$).

3.2. Association of P(inf) with biofilm formation ability

The ability to form biofilm was significantly negatively associated with the size of P(inf) for *S. Infantis* grown in tryptic soy broth (TSB) (value of $p = 0.000$); *S.* Derby and *S.* Montevideo grown in TSB 4% NaCl, pH4.5 (value of $ps = 0.045$ and 0.000, respectively); and *S. Infantis* and *S.* Montevideo grown in TSB 10% NaCl, pH4.5 (value of $ps = 0.030$ and 0.000, respectively). In contrast, the ability to form biofilm was significantly and positively associated with the size of P(inf) for *S.* Hadar grown in TSB 4% NaCl, pH7 (p-value = 0.008) and *S. Enteritidis* and *S.* Hadar grown in TSB 10% NaCl, pH7 (p-values = 0.014 and 0.003, respectively). Significant results are reported in Table 1, extended results are reported in Supplementary Table S3.

3.3. Assessing the similarity of clusters based on virulence genes and genetic characteristics

To investigate potential associations between the mean value of P(inf) and the presence or absence of specific virulence genes, cluster trees were built for both the mean P(inf) of each isolate and the genes presence/absence. Cluster trees were then compared to quantify similarities. Figure 3 shows the cluster trees based on the mean value of P(inf) (Figure 3A) and based on the matrix of presence/absence of virulence genes (Figure 3B). Looking at the cluster trees, it was noticed that both the elements clustered together, and that the branching structures are different. In order to assess the similarity between the two clusters, the B_k statistic was computed and plotted as a function of the number of sub-clusters k in which the two trees could be partitioned into (black dots in Figure 3C). The red line in Figure 3C represents the 95% rejection region under the null hypothesis of no relation between the trees. For the majority of the k partitions, the black dots fall below the red line, indicating that the tree based on the P(inf) and the tree based on the virulence genetic matrix are not related.

3.4. Predicting mean P(inf) from virulence genes and ability to produce biofilm

To assess whether the mean value of P(inf) could be predicted by the presence/absence of specific genes, a Random Forest (RF) model was applied. First, presence/absence of virulence genes was plotted against the mean values of P(inf) for each isolate (Figure 4). No evident pattern(s) were found to link the presence of a given virulence gene(s) and the mean P(inf) of the isolates. The percentage of variance explained for the RF model run in regression mode with 10.000 trees was essentially 0. This low score indicated that the virulence genes were very poor predictors of the mean value of P(inf). This was also confirmed by plotting the out of bag (OOB) predictions versus the true mean values of P(inf) (Figure 5).

The OOB error rate for the model run in classification mode with 10.000 trees (dichotomy variable "low," "high") was 42.5%. For both regression and classification models, increasing the number of trees did not improve the performance. The accuracy of the model in classification mode was 59%, with 95% CI [36–79%]. This showed that

TABLE 1 Significant results of the association test between P(inf) and biofilm formation ability in different experimental conditions for different serovars.

Experimental condition	Serovar	Beta[a]	Bonferroni-corrected 95% CI		p-value
TSB	*S. Infantis*	−6.581	−10.479	−2.682	0.000
TSB 4% NaCl pH 7	*S. Hadar*	7.844	1.312	14.376	0.008
TSB 10% NaCl pH 7	*S. Enteritidis*	12.481	1.656	23.306	0.014
	S. Hadar	11.405	2.548	20.262	0.003
TSB 4% NaCl pH 4.5	*S. Derby*	−15.909	−31.082	−0.736	0.045
	S. Montevideo	−9.378	−15.816	−2.940	0.000
TSB 10% NaCl pH 4.5	*S. Infantis*	−37.142	−72.260	−2.023	0.030
	S. Montevideo	−11.519	−19.258	−3.779	0.0

[a]Beta = coefficient of the GLM with a gamma error distribution and a log link function.

the presence/absence of virulence genes were poor predictors of the mean P(inf) also when treated as dichotomous variable.

The RF analysis was conducted also using the informative sequences, ability to form biofilm and serovar as predictors. Results are detailed in Supplementary material S1.

4. Discussion

For many years, salmonellosis has been the second most commonly reported foodborne bacterial infection in Europe (EFSA and ECDC, 2021a). EU Regulation (CE) No 2160/2003 and national control programs were implemented to lower the prevalence of *Salmonella* serovars relevant for public health, however, the choice of which serovars to be included as relevant in poultry flock has been the recent object of further evaluation, due to the observation that no further significant decrease in human salmonellosis infections has occurred since 2012 in EU (Koutsoumanis et al., 2019b). The large amount of available molecular and genomic data in association with epidemiological data, has allowed the identification of emerging *Salmonella* clones with a potentially high impact on human and public health. Indeed, the emergence of such high-risk clones, especially those characterized by increased virulence or resistance to relevant antimicrobials for human medicine, usually precedes the epidemic spread of a specific serovar, with the majority of the stains within such serovar not belonging to the emergent clone and displaying instead only limited epidemiological relevance (Aviv et al., 2014; Mourão et al., 2014; Worley et al., 2018; Chiou et al., 2019; Liao et al., 2019; Yokoyama et al., 2019). It would therefore be important to identify a panel of biological markers that could predict the relevance of a strain in terms of public health impact, besides the serovars.

In this study we determined the *in vitro* infectivity (probability of infection, or P(inf)), of a panel of *Salmonella* strains, investigated the presence of virulence genes in their genomes and integrated these data to identify potential predictors of P(inf), with the final aim of highlighting potentially relevant *Salmonella* strains for public health.

The use of P(inf) as a proxy of infectivity, and ultimately virulence, of a given strain has been driven by the fact that *Salmonella* can act as intracellular pathogen able to invade the intestinal mucosa through expression of genes encoded in the *Salmonella* Pathogenicity Island (SPI)-1 (Galán, 2001). Moreover, invasive NTS (iNTS), which spreads to host tissues beyond the intestine, can cause bacteremia and infection of usually sterile sites (Uzzau et al., 2000; Santos et al., 2009). Many serovars have been documented to cause iNTS, including *S. Typhimurium*, *S. Enteritidis* and *S.* Dublin (Uzzau et al., 2000; Okoro et al., 2015; Feasey et al., 2016; Mughini-Gras et al., 2020). Although these serovars mainly cause self-limiting gastroenteritis, their potential to cause more severe, invasive infections should not be underestimated. For this reason, P(inf), as derived from the INV to ON ratio, has been considered as an ultimate indicator of infectivity providing a snapshot of the most severe form of *Salmonella* infection.

The set of strains showed a wide range of P(inf) values ranging from 10^{-5} to 10^{-1}, similar to what has been reported for another *Salmonella* strain collection by Kuijpers et al. (2019), thus indicating variability among serovars and individual strains within a serovar. This is not surprising, since the large variability expressed by *Salmonella* serovars and strains in terms of virulence mechanisms (Cheng et al., 2019) could influence their ability to invade epithelial human cells. Indeed, our results suggested that generally P(inf) for food *Salmonella* isolates of a given serovar was higher than P(inf) for animal and human strains within the same serovar., with the exception of *S.* Kentucky, *S.* Livingstone and *S.* Montevideo, where P(inf) of human strains showed higher values. These serovars are uncommon in human infections, accounting for 0.69, 0.25 and 0.31% of the confirmed reported human cases in Europe in 2019, respectively (EFSA and ECDC, 2021b; European Centre for Disease Prevention and Control (ECDC), 2022).

It is interesting to note that in this study, *S.* Kentucky sequence type (ST) 152 strains, usually associated to poultry (Haley et al., 2016; Hawkey et al., 2019), displayed lower P(inf) values than *S.* Kentucky strains ST198, usually associated with humans (le Hello et al., 2013; Hawkey et al., 2019). Indeed, Le Hello et al. (2011) reported that patients infected with ciprofloxacin-resistant (CIP^R) *S.* Kentucky ST198 strains, a clone that rapidly spread in recent years due to the emergence of CIP^R and multidrug resistance (Coipan et al., 2020), were more frequently hospitalized, possibly reflecting the higher invasive potential of this clone. In a different study, using an *in vitro* assays with chicken embryo hepatocytes, *S.* Kentucky strains isolated from poultry sources exhibited equal invasive capabilities to that of other serovars, including *S. enteritidis* and *S. Typhimurium*, while they resulted in less invasion than isolates of *S. Enteritidis*, *S.* Mbandaka, and *S. Typhimurium* in invasion assays with a human ileocecal adenocarcinoma cells line (HCT-8 cells) (Joerger et al., 2009). On the

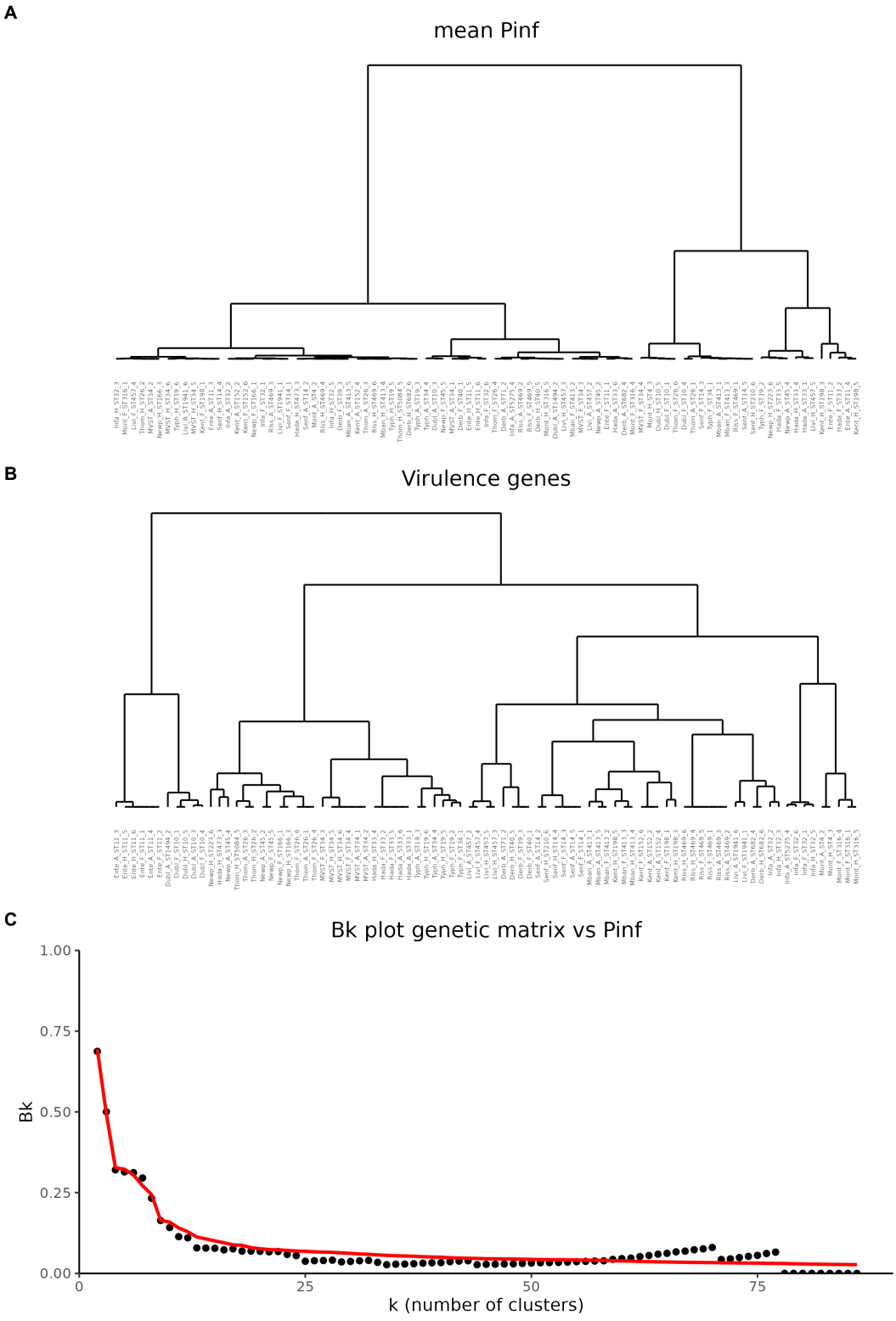

FIGURE 3
Comparison of hierarchical cluster trees. **(A)** Cluster tree based on the mean values of P(inf). **(B)** Cluster based on the matrix of virulence genes. **(C)** Comparison of the two cluster trees based on the B_k statistics. Black dots represent the B_k values plotted against the k number of clusters in which the dendrogram has been portioned. Red line represents the one-sided rejection region based on the asymptotic distribution of B_k for each value of k under the null hypothesis of no relation between the clusters.

basis of its rapid emergence and dissemination in poultry and humans, France has included *S.* Kentucky as a target serovar in poultry flocks (Koutsoumanis et al., 2019b). It is therefore possible that the ability of *S.* Kentucky strains to invade cells depends on the cell line used and also on sequence type, even if the reasons why certain *S.* Kentucky STs are associated with different hosts are not completely elucidated.

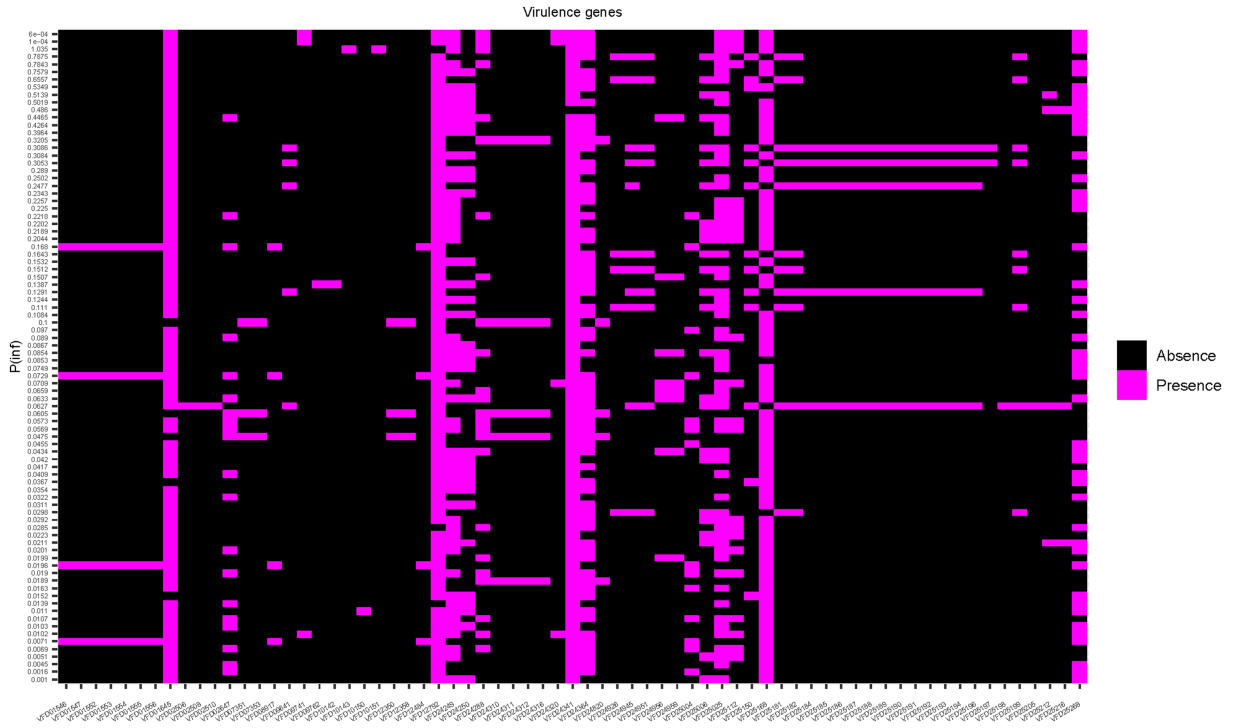

FIGURE 4
Heat map showing the presence/absence of genes for each isolate. Strains are ranked on the Y-axis according to the mean P(inf) values.

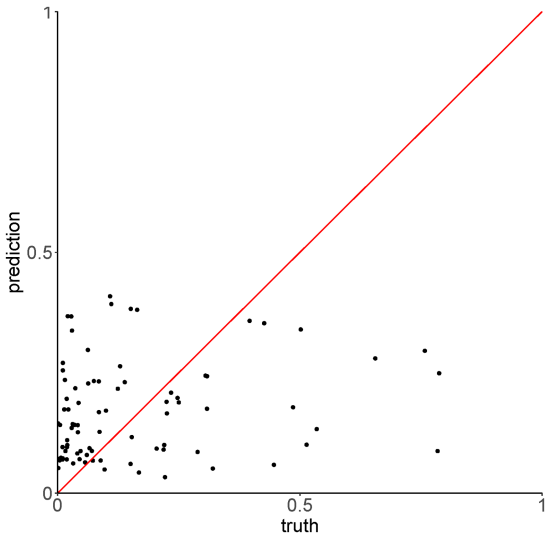

FIGURE 5
Out of bag (OOB) predictions of the Random Forest model run in regression mode versus the true values of P(Inf).

Human cases of salmonellosis caused by *S.* Montevideo are also infrequent, however this serovar has been described as the causative agent in cases of bacteremia (Kim et al., 2004), serous and septic arthritis (Gordon et al., 1949; Katsoulis et al., 2004), and acute myocarditis (O'Connor, 2000), demonstrating its potential as invasive pathogen in human infections. Foodborne outbreaks associated to this serovar have also been documented, with pepper, sesame seeds and their products listed as food vehicles (Unicomb et al., 2005; Willis et al., 2009; D'Oca et al., 2021), and low concentrations of *S.* Montevideo were found sufficient in such products to cause outbreaks (Unicomb et al., 2005; Harada et al., 2011; Stöcker et al., 2011; Paine et al., 2014). In the current study, indeed the two *S.* Montevideo isolates from human sources, despite having different P(inf) values, were among the human strains with the highest ability to invade Caco-2 cells, and showed higher P(inf) values compared to *S. typhimurium*, MVST and *S. Enteritidis* strains isolated from human sources, although such serovars are frequently found in human infections. Furthermore, Lalsiamthara and Lee (2017) demonstrated that the competence of *S.* Montevideo strains in invading chicken epithelial cells is comparable to that of *S. Typhimurium*, with whom *S.* Montevideo shares similar pattern of macrophage uptake and survival (Lalsiamthara and Lee, 2017).

Other serovars often involved in human infections, for which we expected higher ability to invade human cells, on the contrary, showed a higher variability in P(inf) values, and we even observed that the strains isolated from human cases showed lower P(inf) values than strains isolated from animal and food sources.

Salmonella Typhimurium and MVST, for instance have been consistently reported as major cause of human salmonellosis in Europe and worldwide (Ferrari et al., 2019; EFSA and ECDC, 2021b). Consumption of contaminated pork and poultry products was identified as the primary source of infection (EFSA and ECDC, 2021a), even if other food sources have been linked to outbreaks recently (Larkin et al., 2022; Lund et al., 2022). The higher P(inf) values displayed by strains isolated from animal and food sources could suggest that the strains isolated from non-human sources are in fact more efficient in invading human cells and possibly causing an

infection in humans. Further studies are needed to understand why, but the observation may give hints, why human-to-human spread of non-typhoidal *Salmonella* is known to be relatively rare. For instance, Kapperud et al. (1990) demonstrated that infection dose for *S. Typhimurium* in a Norwegian chocolate outbreak was very low in the food vehicle, probably due to the high level of fat, which protects the pathogen from gastric acidity through the stomach. Of note, the recent *Salmonella* outbreak related to chocolate products in Europe, which was characterized by a hospitalization rate of about 40% and some cases with severe clinical symptoms, was caused by MVST ST34, which in the current study also displayed a high P(inf). Similarly the different ability to invade Caco-2 cells in *S.* Kentucky according to ST, *S. Typhimurium* ST19 isolates generally displayed lower P(inf) values compared to *S. Typhimurium* ST34 isolates. Nonetheless, food isolates, irrespectively of the ST, had the highest P(inf). Variability in P(inf) values was also observed in *S. Enteritidis* and *S. Infantis* strains, where isolates from human sources were less invasive than isolates from animal and food sources, despite they were all of ST11 and ST32, respectively. Further research is needed to elucidate the variability within these serovars, since they are often involved in human infections (EFSA and ECDC, 2017, 2021a,b; Sarno et al., 2021).

High values of P(inf) were shown for *S.* Hadar isolates from food sources. Although this serovar is rarely reported from human infections, and caused only 298 human infections in 2019 in Europe (0.41% of the reported cases, European Centre for Disease Prevention and Control (ECDC), 2022), it is included as a target serovar in national programs for *Salmonella* control in breeding flocks of *Gallus gallus*. This serovar has been recently considered for revision due to its low frequency in breeders, broilers, layer flocks and humans; however, our data indicate that *S.* Hadar strains, irrespectively of their origin or ST, are able to efficiently pass through the *in vitro* GIT system and invade human cells, potentially developing an infection. Similar considerations can be drawn for *S.* Dublin isolates that in the current study showed high ability to invade human cells: indeed, human infections with this serovar often present as fatal syndromes (Fang and Fierer, 1991; Helms et al., 2003) and as reported by other researchers, *S.* Dublin isolates showed higher invasiveness and pathogenicity on Caco-2 cells (Bolton et al., 2000; Mughini-Gras et al., 2020).

For the other serovars included in the current study, similar scenarios can be described: *S.* Mbandaka, *S.* Rissen, *S.* Senftenberg and *S.* Thompson displayed variability in their ability to invade human cells after the passages in the GIT system, despite belonging to the same STs. On the contrary, *S.* Livingstone and *S.* Newport, for which we included isolates of different STs, showed similar P(inf) values, while for *S.* Derby we could describe diversity in the ability to invade human cells in the GIT system but no relation to the different STs characterizing our *S.* Derby strains and the circulating clones (Sévellec et al., 2020).

Overall, we did not find statistically significant differences among serovars in the different passages of the GIT system, except for adhesiveness to Caco-2 cells. Adhesion to surfaces and host cells is mediated by fimbriae that are therefore recognized as important virulence factors: since different fimbrial gene clusters exist in *Salmonella* spp. and most of them are sporadic or found only in few strains (Dufresne and Daigle, 2017). It is therefore possible that the different prevalence of certain fimbriae among *Salmonella* serovars influence their ability to adhere to Caco-2 cells. Nonetheless, the higher adhesiveness shown by *S. Typhimurium* strains did not always result in a better ability to invade cells and probably other factors involved in the invasion mechanisms could explain these differences.

The association of P(inf) with biofilm formation ability was also studied and statistically significant associations were found in all the different conditions for a limited number of serovars (*S. Infantis*, *S.* Hadar, *S. Enteritidis*, *S.* Derby, *S.* Montevideo), indicating that the two phenotypes are governed by different mechanisms and for the majority of the serovars tested here the ability to form biofilm does not seem to correlate with the ability to invade epithelial cells. Indeed, it seems that for *S.* Montevideo, *S. Infantis* and *S.* Derby strains, biofilm formation especially if the strains are exposed at pH 4.5, although limited (Petrin et al., 2022), impairs significantly the ability of such strains to invade human Caco-2 cells. On the contrary, from our data, a positive correlation between biofilm formation and P(inf) emerged for *S.* Hadar and *S. Enteritidis* strains. Previous studies demonstrated that high-virulence *S. Enteritidis* strains, incubated at optimal biofilm-forming conditions, release a soluble factor enabling them to disrupt the integrity of Caco-2 monolayer (Solano et al., 2001, 2002), while others found no correlation and suggested that biofilm formation might enhance cell invasiveness, even if this trait is not essential for cell invasiveness of *S. Enteritidis* in cultured epithelial cells (Shah et al., 2011). Most of the *S.* Hadar and few *S. Enteritidis* strains indeed showed high ability to invade human Caco-2 cell in the current study. For all the other tested serovars, no significant correlation was found, supporting the hypothesis that different characteristics other than the ability to form biofilm contribute to *Salmonella* invasiveness.

We then tried to predict the P(inf) from the presence or absence of virulence genes, however, the Random Forest model did not show good performance. It might then be that the differences in P(inf) are not determined by presence or absence of genes, but rather by difference in expression of genes present in all serovars. Similarly, the informative sequences, present only in at least 10% and no more than 95% of the genomes, as well as biofilm formation ability or serovar were only poor predictors of P(inf).

Although the well-differentiated Caco-2 cells closely mimic the differentiated intestinal tract (Hara et al., 1993) and previous studies have used them alone to successfully identify how *Salmonella* invasiveness differs (Solano et al., 2001; Betancor et al., 2009; Yim et al., 2010) or in an *in vitro* GIT system to identify genes potentially associated with P(inf) (Kuijpers et al., 2019), our study did not lead to conclusive results on the identification of specific virulence genes to predict the pathogenicity of a given *Salmonella* strain. Indeed, other factors might be involved in the infection process and these factors may depend on the pathogen itself, but also on other elements, such as the host environment, which is usually complex and cannot be properly reproduced in an *in vitro* model. Indeed, as already discussed by Wijnands et al. (2017), the GIT model used in our study does not take into account, for example the mechanical movements enabling the chyme to pass through the gastrointestinal tract, nor the role of immune system and intestinal microbiota, which can play an essential role in influencing *Salmonella* survival, attachment and invasion abilities.

Different approaches, such as RNAseq or metabolic profiling, together with more complex *in vitro* systems, could be helpful to

understand further the genetic characteristics involved in the invasiveness ability of each *Salmonella* strain.

5. Conclusion

We assessed the virulence of a set of *Salmonella* strains using an *in vitro* gastrointestinal tract model system that also includes attachment to and invasion of cultured human Caco-2 cells. The probability of infection P(inf) was estimated as a quantification of the infectivity of each strain and statistical associations with the ability of such strains to produce biofilm and the presence or absence of virulence genes were studied. Large variability in P(inf) was observed between *Salmonella* strains, and serovars more commonly isolated from human infections did not always show greater P(inf) nor invasiveness. Moreover, it was not possible to identify virulence genes that acted as predictors of P(inf) unambiguously. The use of expression data and/or metabolic profiles could represent a valuable alternative to detect genes highly associated with P(inf) and could be used to test potential association with strain's invasiveness.

Data availability statement

The datasets generated and analyzed during the current study are available in the NCBI database (http://www.ncbi.nlm.nih.gov) under BioProject ID PRJNA817603.

Author contributions

SP performed the experiments and wrote the manuscript. LW and EHMD-vA performed the experiments. EB, LM-G, and MO performed the analyses. CL, LB, and JO contributed to the concept of the work. All authors contributed to the article and approved the submitted version.

Funding

This work was supported by the project 'PRoSPECT': Predicting *Salmonella* Pathogenic Potential to Enhance Targeted Control Strategies', funded by the Italian Ministry of Health (grant no. RF-2018-12366604).

Acknowledgments

Ida Luzzi from the Istituto Superiore di Sanità (ISS, Rome, Italy) is greatly acknowledged for providing part of the human isolates. The authors would also like to thank Josè de Sousa Jorge Ferreira (RIVM) for useful suggestions on the Random Forest analysis.

Conflict of interest

The authors declare that the research was conducted in the absence of any commercial or financial relationships that could be construed as a potential conflict of interest.

Publisher's note

All claims expressed in this article are solely those of the authors and do not necessarily represent those of their affiliated organizations, or those of the publisher, the editors and the reviewers. Any product that may be evaluated in this article, or claim that may be made by its manufacturer, is not guaranteed or endorsed by the publisher.

Supplementary material

The Supplementary material for this article can be found online at: https://www.frontiersin.org/articles/10.3389/fmicb.2023.1184387/full#supplementary-material

References

Andrews, S. (2010). *FastQC: a quality control tool for high throughput sequence data.*

Aviv, G., Tsyba, K., Steck, N., Salmon-Divon, M., Cornelius, A., Rahav, G., et al. (2014). A unique megaplasmid contributes to stress tolerance and pathogenicity of an emergent *S. Enterica* serovar infantis strain. *Environ. Microbiol.* 16, 977–994. doi: 10.1111/1462-2920.12351

Bankevich, A., Nurk, S., Antipov, D., Gurevich, A. A., Dvorkin, M., Kulikov, A. S., et al. (2012). SPAdes: a new genome assembly algorithm and its applications to single-cell sequencing. *J. Comput. Biol.* 19, 455–477. doi: 10.1089/cmb.2012.0021

Bäumler, A. J., Winter, S. E., Thiennimitr, P., and Casadesús, J. (2011). Intestinal and chronic infections: *Salmonella* lifestyles in hostile environments. *Environ. Microbiol. Rep.* 3, 508–517. doi: 10.1111/j.1758-2229.2011.00242.x

Berk, P.A., (2008). *In vitro* and *in vivo* Virulence of *Salmonella typhimurium* DT104: A Parallelogram Approach. PhD Thesis, Wageningen University.

Betancor, L., Yim, L., Fookes, M. C., Martinez, A., Thomson, N. R., Ivens, A., et al. (2009). Genomic and phenotypic variation in epidemic-spanning *S. Enterica* serovar enteritidis isolates. *BMC Microbiol.* 9, 1–16. doi: 10.1186/1471-2180-9-237/FIGURES/2

Bolger, A. M., Lohse, M., and Usadel, B. (2014). Trimmomatic: a flexible trimmer for Illumina sequence data. *Bioinformatics* 30, 2114–2120. doi: 10.1093/bioinformatics/btu170

Bolton, A. J., Osborne, M. P., and Stephen, J. (2000). Comparative study of the invasiveness of *Salmonella* serotypes typhimurium, Choleraesuis and Dublin for Caco-2 cells, HEp-2 cells and rabbit ileal epithelia. *J. Med. Microbiol.* 49, 503–511. doi: 10.1099/0022-1317-49-6-503

Bonardi, S., Blagojevic, B., Belluco, S., Roasto, M., Gomes-Neves, E., and Vågsholm, I. (2021). Food chain information in the European pork industry: where are we? *Trends Food Sci. Technol.* 118, 833–839. doi: 10.1016/J.TIFS.2021.10.030

Buchfink, B., Xie, C., and Huson, D. H. (2015). Fast and sensitive protein alignment using DIAMOND. *Nat. Methods* 12, 59–60. doi: 10.1038/nmeth.3176

Chanamè-Pinedo, L., Franz, E., van den Beld, M., van Goethem, N., Mattheus, W., Veldman, K., et al. (2022a). Changing epidemiology of *Salmonella enteritidis* human infections in the Netherlands and Belgium, 2006 to 2019: a registry-based population study. *Eur. Secur.* 27:2101174. doi: 10.2807/1560-7917.ES.2022.27.38.2101174/CITE/PLAINTEXT

Chanamè-Pinedo, L., Mughini-Gras, L., Franz, E., Hald, T., and Pires, S. M. (2022b). Sources and trends of human salmonellosis in Europe, 2015-2019: an analysis of outbreak data. *Int. J. Food Microbiol.* 379:109850. doi: 10.1016/j.ijfoodmicro.2022.109850

Chen, L., Yang, J., Yu, J., Yao, Z., Sun, L., Shen, Y., et al. (2005). VFDB: a reference database for bacterial virulence factors. *Nucleic Acids Res.* 33, D325–D328. doi: 10.1093/nar/gki008

Cheng, R. A., Eade, C. R., and Wiedmann, M. (2019). Embracing diversity: differences in virulence mechanisms, disease severity, and host adaptations contribute to the success of nontyphoidal *Salmonella* as a foodborne pathogen. *Front. Microbiol.* 10:1368. doi: 10.3389/fmicb.2019.01368

Chiou, C.-S., Hong, Y. P., Liao, Y. S., Wang, Y. W., Tu, Y. H., Chen, B. H., et al. (2019). New multidrug-resistant *Salmonella enterica* serovar Anatum clone, Taiwan, 2015–2017. *Emerg. Infect. Dis.* 25, 144–147. doi: 10.3201/EID2501.181103

Coipan, C. E., Westrell, T., van Hoek, A. H. A. M., Alm, E. J., Kotila, S. M., Berbers, B., et al. (2020). Genomic epidemiology of emerging ESBL-producing *Salmonella* Kentucky blaCTX-M-14b in Europe. *Emerg. Microbes. Infect.* 9, 2124–2135. doi: 10.1080/22221751.2020.1821582

Correia-Gomes, C., Leonard, F., and Graham, D. (2021). Description of control programmes for *Salmonella* in pigs in Europe. Progress to date? *J Food Saf* 41:e12916. doi: 10.1111/JFS.12916

De Masi, L., Yue, M., Hu, C., Rakov, A. V., Rankin, S. C., and Schifferli, D. M. (2017). Cooperation of adhesin alleles in Salmonella-host tropism. *Msphere* 2, e00066–e00017. doi: 10.1128/mSphere.00066-17

D'Oca, M. C., Noto, A. M., Bartolotta, A., Parlato, A., Nicastro, L., Sciortino, S., et al. (2021). Assessment of contamination of *Salmonella* spp. in imported black pepper and sesame seed and *Salmonella* inactivation by gamma irradiation. *Ital J Food Saf* 10:8914. doi: 10.4081/ijfs.2021.8914

Dufresne, K., and Daigle, F. (2017). "*Salmonella* fimbriae: what is the clue to their hairdo?" in *Current Topics in Salmonella and Salmonellosis*. ed. M. Mares (InTechOpen), 59–79.

EFSA and ECDC (2017). Multi-country outbreak of *Salmonella enteritidis* infections linked to polish eggs. *EFSA Support. Publ* 14:21. doi: 10.2903/SP.EFSA.2017.EN-1353

EFSA and ECDC (2021a). The European Union one health 2020 zoonoses report. *EFSA J.* 19:e06971. doi: 10.2903/J.EFSA.2021.6971

EFSA and ECDC (2021b). The European Union one health 2019 zoonoses report. *EFSA J.* 19:e06406. doi: 10.2903/j.efsa.2021.6406

European Centre for Disease Prevention and Control (ECDC). (2022). *Surveillance Atlas of Infectious Diseases*. Stockholm: ECDC. (Accessed November 29, 2022).

Fang, F. C., and Fierer, J. (1991). Human infection with *Salmonella* Dublin. *Medicine* 70, 198–207. doi: 10.1097/00005792-199105000-00004

Feasey, N. A., Hadfield, J., Keddy, K. H., Dallman, T. J., Jacobs, J., Deng, X., et al. (2016). Distinct *Salmonella enteritidis* lineages associated with enterocolitis in high-income settings and invasive disease in low-income settings. *Nat. Genet.* 48, 1211–1217. doi: 10.1038/ng.3644

Ferrari, R. G., Rosario, D. K. A., Cunha-Neto, A., Mano, S. B., Figueiredo, E. E. S., and Conte Junior, C. A. (2019). Worldwide epidemiology of *Salmonella* serovars in animal-based foods: a meta-analysis. *Appl. Environ. Microbiol.* 85:e00591-15. doi: 10.1128/AEM.00591-19/SUPPL_FILE/AEM.00591-19-S0001.PDF

Fowlkes, E. B., and Mallows, C. L. (1983). A method for comparing two hierarchical clusterings. *J. Am. Stat. Assoc.* 78, 553–569. doi: 10.1080/01621459.1983.10478008

Galán, J. E. (2001). *Salmonella* interactions with host cells: type III secretion at work. *Annu. Rev. Cell Dev. Biol.* 17, 53–86. doi: 10.1146/annurev.cellbio.17.1.53

Galili, T. (2015). Dendextend: an R package for visualizing, adjusting and comparing trees of hierarchical clustering. *Bioinformatics* 31, 3718–3720. doi: 10.1093/bioinformatics/btv428

Gordon, H. S., Hoffman, S. J., Schultz, A., and Lomberg, F. (1949). SEROUS ARTHRITIS OF THE KNEE JOINT: report of a case caused by *Salmonella* Typhosa and *Salmonella* Montevideo in a child. *J. Am. Med. Assoc.* 141, 460–461. doi: 10.1001/JAMA.1949.62910070003007B

Gurevich, A. A., Saveliev, V., Vyahhi, N., and Tesler, G. (2013). QUAST: quality assessment tool for genome assemblies. *Bioinformatics* 29, 1072–1075. doi: 10.1093/bioinformatics/btt086

Haley, B. J., Kim, S. W., Pettengill, J., Luo, Y., Karns, J. S., and van Kessel, J. A. S. (2016). Genomic and evolutionary analysis of two *Salmonella enterica* serovar Kentucky sequence types isolated from bovine and poultry sources in North America. *PLoS One* 11:e0161225. doi: 10.1371/JOURNAL.PONE.0161225

Hara, A., Hibi, T., Yoshioka, M., Toda, K., Watanabe, N., Hayashi, A., et al. (1993). Changes of proliferative activity and phenotypes in spontaneous differentiation of a colon cancer cell line. *Jpn. J. Cancer Res.* 84, 625–632. doi: 10.1111/j.1349-7006.1993.tb02022.x

Harada, T., Sakata, J., Kanki, M., Seto, K., Taguchi, M., and Kumeda, Y. (2011). Molecular epidemiological investigation of a diffuse outbreak caused by *Salmonella enterica* serotype Montevideo isolates in Osaka prefecture, Japan. *Foodborne Pathog. Dis.* 8, 1083–1088. doi: 10.1089/FPD.2011.0862/ASSET/IMAGES/LARGE/FIGURE1.JPEG

Hawkey, J., le Hello, S., Doublet, B., Granier, S. A., Hendriksen, R. S., Florian Fricke, W., et al. (2019). Global phylogenomics of multidrug-resistant *Salmonella enterica* serotype Kentucky ST198. *Microb Genom* 5:e000269. doi: 10.1099/MGEN.0.000269

Helms, M., Evans, S., Vastrup, P., and Gerner-Smidt, P. (2003). Short and long term mortality associated with foodborne bacterial gastrointestinal infections: registry based study commentary: matched cohorts can be useful. *BMJ* 326:357. doi: 10.1136/bmj.326.7385.357

Hensel, M., Hinsley, A. P., Nikolaus, T., Sawers, G., and Berks, B. C. (1999). The genetic basis of tetrathionate respiration in *Salmonella Typhimurium*. *Mol. Microbiol.* 32, 275–287. doi: 10.1046/j.1365-2958.1999.01345.x

Hopkins, K. L., and Threlfall, E. J. (2004). Frequency and polymorphism of sopE in isolates of *Salmonella Enterica* belonging to the ten most prevalent serotypes in England and Wales. *J. Med. Microbiol.* 53, 539–543. doi: 10.1099/jmm.0.05510-0

Joerger, R. D., Sartori, C. A., and Kniel, K. E. (2009). Comparison of genetic and physiological properties of *Salmonella enterica* isolates from chickens reveals one major difference between serovar Kentucky and other serovars. *Response Acid.* 6, 503–512. doi: 10.1089/FPD.2008.0144

Katsoulis, E., Pallett, A., and Bowyer, G. W. (2004). Septic arthritis of the knee by *Salmonella* Montevideo. *Ann. R. Coll. Surg. Engl.* 86, 272–274. doi: 10.1308/147870804588

Kapperud, G., Gustavsen, S., Hellesnes, I., Hansen, A. H., Lassen, J., Hirn, J., et al. (1990). Outbreak of *Salmonella Typhimurium* infection traced to contaminated chocolate and caused by a strain lacking the 60-megadalton virulence plasmid. *J. Clin. Microbiol.* 28, 2597–2601. doi: 10.1128/jcm.28.12.2597-2601.1990

Kim, J.-Y. Y., Park, Y.-J. J., Lee, S.-O. O., Song, W., Jeong, S. H., Yoo, Y. A., et al. (2004). Bacteremia due to *Salmonella enterica* Serotype Montevideo producing plasmid-mediated AmpC β-lactamase (DHA-1). *Ann. Clin. Lab. Sci.* 34, 214–217.

Koutsoumanis, K. P., Allende, A., Alvarez-Ordóñez, A., Bolton, D., Bover-Cid, S., Chemaly, M., et al. (2019a). Whole genome sequencing and metagenomics for outbreak investigation, source attribution and risk assessment of food-borne microorganisms. *EFSA J.* 17:e05898. doi: 10.2903/J.EFSA.2019.5898

Koutsoumanis, K. P., Allende, A., Alvarez-Ordóñez, A., Bolton, D., Bover-Cid, S., Chemaly, M., et al. (2019b). *Salmonella* control in poultry flocks and its public health impact. *EFSA J.* 17:e05596. doi: 10.2903/J.EFSA.2019.5596

Kuijpers, A. F. A., Marinovic, A. A. B., Wijnands, L. M., Delfgou-Van Asch, E. H. M., van Hoek, A. H. A. M., Franz, E., et al. (2019). Phenotypic prediction: linking in vitro virulence to the genomics of 59 *Salmonella* enteric strains. *Front. Microbiol.* 10:3182. doi: 10.3389/FMICB.2018.03182/BIBTEX

Lalsiamthara, J., and Lee, J. H. (2017). Pathogenic traits of *Salmonella* Montevideo in experimental infections *in vivo* and *in vitro*. *Sci. Rep.* 7, 1–12. doi: 10.1038/srep46232

Larkin, L., de la Gandara, M. P., Hoban, A., Pulford, C., Jourdan-da Silva, N., de Valk, H., et al. (2022). Investigation of an international outbreak of multidrug-resistant monophasic *Salmonella typhimurium* associated with chocolate products, EU/EEA and United Kingdom, February to April 2022. *Eur. Secur.* 27:2200314. doi: 10.2807/1560-7917.ES.2022.27.15.2200314

le Hello, S., Bekhit, A., Granier, S. A., Barua, H., Beutlich, J., Zając, M., et al. (2013). The global establishment of a highly-fluoroquinolone resistant *Salmonella enterica* serotype Kentucky ST198 strain. *Front. Microbiol.* 4:395. doi: 10.3389/fmicb.2013.00395

le Hello, S., Hendriksen, R. S., Doublet, B., Fisher, I. S. T., Nielsen, E. M., Whichard, J. M., et al. (2011). International spread of an epidemic population of *Salmonella enterica* serotype Kentucky ST198 resistant to ciprofloxacin. *J. Infect. Dis.* 204, 675–684. doi: 10.1093/INFDIS/JIR409

Leati, M., Zaccherini, A., Ruocco, L., D'Amato, S., Busani, L., Villa, L., et al. (2021). The challenging task to select *Salmonella* target serovars in poultry: the Italian point of view. *Epidemiol. Infect.* 149:e160. doi: 10.1017/S0950268821001230

Liao, Y. S., Chen, B. H., Hong, Y. P., Teng, R. H., Wang, Y. W., Liang, S. Y., et al. (2019). Emergence of multidrug-resistant *Salmonella enterica* serovar Goldcoast strains in Taiwan and international spread of the ST358 clone. *Antimicrob. Agents Chemother.* 63:e01122-19. doi: 10.1128/AAC.01122-19/SUPPL_FILE/AAC.01122-19-SD001.XLSX

Lund, S., Tahir, M., Vohra, L. I., Hamdana, A. H., and Ahmad, S. (2022). Outbreak of monophasic *Salmonella typhimurium* sequence type 34 linked to chocolate products. *Ann. Med. Surg.* 82:104597. doi: 10.1016/J.AMSU.2022.104597

Mastrorilli, E., Petrin, S., Orsini, M., Longo, A., Cozza, D., Luzzi, I., et al. (2020). Comparative genomic analysis reveals high intra-serovar plasticity within *Salmonella* Napoli isolated in 2005-2017. *BMC Genomics* 21, 1–16. doi: 10.1186/s12864-020-6588-y

Matthews, T. D., Schmieder, R., Silva, G. G. Z., Busch, J., Cassman, N., Dutilh, B. E., et al. (2015). Genomic comparison of the closely-related *S. Enterica* serovars enteritidis, Dublin and Gallinarum. *PLoS One* 10:e0126883. doi: 10.1371/JOURNAL.PONE.0126883

Mourão, J., Machado, J., Novais, C., Antunes, P., and Peixe, L. (2014). Characterization of the emerging clinically-relevant multidrug-resistant *S. Enterica* serotype 4,[5],12:i:- (monophasic variant of *S. Typhimurium*) clones. *Eur. J. Clin. Microbiol. Infect. Dis.* 33, 2249–2257. doi: 10.1007/s10096-014-2180-1

Mughini-Gras, L., Pijnacker, R., Duijster, J., Heck, M., Wit, B., Veldman, K., et al. (2020). Changing epidemiology of invasive non-typhoid *Salmonella* infection: a nationwide population-based registry study. *Clin. Microbiol. Infect.* 26, 941.e9–941.e14. doi: 10.1016/j.cmi.2019.11.015

O'Connor, K. (2000). Acute myocarditis precipitated by *Salmonella* Montevideo infection: a case report. *Ir. Med. J.* 93, 21–22.

Okoro, C. K., Barquist, L., Connor, T. R., Harris, S. R., Clare, S., Stevens, M. P., et al. (2015). Signatures of adaptation in human invasive *Salmonella typhimurium* ST313 populations from sub-Saharan Africa. *PLoS Negl. Trop. Dis.* 9:e0003611. doi: 10.1371/journal.pntd.0003611

Oliveira, M., Wijnands, L. M., Abadias, M., Aarts, H., and Franz, E. (2011). Pathogenic potential of *Salmonella typhimurium* DT104 following sequential passage through soil, packaged fresh-cut lettuce and a model gastrointestinal tract. *Int. J. Food Microbiol.* 148, 149–155. doi: 10.1016/J.IJFOODMICRO.2011.05.013

Paine, S., Thornley, C., Wilson, M., Dufour, M., Sexton, K., Miller, J., et al. (2014). An outbreak of multiple serotypes of *Salmonella* in New Zealand linked to consumption of contaminated tahini imported from Turkey. *Foodborne Pathog. Dis.* 11, 887–892. doi: 10.1089/FPD.2014.1773/ASSET/IMAGES/LARGE/FIGURE2.JPEG

Parisi, A., Crump, J. A., Glass, K., Howden, B. P., Furuya-Kanamori, L., Vilkins, S., et al. (2018). Health outcomes from multidrug-resistant *Salmonella* infections in high-income countries: a systematic review and Meta-analysis. *Foodborne Pathog. Dis.* 15, 428–436. doi: 10.1089/fpd.2017.2403

Petrin, S., Mancin, M., Losasso, C., Deotto, S., Olsen, J. E., and Barco, L. (2022). Effect of pH and salinity on the ability of *Salmonella* serotypes to form biofilm. *Front. Microbiol.* 13:821679. doi: 10.3389/FMICB.2022.821679/FULL

Pielaat, A., Kuijpers, A. F. A., Delfgou-Van Asch, E. H. M., van Pelt, W., and Wijnands, L. M. (2016). Phenotypic behavior of 35 *Salmonella enterica* serovars compared to epidemiological and genomic data. *Procedia Food Sci* 7, 53–58. doi: 10.1016/J.PROFOO.2016.02.085

Pinto, M., Robine, L., Appay, M.-D., Kedinger, M., Triadou, N., Dussaulx, E., et al. (1983). Enterocyte-like differentiation and polarization of the human colon carcinoma cell line Caco-2 in culture. *Biol. Cell.* 47, 323–330.

Rakov, A. V., Mastriani, E., Liu, S. L., and Schifferli, D. M. (2019). Association of *Salmonella* virulence factor alleles with intestinal and invasive serovars. *BMC genomics* 20, 1–14. doi: 10.1186/s12864-019-5809-8

Rivera-Chávez, F., and Bäumler, A. J. (2015). The pyromaniac inside you: *Salmonella* metabolism in the host gut. *Annu. Rev. Microbiol.* 69, 31–48. doi: 10.1146/annurev-micro-091014-104108

RStudio Team (2021). *RStudio: Integrated Development for R. RStudio*. Boston, MA: PBC. Available at: http://www.rstudio.com/

Santos, R. L., Raffatellu, M., Bevins, C. L., Adams, L. G., Tükel, Ç., Tsolis, R. M., et al. (2009). Life in the inflamed intestine, *Salmonella* style. *Trends Microbiol.* 17, 498–506. doi: 10.1016/j.tim.2009.08.008

Sarno, E., Pezzutto, D., Rossi, M., Liebana, E., and Rizzi, V. (2021). A review of significant European foodborne outbreaks in the last decade. *J. Food Prot.* 84, 2059–2070. doi: 10.4315/JFP-21-096

Sévellec, Y., Granier, S. A., le Hello, S., Weill, F.-X., Guillier, L., Mistou, M.-Y., et al. (2020). Source attribution study of sporadic *Salmonella* Derby cases in France. *Front. Microbiol.* 11:889. doi: 10.3389/FMICB.2020.00889/BIBTEX

Shah, D. H., Zhou, X., Addwebi, T., Davis, M. A., and Call, D. R. (2011). In vitro and in vivo pathogenicity of *Salmonella enteritidis* clinical strains isolated from North America. *Arch. Microbiol.* 193, 811–821. doi: 10.1007/S00203-011-0719-4/FIGURES/3

Solano, C., García, B., Valle, J., Berasain, C., Ghigo, J.-M., Gamazo, C., et al. (2002). Genetic analysis of *Salmonella enteritidis* biofilm formation: critical role of cellulose. *Mol. Microbiol.* 43, 793–808. doi: 10.1046/j.1365-2958.2002.02802.x

Solano, C., Sesma, B., Alvarez, M., Urdaneta, E., Garcia-Ros, D., Calvo, A., et al. (2001). Virulent strains of *Salmonella enteritidis* disrupt the epithelial barrier of Caco-2 and HEp-2 cells. *Arch. Microbiol.* 2000 175, 175, 46–51. doi: 10.1007/S002030000236

Stöcker, P., Rosner, B., Werber, D., Kirchner, M., Reinecke, A., Wichmann-Schauer, H., et al. (2011). Outbreak of *Salmonella* Montevideo associated with a dietary food supplement flagged in the rapid alert system for food and feed (RASFF) in Germany, 2010. *Eur. Secur.* 16:20040. doi: 10.2807/ESE.16.50.20040-EN/CITE/PLAINTEXT

Thornbrough, J. M., and Worley, M. J. (2012). *A naturally occurring single nucleotide polymorphism in the Salmonella SPI-2 type III effector srfH/sseI controls early extraintestinal dissemination*. doi: 10.1371/journal.pone.0045245

Unicomb, L. E., Simmons, G., Merritt, T., Gregory, J., Nicol, C., Jelfs, P., et al. (2005). Sesame seed products contaminated with *Salmonella*: three outbreaks associated with tahini. *Epidemiol. Infect.* 133, 1065–1072. doi: 10.1017/S0950268805004085

Uzzau, S., Brown, D. J., Wallis, T. S., Rubino, S., Leori, G., Bernard, S., et al. (2000). Host adapted serotypes of *Salmonella enterica*. *Epidemiol. Infect.* 125, 229–255. doi: 10.1017/S0950268899004379

Ward, J. H. (1963). Hierarchical grouping to optimize an objective function. *J. Am. Stat. Assoc.* 58:236. doi: 10.2307/2282967

Wijnands, L. M., Teunis, P. F. M., Kuijpers, A. F. A., Delfgou-Van Asch, E. H. M., and Pielaat, A. (2017). Quantification of *Salmonella* survival and infection in an in vitro model of the human intestinal tract as proxy for foodborne pathogens. *Front. Microbiol.* 8:1139. doi: 10.3389/FMICB.2017.01139

Williams, R. L. (2000). A note on robust variance estimation for cluster-correlated data. *Biometrics* 56, 645–646. doi: 10.1111/j.0006-341X.2000.00645.x

Willis, C., Little, C. L., Sagoo, S., de Pinna, E., and Threlfall, E. J. (2009). Assessment of the microbiological safety of edible dried seeds from retail premises in the United Kingdom with a focus on *Salmonella* spp. *Food Microbiol.* 26, 847–852. doi: 10.1016/J.FM.2009.05.007

Worley, J., Meng, J., Allard, M. W., Brown, E. W., and Timme, R. E. (2018). *Salmonella enterica* phylogeny based on whole-genome sequencing reveals two new clades and novel patterns of horizontally acquired genetic elements. *mBio* 9:e02303-18. doi: 10.1128/mBio.02303-18

Yim, L., Betancor, L., Martinez, A., Giossa, G., Bryant, C., Maskell, D. J., et al. (2010). Differential phenotypic diversity among epidemic-spanning *S. Enteritidis* serovar enteritidis isolates from humans or animals. *Appl. Environ. Microbiol.* 76, 6812–6820. doi: 10.1128/AEM.00497-10/ASSET/F46595C5-D370-4902-B986-FAD659877B36/ASSETS/GRAPHIC/ZAM9991014220004.JPEG

Yokoyama, E., Torii, Y., Shigemura, H., Ishige, T., Yanagimoto, K., Uematsu, K., et al. (2019). Isolation of *Salmonella enterica* serovar Agona strains and their similarities to strains derived from a clone caused a serovar shift in broilers. *J. Infect. Chemother.* 25, 71–74. doi: 10.1016/J.JIAC.2018.07.003

Yue, M., Han, X., Masi, L. D., Zhu, C., Ma, X., Zhang, J., et al. (2015). Allelic variation contributes to bacterial host specificity. *Nat. Commun.* 6:8754. doi: 10.1038/ncomms9754

Yue, M., and Schifferli, D. M. (2014). Allelic variation in *Salmonella*: an underappreciated driver of adaptation and virulence. *Front. Microbiol.* 4:419. doi: 10.3389/fmicb.2013.00419

Zhou, Z., Alikhan, N. F., Mohamed, K., Fan, Y., Achtman, M., and Agama Study Group (2020). The EnteroBase user's guide, with case studies on Salmonella transmissions, Yersinia pestis phylogeny, and Escherichia core genomic diversity. *Genome Res.* 30, 138–152. doi: 10.1101/gr.251678.119

frontiers | Frontiers in Microbiology

TYPE Original Research
PUBLISHED 08 June 2023
DOI 10.3389/fmicb.2023.1188679

OPEN ACCESS

EDITED BY
George Grant,
University of Aberdeen, United Kingdom

REVIEWED BY
Arumugam Kamaladevi,
Alagappa University, India
Maria Hoffmann,
US Food and Drug Administration, United States
Haider Abdul-Lateef Mousa,
University of Basrah, Iraq
Thilo Fuchs,
Friedrich-Loeffler-Institute, Germany

*CORRESPONDENCE
Istvan Szabo
✉ istvan.szabo@bfr.bund.de

†PRESENT ADDRESS
Wiebke Burkhardt,
Department of Food, Feed and Commodities,
Federal Office of Consumer Protection and
Food Safety, Berlin, Germany

RECEIVED 17 March 2023
ACCEPTED 10 May 2023
PUBLISHED 08 June 2023

CITATION
Burkhardt W, Salzinger C, Fischer J, Malorny B, Fischer M and Szabo I (2023) The nematode worm *Caenorhabditis elegans* as an animal experiment replacement for assessing the virulence of different *Salmonella enterica* strains. *Front. Microbiol.* 14:1188679. doi: 10.3389/fmicb.2023.1188679

The nematode worm *Caenorhabditis elegans* as an animal experiment replacement for assessing the virulence of different *Salmonella enterica* strains

Wiebke Burkhardt†, Carina Salzinger, Jennie Fischer, Burkhard Malorny, Matthias Fischer and Istvan Szabo*

Department Biological Safety, German Federal Institute for Risk Assessment, Berlin, Germany

Caenorhabditis (*C.*) *elegans* has become a popular toxicological and biological test organism in the last two decades. Furthermore, the role of *C. elegans* as an alternative for replacing or reducing animal experiments is continuously discussed and investigated. In the current study, we investigated whether *C. elegans* survival assays can help in determining differences in the virulence of *Salmonella enterica* strains and to what extent *C. elegans* assays could replace animal experiments for this purpose. We focused on three currently discussed examples where we compared the longevity of *C. elegans* when fed (i) with *S. enterica* serovar Enteritidis vaccination or wild-type strains, (ii) with lipopolysaccharide (LPS) deficient rough or LPS forming smooth *S. enterica* serovar Enteritidis, and (iii) with an *S. enterica* subsp. *diarizonae* strain in the presence or absence of the typical pSASd plasmid encoding a bundle of putative virulence factors. We found that the *C. elegans* survival assay could indicate differences in the longevity of *C. elegans* when fed with the compared strain pairs to a certain extent. Putatively higher virulent *S. enterica* strains reduced the lifespan of *C. elegans* to a greater extent than putatively less virulent strains. The *C. elegans* survival assay is an effective and relatively easy method for classifying the virulence of different bacterial isolates *in vivo*, but it has some limitations. The assay cannot replace animal experiments designed to determine differences in the virulence of *Salmonella enterica* strains. Instead, we recommend using the described method for pre-screening bacterial strains of interest to select the most promising candidates for further animal experiments. The *C. elegans* assay possesses the potential to reduce the number of animal experiments. Further development of the *C. elegans* assay in conjunction with omics technologies, such as transcriptomics, could refine results relating to the estimation of the virulent potential of test organisms.

KEYWORDS

***Caenorhabditis elegans*, *Salmonella*, survival assay, virulence, animal experiments, replace, reduce**

1. Introduction

In the past 20 years, the nematode worm *Caenorhabditis* (*C.*) *elegans* has become one of the most widely used model organisms for nearly every aspect of toxicology and biology (Leung et al., 2008; Meneely et al., 2019). In toxicology, for example, *C. elegans* involves determining the possible harmful effects of chemicals. Although animal tests have traditionally been the backbone of toxicology, currently, a broad range of *in vitro* test methods are available, such as cell cultures, organoids, organs-on-chip, and *in silico* systems (Calonie et al., 2022). The bigger challenge is replacing animal tests in the investigations of more complex biological systems such as the immune system, the circulatory system, or the nervous system. Invertebrate animals offer an alternative to the usual animal tests in mammals for research fields like genetics, physiology, biochemistry, evolution, and neurobiology (Singkum et al., 2019). *C. elegans* is used to study various biological processes, including apoptosis, cell signaling, cell cycle, cell polarity, gene regulation, metabolism, aging, and sex determination (Kaletta and Hengartner, 2006). Infection biology is one of the most complex fields of biological and medical research, and infection models are influenced by a broad range of variables in the host, such as the immune system, the unspecific infection defense, the entrance tissue, and the general immune status (Bulitta et al., 2019). Invertebrate animals such as nematodes or insects provide an *in vivo* research platform that is more complex than cell cultures or organoids. Moreover, these systems are not linked to the ethical and animal welfare concerns that limit the use of the usual animal models (Singkum et al., 2019).

When *C. elegans* was established at the beginning of the 21st century as a model host for studying the pathogenesis of *Pseudomonas aeruginosa*, it was expected that the model would be limited to pathogens with a broad host range. However, a restriction was observed, especially for intracellular pathogen microorganisms such as *Salmonella* and *Listeria*. Nevertheless, at the same time, *Sarratia marcescens* was reported as a second bacterium that was pathogenic to *C. elegans* (Kurz and Ewbank, 2000). Since *C. elegans* came to be used as an infection model, two different effects of *Pseudomonas aeruginosa* have been observed in the nematode. The "fast killing" effect with nematodes dying within 24 h and the "slow killing" effect where the worms survived over several days. The "fast killing" effect was caused by a bacterial toxin, while the "slow killing" effect was seen as an infection-like process (Finlay, 1999). In 2000, the application of the *C. elegans* infection model to *Salmonella* was described for several *Salmonella enterica* serovars, including the serovar Typhimurium (Aballay et al., 2000; Labrousse et al., 2000). In contrast to *Pseudomonas aeruginosa, Salmonella enterica* serotype Typhimurium colonized the intestine of the worm permanently (Aballay and Ausubel, 2002). In 2006, Kaletta and Hengartner regarded *C. elegans* as a system that still needed to prove whether it could be used as a valid and relevant infectious disease model (Kaletta and Hengartner, 2006). In the meantime, *C. elegans* as an infection model has provided many insights into the underlying mechanisms of human diseases, including biological processes such as defensive host response to microorganisms, pathogenic mechanisms, and symbiotic interactions (Kumar et al., 2020).

The role of *C. elegans* as an alternative to animal experiments is being continuously discussed and investigated. The range of applications of the model is extensive and includes nutritional studies on probiotic host interactions, immunity, and infection and studies on the antimicrobial effects of food supplements (Lang et al., 2021; Chakravarty, 2022; Zermeño-Ruiz et al., 2022). The application of genetically modified microorganisms could reveal details on the infection mechanisms, e.g., of *S.* Typhimurium, and the host response of *C. elegans,* where several anti-microbiotic protein pathways have been identified to be linked to the reaction of *Salmonella* virulence factors (Tenor et al., 2004; Sahu et al., 2013). Moreover, different mutants of *C. elegans* can be used to investigate pathogen-host interactions (Aballay and Ausubel, 2002). In animal experiments, different species (e.g., mice, fowl, and pigs) are widely used for studying the general and species-related course of infection by the foodborne pathogen *S. enterica*. The application of a broader range of alternative non-animal-based models could contribute to understanding infection mechanisms and reducing the number of animal experiments.

Salmonella can be host-restricted, be host-adapted, or have a broad host range, but only a relatively small proportion of the ca. 2,600 described serovars are of significant clinical relevance. Depending on the serovar, ingested dose, and immunocompetence of the host, *Salmonella* infections differ substantially in their clinical manifestations, ranging from an asymptomatic state to severe illness (Simon et al., 2023). Many virulence factors (e.g., *Salmonella* pathogenicity islands, endotoxins, and virulence plasmids) have been shown to play different roles in the pathogenesis of *Salmonella* infections in humans and animals. Among the virulence traits and factors of *S. enterica* are the invasion of and intracellular replication inside the host's cells (Jajere, 2019). In several studies, *Salmonella* Typhimurium was found to be pathogenic to *C. elegans* and can be lethal to the nematode (Aballay and Ausubel, 2002; Sem and Rhem, 2012). However, the pathogenesis of *S.* Typhimurium infection in *C. elegans* has not been fully clarified. Both well-known *Salmonella* virulence factors and aspects that do not involve the classical invasive or intracellular phenotype of the pathogen appear to play a role in the pathogenicity for the nematode. For example, *S.* Typhimurium has been shown to provoke overwhelming systemic oxidative stress in *C. elegans* through the redox activity of bacterial thioredoxin (Sem and Rhem, 2012).

The present study aimed to determine whether a *C. elegans* survival assay could help measure differences in the virulence of *Salmonella enterica* strains and determine to what extent *C. elegans* assays could replace animal experiments for this purpose. We accordingly selected three examples currently discussed in the literature where specific *Salmonella* characteristics play a role in the pathogenicity course of the organism with possible consequences to control measurements when detected in livestock. We compared (i) vaccination and wild-type strains of *S. enterica* serovar Enteritidis (hereafter referred to as *S.* Enteritidis) since vaccination plays a vital role in *Salmonella* control programs. However, evidence of vaccine *Salmonella* strains on table eggs is not yet substantial enough to influence foodstuff legislation. We also compared (ii) lipopolysaccharide (LPS) deficient (also known as rough) with functional LPS (also known as smooth) strains of *S.* Enteritidis. The pathogenicity of *Salmonella* is associated with the presence

of the immune-reactive O-chain of the LPS expressed on its surface. Several previous studies have indicated the role of LPS in the pathogenicity of the bacteria in host-pathogen interactions with the innate immune system (Maldonado et al., 2016). Finally, we investigated (iii) the impact of the absence of a type IV secretion system (T4SS)-containing plasmid named pSASd on the pathogenicity of *S. enterica* subsp. *diarizonae* (hereafter referred to as SASd).

2. Methods

2.1. Bacterial strains

SASd (strains 12-01777-0-S2 and 12-01777-0-S3), *S.* Enteritidis (20-SA01872-0), and *S.* Enteritidis (20-SA00671-0 and 09-02812-0) (Table 1) were obtained from the National Reference Laboratory (NRL) for *Salmonella* at the Federal Institute for Risk Assessment, Berlin, Germany (BfR) strain collection. The vaccine strain Salmovac SE (19-SA01616) was obtained from the manufacturer.

To minimize potential variations of results based on the genetic diversity of *S.* Enteritidis strains, we chose isolates belonging to MLST type 11 that showed a close genetic relatedness in whole genome sequencing based on cgMLST analysis.

For the *Salmonella* vaccine and wild-type strain comparative analysis (i), we chose an *S.* Enteritidis isolate from the NRL for *Salmonella* strain collection with a genetic distance of 130 allelic differences (AD) from the vaccine strain to ensure a similar genetic background of both isolates.

To compare the rough and smooth *S.* Enteritidis (ii), we chose two serologically different isolates with a genetic difference of 32 AD.

For the SASd strains (iii), we chose two isolates of ST432, one of which contained a 43 kb large plasmid (pSASd having a T4SS and a toxin/antitoxin system) and one without pSASd (Uelze et al., 2021). The AD between the two strains was 39 in the cgMLST analysis.

Escherichia coli OP50 was derived from the strain collection of the group Strategies for Toxicological Assessments at the BfR. Bacterial strains were cultured aerobically in 5 ml Luria-Bertani (LB) medium under shaking at 37°C overnight. The next day, the entire volume was poured into a bottle containing 200 ml of fresh LB medium and incubated at 37°C for 8 h. The bacterial cells were washed three times in M9 buffer (Wittkowski et al., 2020) and up-concentrated. The optical density at 600 nm (OD_{600}) was measured (Ultrospec 10, Amersham Biosciences, UK), and the suspension was brought to an OD_{600} corresponding to 10^{10} CFU/ml (according to prior growth experiments as described in Wittkowski et al., 2020). This bacterial suspension was used to inoculate nematode growth medium (NGM) agar plates (Wittkowski et al., 2020) overnight at 37°C and subsequently stored at 4°C for later use in the survival assay.

2.2. Serotyping

Strains were serotyped by slide agglutination as described in a previous study (Szabo et al., 2017). Compared to smooth isolates, rough isolates showed a non-specific reaction with all sera and a negative reaction or agglutination with 1 x phosphate-buffered saline.

2.3. Whole genome sequencing of *S. enterica* strains

Genomic DNA was extracted from liquid cultures using a PureLink genomic DNA mini kit Invitrogen (Carlsbad, CA, USA). Sequencing libraries were prepared with the Nextera DNA Flex library preparation kit Illumina (San Diego, CA, USA) according to the manufacturer's protocol. Paired-end sequencing was performed on an Illumina MiSeq benchtop sequencer using the MiSeq reagent kit v3 (600 cycles). Raw reads were trimmed and *de novo* assembled with the Aquamis pipeline v1.3 (git version is v1.0.0–60-g60e9d09) (https://gitlab.com/bfr_bioinformatics/AQUAMIS) (Deneke et al., 2021a), which implements fastp v0.19.5 (Chen et al., 2018) for trimming and shovill v1.1.0 (https://github.com/tseemann/shovill) for assembly.

Draft genome assemblies were characterized with the BakCharak pipeline v2.0 (git version 1.0.0–77-g5b31a01) (https://gitlab.com/bfr_bioinformatics/bakcharak), and allele distances between the paired isolates were computed with the chewieSnake pipeline v1.2 (Deneke et al., 2021b) as described in a previous study (Uelze et al., 2021).

2.4. Nematode strain

The genetically modified strain *C. elegans* SS104 (genotype glp-4(bn2) I.) was provided by the *Caenorhabditis* Genetics Center (CGC), University of Minnesota (USA), which is funded by the NIH Office of Research Infrastructure Programs (P40 OD010440). The nematode was grown at 16°C on NGM agar plates seeded with *E. coli* OP50 as the sole food source and transferred to fresh food plates two times per week (Wittkowski et al., 2020). Genetically modified worms can reproduce at a permissive temperature of 16°C. At higher temperatures of ~25°C, the worms become sterile and thus cannot produce progeny. This allows us to perform survival experiments for several weeks without the bias of new generations.

2.5. Survival assay

C. elegans SS104 was washed from a food plate with 10 ml M9 buffer and synchronized with 12% bleach and 1M NaOH as described in a previous study (Wittkowski et al., 2020). Eggs were incubated overnight at 20°C in M9 buffer under shaking, and the resulting L1 larvae were seeded on a fresh food plate and incubated at 25°C for 48 h. From the resulting L4 larvae, 15 were individually picked and transferred to an NGM plate (in 22.1 cm^2 Petri plates) colonized with the bacterial strain of interest (test plate). The two strains of *Salmonella*, which were meant to be compared, were investigated at the same time on individual plates, while

TABLE 1 Details of the bacterial strains and their characteristics.

Strain	Subspecies	Serovar	Source	Identifier (SRA accession/biosample)	Characteristic	References
Salmonella enterica	*diarizonae*	61:k:1,5, (7)	Sheep	12-01777-0-S2 (SRR13071109/SAMN16814736)*	Carrier of plasmid pSASd	Uelze et al., 2021
			Sheep	12-01777-0-S3 (SRR23581851/SAMN33408750)	Absence of plasmid pSASd	
	enterica	Enteritidis	Vaccine, IDT Biologica GmbH	19-SA01616	Vaccine strain Salmovac SE	IDT Biologica GmbH, Germany (CEVA)
			Chicken	20-SA01872-0 (SRR23581848/SAMN33408753)	Non-vaccination strain	This study
			Bird	20-SA00671-0 (SRR23581850/SAMN33408751)	Smooth surface	This study
			Laying hens	09-02812-0 (SRR23581849/SAMN33408752)	Rough surface	Szabo et al., 2017

Salmonella isolates have been deposited in the National Center for Biotechnology Information (NCBI) Sequence Read Archive (SRA) under the BioProject accession number PRJNA937468, *Isolate 12-01777-0-S2 under BioProject PRJNA678834.

test plates seeded with *E. coli* OP50 were run in parallel as a control. All test plates were incubated at 25°C to avoid the reproduction of the thermo-sterile *C. elegans* strain and counted every weekday until all worms were dead. To discriminate dead from living worms, they were gently poked with a worm picker to observe a touch response. For each bacterial strain, three biological and three technical experiments were carried out. Altogether nine replicate experiments were performed, resulting in a total of 135 worms being used per test strain.

2.6. Statistics

Survival was calculated per day relative to the initial number of worms and presented as mean ± standard error of mean (SEM). For the visualization and statistical analyses, the software GraphPad Prism v8.2 (GraphPad Software, San Diego, CA, USA) was used. Differences in the area under the curve (AUC, reflecting the total lifetime of all worms in an experiment) and survival rate per day were tested for significance using the unpaired *t*-test. Survival curves per group were compared with the Gehan-Breslow-Wilcoxon test. The *P*-values of <0.05 relative to the control (*E. coli* OP50) or between both isolates tested were considered significantly different.

2.7. Sequencing data information

Sequencing data for *Salmonella enterica* isolates originating from the strain collection of the NRL for *Salmonella* used in this study have been deposited in the National Center for Biotechnology Information (NCBI) Sequence Read Archive (SRA) under the BioProject accession numbers PRJNA937468 and PRJNA678834.

3. Results

3.1. Vaccine strain Salmovac SE was less virulent against *C. elegans* than a wildtype *S.* Enteritidis strain

The ability of the vaccine strain 19-SA01616 (licensed under the name Salmovac SE) to shorten the lifespan of *C. elegans* was compared to that of the non-vaccination strain *S. enterica* 20-SA01872. Salmovac SE is a live-vaccine auxotrophic for adenine and histidine that was derived through undirected chemical mutagenesis, leading to a significant virulence attenuation (Martin et al., 1996a,b). As shown in Figure 1, there was no difference in the survival rate of *C. elegans* between the vaccine strain and the commensal *E. coli* OP50 (Gehan-Breslow-Wilcoxon test: $p = 0.3668$). In contrast, the non-vaccine strain 20-SA01872 significantly shortened the lifespan of *C. elegans*, especially between days 6 and 14 (Figure 1, Gehan-Breslow-Wilcoxon test: $p = 0.0008$). A comparison of the AUC of the non-vaccination strain with the control group and the vaccine strain revealed a significantly higher difference between them (Figure 2). While the total lifespan of the worms fed with the vaccine strain was reduced by 32%, those of the worms fed with the non-vaccine strain were only reduced by 2% compared to the control group.

3.2. The effect of rough or smooth *S.* Enteritidis strains on the longevity of *C. elegans* did not differ

When *S.* Enteritidis is found in an environmental, food, or feed sample in the European Union, the measures taken depend on the results of its serotyping (Anonymous, 2011). If not typable, the serotype remains unknown and is referred to as rough (Szabo et al., 2017), and no measures are taken. However, the genetic background might clearly indicate the assignment to *S.* Enteritidis. Therefore, the ability to reduce the lifespan of *C. elegans* was

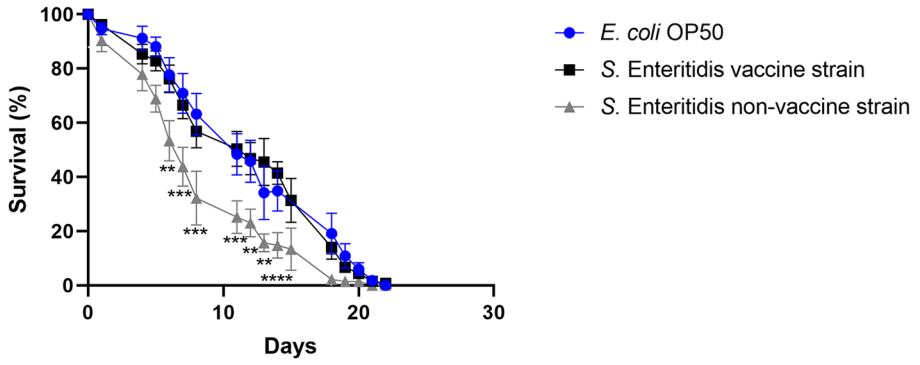

FIGURE 1
Survival over time of *C. elegans* grown on NGM agar either colonized with *E. coli* OP50 (control), Salmovac SE vaccine strain *S.* Enteritidis 19-SA01616, or non-vaccine strain *S.* Enteritidis 20-SA01872. Mean with SEM, $n = 9$, $^{**}p < 0.1$, $^{***}p < 0.01$, $^{****}p < 0.001$.

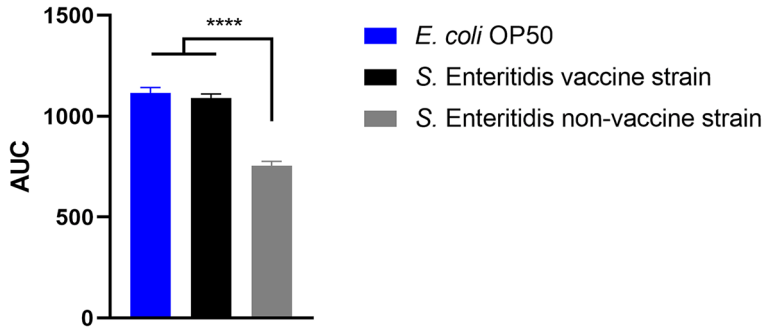

FIGURE 2
Area under the curve (AUC) of *C.* elegans survival curves. The worms were either fed with control strain *E. coli* OP50, Salmovac SE vaccine strain *S.* Enteritidis 19-SA01616, or non-vaccine strain *S.* Enteritidis 20-SA01872. Mean with SEM, $n = 9$, $^{****}p < 0.0001$.

investigated as a surrogate for the pathogenicity of the rough strain 09-2812 and the smooth strain 20-SA00671. As observed in Figures 3, 4, no differences in survival rate were observed for worms fed on the rough or smooth isolate (10 and 11% shorter survival rates compared to the control, respectively). Additionally, differences in virulence were detected between the control *E. coli* strain and the rough and smooth *S. enterica* strains (Figure 4). Overall, the comparison of survival curves revealed a significant difference between the groups in the Gehan-Breslow-Wilcoxon test ($p = 0.0270$).

3.3. *S. enterica* subsp. *diarizonae* isolate with pSASd plasmid did not reduce the lifespan of *C. elegans* more than an isolate without this plasmid

Putative virulence factors and the phylogeny of sheep-derived SASd strain 12-01777-0 were investigated previously (Uelze et al., 2021). The strain belongs to the lineage ST432. Two isolates (S2 and S3) were chosen from our strain collection, and their DNA was sequenced using short-read Illumina technology. Analysis of the genomes revealed that S2 and S3 were separate strains with 40 AD between their core genomes, and they additionally differed by the presence (S2) or absence (S3) of a 43 kb plasmid named pSASd containing a T4SS and a toxin/antitoxin system (Uelze et al., 2021). This led to the assumption that isolate 12-01777-0-S2 could be more virulent during the course of infection than isolate 12-01777-0-S3. We applied the *C. elegans* survival assay to both isolates separately. The assay revealed that both isolates reduced the survival rate of *C. elegans* significantly (Gehan-Breslow-Wilcoxon test: $p = 0.0002$) compared to *E. coli* OP50 (Figures 5, 6). We observed clear differences in the rate between day 10 and day 19 after the challenge of up to 27%. However, no differences in the survival rate were detected between worms grown on isolate 12-01777-0-S2 (21% reduction compared to control) and isolate 12-01777-0-S3 without plasmid (23% reduction compared to control, Figures 5, 6).

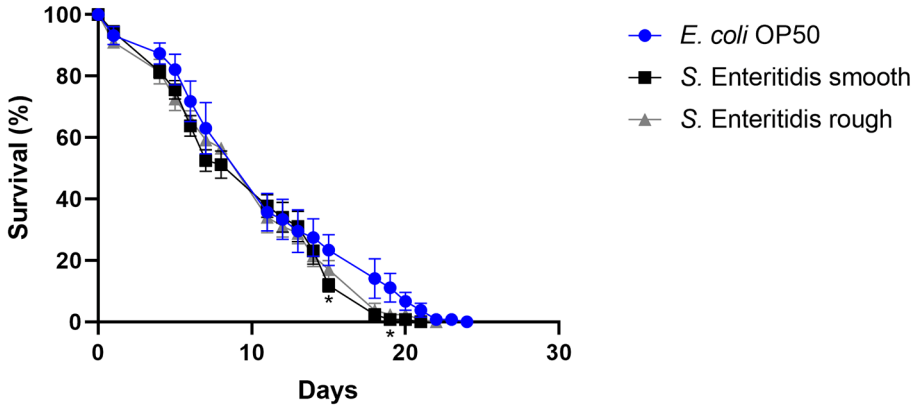

FIGURE 3
Survival over time of *C. elegans* grown on NGM agar either colonized with *E. coli* OP50, smooth *S.* Enteritidis 20-SA00671, or rough *S.* Enteritidis 09-2812. Mean with SEM, $n = 9$, $^{*}p < 0.05$.

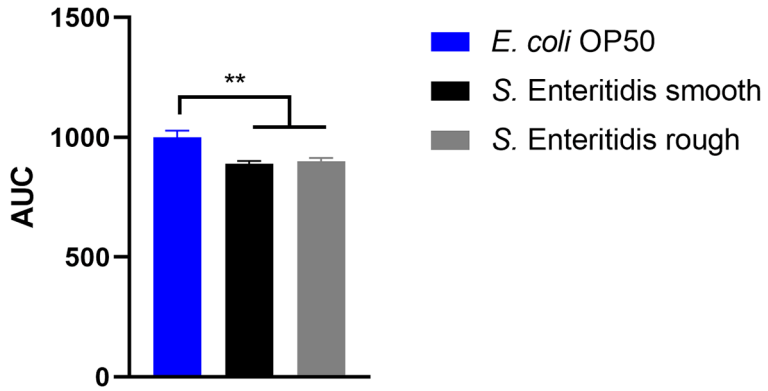

FIGURE 4
Area under the curve (AUC) of C. *elegans* survival curves. The worms were either fed with *E. coli* OP50 (control), *S.* Enteritidis 20-SA00671 (smooth), or *S.* Enteritidis 09-2812 (rough). Mean with SEM, $n = 9$, $^{**}p < 0.01$.

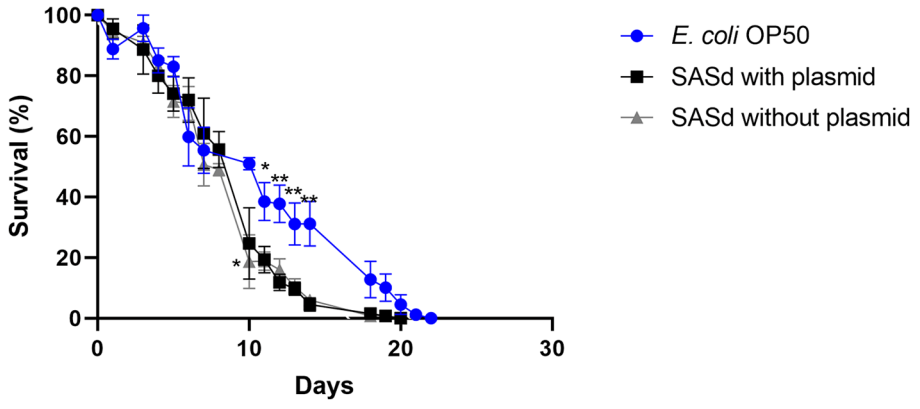

FIGURE 5
Survival over time of *C. elegans* grown on NGM agar either colonized with the control strain *E. coli* OP50, plasmid-equipped SASd isolate 12-01777-0-S2, or plasmid-free SASd isolate 12-01777-0-S3. Mean with SEM, $n = 9$, $^{*}p < 0.05$, $^{**}p < 0.01$.

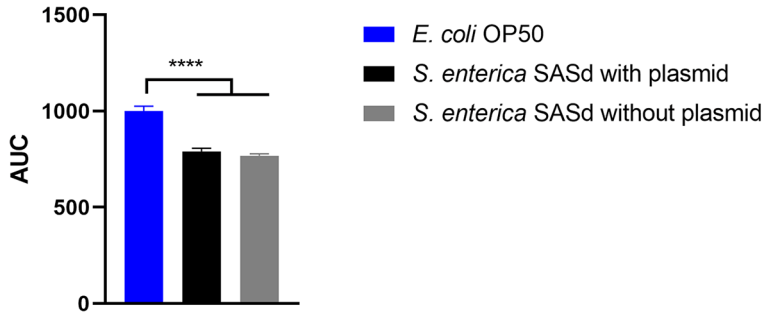

FIGURE 6
Area under the curve (AUC) of *C. elegans* survival curves. The worms were either fed with *E. coli* OP50 (control), SASd isolate 12-01777-0-S2 (with plasmid), or SASd isolate 12-01777-0-S3 (without plasmid). Mean with SEM, $n = 9$, $^{****}p < 0.0001$.

4. Discussion

Approximately 20 years ago, it was shown that broad host range opportunistic pathogens as well as specialized vertebrate pathogens such as *S. enterica* can kill the worm *C. elegans* when it was placed on a lawn of the pathogen (Finlay, 1999; Aballay et al., 2000; Labrousse et al., 2000). The pathogen could proliferate in the *C. elegans* intestine and establish a persistent infection (Aballay et al., 2000). Such a pathogenicity model simplifies scientific studies analyzing the extent of phenotypic traits involved in host-pathogen interactions. It is even conceivable that gene regulatory processes in both the host and the pathogen can be considered for analysis.

In this study, we evaluated the potential of such a *C. elegans* survival assay based on three questions related to the pathogenicity of certain specific *S. enterica* strains. To clarify these questions, animal experiments could also be used and, in the case of vaccination strain Salmovac SE, have been previously reported (Martin et al., 1996b; Theuß et al., 2018).

4.1. Wild-type *S.* Enteritidis strain kills *C. elegans* worms faster than the Salmovac SE vaccination strain

In the European Union (EU), laying hens must be vaccinated against *Salmonella,* and live vaccines are commonly used. The excretion of the *Salmonella* vaccine strains can last for weeks. Therefore, in exceptional cases, young laying hen flocks can contaminate their eggs with *Salmonella* vaccine strains. According to Regulation (EC) No. 178/2002, table eggs contaminated with *Salmonella* are assessed as harmful to health and are considered unsafe food. However, no distinction is made between the evidence of vaccine and wild-type *Salmonella* strains on table eggs. It is currently being discussed whether the detection of a *Salmonella* vaccine strain on eggs should be subject to food law measures. The Salmovac SE vaccine strain is an attenuated strain. Attenuation was achieved in two different ways. The strain was derived from the plasmid-free strain Salmonella Enteritidis 6403 PT4. LD50 increases in mouse experiments from <20 to >106 CFU for the plasmid-free Salmonella enterica variant (Martin et al., 1996b). The attenuation was further augmented by introducing adenine and histidine auxotrophy *via* chemical mutagenesis with N-methyl-N-nitro-N-nitrosoguanidine. This auxotrophy reduced the virulence by a factor of ten. However, attenuation based on the histidine and adenine auxotrophy in the *Salmonella* vaccine strain might be compensated in the worm's intestine through direct uptake of amino acids from the gut, as shown in Kern et al. (2016) for Listeria. Nevertheless, the results showed that the combined attenuation of the *Salmonella* vaccine strain was sufficient to restore the lifespan of *C. elegans* to those of worms fed with *E. coli* OP50.

The current results indicate differences in the virulence of *Salmonella enterica* wild strains and the vaccine strain. Nevertheless, it needs to be clarified whether these differences reflect a lack of virulence. It is possible that the observed reduced virulence in nematodes still poses a hazard to vulnerable groups. It is also possible that the reduced virulence observed in nematodes does not apply to humans. We investigated the survival rate of *C. elegans* in the presence of a wild type and in a vaccine *S.* Enteritidis strain (Salmovac SE) derived from the same lineage using the same experimental setup. There have been two types of lethal effects in *C. elegans*. The so-called "fast killing" effect has been linked to *Pseudomonas aeruginosa,* and the nematodes died within 24 h due to intoxication (Finlay, 1999; Tan and Ausubel, 2000). The "slow killing" effect has been related to a more infection-like process and has been found for *Pseudomonas aeruginosa* and *Serratia marcescens* as a second way of killing *C. elegans* (Finlay, 1999; Kurz and Ewbank, 2000). Our investigations clearly showed a "slow killing" effect, which took the pathogens several days to colonize the nematode's gut and kill *C. elegans*. However, it has been reported that *Salmonella enterica* kills *C. elegans* in an even more prolonged process, as observed for the "slow killing" effect of *P. aeruginosa* (Aballay and Ausubel, 2002).

We observed a differentiable virulence between the two strains in the *C. elegans* survival assay. The higher virulent *S.* Enteritidis wild-type strain reduced the lifespan of *C. elegans* significantly as compared to the less virulent vaccine strain. Similar results have been reported by Martin et al. (1996b) using mice. The diminished pathogenicity is a prerequisite for vaccine strains, but a simple and fast test method for this trait was lacking. The *C. elegans* survival assay can be an effective method for

discriminating between vaccine and wild-type strains. Another group (Sivamaruthi and Balamurugan, 2014) performed a similar study with a different live vaccine strain (Ty21a) and reported similar results. They further claimed that pre-exposure of *C. elegans* to an *S. enterica* vaccine strain rendered the nematode more resistant to an *S. enterica* wild-type strain infection. These results indicate that the *C. elegans* survival assay is an effective method for pre-screening candidate vaccine strains and identifying vaccine strains among those isolated from laying hens and eggs.

4.2. The effect of rough and smooth *S.* Enteritidis strains on the longevity of *C. elegans* did not differ

In total, 60,050 human salmonellosis cases were reported in the EU in 2021, and *Salmonella* Enteritidis was the most commonly isolated (54.6%) serovar (EFSA and ECDC, 2022). Poultry and poultry products are the primary sources of *S.* Enteritidis. Consequently, *S.* Enteritidis is one of the serovars monitored in EU control programs for poultry (Anonymous, 2006, 2008, 2011, 2012). The routine diagnostic determination of *Salmonella* serovars is performed primarily by slide agglutination according to the White-Kauffmann-Le Minor scheme, as outlined in ISO/TR 6579-3:2013. Serotyping is based on the differentiation of the immuno-reactive O-sidechain of the LPS and of two different flagellin(H)antigens. Occasionally, the O-chain reacts non-specifically by classical slide agglutination, leading to non-typeability of the isolates, which are then simply termed "rough". Rough isolates, however, are not part of the EU *Salmonella* control programs. Therefore, when rough isolates are detected on poultry farms, no action is required, even if the *Salmonella* isolates have been shown by molecular methods to belong to *S.* Enteritidis. In the present study, we demonstrated that there is no difference in virulence between rough and smooth strains of *S.* Enteritidis. Both reduced the lifespan of *C. elegans* in a similar fashion. This finding contrasts literature reports that only a smooth strain of *S. enterica* and not a rough strain leads to the death of germ-free piglets colonized with one or both of these bacteria (Dlabac et al., 1997). However, the applicability to humans is not clear. Rough strains are also known for their increased sensitivity to the immune defense. Therefore, it is unclear whether these strains are non-pathogenic only for fully immune-competent individuals (Lalsiamthara et al., 2018). They may still pose a risk for immunocompromised patients. Therefore, more research is needed to clarify the pathogenic potential of rough and smooth *S. enterica* strains and provide guidance on how to deal with the finding of rough *S. enterica* strains in animals, food, or feed. The *C. elegans* approach might be further helpful in analyzing the pathogenic potential of both variants in more detail, for example, by investigating the upregulation and downregulation of virulence genes within the host during the course of the infection. Nevertheless, our initial results established in this study indicate that both variants should be treated in control measurements in the same way to minimize the entry of these bacteria into the food chain.

4.3. The SASd isolate with pSASd plasmid did not reduce the lifespan of *C. elegans* more than an isolate without this plasmid

The SASd isolate is host-adapted to sheep, with a high prevalence in sheep herds worldwide. Infections are usually sub-clinical; however, the serovar has the potential to cause diarrhea, abortions, and chronic proliferative rhinitis. In a previous study (Uelze et al., 2021), we investigated a set of 119 diverse SASd isolates by whole genome sequencing. We found that the serovar was composed of two separate lineages, ST432 and ST439, with different genomic characteristics, of which ST432 was primarily isolated from sheep. We concluded that lineage ST432, in particular, should be considered host-adapted to sheep. In the current study, we investigated two SASd strains of the lineage ST432 in the *C. elegans* survival assay, one with and the other without the pSASd plasmid. Strains of this lineage typically harbor a 43kb large plasmid (pSASd). Although several potential virulence factors are located in this plasmid (Uelze et al., 2021), it does not encode the spv cluster as described for some other virulence plasmids (Gulig et al., 1993; Rotger and Casadesús, 1999). However, the question arises on whether the pSASd plasmid has any influence on the virulence of the strain. We found that the isolates with and without the plasmid both reduced the lifespan of *C. elegans* dramatically, with no difference between them. This indicates that the pSASd plasmid does not have a strong effect on the virulence of the SASd strains under the experimental setup applied in this study. Another group investigated the impact of *S. enterica* strains with and without the pSASd plasmid on macrophages and epithelial cells (Gokulan et al., 2013). They found that plasmid-equipped bacteria showed increased invasion and persistence in those cells and therefore argued that the plasmid enhances the virulence of the *S. enterica* strain. The discrepancy between their and our results can be explained by the fact that *C. elegans* does not have an adaptive immune system or mobile immune cells (Alper et al., 2007; Pukkila-Worley and Ausubel, 2012). Therefore, animal experiments cannot be avoided entirely to elucidate further the role of the pSASd plasmid on the virulence of the strains.

4.4. Limits and potential of *C. elegans* assays in studying the virulence and host interaction of bacterial pathogens

In conclusion, the *C. elegans* survival assay cannot replace animal experiments designed to determine differences in the virulence of *Salmonella enterica* strains. Still, it is an effective and relatively easy method for classifying the virulence of different bacterial isolates *in vivo*, despite some limitations. The divergent immune response to pathogens and differences in the course of infection might lead to discrepancies between results obtained with *C. elegans* assays and those from experiments with higher vertebrates. Therefore, we recommend using the described method to pre-screen bacterial strains of interest to select the most promising candidates for further animal experiments. It has been the traditional concept to substitute an animal test only

with an alternative test that is fully equivalent. This concept is limited to replacing animal tests for complex questions involving interdependent organ systems. The so-called integrated testing strategies were introduced into toxicology by an ECVAM task force to meet the requirements of complex systems (Blaauboer et al., 1999). The idea behind this strategy is to combine different alternative tests, creating a complexity that should overcome the intrinsic limitation of the stand-alone test systems (Calonie et al., 2022). Currently, the range of alternative systems is very broad, ranging from *in silico* simulations, cell cultures, 3D cell cultures, and organoids to non-vertebrate *in vivo* models. An elaborated combination of these options promises testing approaches with a high human prediction value. Moreover, a much larger pool of validation data is available from comparisons between animal tests and alternative methods (Calonie et al., 2022).

Although *C. elegans* has been widely used to study pathogenicity mechanisms of microorganisms for two decades (Sifri et al., 2005), direct comparisons between animal-based infection models and *C. elegans* infection assays are rare. There are different reasons why such a direct comparison is usually not applied. Unlike other approaches, e.g., in toxicology, investigating infectious pathogenicity is not based on standardized animal tests. The animal tests must be chosen according to the microorganism and the host. For example, mice infected with *Salmonella* Typhimurium did not show any signs of diarrhea and are not suitable as an infectious model for human disease (Santos et al., 2001). Moreover, the investigated endpoints in animal tests and *C. elegans* infection assays are very different, making the comparison difficult. The approach usually applied is to use strains of pathogenic microorganisms with a certain proven virulence or a lack of pathogenicity in animal models or patients. If the clinically observed effects are reflected in similar effects in the *C. elegans* infection assay, the assay can be used to investigate the role of specific pathogen factors. This has been quite successfully applied for pathogenic *E. coli*, where the pathogenicity island locus of enterocyte effacement (lee), which is responsible for the virulence in humans, has also been shown to be correlated with the ability to kill the nematode (Anyanful et al., 2005).

Further development of variants of the *C. elegans* assay should encompass deeper investigations of the host and pathogen, e.g., by omics technologies such as transcriptomics. It is anticipated that the results of such studies will improve the estimation of the pathogenic potential of test organisms. This would lead to reduced dependence on vertebrate experiments, which is in agreement with the 3R (refine, replace, reduce) principle.

Data availability statement

The datasets presented in this study can be found in online repositories. The names of the repository/repositories and accession number(s) can be found below: https://www.ncbi.nlm.nih.gov/, PRJNA937468 and PRJNA678834.

Author contributions

WB, BM, and IS designed the study. JF and IS provided the samples and performed pre-analysis and next-generation sequencing. CS and WB performed the experiments with *C. elegans*. WB, IS, and MF interpreted the results and wrote the draft manuscript. WB performed the bioinformatics analysis. JF and BM were involved in manuscript revision prior to the submission of the manuscript. All authors contributed to the article and approved the submitted version.

Funding

This work was supported by the German Federal Institute for Risk Assessment.

Acknowledgments

We thank Mr. Sven Meissner from the Department of Experimental Toxicology and ZEBET of the German Federal Institute for Risk Assessment for introducing us to the *C. elegans* assay.

Conflict of interest

The authors declare that the research was conducted in the absence of any commercial or financial relationships that could be construed as a potential conflict of interest.

Publisher's note

References

Aballay, A., and Ausubel, F. M. (2002). *Caenorhabditis elegans* as a host for the study of host-pathogen interactions. *Curr. Opin. Microbiol.* 5, 97–101. doi: 10.1016/S1369-5274(02)00293-X

Aballay, A., Yorgey, P., and Ausubel, F. M. (2000). *Salmonella* typhimurium proliferates and establishes a persistent infection in the intestine of *Caenorhabditis elegans*. *Curr. Biol.* 10, 1539–1542. doi: 10.1016/S0960-9822(00)00830-7

Alper, S., McBride, S. J., Lackford, B., Freedman, J. H., and Schwartz, D. A. (2007). Specificity and complexity of the *Caenorhabditis elegans* innate immune response. *Mol. Cell. Biol.* 27, 5544–5553. doi: 10.1128/MCB.02070-06

Anonymous (2006). Commission Regulation (EC) No 1168/2006 of 31 July 2006 implementing Regulation (EC) No 2160/2003 as regards a Community target for the reduction of the prevalence of certain *Salmonella* serotypes in laying hens of *Gallus gallus* and amending Regulation (EC) No 1003/2005. Official J.Euro.Union 1.8.2006, L211/214-L170/218.

Anonymous (2008). Commisson Regulation (EC) No 584/2008 of 20 June 2008 implementing Regulation (EC) No 2160/2003 of the European Parliament and of the Council as regards a Community target for the reduction of the prevalence of *Salmonella enteritidis* and *Salmonella typhimurium* in turkeys. Official J.Euro.Union L162, 3–8.

Anonymous (2011). Commission Regulation (EU) No 517/2011 of May 2011 implementing Regulation (EC) No 2160/2003 of the European Parliament and of the Council as regards a Union target for the reduction of the prevalence of certain *Salmonella* serotypes in laying hens of *Gallus gallus* and amending Regulation (EC) No 2160/2003 and Commission Regulation (EU) No 200/2010. Official J.Euro.Union L138, 45–51.

Anonymous (2012). Commission Regulation (EU) No 1190/2012 of 12 December 2012 concerning a Union target for the reduction of *Salmonella* Enteritidis and *Salmonella* Typhimurium in flocks of turkeys, as provided for in Regulation /EC) No 2160/2003 of the European Parliament and of the Council. Official J.Euro.Union L340, 29–34.

Anyanful, A., Dolan-Livengood, J. M., Lewis, T., Sheth, S., DeZalia, M. N., Sherman, M. A., et al. (2005). Paralysis and killing of *Caenorhabditis elegans* by enteropathogenic *Escherichia coli* requires the bacterial tryptophanase gene. *Mol. Microbiol.* 57, 988–1007. doi: 10.1111/j.1365-2958.2005.04739.x

Blaauboer, B., Barratt, M. D., and Houston, J. B. (1999). The Integrated use of alternative methods in toxicological risk evaluation—ECVAM integrated testing strategies task force report 1. *Altern. Lab. Anim.* 27, 229–237. doi: 10.1177/026119299902700211

Bulitta, J. B., Hope, W. W., Eakin, A. E., Guina, T., Tam, V. H., Louie, A., et al. (2019). Generating robust and informative nonclinical in vitro and in vivo bacterial infection model efficacy data to support translation to humans. *Antimicrob. Agents Chemother.* 63, e02307–e02318. doi: 10.1128/AAC.02307-18

Calonie, F., De Angelis, I., and ·Hartung, T. (2022). Replacement of animal testing by integrated approaches to testing and assessment (IATA): a call for in vivitrosi. *Arch. Toxicol.* 96, 1935–1950. doi: 10.1007/s00204-022-03299-x

Chakravarty, B. (2022). The evolving role of the *Caenorhabditis elegans* model as a tool to advance studies in nutrition and health. *Nutr. Res.* 106, 47–59. doi: 10.1016/j.nutres.2022.05.006

Chen, S., Zhou, Y., Chen, Y., and Gu, J. (2018). fastp: an ultra-fast all-in-one FASTQ preprocessor. *Bioinformatics* 34, i884–i890. doi: 10.1093/bioinformatics/bty560

Deneke, C., Brendebach, H., Uelze, L., Borowiak, M., Malorny, B., and Tausch, S. H. (2021a). Species-specific quality control, assembly and contamination detection in microbial isolate sequences with AQUAMIS. *Genes* 12, 644. doi: 10.3390/genes12050644

Deneke, C., Uelze, L., Brendebach, H., Tausch, S. H., and Malorny, B. (2021b). Decentralized investigation of bacterial outbreaks based on hashed cgMLST. *Front. Microbiol.* 12, 649517. doi: 10.3389/fmicb.2021.649517

Dlabac, V., Trebichavsk,ý, I., Rehákov,á, Z., Hofmanov,á, B., Splíchal, I., and Cukrowska, B. (1997). Pathogenicity and protective effect of rough mutants of *Salmonella* species in germ-free piglets. *Infect. Immun.* 65, 5238–5243. doi: 10.1128/iai.65.12.5238-5243.1997

EFSA and ECDC (2022). The European union one health 2021 zoonoses report. *EFSA J.* 20, 273. doi: 10.2903/j.efsa.2022.7666

Finlay, B. B. (1999). Bacterial disease in diverse hosts. *Cell* 96, 315–318. doi: 10.1016/S0092-8674(00)80544-9

Gokulan, K., Khare, S., Rooney, A. W., Han, J., Lynne, A. M., and Foley, S. L. (2013). Impact of plasmids, including those encodingVirB4/D4 type IV secretion systems, on *Salmonella* enterica serovar Heidelberg virulence in macrophages and epithelial cells. *PLoS ONE* 8, e77866. doi: 10.1371/journal.pone.0077866

Gulig, P. A., Danbara, H., Guiney, D. G., Lax, A. J., Norel, F., and Rhen, M. (1993). Molecular analysis of spv virulence genes of the *Salmonella* virulence plasmids. *Mol. Microbiol.* 7, 825–830. doi: 10.1111/j.1365-2958.1993.tb01172.x

Jajere, S. M. (2019). A review of *Salmonella* enterica with particular focus on the pathogenicity and virulence factors, host specificity and antimicrobial resistance including multidrug resistance. *Vet. World* 12, 504–521. doi: 10.14202/vetworld.2019.504-521

Kaletta, T., and Hengartner, M. O. (2006). Finding function in novel targets: *C. elegans* as a model organism. *Nat. Rev. Drug Discov.* 5, 387–398. doi: 10.1038/nrd2031

Kern, T., Kutzner, E., Eisenreich, W., and Fuchs, T. M. (2016). Pathogen-nematode interaction: nitrogen supply of Listeria monocytogenes during growth in *Caenorhabditis elegans*. *Environ. Microbiol. Rep.* 8, 20–29. doi: 10.1111/1758-2229.12344

Kumar, A., Baruah, A., Tomioka, M., Iino, Y., Kalita, M. C., and Khan, M. (2020). Caenorhabditis elegans: a model to understand host-microbe interactions. *Cell. Mol. Life Sci.* 77, 1229–1249. doi: 10.1007/s00018-019-03319-7

Kurz, C. L., and Ewbank, J. J. (2000). Caenorhabditis elegans for the study of host-pathogen interactions. *Trends Microbiol.* 8, 142–144. doi: 10.1016/S0966-842X(99)01691-1

Labrousse, A., Chauvet, S., Couillault, C., Kurz, C. L., and Ewbank, J. J. (2000). *Caenorhabditis elegans* is a model host for *Salmonella* typhimurium. *Curr. Biol.* 10, 1543–1545. doi: 10.1016/S0960-9822(00)00833-2

Lalsiamthara, J., Kim, J. H., and Lee, J. H. (2018). Engineering of a rough auxotrophic mutant *Salmonella* Typhimurium for effective delivery. *Oncotarget* 9, 25441–25457 doi: 10.18632/oncotarget.25192

Lang, M., Montjarret, A., Duteil, E., and Bedoux, G. (2021). Cinnamomum cassia and *Syzygium aromaticum* essential oils reduce the colonization of *Salmonella* Typhimurium in an *in vivo* infection model using *Caenorhabditis elegans*. *Molecules*. 26, 5598. doi: 10.3390/molecules26185598

Leung, M. C., Williams, P. L., Benedetto, A., Au, C., Helmcke, K. J., Aschner, M., et al. (2008). *Caenorhabditis elegans*: an emerging model in biomedical and environmental toxicology. *Toxicol. Sci.* 106, 5–28. doi: 10.1093/toxsci/kfn121

Maldonado, R. F., Correia, I. S, and Valvano, M. A. (2016). Lipopolysaccharide modification in Gram-negative bacteria during chronic infection. *FEMS Microbiol. Rev.* 40, 480–493. doi: 10.1093/femsre/fuw007

Martin, G., Hänel, I., Helmuth, R., Schroeter, A., Erler, W., and Meyer, H. (1996a). Immunization with potential *Salmonella* enteritidis mutants—1. Production and in vitro characterization. *Berl. Munch. Tierarztl. Wochenschr.* 109, 325–329.

Martin, G., Methner, U., Steinbach, G., and Meyer, H. (1996b). Immunization with potential *Salmonella* enteritidis mutants– 2. Investigations on the attenuation and immunogenicity for mice and young hens. *Berl. Munch. Tierarztl. Wochenschr.* 109, 369–374.

Meneely, P., Dahlberg, C. L., and Rose, J. K. (2019). Working with worms: *Caenorhabditis elegans* as a model organism. *Curr. Protokols Essential Lab. Tech.* 19, e35. doi: 10.1002/cpet.35

Pukkila-Worley, R., and Ausubel, F. M. (2012). Immune defense mechanisms in the *Caenorhabditis elegans* intestinal epithelium. *Curr. Opin. Immunol.* 24, 3–9. doi: 10.1016/j.coi.2011.10.004

Rotger, R., and Casadesús, J. (1999). The virulence plasmids of *Salmonella*. *Int. Microbiol.* 2, 177–184.

Sahu, S. N., Anriany, Y., Grim, C. J., Kim, S., Chang, Z., Joseph, S. W., et al. (2013). Identification of virulence properties in *Salmonella* Typhimurium DT104 using *Caenorhabditis elegans*. *PLoS ONE* 8, 76673. doi: 10.1371/journal.pone.0076673

Santos, R. L., Zhang, S., Tsolis, R. M., Kingsley, R. A., Adams, L. G., and Bäumler, A. J. (2001). Animal models of *Salmonella* infections: enteritis versus typhoid fever. *Microbes Infection* 3, 1335–1344. doi: 10.1016/S1286-4579(01)01495-2

Sem, X., and Rhem, M. (2012). Pathogenicity of *Salmonella enterica* in *Caenorhabditis elegans* relies on disseminated oxidative stress in the infected host. *PLoS ONE* 7, e45417. doi: 10.1371/journal.pone.0045417

Sifri, C. D., Begun, J., and Ausubel, F. M. (2005). The worm has turned – microbial virulence modeled in *Caenorhabditis elegans*. *Trends Microbiol.* 13, 119–127. doi: 10.1016/j.tim.2005.01.003

Simon, S., Lamparter, M. C., Pietsch, M., Borowiak, M., Fruth, A., Rabsch, W., et al. (2023). "Zoonoses in food-chain animals with respect to human disease and public health relevance," in *Zoonoses: Infections Affecting Humans and Animals*, ed A. Sing (Cham: Springer).

Singkum, P., Suwanmanee, S., Pumeesat, P., and Luplertlop, N. (2019). A powerful *in vivo* alternative model in scientific research: *Galleria mellonella*. *Acta Microbiol. Immunol. Hung.* 66, 31–55, doi: 10.1556/030.66.2019.001

Sivamaruthi, B. S., and Balamurugan, K. (2014). Physiological and immunological regulations in *Caenorhabditis elegans* infected with *Salmonella* enterica serovar Typhi. *Indian J. Microbiol.* 54, 52–58. doi: 10.1007/s12088-013-0424-x

Szabo, I., Grafe, M., Kemper, N., Junker, E., and Malorny, B. (2017). Genetic basis for loss of immuno-reactive O-chain in *Salmonella* enterica serovar Enteritidis veterinary isolates. *Vet. Microbiol.* 204, 165–173. doi: 10.1016/j.vetmic.2017.03.033

Tan, M. W., and Ausubel, F. M. (2000). Caenorhabditis elegans: a model genetic host to study *Pseudomonas aeruginosa* pathogenesis. *Curr. Opin. Microbiol.* 3, 29–34. doi: 10.1016/S1369-5274(99)00047-8

Tenor, J. L., McCormick, B. A., Ausubel, F. M., and Aballay, A. (2004). Caenorhabditis elegans-based screen identifies *Salmonella* virulence factors required for conserved host-pathogen interactions. *Curr. Biol.* 14, 1018–1024. doi: 10.1016/j.cub.2004.05.050

Theuß, T., Woitow, G., Bulang, M., and Springer, S. (2018). Demonstration of the efficacy of a *Salmonella* Enteritidis live vaccine for chickens according to the current European Pharmacopoeia Monograph. *Heliyon* 4, e01070. doi: 10.1016/j.heliyon.2018.e01070

Uelze, L., Borowiak, M., Deneke, C., Fischer, J., Flieger, A., Simon, S., et al. (2021). Comparative genomics of *Salmonella* enterica subsp. diarizonae serovar 61:k,

1,5, reveals lineage-specific host adaptation of ST432. *Microb. Genom.* 7, 000604. doi: 10.1099/mgen.0.000604

Wittkowski, P., Violet, N., Oelgeschläger, M., Schönfelder, G., and Vogl, S. (2020). A quantitative medium-throughput assay to measure Caenorhabditis elegans development and reproduction. *STAR Protoc.* 1, 100224. doi: 10.1016/j.xpro.2020.100224

Zermeño-Ruiz, M., Rangel-Castañeda, I. A., Suárez-Rico, D. O., Hernández-Hernández, L., Cortés-Zárate, R., Hernández-Hernández, J. M., et al. (2022). Curcumin stimulates the overexpression of virulence factors in *Salmonella enterica* serovar typhimurium: *in vitro* and animal model studies. *Antibiotics* 11, 1230. doi: 10.3390/antibiotics 11091230

frontiers | Frontiers in Microbiology

TYPE Original Research
PUBLISHED 10 August 2023
DOI 10.3389/fmicb.2023.1240458

OPEN ACCESS

EDITED BY
George Grant,
University of Aberdeen, United Kingdom

REVIEWED BY
Ruixi Chen,
Massachusetts Institute of Technology, United States
Lisa Gorski,
Agricultural Research Service (USDA), United States

*CORRESPONDENCE
Debabrata Biswas
dbiswas@umd.edu

†These authors have contributed equally to this work and share first authorship

RECEIVED 15 June 2023
ACCEPTED 31 July 2023
PUBLISHED 10 August 2023

CITATION
Alvarado-Martinez Z, Julianingsih D, Tabashsum Z, Aditya A, Tung C-W, Phung A, Suh G, Hshieh K, Wall M, Kapadia S, Canagarajah C, Maskey S, Sellers G, Scriba A and Biswas D (2023) Assessment of the prevalence, serotype, and antibiotic resistance pattern of *Salmonella enterica* in integrated farming systems in the Maryland-DC area.
Front. Microbiol. 14:1240458.
doi: 10.3389/fmicb.2023.1240458

Assessment of the prevalence, serotype, and antibiotic resistance pattern of *Salmonella enterica* in integrated farming systems in the Maryland-DC area

Zabdiel Alvarado-Martinez[1†], Dita Julianingsih[2†], Zajeba Tabashsum[1], Arpita Aditya[2], Chuan-Wei Tung[2], Anna Phung[3], Grace Suh[3], Katherine Hshieh[3], Matthew Wall[3], Sarika Kapadia[3], Christa Canagarajah[3], Saloni Maskey[3], George Sellers[3], Aaron Scriba[3] and Debabrata Biswas[1,2*]

[1]Biological Sciences Program, Molecular and Cellular Biology, University of Maryland, College Park, College Park, MD, United States, [2]Department of Animal and Avian Sciences, University of Maryland, College Park, College Park, MD, United States, [3]Department of Biology, University of Maryland, College Park, College Park, MD, United States

Implementation of organic/pasture farming practices has been increasing in the USA regardless of official certification. These practices have created an increasingly growing demand for marketing safe products which are produced through these systems. Products from these farming systems have been reported to be at greater risk of transmitting foodborne pathogens because of current trends in their practices. *Salmonella enterica* (SE) is a ubiquitous foodborne pathogen that remains a public health issue given its prevalence in various food products, but also in the environment and as part of the microbial flora of many domestic animals. Monitoring antibiotic resistance and identifying potential sources contamination are increasingly important given the growing trend of organic/pasture markets. This study aimed to quantify prevalence of SE at the pre- and post-harvest levels of various integrated farms and sites in Maryland-Washington D.C. area, as well as identify the most prevalent serovars and antibiotic resistance patterns. Samples from various elements within the farm environment were collected and screened for SE through culture and molecular techniques, which served to identify and serotype SE, using species and serovar-specific primers, while antibiotic resistance was evaluated using an antibiogram assay. Results showed a prevalence of 7.80% of SE pre-harvest and 1.91% post-harvest. These results also showed the main sources of contamination to be soil (2.17%), grass (1.28%), feces (1.42%) and unprocessed produce (1.48%). The most commonly identified serovar was Typhimurium (11.32%) at the pre-harvest level, while the only identified serovar from post-harvest samples was Montevideo (4.35%). With respect to antibiotic resistance, out of the 13 clinically relevant antibiotics tested, gentamycin and kanamycin were the most effective, demonstrating 78.93 and 76.40% of isolates, respectively, to be susceptible. However, ampicillin, amoxicillin and cephradine had the lowest number of susceptible isolates with them being 10.95, 12.36, and 9.83%, respectively. These results help inform farms striving to implement organic practices on how to produce safer products by recognizing areas that pose greater risks as potential sources of contamination, in addition to identifying serotypes of interest, while also showcasing the current state of

10.3389/fmicb.2023.1240458

antibiotic efficacy and how this can influence antibiotic resistance trends in the future.

KEYWORDS

Salmonella enterica, dairy farming, integrated crop-livestock systems, pathogen surveillance, antibiotic resistance

1. Introduction

An increase in consumer demand for both plant and animal food products produced through organic/pasture farming has increased significantly as organic/pasture food producing methods are seen as a healthy and environmentally sustainable alternatives regardless of their certification status (Carlson et al., 2023). Over the last year, this industry has seen a nationwide increase in certified organic sales by 13% from 2019 to 2021, which accounts for $11.2 billion, 54% of which were mainly crops, while 46% were for livestock and related products (NASS, 2022). On the other hand, though many farms lack official certification accredited by relevant regulatory agencies to be properly labeled as organic, they still engage in practices that are compatible with organic farming, such as, limiting or eliminating the use of conventional antibiotics, synthetic antimicrobials, and disinfectants, having alternative animal housing spaces, utilizing natural fertilizers like manure and compost, and practicing animal/crop rotation (USDA National Organic Program, 2010). In keeping with the environmentally friendly approach to farming, numbers of organic/pasture farms grow both fresh produce and livestock in the same facility, commonly known as integrated crop-livestock farm (ICLF) system. This farming method is believed to increase production output and reduce land requirements for farming, while also recycling animal waste materials and repurposing it as a fertilizer for crops in the form of compost (Herrero and Thornton, 2001; Lemaire et al., 2014). Other farms, including dairy farms, have also been known to follow some of the practices laid out by regulatory agencies in order to comply with the organic farming standards. Products from these farming systems are often sold in local farmers markets, stores and roadside stands, with other producers making it to become providers for medium and large sized retail stores (Carlson et al., 2023). This fact has made some of these farms crucial part of the USA economy and supply chain for organic products, as they have become key providers of fresh organic produce, as well as organic meats and other animal products, while those that stay at the local level still manage to have a significant impact as the emergence of new registered farmers markets increase their reach across the entire country (King et al., 2010; Martinez et al., 2010). Considering the prevalence of organic products in the market, their impact on public health and food safety cannot be overlooked. Despite the enthusiasm surrounding organic farming for their progress in promoting sustainability, other findings suggest that the lack of antibiotic and synthetic antimicrobials use within these farms, the use of natural fertilizers like compost and manure, as well as increased contact and exposure to surrounding wildlife that might act as pathogen vectors, are factors that contribute to organic products being more at risk of being contaminated with common foodborne pathogens (Maffei et al., 2016). Further, there is an additional risk of cross-contamination brought about by produce being grown in proximity to different groups of live animals that often harbor pathogenic bacteria as part of their natural flora that can be transferred to food products, other live animals, handlers, and the surrounding environment (Park et al., 2012). On the other hand, other types of farms, such as organic dairy farms do not have to contend with the risk of contaminating produce, but there is still a significant concern for delivering products free from pathogens, while also properly managing animal waste and maintaining the health of the soil and surrounding environment (Lynch, 2022). Both dairy farm and ICLF systems face similar challenges when it comes to maintaining animal welfare and delivering safe products that are free of pathogens, but as the organic farming sector and organic farming practices grow to meet the demand of consumers, so do the risks of outbreaks, especially within markets consisting of limited agricultural space (Adl et al., 2011). In the Mid-Atlantic part of the USA there has been an increase in registered organic farms, (NASS, 2022), however, these numbers neglect the current number of farms that currently lack official organic certification, but are still implementing organic farming practices, or are in the process of transitioning from conventional farming to organic farming. Mid-Atlantic states like Maryland (MD) and Washington, District of Columbia (DC) have seen an increase in organic farming, officially totaling 120 certified farms, with 62 new farms being added as of 2022, all of which contributes to a sector of the local economy that amounts to >$50 million in sales (Maryland State Archives, 2023). Though most of these farms are family-owned businesses that mainly engage in local sales, the MD-DC area has also seen an increment in larger organic retail and wholesale stores, some of which are supplied by the local markets, and import from other states (Dimitri and Greene, 2002).

Considering the growing trend of organic/pasture integrated farming in the MD-DC area and the potential risks that might be involved with the products being produced in these, special attention must be given to specific foodborne pathogens. Among these foodborne pathogens, *Salmonella enterica* (SE) remains a major issue in the USA, as it is the bacterial pathogen responsible for the most amount of yearly cases of foodborne illness, accounting for more than 1.4 million diseases yearly (Scallan et al., 2011), as well as being responsible for a reported 153 single and multi-state outbreaks in 2021 that lead to 3679 illnesses and 768 hospitalizations (Centers for Disease Control and Prevention (CDC), 2021), while also accounting for 44% of outbreaks associate directly with organic products (Harvey et al., 2016). This increase in outbreaks can be attributed to the increase in consumption of these products but could also be associated to farming and processing practices at the pre-harvest and post-harvest levels that are unique to these farms (Iwu and Okoh, 2019; Sosnowski and Osek, 2021). When evaluating MD and DC, there were a reported 18 outbreaks that lead to 1786 illnesses and 450 hospitalizations (Centers for Disease Control and Prevention (CDC),

2021), though it is important to note that, despite improvements in surveillance and reporting, many sporadic outbreaks and illnesses go unreported (Zhang et al., 2022). The risk of SE is aggravated by their prevalence in products both at the pre-harvest and post-harvest levels of farming, particularly attributing them to contaminated fruits, vegetables, and poultry products (Interagency Food Safety Analytics Collaboration, 2022), but also isolating them from various environmental sources (Winfield and Groisman, 2003).

SE is a gram-negative, bacillus shaped facultative anaerobic bacteria that is comprised of over >2500 serotypes that have been identified, many of which can be associated with specific environments, foods, and animal hosts (Jajere, 2019). SE can be found ubiquitously across multiple environments, particularly in soil, water, and other surfaces (Bondo et al., 2016). The 5 most common serovars to be confirmed in cases of illness in the USA are Enteritidis, Newport, Typhimurium, Javiana and monophasic Typhimurium I 4,[5],12:i- (Centers for Disease Control and Prevention (CDC), 2018). The most common foods that have been attributed to causing illness with SE are chicken, produce, pork, beef, turkey, and eggs (Interagency Food Safety Analytics Collaboration, 2022). Some of these food groups have been associated with specific serovars in the USA, such as in the case of chicken being associated with SE Kentucky, beef being found to have Montevideo, turkey with Reading (USDA-FSIS, 2014). However, when looking at the prevalence of specific serotypes to an animal vector, Enteritidis and Typhimurium have been linked to chickens, while Newport and Typhimurium have been linked to cattle, Javiana being linked to equine and turkey sources, and monophasic Typhimurium I 4,[5],12:i- being found in chicken sources (Centers for Disease Control and Prevention (CDC), 2013). SE and many of its serovars can be found as part of the normal microflora of both wild and domestic animals without manifesting any disease or illness, making them vectors that can spread either through direct contact with the animal, through their products, or through their contact with the environment (Rukambile et al., 2019).

When considering the economic loss associated with the burden of SE illness directly associated with various food sources, the costs can amount to over $6.5 billion (Scharff, 2020). Given the importance of monitoring SE within smaller, local, organic farming operations, this study focuses on assessing the prevalence of SE across various farm elements and environments of both dairy farm and ICLF systems within the MD-DC area. After confirmation, SE isolates discovered in this study were serotyped and tested for resistance to various clinically relevant antibiotics. Co-resistance to specific antibiotics among the isolates confirmed in this study was also evaluated. The findings exposed in this research could lead to better facilities management practices at the pre-harvest and post-harvest levels of the local farming industry, as well as offer a detailed assessment of the prevalence of key SE serovars within the area of MD-DC.

2. Materials and methods

2.1. Sample collection by categories and sites

Both pre-harvest and post-harvest samples were collected from various sites within the MD-DC area in the USA, spanning 7 pre-harvest sites comprised of local farms that implement integrated farming practices, as well as other backyard producers, in addition to 3 post-harvest sites comprised of local markets. Farms were selected based on their location within the MD-DC area, as well as their type of farming practices that implement aspects of integrated farming regardless of official organic status certification, such as, but not limited to growing crops in proximity to animals for space maximization, avoidance of synthetic antimicrobials, antibiotics, pesticides and fertilizers in favor of natural fertilization through composing and manure processing, as well as allowing for pasture grazing, rotational grazing and open animal housing. Post-harvest sites were selected based on the same geographic criteria, while also being sites that are associated with the distribution of local produce and markets. A total of 3864 samples were collected (Table 1), with those in the pre-harvest category making up 3028 samples across multiple environmental categories, as well as unprocessed produce, while post-harvest samples made up 836 samples of multiple kinds of produce products. Pre-harvest samples included various elements from the farm environment, including animal feed, water, bedding, soil, grass, manure, and feces that had originated or had contact with poultry (both chicken and turkey), cattle, goat, sheep, and pigs, in addition to pre-processed produce spanning the categories of fruit, capsicum, vegetables, tubers, legumes, grains, leafy greens and herbs. Post-harvest samples were comprised of many kinds of fresh produce, including products within the categories of fruit, capsicum, vegetables, tubers, legumes, grains, leafy greens, and herbs. Sites were visited and sampled at least twice during the summer season (June–September)

TABLE 1 List of sample types and categories collected from pre-harvest and post-harvest sites.

Sites sampled	Sample type	No. of samples per type	No. of samples per site
Pre-harvest*	Bedding	173	3,028
	Compost	219	
	Feces	370	
	Feed	275	
	Grass	269	
	Lagoon	51	
	Produce	874	
	Soil	461	
	Water	336	
Post-harvest**	Leafy greens	120	836
	Tubers	191	
	Fruits	162	
	Capsicum	154	
	Grains	40	
	Legumes	40	
	Herbs	90	
	Other	39	
Total			3,874

* Pre-harvest = 8; samples included environment, pre-harvest produce from various categories and animal samples including chicken, turkey, sheep, pig, and cattle.
** Post-harvest = 3; samples included post-harvest produce from various categories.

between the years of 2019 and 2021, in order to reduce seasonal variability and to comply with enough replicates between farms and sample types.

2.2. Sample processing, enrichment, selection, and growth conditions

All collected samples were placed in sterile plastic sample bags (VWR, PA, USA) and transported to the laboratory for immediate same-day processing. Sample processing was performed as described previously (Salaheen et al., 2015; Peng et al., 2016). Briefly, samples were suspended in sterilized 1 X phosphate buffered solution (PBS) (pH 7.2), while 1 mL of the resulting solution was used to inoculate 9 mL of Luria-Bertani (LB) broth (VWR, OH, USA) enriched with 10% sheep blood (Hemostat Laboratories, CA, USA). The enriched samples were incubated aerobically at 37°C for 24 h. After incubation, samples were streaked in *Salmonella-Shigella* (SS) agar (Difco-BD, MD, USA) and xylose lysine deoxycholate (XLD) agar (Criterion-Hardy Diagnostics, CA, USA) for selection and differentiation of *Salmonella* based on colony morphology (Nye et al., 2002). If present within the same sample, multiple colonies presumed to be *Salmonella* were selected for sub-culturing in LB agar for proper isolation and later used to prepare 20% glycerol stocks for each of the isolates.

2.3. Molecular confirmation, and serotyping of isolates

Molecular confirmation through species-specific and later serotype-specific primers (Table 2) was performed on presumptive positive isolates as described in previous studies (Peng et al., 2016). Briefly, isolates were re-grown in LB agar to isolate single colonies of the isolate. These were collected and resuspended in 1 x PBS to extract total DNA through heat lysis (95°C for 10 min). This solution was centrifuged, while the supernatant was collected and used as template DNA for confirmation and serotyping. Confirmation of SE was done using species-specific primers for genes *aceK* and *Salmonella oriC*, as described previously (O'Regan et al., 2008; Woods et al., 2008). Isolates confirmed to be SE were further serotyped using multiplex PCR with a combination of primers labeled STM 1–5, which are de-signed to identify the 30 most common SE serovars in the USA, by targeting and selectively amplifying specific regions within the bacterial chromosome depending on the serotype, as described previously (Kim et al., 2006). PCR amplification was performed following the manufacturer guidelines form the GoTaq® Green Master Mix (Promega, WI, USA) with the following thermocycler protocol: 1 cycle at 94°C for 5 min, followed by 40 cycles of 94°C for 30 s, 59.8°C for 30 s and 72°C for 1 min, finishing with an ex-tension at 72°C for 5 min. These PCR products were visualized using a 2.5% (w/v) agarose gel prepared with 1 x Tris-Borate-EDTA (TBE) buffer and separated for 90 min at 100 V.

2.4. Determination of antibiotic resistance pattern of confirmed isolates

Antibiotic resistance was evaluated using an antibiogram assay, implementing 13 common antibiotics, and spanning 8 categories (Table 3). This assay was performed as has been describe before, with some modifications (Andrews, 2001). Briefly, several plates of Mullen-Hinton (MH) agar (Difco-BD, MD, USA), were independently prepared by combining a fixed volume of the molten agar with a specific concentration for a given individual antibiotic. Three concentrations were assessed for each antibiotic based on the Minimum Inhibitory concentration (MIC) breakpoints established by the Clinical & Laboratory Standards Institute (CLSI) guidelines manual (CLSI, 2023), which also served to provide the concentrations required to test for whether the isolates were susceptible, intermediate, or resistant to a given antibiotic. After solidifying, inoculation of the

TABLE 2 Primers used for molecular confirmation and serotyping of SE.

Primer name	Primer sequence (5′-3′)		Product size (bp)	References
aceK+	F:	CCGCGCTGGTTGAGTGG	240	O'Regan et al., 2008
	R:	GCGGGGCGAATTTGTCTTTA		
SalOriC+	F:	GCGGTGGATTCTACTCAAC	461	Woods et al., 2008
	R:	AGAAGCGGAACTGAAAGGC		
STM-1*	F:	AACCGCTGCTTAATCCTGATGG	187	Kim et al., 2006
	R:	TGGCCCTGAGCCAGCTTTT		
STM-2*	F:	TCAAAATTACCGGGCGCA	171	
	R:	TTTTAAGACTACATACGCGCATGAA		
STM-3*	F:	TCCAGTATGAAACAGGCAACGTGT	137	
	R:	GCGACGCATTGTTCGATTGAT		
STM-4*	F:	TGGCGGCAGAAGCGATG	114	
	R:	CTTCATTCAGCAACTGACGCTGAG		
STM-5*	F:	TGGTCACCGCGCGTGAT	93	
	R:	CGAACGCCAGGTTCATTTGT		

+ Species-specific primers for confirmation of SE.

* Serotype-specific primers for identifying major SE serovars in the USA.

TABLE 3 Antibiotic used for antibiogram assay with corresponding breakpoints used to test tolerance of isolates.

Antibiotic category	Antibiotic	Breakpoint concentrations (μg/mL)*		
		Susceptible	Intermediate	Resistant
Penicillins	Ampicillin	8	16	32
	Amoxicillin	8	16	32
Macrolides	Azithromycin	16	24	32
Cephalosporins	Cephradine	4	8	16
	Ceftriaxone	1	2	4
Phenolics	Chloramphenicol	8	16	32
Quinolones	Ciprofloxacin	0.06	0.12	1
Aminoglycoside	Gentamycin	4	8	16
	Kanamycin	16	32	64
	Streptomycin	16	24	32
Tetracyclines	Tetracycline	4	8	16
	Oxytetracycline	4	8	16
Folate pathway inhibitors	Trimethoprim-sulfamethoxazole	2–38	3–57	4–76

* Antibiotic breakpoints were selected based on the standards established by the CLSI manual.

MH agar antibiogram plates was done with bacterial colonies that were previously sub-cultured and incubated overnight in LB broth without antibiotics at 37°C. After these isolates grew overnight, the bacterial suspensions were adjusted to an OD_{600} of 0.1, which was later used to inoculation the MH antibiotic agar plates with 2 μL for each isolate into their respective quadrants. After inoculation, MH antibiotic agar plates were also incubated at 37°C overnight for later recording growth pattern of each isolate in the respective MH antibiotic agar plate and compared to the standard breakpoints established by the CLSI guidelines manual for Enterobacterales, which includes standards for bacteria in the *Salmonella* genus.

Further analysis to determine antibiotic co-resistance of isolates was performed by calculating the frequency of isolates that were resistant to two antibiotics. Performing this calculation for every possible antibiotic pair allowed for the determination of co-resistance frequency. These values were represented in a chord plot, using the individual antibiotics as nodes, the existence of a co-resistant isolate forming the edge between nodes, and the weight of these edges being determined by the frequency of isolates sharing the same co-resistance pattern. The data was visualized using the Holoviews package for Python.[1]

2.5. Statistical analysis

Data analysis was performed using the Chi-square statistical analysis to determine significant association between the number of samples positive for SE and the multiple sample categories that were collected for the study (Singhal and Rana, 2015; Barceló, 2018). This test was also later used to determine if there was a significant association regarding the identification of specific SE serotypes from confirmed samples, as well as to analyze their antibiotic resistance pattern. Additional calculations for standard residual values were performed to determine the categories that contributed to driving significance.

3. Results

3.1. Prevalence of *Salmonella enterica* (SE) across collection sites and respective categories

The ecological prevalence of SE within environmental elements and products from the farms that were sampled pre-harvest, as well as post-harvest was assessed through selective and differential culture methods but was later molecularly confirmed (Figure 1). A total of 2237 presumptive SE colonies were collected from the culture plates, spanning 1004 of the samples, as multiple colonies were collected from the plate. After molecular confirmation, it was revealed that 500 of these were confirmed as SE, while at the pre-harvest level, out of 3038 samples a total of 232 samples were found to be positive for SE after molecular confirmation, resulting in a total prevalence of 7.80% (Figure 1A), which was later analyzed by preparing a contingency table that allowed for the use of a Chi-square test for the full data set, showing these results to be significant ($p < 0.05$) and not due to chance within the environmental samples. When specifically analyzing the ecological distribution of SE among the environmental samples collected from the pre-harvest sites, soil was found to be the greatest contributors to the total positivity rate (2.17%), feces (1.42%) and grass (1.28%), which were confirmed as being the major categories driving significance after calculating the standard residual value and finding these to have the largest residuals. Though produce had a numerically similar prevalence of SE compared to other categories (1.48%), the resulting standard residual did not show this category to be a statistically significant contributor to overall prevalence. Further analysis of SE positivity within each of the specific sample categories collected for this study (Figure 1B) elucidated more information

1 https://holoviews.org/

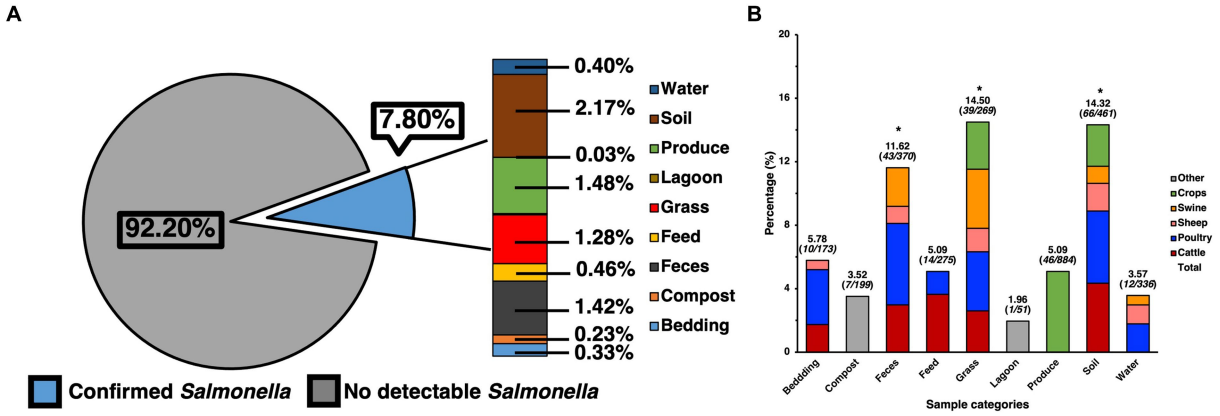

FIGURE 1
Prevalence of SE isolated and confirmed from various samples taken from various farm elements of pre-harvest farm environments and their distribution. **(A)** Prevalence of SE by category and their contribution to total prevalence of pre-harvest samples. **(B)** Ecological distribution of SE within categories based on positivity of SE for the specific category and sample origin. Chi-square analysis was used, along with standard residual analysis and statistical significance ($p < 0.05$) has been denoted by a star a (*).

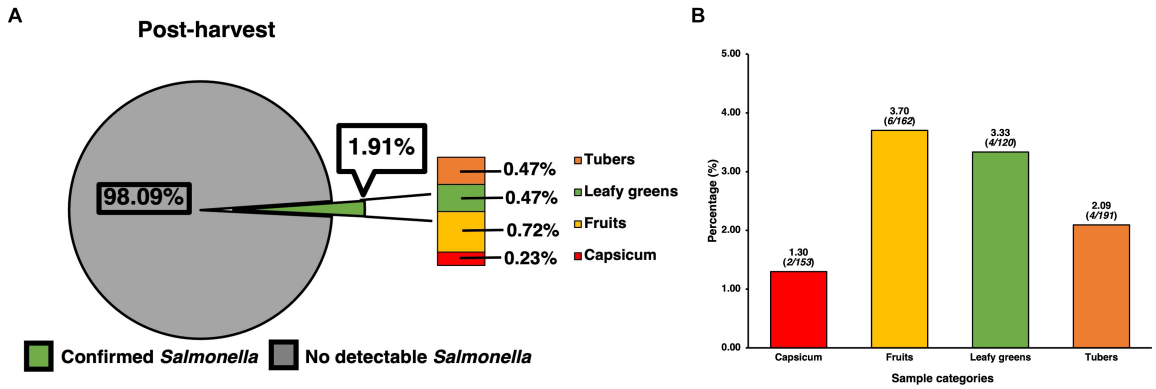

FIGURE 2
Prevalence of SE isolated and confirmed from various post-harvest produce samples and their distribution. **(A)** Prevalence of SE by produce category and their contribution to total prevalence of post-harvest samples. **(B)** Distribution of SE within common produce categories based on the positivity of SE for the specific category. Chi-square analysis was used, along with standard residual analysis and statistical significance ($p < 0.05$) has been denoted by a star a (*).

regarding SE distribution within soil (14.32%, 66/461), feces (11.62%, 43/370), grass (14.50%, 39/269), and produce (5.15%, 45/874), feed (5.09%, 14/275), water (3.57%, 12/336), bedding (5.78%, 10/173), compost (3.52%, 7/199), and lagoon water (1.96%, 1/51). Further analyses were performed to determine the major animal contributors to the categories with the most significant prevalence. These revealed cattle, poultry, and swine to be the most significant ($p < 0.05$) contributors to SE positivity in feces and grass, while cattle and poultry were the most significant contributors in soil.

Prevalence of SE for samples collected at the post-harvest level was found to contain 16 confirmed positives for SE out of 836 samples, resulting in a total prevalence of 1.91% (Figure 2A), though analysis using the chi-square test revealed these to be only numerical and not statistically significant. However, when compared to the pre-harvest produce category alone, post-harvest produce showed a statistically significantly ($p < 0.05$) lower prevalence than pre-harvest (5.09%). In terms of the distribution of SE across sample types, since all post-harvest samples were produce/vegetable, further itemization was done based on the most used classifications for the different kinds of produce samples that were collected. Though many kinds of fresh produce were collected, processed, and assessed for presence of SE, the ones found to be positive were those within the larger categories of fruit (0.72%,), tubers (0.47%), leafy greens (0.47%) and capsicum (0.23%), with standard residual analysis showing fruits and leafy greens having stronger associations. The prevalence of SE within each individual category (Figure 2B) were fruits (3.70%, 6/162), tubers (2.09%, 4/191), leafy greens (3.33%, 4/120), and capsicum (1.30%, 2/153).

3.2. Major SE serotypes identified among confirmed isolates

Serotyping for the top 30 major SE serotypes found in the USA was done for every isolate previously confirmed molecularly by using species-specific primers. Serotype identification was done based on

select amplification, subsequent separation and visualization of primers labeled STM 1–5 (Figure 3). A total of 500 isolates were serotyped, with 477 of these being pre-harvest and 23 being post-harvest, while some were bacteria initially isolated form the same sample. Of the pre-harvest samples, 10 serotypes were identified, namely from most to least numerically prevalent, Typhimurium (11.32%, 54/477), Montevideo (1.05%, 5/477), Derby (0.84%, 4/477), Enteritidis (0.84%, 4/477), Newport (0.84%, 4/477), Munchen (0.63%, 3/477), Hadar (0.42%, 2/477), Heidelberg (0.21%, 1/477), Java (0.21%, 1/477) and Poona (0.21%, 1/477), with 83.44% (398/477) remaining unserotyped, that is the primer combination that were amplified had no match to the serotypes being tested for. Within the post-harvest category, the serotype that was detected was Montevideo (4.35%, 1/23), while the remaining samples remained unserotyped (95.65%, 22/23).

3.3. Antibiotic resistance patter of isolates against major antibiotics

Resistance to specific antibiotics was assessed through an antibiogram assay, in which three concentrations of 13 antibiotics spanning 8 categories (Table 3) where evaluated for their capability to inhibit the growth of the confirmed farm isolates (Figure 4). Concentrations used for each antibiotic in the antibiogram assay were determined using the guidelines from the CLSI manual. Using multiple concentrations allowed for determining the level of tolerance for each of the isolates to a specific antibiotic, leading to categorizing isolates as either being susceptible, intermediately resistant, or resistant to the antibiotics tested, based on the concentration that exhibited growth after incubating for 24 h. The antibiotics to which most isolates were susceptible based on their respective breakpoints were to aminoglycosides like gentamycin (78.93%, 281/356) and kanamycin (76.40%, 272/356), however streptomycin was significantly less effective (54.78%, 195/356). Antibiotics that had a similar percentage of susceptible isolates were the tetracyclines like tetracycline (65.45%, 233/356) and oxytetracycline (66.29%, 236/356), as well as the folate pathway inhibitor mix of trimethoprim-sulfamethoxazole (74.72%, 266/356), with the remaining percentage of isolates being mostly resistant. Slightly more isolates were resistant to the phenolic and quinolone antibiotics tested, namely, chloramphenicol and ciprofloxacin, which still had a majority susceptible isolates (62.08%, 221/356 and 60.11%, 214/356, respectively). Cephalosporines showed to be less effective than other antibiotics, as shown in the samples susceptible to ceftriaxone being only slightly higher than half (55.34%, 197/356), while on the other hand the majority of isolates were resistant to cephradine (82.58%, 303/356). The macrolide, azithromycin had slightly more than half of isolates being susceptible (56.74%, 202/356). As a category, penicillin were the antibiotic group with the most rate of resistance, with amoxicillin and ampicillin having the greatest number of resistant isolates (84.55%, 301/356 and 82.87%, 295/356, respectively). Statistical analysis of the growth pattern exhibited in the antibiogram that there was a statistically significant higher frequency of susceptible isolates, than intermediate or resistant ones, however gentamycin and kanamycin were found to be the main contributors to susceptibility.

3.4. Chord analysis for determining co-occurrence of antibiotic resistance among isolates

To further elucidate the incidence of co-resistance to specific antibiotic pairs within the SE isolates, the number of isolates found to be resistant to the same pair of antibiotics was recorded for every possible antibiotic pair (Supplementary Table 1). These values were used to generate a chord plot for further visualization of the incidence and relationship between resistance to all antibiotic pairs (Figure 5). According to the calculations for incidences of co-resistant isolates, the pairs with the highest amount of co-resistant isolates were amoxicillin-cephradine (281), followed by ampicillin-amoxicillin (278) and ampicillin-cephradine (268), showing penicillin and cephalosporines to have the most cases of co-resistance by antibiotic type. When comparing penicillin to other groups, there were less co-resistant isolates, but notable values were seen for ampicillin-streptomycin (132), amoxicillin-streptomycin (122), amoxicillin-azithromycin (112) and ampicillin-tetracycline (103). Other notable pairs were cephradine-streptomycin (127) and cephradine-azithromycin (112). On the other hand, the best pairings were those with gentamycin, showing the lowest instance of co-resistance,

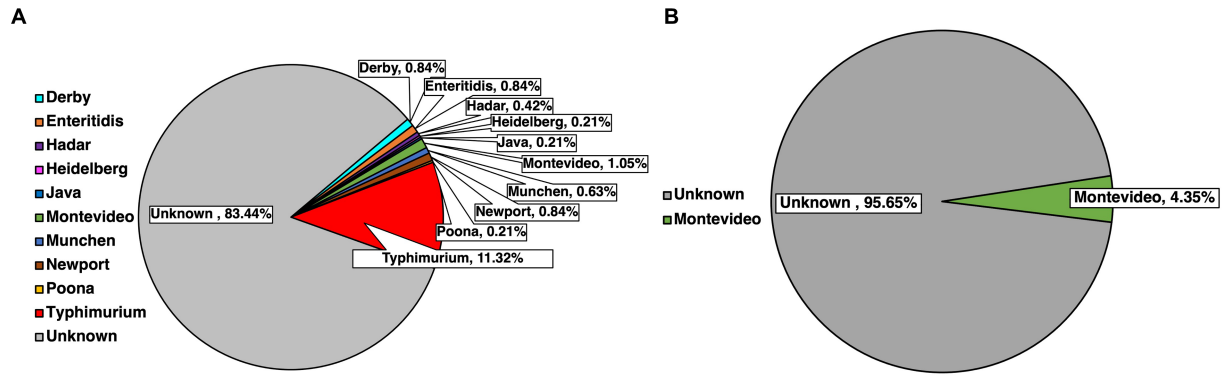

FIGURE 3
Identification of common SE serotypes within confirmed isolates from pre-harvest **(A)** and post-harvest **(B)** samples.

beginning with gentamycin-chloramphenicol (3), followed by gentamycin-trimethoprim-sulfamethoxazole (5), and even including pairings with panicillins like in the case of gentamycin-amoxicillin (8) and gentamycin-ampicillin (9). Other antibiotic pairs that had lower incidences of co-resistance were kanamycin-gentamycin (10), kanamycin-chloramphenicol (10), gentamycin-ceftriaxone (10), gentamycin-azithromycin (10), and gentamycin-oxytetracycline (10).

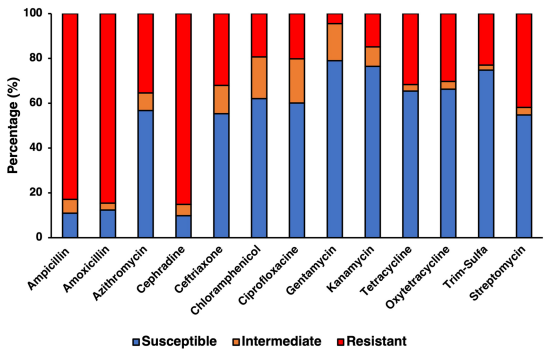

FIGURE 4
Antibiotic resistance profile for confirmed SE isolates determined from antibiogram assay testing for 13 antibiotics using concentrations previously determined to be the breakpoints for susceptible, intermediate, and resistant for *Salmonella*.

4. Discussion

Surveillance of SE in pasture farms specifically backyard and integrated farms withing the Mid-Atlantic region of the USA is merited given the rapid growth of this market in this region of the country (NASS, 2022). As a ubiquitous foodborne pathogen, SE continues to be a burden on the USA healthcare system, as well as an economic burden for food industries and consumers, which could hinder the profitability and viability of smaller producers using alternative farming systems (Ollinger and Houser, 2020). Previous studies have evaluated the prevalence of SE in organic meats, particularly poultry, generated from farms within the MD-DC area (Peng et al., 2016). This study assessed various environmental elements within farms that could be potential sources of SE and serve as transmission pathways, as well as produce samples collected from farms (pre-harvest) and on-farm markets or farmers markets (post-harvest), while also identifying various serotypes of this pathogen in multiple isolates that were previously confirmed to be SE. Compared to the findings of previous studies, there was a lower overall prevalence of SE detected in in the current study. Though environmental factors

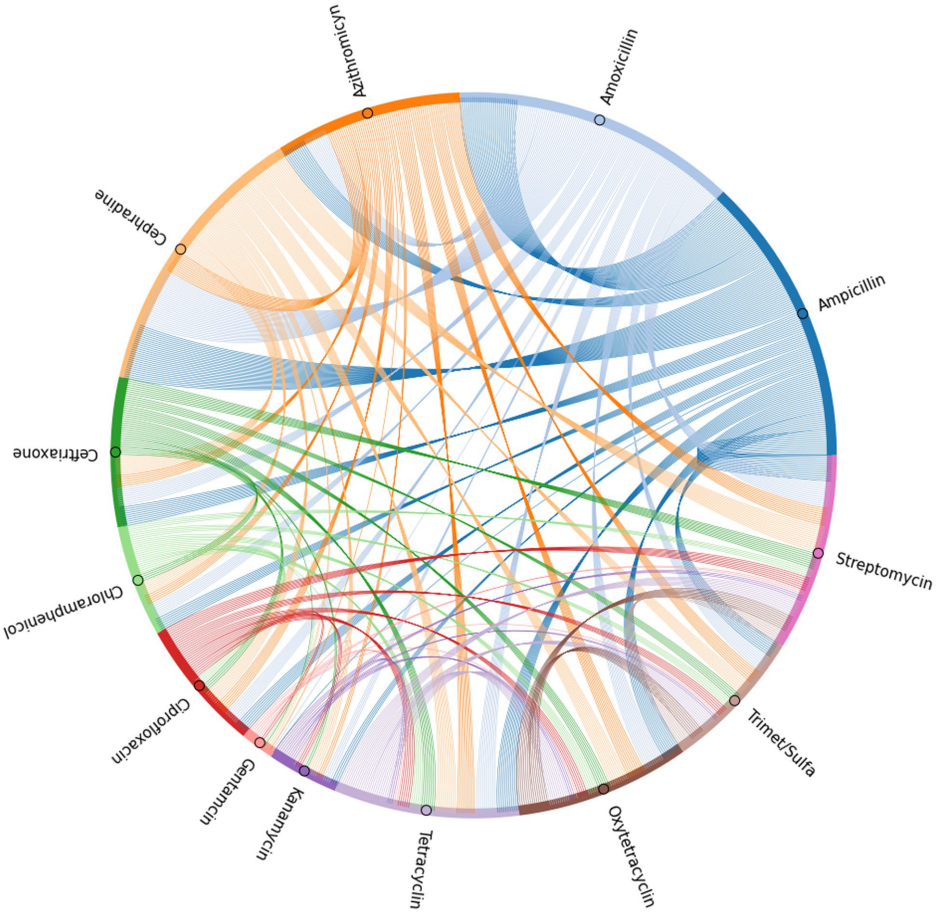

FIGURE 5
Chord plot generated based on the incidence of co-resistance to antibiotic pairs among the isolates tested in the antibiogram.

play an important role SE contamination, meat products are at a particularly higher risk of contamination, post-harvest, due to there being at a higher risk of cross-contamination during processing, as there is potential contact with contaminated equipment and other animal body parts (Golden et al., 2021).

In the current study, notable sources of SE were, soil and grass, especially form fields used for grazing and pasturing cattle and poultry. These results are compatible with previous meta-analyses that have shown soil to be a major reservoir for many common foodborne pathogens, especially SE, as it has been found to survive in this environment for extended periods of time (Wang et al., 2023). Once in soil, SE can spread to other fomites, such as grass, which was observed in the current study, but it is important to note that it could also spread to nearby water sources and crop-fields in the form of runoff. Another major source of SE was fecal matter form various animals, primarily from poultry, cattle and swine, which could be an explanation for the prevalence of the pathogen in soil, as it gets seeded with the bacteria as animals graze, while the soil conversely serves as a source of re-inoculation, as well as cross-contamination for other animals that are rotated to graze on the same land (McAllister and Topp, 2012; Joseph et al., 2021). Many integrate/pasture farms engage in animal rotation, increasing the chances of cross-contamination between the animals that graze on the same plots of land even if the animals are not there simultaneously, which could serve as an explanation as to why chicken and cattle samples were highly positive, since these were two animal groups that were often rotated between the same pasture sites across the farm. Various waste management strategies like composting could also be potential sources of contamination, as studies have shown that when done incorrectly pathogenic bacteria can survive the composing process, making this a potential source of contamination, particularly for plant products and to surrounding soil (Gong et al., 2005; Brinton et al., 2009).

Identifying these sources of SE within alternative and fast-growing farming systems is an important step for generating safer products, but also reducing the negative impact that these farms could pose to the surrounding environment, which often includes other farms, important natural resources, as well as commercial and residential areas (Hudson and Soar, 2023; Wu et al., 2023). On the other hand, when comparing pre-harvest with post-harvest produce, there was a statistically significantly higher prevalence in the pre-harvest samples. This could be attributed to the exposure that these have to the surrounding environment, as well as the lack of processing and screening that these products go through before being sold. However, the prevalence of SE in the post-harvest samples could still be attributed to specific challenges associated with produce processing, in which contamination can occur during the transportation, management, and even washing of the product with reused water (Rahman et al., 2022).

SE is known to have over 2500 serovars, many of which can be attributed to outbreaks within the USA (Andino and Hanning, 2015). Serotyping of the confirmed isolates from this study revealed SE serotype Typhimurium to be the most prevalent out of the isolates that wee serotypeable. This serotype was also found only in pre-harvest samples. *S. typhimurium* is known to be a widely spread serotype, spanning multiple environments and sources, in addition to being associated to multiple vegetable and animal products, including poultry, cattle and swine, while also being capable of causing disease (Ferrari et al., 2019). The next most prevalent serotype was Montevideo, which has been strongly correlated in the past with beef products in North America, as well as with some produce products (Andino and Hanning, 2015). Other serovars that were identified were SE serotypes Derby and Enteritidis, which are also categorized among some of the most common serotypes in the USA. Though previous researchers have been able to attribute the serotype Enteritidis with more outbreaks, the food sources with which it is associated with are narrower, while serotypes like *S. typhimurium* span multiple sources (Jackson et al., 2013). The current study did not find statistically significant association of a given serotype to a specific sample category, however it is important to note that, though Typhimurium was found in samples associated with poultry, cattle, swine, soil and vegetables, other serotypes like Enteritidis, Newport and Derby were mostly found in poultry, while Hadar was only found in cattle, and Montevideo in both cattle and vegetables. Another aspect of the current study was the fact that the majority of isolates for both pre- and post-harvest categories remained unserotyped as they could not be categorized within the 30 most common serotypes found in the USA given their gene expression of the multiplex technique that was used. This lack of identification for the current isolates could account for the lack of statistical significance associated with the isolates that were serotyped. Though multiplex PCR techniques have been used in the past with high accuracy and cover identification many common serovars (Shi et al., 2015), there are still limitation regarding mutations in the bacteria that might affect primer specificity, which is also a contributing factor to many outbreaks not being associated with specific serotypes (Chanamé Pinedo et al., 2022). Another possibility is that the unserotyped isolates belong to serovars other than the main 30 clinically relevant ones that the multiplex PCR assay was designed to detect, which could include other less studied subspecies of SE that might have a lower pathogenicity to humans or are more commonly found in animals as pathogens. Previous research has reported some of these subspecies to also be highly prevalent in farm environments and in some animals, both wild and domestic, and account for a significant percentage of isolates found in some farms (Lamas et al., 2018). Further studies involving the use of whole genome sequencing and *in silico* methods to identify specific genes in these isolates that can reveal their serotype or identify mutations in the genes that were tested that could have led to the primers not being able to properly express (Diep et al., 2019).

Antibiotic resistance of SE isolates was tested for 13 clinically relevant antibiotics, however it is important to note that resistance to some antibiotics can also translate to resistance to others, depending on the mechanism conferring the resistance, as well as the genes involved (Nikaido, 2009). In addition to the intrinsic antibiotic resistance mechanisms that bacteria carry, other antibiotic resistance genes can be transferred horizontally from resistant bacteria to non-resistant ones, including from non-pathogenic to pathogenic bacteria (Dionisio et al., 2023). This dynamic is especially prevalent in the soil, where there is a complex microflora comprised of bacteria, archaea, fungi, and viruses, as well as conglomerate of genes known as the resistome, all of which contribute to bacteria being able to integrate additional antibiotic resistance genes and become increasingly resistant (Walsh, 2013; Von Wintersdorff et al., 2016). In addition to this, the environment also serves as a pressure that helps select for increasingly resistant microbes and in the case of an area that has trace amounts of commonly used antibiotics, these will also serve as a selective force.

The presence of trace amounts of antibiotic in soil can be linked to the overuse of these compounds in healthcare and animal production, with animal farming being of note because of their use as sub-therapeutics, therapeutics, and growth promoters (Chokshi et al., 2019). This created a cycle where trace amounts of antibiotics reached multiple sources in the environment, as well as to other animals, animal products and human consumers (Woolhouse and Ward, 2013). Though many regulatory measures have been put into place for reducing antibiotic resistance in the environment, tackling this issue remains a challenge (Mann et al., 2021). Reducing use of antibiotics has shown to reduce the incidence of antibiotic resistant bacteria (Tang et al., 2017), and in the case of organic farms, they do not use antibiotics in their production practices. Though previous research would suggest that these factors would make organic farms free of antibiotic resistant bacteria, recent findings have shown that there was no significant difference in the presence of antibiotic resistance genes between conventional and long-standing organic farms, though some bacterial isolates were more resistant to a specific type of antibiotic (Sancheza et al., 2016; Armalytė et al., 2019). These findings suggest that regardless of the time that a farm has been engaging in organic practices, it could still be at risk, as it could have trace amounts of antibiotics and other synthetic antimicrobials in their soil, while also having a resistome, and pre-existing bacteria that could potentially harbor antibiotic resistance. In the current study, a significant number of SE isolates showed resistance to each antibiotic, but further genomic analysis would be required to determine the origin of this antibiotic resistance and the genes involved. However, with the exception of ampicillin, amoxicillin and cephradine, all other antibiotics showed that at least more than half of the isolates were susceptible to them.

When analyzing the antibiotic resistance pattern of the isolates form the current study through testing the MIC at various breakpoints for each antibiotic, there were specific groups of antibiotics that were more effective than others. Of all the antibiotic categories tested, penicillins, namely ampicillin and amoxicillin, as well as the cephalosporine, cephradine, were the least effective antibiotics, as most of the isolates were resistant to them. These findings are in accordance with previous groups that have shown a high prevalence of resistance to penicillins in various SE serotypes, but in addition to that, the chord analysis in the current study also showed a high level of co-resistance between ampicillin, amoxicillin and cephradine, which previous researchers have found to be correlated, as they share similar mechanisms of action through the β-lactam site (Nair et al., 2018). Though previous research has identified genes associated with resistance to aminoglycosides like gentamycin, kanamycin and streptomycin, as well as folate pathway inhibitors like the trimethoprim-sulfamethoxazole, these antibiotics are still often prescribed as second line antibiotics in clinical cases (Frye and Jackson, 2013), and the results from the antibiogram of the current study showed gentamycin, kanamycin and a combination of trimethoprim-sulfamethoxazole to be the most effective against most isolates, while streptomycin was not as effective. In terms of co-resistance, the antibiotic pairs with the lowest occurrence were gentamycin-chloramphenicol, gentamycin-trimethoprim-sulfamethoxazole, gentamycin-ciprofloxacin, and even gentamycin-ampicillin and -amoxicillin. This could be attributed to the individual effect of gentamycin, relative to the efficacy of the other antibiotics, as these were not tested simultaneously, as to be able to properly determine any synergistic activity. However, in the past, aminoglycosides have been proposed as potential antibiotics that could be paired with others to achieve a synergistic effect (Umemura et al., 2022). In addition to synergistic mechanisms of action, using antibiotics that require the bacteria to employ multiple mechanisms of resistance could be another approach to antibiotic selection for clinical uses (Kakoullis et al., 2021). Another two groups of antibiotics that are important to mention from this study are tetracycline and ciprofloxacin, as when these were compared to the national average reported by the National Antimicrobial Resistance Monitoring System (NARMS) for the percentage of resistant SE, they were more susceptible bacteria than in NARMS reports, which is important since these are often times used as indicators for multidrug resistance and cases of co-resistance in SE and other coliforms (Hopkins et al., 2005; Food and Drug Administration (FDA), 2022). Though it remains unclear whether antibiotic resistant SE translates to more or less virulent bacteria, recent research has found correlations between specific genes related to virulence and multi-drug resistance, warranting further study into the current effective antibiotic treatments that are available to deliver more accurate and safer treatments (Higgins et al., 2020).

5. Conclusion

Surveillance and risk assessment remain crucial tools for preventing outbreaks and producing safer food, especially in small and medium sized producers within the organic/pasture farming systems. SE remains prevalent in the farm environment, especially within the soil, which serves as a reservoir for the pathogen. The SE serovar Typhimurium remains of the most prevalent serotype, which coincides with the previous knowledge that Typhimurium us ubiquitous across multiple environments and is attributable to multiple animals. This will provide valuable information for tracing and containing outbreaks. On the other hand, the current antibiotic pattern exhibited by the isolates of this study show that, despite the absence of antibiotic use in these farming systems, there is still the presence of antibiotic resistant bacteria. However, some antibiotics were more effective than others, which can be used in the future to further study the mechanisms behind antibiotic resistance in farming environments, while also inform future treatment protocols for clinical cases of SE infections.

Data availability statement

The original contributions presented in the study are included in the article/Supplementary material, further inquiries can be directed to the corresponding author.

Author contributions

DB: conceptualization, supervision, project administration, and funding acquisition. ZA-M and DB: methodology and writing—review and editing. ZA-M and DJ: formal analysis. ZA-M, ZT, AA, C-WT, AP, GSu, and MW: sample acquisition, preparation, and

processing. ZA-M, DJ, AP, GSu, KH, MW, SK, CC, SM, GSe, and AS: execution of experiments. ZA-M: writing—original draft preparation. All authors have read and agreed to the published version of the manuscript.

Funding

This research was funded by the United States Department of Agriculture (USDA), National Institute of Food and Agriculture (NIFA) (grant no. 20185110628809).

Acknowledgments

The authors would like to acknowledge the technical support of Dr. Maria Eduarda Montezzo Coelho in writing the Python scripts for generating the data required to create and designing the chord plot used for determining co-resistance to antibiotics among isolates. We also thank the farmers who have given us the opportunity to collect the samples from their farms.

Conflict of interest

The authors declare that the research was conducted in the absence of any commercial or financial relationships that could be construed as a potential conflict of interest.

Publisher's note

All claims expressed in this article are solely those of the authors and do not necessarily represent those of their affiliated organizations, or those of the publisher, the editors and the reviewers. Any product that may be evaluated in this article, or claim that may be made by its manufacturer, is not guaranteed or endorsed by the publisher.

Supplementary material

The Supplementary material for this article can be found online at: https://www.frontiersin.org/articles/10.3389/fmicb.2023.1240458/full#supplementary-material

References

Adl, S., Iron, D., and Kolokolnikov, T. (2011). A threshold area ratio of organic to conventional agriculture causes recurrent pathogen outbreaks in organic agriculture. *Sci. Total Environ.* 409, 2192–2197. doi: 10.1016/j.scitotenv.2011.02.026

Andino, A., and Hanning, I. (2015). *Salmonella enterica*: survival, colonization, and virulence differences among serovars. *Sci. World J.* 2015, 1–16. doi: 10.1155/2015/520179

Andrews, J. M. (2001). Determination of minimum inhibitory concentrations. *J. Antimicrob. Chemother.* 48, 5–16. doi: 10.1093/jac/48.suppl_1.5

Armalytė, J., Skerniškytė, J., Bakienė, E., Krasauskas, R., Šiugždinienė, R., Kareivienė, V., et al. (2019). Microbial diversity and antimicrobial resistance profile in microbiota from soils of conventional and organic farming systems. *Front. Microbiol.* 10:892. doi: 10.3389/fmicb.2019.00892

Barceló, J. A. (2018). "Chi-Square analysis" in *The encyclopedia of archaeological sciences*. ed. S. L. Lopez (Hoboken: John Wiley & Sons, Inc)

Bondo, K. J., Pearl, D. L., Janecko, N., Boerlin, P., Reid-Smith, R. J., Parmley, J., et al. (2016). Impact of season, demographic and environmental factors on salmonella occurrence in raccoons (*procyon lotor*) from swine farms and conservation areas in southern Ontario. *PLoS One* 11:e0161497. doi: 10.1371/journal.pone.0161497

Brinton, W. F., Storms, P., and Blewett, T. C. (2009). Occurrence and levels of fecal indicators and pathogenic bacteria in market-ready recycled organic matter composts. *J. Food Prot.* 72, 332–339. doi: 10.4315/0362-028X-72.2.332

Carlson, A., Greene, C., Raszap Skorbiansky, S., Hitaj, C., Ha, K., Cavigelli, M., et al. (2023). *U.S. organic production, markets, consumers, and policy, 2000-21, ERR-315*. Washington, DC: United States Department of Agriculture.

Centers for Disease Control and Prevention (CDC) (2013). *An atlas of salmonella in the United States, 1968–2011: laboratory-based enteric disease surveillance*. Atlanta, Georgia: US Department of Health and Human Services, CDC.

Centers for Disease Control and Prevention (CDC) (2018). *National enteric disease surveillance: Salmonella annual summary, 2016*. Atlanta, Georgia: US Department of Health and Human Services, CDC.

Centers for Disease Control and Prevention (CDC) (2021). *National outbreak reporting system dashboard*. Atlanta, Georgia: U.S. Department of Health and Human Services, CDC.

Chanamé Pinedo, L., Mughini-Gras, L., Franz, E., Hald, T., and Pires, S. M. (2022). Sources and trends of human salmonellosis in Europe, 2015–2019: an analysis of outbreak data. *Int. J. Food Microbiol.* 379:109850. doi: 10.1016/j.ijfoodmicro.2022.109850

Chokshi, A., Sifri, Z., Cennimo, D., and Horng, H. (2019). Global contributors to antibiotic resistance. *J Glob Infect Dis.* 11, 36–42. doi: 10.4103/jgid.jgid_110_18

CLSI (2023). *Performance standards for antimicrobial susceptibility testing. 33rd*. Wayne, PA: CLSI Supplement M100 Clinical & laboratory Standards.

Diep, B., Barretto, C., Portmann, A. C., Fournier, C., Karczmarek, A., Voets, G., et al. (2019). Salmonella serotyping; comparison of the traditional method to a microarray-based method and an in silico platform using whole genome sequencing data. *Front. Microbiol.* 10:2554. doi: 10.3389/fmicb.2019.02554

Dimitri, C., and Greene, C. (2002). *Recent growth patterns in the U.S. organic foods market*. Washington, DC: US Department of Agriculture Economic Research Service.

Dionisio, F., Domingues, C. P. F., Rebelo, J. S., Monteiro, F., and Nogueira, T. (2023). The impact of non-pathogenic bacteria on the spread of virulence and resistance genes. *Int. J. Mol. Sci.* 24:1967. doi: 10.3390/ijms24031967

Ferrari, R. G., Rosario, D. K. A., Cunha-Neto, A., Mano, S. B., Figueiredo, E. E. S., and Conte-Juniora, C. A. (2019). Worldwide epidemiology of salmonella serovars in animal-based foods: a meta-analysis. *Appl. Environ. Microbiol.* 85:e00591-19. doi: 10.1128/AEM.00591-19

Food and Drug Administration (FDA) (2022). *NARMS Now. NARMS Now*. Rockville, MD: U.S. Department of Health and Human Services.

Frye, J. G., and Jackson, C. R. (2013). Genetic mechanisms of antimicrobial resistance identified in *Salmonella enterica*, *Escherichia coli*, and *Enteroccocus* spp. isolated from U.S. food animals. *Front. Microbiol.* 4:135. doi: 10.3389/fmicb.2013.00135

Golden, C. E., Rothrock, M. J., and Mishra, A. (2021). Mapping foodborne pathogen contamination throughout the conventional and alternative poultry supply chains. *Poult. Sci.* 100:101157. doi: 10.1016/j.psj.2021.101157

Gong, C. M., Inoue, K., Inanaga, S., and Someya, T. (2005). Survival of pathogenic bacteria in compost with special reference to *Escherichia coli*. *J. Environ. Sci.* 17, 770–774.

Harvey, R. R., Zakhour, C. M., and Gould, L. H. (2016). Foodborne disease outbreaks associated with organic foods in the United States. *J. Food Prot.* 79, 1953–1958. doi: 10.4315/0362-028X.JFP-16-204

Herrero, M., and Thornton, P. K. (2001). Integrated crop livestock simulation models for scenario analysis and impact assessment – Google Scholar. *Agric. Syst.* 70, 581–602. doi: 10.1016/S0308-521X(01)00060-9

Higgins, D., Mukherjee, N., Pal, C., Sulaiman, I. M., Jiang, Y., Hanna, S., et al. (2020). Association of virulence and antibiotic resistance in salmonella—statistical and computational insights into a selected set of clinical isolates. *Microorganisms* 8:1465. doi: 10.3390/microorganisms8101465

Hopkins, K. L., Davies, R. H., and Threlfall, E. J. (2005). Mechanisms of quinolone resistance in *Escherichia coli* and salmonella: recent developments. *Int. J. Antimicrob. Agents* 25, 358–373. doi: 10.1016/j.ijantimicag.2005.02.006

Hudson, C., and Soar, P. J. (2023). Soil erosion risk for farming futures: novel model application and validation to an agricultural landscape in southern England. *Environ. Res.* 219:115050. doi: 10.1016/j.envres.2022.115050

Interagency Food Safety Analytics Collaboration (2022). *Interagency food safety analytics collaboration. Foodborne illness source attribution estimates for 2020 for Salmonella, Escherichia coli O157, and Listeria monocytogenes using multi-year outbreak surveillance data, United States*. Washington, DC: Interagency Food Safety Analytics Collaboration (IFSAC). 157.

Iwu, C. D., and Okoh, A. I. (2019). Preharvest transmission routes of fresh produce associated bacterial pathogens with outbreak potentials: a review. *Int. J. Environ. Res. Public Health* 16:4407. doi: 10.3390/ijerph16224407

Jackson, B. R., Griffin, P. M., Cole, D., Walsh, K. A., and Chai, S. J. (2013). Outbreak-associated *Salmonella enterica* serotypes and food commodities, United States, 1998-2008. *Emerg. Infect. Dis.* 19, 1239–1244. doi: 10.3201/eid1908.121511

Jajere, S. M. (2019). A review of *Salmonella enterica* with particular focus on the pathogenicity and virulence factors, host specificity and adaptation and antimicrobial resistance including multidrug resistance. *Vet World.* 12, 504–521. doi: 10.14202/vetworld.2019.504-521

Joseph, N., Lucas, J., Viswanath, N., Findlay, R., Sprinkle, J., Strickland, M. S., et al. (2021). Investigation of relationships between fecal contamination, cattle grazing, human recreation, and microbial source tracking markers in a mixed-land-use rangeland watershed. *Water Res.* 194:116921. doi: 10.1016/j.watres.2021.116921

Kakoullis, L., Papachristodoulou, E., Chra, P., and Panos, G. (2021). Mechanisms of antibiotic resistance in important gram-positive and gram-negative pathogens and novel antibiotic solutions. *Antibiotics* 10:415. doi: 10.3390/antibiotics10040415

Kim, S., Frye, J. G., Hu, J., Fedorka-Cray, P. J., Gautom, R., and Boyle, D. S. (2006). Multiplex PCR-based method for identification of common clinical serotypes of *Salmonella enterica* subsp. enterica. *J. Clin. Microbiol.* 44, 3608–3615. doi: 10.1128/JCM.00701-06

King, R. P., Hand, M. S., DiGiacomo, G., Clancy, K., Gomez, M. I., Hardesty, S. D., et al. (2010). Comparing the structure, size, and performance of local and mainstream food supply chains. *J. Agric. Food Syst. Commun. Dev.* 1, 187–189. doi: 10.5304/jafscd.2010.012.005

Lamas, A., Miranda, J. M., Regal, P., Vázquez, B., Franco, C. M., and Cepeda, A. (2018). A comprehensive review of non-enterica subspecies of *Salmonella enterica*. *Microbiol. Res.* 206, 60–73. doi: 10.1016/j.micres.2017.09.010

Lemaire, G., Franzluebbers, A., Carvalho, P. C. D. F., and Dedieu, B. (2014). Integrated crop-livestock systems: strategies to achieve synergy between agricultural production and environmental quality. *Agric. Ecosyst. Environ.* 190, 4–8. doi: 10.1016/j.agee.2013.08.009

Lynch, D. H. (2022). Soil health and biodiversity is driven by intensity of organic farming in Canada. *Front Sustain Food Syst* 6:826486. doi: 10.3389/fsufs.2022.826486

Maffei, D. F., Batalha, E. Y., Landgraf, M., Schaffner, D. W., and Franco, B. D. G. M. (2016). Microbiology of organic and conventionally grown fresh produce. *Braz. J. Microbiol.* 47, 99–105. doi: 10.1016/j.bjm.2016.10.006

Mann, A., Nehra, K., Rana, J. S., and Dahiya, T. (2021). Antibiotic resistance in agriculture: perspectives on upcoming strategies to overcome upsurge in resistance. *Curr. Res. Microb Sci.* 2:100030. doi: 10.1016/j.crmicr.2021.100030

Martinez, S., Hand, M., da Pra, M., Pollack, S., Ralston, K., Smith, T., et al. (2010). *Local food systems concepts, impacts, and issues*. USDA-Economic Research Service, Washington, DC, USA.

Maryland State Archives (2023). Maryland manuals on-line. Available at: https://msa.maryland.gov/msa/mdmanual/01glance/html/agri.html#:~:text=In%20Fiscal%20Year%202022%2C%20somegrains%2C%20livestock%2C%20and%20poultry (Accessed May 22, 2023).

McAllister, T. A., and Topp, E. (2012). Role of livestock in microbiological contamination of water: commonly the blame, but not always the source. *Anim. Front.* 2, 17–27. doi: 10.2527/af.2012-0039

Nair, D. V. T., Venkitanarayanan, K., and Johny, A. K. (2018). Antibiotic-resistant salmonella in the food supply and the potential role of antibiotic alternatives for control. *Foods* 7:167. doi: 10.3390/foods7100167

NASS (2022). *Certified organic survey 2021 summary*. Available at: https://www.ers.usda.gov/data-products/chart-gallery/gallery/chart-detail/?chartId=105850#:~:text=Additionally%2C%20the%20number%20of%20certifiedto%2017%2C40920from20about%208%2C978 (Accessed June 13, 2023).

Nikaido, H. (2009). Multidrug resistance in bacteria. *Annu. Rev. Biochem.* 78, 119–146. doi: 10.1146/annurev.biochem.78.082907.145923

Nye, K. J., Fallon, D., Frodsham, D., Gee, B., Graham, C., Howe, S., et al. (2002). An evaluation of the performance of XLD, DCA, MLCB, and ABC agars as direct plating media for the isolation of *Salmonella enterica* from faeces. *J. Clin. Pathol.* 55, 286–288. doi: 10.1136/jcp.55.4.286

O'Regan, E., McCabe, E., Burgess, C., McGuinness, S., Barry, T., Duffy, G., et al. (2008). Development of a real-time multiplex PCR assay for the detection of multiple salmonella serotypes in chicken samples. *BMC Microbiol.* 8:156. doi: 10.1186/1471-2180-8-156

Ollinger, M., and Houser, M. (2020). Ground beef recalls and subsequent food safety performance. *Food Policy* 97:101971. doi: 10.1016/j.foodpol.2020.101971

Park, S., Szonyi, B., Gautam, R., Nightingale, K., Anciso, J., and Ivanek, R. (2012). Risk factors for microbial contamination in fruits and vegetables at the preharvest level: a systematic review. *J. Food Prot.* 75, 2055–2081. doi: 10.4315/0362-028X.JFP-12-160

Peng, M., Salaheen, S., Almario, J. A., Tesfaye, B., Buchanan, R., and Biswas, D. (2016). Prevalence and antibiotic resistance pattern of Salmonella serovars in integrated crop-livestock farms and their products sold in local markets. *Environ. Microbiol.* 18, 1654–1665. doi: 10.1111/1462-2920.13265

Rahman, M., Alam, M. U., Luies, S. K., Kamal, A., Ferdous, S., Lin, A., et al. (2022). Contamination of fresh produce with antibiotic-resistant bacteria and associated risks to human health: a scoping review. *Int. J. Environ. Res. Public Health* 19:360. doi: 10.3390/ijerph19010360

Rukambile, E., Sintchenko, V., Muscatello, G., Kock, R., and Alders, R. (2019). Infection, colonization and shedding of campylobacter and salmonella in animals and their contribution to human disease: a review. *Zoonoses Public Health* 66, 562–578. doi: 10.1111/zph.12611

Salaheen, S., Chowdhury, N., Hanning, I., and Biswas, D. (2015). Zoonotic bacterial pathogens and mixed crop-livestock farming. *Poult. Sci.* 94, 1398–1410. doi: 10.3382/ps/peu055

Sancheza, H. M., Echeverria, C., Thulsiraj, V., Zimmer-Faust, A., Flores, A., Laitz, M., et al. (2016). Antibiotic resistance in airborne bacteria near conventional and organic beef cattle farms in California, USA. *Water Air Soil Pollut.* 227:280. doi: 10.1007/s11270-016-2979-8

Scallan, E., Hoekstra, R. M., Angulo, F. J., Tauxe, R. V., Widdowson, M. A., Roy, S. L., et al. (2011). Foodborne illness acquired in the United States-major pathogens. *Emerg. Infect. Dis.* 17, 7–15. doi: 10.3201/eid1701.P11101

Scharff, R. L. (2020). Food attribution and economic cost estimates for meat- and poultry-related illnesses. *J. Food Prot.* 83, 959–967. doi: 10.4315/JFP-19-548

Shi, C., Singh, P., Ranieri, M. L., Wiedmann, M., and Moreno Switt, A. I. (2015). Molecular methods for serovar determination of Salmonella. *Crit. Rev. Microbiol.* 41, 309–325. doi: 10.3109/1040841X.2013.837862

Singhal, R., and Rana, R. (2015). Chi-square test and its application in hypothesis testing. *J. Pract. Cardiov. Sci.* 1:69. doi: 10.4103/2395-5414.157577

Sosnowski, M., and Osek, J. (2021). Microbiological safety of food of animal origin from organic farms. *J. Vet. Res.* 65, 87–92. doi: 10.2478/jvetres-2021-0015

Tang, K. L., Caffrey, N. P., Nóbrega, D. B., Cork, S. C., Ronksley, P. E., Barkema, H. W., et al. (2017). Restricting the use of antibiotics in food-producing animals and its associations with antibiotic resistance in food-producing animals and human beings: a systematic review and meta-analysis. *Lancet Planet Health* 1, e316–e327. doi: 10.1016/S2542-5196(17)30141-9

Umemura, T., Kato, H., Hagihara, M., Hirai, J., Yamagishi, Y., and Mikamo, H. (2022). Efficacy of combination therapies for the treatment of multi-drug resistant gram-negative bacterial infections based on meta-analyses. *Antibiotics* 11:524. doi: 10.3390/antibiotics11040524

USDA National Organic Program (2010). *NOP handbook: guidance and instructions for accredited certifying agents & certified operations*. Washington, DC: USDA National Organic Program.

USDA-FSIS (2014). *Serotypes profile of salmonella isolates from meat and poultry products January 1998 through December 2014*. Washington, DC: US Department of Agriculture, Food Safety and Inspection Service.

Von Wintersdorff, C. J. H., Penders, J., Van Niekerk, J. M., Mills, N. D., Majumder, S., Van Alphen, L. B., et al. (2016). Dissemination of antimicrobial resistance in microbial ecosystems through horizontal gene transfer. *Front. Microbiol.* 7:173. doi: 10.3389/fmicb.2016.00173

Walsh, F. (2013). Investigating antibiotic resistance in non-clinical environments. *Front. Microbiol.* 4:19. doi: 10.3389/fmicb.2013.00019

Wang, J., Vaddu, S., Bhumanapalli, S., Mishra, A., Applegate, T., Singh, M., et al. (2023). A systematic review and meta-analysis of the sources of Salmonella in poultry production (pre-harvest) and their relative contributions to the microbial risk of poultry meat. *Poult. Sci.* 102:102566. doi: 10.1016/j.psj.2023.102566

Winfield, M. D., and Groisman, E. A. (2003). Role of nonhost environments in the lifestyles of Salmonella and *Escherichia coli*. *Appl. Environ. Microbiol.* 69, 3687–3694. doi: 10.1128/AEM.69.7.3687-3694.2003

Woods, D. F., Reen, F. J., Gilroy, D., Buckley, J., Frye, J. G., and Boyd, E. F. (2008). Rapid multiplex PCR and real-time TaqMan PCR assays for detection of Salmonella enterica and the highly virulent serovars Choleraesuis and Paratyphi C. *J. Clin. Microbiol.* 46, 4018–4022. doi: 10.1128/JCM.01229-08

Woolhouse, M. E. J., and Ward, M. J. (2013). Sources of antimicrobial resistance. *Science* 341, 1460–1461. doi: 10.1126/science.1243444

Wu, Y., Song, S., Chen, X., Shi, Y., Cui, H., Liu, Y., et al. (2023). Source-specific ecological risks and critical source identification of PPCPs in surface water: comparing urban and rural areas. *Sci. Total Environ.* 854:158792. doi: 10.1016/j.scitotenv.2022.158792

Zhang, Y., Simpson, R. B., Sallade, L. E., Sanchez, E., Monahan, K. M., and Naumova, E. N. (2022). Evaluating completeness of foodborne outbreak reporting in the United States, 1998–2019. *Int. J. Environ. Res. Public Health* 19:2898. doi: 10.3390/ijerph19052898

frontiers | Frontiers in Microbiology

TYPE Original Research
PUBLISHED 17 August 2023
DOI 10.3389/fmicb.2023.1252344

OPEN ACCESS

EDITED BY
Sébastien Holbert,
INRA Centre Val de Loire, France

REVIEWED BY
Qiuhe Lu,
Cleveland Clinic, United States
Luke Peter Allsopp,
Imperial College London, United Kingdom
Fernando Navarro-Garcia,
National Polytechnic Institute of Mexico (CINVESTAV), Mexico

*CORRESPONDENCE
Carlos A. Santiviago
✉ csantiviago@ciq.uchile.cl
David Pezoa
✉ dpezoa@udla.cl

†These authors have contributed equally to this work and share first authorship

RECEIVED 03 July 2023
ACCEPTED 03 August 2023
PUBLISHED 17 August 2023

CITATION
Blondel CJ, Amaya FA, Bustamante P, Santiviago CA and Pezoa D (2023) Identification and distribution of new candidate T6SS effectors encoded in *Salmonella* Pathogenicity Island 6.
Front. Microbiol. 14:1252344.
doi: 10.3389/fmicb.2023.1252344

Identification and distribution of new candidate T6SS effectors encoded in *Salmonella* Pathogenicity Island 6

Carlos J. Blondel[1†], Fernando A. Amaya[2†], Paloma Bustamante[3], Carlos A. Santiviago[2*] and David Pezoa[4,5*]

[1]Facultad de Medicina y Facultad de Ciencias de la Vida, Instituto de Ciencias Biomédicas, Universidad Andrés Bello, Santiago, Chile, [2]Laboratorio de Microbiología, Departamento de Bioquímica y Biología Molecular, Facultad de Ciencias Químicas y Farmacéuticas, Universidad de Chile, Santiago, Chile, [3]Facultad de Medicina Veterinaria y Agronomía, Universidad de Las Américas, Santiago, Chile, [4]Núcleo de Investigaciones Aplicadas en Ciencias Veterinarias y Agronómicas, Facultad de Medicina Veterinaria y Agronomía, Universidad de Las Américas, Santiago, Chile, [5]Departamento de Ciencias Químicas y Biológicas, Universidad Bernardo O'Higgins, Santiago, Chile

The type VI secretion system (T6SS) is a contact-dependent contractile multiprotein apparatus widely distributed in Gram-negative bacteria. These systems can deliver different effector proteins into target bacterial and/or eukaryotic cells, contributing to the environmental fitness and virulence of many bacterial pathogens. *Salmonella* harbors five different T6SSs encoded in different genomic islands. The T6SS encoded in *Salmonella* Pathogenicity Island 6 (SPI-6) contributes to *Salmonella* competition with the host microbiota and its interaction with infected host cells. Despite its relevance, information regarding the total number of effector proteins encoded within SPI-6 and its distribution among different *Salmonella enterica* serotypes is limited. In this work, we performed bioinformatic and comparative genomics analyses of the SPI-6 T6SS gene cluster to expand our knowledge regarding the T6SS effector repertoire and the global distribution of these effectors in *Salmonella*. The analysis of a curated dataset of 60 *Salmonella enterica* genomes from the Secret6 database revealed the presence of 23 new putative T6SS effector/immunity protein (E/I) modules. These effectors were concentrated in the variable regions 1 to 3 (VR1-3) of the SPI-6 T6SS gene cluster. VR1-2 were enriched in candidate effectors with predicted peptidoglycan hydrolase activity, while VR3 was enriched in candidate effectors of the Rhs family with C-terminal extensions with predicted DNase, RNase, deaminase, or ADP-ribosyltransferase activity. A global analysis of known and candidate effector proteins in *Salmonella enterica* genomes from the NCBI database revealed that T6SS effector proteins are differentially distributed among *Salmonella* serotypes. While some effectors are present in over 200 serotypes, others are found in less than a dozen. A hierarchical clustering analysis identified *Salmonella* serotypes with distinct profiles of T6SS effectors and candidate effectors, highlighting the diversity of T6SS effector repertoires in *Salmonella enterica*. The existence of different repertoires of effector proteins suggests that different effector protein combinations may have a differential impact on the environmental fitness and pathogenic potential of these strains.

KEYWORDS

***Salmonella*, T6SS, SPI-6, effector, immunity protein**

Introduction

The type VI secretion system (T6SS) is a multiprotein nanomachine composed of 13 structural components and various accessory proteins that deliver protein effectors into target cells through a contractile mechanism (Cherrak et al., 2019; Coulthurst, 2019). The T6SS needle, composed of an inner tube (made of a stack of Hcp hexamer rings) and comprising a trimer of VgrG and a PAAR protein, is wrapped into a contractile sheath formed by the polymerization of TssB/TssC subunits. These are assembled into an extended, metastable conformation (Silverman et al., 2013; Cherrak et al., 2019). Contraction of the sheath upon contact with a target cell or sensing cell envelope damage propels the needle toward the target cell (Brackmann et al., 2017). T6SS effector proteins are classified as either cargo or specialized effectors. Cargo effectors are delivered by non-covalent interaction with some core components (Coulthurst, 2019), while specialized effectors are additional domains of either VgrG, Hcp, or PAAR proteins (Durand et al., 2014; Whitney et al., 2014; Diniz and Coulthurst, 2015; Ma et al., 2017; Pissaridou et al., 2018).

The extensive repertoire of effector proteins makes the T6SS a highly versatile machine that can target prokaryotic or eukaryotic cells (Coulthurst, 2019; Monjarás Feria and Valvano, 2020). Among the antibacterial effector proteins, some target the peptidic or glycosidic bonds of the peptidoglycan (Ma and Mekalanos, 2010; Russell et al., 2012; Srikannathasan et al., 2013; Whitney et al., 2013; Berni et al., 2019; Wood et al., 2019), or the FtsZ cell division ring (Ting et al., 2018). These antibacterial effectors are encoded in bi-cistronic elements with immunity proteins (E/I pairs) that bind tightly and specifically to their cognate effector preventing self-intoxication and killing of sibling cells (Russell et al., 2012). Other T6SS effectors are eukaryote-specific, such as those targeting the actin or microtubule cytoskeleton networks (Monjarás Feria and Valvano, 2020), and others (known as trans-kingdom effectors) can target both bacterial and eukaryotic cells (Jiang et al., 2014). These effectors include those targeting conserved molecules (NAD^+ and $NADP^+$) and macromolecules (DNA, phospholipids) or forming pores in membranes (Whitney et al., 2015; Tang et al., 2018; Ahmad et al., 2019).

Many enteric pathogens (e.g., *Salmonella*, *Shigella*, and *Vibrio*) use the T6SS to colonize the intestinal tract of infected hosts (Sana et al., 2016; Chassaing and Cascales, 2018), while some strains of the gut commensal *Bacteroides fragilis* use their T6SSs only for competition against other Bacteroidales species (Coyne and Comstock, 2019). The T6SS is, therefore, a key player in bacterial warfare.

The *Salmonella* genus includes more than 2,600 serotypes distributed between species *S. enterica* and *S. bongori* (Issenhuth-Jeanjean et al., 2014), which differ in clinical signs and host range (Uzzau et al., 2000). Serotypes are defined based on variations in the somatic, flagellar and capsular antigens, according to the Kauffmann-White-Le Minor serotyping scheme (Grimont and Weill, 2007; Issenhuth-Jeanjean et al., 2014). Worldwide, *Salmonella* infections are responsible for 95.1 million cases of gastroenteritis per year (GBD 2017 Non-Typhoidal Salmonella Invasive Disease Collaborators, 2019). In addition, the World Health Organization (WHO) has also included *Salmonella* as a high-priority pathogen due to the emergence of strains with high levels of fluoroquinolone resistance (GBD 2017 Non-Typhoidal Salmonella Invasive Disease Collaborators, 2019). In *Salmonella*, 5 T6SS gene clusters have been identified within *Salmonella* Pathogenicity Islands (SPIs) SPI-6, SPI-19, SPI-20, SPI-21, and SPI-22 (Blondel et al., 2009; Fookes et al., 2011). These T6SSs are distributed in 4 different evolutionary lineages: $T6SS_{SPI-6}$ belongs to subtype i3, $T6SS_{SPI-19}$ to subtype i1, $T6SS_{SPI-22}$ to subtype i4a, and both $T6SS_{SPI-20}$ and $T6SS_{SPI-21}$ belong to subtype i2 (Bao et al., 2019). Besides their distinct evolutionary origin, these five T6SS gene clusters are differentially distributed among distinct serotypes, subspecies, and species of *Salmonella* (Blondel et al., 2009).

Notably, most of these T6SSs have been shown to contribute to the virulence and pathogenesis of different *Salmonella* serotypes (Blondel et al., 2010; Mulder et al., 2012; Pezoa et al., 2013, 2014; Sana et al., 2016; Xian et al., 2020; Hespanhol et al., 2022; Sibinelli-Sousa et al., 2022). One of the most studied and widely distributed T6SS corresponds to that encoded in SPI-6. Depending on the serotype, the SPI-6 T6SS gene cluster comprises a region of ~35 to 50 kb encoding ~30 to 45 ORFs, including each of the 13 T6SS core components. The genetic architecture of the SPI-6 T6SS gene cluster is highly conserved among serotypes; nonetheless, there are structural differences restricted to three variable regions of the island (herein referred to as VR1, VR2, and VR3, Figure 1) (Blondel et al., 2009). In *S.* Typhimurium and *S.* Dublin, 9 SPI-6 T6SS effector proteins have been described to date (Russell et al., 2012; Benz et al., 2013; Whitney et al., 2013; Koskiniemi et al., 2014; Sana et al., 2016; Sibinelli-Sousa et al., 2020; Amaya et al., 2022; Jurėnas et al., 2022; Lorente-Cobo et al., 2022), most of which are encoded within these variable regions (Figure 1; Table 1).

The VR1 is located downstream of gene *tssC* and encodes the E/I modules Tae2/Tai2 and Tae4/Tai4. Tae2 and Tae4 are peptidoglycan hydrolases able to cleave the DD-crosslinks between D-mDAP and D-alanine or the covalent link between D-Glu and mDAP of the tetrapeptide stem, respectively, thus contributing to interbacterial competition and mice colonization (Russell et al., 2012; Sana et al., 2016). VR2 is located downstream of gene *tssM* and encodes many proteins of unknown function and two E/I modules with peptidoglycan hydrolase activity: Tge2/Tgi2P is predicted to have N-acetylglucosaminidase activity (Whitney et al., 2013), while Tlde1/Tldi shows L,D carboxypeptidase activity against the peptide stems of the peptidoglycan layer (Sibinelli-Sousa et al., 2020; Lorente-Cobo et al., 2022). Finally, the VR3 is located downstream of gene *tssI* and encodes a variable number of Rhs elements, some of them harboring endonuclease domains such as HNHc (DNase) and Ntox47 (RNase), and an ART domain (ADP-ribosyltransferase) linked to the C-terminal of these Rhs proteins (Koskiniemi et al., 2014; Amaya et al., 2022; Jurėnas et al., 2022).

Most of our knowledge regarding the presence and distribution of SPI-6 T6SS effector proteins comes from studies using reference strains of a limited number of serotypes (e.g., *S.* Typhimurium and *S.* Dublin) (Russell et al., 2012; Benz et al., 2013; Whitney et al., 2013; Koskiniemi et al., 2014; Sana et al., 2016; Sibinelli-Sousa et al., 2020; Amaya et al., 2022; Jurėnas et al., 2022; Lorente-Cobo et al., 2022). In this study, we performed a bioinformatic prediction analysis searching for putative T6SS effectors in a dataset of 60 genomes covering 37 *S. enterica* serotypes retrieved from the curated Secret6 database. Our analysis identified 23 new putative antibacterial effectors encoded in E/I modules within the 3 VRs of the SPI-6 T6SS gene cluster. These candidates include 5 effectors with putative peptidoglycan hydrolase activity, 16 effectors with potential nuclease activity and 2 effectors

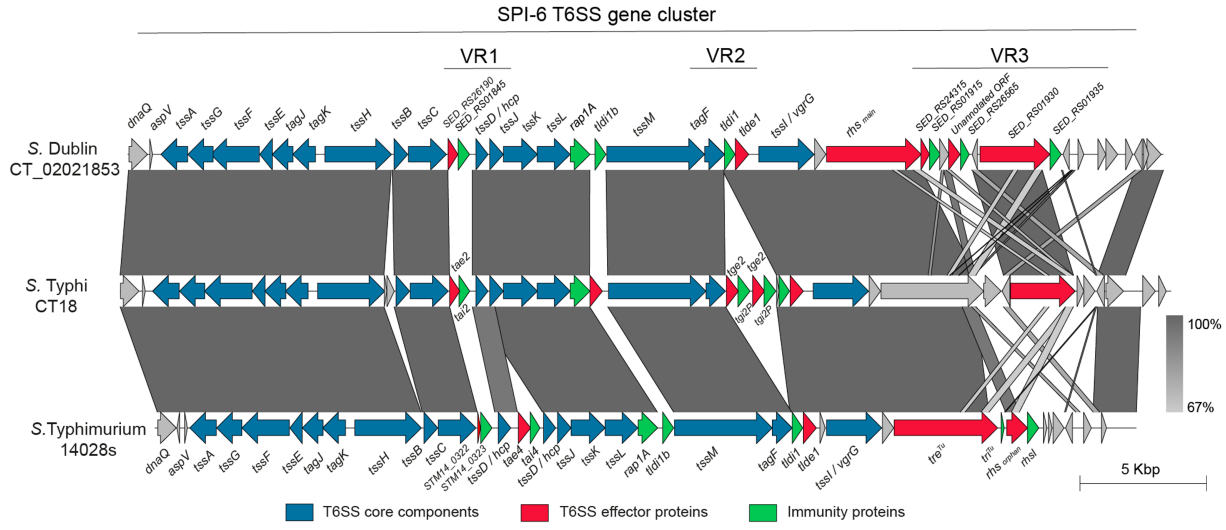

FIGURE 1
Schematic representation of selected SPI-6 T6SS gene clusters. The figure shows an alignment of the SPI-6 T6SS gene cluster of *S.* Dublin CT_02021853, *S.* Typhi CT18 and *S.* Typhimurium 14028s. The location of variable regions 1–3 is shown. ORFs encoding previously described T6SS effectors and cognate immunity proteins are shown in red and green, respectively. ORFs encoding T6SS core components are shown in blue. Grayscale represents the percentage of identity between nucleotide sequences.

targeting the bacterial translation machinery. Finally, we expanded our analysis to include all available *Salmonella* genomes deposited in the NCBI database and determined the global distribution of these new putative effectors. A hierarchical clustering analysis identified that some effectors are conserved in most *Salmonella* serotypes. In contrast, most other effectors are differentially distributed in different serotypes. The presence of different sets of T6SS effectors suggests that distinct repertoires of these proteins may have a differential impact on the pathogenicity and environmental adaptation of *Salmonella* serotypes.

Materials and methods

Identification of candidate SPI-6 T6SS effectors

First, we searched the Secret6 database[1] for *Salmonella* genomes encoding the minimal 13 core components of a T6SS and identified a total of 60 genomes that met this requirement. Then, to identify putative T6SS effectors encoded within SPI-6 of *Salmonella*, each ORF of this island was analyzed with the Bastion6 pipeline (Wang et al., 2018) excluding the 13 T6SS core components. ORFs presenting a Bastion6 score ≥ 0.7 were considered as candidate T6SS effectors. Each Bastion6 prediction was further analyzed with tools implemented in the Operon-Mapper web server (Taboada et al., 2018) to determine if it was likely part of a bi-cistronic unit also encoding a putative immunity protein [i.e., a small protein with potential signal peptides (SignalP 6.0) and/or transmembrane domains (TMHMM 2.0)]. Conserved functional domains and motifs in the candidate T6SS effectors were identified using the PROSITE, NCBI-CDD, Motif-finder, and Pfam databases (Kanehisa et al., 2002; Sigrist et al., 2013; Finn et al., 2014; Lu et al., 2019) implemented in the GenomeNet[2] search engine. An e-value cutoff score of 0.01 was used. Finally, a biochemical functional prediction for each putative effector and immunity protein identified was performed by HMM homology searches using the HHpred HMM-HMM comparison tool (Zimmermann et al., 2017). It is worth mentioning that most genes (ORFs) identified do not have formal names, making extremely difficult referring to them using conventional genetic nomenclature. Thus, in figures and tables we will refer to ORFs encoding effectors and immunity proteins according to the corresponding protein name (in the case of those previously reported in the literature) or the functional domains present in the predicted proteins (in the case of ORFs encoding new candidate effectors and immunity proteins).

Hierarchical clustering analysis of the new SPI-6 T6SS effectors

For hierarchical clustering analysis, a presence/absence matrix of each T6SS effector and candidate effector was constructed for each bacterial genome by means of BLASTn analyses and manual curation of the data. A 90% identity and 90% sequence coverage threshold was used to select positive matches. The matrix generated was uploaded as a csv file to the online server MORPHEUS[3] using default parameters (i.e., one minus Pearson's correlation, average linkage method).

1 https://bioinfo-mml.sjtu.edu.cn/SecReT6/download.html

2 https://www.genome.jp

3 https://software.broadinstitute.org/morpheus

TABLE 1 T6SS effectors and cognate immunity proteins encoded in SPI-6 previously identified in *Salmonella enterica*.

E/I pair	Effector activity	Paper highlights	References
Effectors targeting peptidoglycan			
Tae2/Tai2	Peptidoglycan hydrolase (Amidase that cleaves DD-crosslinks between D-mDAP and D-alanine)	Toxicity against the target-cell peptidoglycan in interbacterial competition	Russell et al. (2012)
Tae4-Tai4	Peptidoglycan hydrolase (Amidase that cleaves between D-mDAP and D-Glu)	Tae4 contributes to interbacterial competition and mice colonization	Sana et al. (2016)
Tge2/Tgi2P	Peptidoglycan glycoside hydrolase (N-acetylglucosaminidase)	Identified by bioinformatic analyses	Whitney et al. (2013)
Tlde1/Tldi1	Peptidoglycan L,D carboxypeptidase	Toxicity against the target-cell peptidoglycan in interbacterial competition	Sibinelli-Sousa et al. (2020)
Effectors targeting nucleic acids			
SED_RS01930/SED_RS01935	Ntox47 endonuclease (RNase)	SED_RS01930 contributes to interbacterial competition	Amaya et al. (2022)
SED_RS24315/SED_RS01915	Predicted Tox-URI2 endonuclease (DNase)	Identified by bioinformatic analyses	Amaya et al. (2022)
Unannotated ORF/SED_RS26565	Predicted HNH endonuclease (DNase)	Identified by bioinformatic analyses	Amaya et al. (2022)
Rhs^{orphan}/RhsI	Ntox47 endonuclease (RNase)	Rhs^{orphan} contributes to bacterial killing during mice infection	Koskiniemi et al. (2014)
Effectors targeting translation machinery			
Tre^{Tu}/Tri^{Tu}	ART (ADP-ribosyltransferase)	Rhs^{main}-type effector Tre^{Tu} arrests bacterial translation by ADP-ribosyltation of EF-Tu	Jurėnas et al. (2022)

Salmonella 16S rDNA phylogenetic analyses

The 16S rDNA sequences were obtained from the 60 *Salmonella* genomes previously analyzed. The sequences were concatenated and aligned with ClustalW using the Molecular Evolutionary Genetics Analysis (MEGA) software version 7.0 (Kumar et al., 2016). A phylogenetic tree was built from the alignments obtained from MEGA by performing a bootstrap test of phylogeny (1,000 replications) using the maximum-likelihood method with a Jones-Taylor-Thornton correction model.

Sequence and phylogenetic analyses

The DNA sequence encoding each T6SS effector identified in this study was subjected to BLASTn analyses to find orthologs in all *Salmonella* genome sequences deposited in the NCBI database (October 2022). For selection of positive matches, a 90% identity and 90% sequence coverage threshold was used. Conservation of sequences was determined by multiple sequence alignments using T-Coffee Expresso (Notredame et al., 2000), MAFFT (Katoh et al., 2017), and ESPript 3 (Robert and Gouet, 2014). Comparative genomic analysis of SPI-6 T6SS gene clusters was performed using Mauve (Darling et al., 2004) and EasyFig v2.2.5 (Sullivan et al., 2011). Nucleotide sequences were analyzed using Artemis version 18 (Rutherford et al., 2000).

Results

Analysis of a curated dataset of *Salmonella* genomes reveals 23 new putative E/I modules encoded within the SPI-6 T6SS gene cluster

To identify new T6SS effectors with high confidence, we first screened the SPI-6 T6SS gene clusters of a dataset of 60 *Salmonella enterica* genomes from the Secret6 curated database (Zhang et al., 2023). This database includes 60 strains covering 37 *Salmonella* serotypes (Supplementary Table S1). Each ORF within SPI-6 T6SS gene clusters was analyzed based on four criteria: (i) identification of candidate effectors through Bastion6 analysis (a bioinformatic tool that predicts T6SS effectors based on amino acid sequence, evolutionary information, and physicochemical properties); (ii) identification of putative immunity proteins by detection of signal peptides (SignalP 6.0), transmembrane domains (TMHMM 2.0) and operon prediction (Operon-mapper; Taboada et al., 2018); (iii) identification of conserved functional domains associated with *bona fide* T6SS effectors (INTERPROSCAN, PROSITE, NCBI-CDD, MOTIF, and Pfam) and (iv) functional biochemical prediction using the HHpred HMM-HMM server. In addition, we analyzed these gene clusters to identify potential unannotated ORFs which could encode putative effectors and cognate immunity proteins.

Our analysis identified 23 new putative effector proteins and cognate immunity proteins (Table 2). These candidates included both cargo and specialized effector proteins with diverse predicted

10.3389/fmicb.2023.1252344

TABLE 2 New putative T6SS effectors and cognate immunity proteins encoded in SPI-6 of *Salmonella enterica*.

T6SS effector genes					Cognate T6SS immunity protein genes	
ORF(s)	Size (aa)	Serotype-strain	Variable region	Predicted activity/domain	ORF(s)	TM or signal peptide/ domain
Effectors targeting peptidoglycan						
Unannotated ORF	32	*S.* Bareilly RSE03	1	Peptidoglycan hydrolase (Amidase)/L-Ala, D-Glu endopeptidase	ELZ70_17800	Signal peptide (Sec/SPI)/No
		S. Bredeney CVM24358			HFS03_00580	
		S. Daytona NCTC7102			NCTC7102_04795	
		S. Florida NCTC6480			NCTC6480_03851	
		S. Give NCTC5778			NCTC5778_03432	
		S. India SA20085604			Unannotated ORF	
		S. Mikawasima RSE13			Unannotated ORF	
		S. Paratyphi A ATCC9150			SPA_RS12640	
		S. Poona NCTC4840			NCTC4840_03690	
		S. enterica LHST_2018			Unannotated ORF	
		S. enterica NCTC7404			NCTC7404_03579	
		S. enterica NCTC7411			NCTC7411_03668	
		S. enterica NCTC7831			NCTC7831_03115	
		S. enterica NCTC8272			NCTC8272_03056	
		S. Sanjuan NCTC7406			NCTC7406_04092	
		S. Schwarzengrund CMV19633			SESA_RS02015	
		S. Senftenberg ATCC 43845			SEES3845_018760	
		S. Typhi CT18			STY_RS01380	
NCTC7406_04082	122	*S.* Sanjuan NCTC7406	2	Peptidoglycan hydrolase (L,D transpeptidase)/ Pgp2	NCTC7406_04081	Signal peptide (Sec/SPI)/No
G9X22_18260	279	*S.* Adjame 353,868	2	Peptidoglycan hydrolase (Amidase)/TseH-like	Unannotated ORF	2 TM/DUF4229
NCTC5778_03416		*S.* Give NCTC5778			NCTC5778_03415	
LFZ16_04210		*S.* India SA20085604			LFZ16_04215	
SESA_RS02090		*S.* Schwarzengrund CMV19633			Unannotated ORF	
SESEF3709_03438	243	*S. enterica* SESen3709	2	Peptidoglycan hydrolase (Amidase)/Reprolysin_4	SESEF3709_03437	Signal peptide (Sec/SPI)/No
EOS97_RS15095		*Salmonella* sp. SSDFZ54			EOS97_RS15100	No/No
SEES3845_018655		*S.* Senftenberg ATCC 43845			SEES3845_018650	No/No
CS349_18880		*S.* Tennessee CFSAN070645			CS349_18875	No/No
NCTC7411_03656	243	*S. enterica* NCTC7411	2	Peptidoglycan hydrolase (Amidase)/Peptidase_ M64	NCTC7411_03655	1 TM/No
NCTC7831_03138		*S. enterica* NCTC7831			NCTC7831_03139	1 TM/No
NCTC7406_04078		S. Sanjuan NCTC7406			NCTC7406_04077	1 TM/No

(Continued)

TABLE 2 (Continued)

T6SS effector genes					Cognate T6SS immunity protein genes	
ORF(s)	Size (aa)	Serotype-strain	Variable region	Predicted activity/domain	ORF(s)	TM or signal peptide/ domain
Effectors targeting nucleic acids						
Unannotated ORF	149	*S.* Kedougo Sal162	3	RNase and DNase/ RhsA-Ntox47-Tox-HNH-EHHH	Unannotated ORF	No/Imm50
CS349_18795		*S.* Tennessee CFSAN070645			CS349_18790	
NCTC7836_04182	970	*S. enterica* NCTC7836	3	DNase/RhsA-PDEEXK	NCTC7836_04181	No/No
NCTC7836_04194	616	*S. enterica* NCTC7836	3	DNase/RhsA-Tox-HNH-EHHH	NCTC7836_04193	No/No
NCTC8272_03019	589	*S. enterica* NCTC8272			NCTC8272_03018	No/No
SESEF3709_03428	592	*S. enterica* SESen3709			SESEF3709_03427	No/Imm50
G9X22_18245	1,501	*S.* Adjame 353,868	3	DNase/PAAR-RhsA-Tox-HNH-EHHH	G9X22_18240	No/Imm50
CFSAN002050_RS06455	1,499	*S.* Cubana CFSAN002050			CFSAN002050_RS06460	No/No
HFQ57_17525		*S.* Havana CVM20761			HFQ57_17520	No/No
SEES3845_018630		*S.* Senftenberg ATCC 43845			Unannotated ORF	No/No
HFQ45_19990	1,377	*S.* Anatum CVM20746	3	DNase/PAAR-RhsA-HNHc	HFQ45_19995	No/SMI1_KNR4
NCTC5778_03412	1,382	*S.* Give NCTC5778			NCTC5778_03411	No/SMI1_KNR4
E4T58_01505	1,580	*S.* Infantis L41			E4T58_01510	No/No
SPA_RS12520	1,570	*S.* Paratyphi A ATCC9150			SPA_RS12515	No/No
NCTC7831_03143	1,382	*S. enterica* NCTC7831			NCTC7831_03144	No/SMI1_KNR4
SEES3845_018590	1,377	*S.* Senftenberg ATCC 43845			SEES3845_018585	No/SMI1_KNR4
NCTC7102_04762	1,044	*S.* Daytona NCTC7102	3	DNase/RhsA-WHH	NCTC7102_04761	No/SMI1_KNR4
SESEF3709_03422	1,575	*S. enterica* SESen3709	3	DNase/PAAR-RhsA-WHH	SESEF3709_03421	No/SMI1_KNR4
ELZ70_17690	1,354	*S.* Bareilly RSE03	3	DNase/PAAR-RhsA-AHH	ELZ70_17685	No/No
HFQ57_17490	1,368	*S.* Havana CVM20761			HFQ57_17485	
HI825_06260	1,317	*S. enterica* LHST_2018			HI825_06265	
STY_RS01485	1,354	*S.* Typhi CT18			STY_RS01490	
HF553_RS18710	1,374	*Salmonella* sp. SCFS4	3	DNase/PAAR-RhsA-GIY-YIG	HF553_RS18705	No/CdiI
HU143_RS17590		*Salmonella* sp. SJTUF14076			HU143_RS17585	
IVP14_RS17960		*Salmonella* sp. SJTUF14146			IVP14_RS17955	
IVP15_RS18860		*Salmonella* sp. SJTUF14152			IVP15_RS18855	
IVP16_RS17665		*Salmonella* sp. SJTUF14154			IVP16_RS17660	
IVP17_RS17925		*Salmonella* sp. SJTUF14170			IVP17_RS17920	
IVP18_RS17920		*Salmonella* sp. SJTUF14178			IVP18_RS17915	
HFQ45_20000	174	*S.* Anatum CVM20746	3	RNase/RhsA-DUF4329	HFQ45_20005	No/CdiI
ELZ68_18315	267	*S.* Stanleyville RSE01			ELZ68_18310	No/No

(Continued)

TABLE 2 (Continued)

T6SS effector genes					Cognate T6SS immunity protein genes	
ORF(s)	Size (aa)	Serotype-strain	Variable region	Predicted activity/domain	ORF(s)	TM or signal peptide/ domain
SCH_RS26875	1,593	*S.* Choleraesuis SC-B67	3	RNase/PAAR-RhsA-DUF4329	SCH_RS01475	No/CdiI
SPC_RS25995		*S.* Paratyphi C RSK4594			SPC_RS01475	
NCTC13175_03561	352	*S.* Goldcoast NCTC13175	3	RNase/RhsA-Ribonuclease/Microbial Rnase	NCTC13175_03560	No/Barstar
Unannotated ORF	1,564	*S.* Derby Sa64	3	RNase/PAAR-RhsA-Ribonuclease/Microbial Rnase	EIC79_17405	No/Barstar
SEBLO3795_03484	1,564	*S. enterica* SEHaa3795			SEBLO3795_03483	
EOS98_RS24920	1,560	*Salmonella* sp. SSDFZ69			EOS98_RS17735	
HLB37_13055	1,560	*S.* Kedougo Sal162	3	RNase/PAAR-RhsA-EndoU_bacteria	HLB37_13060	No/MafI
SEHA_RS26915	102	*S.* Heidelberg SL476	3	RNase/CdiA	SEHA_RS02130	No/Imm42
IA1_RS24740		*S.* Thompson RM6836			IA1_RS01635	
HI825_06280	106	*S. enterica* LHST_2018	3	Deaminase/Tox-Deaminase	HI825_06285	No/SUKH_5
STY_RS01505	86	*S.* Typhi CT18			STY_RS01510	
Effectors targeting translation machinery						
DYN42_004080	943	*S.* London CVM N17S347	3	ADP-ribosyltransferase/RhsA-Tox-ART-HYD1	DYN42_004085	No/No
NCTC8271_04564	194	*S. enterica* NCTC8271			Unannotated ORF	
NCTC5741_00975	943	*S. enterica* NCTC5741			NCTC5741_00976	
SESEF3709_03418	402	*S. enterica* SESen3709			SESEF3709_03417	
IA1_RS01605	959	*S.* Thompson RM6836			IA1_RS01610	
NCTC4840_03667	1,566	*S.* Poona NCTC4840	3	ADP-ribosyltransferase/PAAR-RhsA-Tox-ART-HYD1	NCTC4840_03666	No/No

biochemical functions, including peptidoglycan hydrolases (5), DNases (8), RNases (6), deaminases (1), ADP-ribosyltransferases (2) and hybrid DNases/RNases (1) (Table 2). In addition, our analysis showed that the repertoire of E/I modules in SPI-6 vary considerably between closely related strains (Figure 2). Of note, comparative genomic analyses revealed that each identified E/I module is encoded within one of the 3 VRs previously described (Blondel et al., 2009). One E/I module is encoded within VR1, four within VR2, and 18 are encoded within VR3 (Figure 3).

Putative T6SS cargo effectors with predicted peptidoglycan hydrolase activity are confined to VR1 and VR2

Our bioinformatic analysis identified 5 predicted T6SS cargo effectors with putative peptidoglycan hydrolase activity (Table 2; Figure 4). One effector corresponds to an unannotated ORF encoded within VR1. This ORF was identified in 30% (18/60) of the genomes analyzed, is located between genes *tssH* and *tssB* (*ELZ70_17805* and *ELZ70_17795* ORFs in *S.* Bareilly strain RSE03) and is predicted to encode a 32 amino acids protein with a putative L-Ala-D-Glu-endopeptidase protein domain (Figure 4). This ORF is predicted to be co-transcribed with a downstream unannotated ORF that encodes a 146 amino acids protein with a periplasmic-targeting signal peptide (Table 2), suggesting that this latter ORF encodes the cognate immunity protein of the new candidate effector.

In addition, our analysis identified four putative E/I modules encoded in VR2. The first putative effector (NCTC7406_04082 in *S.* Sanjuan strain NCTC7406) is a 122 amino acid protein that harbors a predicted PgP2 protein domain with putative L,D transpeptidase activity (Table 2; Figure 4). *NCTC7406_04082* is part of a bi-cistronic unit with *NCTC7406_04081*. This latter ORF encodes a 147 amino acid protein with a signal peptide targeting the periplasmic space that may correspond to its cognate immunity protein (Table 2). The second VR2 candidate effector (G9X22_18260 in *S.* Adjame strain 353868) is a 279 amino acids protein that harbors a putative amidase domain similar to the NlpC/P60 endopeptidase domain of the TseH T6SS effector of

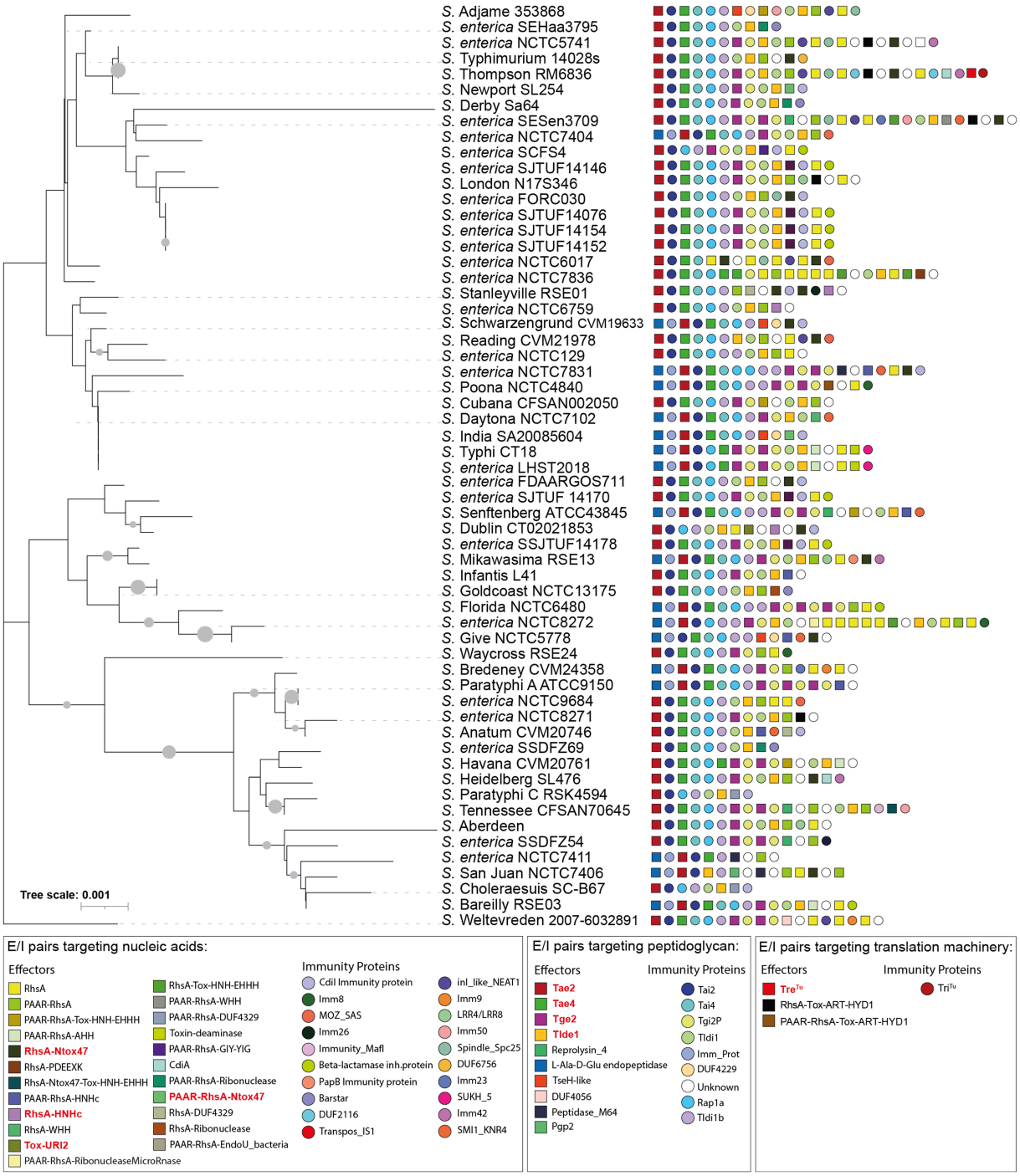

FIGURE 2
16S rDNA phylogeny and T6SS E/I module composition of *Salmonella enterica* SPI-6. Concatenated 16S rDNA nucleotide sequences from 60 *Salmonella* genomes deposited in Secret6 database were aligned with ClustalW using MEGA version 7.0. Next, a maximum-likelihood phylogenetic tree was built from the alignment using a bootstrap test of phylogeny (1,000 replications) with a Jones-Taylor-Thornton correction model. In the figure, we refer to ORFs encoding effectors and immunity proteins according to the corresponding protein name (in the case of those previously reported in the literature) or the functional domains present in the predicted proteins (in the case of ORFs encoding new candidate effectors and immunity proteins). Squares and circles next to each strain name correspond to ORFs encoding an effector or an immunity protein, respectively. Different colors represent confirmed or predicted functions, as indicated in the figure.

Vibrio cholerae (Altindis et al., 2015). This candidate effector is also encoded next to a putative immunity protein of 86 amino acids harboring a DUF4229 protein domain and 2 transmembrane helices that may target this protein to the periplasmic space (Table 2).

The third candidate effector (SESEF3709_03438 in *S. enterica* strain SESen3709) is a 243 amino acids protein that harbors a Reprolysin_4 domain with putative amidase activity (Figure 4). *SESEF3709_03438* is predicted to be part of a bi-cistronic unit with

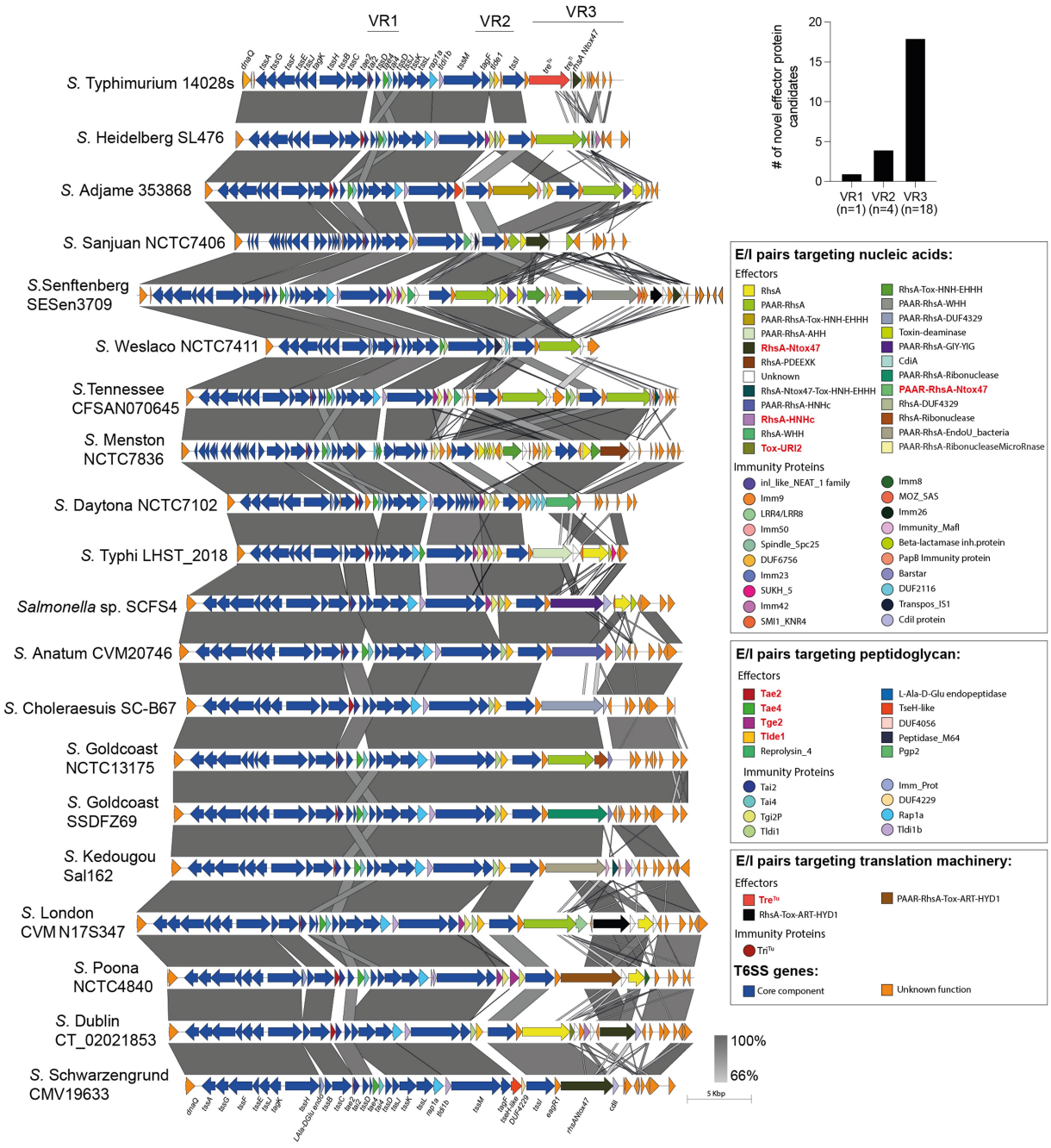

FIGURE 3
Comparative genomic analysis of SPI-6 T6SS gene clusters in representative *Salmonella* serotypes reveals new effector encoding genes. The location of variable regions 1–3 is shown. In the figure, we refer to ORFs encoding effectors and immunity proteins according to the corresponding protein name (in the case of those previously reported in the literature) or the functional domains present in the predicted proteins (in the case of ORFs encoding new candidate effectors and immunity proteins). ORFs encoding T6SS core components are shown in blue. ORFs encoding E/I modules are presented in different colors according to the confirmed or predicted functions, as indicated in the figure. Grayscale represents the percentage of identity between nucleotide sequences. Previously described *Salmonella* T6SS effectors are highlighted in red.

SESEF3709_03437, that encodes a putative cognate immunity protein with a signal peptide for periplasmic targeting.

The final candidate effector of VR2 corresponds to a 243 amino acid protein with a predicted M64 peptidase domain (NCTC7411_03656 in *S. enterica* strain NCTC7411) (Table 2; Figure 4). Our analysis also revealed that *NCTC7411_03656* is likely to be part of bi-cistronic unit with their respective putative immunity protein gene (*NCTC7411_03655* in *S. enterica* strain NCTC7411) (Table 2). In other serotypes, the putative immunity protein gene encodes a protein of 84–144 amino acids harboring a transmembrane domain that targets this protein to the periplasmic space (Table 2).

10.3389/fmicb.2023.1252344

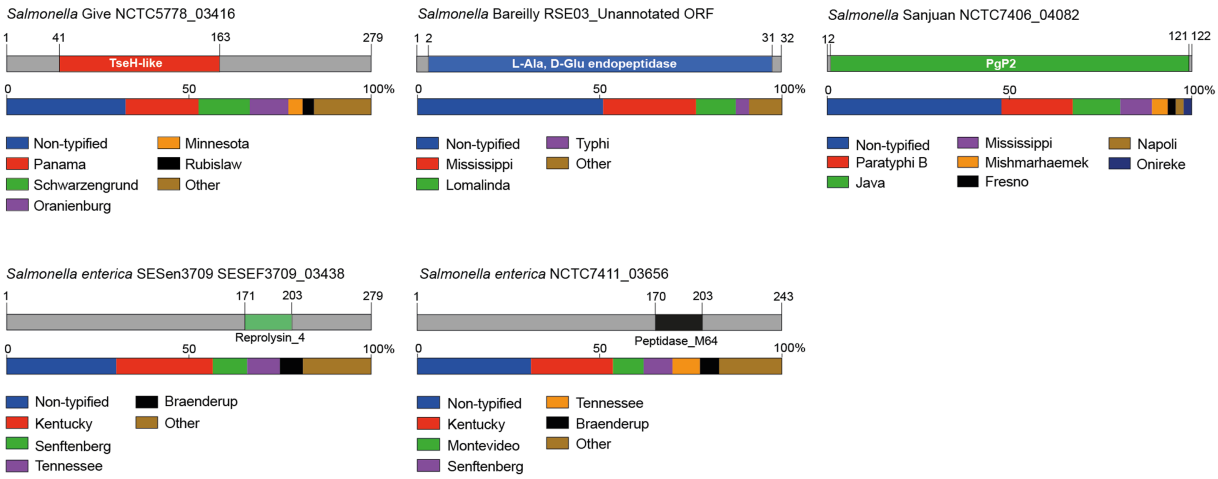

FIGURE 4
The variable regions 1 and 2 of the SPI-6 T6SS gene cluster encode 5 new putative effectors. Schematic representation and distribution of new putative effectors among *Salmonella* genomes. Predicted functional domains are show in different colors. Homologs for each candidate effector were identified by BLASTn analyses, as described in Materials and Methods.

Putative T6SS specialized effectors with polymorphic nuclease and ADP-ribosyltransferase toxin domains associated to Rhs proteins are restricted to the VR3

Our analysis revealed the presence of 18 candidate effectors encoded within the VR3 of SPI-6, including 16 in the Rhs family of proteins, 1 RNase and 1 deaminase. The size of the Rhs proteins ranged from 500 to 1,500 amino acids harboring different nuclease and ADP-ribosyltransferases domains (Table 2; Figure 5).

Eight of the 16 Rhs proteins harbored distinct C-terminal DNase domains, including domains of the HNH/ENDO VII superfamily of nucleases (IPR028048) such as WHH (IPR032869), Tox-HNH-EHH5H (IPR028048) or AHH (IPR032871), and nuclease domains of the GIY-YIG (IPR000305) and PDEEXK (IPR009362) families (Figure 5). In addition, 4 of these 8 candidates also harbored N-terminal PAAR motifs (IPR008727) (Figure 5). The presence of PAAR motifs suggests that these candidates correspond to specialized effector proteins. Each of these candidates were also predicted to be encoded in bi-cistronic units with ORFs encoding their respective immunity protein. Several of these proteins harbored domains previously found in cognate immunity proteins of bacterial toxin systems such as Imm50 (IPR028957), SMI1_KNR4 (PF09346) and CdI (IPR041256), among others (Table 2).

Our bioinformatics analyses also predicted 5 Rhs effectors with C-terminal extensions harboring different RNase protein domains (Table 2; Figure 5). These include Rhs proteins with Guanine-specific ribonuclease N1/T1/U2 (IPR000026), EndoU (IPR029501), and DUF4329 (IPR025479) domains. In addition, three of these proteins also harbored N-terminal PAAR motifs (IPR008727). The gene encoding each of these proteins was also predicted to be co-transcribed with genes encoding putative immunity proteins (Table 2). Remarkably, our analysis also identified a hybrid Rhs effector with predicted C-terminal RNase (Ntox47 domain) and DNase (Tox-HNH-EHHH) domains (CS349_18795 in *S.* Tennessee strain CFSAN070645). The gene encoding this protein is also predicted to be part of bi-cistronic unit with an ORF encoding a 129 amino acid protein with an Imm50 (IPR028957) domain. We also identified two putative Rhs effectors with a TOX-ART-HYD1 (pfam15633) ADP-ribosyltransferase domain, one of which also includes an N-terminal PAAR motif (NCTC4840_03667 in *S.* Poona strain NCTC4840). This protein shares 32% identity with STM0291, a recently described Rhs effector with an ART protein domain of *S.* Typhimurium named Tre^{Tu} (type VI ribosyltranferase effector targeting EF-Tu; Jurėnas et al., 2022). The low percentage of sequence identity (Supplementary Figure S1) suggests that this could be a divergent STM0291 homolog.

Finally, in VR3 we identified a putative effector with the CdiA RNase domain (IPR041620) not associated to Rhs elements (SEHA_RS26915 in *S.* Heidelberg SL476) (Table 2; Figure 5). In addition, we also identified a candidate effector harboring potential adenosine deaminase activity (STY_RS01505 in *S.* Typhi CT18). This effector is a small 86 amino acid protein with a TOX-deaminase domain of the BURPS668_1122 family (IPR032721) found in polymorphic toxin systems (Table 2; Figure 5). The gene encoding this effector is predicted to be co-transcribed with an ORF encoding a putative immunity protein with a SUKH_5 (PF14567) domain (Table 2; Figure 5).

Genome-wide analysis of the distribution of SPI-6 T6SS effectors and candidate effectors in *Salmonella*

Identifying new putative T6SS effectors encoded within VR1-3 of SPI-6 encouraged us to determine the presence and distribution of the

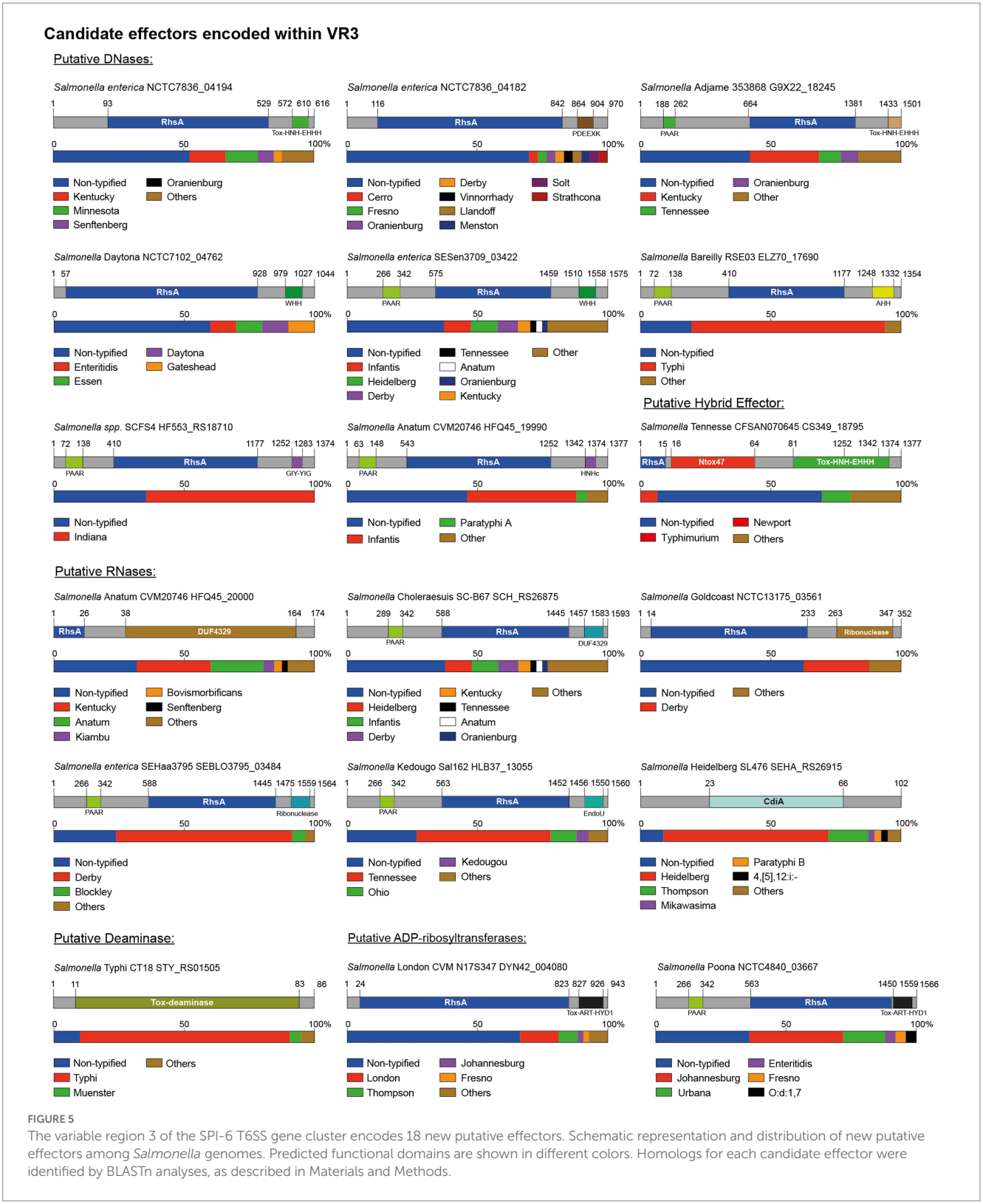

FIGURE 5
The variable region 3 of the SPI-6 T6SS gene cluster encodes 18 new putative effectors. Schematic representation and distribution of new putative effectors among *Salmonella* genomes. Predicted functional domains are shown in different colors. Homologs for each candidate effector were identified by BLASTn analyses, as described in Materials and Methods.

genes encoding these proteins across *Salmonella enterica*. The nucleotide sequence corresponding to each effector and candidate effector was used in BLASTn searches examining publicly available *Salmonella enterica* genome sequences deposited in the NCBI database, and the distribution of each effector protein was determined (Supplementary Table S2).

The analysis of the 9 T6SS effector proteins previously reported in the literature (i.e., Tae2, Tae4, Tge2, Tlde1, RhsA-HNHc, RhsA-Ntox47, PAAR-RhsA-Ntox47, Tre^{Tu} and Tox-URI2) and the 23 candidate effectors described in this study showed that they are widely and differentially distributed among *Salmonella* genomes (Supplementary Table S2). Interestingly, we identified these effectors

10.3389/fmicb.2023.1252344

and candidates effector in many non-typified *Salmonella* strains (Figure 6A).

Some effector and candidate effectors were more widespread across different serotypes than others (Figure 6B). Within VR1 and VR2, the previously reported effectors Tae2, Tae4, Tge2, and Tlde1 were identified across 150–240 serotypes, while the five candidate effector proteins identified in this study were found in 5–50 distinct serotypes. A different scenario was observed for effectors and candidate effectors encoded within VR3. In this case, the previously reported effectors were identified in less than 50 serotypes, while some new candidate effectors, such as PAAR-RhsA-WHH and PAAR-RhsA-DUF4329, were identified in over 150 serotypes. The distribution of each candidate effector in different *Salmonella* serotypes is highlighted in Figures 4, 5.

Finally, we performed a hierarchical clustering analysis to gain further insight into the distribution of effector and candidate effectors identified in 340 *Salmonella* genomes (Supplementary Table S3). As shown in Figure 6C, the four *bona fide* effectors encoded within VR1-2 (Tae2, Tae4, Tge2, and Tlde1) were the most conserved across the genomes of 113 different *Salmonella* serotypes. Nevertheless, these effectors are absent in the genome of 78 *Salmonella* serotypes, all of which include the genes encoding candidate effectors PAAR-RhsA-WHH and PAAR-RhsA-DUF4329 located within VR3. Furthermore, these candidate effectors are also distributed in the genome of 73 other *Salmonella* serotypes, suggesting that they play important roles in the biology of this pathogen.

Discussion

The T6SS has emerged as an important virulence and environmental fitness factor for *Salmonella* (Blondel et al., 2010; Mulder et al., 2012; Pezoa et al., 2013, 2014; Sana et al., 2016; Xian et al., 2020; Hespanhol et al., 2022; Sibinelli-Sousa et al., 2022). However, information regarding the complexity and diversity of effector proteins for each distinct *Salmonella* T6SS is still lacking. In this context, even though the T6SS encoded in SPI-6 has been shown to contribute to host colonization by *S.* Typhimurium and *S.* Dublin (Mulder et al., 2012; Pezoa et al., 2013, 2014; Sana et al., 2016) and to interbacterial competition of *S.* Typhimurium against the intestinal

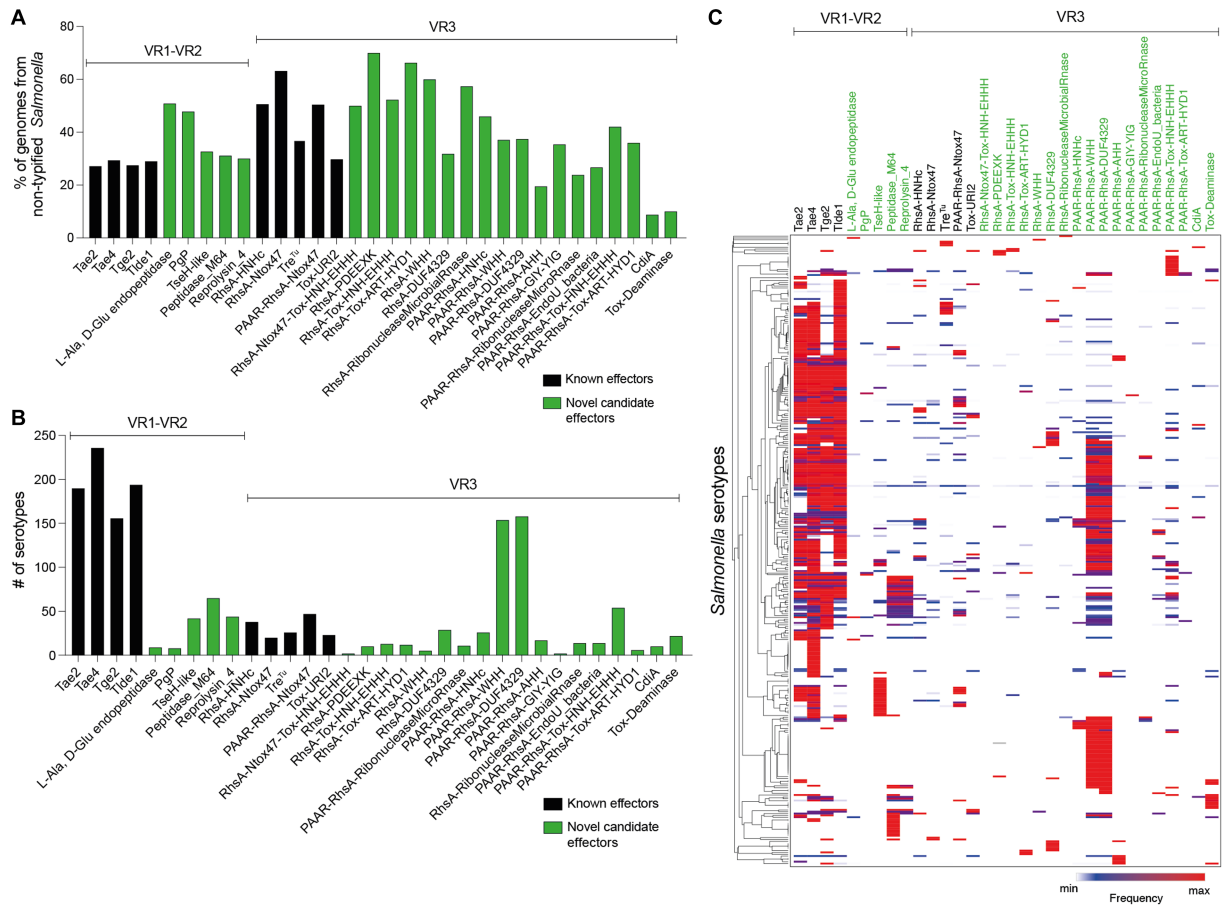

FIGURE 6
Prevalence of ORFs encoding T6SS effectors and candidate effectors in SPI-6. In the figure, we refer to ORFs encoding effectors according to the corresponding protein name (in the case of those previously reported in the literature) or the functional domains present in the predicted proteins (in the case of ORFs encoding new candidate effectors). Distribution of ORFs encoding T6SS effectors and candidate effectors in non-typified **(A)** and serotyped **(B)** *Salmonella* strains. **(C)** Prevalence of ORFs encoding T6SS effectors and candidate effectors in the genome of 340 *Salmonella* serotypes. A hierarchical clustering analysis was performed using MORPHEUS, as described in Materials and Methods. Color code in the heatmap indicates the presence of a given ORF (frequency) among all analyzed strains of a particular *Salmonella* serotype.

microbiota (Sibinelli-Sousa et al., 2022), only 9 effector proteins have been identified and characterized so far (Russell et al., 2012; Benz et al., 2013; Whitney et al., 2013; Koskiniemi et al., 2014; Sana et al., 2016; Sibinelli-Sousa et al., 2020; Amaya et al., 2022; Jurėnas et al., 2022; Lorente-Cobo et al., 2022).

In this study, by means of bioinformatic and comparative genomic analyses, we identified a subset of 23 new SPI-6 T6SS candidate effectors, including peptidoglycan hydrolases, DNases, RNases, deaminases, and ADP-ribosyltransferases. Despite being well conserved, the SPI-6 T6SS gene cluster encodes a variable number of ORFs of unknown function restricted to three variable regions (VR1-3), that include the T6SS effectors previously identified in this species (Blondel et al., 2009). Notably, our analysis showed that every new T6SS effector identified is encoded within one of these variable regions. An interesting observation was that all predicted peptidoglycan targeting effectors are confined to VR1 and VR2. The reason behind this observation remains unclear; however, it is possible that VR1 and VR2 are hot-spots for gene recombination during *Salmonella* evolution, but the lack of mobile genetic elements surrounding these regions does not support this hypothesis. Importantly, in addition to the 4 peptidoglycan targeting effectors reported so far (Tae2, Tae4, Tge2, and Tlde1) (Russell et al., 2012; Benz et al., 2013; Whitney et al., 2013; Sana et al., 2016; Sibinelli-Sousa et al., 2020; Lorente-Cobo et al., 2022), we identified 5 candidate effectors encoded in VR1 and VR2 that presumably degrade peptidoglycan, indicating that this macromolecule is a common target site for *Salmonella* T6SS effectors. Of note, the unannotated ORF encoded in VR1 is the first putative effector that likely cleaves the link between L-Ala and D-Glu of the peptidoglycan peptide stems reported in *Salmonella* and shares homology to the peptidoglycan hydrolase ChiX of *Serratia marcescens* (30% identity and 45.2% similarity at amino acid sequence level) (Owen et al., 2018). This finding expands the peptidoglycan target sites exploited by *Salmonella* T6SS effectors against competing bacteria. On the other hand, the PgP2 and TseH-like candidate effectors are predicted to have redundant peptidoglycan degrading functions with other *Salmonella* T6SS effectors. PgP2 is predicted to have the same L,D transpeptidase exchange activity reported for Tlde1 (Sibinelli-Sousa et al., 2020; Lorente-Cobo et al., 2022), replacing D-Ala by a non-canonical D-amino acid preventing the normal crosslink between mDAP and D-Ala. In addition, the TseH-like candidate effector is a NlpC/P60 endopeptidase family protein (Xu et al., 2010; Altindis et al., 2015; Squeglia et al., 2019) predicted to cleave the covalent link between D-Glu and mDAP, as reported for Tae4 (Benz et al., 2013). These redundant functions suggests that the peptide stems are the main peptidoglycan target sites of *Salmonella* T6SS effectors, as only one identified effector targets the glycoside bonds in this macromolecule corresponds to Tge2 (Whitney et al., 2013). Remarkably, most serotypes encode combinations of T6SS effectors predicted to have hydrolytic activity toward different regions of the peptidoglycan structure. We hypothesize that this assortment of seemingly redundant effectors may improve the efficiency of the bacterial killing process.

The Reprolysin_4 domain found in some candidate effectors is present in zinc-binding metallo-peptidases harboring the binding motif HExxGHxxGxxH of family M12B peptidases. Of note, this motif is also present in the T6SS antibacterial effector SED_RS06335 with putative peptidoglycan hydrolase activity encoded in SPI-19 of *Salmonella* Dublin CT_02021853 (Amaya et al., 2022). The last candidate effector targeting the peptidoglycan identified in our study harbors the Peptidase_M64 protein domain that is also present in the IgA proteinase of *Clostridium ramosum* (Kosowska et al., 2002), recently reclassified as *Thomasclavelia ramosa* (Lawson et al., 2023). The putative immunity proteins of Reprolysin_4 and Peptidase_M64 have a signal peptide and a transmembrane domain, respectively. This suggests that both candidate effectors target the bacterial periplasm.

On the other hand, the VR3 of the SPI-6 T6SS gene cluster encodes a wide variety of effector proteins including domains found in DNases, RNases, deaminases and ADP-ribosyltransferases. Interestingly, most of these domains are fused to the C-terminal of Rhs proteins contributing to diversify the molecular targets of T6SSs in *Salmonella*. This was not unexpected since we have previously shown that the VR3 of SPI-6 encodes a variable number of Rhs elements (Blondel et al., 2009; Amaya et al., 2022) and many Rhs proteins have C-terminal polymorphic endonuclease domains associated with T6SS effectors in *Salmonella* and other bacteria (Zhang et al., 2012; Koskiniemi et al., 2014; Amaya et al., 2022). It is known that Rhs proteins have YD-peptide repeats, which fold into a large β-cage structure that surrounds and protects the C-terminal toxin domain increasing T6SS secretion efficiency (Donato et al., 2020; Jurėnas et al., 2021; Günther et al., 2022). This could explain why many T6SS effectors are associated to these elements.

Altogether, our work expands the repertoire of *Salmonella* T6SS effectors and provides evidence that the SPI-6 T6SS gene cluster harbors a great diversity of antibacterial effectors encoded in three variable regions. One interesting finding of our study is that peptidoglycan hydrolyzing effectors restricted to VR1 and VR2 are highly conserved in *Salmonella* genomes, while effectors targeting nucleic acids and the translation machinery encoded in VR3 are broadly distributed in *Salmonella* serotypes. This suggests that different repertoires of effectors could have an impact on the pathogenic potential and environmental fitness of these bacteria. Importantly, although this study increases the number of putative *Salmonella* antibacterial effectors against competing bacteria, we could not rule out that those targeting nucleic acids encoded in VR3 may also affect eukaryotic cells. This is an important knowledge gap, since no T6SS effector protein identified to date in *Salmonella* has been confirmed to target eukaryotic organisms, despite the clear contribution of *Salmonella* T6SSs to intracellular replication, survival and cytotoxicity inside the host immune cells (Mulder et al., 2012; Blondel et al., 2013; Schroll et al., 2019). Further research is required to address this issue. Finally, we are currently performing experimental work to confirm that each of the 23 candidates identified in our study correspond to *bona fide* T6SS effector proteins.

Data availability statement

The original contributions presented in the study are included in the article/Supplementary material, further inquiries can be directed to the corresponding author.

Author contributions

CB, FA, PB, CS, and DP: conceptualization, formal analysis, validation, writing-original draft preparation, writing review and editing, resources, project administration, and funding acquisition. CB and DP: methodology, investigation, and visualization. CS and DP: supervision. All authors contributed to the article and approved the submitted version.

Funding

DP was supported by Fondo Concursable Proyectos de Investigación Regulares UDLA 2023 DI-13/23. CS was supported by FONDECYT grant 1212075. CB was supported by FONDECYT grant 1201805, ECOS-ANID ECOS200037 and HHMI-Gulbenkian International Research Scholar Grant #55008749. FA was supported by CONICYT/ANID fellowship 21191925.

Conflict of interest

The authors declare that the research was conducted in the absence of any commercial or financial relationships that could be construed as a potential conflict of interest.

Publisher's note

Supplementary material

The Supplementary material for this article can be found online at: https://www.frontiersin.org/articles/10.3389/fmicb.2023.1252344/full#supplementary-material

References

Ahmad, S., Wang, B., Walker, M. D., Tran, H.-K. R., Stogios, P. J., Savchenko, A., et al. (2019). An interbacterial toxin inhibits target cell growth by synthesizing (p)ppApp. *Nature* 575, 674–678. doi: 10.1038/s41586-019-1735-9

Altindis, E., Dong, T., Catalano, C., and Mekalanos, J. (2015). Secretome analysis of *Vibrio cholerae* type VI secretion system reveals a new effector–immunity pair. *mBio* 6:e00075. doi: 10.1128/mBio.00075-15

Amaya, F. A., Blondel, C. J., Barros-Infante, M. F., Rivera, D., Moreno-Switt, A. I., Santiviago, C. A., et al. (2022). Identification of type VI secretion systems effector proteins that contribute to interbacterial competition in *Salmonella* Dublin. *Front. Microbiol.* 13:811932. doi: 10.3389/fmicb.2022.811932

Bao, H., Zhao, J.-H., Zhu, S., Wang, S., Zhang, J., Wang, X.-Y., et al. (2019). Genetic diversity and evolutionary features of type VI secretion systems in *Salmonella*. *Future Microbiol.* 14, 139–154. doi: 10.2217/fmb-2018-0260

Benz, J., Reinstein, J., and Meinhart, A. (2013). Structural insights into the effector - immunity system Tae4/Tai4 from *Salmonella typhimurium*. *PLoS One* 8:e67362. doi: 10.1371/journal.pone.0067362

Berni, B., Soscia, C., Djermoun, S., Ize, B., and Bleves, S. (2019). A type VI secretion system trans-kingdom effector is required for the delivery of a novel antibacterial toxin in *Pseudomonas aeruginosa*. *Front. Microbiol.* 10:1218. doi: 10.3389/fmicb.2019.01218

Blondel, C. J., Jiménez, J. C., Contreras, I., and Santiviago, C. A. (2009). Comparative genomic analysis uncovers 3 novel loci encoding type six secretion systems differentially distributed in *Salmonella* serotypes. *BMC Genomics* 10:354. doi: 10.1186/1471-2164-10-354

Blondel, C. J., Jiménez, J. C., Leiva, L. E., Alvarez, S. A., Pinto, B. I., Contreras, F., et al. (2013). The type VI secretion system encoded in *Salmonella* Pathogenicity Island 19 is required for *Salmonella enterica* serotype Gallinarum survival within infected macrophages. *Infect. Immun.* 81, 1207–1220. doi: 10.1128/iai.01165-12

Blondel, C. J., Yang, H.-J., Castro, B., Chiang, S., Toro, C. S., Zaldívar, M., et al. (2010). Contribution of the type VI secretion system encoded in SPI-19 to chicken colonization by *Salmonella enterica* serotypes Gallinarum and Enteritidis. *PLoS One* 5:e11724. doi: 10.1371/journal.pone.0011724

Brackmann, M., Nazarov, S., Wang, J., and Basler, M. (2017). Using force to punch holes: mechanics of contractile nanomachines. *Trends Cell Biol.* 27, 623–632. doi: 10.1016/j.tcb.2017.05.00

Chassaing, B., and Cascales, E. (2018). Antibacterial weapons: targeted destruction in the microbiota. *Trends Microbiol.* 26, 329–338. doi: 10.1016/j.tim.2018.01.006

Cherrak, Y., Flaugnatti, N., Durand, E., Journet, L., and Cascales, E. (2019). Structure and activity of the type VI secretion system. *Microbiol. Spectr.* 7:10.1128/microbiolspec.PSIB-0031-2019. doi: 10.1128/microbiolspec.PSIB-0031-2019

Coulthurst, S. (2019). The type VI secretion system: a versatile bacterial weapon. *Microbiology* 165, 503–515. doi: 10.1099/mic.0.000789

Coyne, M. J., and Comstock, L. E. (2019). Type VI secretion systems and the gut microbiota. *Microbiol. Spectr.* 7:10.1128/microbiolspec.PSIB-0009-2018. doi: 10.1128/microbiolspec.PSIB-0009-2018

Darling, A. C. E., Mau, B., Blattner, F. R., and Perna, N. T. (2004). Mauve: multiple alignment of conserved genomic sequence with rearrangements. *Genome Res.* 14, 1394–1403. doi: 10.1101/gr.2289704

Diniz, J. A., and Coulthurst, S. J. (2015). Intraspecies competition in *Serratia marcescens* is mediated by type VI-secreted Rhs effectors and a conserved effector-associated accessory protein. *J. Bacteriol.* 197, 2350–2360. doi: 10.1128/jb.00199-15

Donato, S. L., Beck, C. M., Garza-Sánchez, F., Jensen, S. J., Ruhe, Z. C., Cunningham, D. A., et al. (2020). The β-encapsulation cage of rearrangement hotspot (Rhs) effectors is required for type VI secretion. *Proc. Natl. Acad. Sci. U. S. A.* 117, 33540–33548. doi: 10.1073/pnas.1919350117

Durand, E., Cambillau, C., Cascales, E., and Journet, L. (2014). VgrG, Tae, Tle, and beyond: the versatile arsenal of type VI secretion effectors. *Trends Microbiol.* 22, 498–507. doi: 10.1016/j.tim.2014.06.004

Finn, R. D., Bateman, A., Clements, J., Coggill, P., Eberhardt, R. Y., Eddy, S. R., et al. (2014). Pfam: the protein families database. *Nucleic Acids Res.* 42, D222–D230. doi: 10.1093/nar/gkt1223

Fookes, M., Schroeder, G. N., Langridge, G. C., Blondel, C. J., Mammina, C., Connor, T. R., et al. (2011). *Salmonella bongori* provides insights into the evolution of the salmonellae. *PLoS Pathog.* 7:e1002191. doi: 10.1371/journal.ppat.1002191

GBD 2017 Non-Typhoidal *Salmonella* Invasive Disease Collaborators (2019). The global burden of non-typhoidal *Salmonella* invasive disease: a systematic analysis for the global burden of disease study 2017. *Lancet Infect. Dis.* 19, 1312–1324. doi: 10.1016/s1473-3099(19)30418-9

Grimont, P. A. D., and Weill, F.-X. (2007). *Antigenic formulae of the Salmonella serovars*. *9* WHO Collaborating Centre for Reference and Research on *Salmonella*, Institut Pasteur, Paris.

Günther, P., Quentin, D., Ahmad, S., Sachar, K., Gatsogiannis, C., Whitney, J. C., et al. (2022). Structure of a bacterial Rhs effector exported by the type VI secretion system. *PLoS Pathog.* 18:e1010182. doi: 10.1371/journal.ppat.1010182

Hespanhol, J. T., Sanchez-Limache, D. E., Nicastro, G. G., Mead, L., Llontop, E. E., Chagas-Santos, G., et al. (2022). Antibacterial T6SS effectors with a VRR-Nuc domain are structure-specific nucleases. *eLife* 11:e82437. doi: 10.7554/eLife.82437

Issenhuth-Jeanjean, S., Roggentin, P., Mikoleit, M., Guibourdenche, M., de Pinna, E., Nair, S., et al. (2014). Supplement 2008–2010 (no. 48) to the white–Kauffmann–Le minor scheme. *Res. Microbiol.* 165, 526–530. doi: 10.1016/j.resmic.2014.07.004

Jiang, F., Waterfield, N. R., Yang, J., Yang, G., and Jin, Q. (2014). A *Pseudomonas aeruginosa* type VI secretion phospholipase D effector targets both prokaryotic and eukaryotic cells. *Cell Host Microbe* 15, 600–610. doi: 10.1016/j.chom.2014.04.010

Jurėnas, D., Rey, M., Byrne, D., Chamot-Rooke, J., Terradot, L., and Cascales, E. (2022). *Salmonella* antibacterial Rhs polymorphic toxin inhibits translation through ADP-ribosylation of EF-Tu P-loop. *Nucleic Acids Res.* 50, 13114–13127. doi: 10.1093/nar/gkac1162

Jurėnas, D., Rosa, L. T., Rey, M., Chamot-Rooke, J., Fronzes, R., and Cascales, E. (2021). Mounting, structure and autocleavage of a type VI secretion-associated Rhs polymorphic toxin. *Nat. Commun.* 12:6998. doi: 10.1038/s41467-021-27388-0

Kanehisa, M., Goto, S., Kawashima, S., and Nakaya, A. (2002). The KEGG databases at GenomeNet. *Nucleic Acids Res.* 30, 42–46. doi: 10.1093/nar/30.1.42

Katoh, K., Rozewicki, J., and Yamada, K. D. (2017). MAFFT online service: multiple sequence alignment, interactive sequence choice and visualization. *Brief. Bioinform.* 20, 1160–1166. doi: 10.1093/bib/bbx108

Koskiniemi, S., Garza-Sánchez, F., Sandegren, L., Webb, J. S., Braaten, B. A., Poole, S. J., et al. (2014). Selection of orphan Rhs toxin expression in evolved *Salmonella enterica* serovar Typhimurium. *PLoS Genet.* 10:e1004255. doi: 10.1371/journal.pgen.1004255

Kosowska, K., Reinholdt, J., Rasmussen, L. K., Sabat, A., Potempa, J., Kilian, M., et al. (2002). The *Clostridium ramosum* IgA proteinase represents a novel type of metalloendopeptidase. *J. Biol. Chem.* 277, 11987–11994. doi: 10.1074/jbc.M110883200

Kumar, S., Stecher, G., and Tamura, K. (2016). MEGA7: molecular evolutionary genetics analysis version 7.0 for bigger datasets. *Mol. Biol. Evol.* 33, 1870–1874. doi: 10.1093/molbev/msw054

Lawson, P. A., Saavedra-Perez, L., and Sankaranarayanan, K. (2023). Reclassification of *Clostridium cocleatum*, *Clostridium ramosum*, *clostridium spiroforme* and *Clostridium saccharogumia* as *Thomasclavelia cocleata* gen. Nov., comb. nov., *Thomasclavelia ramosa* comb. nov., gen. Nov., *Thomasclavelia spiroformis* comb. nov. and *Thomasclavelia saccharogumia* comb. nov. *Int. J. Syst. Evol. Microbiol.* 73:10.1099/ijsem.0.005694. doi: 10.1099/ijsem.0.005694

Lorente-Cobo, N., Sibinelli-Sousa, S., Biboy, J., Vollmer, W., Bayer-Santos, E., and Prehna, G. (2022). Molecular characterization of the type VI secretion system effector Tlde1a reveals a structurally altered LD-transpeptidase fold. *J. Biol. Chem.* 298:102556. doi: 10.1016/j.jbc.2022.102556

Lu, S., Wang, J., Chitsaz, F., Derbyshire, M. K., Geer, R. C., Gonzales, N. R., et al. (2019). CDD/SPARCLE: the conserved domain database in 2020. *Nucleic Acids Res.* 48, D265–D268. doi: 10.1093/nar/gkz991

Ma, A. T., and Mekalanos, J. J. (2010). *In vivo* actin cross-linking induced by *Vibrio cholerae* type VI secretion system is associated with intestinal inflammation. *Proc. Natl. Acad. Sci.* 107, 4365–4370. doi: 10.1073/pnas.0915156107

Ma, J., Sun, M., Dong, W., Pan, Z., Lu, C., and Yao, H. (2017). PAAR-Rhs proteins harbor various C-terminal toxins to diversify the antibacterial pathways of type VI secretion systems. *Environ. Microbiol.* 19, 345–360. doi: 10.1111/1462-2920.13621

Monjarás Feria, J., and Valvano, M. A. (2020). An overview of anti-eukaryotic T6SS effectors. *Front. Cell. Infect. Microbiol.* 10:584751. doi: 10.3389/fcimb.2020.584751

Mulder, D. T., Cooper, C. A., and Coombes, B. K. (2012). Type VI secretion system-associated gene clusters contribute to pathogenesis of *Salmonella enterica* serovar Typhimurium. *Infect. Immun.* 80, 1996–2007. doi: 10.1128/iai.06205-11

Notredame, C., Higgins, D. G., and Heringa, J. (2000). T-coffee: a novel method for fast and accurate multiple sequence alignment. *J. Mol. Biol.* 302, 205–217. doi: 10.1006/jmbi.2000.4042

Owen, R. A., Fyfe, P. K., Lodge, A., Biboy, J., Vollmer, W., Hunter, W. N., et al. (2018). Structure and activity of ChiX: a peptidoglycan hydrolase required for chitinase secretion by *Serratia marcescens*. *Biochem. J.* 475, 415–428. doi: 10.1042/BCJ20170633

Pezoa, D., Blondel, C. J., Silva, C. A., Yang, H.-J., Andrews-Polymenis, H., Santiviago, C. A., et al. (2014). Only one of the two type VI secretion systems encoded in the *Salmonella enterica* serotype Dublin genome is involved in colonization of the avian and murine hosts. *Vet. Res.* 45:2. doi: 10.1186/1297-9716-45-2

Pezoa, D., Yang, H.-J., Blondel, C. J., Santiviago, C. A., Andrews-Polymenis, H. L., and Contreras, I. (2013). The type VI secretion system encoded in SPI-6 plays a role in gastrointestinal colonization and systemic spread of *Salmonella enterica* serovar Typhimurium in the chicken. *PLoS One* 8:e63917. doi: 10.1371/journal.pone.0063917

Pissaridou, P., Allsopp, L. P., Wettstadt, S., Howard, S. A., Mavridou, D. A. I., and Filloux, A. (2018). The *Pseudomonas aeruginosa* T6SS-VgrG1b spike is topped by a PAAR protein eliciting DNA damage to bacterial competitors. *Proc. Natl. Acad. Sci.* 115, 12519–12524. doi: 10.1073/pnas.1814181115

Robert, X., and Gouet, P. (2014). Deciphering key features in protein structures with the new ENDscript server. *Nucleic Acids Res.* 42, W320–W324. doi: 10.1093/nar/gku316

Russell, A. B., Singh, P., Brittnacher, M., Bui, N. K., Hood, R. D., Carl, M. A., et al. (2012). A widespread bacterial type VI secretion effector superfamily identified using a heuristic approach. *Cell Host Microbe* 11, 538–549. doi: 10.1016/j.chom.2012.04.007

Rutherford, K., Parkhill, J., Crook, J., Horsnell, T., Rice, P., Rajandream, M.-A., et al. (2000). Artemis: sequence visualization and annotation. *Bioinformatics* 16, 944–945. doi: 10.1093/bioinformatics/16.10.944

Sana, T. G., Flaugnatti, N., Lugo, K. A., Lam, L. H., Jacobson, A., Baylot, V., et al. (2016). *Salmonella* Typhimurium utilizes a T6SS-mediated antibacterial weapon to establish in the host gut. *Proc. Natl. Acad. Sci.* 113, E5044–E5051. doi: 10.1073/pnas.1608858113

Schroll, C., Huang, K., Ahmed, S., Kristensen, B. M., Pors, S. E., Jelsbak, L., et al. (2019). The SPI-19 encoded type-six secretion-systems (T6SS) of *Salmonella enterica* serovars Gallinarum and Dublin play different roles during infection. *Vet. Microbiol.* 230, 23–31. doi: 10.1016/j.vetmic.2019.01.006

Sibinelli-Sousa, S., de Araújo-Silva, A. L., Hespanhol, J. T., and Bayer-Santos, E. (2022). Revisiting the steps of *Salmonella* gut infection with a focus on antagonistic interbacterial interactions. *FEBS J.* 289, 4192–4211. doi: 10.1111/febs.16211

Sibinelli-Sousa, S., Hespanhol, J. T., Nicastro, G. G., Matsuyama, B. Y., Mesnage, S., Patel, A., et al. (2020). A family of T6SS antibacterial effectors related to L,D-transpeptidases targets the peptidoglycan. *Cell Rep.* 31:107813. doi: 10.1016/j.celrep.2020.107813

Sigrist, C. J. A., de Castro, E., Cerutti, L., Cuche, B. A., Hulo, N., Bridge, A., et al. (2013). New and continuing developments at PROSITE. *Nucleic Acids Res.* 41, D344–D347. doi: 10.1093/nar/gks1067

Silverman, J. M., Agnello, D. M., Zheng, H., Andrews, B. T., Li, M., Catalano, C. E., et al. (2013). Haemolysin coregulated protein is an exported receptor and chaperone of type VI secretion substrates. *Mol. Cell* 51, 584–593. doi: 10.1016/j.molcel.2013.07.025

Squeglia, F., Moreira, M., Ruggiero, A., and Berisio, R. (2019). The cell wall hydrolytic NlpC/P60 endopeptidases in mycobacterial cytokinesis: a structural perspective. *Cells* 8:609. doi: 10.3390/cells8060609

Srikannathasan, V., English, G., Bui, N. K., Trunk, K., O'Rourke, P. E. F., Rao, V. A., et al. (2013). Structural basis for type VI secreted peptidoglycan DL-endopeptidase function, specificity and neutralization in *Serratia marcescens*. *Acta Crystallogr. Sect. D Biol. Crystallogr.* 69, 2468–2482. doi: 10.1107/s0907444913022725

Sullivan, M. J., Petty, N. K., and Beatson, S. A. (2011). Easyfig: a genome comparison visualizer. *Bioinformatics* 27, 1009–1010. doi: 10.1093/bioinformatics/btr039

Taboada, B., Estrada, K., Ciria, R., and Merino, E. (2018). Operon-mapper: a web server for precise operon identification in bacterial and archaeal genomes. *Bioinformatics* 34, 4118–4120. doi: 10.1093/bioinformatics/bty496

Tang, J. Y., Bullen, N. P., Ahmad, S., and Whitney, J. C. (2018). Diverse NADase effector families mediate interbacterial antagonism via the type VI secretion system. *J. Biol. Chem.* 293, 1504–1514. doi: 10.1074/jbc.ra117.000178

Ting, S.-Y., Bosch, D. E., Mangiameli, S. M., Radey, M. C., Huang, S., Park, Y.-J., et al. (2018). Bifunctional immunity proteins protect bacteria against FtsZ-targeting ADP-ribosylating toxins. *Cells* 175, 1380–1392.e14. doi: 10.1016/j.cell.2018.09.037

Uzzau, S., Brown, D. J., Wallis, T., Rubino, S., Leori, G., Bernard, S., et al. (2000). Host adapted serotypes of *Salmonella enterica*. *Epidemiol. Amp. Infect.* 125, 229–255. doi: 10.1017/s0950268899004379

Wang, J., Yang, B., Leier, A., Marquez-Lago, T. T., Hayashida, M., Rocker, A., et al. (2018). Bastion6: a bioinformatics approach for accurate prediction of type VI secreted effectors. *Bioinformatics* 34, 2546–2555. doi: 10.1093/bioinformatics/bty155

Whitney, J. C., Beck, C. M., Goo, Y. A., Russell, A. B., Harding, B. N., Leon, J. A. D., et al. (2014). Genetically distinct pathways guide effector export through the type VI secretion system. *Mol. Microbiol.* 92, 529–542. doi: 10.1111/mmi.12571

Whitney, J. C., Chou, S., Russell, A. B., Biboy, J., Gardiner, T. E., Ferrin, M. A., et al. (2013). Identification, structure, and function of a novel type VI secretion peptidoglycan glycoside hydrolase effector-immunity pair. *J. Biol. Chem.* 288, 26616–26624. doi: 10.1074/jbc.m113.488320

Whitney, J. C., Quentin, D., Sawai, S., LeRoux, M., Harding, B. N., Ledvina, H. E., et al. (2015). An interbacterial NAD(P)$^+$ glycohydrolase toxin requires elongation factor Tu for delivery to target cells. *Cells* 163, 607–619. doi: 10.1016/j.cell.2015.09.027

Wood, T. E., Howard, S. A., Förster, A., Nolan, L. M., Manoli, E., Bullen, N. P., et al. (2019). The *Pseudomonas aeruginosa* T6SS delivers a periplasmic toxin that disrupts bacterial cell morphology. *Cell Rep.* 29, 187–201.e7. doi: 10.1016/j.celrep.2019.08.094

Xian, H., Yuan, Y., Yin, C., Wang, Z., Ji, R., Chu, C., et al. (2020). The SPI-19 encoded T6SS is required for *Salmonella* Pullorum survival within avian macrophages and initial colonization in chicken dependent on inhibition of host immune response. *Vet. Microbiol.* 250:108867. doi: 10.1016/j.vetmic.2020.108867

Xu, Q., Abdubek, P., Astakhova, T., Axelrod, H. L., Bakolitsa, C., Cai, X., et al. (2010). Structure of the γ-D-glutamyl-L-diamino acid endopeptidase YkfC from *Bacillus cereus* in complex with L-ala-γ-D-Glu: insights into substrate recognition by NlpC/P60 cysteine peptidases. *Acta crystallographica. Sect. F Struct. Biol. Crystallizat. Commun.* 66, 1354–1364. doi: 10.1107/S1744309110021214

Zhang, D., de Souza, R. F., Anantharaman, V., Iyer, L. M., and Aravind, L. (2012). Polymorphic toxin systems: comprehensive characterization of trafficking modes, processing, mechanisms of action, immunity and ecology using comparative genomics. *Biol. Direct* 7:18. doi: 10.1186/1745-6150-7-18

Zhang, J., Guan, J., Wang, M., Li, G., Djordjevic, M., Tai, C., et al. (2023). SecReT6 update: a comprehensive resource of bacterial type VI secretion systems. *Sci. China Life Sci.* 66, 626–634. doi: 10.1007/s11427-022-2172-x

Zimmermann, L., Stephens, A., Nam, S.-Z., Rau, D., Kübler, J., Lozajic, M., et al. (2017). A completely reimplemented MPI bioinformatics toolkit with a new HHpred server at its core. *J. Mol. Biol.* 430, 2237–2243. doi: 10.1016/j.jmb.2017.12.007

frontiers | Frontiers in Microbiology

TYPE Original Research
PUBLISHED 23 August 2023
DOI 10.3389/fmicb.2023.1232490

OPEN ACCESS

EDITED BY
Patrick J. Naughton,
Ulster University, United Kingdom

REVIEWED BY
Martine Denis,
de l'Environnement et du Travail (ANSES), France
Veronica Cibin,
Experimental Zooprophylactic Institute of the Venezie (IZSVe), Italy

*CORRESPONDENCE
Raúl Carlos Mainar-Jaime
✉ rcmainar@unizar.es

RECEIVED 31 May 2023
ACCEPTED 25 July 2023
PUBLISHED 23 August 2023

CITATION
Bernad-Roche M, Marín-Alcalá CM, Cebollada-Solanas A, de Blas I and Mainar-Jaime RC (2023) Building a predictive model for assessing the risk of *Salmonella* shedding at slaughter in fattening pigs. *Front. Microbiol.* 14:1232490. doi: 10.3389/fmicb.2023.1232490

Building a predictive model for assessing the risk of *Salmonella* shedding at slaughter in fattening pigs

María Bernad-Roche[1], Clara María Marín-Alcalá[2], Alberto Cebollada-Solanas[3], Ignacio de Blas[1] and Raúl Carlos Mainar-Jaime[1]*

[1]Departamento de Patología Animal, Facultad de Veterinaria, Instituto Agroalimentario de Aragón-IA2, Universidad de Zaragoza-CITA, Zaragoza, Spain, [2]Departamento de Ciencia Animal, Centro de Investigación y Tecnología Agroalimentaria de Aragón, Instituto Agroalimentario de Aragón-IA2, Universidad de Zaragoza-CITA, Zaragoza, Spain, [3]Unidad de Biocomputación, Instituto Aragonés de Ciencias de la Salud (IACS/IIS Aragón), Centro de Investigación Biomédica de Aragón (CIBA), Zaragoza, Spain

Salmonellosis continues to be a major cause of foodborne outbreaks worldwide, and pigs are one of the main sources of human infection. *Salmonella* pork contamination is a major concern for abattoirs and is related to the presence of *Salmonella* in pigs' feces at slaughter. Being able to predict the risk of *Salmonella* shedding in pigs arriving at the slaughterhouse could help mitigate abattoir and carcass contamination. For this purpose, 30 batches of 50 pigs each were selected from 30 different fattening units. The pigs were tagged and bled for the detection of antibodies against *Salmonella* approximately one month before slaughter. Pooled floor fecal samples were also collected from 10 pens per unit for *Salmonella* detection, and a questionnaire on biosecurity was administered to each farm. At the abattoir, colon content was collected from each tagged pig for the *Salmonella* shedding assessment. A predictive model for *Salmonella* shedding at slaughter was built with two-third of the pigs by employing random-effects logistic regression analysis, with *Salmonella* shedding as the dependent variable and pig serology and other farm/environmental characteristics as the independent variables. The model included farm as the grouping factor. Data from the remaining one-third of the pigs were used for model validation. Out of 1,500 pigs initially selected, 1,341 were identified at the abattoir and analyzed. *Salmonella* was detected in 13 (43.3%; 95%CI = 27.4–60.8) of the fattening units. The mean batch seroprevalence (cut-off OD% ≥40) among the fattening units was 31.7% (95%CI = 21.8–41.0), and a total of 316 pigs (23.6%; 95%CI = 21.4–25.9) shed *Salmonella* at slaughter. The model predicted reasonably well (Area under the curve = 0.76; $P < 0.05$) whether a pig would shed *Salmonella* at slaughter, with estimates of sensitivity and specificity at 71.6% and 73.6%, respectively. Serology, the percentage of *Salmonella*-positive pens on the farm, and the internal biosecurity score were significantly associated ($P < 0.05$) with *Salmonella* shedding at the abattoir, and several scenarios were observed by the model. The study highlighted that although serology may be helpful for identifying batches of pigs at risk of shedding *Salmonella* upon their arrival at the abattoir, it may not be necessary in some scenarios.

KEYWORDS

prediction model, *salmonella* control, abattoir, shedding, swine

1. Introduction

Salmonellosis remains one of the most frequent foodborne zoonoses in the EU, with 60,050 human cases (15.7/100,000 inhabitants) in 2021. In the last year, *S.* Enteritidis, *S.* Typhimurium, and the monophasic variant of *S.* Typhimurium (mST) were among the most reported serovars, with the latter two mainly associated with contaminated pork (EFSA and ECDC, 2022).

In contrast to the fowl industry, to date, few EU countries have established National Control Programs (NCPs) against pig salmonellosis. On-farm *Salmonella* control programs in fattening swine were expected to be initiated in all EU after Regulation EC No. 2160/2003. However, most EU countries did not implement them, likely because they were not considered cost-effective (Anonymous, 2011).

The first comprehensive *Salmonella* NCP for pigs in Europe was established in Sweden in the 60s (Wierup, 2006) after a major food-borne outbreak in 1953 (Lundbeck et al., 1955), which was followed later by Norway, Finland, and Denmark in 1995 (Mousing et al., 1997; Maijala et al., 2005; Lyngstad et al., 2007). All but Denmark's were focused on eradication and had bacteriological analyses as the keystone. Denmark developed its own NCP based on both bacteriological and serological analyses, and its focus was mainly on *Salmonella* control. In all cases, the farm-level prevalence was initially low, and strict measures were enforced when *Salmonella* was found. These measures included the application of economic penalties. Positive results were observed in reducing the overall *Salmonella* prevalence in pig carcasses but at a high cost (Anonymous, 2011).

After the success of the Scandinavian action plans and along with EU regulation, new NCPs followed suit in other European countries: Germany and United Kingdom in 2002 (Osterkorn et al., 2001; BPEX, 2002; Snary et al., 2010), Ireland in 2003 (Statutory Instrument No. 165/2002), the Netherlands in 2005 (Hanssen et al., 2007), and Belgium in 2007 (Méroc et al., 2012). In general, these programs were similar to the Danish NCP, focusing on control, but they were based mostly on serological analysis of a relatively small number of pigs per batch slaughtered. Thus, pig herds were categorized into three different risk groups: low-risk (I), medium-risk (II), and high-risk herds (III). Category III herds had to undertake farm-specific activities aimed at reducing their *Salmonella* exposure and, accordingly, their *Salmonella* seroprevalence. Although no penalties were generally applied, incentives were offered to farmers in some countries, such as to be included in pork quality assurance schemes, particularly, the Qualität und Sicherheit (QS) in Germany, the British Quality Assured Pork (BQAP) in the UK, the Bord Bía Quality Assurance Scheme in Ireland, and the IKB Nederland Varkens in The Netherlands.

Despite these efforts, there is no evidence in the scientific literature of any significant change in swine *Salmonella* infection reduction in pigs or in human cases related to pork consumption, and the overall *Salmonella* seroprevalence remains stable in pigs in many of these non-Scandinavian countries (Correia-Gomes et al., 2021). Only Germany recently reported some positive results after more than 20 years since the implementation of its program (Anonymous, 2021). Meanwhile, the United Kingdom suspended its serological monitoring in 2012 (Anonymous, 2012), and Belgium, which also suspended its serological monitoring, only has maintained veterinary advice on the control of pig salmonellosis (Anonymous, 2015).

The overall lack of efficacy and the high cost of the on-farm control of pig salmonellosis, especially for countries with large pig census (Anonymous, 2011; Gavin et al., 2018), suggest the need to revisit these NCPs. Since in the EU, pig salmonellosis is by far a public health problem, not a pig health problem, a change in the programs' main objective would be advisable. Asymptomatic *Salmonella*-infected pigs commonly arrive at the abattoir for slaughter [European Food Safety Authority (EFSA), 2011], and they are particularly prone to *Salmonella* shedding (Rostagno et al., 2010). Thus, live pigs, through their feces, are a major source of abattoir environmental *Salmonella* contamination, likely being the main source of carcass contamination and, consequently, pork and related products (Argüello et al., 2013a; Swart et al., 2016; Marin et al., 2020). Thus, the main objective of a NCP aimed at reducing the incidence of human salmonellosis may be to focus on finding ways to minimize *Salmonella* contamination in abattoirs, which in the short term, could be more cost-effective than trying to stop the infection within pig farms. Being able to predict the likelihood that a pig will shed *Salmonella* upon its arrival at the abattoir may be the first step to reaching this objective.

Casanova-Higes et al. (2017) observed that pigs shedding *Salmonella* at slaughter seroconverted earlier during the fattening period than non-shedder pigs. A subsequent study showed that on-farm serology could, to some extent, help predict the probability of a pig shedding *Salmonella* at slaughter, thus allowing for the prompt implementation of on-farm and slaughter interventions to reduce the likelihood of abattoir environmental contamination with *Salmonella* (Mainar-Jaime et al., 2018). However, since these studies were carried out on a small number of pig batches from a single *Salmonella*-positive farm and with no additional information, their results should be confirmed further.

Thus, the main objective of this study was to assess whether serology and other farm and/or environmental characteristics (*Salmonella* pen contamination, farm biosecurity, season, etc.) could be used as predictors of *Salmonella* shedding at the abattoir. By predicting the risk of *Salmonella* shedding for a given batch of pigs upon their arrival at the abattoir, subsequent carcass contamination could be prevented by implementing both on-farm and abattoir control strategies.

2. Materials and methods

2.1. Animal selection and sampling

Between December 2019 and March 2022, 30 batches of 50 pigs each (a total of 1,500 pigs) from 30 different fattening units (average size ≈1,000 pigs/unit) were chosen for this study. Farms were selected based on farmers' willingness to collaborate and the availability of veterinary services.

The 50 animals from each fattening unit were selected approximately 3-4 weeks before slaughter, as suggested in a previous study (Mainar-Jaime et al., 2018). They were chosen from

different pens along the fattening units (from 1 to 3 pigs/pen) among the first pigs of the unit to be sent for slaughter (the heaviest ones). At that moment, pigs were ear-tagged, and their blood samples were taken for the detection of specific antibodies against *Salmonella*. In addition, pooled floor fecal (FF) samples were collected from 10 pens distributed at different points of the fattening unit (corners, middle areas, and right and left to aisles) for the detection of *Salmonella* on the farm.

The selected pigs were loaded onto a clean and disinfected truck along with other pigs from the same fattening unit (up to approximately 200 pigs/truck); thus, they were not mixed with pigs from other different units. Transport to slaughter usually occurred on Monday mornings, but they were not necessarily the first batches to be slaughtered that day. In general, farms were not more than 2 h away from the abattoir (mean distance farm to abattoir: 33 km; 95%CI = 25.4–40.5). At the abattoir, pigs were kept in a clean pen without mixing them with pigs of other origins. Slaughtering was performed within the first two hours after arrival. All the procedures followed the usual abattoir routine, and no specific changes were made for this study. Tagged animals were identified at the slaughter line, and after evisceration, a minimum of 25 g of intestinal (colon) content (IC) was collected from the gastrointestinal package of each of these pigs for assessing their *Salmonella* shedding status. After collection, all samples were transported directly to the laboratory for immediate processing.

2.2. Farm biosecurity questionnaire

A questionnaire on the different aspects of farm biosecurity was filled in by the veterinarian responsible for each farm included in the study. This questionnaire was based on that available through Biocheck. Gent BV, Belgium (https://biocheckgent.com/en). Briefly, it consisted of a risk-based scoring system and retrieved information on external and internal farm biosecurity. Regarding external biosecurity, the factors considered were the purchase of animals, transport of animals, removal of manure and dead animals, feed, water and equipment supply, personnel and visitors, vermin and bird control, and environmental region. Regarding internal biosecurity, the factors considered were disease management, fattening unit management, measures between compartments and the use of equipment, and cleaning and disinfection. For each category, a score between 0 for the worst scenario and 100 for the best biosecurity level was obtained. A final score on the overall farm biosecurity level, which was computed as the average of external and internal biosecurity scores, could then be calculated. These results could be further compared to national score averages.

2.3. Serological analysis

Sera were analyzed by an indirect enzyme-linked immunosorbent assay (ELISA) for the presence of specific antibodies against *Salmonella* (Herdcheck Swine *Salmonella* test, IDEXX Laboratories, Westbrook, ME, USA). This test is designed to detect antibodies to the LPS *Salmonella* B, C1, and D serogroups (O-antigens 1, 4, 5, 6, 7, and 12), which are the most common serotypes isolated in pigs. Individual results were presented as optical density percentages (OD%) as compared to the control sera. For farm seroprevalence estimates, a high cut-off value (OD% $\geq$40) was used to deem a pig as seropositive. Given the limited test's sensitivity and specificity on field samples (73% and 95%, respectively; Mainar-Jaime et al., 2008), high OD% values allowed for the minimization of the number of false-positive individual results.

2.4. *Salmonella* isolation and identification of the main serotypes

Salmonella identification from FF and IC samples was carried out following the standard ISO 6579-1:2017 method. A colony from each *Salmonella*-positive culture was selected for PCR identification of the two major serotypes of concern in the pig industry, i.e., *S.* Typhimurium and the mST. These two serotypes are the second and third most prevalent in human cases, and a high proportion of them are related to pig sources (EFSA and ECDC, 2022). For that purpose, a duplex PCR that simultaneously amplifies a fragment between the genes *fljB* and *fljA* and the phase-2 flagellar gene (*fljB*) was used (Tennant et al., 2010; Barco et al., 2011).

2.5. Pulsed-field gel electrophoresis

Cross-contamination may occur during transport and lairage (Argüello et al., 2013a). Therefore, to confirm the spread of isolates from the farm to the slaughter, the genetic relationship between the *Salmonella* strains shed by pigs at slaughter (IC samples) and those isolated from farm FF samples was assessed by performing PFGE analysis (Ribot et al., 2006). PFGE analysis was performed on isolates identified as *S.* Typhimurium or mST.

Only isolates from FF samples and IC samples from the same farm that showed the same serotype were analyzed. If several isolates met this criterion, then a maximum of three pig isolates and three FF isolates per farm were analyzed. PFGE pattern analysis was performed using the BIONUMERICS software (version 6; Applied Maths, Sint-Martens-Latem, Belgium) with Dice's coefficient and the unweighted pair group method with arithmetic averages (UPGMA dendrogram type), employing a position tolerance of 2.0% and optimization of 2.0%. Fragments less than 30 kb long were not included in the final analysis as they are produced by plasmid DNA (Kariuki et al., 2000; Peters et al., 2003; Cooke et al., 2008).

2.6. Statistical analyses and *Salmonella* shedding predictive model development

Estimates of on-farm *Salmonella* seroprevalence, pen prevalence, and prevalence of *Salmonella* shedding at slaughter with their corresponding 95% confidence intervals (95%CI) were calculated for the fattening units.

To create the predictive model for *Salmonella* shedding at slaughter, a random-effects logistic regression analysis was conducted, with *Salmonella*-shedding pigs at the abattoir (yes/no) as the dependent variable. Serology (OD% values), internal, external, and total biosecurity, percentage of *Salmonella*-positive pens in the farm (three categories: no positive pens, less than 20% of positive pens, ≥30% of positive pens), and other farm and/or environmental characteristics that may be related to *Salmonella* infection, such as the season of sampling (spring, summer, autumn, and winter), the distance (in km) and time (in minutes) of transport from the farm to the abattoir, and the time elapsed between farm and abattoir samplings (in days) were the independent variables. The presence of *S.* Typhimurium/mST in the farm (yes/no) was also included in the model as *Salmonella* shedding, and immune response could be related to these serotypes (Ivanek et al., 2012). Since animals were grouped within farms, the farm was considered a random (grouping) variable to account for the correlation between individual pigs coming from the same farm (i.e., intraclass correlation, ICC). Two-thirds of the study population, which was defined as the total number of pigs for which all required information was obtained, were randomly selected to run the main model. The remaining third of the pigs were used for model validation (reproducibility).

Receiver operating characteristic (ROC) curves were built from potential logistic models, and the area under the curve (AUC) was used as a method for selecting the best predictive model (Greiner et al., 2000). Final estimates of the probability of shedding *Salmonella* were calculated for each pig from the selected logistic regression equation, and different scenarios were identified according to the different levels of the variables included in the model. Furthermore, a cut-off value was selected, based on Pythagoras' theorem-based method, which is a new approach based on the smallest sum of squares of 1-sensitivity and 1-specificity, to assess the diagnostic accuracy of the prediction when sensitivity (Se) and specificity (Sp) were valued equally. The cut-point chosen by this method always selects the one closest to the top-left corner of the ROC curve, regardless of its shape (Froud and Abel, 2014).

Statistical analyses were performed using the STATA software (STATA/IC 12.1. StataCorp. LP, College Station, TX, USA) and MedCalc® statistical software version 20.215 (MedCalc Software Ltd, Ostend, Belgium).

3. Results

3.1. Farm biosecurity and *Salmonella* contamination at the farm

The 30 selected farms presented a mean overall biosecurity score of 73.31% (ranging from 51% to 84%) (Figure 1). The mean internal biosecurity score for these farms was 67.80% (min.: 40%, max.: 82%), while their mean external biosecurity score was 78.98% (min.: 62%, max.: 89%).

Salmonella was detected in 13 (43.3%; 95%CI = 27.4–60.8) of the fattening units sampled, with a mean pen prevalence of 36.9% (95%CI = 22.6–51.2) in the *Salmonella*-positive units. *S.* Typhimurium was present in six (46.2%), the mST in eight (61.5%), and other serotypes in only two (15.4%) of the pig units. Seven (53.8%) of the *Salmonella*-positive units showed ≥30% of positive pens.

Salmonella was recovered from 48 out of 300 pooled FF samples (16%; 95%CI = 12.3–20.6) analyzed. Among the positive FF samples, *S.* Typhimurium was isolated in 21 samples (43.7%; 95%CI = 30.7–57.7), and the mST was isolated in 20 samples (41.7%, 95%CI = 28.9–55.7). *Salmonella* isolates belonging to serotypes other than these two were found in only seven FF samples (14.6%; 95%CI = 7.3–27.2).

3.2. *Salmonella* farm seroprevalence

Out of the 1,500 pigs initially ear-tagged at the farm, a total of 1,341 (89.4%) were further identified at slaughter, and IC samples were collected (an average of 44.7 pigs/fattening unit; 95%CI = 42.6–46.8). Serological analyses were performed on these 1,341 pigs. The mean seroprevalence (cut-off value OD% ≥40) among the 30 units was 31.7% (95%CI = 21.8–41.0), but it differed significantly among farms, ranging from a minimum of 2.3% to a maximum of 87.0%. Only six of these farms showed seroprevalences below 10%. The distribution of the seroprevalence among pig farms is shown in Figure 2.

3.3. Prevalence of *Salmonella* shedding at the slaughterhouse

A total of 316 pigs (23.6%; 95%CI = 21.4–25.9) were shedding *Salmonella* at slaughter. The prevalence of shedding differed significantly among farm batches, ranging from 0% to a maximum of 79.4%. All pigs were *Salmonella* negative only in three of these batches. The distribution of *Salmonella* shedding prevalence among pig batches is shown in Figure 2.

The major serotype identified was the mST, which was isolated in 151 pigs (47.8%; 95%CI = 42.3–53.3). *S.* Typhimurium was isolated in 71 pigs (22.5%; 95%CI = 18.2–27.4). Serotypes other than *S.* Typhimurium and the mST were identified in 94 pigs (29.7%; 95%CI = 25.0–35.0).

3.4. PFGE

Since *S.* Typhimurium and the mST were the two major serotypes involved (isolated in >80% PFF samples and 70% IC samples), PFGE analysis was performed on these *Salmonella* serotypes but only when the same *Salmonella* serotype was detected in both FF and IC samples from the same fattening unit. A total of 20 *Salmonella* isolates from FF samples and 26 isolates from IC samples from nine *Salmonella*-positive units were submitted for PFGE analysis.

PFGE analysis showed 11 different *XbaI* patterns (based on a similarity cut-off of ≥90%) (Figure 3). The observed PFGE clusters matched well with the serotypes. Four main clusters were observed for *S.* Typhimurium (clusters IV, V, VI, and XI), including only

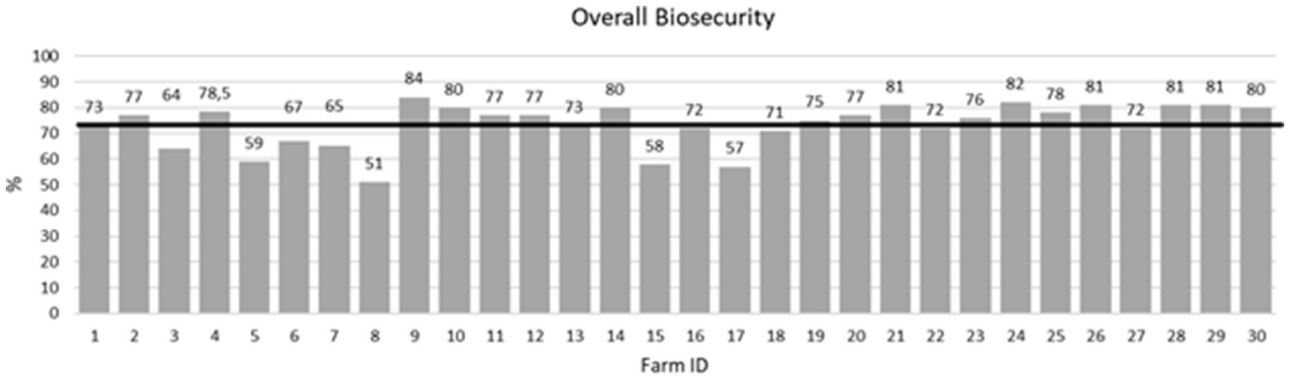

FIGURE 1
Individual overall biosecurity scores for the 30 pig farms included in the study and the mean value (solid black line) of all farms.

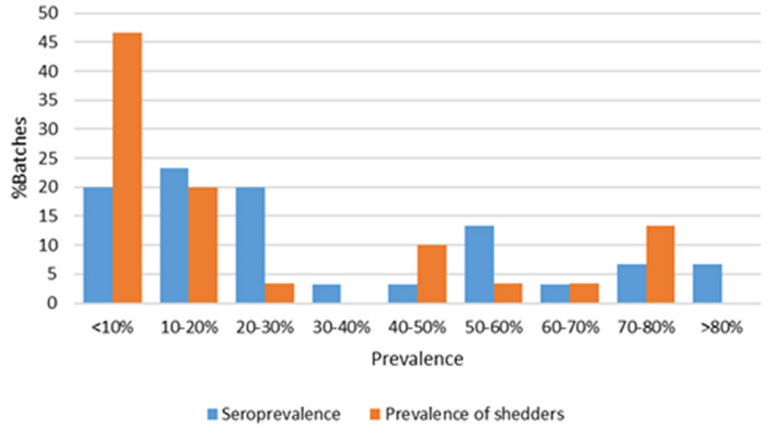

FIGURE 2
Distribution of *Salmonella* seroprevalence and the prevalence of *Salmonella* shedders among the 30 pig batches. Spearman's coefficient of rank correlation (rho) between on-farm seroprevalence and the prevalence of *Salmonella* shedders at slaughter: 0.451; 95%CI = 0.11–0.69; $P = 0.012$.

three farms, and seven for mST (clusters I, II, III, VII, VIII, IX, and X).

Salmonella isolates from FF samples were grouped into four different PFGE patterns (I, V, VI, and XI). Clusters VI and XI were composed only of isolates from FF samples. Within the other two clusters (clusters I and V), isolates from IC samples obtained from pigs from the corresponding fattening unit were also included. Overall, 65.4% of the IC isolates analyzed were included within these two clusters. At least one genetic relationship between *Salmonella* isolates from IC and FF samples was detected in 77.7% of the pig units.

3.5. *Salmonella* shedding prediction model development and validation

Two-thirds (885 animals) of the 1,341 pigs were randomly selected for building the predictive model. The results of the random-effects logistic regression analysis showed three variables related to *Salmonella* shedding at the abattoir, namely, serology (included as the logarithm of OD% values), the percentage of *Salmonella*-positive pens in the farm (used as a categorical variable based on percentiles: no positive pens; low percentage of positive pens, ≤20%; and high percentage of positive pens, >20%), and the internal biosecurity score (also used as a categorical variable based on percentiles: low score, <64%; medium score, from 64 to 77%; and high score, >77%) (Table 1). The random-effects logistic regression analysis indicated a significant clustering effect of "Farm" (ICC = 0.33; $P < 0.001$).

Individual serology was positively related to *Salmonella* shedding at the abattoir as increasing OD% values increased the odds of shedding (OR = 1.75; 95%CI = 1.06-2.87). Pigs from fattening units in which *Salmonella* was isolated from 10 to 20% of the pens had approximately five times higher odds of shedding *Salmonella* at the abattoir than pigs from units where *Salmonella* was not isolated from any pen (OR = 5.46; 95%CI = 1.19–24.95). These odds were even higher when *Salmonella* was detected in ≥30% of the pens in the unit (OR = 8.18; 95%CI = 2.07–32.33; $P < 0.01$). Regarding farm biosecurity, medium and high internal biosecurity scores significantly decreased the odds of a pig shedding *Salmonella* when compared to low biosecurity scores

10.3389/fmicb.2023.1232490

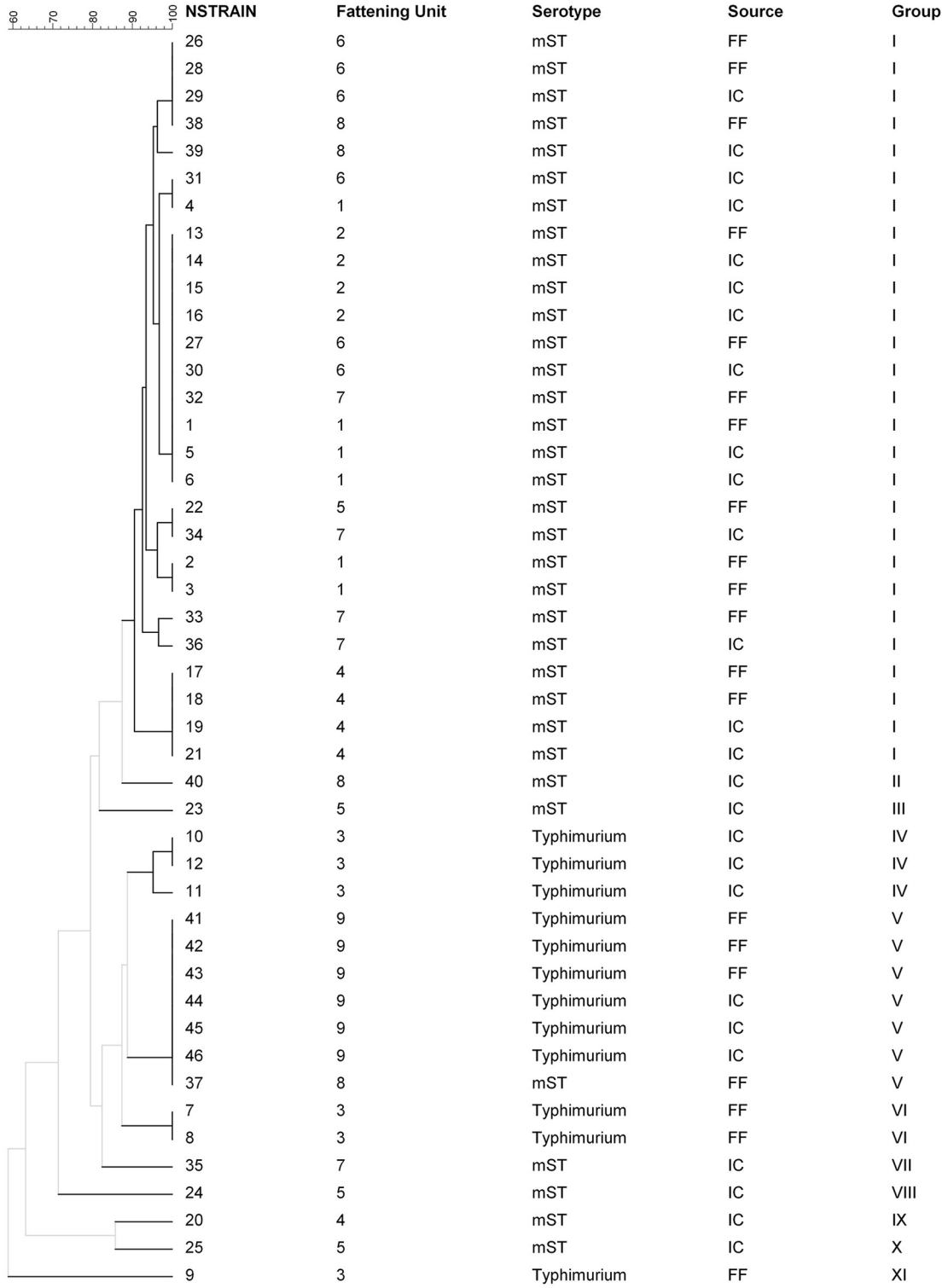

NSTRAIN	Fattening Unit	Serotype	Source	Group
26	6	mST	FF	I
28	6	mST	FF	I
29	6	mST	IC	I
38	8	mST	FF	I
39	8	mST	IC	I
31	6	mST	IC	I
4	1	mST	IC	I
13	2	mST	FF	I
14	2	mST	IC	I
15	2	mST	IC	I
16	2	mST	IC	I
27	6	mST	FF	I
30	6	mST	IC	I
32	7	mST	FF	I
1	1	mST	FF	I
5	1	mST	IC	I
6	1	mST	IC	I
22	5	mST	FF	I
34	7	mST	IC	I
2	1	mST	FF	I
3	1	mST	FF	I
33	7	mST	FF	I
36	7	mST	IC	I
17	4	mST	FF	I
18	4	mST	FF	I
19	4	mST	IC	I
21	4	mST	IC	I
40	8	mST	IC	II
23	5	mST	IC	III
10	3	Typhimurium	IC	IV
12	3	Typhimurium	IC	IV
11	3	Typhimurium	IC	IV
41	9	Typhimurium	FF	V
42	9	Typhimurium	FF	V
43	9	Typhimurium	FF	V
44	9	Typhimurium	IC	V
45	9	Typhimurium	IC	V
46	9	Typhimurium	IC	V
37	8	mST	FF	V
7	3	Typhimurium	FF	VI
8	3	Typhimurium	FF	VI
35	7	mST	IC	VII
24	5	mST	IC	VIII
20	4	mST	IC	IX
25	5	mST	IC	X
9	3	Typhimurium	FF	XI

FIGURE 3
Dendrogram showing the main *XbaI* pulsed-field gel electrophoresis (PFGE) patterns (≥90% homology) for 46 *Salmonella* strains isolated from slaughtered pigs' intestinal content (IC) and pen floor fecal (FF) samples from 9 fattening units.

TABLE 1 Results of the random-effects logistic regression analysis* for predicting *Salmonella* shedding at the abattoir.

	Odds ratio (OR)	*P*-value	95% CI(OR)
Serology (LogOD%)	1.74	0.028	1.06–2.87
% *Salmonella*-positive pens			
0[a]	1	-	-
10–20	5.46	0.029	1.19–24.95
≥30	8.18	0.003	2.07–32.33
Internal biosecurity score			
<64%[a]	1	-	-
64–77%	0.25	0.043	0.07–0.96
>77%	0.20	0.050	0.04–0.99
Constant	0.11	0.005	0.03–0.52

*Farm regarded as a grouping (random) variable.
[a]Reference category. Intraclass correlation coefficient (ICC): 0.33 (95%CI = 0.19–0.50).

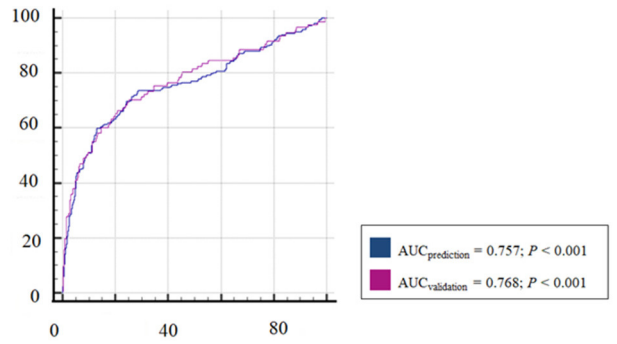

FIGURE 4
Receiver operating characteristic curves (ROC) and the corresponding areas under the curve (AUC) for the estimated (blue) model and the validation model (purple).

(OR = 0.25; 95%CI = 0.07–0.96 and OR = 0.20; 95%CI = 0.04–0.99, respectively).

The prediction model built with these three factors showed a good ability to predict whether an animal will shed *Salmonella* at the abattoir. The AUC (0.76) was significantly different from that for a non-discriminatory model (Figure 4). The best cut-off value for maximizing Se (i.e., its ability to correctly identify an animal that will be shedding *Salmonella* after its arrival to the abattoir) and Sp (i.e., its ability to correctly identify an animal that will not shed *Salmonella* at the abattoir) was 25.9%. The associated diagnostic Se and Sp for that cut-off value were 71.6% and 73.6%, respectively (Table 2).

The model was rerun using data from the one-third left of the pig population ($N = 456$) for validation purposes. The comparison between the predictive and the validation models showed non-significant differences (Table 2 and Figure 4).

Figure 5 shows the predicted probability of shedding *Salmonella* at the abattoir according to serological values (ELISA OD%) after considering the proportion of *Salmonella*-positive pens in the fattening units and their internal biosecurity scores. In two scenarios, serology would not add significant information for considering whether a pig would shed *Salmonella* at the abattoir: in the case of farms with high or medium internal biosecurity with no *Salmonella*-positive pens or in the case of farms with low internal biosecurity with at least one *Salmonella*-positive pen.

TABLE 2 Prediction parameters for the estimated model and the validation model.

	Estimated model	Validation model
AUC	0.757	0.768
95% CI (AUC)	0.728–0.785	0.727–0.806
Pythagoras cut-off*	25.88	26.47
Sensitivity	71.56	70.41
95% CI (sensitivity)	65.1–77.4	60.3–79.2
Specificity	73.61	74.58
95% CI (specificity)	70.1–76.9	69.7–79.0

AUC, Area under the curve.
*Estimated as the smallest sum of squares of 1-sensitivity and 1-specificity (Froud and Abel, 2014).

4. Discussion

In this study, a total of 1,341 pigs from 30 farms that were willing to participate and were located in Northeast Spain, the largest pig production region in Spain (MAGRAMA, 2021), were selected. Even though pig salmonellosis is considered a public health concern, *Salmonella* contamination was detected in 43.3% of the farms, a figure comparable to that reported in 2003-2004 in a similar study on the entire country (García-Feliz et al., 2007). More concerning, the proportion of pigs shedding *Salmonella* at the abattoir was also high (23.6%), with some pig batches reaching up to 80% and with zoonotic *S.* Typhimurium and the mST being the predominant serotypes. These pigs are likely major sources of carcass contamination (Argüello et al., 2013a; Marin et al., 2020), and finding ways to prevent this shedding should be of utmost importance.

As indicated by the random-effects logistic model, the proportion of pigs shedding *Salmonella* at the abattoir was strongly related to the presence of *Salmonella* in the fattening unit from which pigs came (Table 1). This relationship was supported to some extent by the identification through PFGE analyses of genetic matches between *Salmonella* isolates from pen FF and pig IC samples in most of the analyzed batches (Figure 3), despite the possibility of cross-contamination during transport or lairage (Argüello et al., 2013a). These findings emphasized the role that *Salmonella* farm contamination plays in *Salmonella* shedding at slaughter and suggested that *Salmonella* control should begin at the farm (de Busser et al., 2013).

A thorough biosecurity questionnaire was carried out on all the pig farms to describe their overall biosecurity level. On average, they presented good biosecurity levels. The mean biosecurity score for these farms was 73%, which appears to be somewhat higher than the Spanish national average (68%, from 275

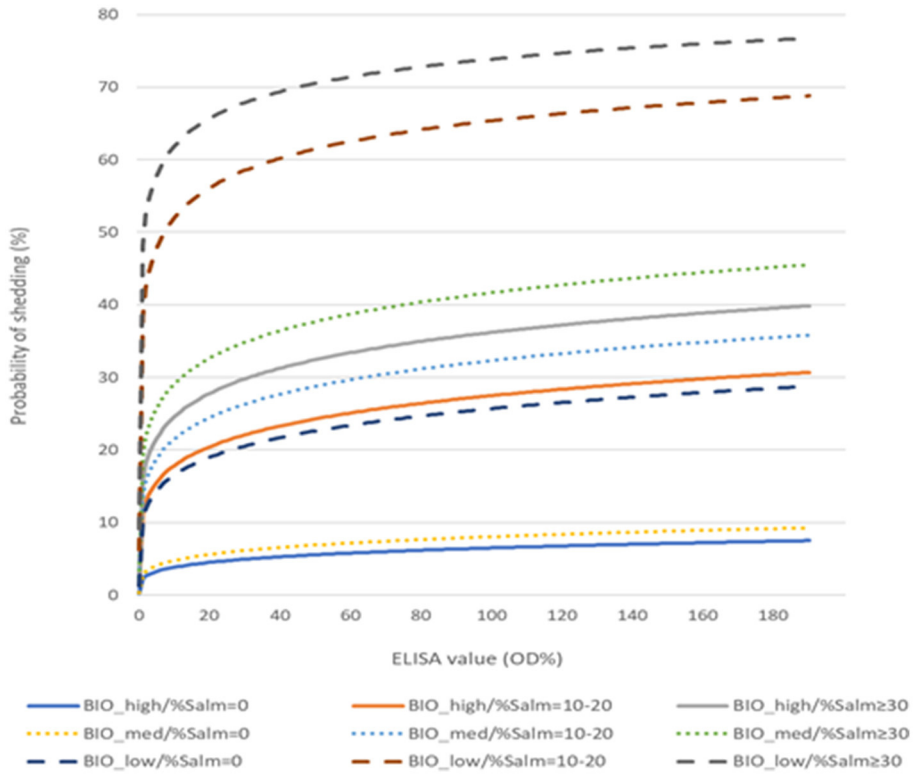

FIGURE 5
Probability of *Salmonella* shedding at the abattoir as a function of serology (ELISA OD% values), farm internal biosecurity (BIO: high, medium, and low), and the percentage of *Salmonella*-positive pens in the farm (%Salm: 0%, 10–20% and ≥30%).

questionnaires) and even higher than the national average for other big European pig-producer countries such as Germany (64%; 180 questionnaires), The Netherlands (69%; 198 questionnaires), Italy (71%; 353 questionnaires), or Ireland (72%; 486 questionnaires). However, the score was lower than that in Belgium (75%; 10,068 questionnaires) (as checked at biocheck.ugent.be on 31 January 2023). However, despite this good level of overall biosecurity, serological results suggested that *Salmonella* was circulating within most farms, highlighting the difficulties in controlling it at the farm level. On average, 32.9% of the pigs presented high ELISA OD% values (≥40%). Based on these results, one-third of the farms would be classified within the high-seroprevalence category (≥40% seroprevalence), and another one-third would be classified within the medium category (between 20% and 40% seroprevalence), according to the main NCPs. Only six farms showed seroprevalence levels below 10%. These results might also explain to some extent the high proportion of pigs shedding *Salmonella* at the abattoir, as a significant positive but weak association was observed in the logistic model between pig serology and *Salmonella* shedding at slaughter (Table 1). Pigs with much higher ELISA OD% values would have somewhat higher odds of shedding *Salmonella* at slaughter (Kranker et al., 2003; Sørensen et al., 2004; Korsak et al., 2006; Mainar-Jaime et al., 2018).

In this study, neither the overall nor the external biosecurity scores were related to the reduction of *Salmonella* shedding at the abattoir (Table 1). Although the biosecurity level of farms is, in general, considered to be beneficial to reducing bacterial transmission, it appears that biosecurity cannot reduce *Salmonella* prevalence by itself (Alarcón et al., 2021; Youssef et al., 2021). The implementation of efficient on-farm *Salmonella* control measures will depend on farmers' perception of the disease and their motivation to maintain them on an ongoing basis (Fraser et al., 2010; Marier et al., 2016). However, pig salmonellosis is usually asymptomatic, that is, of low concern for farmers and swine production veterinarians.

The predictive model built with these three factors, i.e., serology, farm internal biosecurity, and *Salmonella* pen prevalence, showed an acceptable ability to predict whether an animal will shed *Salmonella* at the abattoir. Thus, according to the model, a pig with a predicted probability of shedding *Salmonella* greater than 26% would have a 71.6% probability of being a true shedder. If the predicted probability was ≤26%, the animal would have a 73.6% probability of being a true non-shedder. Therefore, estimating the proportion of animals with a model probability higher than 26% in a given batch of pigs intended for slaughter would allow for the assessment of the overall risk of shedding for that batch. Once the potential risk of *Salmonella* shedding has been assessed 3-4 weeks before slaughter, stakeholders could act according to the results obtained. At the farm level, control measures could be implemented to minimize the likelihood of *Salmonella* shedding at slaughter. For instance, the addition of organic acids in food/water could help reduce shedding (de Busser et al., 2009; Argüello et al., 2013b; Lynch et al., 2017; Bernad-Roche et al., results to be published). Additionally, the abattoir, being aware of the risk, could implement

mitigation measures such as logistic slaughter (Swanenburg et al., 2001; Hotes et al., 2011) or even the addition of organic acids to the water at lairage (Bernad-Roche et al., 2022), to attempt to reduce the risk of *Salmonella* shedding. These interventions will only be required on those batches of pigs that present probabilities of *Salmonella* shedding above an established threshold.

It is interesting to note that in farms with high or medium internal biosecurity scores (i.e., scores >64%) and where no *Salmonella*-positive pens were detected, no animals could be considered shedders at slaughter (i.e., with predicted probability >26%), regardless of the ELISA OD% values (Figure 5). Likewise, serology would be unnecessary in the case of farms with low internal biosecurity when at least one pen is positive for *Salmonella*, as all pigs would show high predicted probabilities of shedding the bacterium at slaughter. In this second scenario, the likelihood of a pig becoming infected will be high, since *Salmonella* should be able to circulate easily among pens in farms with low internal biosecurity (Baptista et al., 2010).

These results emphasized the importance of internal biosecurity in the transmission of *Salmonella* within the farm. The internal biosecurity questionnaire included factors such as disease management (i.e., vaccination and treatment protocols and frequency of health status assessment), fattening unit management (i.e., all-in/all-out system and pig mix and density), measures between compartments and the use of equipment (i.e., foot baths, cleaning and disinfection after equipment usage, workflow from younger to older pigs, and sharing equipment with other farms), and cleaning and disinfection (i.e., after every production cycle, protocols, and drying after cleaning and disinfection). Cleaning and disinfection along with feed, water, and bedding are considered by experts some of the most important biosecurity measures to control *Salmonella* in indoor settings (De Lucia and Ostanello, 2020; Galipó et al., 2023). However, more research is required to determine with more certainty the most-effective measures from the human health perspective (Youssef et al., 2021).

In contrast to the two previous scenarios, in the case of any of the other situations (i.e., acceptable internal biosecurity with the presence of *Salmonella*-positive pens or low internal biosecurity and no *Salmonella*-positive pens), serology would add useful information to the decision of whether a pig should be considered of risk for *Salmonella* shedding at the abattoir. As an example, pigs with ELISA values >30% would be associated with abattoir *Salmonella* shedding if they belong to farms with medium internal biosecurity, along with the presence of *Salmonella* in 10–20% of the pens. If they belong to a similar farm but with high internal biosecurity, the pigs of risk would be those showing much higher ELISA values (close to 80%). ELISA values would also help interpret the possible shedding status of a pig from a low internal biosecurity farm when no *Salmonella*-positive pens are detected (Figure 5). Therefore, considering the different scenarios that are possible according to the model, the simplest way to proceed with the estimation of the risk of *Salmonella* shedding at slaughter would be to start with an assessment of the farms' internal biosecurity and the *Salmonella* pen prevalence. Depending on the results, additional serological analyses should be carried out on a representative sample of the pigs from the batch.

Although many studies have shown the lack of reliability of indirect ELISA tests for ascertaining the individual *Salmonella* status of a pig, either infection or shedding (Nollet et al., 2005; Farzan et al., 2007; Gradassi et al., 2015), they could be of relative value when used on groups of pigs (Sørensen et al., 2004; Korsak et al., 2006; Farzan et al., 2007). In this study, a significant but low correlation was observed between the *Salmonella* seroprevalence of a given batch and the proportion of shedding pigs at the abattoir for that batch (Figure 2), when no other factors were taken into account. This simple approach might not be sufficient for accurately predicting *Salmonella* shedding at the abattoir.

It appears that the value of serology for predicting shedding depends on the context in which it is used. Similar to the results of a previous study (Mainar-Jaime et al., 2018), the model in this study indicated that higher individual OD% values were related to higher odds of *Salmonella* shedding at slaughter. This was likely due to the presence of stressful factors such as the transport and waiting (lairage) times that pigs went through, which would favor the shedding among the infected pigs (Duggan et al., 2010; Simons et al., 2016). In addition, other factors, such as the internal biosecurity of the farm and the presence of *Salmonella* in the farm, would also play a significant role in interpreting ELISA values in this context. Thus, these results might help explain, at least in part, the difficulties that many NCPs face in properly assessing the *Salmonella* status of pig farms, as many of them are based exclusively on serological results usually obtained from a small and hardly representative number of animals, without considering other factors (Mainar-Jaime et al., 2018; Correia-Gomes et al., 2021).

5. Conclusion

This study highlighted the importance of the context in which serology is used for pig salmonellosis control. Using it 3-4 weeks prior to sending the pigs to slaughter might be helpful for identifying batches of pigs at risk of shedding *Salmonella* upon their arrival at the abattoir. In some cases, being aware of the farm's internal biosecurity level and performing a bacteriological sampling of a representative number of pens might be sufficient for estimating the risk of *Salmonella* shedding for a given batch of pigs ready for slaughter. In others, serology would be required for a more accurate interpretation of the results, but in both situations, an acceptable level of knowledge about the risk of *Salmonella* shedding for a given batch of slaughter pigs could be achieved. Reducing the likelihood of *Salmonella* shedding at this stage would be an important step for reducing *Salmonella* carcass contamination.

An additional advantage of this approach is that *Salmonella* control would not initially rely on the farmer's work but on the farm's data collection, as farmer's engagement seems to be one of the main obstacles NCPs face, especially when dealing with animal infections of no clinical concern (Fraser et al., 2010; Marier et al., 2016; Alarcón et al., 2021). Moreover, this approach would also allow for a combined farm/abattoir strategy that would likely have cumulative benefits (Swart et al., 2016), as it would make both abattoirs and farmers aware of the risk of the pigs coming to the

slaughter. Thus, a more precise characterization of the *Salmonella* status of pig farms would be obtained from routine sampling, with the collection of proper representative samples, which would also help encourage a good attitude among farmers toward *Salmonella* control in the short/medium term.

Data availability statement

The raw data supporting the conclusions of this article will be made available by the authors, without undue reservation.

Ethics statement

The animal study was approved by Ethical Advisory Commission for Animal Experimentation of the University of Zaragoza (permit no. PI13/20). The study was conducted in accordance with the local legislation and institutional requirements.

Author contributions

RM-J: conceptualization, supervision, project administration, and funding acquisition. RM-J and MB-R: methodology, investigation, and writing-original draft preparation. RM-J, MB-R, IB, and AC-S: formal analysis. MB-R, RM-J, and CM-A: writing-review and editing. All authors have read and agreed to the published version of the manuscript.

Funding

This work was supported by grant RTI2018-093915-B-I00 funded by MCIN/AEI/10.13039/501100011033 and ERDF A way of making Europe from the European Union.

Acknowledgments

We thank the pig production companies and their technical staff and farmers, as well as the abattoirs, for their support and collaboration in carrying out the fieldwork.

Conflict of interest

The authors declare that the research was conducted in the absence of any commercial or financial relationships that could be construed as a potential conflict of interest.

Publisher's note

References

Alarcón, L. V., Allepuz, A., and Mateu, E. (2021). Biosecurity in pig farms: a review. *Porcine Health Manag.* 7, 5. doi: 10.1186/s40813-020-00181-z

Anonymous (2011). FCC Consortium, Final Report. Analysis of the costs and benefits of setting a target for the reduction of *Salmonella* in breeding pigs for European Commission Health and Consumers Directorate-General SANCO/2008/E2/056. Brussels: SANCO/2008/E2/056. Available online at: https://ec.europa.eu/food/sites/food/files/safety/docs/biosafety_food-bornedisease_salmonella_breeding-pigs_salm-cost-benefit.pdf (accessed April 3, 2023).

Anonymous (2012). UK: New direction for Zoonoses National Control Programme (ZNCP). Available online at: https://www.pigprogress.net/Health-Diseases/Health/2012/6/UK-New-direction-for-Zoonoses-National-Control-Programme-ZNCP-PP008961W/ (accessed April 3, 2023).

Anonymous (2015). Koninklijk besluit tot opheffing van het koninklijk en het ministerieel besluit van 27 april 2007 betreffende de bewaking van Salmonella bij varkens. In: Voedselketen, F.A.v.d.V.v.d. (Ed.). Available online at: https://etaamb.openjustice.be/fr/arrete-royal-du-27-avril-2007_n2007022865 (accessed June 27, 2023).

Anonymous (2021). QS Qualität und Sicherheit GmbH. 20 Jahre QS: Salmonellenrisiko Um Über 70% Gesunken. Available online at: https://www.q-s.de/pressemeldungen/20-jahre-qs-salmonellenrisiko-um-ueber-70-prozent.html (accessed April 3, 2023).

Argüello, H., Alvarez-Ordoñez, A., Carvajal, A., Rubio, P., and Prieto, M. (2013a). Role of slaughtering in *Salmonella* spreading and control in pork production. *J. Food Prot.* 76, 899–911. doi: 10.4315/0362-028X.JFP-12-404

Argüello, H., Carvajal, A., Costillas, S., and Rubio, P. (2013b). Effect of the addition of organic acids in drinking water or feed during part of the finishing period on the prevalence of *Salmonella* in finishing pigs. *Foodborne Pathog Dis.* 10, 842–9. doi: 10.1089/fpd.2013.1497

Baptista, F. M., Alban, L., Nielsen, L. R., Domingos, I., Pomba, C., Almeida, V., et al. (2010). Use of herd information for predicting *Salmonella* status in pig herds. *Zoonoses Public Health* 1, 49–59. doi: 10.1111/j.1863-201001354.x

Barco, L., Lettini, A. A., Ramon, E., Longo, A., Saccardin, C., Pozza, M. C., et al. (2011). A rapid and sensitive method to identify and differentiate *Salmonella* enterica serotype *Typhimurium* and *Salmonella* enterica serotype 4,[5],12:i:- by combining traditional serotyping and multiplex polymerase chain reaction. *Foodborne Pathog. Dis.* 8, 741–743. doi: 10.1089/fpd.2010.0776

Bernad-Roche, M., Casanova-Higes, A., Marín-Alcalá, C. M., and Mainar-Jaime, R. C. (2022). *Salmonella* shedding in slaughter pigs and the use of esterified formic acid in the drinking water as a potential abattoir-based mitigation measure. *Animals* 12, 1620. doi: 10.3390/ani12131620

BPEX (2002). The British Pig Executive. ZAP *Salmonella*—A zoonosis action plan for the Brithis Pig Industry. https://www.porcat.org/download/ZAP-Salmonella.pdf (accessed April 3, 2023).

Casanova-Higes, A., Andrés-Barranco, S., and Mainar-Jaime, R. C. (2017). Influence of On-farm pig *Salmonella* status on *Salmonella* Shedding at Slaughter. *Zoonoses Public Health* 64, 328–336. doi: 10.1111/zph.12301

Cooke, F. J., Brown, D. J., Fookes, M., Pickard, D., Ivens, A., Wain, J., et al. (2008). Characterization of the genomes of a diverse collection of *Salmonella* enterica serovar Typhimurium definitive phage type 104. *J. Bacteriol.* 190, 8155–62. doi: 10.1128/JB.00636-08

Correia-Gomes, C., Leonard, F., and Graham, D. (2021). Description of control programmes for *Salmonella* in pigs in Europe. Progress to date? *J. Food Saf.* 41, e12916. doi: 10.1111/jfs.12916

de Busser, de Zutter, E. V., Dewulf, L., Houf, J., and Maes, K. (2013). *Salmonella* control in live pigs and at slaughter. *Vet. J.* 196, 20–7. doi: 10.1016/j.tvjl.01002

de Busser, Dewulf, E. V., Nollet, J., Houf, N., Schwarzer, K., de Sadeleer, K., et al. (2009). Effect of organic acids in drinking water during the last 2 weeks prior to

slaughter on *Salmonella* shedding by slaughter pigs and contamination of carcasses. *Zoonoses Public Health*. 56, 129–36. doi: 10.1111/j.1863-200801172.x

De Lucia, A., and Ostanello, F. (2020). On-farm risk factors associated with *Salmonella* in pig herds. *Large Animal Rev*. 26, 133–140.

Duggan, S. J., Mannion, C., Prendergast, D. M., Leonard, N., Fanning, S., Gonzales-Barron, U., et al. (2010). Tracking the *Salmonella* status of pigs and pork from lairage through the slaughter process in the Republic of Ireland. *J. Food Prot*. 73, 2148–60. doi: 10.4315/0362-028x-73.12.2148

EFSA and ECDC (2022). European food safety authority and European Centre for disease prevention and control. The European Union one health 2021 zoonoses report. *EFSA J*. 20, 7666. doi: 10.2903/j.efsa.2022.7666

European Food Safety Authority (EFSA). (2011). Analysis of the baseline survey of *Salmonella* in holdings with breeding pigs, in the EU, 2008; Part B: analysis of factors potentially associated with *Salmonella* pen positivity. *EFSA J*. 9, 2329. doi: 10.2903/j.efsa.2011.2329

Farzan, A., Friendship, R. M., and Dewey, C. E. (2007). Evaluation of enzyme-linked immunosorbent assay (ELISA) tests and culture for determining *Salmonella* status of a pig herd. *Epidemiol. Infect*. 135, 238–44. doi: 10.1017/S0950268806006868

Fraser, R. W., Williams, N. T., Powell, L. F., and Cook, A. J. (2010). Reducing *Campylobacter* and *Salmonella* infection: two studies of the economic cost and attitude to adoption of on-farm biosecurity measures. *Zoonoses Public Health*. 57, e109–15. doi: 10.1111/j.1863-200901295.x

Froud, R., and Abel, G. (2014). Using ROC curves to choose minimally important change thresholds when sensitivity and specificity are valued equally: the forgotten lesson of pythagoras. theoretical considerations and an example application of change in health status. *PLoS ONE*. 9, e114468. doi: 10.1371/journal.pone.0114468

Galipó, E., Zoche-Golob, V., Sassu, E. L., Prigge, C., Sjölund, M., Tobias, T., et al. (2023). Prioritization of pig farm biosecurity for control of *Salmonella* and hepatitis E virus infections: results of a European expert opinion elicitation. *Porcine Health Manag*. 9, 8. doi: 10.1186/s40813-023-00306-0

García-Feliz, C., Collazos, J. A., Carvajal, A., Vidal, A. B., Aladueña, A., Ramiro, R., et al. (2007). *Salmonella enterica* infections in Spanish swine fattening units. *Zoonoses Public Health* 54, 294–300. doi: 10.1111/j.1863-200701065.x

Gavin, C., Simons, R. R. L., Berriman, A. D. C., Moorhouse, D., Snary, E. L., Smith, R. P., et al. (2018). A cost-benefit assessment of *Salmonella*-control strategies in pigs reared in the United Kingdom. *Prev Vet Med*. 160, 54–62. doi: 10.1016/j.prevetmed.09022

Gradassi, M., Caminiti, A., Galletti, G., Santi, A., Paternoster, G., Tamba, M., et al. (2015). Suitability of a *Salmonella* control programme based on serology in slaughter heavy pigs. *Res. Vet. Sci*. 101, 154–60. doi: 10.1016/j.rvsc.06015

Greiner, M., Pfeiffer, D., and Smith, R. D. (2000). Principles and practical application of the receiver-operating characteristic analysis for diagnostic tests. *Prev. Vet. Med*. 45, 23–41. doi: 10.1016/s0167-5877(00)00115-x

Hanssen, E. J., Swanenburg, M., and Maassen, C. B. M. (2007). The Dutch *Salmonella* monitoring programme for pigs and some recommendations for control plans in the future. *Proceedings from Safepork 2007, 7th. Sym Epidemiol and Control Foodborne Pathogens in pork*. Verona, Italy, pp. 169–172.

Hotes, S., Traulsen, I., and Krieter, J. (2011). *Salmonella* control measures with special focus on vaccination and logistic slaughter procedures. *Transbound Emerg. Dis*. 58, 434–44. doi: 10.1111/j.1865-201101226.x

Ivanek, R., Österberg, J., Gautam, R., and Sternberg Lewerin, S. (2012). *Salmonella* fecal shedding and immune responses are dose- and serotype- dependent in pigs. *PLoS ONE* 7, e34660. doi: 10.1371/journal.pone.0034660

Kariuki, S., Oundo, J. O., Muyodi, J., Lowe, B., Threlfall, E. J., Hart, C. A., et al. (2000). Genotypes of multidrug-resistant *Salmonella* enterica serotype typhimurium from two regions of Kenya. *FEMS Immunol. Med. Microbiol*. 29, 9–13. doi: 10.1111/j.1574-695X.2000.tb01498.x

Korsak, N., Degeye, J. N., Etienne, G., Beduin, J. M., China, B., Ghafir, Y., et al. (2006). Use of a serological approach for prediction of *Salmonella* status in an integrated pig production system. *Int. J. Food Microbiol*. 108, 246–54. doi: 10.1016/j.ijfoodmicro.09013

Kranker, S., Alban, L., Boes, J., and Dahl, J. (2003). Longitudinal study of *Salmonella enterica* serotype Typhimurium infection in three Danish farrow-to-finish swine herds. *J. Clin. Microbiol*. 41, 2282–8. doi: 10.1128/JCM.41.6.2282-2288.2003

Lundbeck, H., Plazikowski, U., and Silverstolpe, L. (1955). The Swedish *Salmonella* outbreak of 1953. *J. Appl. Microbiol*. 18, 535–548.

Lynch, H., Leonard, F. C., Walia, K., Lawlor, P. G., Duffy, G., Fanning, S., et al. (2017). Investigation of in-feed organic acids as a low cost strategy to combat *Salmonella* in grower pigs. *Prev. Vet. Med*. 139, 50–57. doi: 10.1016/j.prevetmed.02008

Lyngstad, T. M., Hopp, P., Hofshagen, M., Bergsjø, B., Bruheim, T., Eikenæs, O., et al. (2007). *The Surveillance and Control Programmes for Salmonella in Live Animals, Eggs and Meat in Norway*. Oslo: National Veterinary Institute.

MAGRAMA (2021). El sector de la carne de cerdo en cifras: Principales indicadores económicos. Available online at: https://www.mapa.gob.es/es/ganaderia/estadisticas/indicadoressectorporcino2021_tcm30-564427.pdf (accessed April 3, 2023).

Maijala, R., Ranta, J., Seuna, E., and Peltola, J. (2005). The efficiency of the Finnish *Salmonella* control programme. *Food Control*. 16, 669–675. doi: 10.1016/j.foodcont.06003

Mainar-Jaime, R. C., Atashparvar, N., Chirino-Trejo, M., and Blasco, J. M. (2008). Accuracy of two commercial enzyme-linked immunosorbent assays for the detection of antibodies to *Salmonella* spp. *in slaughter pigs from Canada. Prev. Vet. Med*. 85, 41–51. doi: 10.1016/j.prevetmed.12015

Mainar-Jaime, R. C., Casanova-Higes, A., Andrés-Barranco, S., and Vico, J. P. (2018). Looking for new approaches for the use of serology in the context of control programmes against pig salmonellosis. *Zoonoses Public Health*. 65, e222–e228. doi: 10.1111/zph.12432

Marier, E., Piers Smith, R., Ellis-Iversen, J., Watson, E., Armstrong, D., Hogeveen, H., et al. (2016). Changes in perceptions and motivators that influence the implementation of on-farm *Salmonella* control measures by pig farmers in England. *Prev. Vet. Med*. 133, 22–30. doi: 10.1016/j.prevetmed.09009

Marin, C., Chinillac, M. C., Cerdà-Cuéllar, M., Montoro-Dasi, L., Sevilla-Navarro, S., Ayats, T., et al. (2020). Contamination of pig carcass with *Salmonella* enterica serovar Typhimurium monophasic variant 1,4[5],12:i:- originates mainly in live animals. *Sci. Total Environ*.703, 134609. doi: 10.1016/j.scitotenv.2019.134609

Méroc, E., Strubbe, M., Vangroenweghe, F., Czaplicki, G., Vermeersch, K., Hooyberghs, J., et al. (2012). Evaluation of the *Salmonella* surveillance program in Belgian pig farms. *Prev. Vet. Med*. 105, 309–14. doi: 10.1016/j.prevetmed.03006

Mousing, J., Jensen, P. T., Halgaard, C., Bager, F., Feld, N., Nielsen, B., et al. (1997). Nation-wide *Salmonella* enterica surveillance and control in Danish slaughter swine herds. *Prev. Vet. Med*. 29, 247–61. doi: 10.1016/s0167-5877(96)01082-3

Nollet, N., Maes, D., Duchateau, L., Hautekiet, V., Houf, K., van Hoof, J., et al. (2005). Discrepancies between the isolation of *Salmonella* from mesenteric lymph nodes and the results of serological screening in slaughter pigs. *Vet. Res*. 36, 545–55. doi: 10.1051/vetres:2005014

Osterkorn, K., Czerny, C. P., Wittkowski, G., and Huber, M. (2001). Stichprobenplanung für die Etablierung eines serologischen Salmonellen-Monitoringprogramms bei Mastschweinen mittels Fleischsaft-ELISA [Sampling plan for the establishment of a serologic *Salmonella* surveillance for slaughter pigs with meat juice ELISA]. *Berl. Munch. Tierarztl. Wochenschr*. 114, 30–4.

Peters, T. M., Maguire, C., Threlfall, E. J., Fisher, I. S., Gill, N., Gatto, A. J., et al. (2003). Salm-gene project. The Salm-gene project—A European collaboration for DNA fingerprinting for food-related salmonellosis. *Euro. Surveill*. 8, 46–50. doi: 10.2807/esm.08.02.00401-en

Ribot, E. M., Fair, M. A., Gautom, R., Cameron, D. N., Hunter, S. B., Swaminathan, B., et al. (2006). Standardization of pulsed-field gel electrophoresis protocols for the subtyping of *Escherichia coli* O157:H7, *Salmonella*, and *Shigella* for PulseNet. *Foodborne Pathog. Dis*. 3, 59–67. doi: 10.1089/fpd.359

Rostagno, M. H., Eicher, S. D., and Lay, D. C. (2010). Does pre-slaughter stress affect pork safety risk? in *Proceedings of the 21st International Pig Veterinary Society (IPVS) Congress*, July 18–21, 2010. Vancouver, Canada. *p*. 176.

Simons, R. R., Hill, A. A., Swart, A., Kelly, L., and Snary, E. L. (2016). A transport and lairage model for *Salmonella* transmission between pigs applicable to EU member states. *Risk Anal*. 36, 482–97. doi: 10.1111/risa.12390

Snary, E. L., Munday, D. K., Arnold, M. E., and Cook, A. J. C. (2010). Zoonoses action plan *Salmonella* monitoring programme: an investigation of the sampling protocol. *J. Food Prot*. 73, 488–494. doi: 10.4315/0362-028X-73.3.488

Sørensen, L. L., Alban, L., Nielsen, B., and Dahl, J. (2004). The correlation between *Salmonella* serology and isolation of *Salmonella* in Danish pigs at slaughter. *Vet. Microbiol*. 101, 131–41. doi: 10.1016/j.vetmic.02016

Swanenburg, M., van der Wolf, P. J., Urlings, H. A., Snijders, J. M., and van Knapen, F. (2001). *Salmonella* in slaughter pigs: the effect of logistic slaughter procedures of pigs on the prevalence of *Salmonella* in pork. *Int. J. Food Microbiol*. 70, 231–42. doi: 10.1016/s0168-1605(01)00546-3

Swart, A. N., Evers, E. G., Simons, R. L., and Swanenburg, M. (2016). Modeling of *Salmonella* Contamination in the Pig Slaughterhouse. *Risk Anal*. 36, 498–515. doi: 10.1111/risa.12514

Tennant, S. M., Diallo, S., Levy, H., Livio, S., Sow, S. O., Tapia, M., et al. (2010). Identification by PCR of non-typhoidal *Salmonella* enterica serovars associated with invasive infections among febrile patients in Mali. *PLoS Negl. Trop. Dis*. 4, e621. doi: 10.1371/journal.pntd.0000621

Wierup, M. (2006). *The Swedish Salmonella Control in Primary Production—An overview of its Background, Strategy, and Development: Salmonella Workshop—Control in Poultry From Feed to Farm*. Uppsala: National Veterinary Institutepp. p. 11–14.

Youssef, D. M., Wieland, B., Knight, G. M., Lines, J., and Naylor, N. R. (2021). The effectiveness of biosecurity interventions in reducing the transmission of bacteria from livestock to humans at the farm level: a systematic literature review. *Zoonoses Public Health*. 68, 549–562. doi: 10.1111/zph.12807

frontiers | Frontiers in Microbiology

TYPE Original Research
PUBLISHED 14 September 2023
DOI 10.3389/fmicb.2023.1210358

OPEN ACCESS

EDITED BY
Patrick J. Naughton,
Ulster University, United Kingdom

REVIEWED BY
Amit K. Singh,
Albany Medical College, United States
Anna Jarzab,
Technical University of Munich, Germany
Alexey V. Rakov,
Central Research Institute of Epidemiology (CRIE), Russia
Kuang-Sheng Yeh,
National Taiwan University, Taiwan

*CORRESPONDENCE
Guoping Liu
✉ guoping.liu@yangtzeu.edu.cn
Bin Wu
✉ wub@mail.hzau.edu.cn

†These authors have contributed equally to this work and share first authorship

RECEIVED 22 April 2023
ACCEPTED 31 August 2023
PUBLISHED 14 September 2023

CITATION
Liu G, Li C, Liao S, Guo A, Wu B and Chen H (2023) C500 variants conveying complete mucosal immunity against fatal infections of pigs with *Salmonella enterica* serovar Choleraesuis C78-1 or F18+ Shiga toxin-producing *Escherichia coli*. *Front. Microbiol.* 14:1210358. doi: 10.3389/fmicb.2023.1210358

C500 variants conveying complete mucosal immunity against fatal infections of pigs with *Salmonella enterica* serovar Choleraesuis C78-1 or F18+ Shiga toxin-producing *Escherichia coli*

Guoping Liu[1,2,3*†], Chunqi Li[1,3†], Shengrong Liao[2,4†], Aizhen Guo[4], Bin Wu[4*] and Huanchun Chen[4]

[1]College of Animal Science, Yangtze University, Jingzhou, China, [2]Key Laboratory of Preventive Veterinary Medicine in Hubei Province, The Cooperative Innovation Center for Sustainable Pig Production, Wuhan, China, [3]Hubei Institute of Cross Biological Health Industry Technology, Jingzhou, China, [4]State Key Laboratory of Agricultural Microbiology, College of Veterinary Medicine, Huazhong Agricultural University, Wuhan, China

Salmonella enterica serovar Choleraesuis (*S.* Choleraesuis) C500 strain is a live, attenuated vaccine strain that has been used in China for over 40 years to prevent piglet paratyphoid. However, this vaccine is limited by its toxicity and does not offer protection against diseases caused by F18+ Shiga toxin-producing *Escherichia coli* (STEC), which accounts for substantial economic losses in the swine industry. We recently generated a less toxic derivative of C500 strain with both *asd* and *crp* deletion (*S.* Choleraesuis C520) and assessed its efficacy in mice. In addition, we demonstrate that C520 is also less toxic in pigs and is effective in protecting pigs against *S.* Choleraesuis when administered orally. To develop a vaccine with a broader range of protection, we prepared a variant of C520 (*S.* Choleraesuis C522), which expresses rSF, a fusion protein comprised of the fimbriae adhesin domain *Fed*F and the Shiga toxin-producing IIe B domain antigen. For comparison, we also prepared a control vector strain (*S.* Choleraesuis C521). After oral vaccination of pigs, these strains contributed to persistent colonization of the intestinal mucosa and lymphoid tissues and elicited both cytokine expression and humoral immune responses. Furthermore, oral immunization with C522 elicited both *S.* Choleraesuis and rSF-specific immunoglobulin G (IgG) and IgA antibodies in the sera and gut mucosa, respectively. To further evaluate the feasibility and efficacy of these strains as mucosal delivery vectors via oral vaccination, we evaluated their protective efficacy against fatal infection with *S.* Choleraesuis C78-1, as well as the F18+ Shiga toxin-producing *Escherichia coli* field strain Ee, which elicits acute edema disease. C521 conferred complete protection against fatal infection with C78-1; and C522 conferred complete protection against fatal infection with both C78-1 and Ee. Our results suggest that C520, C521, and C522 are competent to provide complete mucosal immune protection against fatal infection

with *S.* Choleraesuis in swine and that C522 equally qualifies as an oral vaccine vector for protection against F18+ Shiga toxin-producing *Escherichia coli*.

KEYWORDS

Salmonella enterica* serovar Choleraesuis C500, mucosal immunity, edema disease of swine, host, *in vivo

1. Introduction

F18+ Shiga toxin-producing *Escherichia coli* (*E. coli*) will cause either post-weaning diarrhea (PWD) or edema disease of swine (ED) (Niewerth et al., 2001). It is also an important causative agent of diarrhea syndrome in swine, which has emerged over the past 3 to 5 years (Nadeau et al., 2017). These two diseases are the most widespread causes of death in weaned pigs or newborn piglets and account for substantial economic losses in the swine industry (Johansen et al., 1997). Although vaccines against F4 provide good protection from the PWD caused by F4 + enterotoxigenic *Escherichia coli* (ETEC), vaccines against F18 have not shown promising results due to poor immune response and difficulty producing specific antibodies (Verdonck et al., 2007; Delisle et al., 2012; Melkebeek et al., 2013; Okello et al., 2021). Hence, there is an unmet need for research on increasing the immune response of F18 as well as providing complete protection from PWD.

ST-II e (Shiga toxin-producing two variant) and F18 fimbriae (adhesion factor) are two virulence factors that are immunogenic and are regarded as the most important components of new generation vaccines against F18+ STE C (Johansen et al., 1997; Zhao et al., 2009b; Rossi et al., 2014; Cai et al., 2019). Although the single immunogenicity of F18 fimbriae and the ST-II e is not so great, their immunogenicity is enhanced through their fusion expression (Liu et al., 2007a). ST-II e has two domains: an enzymatic subunit (A) and five copies of a cell-binding subunit (the B pentamer; 7.5 kDa × 5) (Ling et al., 1998, 2000). The B pentamer is responsible for toxin attachment to a series of glycolipids on the cell surface and has been defined as an immunodominant protective epitope (Cai and Yang, 2003). Additionally, F18 fimbriae harbor two major structural adhesin genes, *fed*A and *fed*F. Although *fed*A subunit is immunodominant as compared to *fed*F, whereas *fed*A gene is not a shared sequence and there are more variations between the antigenic variants F18ab and F18ac, the latter containing an extra proline (Snoeck et al., 2004; Facinelli et al., 2019). Another adhesion of F18 fimbriae, *fed*F gene is highly conserved among F18+ *E. coli* strains isolated in different countries, and serves as a common receptor binding site for both F18ab and F18ac, and there is no specific variation in F18ab and F18ac (Tiels et al., 2005, 2008). Furthermore, anti-*fed*F antibodies are able to inhibit F18+ *E. coli* adhesion to porcine enterocytes (O'Brien et al., 2001; Moonens et al., 2014). These facts indicate that *fed*F is another good immunogenic candidate. Further study has demonstrated rSF that fusion proteins of the fimbriae adhesin domain of *fed*F with the Shiga toxin-producing IIe B domain antigen (rSF) result in high levels of neutralizing antibody against F18+ STEC in rabbits, conferring higher immunogenicity than *fed*F or ST-IIe B subunit alone under *in vivo* conditions (Liu et al., 2007a). Therefore, rSF provides a stable foundation for the development of a novel vaccine design.

Over the last decade, recombinant attenuated *Salmonella* vaccine strains have been increasingly employed for heterologous antigen delivery (DiGiandomenico et al., 2004; Su et al., 2021). The advantage of oral delivery of these strains is their ability to activate systemic immunity including cellular immunity, humoral immunity and mucosal immunity without causing significant side effects (DiGiandomenico et al., 2004). Varied vaccine components can affect the immune responses elicited by live *Salmonella*-vectors, including expression level, location and time of antigens (Isoda et al., 2007). Diverse methods have been developed to allow well-monitored and stable delivery of antigens and augmented immunogenicity where required. This includes the selection of heterologous protective fragments and their expression under the control of suitable plasmids within the vector strains (Spreng et al., 2006). The availability of well-characterized attenuated mutants of *Salmonella* supports fine-tuning of the immune response elicited by heterologous immunogenic fragments (Spreng et al., 2006).

The C500 strain of *S.* Choleraesuis is an attenuated vaccine strain attenuated by chemical methods (Xu et al., 2006). This strain exhibits efficacy and safety and has been used to prevent and control piglet paratyphoid in China for over 40 years (Zhao et al., 2009a). It has also been developed as a potential live oral vaccine vector for heterologous antigen delivery (Zhao et al., 2008; Li et al., 2014). Although the complete genome of C500 has been characterized (Han et al., 2014), the molecular mechanism of virulence attenuation of C500 remains obscure (Ji et al., 2015). Moreover, it has residual toxicity, which limits its utility. Therefore, a more effective, more stable, and safer strain is desirable. The C500 *asd*- vaccine strain was created by the introduction of an aspartate-semialdehyde dehydrogenase (*asd*) deletion mutant, which was employed to deliver foreign antigens utilizing the *Asd* + balanced-lethal host-vector system without any antibiotic resistance gene markers (Xu et al., 2006). Zhao et al. (2009a) have developed a version of C500 based on this mutant that efficiently and consistently expresses the recombinant filamentous hemagglutinin type I domain and pertactin region 2 domain antigens (rF1P2) of *Bordetella bronchiseptica* (*Bb*). Though this variant demonstrated complete protection efficacy against lethal dose challenge via subcutaneous injection in mice, it did not exhibit satisfactory efficacy of systemic and mucosal immunity after oral administration (Zhao et al., 2009a; Fan et al., 2021).

It is not known why the C500 *asd*- vaccine strain was less effective when administered orally than subcutaneous injection; however, this strain has a weakened colonizing ability, which may explain its poor immunity in mice (Xu et al., 2006; Han et al., 2014). Notably, the latter was not performed in the natural host, swine. The digestive system of pigs is different from that of mice, and the GI (gastrointestinal) tract is not only threatened by host defenses, but also more impacted by various small molecular compounds, such as glucose and other sugars. Moreover, glucose is the best carbon source for *Salmonella* and facilitates growth in culture. In the vaccine design, the Cyclic Adenosine monophosphate (cAMP)-independent cAMP receptor protein (Crp) is postulated to protect interference by glucose, which decreases synthesis of cAMP and enhances the colonizing ability and immunogenicity of the vaccine strains (Curtiss and Kelly, 1987). *Crp* deletion augments colonizing ability and immunogenicity of *Salmonella* vaccine constructs both in mice and in pigs (Curtiss et al., 2009). To maximize the colonizing ability and induction of immune responses, guarantee attenuation, prevent reversion of virulence, and eliminate potential side effects, vaccine strains typically integrate more than one advantage for genetic constructs. Therefore, C500 with both *asd* and *crp* deletion was designed and constructed as a new vaccine strain (named "C520") (Xu et al., 2006). However, no data regarding the *in vivo* function of this engineered strain in pigs have been reported.

In this study, we evaluated the colonization, virulence and systemic immunity of C520 in pigs and determined whether this strain elicits robust immune response and confers effective protection against challenge with homologous strains via the oral administration in swine. Additionally, we constructed a C500Δ*asd*Δ*crp* strain expressing rSF (C522) and initiated a comprehensive evaluation to determine whether C522 can provide robust immunity either to STEC or to *Salmonella* itself in an ED infection model in swine. Our results demonstrate that these vaccine strains provided improved practicable vaccine candidates against STEC.

2. Materials and methods

2.1. Bacterial strains, plasmids, primers, media, and growth conditions

The bacterial strains and plasmids used in this study are listed in **Table 1**. The STEC Ee strain (O139, positive for ST-IIe, F18ab) is a virulent field-type strain isolated from pigs in a farm in Wuhan during an outbreak of ED (Liu et al., 2007b). The attenuated *S.* Choleraesuis vaccine strain C500 and the wild-type, virulent parental strain C78-1 were supplied by the China Institute of Veterinary Drug Control (CIVDC, Beijing, China). C500 was chosen as the parent strain for the generation of genetically modified strains. *E. coli* and *S.* Choleraesuis cultures were grown at 37°C in Luria-Bertani (Alborali et al., 2017) broth or on LB agar plates. When required, D L-α, ε-diaminopimelic acid (D L-α, ε-DAP) (Liu et al., 2007a; Gangaiah et al., 2022) was added (50 μg/ml) for the growth of *asd*- strains (Xu et al., 2006).

TABLE 1 Strains and plasmids used in this study.

Strain, plasmid	Relevant characteristics	Source or references
E. coli DH5a	supE44 ΔlacU169 (φ80 lacZΔM15) hsdR17 recA1 endA1 gyrA96 thi-1 relA1	Takara
BL21 (DE3)	F^- *ompT* r^-_B m^-_B; DE3 is a λ derivative carrying *lacI* and T7 RNA polymerase genes under placUV5 control	Takara
χ7213	Thi-1 thr-1 leuB6 fhuA21 lacY1 glnV44 Δ*asd*A4 recA1 RP4 2-Tc: Mu[λpir] Kmr	Curtiss and Kelly, 1987; Curtiss et al., 2009
χ6097 *S.* Choleraesuis	F- ara Δ(pro-lac) rpsL Δ*asd*A4 Δ [zhf-2:Tn10] thi φ80 days lacZΔM15	Curtiss and Kelly, 1987; Curtiss et al., 2009
C500	A live vaccine attenuated from C78-1 by chemical methods, used to prevent piglet paratyphoid in China; serovar 6,7:C:1,5	CIVDC[a]
C78-1	Wild type, virulent strain	CIVDC[a]
C520	Δ*asd* Δ*crp* derivative of C500	This work
C521	C500Δ*asd*Δ*crp* vaccine expressing a control vector	This work
C522	C500Δ*asd*Δ*crp* vaccine expressing rSF	This work
E. coli Ee	Wild type, virulent strain, originally isolated from a pig suffering from edema disease of swine	Lab stock
Plasmid pBluescript SK (+)	Phagemid cloning vector, oriColE1 oriF1(+) bla lacZa	Stratagene
pRE112	oriT oriV Δ*asd* Cmr, sacB, counterselectable suicide plasmid	Curtiss and Kelly, 1987; Curtiss et al., 2009
pYA3493	*Asd* + vector; pBR322 ori; derivative β-lactamase signal sequence-based periplasmic secretion plasmid	Curtiss and Kelly, 1987; Curtiss et al., 2009
pYA-SF	1095-bp DNA encoding the ST-IIeB and *Fed*F in pYA3493	This work

[a]China institute of veterinary drug control (Beijing, China).

2.2. Construction of variants of the *S. enterica* serovar Choleraesuis C500 vaccine strain

The primers used for preparation of the recombinant a virulent vaccine strains are listed in **Table 2**. *S.* Choleraesuis C520, which has deletions in both *crp* and *asd*, was generated from the *S.*

TABLE 2 The primer sets used for the recombinant attenuated vaccine constructs.

Gene amplified	Primer names	Primer sequences (5′-3′)	Fragment length (bp)	Underline
Upstream of *crp*	pr1	TTTTCTAGAGCTGGATGAGAGTTTTGTGG	1048	*Xba*I
	pr2	TTTGGATCCCCATTCAAGAGTCGGGTCT		*Bam*HI
Downstream of *crp*	pr3	TTTCTCGAGGCTCGTCGCTTACAAGTCAC	1743	*Xho*I
	pr4	TTTGGTACCCAGTAACTGGATGGTGTATA		*Kpn*I
crp/*crp*-	pr5	GCCATTCTGACGGAATTAACGGG	1412 (*crp*$^-$)	
	pr6	TCGCGTACCCATATCAACTT	1731 (wt)	
Upstream of *asd*	pr1	TTTCTAGACGCTTTGAGCACGACTAA	2112	*Xba*I
	Pr2	TTGGATCCTGCGTTAGGAAGGGAATC		*Bam*HI
Downstream of *asd*	pr3	TTGGATCCAGGGTAGCTTAATCCCAC	2069	*Xho*I
	pr4	TTGGTACCACCGAGCGTTCATTGTCA		*Kpn*I
asd/*asd*-	pr5	TTGCTTTCCAACTGCTGAGC	1803 (wt)	
	pr6	TCCTATCTGCGTCGTCCTAC	315 (*asd*-)	
ST-IIeB	pr1	TTTGAATTCAAAGGTAAAAATTGAGTT	207	*Eco*RI
	pr2	TTTGAGCTCGTTAAACTTCACCTGGGC		*Sac*I
fedF	pr1	TTTGAGCTCACTCTACAAGTAGAC	894	*Sac*I
	pr2	TTAAGCTTTGGTCTACTTATTACGCGATG		*Hin*dIII

Choleraesuis C500 vaccine strain as described previously (Xu et al., 2006). Briefly, DNA was introduced into the bacteria by electroporation. A 1048 bp upstream fragment of the *crp* gene was amplified by PCR as described, with the exception that polymerization was performed at 72°C for 2.5 min from the genomic DNA of *S.* Choleraesuis C500 strain using two pairs of primers (Accession No: AE008863; N terminal, crp1, pr1 and pr2, crp2, pr3, and pr4). The amplified fragment was cloned into the *Xba*I and *Bam*HI sites of the pBluescript II SK (+) vector to construct pSK-*crp*up. Then, the 1743-bp downstream fragment of the *crp* gene was PCR-amplified using a pair of primers (pr3 and pr4) and cloned into the *Xho*I and *Kpn*I sites of pSK-*crp*up to obtain pSKΔ*crp*, which resulted in a 320-bp deletion, including the *crp* gene fragment. The 2890-bp fragment, including composed of the upstream and downstream fragments of the *crp* gene, from an *Xba*I- and *Kpn*I-digested pSKΔ*crp* plasmid was ligated to pRE112 plasmid to yield the pREΔ*crp* suicide plasmid. Transfer of the recombinant suicide plasmid to *S.* Choleraesuis C500 was accomplished by conjugation using *E. coli* χ7213 (pRE*crp*) as the plasmid donor. Strains containing single-crossover plasmid insertions (C500*crp*: pREΔ*crp*) were isolated on plates containing chloramphenicol and DAP. Loss of the suicide vector after the second recombination event between homologous regions (i.e., allelic exchange) was selected for by using a *sacB*-based sucrose sensitivity counter selection system. The presence of the 320-bp *crp* deletion in *S.* Choleraesuis C500 was confirmed by sucrose-sensitive growth on media and by PCR using a flanking *crp* primer set (pr5 + pr6). A pRE*asd* plasmid was constructed by the same method. Then C500Δ*crp* as recipient bacterium was conjugated with the *E. coli* χ7213 (pREasd) donor. The presence of the 1,408-bp *asd* deletion in *S.* Choleraesuis C520 was confirmed by the inability of the strain to grow on media without DAP and by PCR using a flanking *asd* primer set (pa5 and pa6).

To construct *S.* Choleraesuis C522, which is a derivative of C520 that expresses rSF, fragments encoding mature ST-IIe B and *fed*F were amplified from the genomic DNA of Ee *E. coli* using two pairs of primers (pB1, pB2, and pF1, pF2) that were designed according to the ST-IIeB gene sequence (GenBank accession no: AY332411) and the *fed*F gene sequence (GenBank accession no: AFZ26250) (Liu et al., 2007a). These primers contain restriction sites (*Eco*I, *Sac*I, *Sac*I, and *Hin*dIII) to allow the direct cloning of the PCR product into pYA-3493 plasmid. Two rounds of amplification were performed in a total volume of 50 μl containing 200 μM deoxynucleoside triphosphates (dATP, dCTP, dGTP, and dTTP), 1 pmol of each primer, 5 μl of dilution buffer, and 2.5 U of Taq polymerase. Thirty cycles were performed, each consisting of a denaturing step of 1 min at 94°C, an annealing step of 60 s at 55°C, and a 60 s extension step at 72°C. The 1095 bp PCR fragment of ST-IIeB and the *fed*F fragment were purified and cloned into the *Eco*RI and *Hin*dIII sites of pYA3493, resulting in pYA-SF. In-frame cloning of pYA-SF was confirmed by nucleotide sequencing. pYA-SF (encoding rSF) was electroporated into the C500Δ*asd*Δ*crp* strain (named C520), to construct the recombinant *S.* Choleraesuis C522 (pYA-SF). To prepare a control strain, pYA3493 (vector control) was electroporated into C520, resulting in C521 (pYA3493) being constructed.

2.3. Characterization of bacterial phenotypes

The growth curves of the strains in LB were determined, and carbohydrate fermentation or utilization assays were processed according to the manufacturer's protocol. MH medium, sugar fermentation tube purchased from Tianhe Microbial Reagent Co., Ltd (Hangzhou, China). The group O serovar and H antigen were identified by slide agglutination with antisera supplied by

the CIVDC (Beijing, China). The rSF fragment expression in the cytoplasm and culture supernatant of C522 was monitored by 12% SDS-PAGE, and immunoblot analyses were performed with the anti-rSF rabbit polyclonal antibody as previously described (Liu, 2008). Specific band intensities were further analyzed by densitometry using the Quant Studio™ 5 real-time PCR instrument (MA, USA).

2.4. Immunization and sampling

Duroc × Landrace × Yorkshire (DLY) Hybrid Pigs (F18R+, 28–30 days of age) were obtained from a breeding farm in Shandong Province, China to the experimental animal house of Huazhong Agricultural University. All pigs were confirmed either to be without antibody against both O antigen of *S.* Choleraesuis and rSF by their individual ELISA or to be culture-negative for both *S.* Choleraesuis and STEC by the enrichment of rectal swabs. In the process of the study, all animal experiments were approved by the Animal Ethics Committee (AEC) of the Huazhong Agricultural University, ethics number HZAUSW-2006-0005 and were performed according to the ARRIVE guidelines. When immunizing pigs (30 days of age), 2.0×10^9 CFU immunization doses of vaccine strain was administered orally in accordance with the vaccine instructions for the use of the C500 strain. A total of 128 pigs were randomly assigned to four groups, as follows: group 1 (pigs 1–32) received C522; group 2 (pigs 33–64) received C521; group 3 (pigs 65–96) received C500; group 4 (pigs 97–128) was non-infected controls, respectively, via the oral route (Narita and Ishii, 2004). Twelve pigs per group, group B, group C and group D were used for the evaluation of C521 to evaluate whether or not having ability to elicit a mucosal immune response via the oral route in swine. In addition, twelve pigs in group A were monitored as well as other three groups. Clinical manifestations and rectal temperature changes were observed daily over the first 5 days and on day 14 and 21 post-vaccination. And fecal consistency score was evaluated on a continuous scale (0–4/4) as described by Fairbrother et al. (2017). Fecal consistency scores of 2, 3, and 4 were considered as indicative of mild, moderate and severe diarrhea. Pigs with rectal temperature ≥41°C are fever (Yu et al., 2012). Additionally, rectal swabs and blood samples from each pig were collected. Autopsies were conducted as presently as possible for simultaneous death or on day 0, day 1, day 14, and day 21 post-vaccination. Three grams of spleen, mesenteric lymph nodes and Peyer's patches were immediately prepared in triplicates for cytokine determination. To determine the bacteria counts and antibody titers in the infected organs, 1 g of tissue samples from the spleen, mesenteric lymph nodes and Peyer's patches were homogenized in 10 ml phosphate-buffered saline (PBS). Enumeration of the bacteria strains in these organs or tissues was performed by plating a dilution series of lysates on MacConkey agar after overnight incubation at 37°C. Also, 2 ml PBS were used to wash the intestinal mucosa of the part of terminal ileum and then the wash fluid was collected. Antibody titers were determined in supernatants of homogenized organs and wash fluid. The other organ samples were fixed in 10% (w/v) buffered formalin and then subjected to histopathological examination.

An additional 20 pigs in each group were selected for protection studies. After 3 weeks of inoculation, 10 pigs were challenged with 2×10^{10} CFU of C78-1 and another 10 pigs with 2.5×10^{11} CFU of Ee strain. Monitoring and sample collection from challenged pigs were performed as described above in the post-vaccination and post-challenge periods. Necropsies were performed after simultaneous death on day 21 post-infection. Organ and tissue samples were prepared as described above. Rectal swabs and organs were examined to determine whether the orally administered live vaccine candidates or challenge strain were shed in the feces or located in the organs. Isolation and identification of the vaccine candidates and challenge strains were performed according to previously described methods (Xu et al., 2006). Blood and other samples were collected and stored at −80°C until use.

2.5. Cytokine response in the spleens of swine

Total RNA was extracted from the spleens of the vaccinated pigs using ISOGEN (Invitrogen). Reverse transcriptase-PCR (RT-PCR) was monitored using a one-step RNA PCR kit (Takara) with three pairs of primers according to the operating instructions. Primers are listed below: IFN-ϒ (5′-GTTTTTCTGGCTCTTACTGC-3′; 5′-CTTCCGCTT TCTTAGGTTAG-3′) (Chaoprasid and Dersch, 2021); TNF-α (5-ACTGCACTTCGAGGTTATCGG-3′, 5′-GGCGACGGGCTTATCTGA-3′) (Meissonnier et al., 2008); interleukin (IL)-4 (5′-GTCTGCTTACTGGCATGTACCA-3′; 5′-GCTCCATGCACGAGTTCTTTCT-3′) (Duvigneau et al., 2005); GAPDH (5′-AACGACCCCTTCATTGAC-3′; 5′-TCCACGACATACTCAGCAC-3′).

Quantitative reverse transcriptase-PCR (qRT-PCR) was performed on the 7900HT Sequence Detection System (Applied Biosystems) using SYBR Green (Meissonnier et al., 2008). Each sample was analyzed in triplicate. Data were analyzed by a comparative CT method (Applied Biosystems). Transcript levels were calculated by normalizing to the levels of GAPDH mRNA. In addition, cytokines (IFN-γ, IL 4, TNF-α) in the spleen were analyzed in relation to the expression of antibodies (IgG, IgA) in the mucus, MLN and serum utilizing JMP software.[1]

2.6. ELISA for *Salmonella* and rSF

Salmonella Somatic or rSF ELISA was used to monitor antibodies in serum samples, lymphoid-associated tissue and intestinal mucosal from each piglet. For the determination of anti-rSF titers, 100 ng of purified rSF dissolved in 100 μl 0.1 M carbonate buffer (pH 9.6) was coated in each well of polystyrene 96-well flat-bottomed microtiter plates (Kangjia Ltd., China). For determining the anti-*Salmonella* Somatic antibody level, *S.* Choleraesuis C500 cells were diluted in PBS at 3×10^{11} CFU/ml and grown overnight. The cells were then harvested by centrifugation, inactivated for 10 min at 80°C and stored at −80°C. Plates coated with 100 μl of this suspension at 100-fold dilution in carbonate buffer were incubated at 37°C for 1 h, followed by overnight incubation at 4°C. Then they were blocked with a blocking buffer (PBS, 0.1% tween

1 https://www.jmp.com/zhcn/software.html

20, and 5% skimmed milk). Samples of serum, lymphoid associated tissue and intestinal mucosa were diluted at the optimal dilution factor and added to each well and incubated at 37°C for 30 min. After three washes, plates were treated with biotinylated goat anti-pig IgG (Southern Biotechnology Inc., Birmingham, AL, USA) and lymphoid associated tissue homogenates or IgA at 37°C for 30 min, followed by five washes. The substrate solution TMB and H_2O_2 (50 μl) were then added to each well, and the plates were incubated at room temperature in the dark for approximately 10 min. The catalytic reactions were stopped with 50 μl 1% SDS. The optical densities were read at 630 nm using an ELISA reader (Liu, 2008).

2.7. Oral infection with *S.* Choleraesuis and STEC

The wild-type *S.* Choleraesuis strain C78-1 and the STEC field strain Ee were cultured in tryptose soy agar medium for 24 h at 37°C. The cultures were diluted of 1:100 in the tryptose soy broth and was incubated for 6 h with gentle shaking. All the pigs were fasted for 24 h prior to infection. The pigs were then intramuscularly injected with azaperone (stresnil, 4 mg/kg body weight), and 10 ml of a 10% (w/v) sodium bicarbonate solution was imported via gastric intubations followed by administration of bacterial emulsion. The Ee strain infection model was applied according to the method of B. T. Bosworth (Cornick et al., 1999). All of the pigs in this model were fed commercial rations containing 21.0% crude protein *ad libitum*, and until day 21 after the challenge, feed consumption, diarrhea, disorientation, abnormal behavior, and histopathology were all regularly assessed. For light microscopy, lungs and intestines were fixed in 10% formaldehyde solution embedded in paraffin and sections stained with Hematoxylin and eosin. Microscopically histological changes of these tissues caused by C78-1 and the Ee were the representative.

2.8. Statistical analysis

All data analysis was performed using the T Test or ANOVA in the SPSS 27 software[2] for comparison of the differences in specific antibody levels between different groups. *P*-value less than 0.05 (typically < 0.05) was statistically significant.

3. Results

3.1. Preparation of recombinant *S.* Choleraesuis C520 (C500ΔasdΔcrp), C522 (C500ΔasdΔcrp vaccine expressing rSF), and C521 (C500ΔasdΔcrp vaccine expressing a control vector)

To improve the *S.* Choleraesuis C500 vaccine, we introduced deletion mutations in both *asd* and *crp* genes. The resulting strain, C520, lacked the ability to synthesize DAP and was unable to grow on media without DAP, as expected. Its ability was restored when transfected with the control vector pYA3493, resulting in the creation of C521; or with the rSF expression vector pYA-SF, resulting in the creation of C522 (**Figure 1D**). The mean generation in Luria broth of the recombinant *S.* Choleraesuis strains C522 (31.2 min) and C521 (28.1 min) were similar to that of the parent attenuated C500 vaccine (27.9 min). We further compared their fermentation patterns on different carbohydrates. As expected, *S.* Choleraesuis C500, but not C521 and C522, was able to use maltose, glucose, mannose and xylose. Moreover, C521, C522 and the parent C500 strain were confirmed to share the same O and H antigenic type, 6, 7: C: 1, 5.

To confirm that *S.* Choleraesuis C522 expressed rSF we performed immunoblotting and Coomassie blue staining of SDS-polyacrylamide gels. C522 expressed the rSF of a molecular weight of 37 kDa, which is consistent with the calculated size of rSF (**Figure 1A**). Analysis of Coomassie blue-stained SDS-polyacrylamide gels showed that the amount of the rSF protein accounted for up to approximately 2.1% of the total C522 (pYA-SF) protein (**Figures 1B, C**). Approximately 69.8% of the rSF was detected in the cell lysates and 30.2% in the culture supernatants. To examine the stability of plasmids pYA3493 and pYA-SF in C522 and C521 *in vitro*, cells were cultured with daily passage of 1:1,000 dilution for five consecutive days in LB broth containing DAP. The last day, the amounts of the 37-kDa rSF that were expressed were similar to those from the first day, suggesting that the expression of rSF is stable from rearrangements.

3.2. The vaccine strains can colonize both the intestinal mucosa and lymphoid tissues

To evaluate the colonization abilities of the engineered strains, we vaccinated swine. All C500-inoculated piglets had diarrhea from day 1 to day 3 post-vaccination, and 20% of C500-inoculated piglets had fever after 14 days post vaccination; however, piglets inoculated with C520, C522, or C521 did not show side effects such as diarrhea, fever, depressed spirit, or abnormal behavior during the corresponding period (**Figure 2A**). The vaccine strains were detected in rectal swabs collected from immunized piglets from day 1 to day 10 after oral immunizations, but only the C500 strain was recovered from shedding fecal samples from day 1 to day 3 post-vaccination. These findings suggest that the vaccine strains have the ability to colonize the intestine, which is vital to the mucosal immunity and also suggests that C521 and C522 are safer than their parent strain C500.

To verify that the vaccine strains can settle in lymphoid tissue and to assess the residence time, we monitored the quantities of vaccine strain in the Peyer's patches, mesenteric lymph nodes and spleen at different times after inoculation. Between 0 and 1.4×10^3 CFU were detected from day 0 to day 21 post-inoculation (**Figure 2B**). These results confirm that the vaccine strains can colonize both the intestinal mucosa and lymphoid tissues.

2 https://www.ibm.com/docs/en/spss-statistics/27.0.0

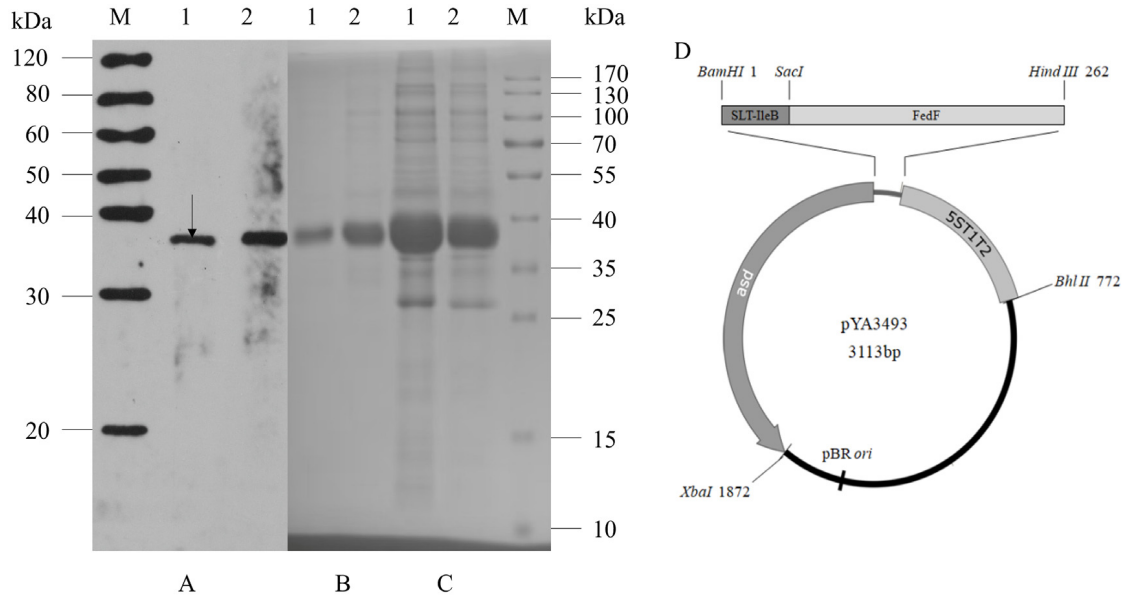

FIGURE 1
Expression of rSF by *S.* Choleraesuis C520, C522 and construction of vector pYA3493. C522 (pYA-SF; vaccine strain; rSF expression) and C521 (pYA3493; vector control) vaccine strains were cultured in LB broth at 37°C. Total cells (1.2×10^9) and concentrated culture supernatants (750 μl at an OD600 of 0.8) were subjected to SDS-PAGE analysis, and rSF was detected by Coomassie blue staining or immunoblotting with anti-rSF rabbit polyclonal antibody. **(A)** Immunoblot of concentrated culture supernatants (lane 1) and total cell extracts (lane 2) of the C522 strain detected with anti-rSF rabbit polyclonal antibody. **(B)** Coomassie brilliant blue gel staining of concentrated culture supernatant from C522 (lane 1) and inclusion bodies from C522 (lane 2). **(C)** Coomassie brilliant blue-stained gel of total cell extracts from C522 (pYA-SF) (lane 1) and C521 (pYA3493) (lane 2). Molecular markers are indicated to the right. The position corresponding to the predicted MW of rSF protein is indicated by an arrow. **(D)** Construction of vector pYA3493.

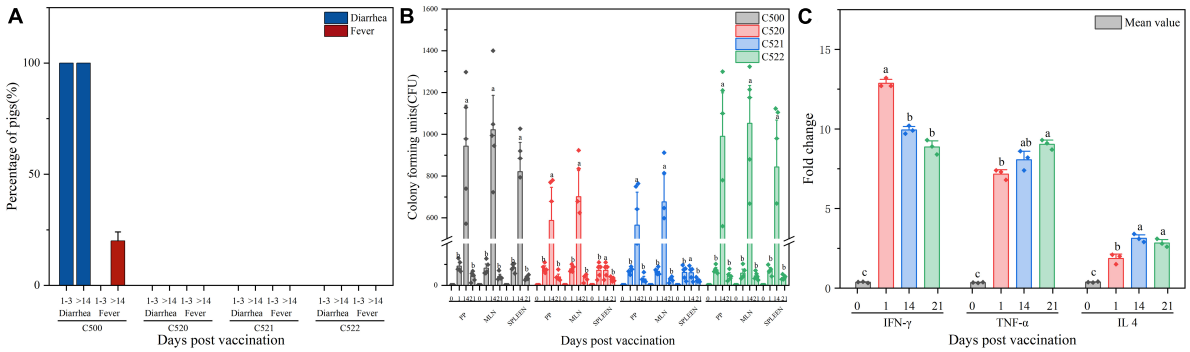

FIGURE 2
(A) Percentage of pigs experiencing diarrhea and fever 1–3 days and more than 14 days (>14) after vaccination C500, C520, C521, and C522. **(B)** Enumeration of the vaccine strains in lymphoid tissue after vaccination (day 0, day 1, day 14, and day 21). Pigs were orally vaccinated with 2.0×10^9 CFU of C522 (pYA-SF) vaccine strain, C521 (pYA3493) vector control strain or C500 parental vaccine strain. Colonization of each vaccine strain from the Peyer's patches (Facinelli et al., 2019). Facinelli et al. (2019), mesenteric lymph nodes (MLN) and spleen were measured on day 0, day 1, day 14, and day 21 post-vaccination. **(C)** Cytokine expression in the spleen from spleens of pigs immunized with C521. Pigs were orally vaccinated with 2.0×10^9 CFU of C521 (pYA3493) vector control strain. Quantitative RT-PCR was performed to measure the level of interferon Y (IFN-Y), tumor necrosis factor-α (TNF-α) and interleukin 4 (IL 4) on day 0, day 1, day 14, and day 21 post-vaccination. Day 0 as a control group means that the pigs have been unvaccinated. The level of each cytokine gene was normalized to the corresponding GAPDH value. Data represent the means ± SE ($n = 3$). The alphabet indicate the statistically significant differences between CFU of Cytokine at 0, 1, 14, and 21 days post-vaccination. $P < 0.05$ was considered significant. Error bars indicate standard deviations.

3.3. Vaccination with strain C521 induces proinflammatory cytokines

To further evaluate the cellular immune response to the C521 vaccine strain, we assessed the expression of inflammatory cytokines in the spleen of vaccinated piglets and naive piglets. On days 1, 14, and 21 after inoculation, the expression of IFN-γ, IL4, and TNF-α were elevated as assessed by qRT-PCR in the vaccinated piglets in contrast to piglets without inoculation of C521, on day 0. From day 1 to day 21 post-vaccination, IFN-γ expression level declined from day 1 to day 21 post-vaccination, whereas for TNF-α expression level increased. As for the expression

of IL4, it sustains a certain level at three timepoints, day 1, 14, and 21 (Figure 2C). In addition, the correlation analysis showed that the Pearson correlation between the expression of cytokines (IFN-γ, IL 4, TNF-α) in the spleen and the expression of antibodies (IgG, IgA) in the mucus (Supplementary Table 1), MLN (Supplementary Table 2) and serum (Supplementary Table 3) was between 0.4 and 0.8, indicating better correlation. These results indicate that inoculation with strain C521 may elicit cellular immunity in swine.

3.4. The vaccine strains are potent at inducing an *S.* Choleraesuis-specific antibody response

To further assess the immunogenicity of the vaccine strains, we evaluated the formation of antibodies against *S.* Choleraesuis in the sera, gut mucosa and mesenteric lymph nodes (MLN) of piglets that were orally vaccinated with C522, C521, and C500. ELISA was performed using whole cell *S.* Choleraesuis as antigen. C522, C521, and C500 vaccine elicited IgA and IgG antibody responses in the sera (Figures 3A, B), gut mucus (Figures 3C, D) and MLN (Figures 3E, F) on days 14 and 21 that were 7–9-fold higher than on day 0 ($P < 0.01$). Additionally, the antibody response to C522 was similar to that elicited by vaccination with C500 and C521. These results suggest C521 and C522 confer a vigorous systemic immune response, which verifies that the *asd* and *crp* deletions in these strains had a minimal influence on the immune response to *Salmonella* itself.

3.5. C522 elicits antibodies against rSF

We also assessed the production of antibodies against rSF by C522, C520, and C521, which is the only vaccine strain that expresses rSF. Our results demonstrate that C522-vaccinated pigs produced IgA and IgG antibody responses in the sera (Figures 4A, B), gut mucus (Figures 4C, D), and MLN (Figures 4E, F) at days 14 and 21.

3.6. Challenge of vaccinated pigs against *S.* Choleraesuis and STEC Ee

As a test of the efficacy of the vaccine strains, we assessed the ability of oral administration of the recombinant C521 vaccine, C522 vaccine, and the parental C500 vaccine to induce immunity in swine against oral challenge with an absolute lethal dose of the wild type, virulent parent strain, C78-1 (2×10^{10} CFU) or the STEC Ee strain (2.5×10^{11} CFU) (Zhao, 2009). Animals were fed a high-protein diet (comparable to commonly used commercial weaning rations). Complete protection against C78-1 was afforded by C521, C522, and C500, whereas there were no survivors in a group of ten naïve piglets in the PBS group (Table 3). Furthermore, almost no Ee strain was detected in rectal swabs from pigs orally vaccinated with C522 from day 3 until day 21 post-challenge, whereas large quantities were detected in the blank control group (Figure 5A). Only the C522 strain provided protection against STEC Ee. The other groups of animals showed clinical signs that were consistent with ED. Three pigs in the PBS group died of ED after seven days, and two were in lateral recumbence for 2 days and were euthanized. These results indicate that oral immunization with C521 or C522 (pYA-SF) can provide complete protection from *S.* Choleraesuis infection, and that C522 can additionally provide protection against STEC Ee.

Continual fevers typically occur in pigs undergoing necrotic enteritis. To further determine the *in vivo* efficiency of the recombinant strains, we monitored the temperatures during the entire animal experiment. Vaccinated pigs had marginally increased in body temperature 1 day after inoculation, followed by temperatures that immediately return to basal levels (Figure 5B), which suggests that continued necrotic enteritis was not present.

We also directly examined tissues for pathologic signs of necrotic enteritis in 21 days after vaccination. Naive pigs (PBS) inoculated with C78-1 and Ee showed severe pathological changes in the lungs and intestines (Figures 6A1–8). All of these pigs had extensive systemic lesions including focal necrosis in the liver and lymph nodes, fibrous necrotic enteritis in the ileum and caecum and mild interstitial pneumonia. In contrast, no significant pathological lesions were observed for the vaccinated groups upon challenge with C78-1 and Ee (Figures 6B1–6). These findings confirm the efficacy of C522 in protection swine against both *S.* Choleraesuis and STEC Ee.

To verify the protective response in C522-vaccinated pigs, the IgG and IgA responses in the MLN were assessed on day 21. C522 induced high antibody (IgG and IgA) response against both rSF and *S.* Choleraesuis Somatic (Figure 5C). Similar results were observed in the sera and mucosa (Figure 4). These results demonstrate that rSF fusion protein expressed by the strain C522 confers systemic rSF-specific immunity.

4. Discussion

Attenuated *S.* Choleraesuis strains have been developed over the past decade as live vaccines for humans and animals to prevent diseases caused by *Salmonella* infection (Alborali et al., 2017). Recombinant *Salmonella* strains have also been developed as multivalent vaccines for delivering recombinant antigens that originate from viruses, bacteria and parasites (Atul et al., 2011). The advantage of mucosal delivery of these strains remain their ability to activate systemic as well as local and distant compartments of the immune system (DiGiandomenico et al., 2004). Additionally, to avoid safety problems associated with the usage of antibiotics for selection of expression vectors, a host-vector system called "balanced-lethal system," based on the essential bacterial gene for aspartate β-semialdehyde dehydrogenase (*asd*), has been introduced to stabilize *Asd* + plasmids that carry foreign antigen genes (Santander et al., 2010). The *Asd* + plasmid pYA3493, which contains a DNA fragment encoding the β-lactamase signal sequence and 12 amino acid residues of the N terminus of mature β-lactamase from *Salmonella*, was designed and constructed for use in the periplasmic secretion of recombinant antigens for antigen delivery by *Salmonella* vaccines (Liang et al., 2008).

S. Choleraesuis C500, an attenuated vaccine strain attenuated by chemical methods, is highly immunogenic and relatively safe

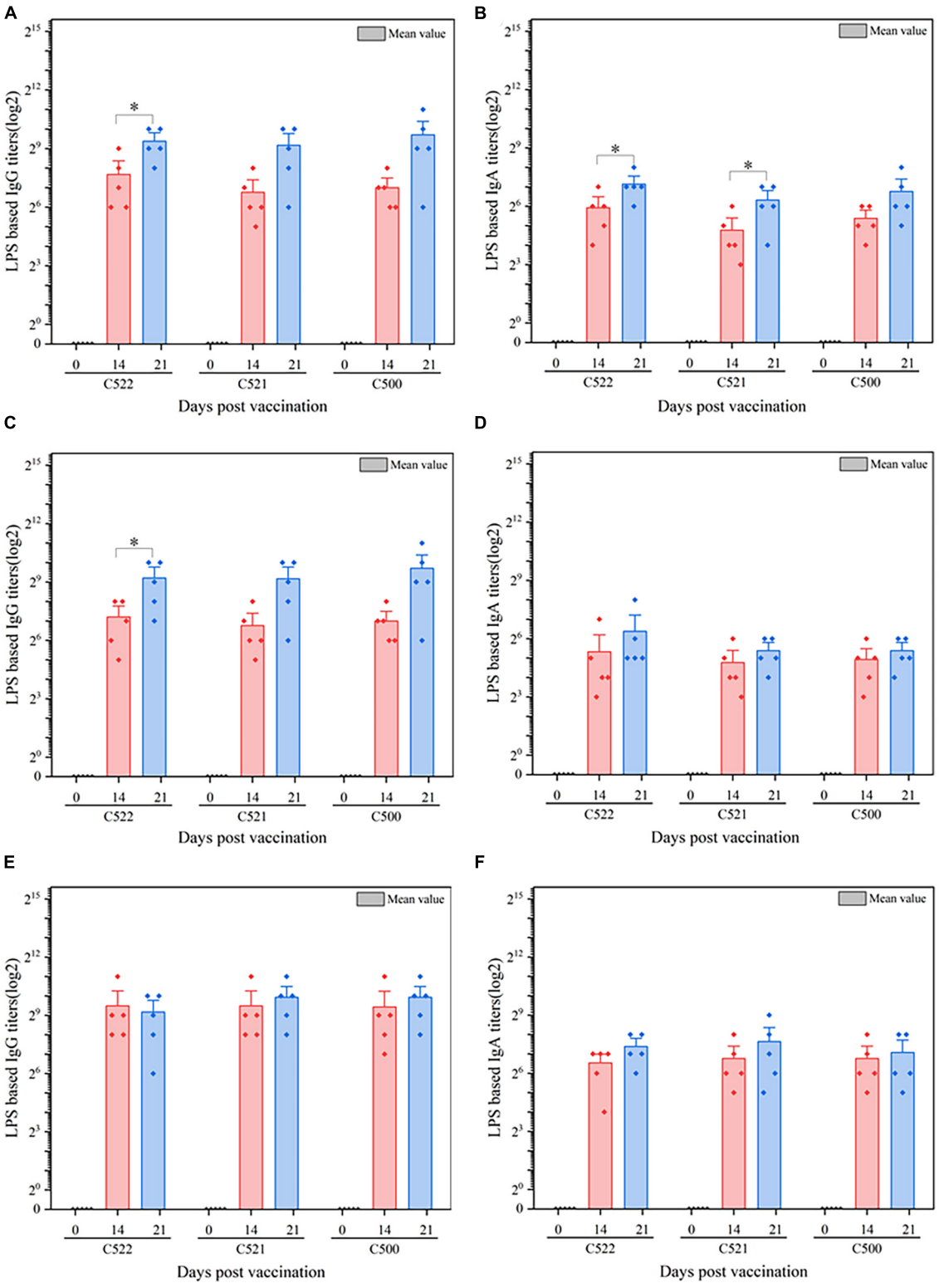

FIGURE 3
ELISA analysis of the anti-*S.* Choleraesuis immune response after oral vaccination of pigs with C521, C522 (pYA-SF) and C500-vaccinated pigs after oral vaccinations. Pigs were inoculated with the recombinant vaccine C522 (pYA-SF), C521 or parent (vector control) or the parental vaccine C500. Samples from 5 pigs were collected on day 0, day 14, and day 21. Individual pig serum, gut mucus (wash fluid from mucosa of terminal ileum) and MLN samples were tested for total IgG antibody or IgA antibody against whole *Salmonella* cells by ELISA. **(A,B)** Anti-*Salmonella* IgG or IgA titers obtained in serum; **(C,D)** anti-*Salmonella* IgG or IgA titers obtained in gut mucus; **(E,F)** anti-*Salmonella* IgG or IgA titers obtained in MLN. The data show the mean maximum end-point dilutions from the serum generating an optical density at 630 nm (OD630) two times that of undiluted pre-immune serum from the PBS-treated group (OD630 < 0.1). Statistical differences between groups were analyzed by the *T*-Test. The asterisk indicates the statistically significant differences ($P < 0.05$) between lipopolysaccharide (LPS) titers at 14 and 21 days post-vaccination. Error bars indicate standard deviations.

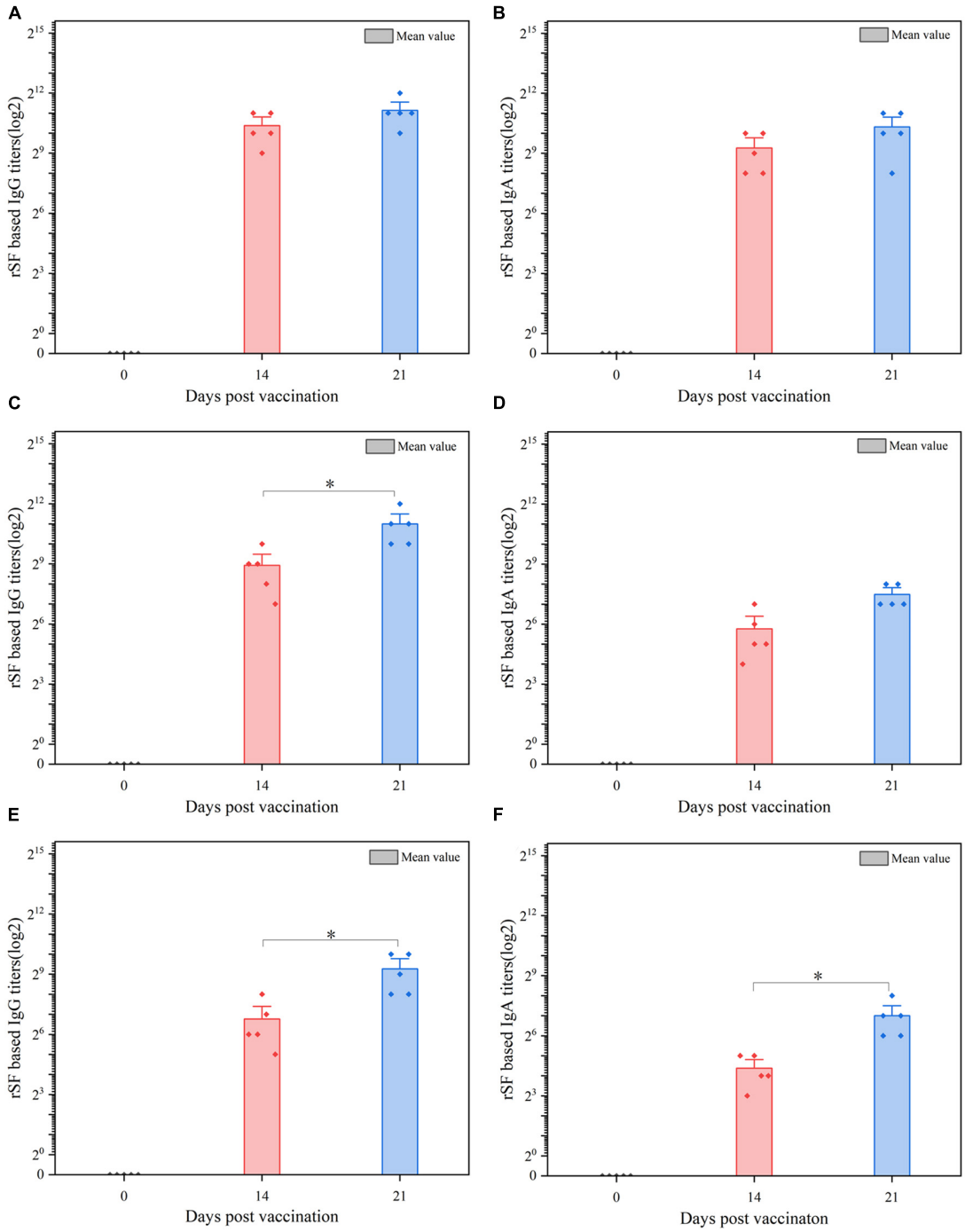

FIGURE 4
ELISA analysis of the anti-rSF immune response for pigs vaccinated orally with C522 (pYA-SF). Pigs were inoculated with the recombinant vaccine C522 (pYA-SF) on day 0, day 14, and day 21. Samples from 5 pigs in each group were collected at each time point. Individual pig serum, gut mucus and MLN samples were tested for total IgG antibody or IgA antibody against rSF by ELISA. **(A,B)** Anti-rSF IgG or IgA titers obtained in serum; **(C,D)** anti-rSF IgG or IgA titers obtained in gut mucus; **(E,F)** anti-rSF IgG or IgA titers obtained in MLN. The titers represent the maximum end-point dilutions from the sample yielding an optical density at 630 nm (OD630) two times that of undiluted pre-immune serum from the PBS-treated group (OD630 < 0.1). Mean values from each group were compared using the *T*-Test. The asterisk indicates the statistically significant differences ($P < 0.05$) between rSF titers at 14 and 21 days post-vaccination. Error bars indicate standard deviations.

and has been used to prevent piglet paratyphoid in China for over 40 years (Zhao et al., 2009a). As yet, its mechanism of immune protection has been unclear (Ji et al., 2015). Moreover, it has residual toxicity, which limits its utility. A previous study demonstrated that the systemic immune response to C500 Δ*asd* is elicited via subcutaneous injection, but not via oral vaccination in mice (Zhao et al., 2009a). The primary reason for the reduced immunogenicity is that C500 Δ*asd* has a weakened colonizing ability compared to its parental C500 strain. On the other hand, the mechanism of antigen presentation of attenuated *S.* Choleraesuis

TABLE 3 Effectiveness of oral immunization with the recombinant *S.* Choleraesuis C520 (pYA-SF) vaccine strain, the recombinant *S.* Choleraesuis C520 (pYA-3493), compared with the parental vaccine C500 and PBS, in protecting swine against challenge with wild-type parent C78-1 and STEC Ee.

Group	Immunizing strain	Immunizing dose (CFU)	Challenge dose (CFU)	Challenge strain	Survived pigs/total
A	C522	2.0×10^9	2×10^{10}	Ee	10/10
			2.5×10^{11}	C78-1	10/10
B	C521	2.0×10^9	2×10^{10}	C78-1	10/10
			2.5×10^{11}	Ee	0/10
C	C500	2.0×10^9	2×10^{10}	C78-1	10/10
			2.5×10^{11}	Ee	0/10
D	PBS	200 μl	2×10^{10}	C78-1	0/10
			2.5×10^{11}	Ee	0/10

A: piglets were orally immunized once with the three vaccine strains or with PBS control and infected 3 weeks after the infections with wild-type *S. enterica* serovar Choleraesuis C78-1 and STEC Ee. Morbidity and mortality were observed and recorded daily for 21 days post-challenge. B: 2.0×10^{10} CFU is representative of about 5 times the LD50 of C78-1 in non-immunized piglets. C: 2.5×10^{11} CFU is representative of about 5 times the LD50 of Ee in non-immunized piglets.

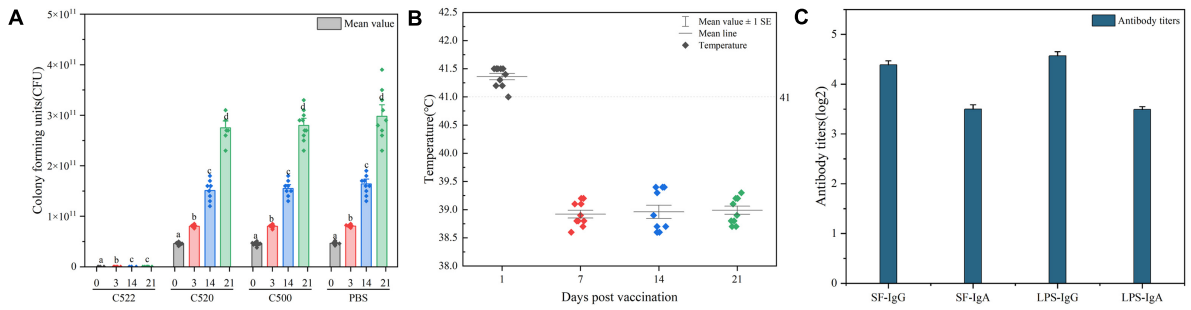

FIGURE 5

(A) CFU of Ee strain was detected in rectal swabs from pigs orally vaccinated with C522, C520, C500, and PBS from day 0 until day 21 post-challenge. The asterisk indicates the statistically significant differences between CFU of Ee strain at 0, 3, 14, and 21 days post-vaccination. $P < 0.05$ was considered significant. Error bars indicate standard deviations. **(B)** Temperatures of pigs during the 21 days post-vaccination. Pigs with temperatures above 41 degrees have an increase in body temperature. **(C)** ELISA analysis of the anti-rSF immune response in pigs vaccinated orally with C522 (pYA-SF) at 21 days after C78-1 and Ee challenge. Somatic of *S.* Choleraesuis C500-based IgG or IgA in mesenteric lymph nodes (MLN) from the C522-vaccinated pigs 21 days after C78-1 challenge and rSF-based IgG or IgA in MLN from the C522 vaccinated pigs 21 days after Ee challenge were determined by ELISA.

is not always consistent in mice and in pigs (Dominguez-Bernal et al., 2008). In this study, we have shown that orally administered *Salmonella* C500 with both *asd* and *crp* deletions (C520) elicited a strong immune response and conferred protection against challenge with homologous strains in the natural host. C520 showed immunity that is similar to that of its parent strain C500 in pigs. Another recombinant strain, C522 (C500Δ*asd*Δ*crp*SF) was constructed to allow vector delivery of the rSF fragment, and our results show that it provided robust immunity either to STEC or to *Salmonella* itself. These findings support the use of C520 and its derivatives to confer mucosal and systemic immune response in swine (Burda et al., 2018).

To verify the efficacy of the strains that were derived from C500, we addressed their colonization ability in pigs. Large quantities of the vector control strain C521 invaded and colonized in intestinal mucosa, lymphatic related tissues (Peyer's patches, MLN and spleen) at four time points post-vaccination. We also observed increased expression of IFN-γ, IL4 and TNF-α in spleens from pigs after oral vaccination of C521 and C500, suggesting that C521 may induce both humoral and cellular immunity in pigs. Because IL-4 can enhance CD8 T cell expansion during an immune response and IFN-γ can reciprocally counteract IL-4 induced reduction in IFN-γ production (Riber et al., 2015), the recombinant bacteria may induce a systemic immune response in pigs (Orndorff et al., 2000). Spleen levels of IL-4, TNF-α, and IFN-γ play a vital role in immune regulation, host defense against bacterial pathogens and protection from lethal bacterial infection (Ren et al., 2013). A simultaneous elevation of cytokines (IFN-γ and IL-4), which peaked at day 14 post-vaccination, may play a vital role in immune regulation, host defense against bacterial pathogens and protection at an early infection stage and thus complement the humoral immunity (Meissonnier et al., 2008; Ren et al., 2013). TNF-α level maintain a gently rising from day 1 to day 21 showing C522 can sustainedly attack host cell and live in the cell or colonize in the interstitial space, which contribute to the ability of triggering systemic immune response of C522. As expected, C521 conferred high antibody titers of *S.* Choleraesuis C500 Somatic IgA and IgG in intestinal mucosa, lymphoid associated tissues and sera. As a result, the vaccine provided complete protection efficiency against lethal challenge by C78-1.

A recombinant fusion gene, rSF, which is comprised of the B subunit of ST-IIe toxin fused to *fed*F adhesion of F18 fimbriae by

10.3389/fmicb.2023.1210358

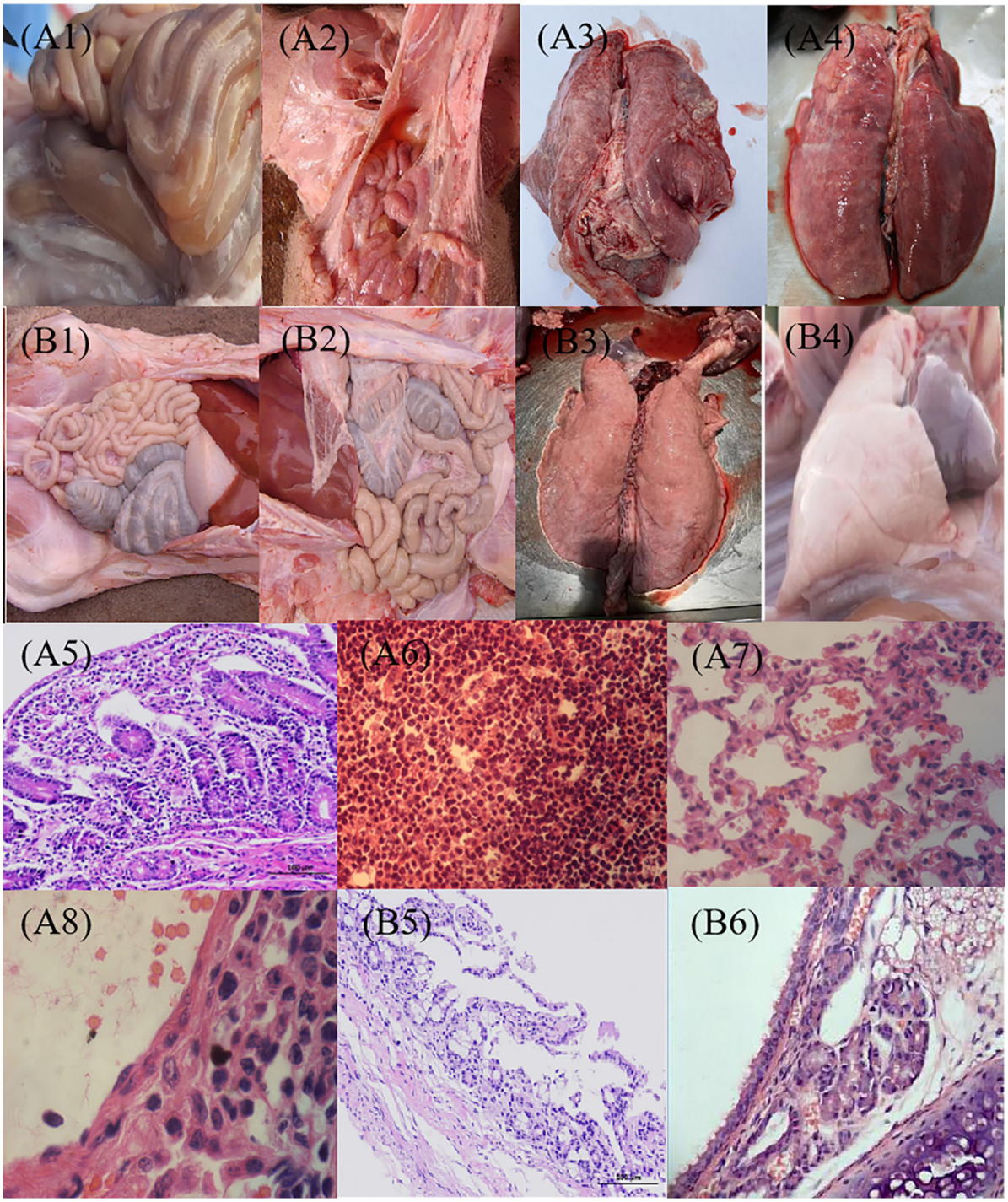

FIGURE 6
Pathological observation post-challenge with C78-1 and STEC Ee strains. Piglets were vaccinated orally with 1 dose of 2×10^9 CFU of C522 live vaccine, or PBS as blank control. Three weeks later, the piglets were challenged orally with 2.0×10^{10}CFU of virulent Salmonella C78-1 or 25×10^{10} CFU of STEC Ee field strain. **(A1,A2)** The PBS control of C78-1 and Ee on the gut, respectively. **(A1)** Mesenteric lymph nodes are diffusely hyperemic and mildly enlarged. **(A2)** There is moderate amount of yellowish fluid in the intestine, and the small intestine is hyperemic and bleeding. **(A3,A4)** The PBS control of C78-1 and Ee on the lung, respectively. **(A3)** Interstitial pneumonia, alveolar septal hyperemia, edema, inflammatory cell infiltration, septum widening, and alveolar shrinkage were seen in the lungs of piglets that challenged C78-1. **(A4)** The piglets that challenged Ee had fibrinous exudate on the apical lobes of their lungs, and the entire lung was covered with rubber-like exudate. **(A5)** The intestinal mucosal wall of piglets that challenged C78-1 is destroyed, the intestinal mucosa is detached, and inflammatory cells are infiltrated. **(A6)** The small intestinal lymph nodes of piglets that challenged Ee showed hemorrhagic and necrotic pathological manifestations. **(A7,A8)** The piglets that challenged C78-1 and Ee had hyperemia and thickened capillaries in the alveolar wall, and a large number of neutrophils and serous and fibrinous exudation in the alveolar cavity. **(B1,B2)** The protective effects of C78-1 and Ee on the gut after vaccination with C522, respectively. **(B3,B4)** The protective effects of C78-1 and Ee on the lung after vaccination with C522, respectively. **(B5)** The intestinal tissue of piglets in the C522 immune group had no lesions and the intestinal mucosa was intact. **(B6)** The lungs of piglets in the C522 immune group had no lesions. Magnification, 10×4 **(A5,B5)**, 10×40 (others).

a rigid linker, has previously been reported as an effective vaccine candidate (Liu, 2008). Therefore, in this study, we constructed a recombinant C520 strain using the C522 host strain that express rSF based on the *Asd* + balanced-lethal host-vector system.(Yan et al., 2013). As a model to further test the feasibility of C520-derived strains as mucosal vaccine vectors, we investigated the efficacy of C522 in preventing ED, a classical GI infectious disease caused by STEC that has a mortality rate of 90–100% and causes considerable economic loss in the swine industry (Hamabata et al., 2019). Although vaccines against F4 provide good protection from the PWD caused by F4 + ETEC, vaccines against F18 have not shown promising results due to insufficient immune response and difficulty producing specific antibodies (Okello et al., 2021). pYA-SF was stable (100% recovery) over 50 generations in the C522 vaccine strain grown in the presence of DAP. C520 contains pYA-SF expressed the rSF protein with an apparent molecular mass of about 37 kDa, and this protein was detected in the cytoplasm and in the culture supernatant. These results suggest that the signal peptide and 12 residues of the N terminus of β-lactamase (present in pYA-SF) promote periplasmic secretion of rSF. Kang et al. reported that the immunogenicity and appropriate sub-cellular localization of recombinant heterologously expressed antigen in a *Salmonella* vaccine strain augments immune responses by facilitating adequate exposure of rSF antigen to antigen-presenting cells for processing (Kang et al., 2002). Consistently, this study shows elevated protection efficacy against Ee strain and fecal excretion was also prevented when C522 was administered orally in pigs. Similar levels of anti-*S.* Choleraesuis IgG in the sera and IgA in the gut mucosa were induced by strains C500 and C522, suggesting that rSF-specific immunity, including mucosal and humoral immunity conferred by C522, did not interfere with immunity against *Salmonella* C520 itself. Additionally, the C522 strain elicited IgG and IgA that was specific to rSF. The results indicate that oral vaccination with this strain provides complete protection against challenge with Ee strain in a gastrointestinal tract model, suggesting that effective immunization might be achieved via the oral route based on this principle. Infection is initiated by the attachment of STEC organisms to intestinal brush border cells of the gastrointestinal tract; the bacteria then cause local damage to the gastrointestinal tract and systemic manifestations of disease (Cornick et al., 1999). Therefore, protection may correlate with the presence of protective antibodies in the intestinal mucosa, and induction of local immunity to this pathogen appears to be an ideal strategy for the prevention of infection (Melkebeek et al., 2013).

The efficacy of C522 in our study is in contrast to the results of another study in which a Δ*asd* strain harboring F1P2 could not provide sufficient immunity against *Bb* challenge via the oral inoculation route in mice (Han et al., 2014). Furthermore, only trace amounts of Ee strain was detected in rectal swabs from pigs orally vaccinated with C522 from day 3 until day 21 post-challenge, whereas copious quantities were detected in the blank control group. These findings suggest that protection correlates with the presence of specific IgG and IgA for rSF in the mucosa of the gastrointestinal tract, and protection against infection was apparently associated with the local systemic responses elicited by vaccination. In addition, these findings suggest that the degree of activation of gut-associated lymphoid tissue by oral vaccination is sufficient for antibody-secreting B cells to localize to the gastrointestinal tract lymphoid tissue (Liu, 2008). And these results also indicate that local lymphoid tissue is one of the sources of the protective antibodies. C522 conferred slightly higher IgA or IgG titers of the antibody against Somatic of *S.* Choleraesuis than did C520 in pigs, which verified that the rSF fragment delivery contributed to the elevated immunogenicity of the C520 vector.

5. Conclusion

C520 and the C522 antigen vector confer mucosal immune and systemic immune response in its natural host, swine. We showed that both C520 and C522 protect pigs against fatal infection with *S.* Choleraesuis. Furthermore, C522 provides a safe and promising vaccine candidate against STEC, which may be useful in practice in the future. This vaccine could also be easily adapted to develop multivalent recombinant *Salmonella* vaccines against other homologous strains.

Data availability statement

The original contributions presented in this study are included in the article/**Supplementary material**, further inquiries can be directed to the corresponding authors.

Ethics statement

The animal study was approved by the Animal Ethics Committee (AEC) of the Huazhong Agricultural University. The study was conducted in accordance with the local legislation and institutional requirements.

Author contributions

GL, CL, and SL provided conceptualization, methodology, writing, reviewing, and editing. GL and SL provided methodology and investigation. CL and GL provided data analysis. AG provided methodology and visualization. BW provided project administration and manuscript checking. BW and HC provided supervision and visualization. All authors contributed to the manuscript and approved the submitted version.

Funding

This research was funded by grants from the National Nature Science Foundation of China (No. 30471292), and the Special Fund for Agro-scientific Research in the Public Interest of the Ministry of China (No. 201503226).

Acknowledgments

We thank Roy Curtiss III (at the Department of Biology, Washington University, MO, USA) for the generous donation of strains and plasmids.

Conflict of interest

The authors declare that the research was conducted in the absence of any commercial or financial relationships that could be construed as a potential conflict of interest.

Publisher's note

All claims expressed in this article are solely those of the authors and do not necessarily represent those of their affiliated organizations, or those of the publisher, the editors and the reviewers. Any product that may be evaluated in this article, or claim that may be made by its manufacturer, is not guaranteed or endorsed by the publisher.

Supplementary material

The Supplementary Material for this article can be found online at: https://www.frontiersin.org/articles/10.3389/fmicb.2023.1210358/full#supplementary-material

References

Alborali, G. L., Ruggeri, J., Pesciaroli, M., Martinelli, N., Chirullo, B., Ammendola, S., et al. (2017). Prime-boost vaccination with attenuated *Salmonella typhimurium* ΔznuABC and inactivated *Salmonella choleraesuis* is protective against *Salmonella choleraesuis* challenge infection in piglets. *BMC Vet. Res.* 13:284. doi: 10.1186/s12917-017-1202-5

Atul, A. C., Sam Woong, K., Kiku, M., and John Hwa, L. (2011). Safety evaluation and immunogenicity of arabinose-based conditional lethal *Salmonella Gallinarum* mutant unable to survive ex vivo as a vaccine candidate for protection against fowl typhoid. *Avian Dis.* 55, 165–171. doi: 10.1637/9512-083010-Reg.1

Burda, W. N., Brenneman, K. E., Gonzales, A., and Curtiss, R. (2018). Conversion of RpoS(-) Attenuated *Salmonella enterica* serovar typhi vaccine strains to RpoS(+) improves their resistance to host defense barriers. *mSphere* 3, e00006–e00018. doi: 10.1128/mSphere.00006-18

Cai, X., Yu, N., Ma, J., Li, W. Y., Xu, M., Li, E., et al. (2019). Altered pulmonary capillary permeability in immunosuppressed guinea pigs infected with *Legionella pneumophila* serogroup 1. *Exp. Ther. Med.* 18, 4368–4378. doi: 10.3892/etm.2019.8102

Cai, X. E., and Yang, J. (2003). The Binding Potential between the Cholera Toxin B-Oligomer and Its Receptor. *Biochemistry* 42, 4028–4034. doi: 10.1021/bi027016h

Chaoprasid, P., and Dersch, P. (2021). The Cytotoxic Necrotizing Factors (CNFs)-A Family of Rho GTPase-Activating Bacterial Exotoxins. *Toxins* 13, 901. doi: 10.3390/toxins13120901

Cornick, N. A., Matise, I., Samuel, J. E., Bosworth, B. T., and Moon, H. W. (1999). Edema disease as a model for systemic disease induced by Shiga toxin-producing E. coli. *Adv. Exp. Med. Biol.* 473, 155–161. doi: 10.1007/978-1-4615-4143-1_14

Curtiss, R., and Kelly, S. M. (1987). *Salmonella typhimurium* deletion mutants lacking adenylate cyclase and cyclic AMP receptor protein are avirulent and immunogenic. *Infect. Immun.* 55, 3035–3043. doi: 10.1128/iai.55.12.3035-3043.1987

Curtiss, R., Wanda, S.-Y., Gunn Bronwyn, M., Zhang, X., Tinge Steven, A., Ananthnarayan, V., et al. (2009). *Salmonella enterica* serovar typhimurium strains with regulated delayed attenuation *in vivo*. *Infect. Immun.* 77, 1071–1082. doi: 10.1128/IAI.00693-08

Delisle, B., Calinescu, C., Mateescu, M. A., Fairbrother, J. M., and Nadeau, E. (2012). Oral immunization with F4 fimbriae and CpG formulated with carboxymethyl starch enhances F4-specific mucosal immune response and modulates Th1 and Th2 cytokines in weaned pigs. *J. Pharmacy Pharm. Sci.* 15, 642–656. doi: 10.18433/J30W32

DiGiandomenico, A., Rao, J., and Goldberg, J. B. (2004). Oral vaccination of BALB/c mice with *Salmonella enterica* serovar Typhimurium expressing *Pseudomonas aeruginosa* O antigen promotes increased survival in an acute fatal pneumonia model. *Infect. Immun.* 72, 7012–7021. doi: 10.1128/IAI.72.12.7012-7021.2004

Dominguez-Bernal, G., Tierrez, A., Bartolome, A., Martinez-Pulgarin, S., Salguero, F. J., Orden, J. A., et al. (2008). *Salmonella enterica* serovar Choleraesuis derivatives harbouring deletions in rpoS and phoP regulatory genes are attenuated in pigs, and survive and multiply in porcine intestinal macrophages and fibroblasts, respectively. *Vet. Microbiol.* 130, 298–311. doi: 10.1016/j.vetmic.2008.01.008

Duvigneau, J. C., Hartl, R. T., Groiss, S., and Gemeiner, M. (2005). Quantitative simultaneous multiplex real-time PCR for the detection of porcine cytokines. *J. Immunol. Methods* 306, 16–27. doi: 10.1016/j.jim.2005.06.021

Facinelli, B., Marini, E., Magi, G., Zampini, L., Santoro, L., Catassi, C., et al. (2019). Breast milk oligosaccharides: effects of 2′-fucosyllactose and 6′-sialyllactose on the adhesion of *Escherichia coli* and *Salmonella fyris* to Caco-2 cells. *J. Matern. Fetal Neonatal Med.* 32, 2950–2952. doi: 10.1080/14767058.2018.1450864

Fairbrother, J. M., Nadeau, E., Belanger, L., Tremblay, C. L., Tremblay, D., Brunelle, M., et al. (2017). Immunogenicity and protective efficacy of a single-dose live non-pathogenic *Escherichia coli* oral vaccine against F4-positive enterotoxigenic *Escherichia coli* challenge in pigs. *Vaccine* 35, 353–360. doi: 10.1016/j.vaccine.2016.11.045

Fan, Y., Bai, T., Tian, Y., Zhou, B., Wang, Y., and Yang, L. (2021). H2O2-Inactivated *Salmonella typhimurium* RE88 strain as a new cancer vaccine carrier: Evaluation in a mouse model of cancer. *Drug Des. Devel Ther.* 15, 209–222. doi: 10.2147/DDDT.S282660

Gangaiah, D., Ryan, V., Van Hoesel, D., Mane, S. P., McKinley, E. T., Lakshmanan, N., et al. (2022). Recombinant *Limosilactobacillus* (*Lactobacillus*) delivering nanobodies against *Clostridium perfringens* NetB and alpha toxin confers potential protection from necrotic enteritis. *MicrobiologyOpen* 11, e1270. doi: 10.1002/mbo3.1270

Hamabata, T., Sato, T., Takita, E., Matsui, T., Imaoka, T., Nakanishi, N., et al. (2019). Shiga toxin 2eB-transgenic lettuce vaccine is effective in protecting weaned piglets from edema disease caused by Shiga toxin-producing *Escherichia coli* infection. *Anim. Sci. J.* 90, 1460–1467. doi: 10.1111/asj.13292

Han, L., Zhen, Y.-H., Liang, A.-X., Zhang, J., Riaz, H., Xiong, J.-J., et al. (2014). Oral vaccination with inhibin DNA delivered using attenuated *Salmonella choleraesuis* for improving reproductive traits in mice. *J. Basic Microbiol.* 54, 962–968. doi: 10.1002/jobm.201300052

Isoda, R., Simanski, S. P., Pathangey, L., Stone, A. E., and Brown, T. A. (2007). Expression of a *Porphyromonas gingivalis* hemagglutinin on the surface of a *Salmonella* vaccine vector. *Vaccine* 25, 117–126. doi: 10.1016/j.vaccine.2006.06.085

Ji, Z., Shang, J., Li, Y., Wang, S., and Shi, H. (2015). Live attenuated *Salmonella enterica* serovar Choleraesuis vaccine vector displaying regulated delayed attenuation and regulated delayed antigen synthesis to confer protection against Streptococcus suis in mice. *Vaccine* 33, 4858–4867. doi: 10.1016/j.vaccine.2015.07.063

Johansen, M., Andresen, L. O., Jorsal, S. E., Thomsen, L. K., Waddell, T. E., and Gyles, C. L. (1997). Prevention of edema disease in pigs by vaccination with verotoxin 2e toxoid. *Can. J. Vet. Res.* 61, 280–285.

Kang, H. Y., Srinivasan, J., and Curtiss, R. (2002). Immune responses to recombinant pneumococcal PspA antigen delivered by live Attenuated *Salmonella enterica* serovar typhimurium vaccine. *Infect. Immun.* 70, 1739–1749. doi: 10.1128/IAI.70.4.1739-1749.2002

Li, Q., Hu, Y., Xu, L., Xie, X., Tao, M., and Jiao, X. (2014). Complete genome sequence of *Salmonella enterica* Serovar Choleraesuis Vaccine Strain C500 Attenuated by Chemical Mutation. *Genome Announce.* 2, e1022–e1014. doi: 10.1128/genomeA.01022-14

Liang, A., Feng, X., Han, L., Hua, G., Sang, L., Liu, X., et al. (2008). Construction and characterization of a novel somatostatin prokaryotic expression. *Chin. J. Biotechnol.* 24, 995–998.

Ling, H., Boodhoo, A., Hazes, B., Cummings, M. D., Armstrong, G. D., Brunton, J. L., et al. (1998). Structure of the shiga-like toxin I B-pentamer complexed with an analogue of its receptor Gb3. *Biochemistry* 37, 1777–1788. doi: 10.1021/bi971806n

Ling, H., Pannu, N. S., Boodhoo, A., Armstrong, G. D., Clark, C. G., Brunton, J. L., et al. (2000). A mutant Shiga-like toxin IIe bound to its receptor Gb(3): structure of a group II Shiga-like toxin with altered binding specificity. *Structure* 8, 253–264. doi: 10.1016/S0969-2126(00)00103-9

Liu, G., Wu, B., Lin, Y., Liu, M., Chen, H., and Hu, C. (2007a). Fusion expression of SLT-IIeB gene and FedF gene of Ee in *Escherichia coli* and its immunogenicity. *J. Microbiol.* 6, 1044–1049. doi: 10.13343/j.cnki.wsxb.2007.06.027

Liu, G. P., Wu, B., Lin, Y. Y., Jin, M. L., and Chen, H. C. (2007b). Expression of GST-3B fusion protein of *Escherichia coli* of Ee strain producing SLT-IIe toxin and study on its biological activities and immunogenicity. *Acta Microbiol. Sin.* 47, 686–691. doi: 10.13343/j.cnki.wsxb.2007.04.023

Liu, G. P. (2008). Study on Gene Engineering Submit Bacterin against Oedema Disease of Swine and Etiology of F18+E.coli. *Huazhong Agric. Univ.* 2, 1–129.

Meissonnier, G. M., Pinton, P., Laffitte, J., Cossalter, A. M., Gong, Y. Y., Wild, C. P., et al. (2008). Immunotoxicity of aflatoxin B1: impairment of the cell-mediated response to vaccine antigen and modulation of cytokine expression. *Toxicol. Appl. Pharmacol.* 231, 142–149. doi: 10.1016/j.taap.2008.04.004

Melkebeek, V., Goddeeris, B. M., and Cox, E. (2013). ETEC vaccination in pigs. *Vet. Immunol. Immunopathol.* 152, 37–42. doi: 10.1016/j.vetimm.2012.09.024

Moonens, K., De Kerpel, M., Coddens, A., Cox, E., Pardon, E., Remaut, H., et al. (2014). Nanobody mediated inhibition of attachment of F18 Fimbriae expressing *Escherichia coli*. *PLoS One* 9:e114691. doi: 10.1371/journal.pone.0114691

Nadeau, E., Fairbrother, J. M., Zentek, J., Belanger, L., Tremblay, D., Tremblay, C. L., et al. (2017). Efficacy of a single oral dose of a live bivalent E. coli vaccine against post-weaning diarrhea due to F4 and F18-positive enterotoxigenic *E. coli*. *Vet. J.* 226, 32–39. doi: 10.1016/j.tvjl.2017.07.004

Narita, M., and Ishii, M. (2004). Encephalomalacic lesions in pigs dually infected with porcine reproductive and respiratory syndrome virus and pseudorabies virus. *J. Comp. Pathol.* 131, 277–284. doi: 10.1016/j.jcpa.2004.05.001

Niewerth, U., Frey, A., Voss, T., Le Bouguenec, C., Baljer, G., Franke, S., et al. (2001). The AIDA autotransporter system is associated with F18 and stx2e in *Escherichia coli* isolates from pigs diagnosed with edema disease and postweaning diarrhea. *Clin. Diagn. Lab. Immunol.* 8, 143–149. doi: 10.1128/CDLI.8.1.143-149.2001

O'Brien, A. D., Smeds, A., Hemmann, K., Jakava-Viljanen, M., Pelkonen, S., Imberechts, H., et al. (2001). Characterization of the adhesin of *Escherichia coli* F18 fimbriae. *Infect. Immun.* 69, 7941–7945. doi: 10.1128/IAI.69.12.7941-7945.2001

Okello, E., Moonens, K., Erume, J., and De Greve, H. (2021). Orally fed recombinant *Lactococcus lactis* displaying surface anti-fimbrial nanobodies protects piglets against *Escherichia coli* causing post-weaning diarrhea. *Agriculture* 11, 186. doi: 10.3390/agriculture11030186

Orndorff, P. E., Fournout, S., Dozois, C. M., Odin, M., Desautels, C., Pérès, S., et al. (2000). Lack of a role of cytotoxic necrotizing factor 1 toxin from *Escherichia coli* in bacterial pathogenicity and host cytokine response in infected germfree piglets. *Infect. Immun.* 68, 839–847. doi: 10.1128/IAI.68.2.839-847.2000

Ren, W. K., Yu, R., Liu, G., Li, N. Z., Peng, Y. Y., Wu, M. M., et al. (2013). DNA vaccine encoding the major virulence factors of Shiga toxin type 2e (Stx2e)-expressing *Escherichia coli* induces protection in mice. *Vaccine* 31, 367–372. doi: 10.1016/j.vaccine.2012.10.107

Riber, U., Heegaard, P. M., Cordes, H., Stahl, M., Jensen, T. K., and Jungersen, G. (2015). Vaccination of pigs with attenuated *Lawsonia intracellularis* induced acute phase protein responses and primed cell-mediated immunity without reduction in bacterial shedding after challenge. *Vaccine* 33, 156–162. doi: 10.1016/j.vaccine.2014.10.084

Rossi, L., Dell'Orto, V., Vagni, S., Sala, V., Reggi, S., and Baldi, A. (2014). Protective effect of oral administration of transgenic tobacco seeds against verocytotoxic *Escherichia coli* strain in piglets. *Vet. Res. Commun.* 38, 39–49. doi: 10.1007/s11259-013-9583-9

Santander, J., Xin, W., Yang, Z., and Curtiss, R. (2010). The aspartate-semialdehyde dehydrogenase of *Edwardsiella ictaluri* and its use as balanced-lethal system in fish vaccinology. *PLoS One* 5:e15944. doi: 10.1371/journal.pone.0015944

Snoeck, V., Verdonck, F., Cox, E., and Goddeeris, B. M. (2004). Inhibition of adhesion of F18+ *Escherichia coli* to piglet intestinal villous enterocytes by monoclonal antibody against blood group H-2 antigen. *Vet. Microbiol.* 100, 241–246. doi: 10.1016/j.vetmic.2004.03.001

Spreng, S., Dietrich, G., and Weidinger, G. (2006). Rational design of *Salmonella*-based vaccination strategies. *Methods* 38, 133–143. doi: 10.1016/j.ymeth.2005.09.012

Su, H. L., Liu, Q., Bian, X. P., Wang, S. F., Curtiss, R., and Kong, Q. K. (2021). Synthesis and delivery of *Streptococcus pneumoniae* capsular polysaccharides by recombinant attenuated *Salmonella* vaccines. *Proc. Natl. Acad. Sci. U. S. A.* 118, 2013350118. doi: 10.1073/pnas.2013350118

Tiels, P., Verdonck, F., Coddens, A., Goddeeris, B., and Cox, E. (2008). The excretion of F18+ E. coli is reduced after oral immunisation of pigs with a FedF and F4 fimbriae conjugate. *Vaccine* 26, 2154–2163. doi: 10.1016/j.vaccine.2008.01.054

Tiels, P., Verdonck, F., Smet, A., Goddeeris, B., and Cox, E. (2005). The F18 fimbrial adhesin FedF is highly conserved among F18(+) *Escherichia coli* isolates. *Vet. Microbiol.* 110, 277–283. doi: 10.1016/j.vetmic.2005.08.004

Verdonck, F., Tiels, P., van Gog, K., Goddeeris, B. M., Lycke, N., ClementSd, J., et al. (2007). Mucosal immunization of piglets with purified F18 fimbriae does not protect against F18(+) *Escherichia coli* infection. *Vet. Immunol. Immunopathol.* 120, 69–79. doi: 10.1016/j.vetimm.2007.06.018

Xu, Y. D., Guo, A. Z., Liu, W. H., Jia, A. Q., and Chen, H. C. (2006). Construction and characterization of delta crp delta asd mutant host-vector balanced lethal system of *Salmonella choleraesuis* C500 strain. *Chin. J. Biotechnol.* 22, 366–372. doi: 10.13345/j.cjb.2006.03.003

Yan, Y. J., Mu, W., Zhang, L. Z., Guan, L. Y., Liu, Q., and Zhang, Y. X. (2013). Asd-based balanced-lethal system in attenuated Edwardsiella tarda to express a heterologous antigen for a multivalent bacterial vaccine. *Fish Shellfish Immunol.* 34, 1188–1194. doi: 10.1016/j.fsi.2013.01.027

Yu, X., Chen, N., Wang, L., Wu, J., Zhou, Z., Ni, J., et al. (2012). New genomic characteristics of highly pathogenic porcine reproductive and respiratory syndrome viruses do not lead to significant changes in pathogenicity. *Vet. Microbiol.* 158, 291–299. doi: 10.1016/j.vetmic.2012.02.036

Zhao, Z., Xu, Y., Wu, B., Cheng, X., Li, Y., Tang, X., et al. (2009a). Characterization of attenuated *Salmonella* C500 strain with a delta asd mutant and use as an Asd+ balanced-lethal host-vector system. *Chin. j. Biotechnol.* 25, 29–36.

Zhao, Z. Q., Xue, Y., Tang, X. B., Wu, B., Cheng, X. C., He, Q. G., et al. (2009b). Immunogenicity of recombinant protective antigen and efficacy against intranasal challenge with *Bordetella bronchiseptica*. *Vaccine* 27, 2523–2528. doi: 10.1016/j.vaccine.2008.09.091

Zhao, Z., Xue, Y., Wu, B., Tang, X., Hu, R., Xu, Y., et al. (2008). Subcutaneous vaccination with attenuated *Salmonella enterica* Serovar Choleraesuis C500 expressing recombinant filamentous hemagglutinin and pertactin antigens protects mice against fatal infections with both *S. enterica* Serovar Choleraesuis and *Bordetella bronchiseptica*. *Infect. Immun.* 76, 2157–2163. doi: 10.1128/IAI.01495-07

Zhao, Z. Q. (2009). Development of a recombinant *Salmonella* vaccine against both *B. bronchiseptica* and *Salmonella* infections in Swine. *Huazhong Agric. Univ.* 1, 1–130.

frontiers | Frontiers in Microbiology

TYPE Original Research
PUBLISHED 29 September 2023
DOI 10.3389/fmicb.2023.1218864

OPEN ACCESS

EDITED BY
Maurizio Sanguinetti,
Catholic University of the Sacred Heart, Italy

REVIEWED BY
Danilo Buonsenso,
Catholic University of the Sacred Heart, Italy
Moataz Abd El Ghany,
The University of Sydney, Australia
Lok Bahadur Shrestha,
University of New South Wales, Australia

*CORRESPONDENCE
Nayanum Pokhrel
✉ nayanumpr@gmail.com

RECEIVED 08 May 2023
ACCEPTED 10 July 2023
PUBLISHED 29 September 2023

CITATION
Pokhrel N, Chapagain R, Thakur CK, Basnet A, Amatya I, Singh R and Ghimire R (2023) *Salmonella* infection among the pediatric population at a tertiary care children's hospital in central Nepal: a retrospective study. *Front. Microbiol.* 14:1218864. doi: 10.3389/fmicb.2023.1218864

Salmonella infection among the pediatric population at a tertiary care children's hospital in central Nepal: a retrospective study

Nayanum Pokhrel[1]*, Ramhari Chapagain[2], Chandan Kumar Thakur[1], Ajaya Basnet[3], Isha Amatya[1], Rajan Singh[4] and Raghav Ghimire[5]

[1]Nepal Health Research Council, Kathmandu, Nepal, [2]Department of Pediatrics, Kanti Children's Hospital, Kathmandu, Nepal, [3]Shi-Gan International College of Science and Technology, Kathmandu, Nepal, [4]Provincial Hospital, Malangwa, Nepal, [5]Department of Pediatric Cardiology, Shahid Gangalal National Heart Centre, Kathmandu, Nepal

Background: Typhoid fever, an infective bacterial disease, is capable of causing fatal systemic infection in humans, and in an era of antimicrobial resistance, it has become of public health importance. This study aimed to investigate the laboratory diagnosis of *Salmonella* bloodstream infection, its serotype, antimicrobial resistance pattern, and seasonal variation at a tertiary care children's hospital.

Methods: We undertook a retrospective, cross-sectional study by reviewing hospital-based laboratory records of patients whose blood culture samples were submitted from the outpatient department to the laboratory of a tertiary care children's hospital in Kathmandu, Nepal, from January 2017 to January 2019.

Results: Among the total blood culture samples obtained (n=39,771), bacterial isolates (n=1,055, 2.65%) belonged either to the Genus *Enterobacteriaceae* or Genus *Acinetobacter*. Altogether (n=91, 8.63%), isolates were positive for *Salmonella* spp., which were further identified as *Salmonella enterica* subsp. *enterica* ser. Typhi (n=79, 7.49%), *Salmonella enterica* subsp. *enterica* ser. Paratyphi A (n=11, 1.04%), and *Salmonella enterica* subsp. *enterica* ser. Paratyphi B (n=1, 0.1%). The median age of patients was 6 years (IQR: 4–9), with male and female patients constituting (n=53, 58.24%; OR, 1.0; 95% CI, 0.60–1.67) and (n=38, 41.76%; OR, 0.98; 95% CI, 0.49–2.05) cases, respectively. The disease was observed throughout the year, with a high prevalence toward the spring season (March–May). An antibiogram showed resistance more toward nalidixic acid with *S.* Typhi, comprising half the isolates (n=52, 65.82%; p=0.11). Resistance toward β-lactams with β-lactamase inhibitors (amoxicillin/clavulanate; 1.27%) was seen in a single isolate of *S.* Typhi. The multidrug resistance pattern was not pronounced. The multiple antibiotic resistance (MAR) index was in the range between 0.14 and 0.22 in *S.* Typhi and 0.22 and 0.23 in *S.* Paratyphi.

Conclusion: *Salmonella* Typhi was the predominant ser. Infection was common among children between 1 and 5 years of age, showing male predominance and with the spring season contributing to a fairly higher number of cases. Antimicrobial susceptibility testing of *S.* Typhi showed more resistance toward nalidixic acid, with only a single isolate resistant to β-lactamase inhibitors (amoxicillin/clavulanate). Alarming multidrug resistance patterns were not observed. The MAR index in this study indicates the importance of the judicious use of antimicrobials and hospital infection prevention and control practices.

KEYWORDS

antibiogram, blood culture, enteric fever, pediatric population, serotypes, salmonella infection

1. Introduction

Typhoid fever is a life-threatening systemic infection affecting 11–20 million people and with almost 128,000 to 161,000 people dying from it each year in numerous growing parts of the WHO African, Eastern Mediterranean, South-East Asia, and Western Pacific Regions (WHO, 2018). This disease is associated with the bacterium *Salmonella enterica* serotype Typhi, a member of the family *Enterobacteriaceae*, which shows seropositivity for a range of both capsular and flagellar antigens that include lipopolysaccharide antigens O9 and O12, protein flagellar antigen Hd, and polysaccharide capsular antigen Vi (Parry et al., 2002). Typhoid fever is a disease of significant importance in overcrowded and unsanitary conditions, as seen in many developing countries and, infrequently, in developed nations, where only sporadic cases are reported among travelers returning from endemic areas (Osler, 1912; Ackers et al., 2000). Several factors come into play for the transmission of this infection, some of which include food consumption from street vendors such as ice cream or flavored iced drinks (Black et al., 1985; Luby et al., 1998), substandard housing conditions, and personal hygiene, as well as the recent use of antimicrobial drugs (Luby et al., 1998).

The symptoms of the disease include protracted fever, lassitude, headache, nausea, abdominal pain, constipation or diarrhea, and an occasional rash, with death in severe and complicated cases. Chloramphenicol, once regarded as a game changer in the management of severe, incapacitating, and frequently lethal disease into a treatable illness, saw a shift in its treatment guidelines, including management with the fluoroquinolone group of drugs, paving the path for newer-generation cephalosporins and azithromycin in affected areas (Woodward et al., 2004; WHO, 2014).

Nonetheless, among the preventive measures aimed at reducing the risk of typhoid fever, vaccination also serves as a good strategy for *S.* Typhi prevention.

The first identification of typhoid infection in Nepal was in a British-Nepalese soldier in 1984, followed by an infant in 1989 (Klonin et al., 1989). Since then, the disease has been reported in all regions of Nepal and has affected individuals of all ages, with a disproportionately high number of cases occurring among children and young adults (Gupta et al., 2021). Moreover, the growing concern about the rise of antimicrobial resistance in all infectious diseases has made *S.* Typhi an important bacterium of concern for treatment in endemic regions such as Nepal. Therefore, the primary objective of this study was to determine the presence of typhoidal *Salmonella* in the blood culture of pediatric patients attending the outpatient department of a tertiary care children's hospital. The study also aimed to identify the serotype of *Salmonella*, analyze its antimicrobial resistance pattern, and assess any seasonal variations over 2 years.

2. Methods

2.1. Study design and patients

A retrospective, cross-sectional study was conducted by retrieving documented paper-based hospital laboratory records from the Department of Microbiology at Kanti Children's Hospital, Kathmandu, Nepal. The main catchment area for the hospital is the Kathmandu Valley (population ~3,025,386; Central Bureau of Statistics, 2021), but as the only government-run children's hospital in Nepal, it also caters to children from all other regions of the country. Blood culture samples collected from pediatric patients visiting the outpatient department of the hospital were reviewed. The demographic data of the patients, isolated organisms, and their respective antibiograms within 2 years duration (January 2017 to January 2019) were included. Any incomplete data were excluded from the study. The study was approved by the Institutional Review Committee (IRC) of Kanti Children's Hospital, Maharajgunj, Kathmandu, Nepal (IRC No: 969). Laboratory tests were performed as a part of routine diagnostic procedures based on the clinician's need. Hence, patient-informed consent was not applicable.

2.2. Laboratory procedure

Approximately 3 mL of blood sample was inoculated in Bactalert culture bottles. Once growth was indicated by the Bactalert system, biochemical tests using commercially available media preparations (Hi-Media Laboratories, Mumbai, India) were prepared in-house using standard methods and techniques (Collee et al., 1996) for bacterial identification. A slide agglutination test using commercially available antisera was performed for *Salmonella* spp. following the manufacturer's instruction (Denka Seiken Co., Ltd., Chuo-Ku, Tokyo, Japan), and the Genus *Salmonella* and its serogroups were identified using the antigenic classification of the Kauffmann–White Scheme. An antimicrobial susceptibility test by the Kirby–Bauer disc diffusion method was performed using a Muller Hinton agar (Hi-Media Laboratories, Mumbai, India) following the 29th edition CLSI guidelines (Weinstein et al., 2019). Antibiotic discs included in this study were Ampicillin (10 µg), Amoxicillin (10 µg), Cefixime (5 µg), Cefotaxime (30 µg), Cefpodoxime (30 µg), Ceftriaxone (30 µg), Ceftazidime (30 µg), Cefepime (30 µg), Ciprofloxacin (5 µg), Ofloxacin (5 µg), Trimethoprim/sulfamethoxazole (Cotrimoxazole; 1.25/23.75 µg), Chloramphenicol (30 µg), Nalidixic acid (30 µg), Amoxicillin/clavulanate (20/10 µg), Ampicillin/sulbactam (10/10 µg), and Imipenem (10 µg; Hi-Media Laboratories, Mumbai, India). An antimicrobial susceptibility pattern was determined as sensitive, intermediate, and resistant according to the 29th edition CLSI guidelines (Weinstein et al., 2019). Furthermore, the multiple antibiotic resistance (MAR) index was calculated as the ratio of the number of resistant antibiotics to which the organism is resistant to the total number of antibiotics the organism is exposed to. MAR index values more than 0.2 specify high-risk sources of contamination where antibiotics are frequently used (Krumperman, 1983).

2.3. Sample workflow

See Figure 1.

2.4. Statistical analysis

All the data were entered into a Microsoft Excel 2007 spreadsheet from the paper-based hospital records and further analyzed by SPSS software version 17. All the descriptive and inferential data were calculated using SPSS software. The Chi-square test was used to analyze the categorical data.

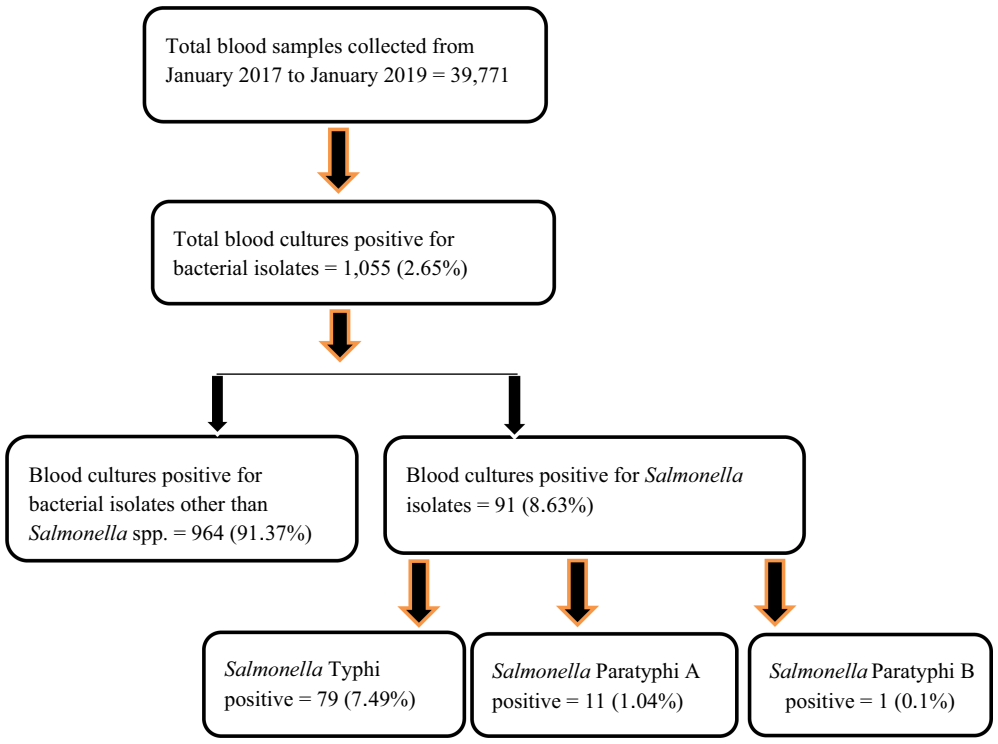

FIGURE 1
Sample workflow of *Salmonella* isolates from blood samples of pediatric patients' ($n = 91$).

3. Results

Enteric fever is common in Nepal, and Kathmandu Valley is an endemic region for this infection due to its known risk of substandard water quality at the community level and its poor sanitation and hygiene, jeopardizing the health of individuals and increasing their chances of acquiring infection (Karkey et al., 2013). Our hospital is the only tertiary-level, government-run children's hospital, located in Maharajgunj, Kathmandu, and it caters to hundreds of children from different socio-economic statuses coming to receive quality treatment. Among the total blood culture samples ($n = 39,771$) collected, ($n = 1,055$, 2.65%) samples tested positive for bacteria belonging either to the Genus *Enterobacteriaceae* or Genus *Acinetobacter*. The culture-positive isolates ($n = 1,055$, 2.65%) were further distributed into two groups. The first group constituted of the Genus *Enterobacteriaceae* (excluding *Salmonella* spp.) and Genus *Acinetobacter* ($n = 964$, 91.37%), with the second group constituting of the Genus *Enterobacteriaceae* comprising exclusively of *Salmonella* spp. ($n = 91$, 8.63%). The *Salmonella* spp. ($n = 91$, 8.63%) were further identified as *Salmonella* ser. Typhi ($n = 79$, 7.49%), Paratyphi A ($n = 11$, 1.04%), and Paratyphi B ($n = 1$, 0.1%). The affected age group was 1–5 years of age, followed by 6–10 years, with the least being 11–15 years. The median age of the patients was 6 years, with an interquartile range of (IQR: 4–9) years (Figure 2). Sex-wise distribution showed the prevalence of *Salmonella* infection among both male ($n = 53$, 58.24%; OR, 1.0; 95% CI, 0.60–1.67), and female patients ($n = 38$, 41.76%; OR, 0.98; 95% CI, 0.49–2.05; Figure 2). Between 2017 and 2019, the highest number of cases was seen during the spring season (March–May; OR, 1.84; 95% CI, 0.46–7.33) and the least during autumn (September to November; OR, 0.51; 95% CI, 0.60–4.30; Figure 3).

Among the tested antimicrobials, resistance was observed in quinolones and their derivatives (nalidixic acid), showing ($n = 60$, 88.23%) resistance to all the *Salmonella* isolates, followed by fluoroquinolone resistance (ciprofloxacin; $n = 29$, 34.11%) and ofloxacin ($n = 11$, 13.92%). Moreover, the penicillin group of antimicrobials was second in line with the overall resistance pattern observed, which was more among amoxicillin ($n = 7$, 24.13%) and ampicillin ($n = 5$, 10.41%). Among the combination drugs, β-lactams with β-lactamase inhibitors (amoxicillin/clavulanate) showed ($n = 1$, 20%) resistant isolate (Table 1). Among the total *Salmonella* ser. isolated, ser. Typhi ($n = 79$, 86.81%) exhibited ($n = 52$, 65.82%) resistance to quinolones and their derivatives (nalidixic acid) and resistance to fluoroquinolones such as ciprofloxacin ($n = 24$, 30.38%). Similarly, the bacterium also showed resistance toward the penicillin group of drugs, such as amoxicillin ($n = 6$, 7.59%) and ampicillin ($n = 3$, 3.8%). Furthermore, β-lactams with β-lactamase inhibitors had a single isolate of *S.* Typhi resistant to amoxicillin/clavulanate ($n = 1$, 1.27%; Table 1). The median multiple antibiotic resistance index or the MAR index values for *S.* Typhi were in the range between 0.14 and 0.22. Likewise, for *S.* Paratyphi, 0.22–0.23 was the mean MAR index (Table 2). There were no clinical outcomes in the form of hospital admission for any of the known complications of typhoid fever among the outpatients visiting the hospital, who were clinically diagnosed with enteric fever in the 2-year study duration.

4. Discussion

Enteric fever is considered one of the leading causes of febrile bacterial illness among adults and children in both developing and

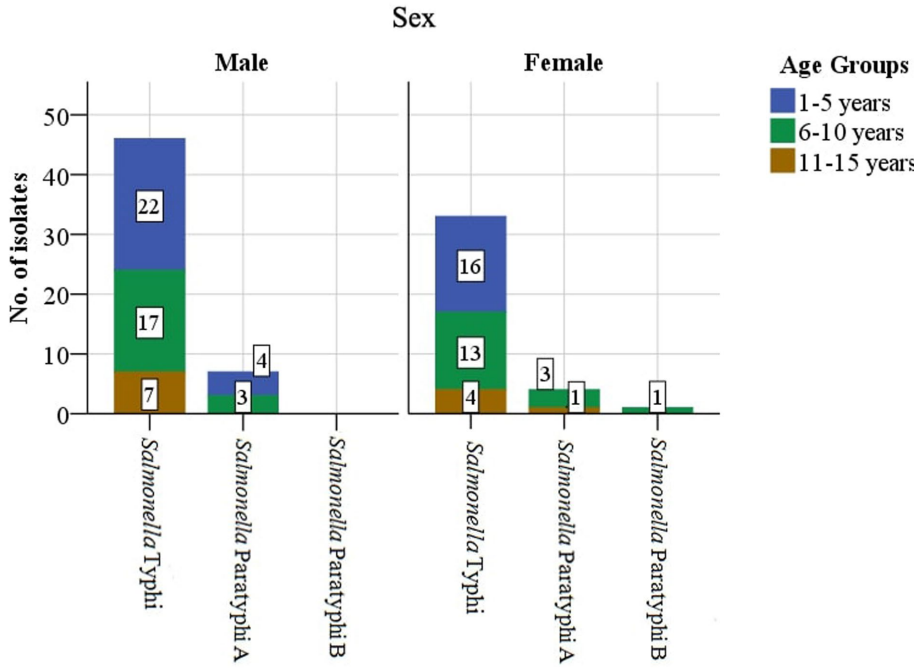

FIGURE 2
Isolation of *Salmonella* spp. based on the patients' demographics ($n = 91$).

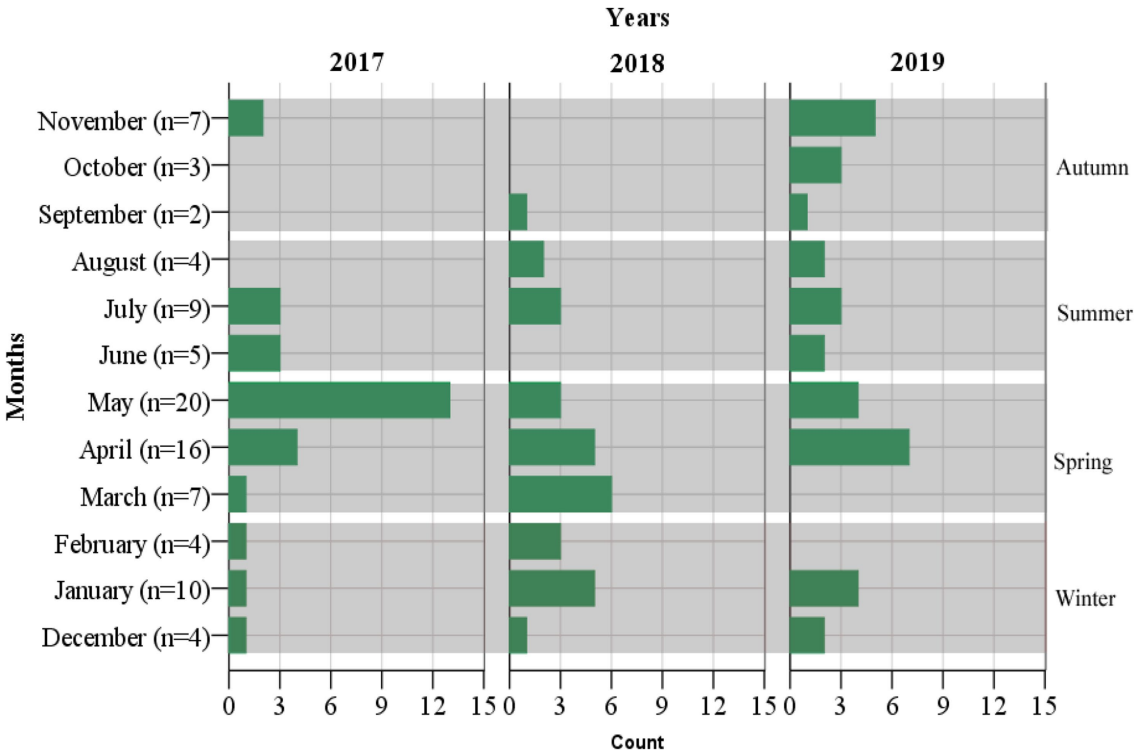

FIGURE 3
Incidence of enteric fever based on months, seasons, and years ($n = 91$).

developed nations (Sánchez-Vargas et al., 2011). The genetic constitution of *Salmonella* spp. enhances their adaptability in both mammalian and non-mammalian hosts, including non-animated reservoirs, thereby challenging their eradication by conventional methods. In an era of antimicrobial resistance, *Salmonella* strains face a similar fate to any other microorganisms exhibiting resistance to

10.3389/fmicb.2023.1218864

TABLE 1 Antimicrobial susceptibility pattern among the isolates of *Salmonella* spp. ($n = 91$).

Antibiotics			*Salmonella* spp.					
			S. Paratyphi A ($n = 11$)	*p*-value	*S.* Paratyphi B ($n = 1$)	*p*-value	*S.* Typhi ($n = 79$)	*p*-value
Penicillins	Ampicillin	Resistant ($n = 5$)	2 (18.18%)	0.15	0 (0%)		3 (3.80%)	0.15
		Intermediate ($n = 3$)	1 (9.09%)		0 (0%)		2 (2.53%)	
		Susceptible ($n = 40$)	4 (36.36%)		0 (0%)		36 (45.57%)	
	Amoxicillin	Resistant ($n = 7$)	1 (9.09%)	1.00	0 (0%)		6 (7.59%)	1.00
		Susceptible ($n = 22$)	2 (18.18%)		1 (100%)		19 (24.05%)	
β-lactams with β-lactamase inhibitors	Amoxicillin/ clavulanate	Resistant ($n = 1$)	0 (0%)		0 (0%)		1 (1.27%)	-*
		Susceptible ($n = 4$)	0 (0%)		0 (0%)		4 (5.06%)	
	Ampicillin/ sulbactam	Susceptible ($n = 3$)	0 (0%)		0 (0%)		3 (3.80%)	
Cephalosporins	Cefotaxime	Susceptible ($n = 11$)	1 (9.09%)		0 (0%)		10 (12.66%)	
	Ceftriaxone	Resistant ($n = 1$)	0 (0%)		0 (0%)		1 (1.27%)	1.00
		Susceptible ($n = 57$)	7 (63.63%)		0 (0%)		50 (63.29%)	
	Cefpodoxime	Intermediate ($n = 1$)	0 (0%)		0 (0%)		1 (1.27%)	
		Susceptible ($n = 5$)	0 (0%)		0 (0%)		5 (6.33%)	
	Cefexime	Resistant ($n = 1$)	0 (0%)		0 (0%)		1 (1.27%)	1.00
		Susceptible ($n = 79$)	11 (100%)		0 (0%)		68 (86.08%)	
	Ceftazidime	Susceptible ($n = 16$)	1 (9.09%)		0 (0%)		15 (18.99%)	
	Cefepime	Susceptible ($n = 10$)	0 (0%)		1 (100%)		9 (11.39%)	
Aminoglycosides	Amikacin	Resistant ($n = 10$)	1 (9.09%)	-*	0 (0%)		9 (11.39%)	-*
	Gentamicin	Resistant ($n = 2$)	0 (0%)		1 (100%)	-*	1 (1.27%)	-*
Quinolones and their derivatives	Nalidixic acid	Resistant ($n = 60$)	7 (63.63%)	0.09	1 (100%)	1.00	52 (65.82%)	0.11
		Susceptible ($n = 8$)	3 (27.27%)		0 (0%)		5 (6.33%)	
	Ofloxacin	Resistant ($n = 11$)	0 (0%)		0 (0%)		11 (13.92%)	0.34
		Intermediate ($n = 2$)	1 (9.09%)		0 (0%)		1 (1.27%)	
		Susceptible ($n = 66$)	9 (81.81%)		0 (0%)		57 (72.15%)	
	Ciprofloxacin	Resistant ($n = 29$)	5 (45.45%)	0.50	0 (0%)		24 (30.38%)	0.53
		Intermediate ($n = 1$)	0 (0%)		0 (0%)		1 (1.27%)	
		Susceptible ($n = 55$)	6 (54.55%)		1 (100%)		48 (60.76%)	
Trimethoprim/ sulfamethoxazole		Resistant ($n = 4$)	0 (0%)		0 (0%)		4 (5.06%)	1.00
		Susceptible ($n = 80$)	11 (100%)		1 (100%)		68 (86.08%)	
Chloramphenicol		Resistant ($n = 3$)	0 (0%)		0 (0%)		3 (3.80%)	1.00
		Susceptible ($n = 22$)	2 (18.18)		1 (100%)		19 (24.05%)	

-*, Data not applicable.

multiple drugs, making treatment an uphill task (Sánchez-Vargas et al., 2011). Our study found that *Salmonella enterica* ser. Typhi is the most common isolate ($n = 79$, 7.49%), followed by *Salmonella enterica* ser. Paratyphi A ($n = 11$, 1.04%) and *Salmonella enterica* ser. Paratyphi B in a single ($n = 1$, 0.1%) case. Historically, a high proportion of *Salmonella* Typhi infections have been reported in Nepal, with a relatively lower proportion of *Salmonella* Paratyphi (Karkey et al., 2010; Shrestha et al., 2014; Thompson et al., 2017), but the trends have been changing over the past two decades, with an increase in *Salmonella* Paratyphi A in some parts of Asia (Karkey et al., 2010; Zellweger et al., 2017).

Among the *Salmonella* isolates, a lower proportion ($n = 79$, 7.49%) of ser. Typhi in our study was comparable to those conducted in various parts of Nepal, contributing to 5.1% and 5.4% of cases (Khanal et al., 2007; Pokharel et al., 2009), but was in contrast (higher, 12.3%, 55.7%, 77.7,% and 85%) to studies published in Pakistan, Nepal, and India, along with population-based surveillance, respectively (Siddiqui et al., 2006; Petersiel et al., 2018; Biswas et al., 2022; Garrett et al., 2022). The findings from our study could be attributed to prior antimicrobial treatment received by the affected age group (1–5 years) before obtaining a blood sample for culture and sensitivity (Britto et al., 2018). Additionally, only 1.04% of Paratyphi A cases according

TABLE 2 Median multiple antibiotic resistance index among the *Salmonella* spp. ($n = 91$).

S.N.	*Salmonella* spp.	Strain-overall	Strain-specific
1.	*S.* Typhi	0.22	0.14
2.	*S.* Paratyphi	0.23	0.22

to our estimates are comparable to a publication from Pakistan (Siddiqui et al., 2006) but discordant (higher, 17% and 12%) to few studies from Nepal (Prajapati et al., 2008; Budhathoki et al., 2020) and another population-based enteric fever surveillance (higher, >99%), respectively (Garrett et al., 2022). The variation in Paratyphi A cases in our findings could be attributed to the asymptomatic infections manifested by this ser. (Sood et al., 1999), with relatively young male adults becoming infected (Karkey et al., 2010), which differed from our study population. Only 3% of *Salmonella* ser. Paratyphi B infection cases among the Nepalese population have been reported, rendering it an uncommon bloodstream infection (Pokhrel et al., 2009; Karkey et al., 2010; Zellweger et al., 2017; Garrett et al., 2022), which is quite similar ($n = 1$, 0.1%) to our study observation but differs (higher, 10%) from another scientific publication in Nepal (Budhathoki et al., 2020). The higher proportion of ser. Paratyphi B infection in the latter study reflects the greater predisposition to this infection among older children (11–15 years), who comparatively have a higher exposure to the external environment and outdoor activities than younger ones (1–5 years).

Children in the age group between 1 and 5 years were the most commonly infected ($n = 42$, 46.1%), with the least among those aged between 11 and 15 years ($n = 12$, 13.2%), similarly to the findings in India (Das et al., 2016), Pakistan (Rafiq et al., 2009; Britto et al., 2017), and other studies in the series (Mahle and Levine, 1993; Pang et al., 1995). However, this was in contrast (lower, 26.5%, 21.3%, and 14%,) to other publications in Pakistan, Nepal, and India for the age group between 1 and 5 years, respectively (Siddiqui et al., 2006; Budhathoki et al., 2020; Behera et al., 2021). The age-related variation in our findings highlights the possibility of reduced documentation of the disease, poor clinical suspicion, prior antimicrobial treatment before blood culture, and difficulty in withdrawing blood resulting in poor laboratory and clinical outcomes (Britto et al., 2018), along with immunological reasons such as immature and unstable gut microbiome and gut immune function in children between 1 and 5 years of age, easily exposing them to bacterial infections such as *S.* Typhi in comparison to older ones (Nuriel-Ohayon et al., 2016).

Enteric fever was more common in the male population, constituting more than half ($n = 53$, 58.24%) of the cases, with similar observations made in countries such as India, Nepal, and African countries, as well as in a population-based enteric fever surveillance (Ramaswamy et al., 2010; Rabasa et al., 2012; Singh et al., 2012; Garrett et al., 2022). The variation in sex proportion in our results could be attributed to factors such as prioritizing a male child over a female for treatment in our context and more outdoor activities seen among male children exposing them to the root of infection.

The wet season in Nepal begins from May to November and the dry season from December to February (Sharma et al., 2021). The frequency of typhoid infections in our study is seen throughout the year, but the incidence was high toward the spring season (end of dry season and beginning of wet season) throughout the two-year duration (March 2017 to May 2019). Our findings were concordant with studies conducted in Nepal (Petersiel et al., 2018), India (Ramaswamy et al., 2010), and Vietnam (Lin et al., 2000) but discordant with other studies conducted in Nepal (Karkey et al., 2010), Bangladesh (Dewan et al., 2013), Pakistan (Siddiqui et al., 2006), and Africa (Rabasa et al., 2012), where cases were seen throughout the year with increased frequency during the peak of the wet months (July–October). The isolation of the bacteria throughout the year in our study with comparatively higher prevalence during spring could be subjected to the microbial contamination of drinking water above the recommended levels in Nepal, thereby impacting the health of Nepalese people and specifically children (Farooqui et al., 1991; Parry et al., 2011; UNICEF Nepal, 2018) via various waterborne diseases (Butler et al., 1991; MR and Nair, 2010).

The treatment for enteric fever over the years has become challenging due to multidrug resistance, with the choice of the drug depending on local patterns of antimicrobial resistance, the severity of the disease, availability, and cost of antimicrobials (JA and Mintz, 2010; WHO, 2014). Our results displayed the occurrence of nalidixic acid-resistant *S.* Typhi ($n = 52$, 65.82%; $p = 0.11$), which was low in comparison to other studies in Nepal (Singh et al., 2011; Petersiel et al., 2018) and India (Walia et al., 2006) but high compared to other similar studies within the nation (Singh et al., 2012) and India (Ramaswamy et al., 2010; Bhumbla et al., 2022). Population-based enteric fever surveillance revealed nalidixic acid resistance in 59% of isolates from Pakistan, 57% from India, 44% from Vietnam, and none from Chinese or Indonesian sites in 2008 (Ochiai et al., 2008). Susceptibility to nalidixic acid is thought to be the best interpreter of clinical response to fluoroquinolones (Parry, 2004), and there have been pleas to adjust the fluoroquinolone breakpoints for all *Salmonella* spp. (Aarestrup et al., 2003). The resistance to nalidixic acid in our results indicates reduced susceptibility and poor clinical response to older-generation fluoroquinolones, which is still considered a first-line treatment for enteric fever in Nepal (Maskey et al., 2008), with our study revealing *S.* Typhi ($n = 24$, 30.38%; $p = 0.53$) being resistant to ciprofloxacin. Systematic reviews on antimicrobial resistance in *S.* Typhi conducted worldwide have witnessed 15% resistance to ciprofloxacin, which is lower than our study estimates but analogous to fluoroquinolones resistance observed within the vicinity (Pham et al., 2016). Resistance toward older drugs such as Amoxicillin ($n = 6$, 7.59%; $p = 1.00$), Ampicillin ($n = 3$, 3.80%; $p = 0.13$), Trimethoprim/sulfamethoxazole ($n = 4$, 5.06%; $p = 1.00$), and Chloramphenicol ($n = 3$, 3.80%; $p = 1.00$) was more toward *S.* Typhi, but none of these were statistically significant. Fairly low resistance toward these antimicrobials has been reported in India and Nepal too (Walia et al., 2006; Petersiel et al., 2018). A systematic review on antimicrobial resistance globally among *S.* Typhi reported 25.9%, 37.9%, and 38.8% resistance toward chloramphenicol, cotrimoxazole, and ampicillin and higher resistance (61.2%) toward amoxicillin (Marchello et al., 2020). The lower level of resistance toward chloramphenicol from our findings could also be due to the lower usage of this drug among the pediatric population due to its known adverse events. Evidence showing more sensitivity toward first-line drugs has created a dilemma in the re-usage and recycling concept of the first-line therapy for enteric fever (Pham et al., 2016), with our study results agreeing with this concept. Cephalosporins are the current drug of choice for the treatment of enteric fever in Nepal (Britto et al., 2018), with our laboratory findings showing resistance to

only one isolate each of Ceftriaxone ($n = 1$, 1.27%; $p = 1.00$) and Cefixime ($n = 1$, 1.27%; $p = 1.0$) among ser. Typhi, resembling the findings of Prajapati et al. (2008) and Marchello et al. (2020). Minimal resistance was observed in beta-lactam with beta-lactamase inhibitors (amoxicillin/clavulanate; $n = 1$, 1.27%) and was parallel to the results from India (Bhumbla et al., 2022; Biswas et al., 2022) and the findings of a systematic review exhibiting 8.0% resistance toward amoxicillin/clavulanate (Marchello et al., 2020). Among the ser. Paratyphi A isolates, resistance was seen toward Ampicillin ($n = 2$, 18.18%; $p = 0.13$), Amoxicillin ($n = 1$, 9.09%; $p = 1.00$), Nalidixic acid ($n = 2$, 63.63%; $p = 0.09$), and Ciprofloxacin ($n = 5$, 45.45%; $p = 0.50$), with only a single isolate of ser. Paratyphi B resistant only to Nalidixic acid ($n = 1$, 100%; $p = 1.00$). These findings were in line with studies from India and Nepal (Petersiel et al., 2018; Biswas et al., 2022) but were not statistically significant for both the bacteria.

MAR analysis is a risk evaluation tool that differentiates low- and high-risk regions of antibiotic overuse. The MAR index was in the range between 0.14 and 0.22 in *S.* Typhi and 0.22 and 0.23 in *S.* Paratyphi. The MAR index of >0.2 in *S.* Paratyphi and about 0.2 in *S.* Typhi indicates the presence of a high-risk source of contamination from the environment where several antimicrobials are used (Osundiya et al., 2013; Davis and Brown, 2016; Ayandele et al., 2020). The findings from our observations could be attributed to high antibiotic use and high selective pressure in the given environment and insufficient infection prevention and control practices, followed by poor surveillance of antimicrobial susceptibility patterns. Bacterial strains resistant to most classes of antimicrobials are emerging from time to time, hinting at various problems such as the injudicious use of antimicrobials and the lack of rigorous training and workshops on infection prevention and control practices (Osundiya et al., 2013); these need to be acknowledged, and measures to reduce these problems should be addressed. Our data limit the clinical characteristics of the patients, MIC data, and antimicrobial-resistant genes, specifically fluoroquinolones. Moreover, genotyping of the isolates would have enhanced the genetic understanding of the antimicrobials and also compared the lineage drift over the years, specifically in the pediatric population, as reported by other studies within the country.

5. Conclusion

In conclusion, this study reveals the prevalence of enteric fever predominantly in children between 1 and 5 years of age, with *S.* Typhi being the most common causative pathogen, the majority of which are nalidixic acid resistant (NARST). Moreover, the multidrug resistance pattern toward *Salmonella* isolates was not apparent, but a comparatively acceptable susceptibility was seen toward the cephalosporin and beta-lactamase inhibitor classification of drugs. Therefore, as far as antimicrobial resistance is concerned, the antimicrobial susceptibility situation does not look alarming. The existence of this bacterium in children raises a general concern regarding hand and food hygiene, along with clean and safe drinking water. It also focuses on the need for public health intervention to raise awareness among children, adults, and food vendors about the disease. The inclusion of typhoid vaccines under the routine immunization program in Nepal for children from 15 months to 15 years of age since 8 April 2022 (UNICEF Nepal, 2022) is a great initiative taken toward controlling the disease, and hopefully, in years to come, we can witness a significantly lesser number of cases.

Data availability statement

The raw data supporting the conclusions of this article will be made available by the authors, without undue reservation.

Ethics statement

The studies involving human participants were reviewed and approved by Institutional Review Committee (IRC) of Kanti Children's Hospital, Maharajgunj, Kathmandu, Nepal (IRC No: 969). Written informed consent from the participants' legal guardian/next of kin was not required to participate in this study in accordance with the national legislation and the institutional requirements.

Author contributions

NP: conceptualization, literature search, data curation, and writing—original draft and editing. RC: conceptualization, reviewing, and editing. CT: validation, reviewing, and editing. AB: data analysis, reviewing, and editing. IA: reviewing and editing. RS: reviewing and editing. RG: reviewing and editing. All authors contributed to the article and approved the submitted version.

Acknowledgments

The authors thank Anita K. C. for helping us with the data collection. Moreover, the support of Saroj Sharma, Head of Clinical Laboratory, Kanti Children's Hospital, Maharajgunj, Kathmandu, Nepal, without whom this endeavor would not have been possible, cannot be disregarded. Lastly, we thank laboratory technician, laboratory assistant, and laboratory helper Gyani Singh, Parbati Shrestha, and Ishwari Manandhar for their roles in the sample collection and processing, bacterial isolation, and preparation of the culture media, respectively, which were some of the noteworthy activities carried out at Kanti Children's Hospital.

Conflict of interest

The authors declare that the research was conducted in the absence of any commercial or financial relationships that could be construed as a potential conflict of interest.

Publisher's note

References

Aarestrup, F. M., Wiuff, C., Mølbak, K., and Threlfall, E. J. (2003). Is it time to change fluoroquinolone breakpoints for Salmonella spp.? *Antimicrob. Agents Chemother.* 47, 827–829. doi: 10.1128/AAC.47.2.827-829.2003

Ackers, M. L., Puhr, N. D., Tauxe, R. V., and Mintz, E. D. (2000). Laboratory-based surveillance of Salmonella serotype typhi infections in the United States: antimicrobial resistance on the rise. *JAMA* 283, 2668–2673. doi: 10.1001/jama.283.20.2668

Ayandele, A., Oladipo, E. K., Oyebisi, O., and Kaka, M. O. (2020). Prevalence of multi-antibiotic resistant Escherichia coli and Klebsiella species obtained from a tertiary medical institution in Oyo state Nigeria. *Qatar Med J* 2020, 1–6. doi: 10.5339/qmj.2020.9

Behera, J. R., Rup, A. R., Dash, A. K., Sahu, S. K., Gaurav, A., and Gupta, A. (2021). Clinical and laboratory profile of enteric fever in children from a tertiary Care Centre in Odisha, eastern India. *Cureus.* 13:e12826. doi: 10.7759/cureus.12826

Bhumbla, U., Chaturvedi, P., and Jain, S. (2022). Prevalence of *Salmonella typhi* in among febrile patients in a tertiary care hospital of south West Rajasthan. *J. Fam. Med. Prim. Care* 11, 2852–2855. doi: 10.4103/jfmpc.jfmpc_1976_21

Biswas, M., Biswas, S., Gupta, B., Mascellino, M. T., Rakshit, A., and Chakraborty, B. (2022). Changing paradigms in antibiotic resistance in Salmonella species with focus on fluoroquinolone resistance: a 5-year retrospective study of enteric fever in a tertiary Care Hospital in Kolkata, India. *Antibiotics* 11:1308. doi: 10.3390/antibiotics11101308

Black, R. E., Cisneros, L., Levine, M. M., Banfi, A., Lobos, H., and Rodriguez, H. (1985). Case-control study to identify risk factors for paediatric endemic typhoid fever in Santiago, Chile. *Bull. World Health Organ.* 63, 899–904.

Britto, C. D., Dyson, Z. A., Duchene, S., Carter, M. J., Gurung, M., Kelly, D. F., et al. (2018). Laboratory and molecular surveillance of paediatric typhoidal Salmonella in Nepal: antimicrobial resistance and implications for vaccine policy. *PLoS Negl. Trop. Dis.* 12:e0006408. doi: 10.1371/journal.pntd.0006408

Britto, C., Pollard, A. J., Voysey, M., and Blohmke, C. J. (2017). An appraisal of the clinical features of Pediatric enteric fever: systematic review and Meta-analysis of the age-stratified disease occurrence. *Clin. Infect. Dis.* 64, 1604–1611. doi: 10.1093/cid/cix229

Budhathoki, S., Rimal, S., Lama, L., Shrestha, S., Sanjel, S., and Amgain, K. (2020). Clinical profile of enteric fever in children of a tertiary Care Centre in Kathmandu, Nepal. *J. Karnali Acad. Heal. Sci.* 3, 122–127. doi: 10.3126/jkahs.v3i2.31327

Butler, T., Islam, A., Kabir, I., and Jones, P. (1991). Patterns of morbidity and mortality in typhoid fever dependent on age and gender: review of 552 hospitalized patients with diarrhea. *Rev. Infect. Dis.* 13, 85–90. doi: 10.1093/clinids/13.1.85

Central Bureau of Statistics (2021). Population|National Population and housing census 2021 results. Central Bureau of Statistics. Available at: https://censusnepal.cbs.gov.np/results.

Collee, J. G., Mackie, T. J., and McCartney, J. E. (1996) in *Mackie & Mccartney practical medical microbiology*. ed. J. G. Collee. *14th* ed (New York: Churchill Livingstone)

Das, S., Ray, U., Akhter, I., Chattopadhyay, A., Paul, D. K., and Dutta, S. (2016). Evaluation of fliC-d based direct blood PCR assays for typhoid diagnosis. *BMC Microbiol.* 16:108. doi: 10.1186/s12866-016-0723-6

Dewan, A. M., Corner, R., Hashizume, M., and Ongee, E. T. (2013). Typhoid fever and its association with environmental factors in the Dhaka metropolitan area of Bangladesh: a spatial and time-series approach. *PLoS Negl. Trop. Dis.* 7:e1998. doi: 10.1371/journal.pntd.0001998

Farooqui, B. J., Khurshid, M., Ashfaq, M. K., and Ata Khan, M. (1991). Comparative yield of *Salmonella typhi* from blood and bone marrow cultures in patients with fever of unknown origin. *J. Clin. Pathol.* 44, 258–259. doi: 10.1136/jcp.44.3.258

Garrett, D. O., Longley, A. T., Aiemjoy, K., Yousafzai, M. T., Hemlock, C., Yu, A. T., et al. (2022). Incidence of typhoid and paratyphoid fever in Bangladesh, Nepal, and Pakistan: results of the surveillance for enteric fever in Asia project. *Lancet Glob. Health* 10, e978–e988. doi: 10.1016/S2214-109X(22)00119-X

Gupta, B. P., Saluja, T., and Sahastrabuddhe, S. (2021). Epidemiology of typhoid in Nepal: review of literature to identify high burden area for potential use of typhoid vaccine. *Pediatr. Infect. Dis.* 3, 51–56. doi: 10.5005/jp-journals-10081-1297

Ja, C., and Mintz, E. (2010). Global trends in typhoid and paratyphoid fever. *Clin. Infect. Dis.* 50, 241–246. doi: 10.1086/649541

Karkey, A., Arjyal, A., Anders, K. L., Boni, M. F., Dongol, S., Koirala, S., et al. (2010). The burden and characteristics of enteric fever at a healthcare facility in a densely populated area of Kathmandu. *PloS One* 5:e13988. doi: 10.1371/journal.pone.0013988

Karkey, A., Thompson, C. N., Tran Vu Thieu, N., Dongol, S., Le Thi Phuong, T., Voong Vinh, P., et al. (2013). Differential epidemiology of Salmonella typhi and Paratyphi a in Kathmandu, Nepal: a matched case control investigation in a highly endemic enteric fever setting. *PLoS Negl. Trop. Dis.* 7:e2391. doi: 10.1371/journal.pntd.0002391

Khanal, B., Sharma, S. K., Bhattacharya, S. K., Bhattarai, N. R., Deb, M., and Kanungo, R. (2007). Antimicrobial susceptibility patterns of *Salmonella enterica* serotype typhi in eastern Nepal. *J. Health Popul. Nutr.* 25, 82–87.

Klonin, H., Minelli, E., and Adhikari, N. (1989). Three unusual cases of Salmonella infection in infants. *Ann. Trop. Paediatr.* 9, 240–242. doi: 10.1080/02724936.1989.11748639

Krumperman, P. H. (1983). Multiple antibiotic resistance indexing of *Escherichia coli* to identify high-risk sources of fecal contamination of foods. *Appl. Environ. Microbiol.* 46, 165–170. doi: 10.1128/aem.46.1.165-170.1983

Lin, F., Vo, A., Phan, V., TT, N., D, B., CT, T., et al. (2000). The epidemiology of typhoid fever in the Dong Thap Province, Mekong Delta region of Vietnam. *Am. J. Trop. Med. Hyg.* 62, 644–648. doi: 10.4269/ajtmh.2000.62.644

Luby, S. P., Faizan, M. K., Fisher-Hoch, S. P., Syed, A., Mintz, E. D., Bhutta, Z. A., et al. (1998). Risk factors for typhoid fever in an endemic setting, Karachi, Pakistan. *Epidemiol. Infect.* 120, 129–138. doi: 10.1017/S0950268897008558

Mahle, W. T., and Levine, M. M. (1993). *Salmonella typhi* infection in children younger than five years of age. *Pediatr. Infect. Dis. J.* 12, 627–631. doi: 10.1097/00006454-199308000-00001

Marchello, C. S., Carr, S. D., and Crump, J. A. (2020). A systematic review on antimicrobial resistance among *salmonella typhi* worldwide. *Am. J. Trop. Med. Hyg.* 103, 2518–2527. doi: 10.4269/ajtmh.20-0258

Maskey, A. P., Basnyat, B., Thwaites, G. E., Campbell, J. I., Farrar, J. J., and Zimmerman, M. D. (2008). Emerging trends in enteric fever in Nepal: 9124 cases confirmed by blood culture 1993-2003. *Trans. R. Soc. Trop. Med. Hyg.* 102, 91–95. doi: 10.1016/j.trstmh.2007.10.003

MR, C., and Nair, D. (2010). Quinolone and cephalosporin resistance in enteric fever. *J. Glob. Infect.* 2, 258–262. doi: 10.4103/0974-777X.68529

Nuriel-Ohayon, M., Neuman, H., and Koren, O. (2016). Microbial changes during pregnancy, birth, and infancy. *Front. Microbiol.* 14:1031. doi: 10.3389/fmicb.2016.01031

Ochiai, R. L., Acosta, C. J., Danovaro-Holliday, M. C., Baiqing, D., Bhattacharya, S. K., Agtini, M. D., et al. (2008). A study of typhoid fever in five Asian countries: disease burden and implications for controls. *Bull. World Health Organ.* 86, 260–268. doi: 10.2471/BLT.06.039818

Osler, W. (1912). *The principles and practice of medicine: Designed for the use of practitioners and students of medicine*. *8th* Edn. New York: D. Appleton.

Osundiya, O., Oladele, R., and Oduyebo, O. (2013). Multiple antibiotic resistance (MAR) indices of Pseudomonas and Klebsiella species isolates in Lagos university teaching hospital. *African J. Clin. Exp. Microbiol.* 14, 164–168. doi: 10.4314/ajcem.v14i3.8

Pang, T., Bhutta, Z., Finlay, B., and Altwegg, M. (1995). Typhoid fever and other salmonellosis: a continuing challenge. *Trends Microbiol.* 3, 253–255. doi: 10.1016/s0966-842x(00)88937-4

Parry, C. M. (2004). Typhoid fever. *Curr. Infect. Dis. Rep.* 6, 27–33. doi: 10.1007/s11908-004-0021-6

Parry, C. M., Hien, T. T., Dougan, G., White, N. J., and Farrar, J. J. (2002). Typhoid fever. *N. Engl. J. Med.* 347, 1770–1782. doi: 10.1056/NEJMra020201

Parry, C. M., Wijedoru, L., Arjyal, A., and Baker, S. (2011). The utility of diagnostic tests for enteric fever in endemic locations. *Expert Rev. Anti Infect. Ther.* 9, 711–725. doi: 10.1586/eri.11.47

Petersiel, N., Shresta, S., Tamrakar, R., Koju, R., Madhup, S., Shresta, A., et al. (2018). The epidemiology of typhoid fever in the Dhulikhel area, Nepal: a prospective cohort study. *PloS One* 13:e0204479. doi: 10.1371/journal.pone.0204479

Pham, T. D., Karkey, A., Dongol, S., Ho, T. N., Thompson, C., Rabaa, M., et al. (2016). A novel ciprofloxacin-resistant subclade of H58 *Salmonella Typhi* is associated with fluoroquinolone treatment failure. *Elife* 5:e14003. doi: 10.7554/eLife.14003

Pokharel, P., Rai, S. K., Karki, G., Katuwal, A., Vitrakoti, R., and Shrestha, S. K. (2009). Study of enteric fever and antibiogram of Salmonella isolates at a teaching hospital in Kathmandu Valley. *Nepal Med. Coll. J.* 11, 176–178.

Pokhrel, B. M., Karmacharya, R., Mishra, S. K., and Koirala, J. (2009). Distribution of antibody titer against *Salmonella enterica* among healthy individuals in Nepal. *Ann. Clin. Microbiol. Antimicrob.* 8:1. doi: 10.1186/1476-0711-8-1

Prajapati, B., Rai, G. K., Rai, S. K., Upreti, H. C., Thapa, M., Singh, G., et al. (2008). Prevalence of Salmonella typhi and paratyphi infection in children: a hospital based study. *Nepal Med. Coll. J.* 10, 238–241.

Davis, R., and Brown, P. (2016). Multiple antibiotic resistance index, fitness and virulence potential in respiratory *Pseudomonas aeruginosa* from Jamaica. *J. Med. Microbiol.* 65, 261–271. doi: 10.1099/jmm.0.000229

Rabasa, A., Mava, Y., Pius, S., Timothy, S., and Baba, U. (2012). Typhoid fever in children: clinical presentation and risk factors. *Niger. J. Paediatr.* 40:11. doi: 10.4314/njp.v40i1.11

Rafiq, H., Zia, R., and Naeem, S. (2009). Typhoid fever—continues as a major threat in children. *Signs* 25, 1–2.

Ramaswamy, G., Janakiraman, L., Thiruvengadam, V., and Sathiyasekeran, M. (2010). Profile of typhoid fever in children from a tertiary care hospital in Chennai-South India. *Indian J. Pediatr.* 77, 1089–1092. doi: 10.1007/s12098-010-0196-9

Sánchez-Vargas, F. M., Abu-El-Haija, M. A., and Gómez-Duarte, O. G. (2011). Salmonella infections: an update on epidemiology, management, and prevention. *Travel Med. Infect. Dis.* 9, 263–277. doi: 10.1016/j.tmaid.2011.11.001

Sharma, S., Khadka, N., Nepal, B., Ghimire, S. K., Luintel, N., and Hamal, K. (2021). Elevation dependency of precipitation over southern slope of central Himalaya. *Jalawaayu* 1, 1–14. doi: 10.3126/jalawaayu.v1i1.36446

Shrestha, S., Amatya, R., Shrestha, R. K., and Shrestha, R. (2014). Frequency of blood culture isolates and their antibiogram in a teaching hospital. *J. Nepal Med. Assoc.* 52, 692–696. doi: 10.31729/jnma.2295

Siddiqui, F. J., Rabbani, F., Hasan, R., Nizami, S. Q., and Bhutta, Z. A. (2006). Typhoid fever in children: some epidemiological considerations from Karachi, Pakistan. *Int. J. Infect. Dis.* 10, 215–222. doi: 10.1016/j.ijid.2005.03.010

Singh, U. K., Neopane, A. K., Thapa, M., Aryal, N., and Agrawal, K. (2011). *Salmonella typhi* infections and effect of fluroquinolones and third generation cephalosporins in clinical outcome. doi: 10.3126/jnps.v31i3.5361

Singh, D. S., Shrestha, S., Shrestha, N., and Manandhar, S. (2012). Enteric fever in children at Dhulikhel hospital. *J. Nepal Paediatr. Soc.* 32, 216–220. doi: 10.3126/jnps.v32i3.6682

Sood, S., Kapil, A., Dash, N., Das, B. K., Goel, V., and Seth, P. (1999). Paratyphoid fever in India: an emerging problem [3]. *Emerg. Infect. Dis.* 5, 483–485. doi: 10.3201/eid0503.990329

Thompson, C. N., Karkey, A., Dongol, S., Arjyal, A., Wolbers, M., Darton, T., et al. (2017). Treatment response in enteric fever in an era of increasing antimicrobial resistance: an individual patient data analysis of 2092 participants enrolled into 4 randomized, controlled trials in Nepal. *Clin. Infect. Dis.* 64, 1522–1531. doi: 10.1093/cid/cix185

UNICEF Nepal (2018). Water and sanitation (WASH). UNICEF Nepal. Available at: https://www.unicef.org/nepal/water-and-sanitation-wash (Accessed 2 April 2023).

UNICEF Nepal (2022). Nepal introduces typhoid vaccine into routine immunisation across the country. UNICEF Nepal. Available at: https://www.unicef.org/nepal/press-releases/nepal-introduces-typhoid-vaccine-routine-immunisation-across-country#:~:text=Thethree-weekcampaign%2Cwhich,theriseofantimicrobialresistance.

Walia, M., Gaind, R., Paul, P., Mehta, R., Aggarwal, P., and Kalaivani, M. (2006). Age-related clinical and microbiological characteristics of enteric fever in India. *Trans. R. Soc. Trop. Med. Hyg.* 100, 942–948. doi: 10.1016/j.trstmh.2006.02.015

Weinstein, M., Patel, J., Bobenchik, A., Campeau, S., Cullen, S., Galas, M., et al. (2019). Performance standards for antimicrobial susceptibility testing performance standards for antimicrobial susceptibility testing. *CLSI* M100, 1–25.

WHO (2014). Background doc: The diagnosis, treatment and prevention of typhoid fever 2014. Geneva, Switzerland, 1–38. Available at: https://www.glowm.com/pdf/WHO-diagnosis%20treatment%20prevention%20of%20typhoid%20fever-2003-CustomLicense.pdf.

WHO (2018). Typhoid. WHO. Available at: https://www.who.int/news-room/fact-sheets/detail/typhoid?

Woodward, T. E., Smadel, J. E., Ley, H. L., Green, R., and Mankikar, D. S. (2004). Preliminary report on the beneficial effect of chloromycetin in the treatment of typhoid fever. 1948. *Wilderness Environ. Med.* 15, 218–220. doi: 10.1580/1080-6032(2004)15[218,protbe]2.0.co;2

Zellweger, R. M., Basnyat, B., Shrestha, P., Prajapati, K. G., Dongol, S., Sharma, P. K., et al. (2017). A 23-year retrospective investigation of Salmonella typhi and *Salmonella Paratyphi* isolated in a tertiary Kathmandu hospital. *PLoS Negl. Trop. Dis.* 11:e0006051. doi: 10.1371/journal.pntd.0006051

frontiers | Frontiers in Microbiology

TYPE Original Research
PUBLISHED 03 October 2023
DOI 10.3389/fmicb.2023.1258796

OPEN ACCESS

EDITED BY
Sébastien Holbert,
INRA Centre Val de Loire, France

REVIEWED BY
Jonathan Lalsiamthara,
Oregon Health and Science University, United States
Edwin Veldhuizen,
Utrecht University, Netherlands

*CORRESPONDENCE
Kate Sutton
✉ kate.sutton@roslin.ed.ac.uk
Lonneke Vervelde
✉ lonneke.vervelde@roslin.ed.ac.uk

RECEIVED 14 July 2023
ACCEPTED 19 September 2023
PUBLISHED 03 October 2023

CITATION
Sutton K, Nash T, Sives S, Borowska D, Mitchell J, Vohra P, Stevens MP and Vervelde L (2023) Disentangling the innate immune responses of intestinal epithelial cells and lamina propria cells to *Salmonella* Typhimurium infection in chickens. *Front. Microbiol.* 14:1258796. doi: 10.3389/fmicb.2023.1258796

Disentangling the innate immune responses of intestinal epithelial cells and lamina propria cells to *Salmonella* Typhimurium infection in chickens

Kate Sutton[1]*, Tessa Nash[1], Samantha Sives[1], Dominika Borowska[1], Jordan Mitchell[1], Prerna Vohra[2], Mark P. Stevens[3] and Lonneke Vervelde[1]*

[1]Division of Immunology, The Roslin Institute, Royal (Dick) School of Veterinary Studies, University of Edinburgh, Edinburgh, United Kingdom, [2]Institute for Immunology and Infection Research, School of Biological Sciences, University of Edinburgh, Edinburgh, United Kingdom, [3]Division of Bacteriology, The Roslin Institute, Royal (Dick) School of Veterinary Studies, University of Edinburgh, Edinburgh, United Kingdom

Salmonella enterica serovar Typhimurium (STm) is a major foodborne pathogen and poultry are a key reservoir of human infections. To understand the host responses to early stages of *Salmonella* infection in poultry, we infected 2D and 3D enteroids, the latter of which contains leukocytes, neurons, and mesenchymal cells that are characteristic of the lamina propria. We infected these enteroids with wild-type (WT STm), a non-invasive mutant lacking the *prgH* gene (Δ*prgH* STm), or treated them with STm lipopolysaccharide (LPS) and analyzed the expression of innate immune related genes by qPCR at 4 and 8 h. The localization of the tight junction protein, ZO-1, expression was disrupted in WT STm infected enteroids but not Δ*prgH* STm or LPS treated enteroids, suggesting a loss of epithelial barrier integrity. The innate immune response to LPS was more pronounced in 2D enteroids compared to 3D enteroids and by 8 hpi, the response in 3D enteroids was almost negligible. However, when STm adhered to or invaded the enteroids, both 2D and 3D enteroids exhibited an upregulation of inflammatory responses. The presence of lamina propria cells in 3D enteroids resulted in the unique expression of genes associated with immune functions involved in regulating inflammation. Moreover, 2D and 3D enteroids showed temporal differences in response to bacterial invasion or adherence. At 8 hpi, innate responses in 3D but not 2D enteroids continued to increase after infection with WT STm, whereas the responses to the non-invasive strain decreased at 8 hpi in both 2D and 3D enteroids. In conclusion, STm infection of chicken enteroids recapitulated several observations from *in vivo* studies of *Salmonella*-infected chickens, including altered epithelial barrier integrity based on ZO-1 expression and inflammatory

responses. Our findings provide evidence that *Salmonella*-infected enteroids serve as effective models for investigating host-pathogen interactions and exploring the molecular mechanisms of microbial virulence although the 3D model mimics the host more accurately due to the presence of a lamina propria.

KEYWORDS

intestine, enteroid, innate immunity, *Salmonella*, Typhimurium

1. Introduction

Salmonella enterica are Gram-negative rod-shaped facultative anaerobic bacteria that are comprised of over 2,600 antigenically distinct serovars. *Salmonella enterica* serovar Typhimurium (STm), typically has a broad host range and transmits via contaminated food or water, causing severe gastroenteritis. The consumption of poultry meat and eggs contaminated with STm is a significant contributor to human infections. Intestinal inflammation that characterizes *Salmonella* gastrointestinal infection is caused by the infection of effector proteins into host cells by a Type 3 secretion system (T3SS-1) encoded by *Salmonella* pathogenicity island 1 (SPI-1) (Mills et al., 1995). Effector proteins delivered by T3SS-1 promote bacterial invasion by orchestrating rearrangements in the subcortical actin cytoskeleton and activate inflammatory responses (Raffatellu et al., 2005; Boyle et al., 2006). In mammals, mutations in T3SS-1 genes, such as *prgH*, reduce the ability of STm to colonize the intestine and induce inflammatory and secretory responses (Klein et al., 2000). T3SS-1 contributes to colonization of the avian intestine by STm (Chaudhuri et al., 2013). However, inflammation is less pronounced than in mammals, with STm typically being carried asymptomatically in chickens over 1-week-old and shed persistently in the faeces (Raffatellu et al., 2005). Neonatal chicks are highly susceptible to STm infection, which causes systemic infection and death (Barrow et al., 1987; Withanage et al., 2005). Although adults are less susceptible, STm can colonise the gastrointestinal tract without an associated clinical disease.

In vivo studies have provided considerable knowledge about the nature and consequences of mucosal immune responses to STm in the chicken intestine (Withanage et al., 2004, 2005; Iqbal et al., 2005; Fasina et al., 2008; Bescucci et al., 2022). An *in vitro* analysis of Salmonella - host interactions in a system containing all cells, such as epithelial cells and lamina propria cells including leukocytes, glial and mesenchymal cells are lacking. In mammals the interplay between cells relies on co-culture systems with either monocyte or bone marrow-derived mononuclear phagocytes which do not fully encompass the heterogeneity of the intestinal tissue (Noel et al., 2017; Staab et al., 2020). Three-dimensional (3D) intestinal organoids, when derived from primary tissue are known as enteroids, closely mimic the morphology and physiology of the intestine, and are emerging as *in vitro* models to study host-pathogen interactions. Intestinal enteroids grown in an extracellular matrix consist of a central lumen lined by a single layer of polarized epithelial cells with their basolateral surface in contact with the extracellular matrix scaffold (Sato et al., 2009). In contrast to cell lines, enteroids recapitulate all major differentiated epithelial cell lineages, including enterocytes, goblet cells, enteroendocrine cells, Paneth cells, and tuft cells. Zhang et al. (2014) were the first to analyze STm infection in murine enteroids demonstrating epithelial cell invasion, disruption of tight junctions and NFκB related pro-inflammatory responses. Human, bovine and porcine enteroids have since been reported to be susceptible to STm (Zhang et al., 2014; Forbester et al., 2015; Derricott et al., 2019). However, the fully enclosed lumen of mammalian enteroids poses a challenge to deliver the pathogens to the epithelial surface. Recently, apical-out enteroids derived from basal-out human, porcine, bovine and ovine enteroids have been developed (Co et al., 2021; Smith et al., 2021; Blake et al., 2022; Joo et al., 2022). A study has shown that human apical-out enteroids recapitulate specific morphological hallmarks of STm infection in humans including epithelial barrier disruption and cytoskeletal reorganization (Co et al., 2021).

Avian floating 3D enteroids naturally develop in an advantageous apical-out conformation with apical microvilli facing the media and an inner core resembling the lamina propria, containing leukocytes, and mesenchymal and neuronal cells (Nash et al., 2021, 2023). In addition, a chicken 2D enteroid model that self-organizes into an epithelial and mesenchymal sub-layer but lacks the underlying lamina propria cells has been developed (Orr et al., 2021). The aim of this study was to disentangle the innate immune response between a system with (3D) and without (2D) lamina propria cells to STm infection by comparing the gene expression profiles between uninfected and infected enteroids. In addition, we analyzed the effects of an invasion deficient strain, a Δ*prgH* mutant of STm, on the innate immune response in each enteroid model. Our study reveals marked differences in the response to STm infection in both models. Therefore, these models provide valuable insights into deciphering the distinct responses in systems where lamina propria cells are present or absent, such that findings with simpler cell-based models should be interpreted with caution.

2. Materials and methods

2.1. Animals

Experiments were performed using embryonic day 18 (ED18) Hy-Line Brown fertile embryos (*Gallus gallus*) obtained from the National Avian Research Facility, University of Edinburgh, UK. Embryos were humanely culled under the authority of a UK Home Office Project License (PE263A4FA) in accordance

with the guidelines and regulations of the Animals (Scientific Procedures) Act 1986.

2.2. Generation of chicken 2D and 3D enteroids

Tissue from duodenum, jejunum and ileum of ED18 chickens were retrieved and placed in phosphate buffered saline (PBS, Mg^{2+} and Ca^{2+} free) until use. For each independent culture, the intestines from five embryos were pooled. For the generation of 3D enteroids, the villi were released from the tissue as previously described (Nash et al., 2021). In brief, intestinal tissue was cut open longitudinally and cut into 3 mm pieces. The tissues were digested with *Clostridium histolyticum* type IA collagenase (0.2 mg/mL, Merck, Gillingham, UK) at 37°C for 50 min with shaking at 200 rpm. Single cells were removed by filtering the digestion solution through a 70 μM cell strainer (Corning, Loughborough, UK). The villi were obtained by rinsing the inverted strainer. The collected villi were centrifuged at 100 *g* for 4 min. The 3D enteroids were seeded at 200 villi per well in 24 well plates with 400 μl of Floating Organoid Media (FOM media); Advanced DMEM/F12 supplemented with 1X B27 Plus, 10 mM HEPES, 2 mM L-Glutamine and 50 U/mL Penicillin/Streptomycin [Thermo Fisher Scientific (TFS), Paisley, UK]. For 2D enteroid generation, freshly isolated intestinal villi were enzymatically digested with Accutase (TFS) as previously described (Orr et al., 2021). To remove the majority of the fibroblasts, cells were resuspended in FOM media supplemented with 1X N2 supplement (TFS), 100 ng/mL human (hu) epidermal growth factor (huEGF, TFS), 10 μM CHIR 99021 (Stratech Scientific), 10 μM Y27632 (Stem Cell Technologies) and 100 nM LDN193189 (Cambridge Bioscience). Cells were incubated for 3 h at 37°C, 5% CO_2 in 6 well plates. Non-adherent cells were removed, counted and seeded at 2×10^5 cells in uncoated 24 well plates with 350 μl of FOM media supplemented with 1X N2 supplement, 100 ng/mL huEGF, 100 ng/mL huR-spondin, 50 ng/mL huNoggin (R&D Systems), 10 μM CHIR 99021 and incubated at 37°C, 5% CO_2.

2.3. Preparation of *Salmonella*

Salmonella Typhimurium strain ST4/74 nal^R (WT) is known to colonize the chicken intestine proficiently (Chaudhuri et al., 2013) and was routinely cultured in Luria-Bertani broth containing 20 μg/mL of naladixic acid (TFS). An isogenic ST4/74 nal^R Δ*prgH:kan* mutant, deficient in bacterial invasion, was additionally cultured in the presence of 20 μg/mL of kanamycin (Merck) and has been described previously (Balic et al., 2019). Both strains were transformed with a plasmid that constitutively expresses green fluorescent protein (GFP), pFVP25.1 (Valdivia and Falkow, 1996; Vohra et al., 2019), which was maintained in the presence of 50 μg/mL of ampicillin (Merck). Bacteria were incubated for 18 h at 37°C with shaking at 180 rpm to an optical density of 1 at 600 nm and pelleted at 2,000 *g* for 10 min. Bacteria were washed twice with PBS and resuspended in 10 mL of PBS. Ten-fold serial dilutions were plated in duplicate on LB agar containing 20 μg/mL of naladixic acid incubated at 37°C overnight to determine viable counts retrospectively.

2.4. Bacterial infection and LPS treatment of 2D and 3D enteroids

On day 2 of culture, 3D enteroids were pelleted at 100 *g* for 4 min and reseeded at 200 enteroids per well on 24 well plates (Corning) in 400 μL of FOM media without antibiotics. Similarly, on day 2 of culture, 2D enteroids were washed twice with PBS and cultured for a further 24 h in FOM without antibiotics, CHIR and Y27632. After 24 h, on day 3 of culture, the 3D and 2D enteroids were treated with WT or Δ*prgH* STm strains (2×10^5), LPS (1 ug/mL) derived from STm (product code L6143, Merck) or media only. At 4 and 8 h post-infection (hpi) the supernatant was removed and cells washed with PBS and lysed in RLT Plus buffer (Qiagen) containing 10 μg/mL 2-mercaptoethanol (Merck). For increasing bacterial dose analysis, 3D enteroids were infected with 1×10^3, 500 or 250 CFU of WT STm for 3 h. The 3D enteroids were further homogenized using QIAshredder columns (Qiagen). Samples were stored at −20°C until use.

2.5. Immuno-fluorescent staining and microscopy

For immuno-fluorescent staining, chicken 2D enteroids were grown on 2% Matrigel (Corning) coated transwell inserts (VWR, 0.33 cm^2) in 24 well plates (Orr et al., 2021) while 3D enteroids were grown as outlined above. Chicken 2D and 3D enteroids were treated with WT or Δ*prgH* STm, LPS or media alone as outlined above. At 4 and 8 h post-treatment, cells were gently washed with PBS and fixed with 4% w/v paraformaldehyde (TFS) for 15 min at room temperature and blocked with 5% v/v goat serum in permeabilization buffer (0.5% w/v bovine serum albumin and 0.1% w/v Saponin in PBS; Sigma-Aldrich). Permeabilization buffer was used to dilute all antibodies. Cells were stained with mouse anti-human ZO-1 (Abcam, IgG1, clone A12) overnight at 4°C followed by the secondary antibody, goat anti-mouse IgG1 Alexa Fluor®594 (TFS) for 2 h on ice. Cells were counterstained with Hoechst 33,258 and Phalloidin Alexa Fluor®647 (TFS) to stain for nuclei and F-actin, respectively. Slides were mounted using ProLong™ Diamond Antifade medium (TFS). Controls comprising of secondary antibody alone were prepared for each sample. Images and Z-stacks were captured using an inverted LSM880 (Zeiss) with 40X and 63X oil lenses using ZEN 2012 (Black Edition) software and were analyzed using ZEN 2012 (Blue Edition). Z-stack modeling was performed using IMARIS software (V9).

2.6. Isolation of RNA and reverse transcription

Total RNA from the enteroids was extracted using an RNeasy Plus Mini Kit (Qiagen) consisting of a genomic DNA column eliminator according to manufacturer's instructions and quantified spectrophotometrically. Five independent 3D enteroids samples and three independent 2D enteroids samples that were of

high quality were used for qPCR analysis (RNA concentration of > 100 ng and a 260/230 ratio of 2). Reverse transcription was performed using the High Capacity Reverse Transcription Kit (Applied Biosystems) according to manufacturer's instructions with random hexamers and oligo (dT)18, containing 100 ng of total RNA. The cDNA samples were stored in −20°C until use.

2.7. Pre-amplification and quantitative PCR using 96.96 Integrated Fluid Circuits dynamic array

Pre-amplification of cDNA was performed as previously described (Borowska et al., 2019; Bryson et al., 2023). In brief, 2.5 µl of a 200 nM stock pool of each primer pair (**Supplementary Material 1**) was added to 5 µl of TaqMan PreAmp Master Mix (Applied Biosystems) and 2.5 µl of 1:5 dilution of cDNA. Due to its high level of expression, the ribosomal 28S (r28S) primer pair were excluded from the stock primer mix. Samples were incubated at 95°C for 10 min followed by 14 cycles of 95°C for 15 s and 60°C for 4 min. Unincorporated primers were digested from the pre-amplified samples using 16 U/µl Exonuclease I (*E. coli*, New England Biolabs) at 37°C for 30 min. High-throughput qPCR was performed with the microfluidic 96.96 Dynamic array (Standard BioTools UK) as previously described (Borowska et al., 2019; Bryson et al., 2023). Each sample was run in duplicate with 89 target genes and 5 reference gene primers. In order to reduce inter-plate variation, an inter-plate calibrator (IPC) sample was employed on each array. The IPC sample comprised of pre-amplified cDNA derived from splenocytes stimulated with Concanavalin A (10 µg/mL, Sigma-Aldrich) for 4 h. Quantitative PCR was performed on the BioMark HD instrument (Fluidigm) using the thermal cycling conditions as previously reported (Borowska et al., 2019). The fluorescence emission was recorded after each cycling step. Raw qPCR data quality threshold was set to 0.65-baseline correction to linear (derivative) and quantitation cycle (Cq) threshold method to auto (global) using the Real-Time PCR Analysis software 3.1.3 (Fluidigm).

2.8. RT-qPCR data analysis

Data pre-processing, normalization, relative quantification and statistics were performed using GenEx6 and GenEx Enterprise (MultiD Analyses AB). The qPCR performance base-line correction and set threshold of the instrument was compensated across the two array runs using the IPC samples. Delta Ct values were obtained by normalizing the Ct values of the target genes with the geometric mean of three reference genes, GAPDH, TBP and r28S, identified from a panel of five references using NormFinder. The technical repeats were averaged and relative quantities were set to the maximum Cq value for a given gene. Relative quantities were log transformed (log2) and differentially expressed genes (DEG) between uninfected and infected enteroids was calculated by the $-2^{-\Delta\Delta CT}$ method (Livak and Schmittgen, 2001). Principal component analysis was performed using *prcomp* function and plots were generated using *ggplot* in RStudio (V1.1.442).

2.9. Statistical analysis

Statistical analysis of the differentially expressed genes (DEGs) between control (untreated) and LPS treated or between control and STm infected 2D or 3D enteroids was performed using GENEx5 and GenEx Enterprise (MultiD Analyses AB). Correction for multiple testing was performed with the estimation of false discovery rate using Dunn-Bonferroni correction threshold of 0.00054. After correction, DEG with a significant difference ($P < 0.05$) and a fold change of ≥ 1.5 were identified. Finally, for each comparison, the fold change of untreated and treated samples at their respective timepoint was calculated. Graphs were prepared using GraphPad Prism 9.

3. Results

3.1. *Salmonella* Typhimurium alters tight junctions in chicken enteroids

We studied the early response of chicken 2D and 3D enteroid cultures to infection with STm in order to understand the relative contribution of epithelial and lamina propria cells to the response. In untreated and LPS-treated 2D and 3D enteroids actin expression was evenly distributed between cells and at the apical surface (**Figures 1A, B**). Images taken using a low objective, show the non-planar surface of 2D enteroids and demonstrates that in a certain planar view, both the epithelial and the underlying mesenchymal cells, with long F-actin filaments, can be observed (**Figures 1A, B**). At 4 hpi with WT STm, raised F-actin structures were observed around the bacteria at the apical surface (**Figure 2A**). Z-stack modeling of 2D enteroids

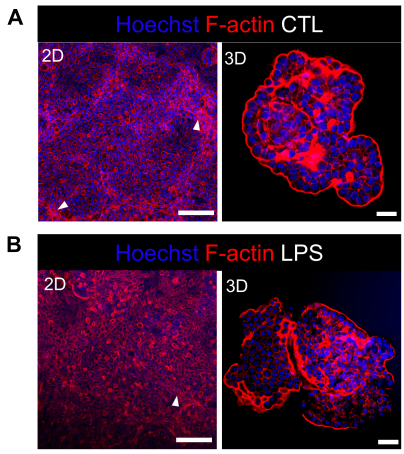

FIGURE 1
Untreated and LPS-treated 2D and 3D enteroids exhibit unaltered organization of F-actin. Confocal micrographs of F-actin organization in **(A)** untreated or **(B)** LPS-treated 2D and 3D enteroids. Chicken 2D enteroids were cultured on Matrigel coated transwell inserts and images were retrieved using 20X objective. In one planar view, both epithelial cells and the underlying mesenchymal cells with long F-actin filaments can be observed (white arrow). Images are representative of 3 independent experiments. Scale bars = 200 µm (2D) and 100 µm (3D).

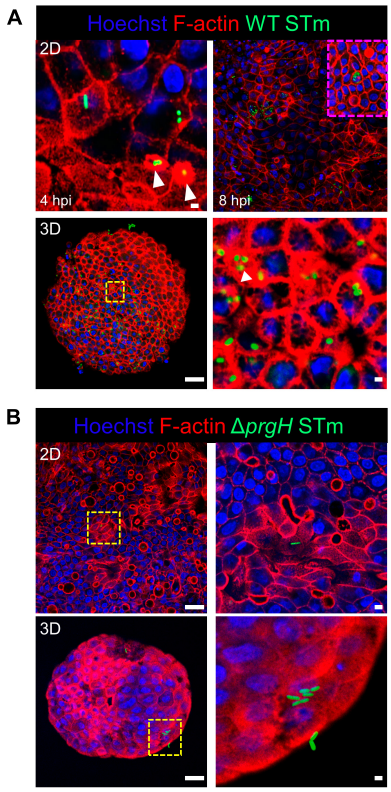

FIGURE 2
WT STm infection remodels F-actin in chicken enteroids. Confocal micrographs showing F-actin remodeling in **(A)** WT STm infected 2D and 3D enteroids. At 4 hpi, dense F-actin staining can be observed surrounding the invading bacteria consistent with reorganization of subcortical actin stimulating membrane ruffling (white arrows). By 8 hpi, numerous bacteria can be observed within epithelial cells. At 8 hpi the number of internalized bacteria was markedly higher in 3D enteroids inoculated with the same bacterial dose. **(B)** No F-actin remodeling was observed in Δ*prgH* STm infected 2D and 3D enteroids at 8 hpi, although bacteria were observed in close association with the apical surface of epithelial cells. Images are representative of 3 independent experiments. Scale bars = 100 μm and 50 μm.

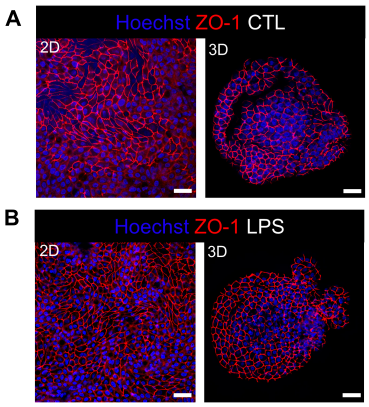

FIGURE 3
Distribution of the tight junction protein ZO-1 at cell-cell junctions in untreated and LPS treated enteroids. Confocal micrographs of ZO-1 distribution in **(A)** untreated or **(B)** LPS treated 2D and 3D enteroids show typical ZO-1 distribution at 8 h. Images are representative of 3 independent experiments. Scale bars = 100 μm.

demonstrates punctuated F-actin expression on the apical surface of a WT STm infected cell (Supplementary Video 1). At 8 hpi, bacteria could be detected within individual cells in 2D enteroids (Figure 2A). Despite the same inoculum used in WT STm infected 3D enteroids, we observed more remodeled F-actin around invading bacteria (Figure 2A). In contrast, no actin remodeling was observed in Δ*prgH* STm infected 2D and 3D enteroids although on occasion, bacteria were observed in close proximity to the apical surface of epithelial cells (Figure 2B) or found trapped in the folds of the epithelial buds (Supplementary Figure 1). This is consistent with the known role of T3SS-1 in promoting membrane ruffling and invasion.

Integrity of the epithelial barrier was analyzed by immunofluorescent staining of the tight junction protein ZO-1. In untreated and LPS treated 2D and 3D enteroids, ZO-1 expression was localized to the lateral membrane, showing a typical polygonal shape of enterocytes and demonstrates that LPS had no effect on ZO-1 localization (Figures 3A, B). No difference in the localization of ZO-1 was observed at 4 hpi across each model after WT or Δ*prgH* STm infection (Supplementary Figure 2). At 8 hpi, ZO-1 localization became discontinuous in WT STm infected 2D enteroids (Supplementary Video 2). In addition to being discontinuous, ZO-1 in 3D enteroids formed dense strands, which was not observed in 2D enteroids following infection. In addition to being discontinuous, ZO-1 in 3D enteroids formed dense strands, which was not observed in 2D enteroids following infection (Figure 4A). The Δ*prgH* STm strain did not elicit changes in ZO-1 distribution, which resembled that observed in the untreated 2D and 3D enteroids (Figure 4B). Occasionally, the Δ*prgH* STm strain was observed in close proximity to the apical surface of epithelial cells, but it did not cause any disruption to ZO-1 localization (Supplementary Video 3).

3.2. Global transcriptional profiles cluster by treatment and culture model

To disentangle the innate immune responses of 2D and 3D chicken enteroids to *Salmonella* or its LPS, the mRNA expression levels of 89 innate-immune related genes were analyzed using Fluidigm Biomark high-throughput qPCR at 4 and 8 h post-treatment. To assess the degree of heterogeneity between replicates and treatments, the global transcriptional profiles were compared using Principal Component Analysis (PCA). This analysis demonstrated that sample clustering was primarily by treatment as the uninfected and infected enteroids segregated from each other along the first principal component (PC1, Figures 5A, B). This difference accounted for 48–49% of the total variance in 2D and 3D enteroids, respectively, and suggested that treatment is a greater determinant of transcriptional variance rather than time post-infection (PC2). PCA of the total dataset shows sample clustering based on the culture system, 2D versus 3D (Figure 5C, PC2), corresponding to the presence of different cell types such as immune cell in 3D enteroids while the effect of treatment (PC1) was preserved.

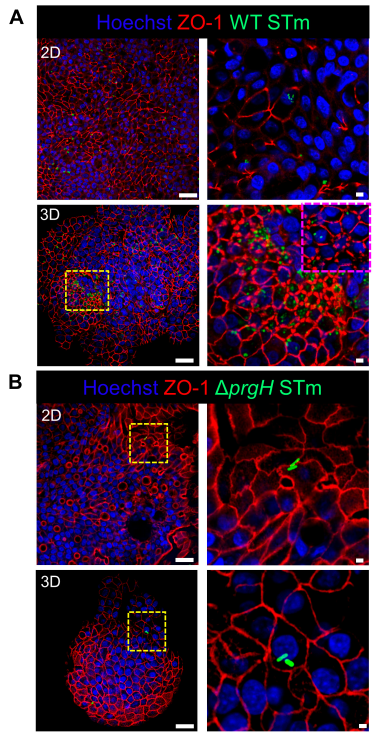

FIGURE 4
WT STm but not Δ*prgH* STm infection alters the distribution of the tight junction protein ZO-1 in chicken enteroids. Confocal micrographs showing the distribution of ZO-1 in **(A)** WT STm infected 2D and 3D enteroids, which leads to reduced ZO-1 expression in 2D enteroids and altered ZO-1 distribution in 3D enteroids at 8 hpi (yellow/magenta dash insert images). **(B)** ZO-1 distribution were unaltered in Δ*prgH* STm infected 2D and 3D enteroids at 8 hpi. Images are representative of 3 independent experiments. Scale bars = 100 μm and 50 μm.

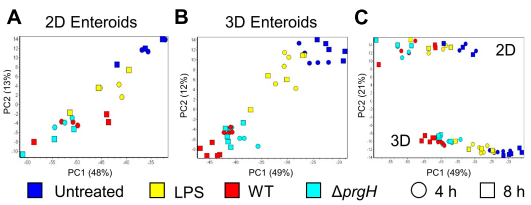

FIGURE 5
Principal component analysis (PCA) of gene expression profiles. PCA analysis of untreated, LPS treated, and WT and Δ*prgH* STm infected **(A)** 2D enteroids (n = 3) and **(B)** 3D enteroids (n = 5) at 4 hpi and 8 hpi alone and **(C)** with both datasets.

3.3. Chicken 2D enteroids exhibit a more pronounced innate immune response to *Salmonella* LPS than 3D enteroids

Chicken 2D and 3D enteroids were treated with STm-derived LPS for 4 and 8 h. Firstly, the number of statistically differentially expressed genes (DEGs) with a fold change ≥ 1.5 at $P < 0.05$ compared to their respective time-matched controls was analyzed (Figure 6A). The number of DEGs was higher at 4 and 8 h in the 2D compared to 3D enteroids and the number of DEG

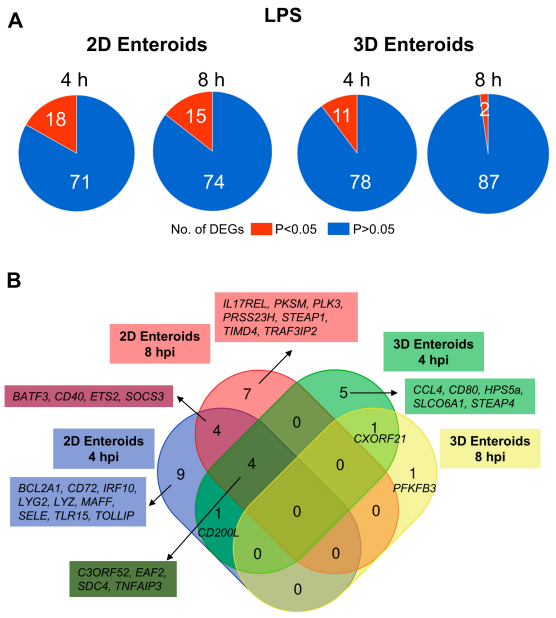

FIGURE 6
Chicken 2D enteroids exhibit more pronounced responses to LPS treatment. **(A)** Pie charts indicating the number of statistically significant ($P < 0.05$) and non-significant ($P > 0.05$) DEGs in LPS treated 2D enteroids (n = 3) and 3D enteroids (n = 5) at 4 h and 8 h compared to time-matched, respective controls. DEGs with a significant difference ($P < 0.05$) and a fold change of ≥ 1.5 were identified. **(B)** Venn diagram showing common and unique DEGs across each enteroid model and timepoint.

substantially decreased with time in the 3D enteroids compared to the 2D enteroids. Next, the commonality and difference in the genes regulated in 2D and 3D enteroids were compared (Figure 6B). There was no core set of common DEGs between 2D and 3D enteroids at 4 and 8 h post-LPS treatment. Of the 11 DEGs regulated by 3D enteroids at 4 h post-LPS treatment, four were common to 2D enteroids, *C3ORF52*, *TNFAIP3*, *EAF2*, and *SDC4*. DEGs specifically regulated in 2D enteroids were related to TLR signaling (*TOLLIP, TRAF3IP2, TLR15*), effector protein functions (*LYZ*, *LYG2*) and regulation of immune responses (*BATF3, CD200L, IRF9, IL17REL, SOCS3*).

The mRNA expression levels of a majority of the DEGs increased by 2-7-fold at *P*-values of less than 0.05 in LPS treated enteroids compared to untreated enteroids except for *SELE* and *TIMD4*, which decreased in expression in 2D enteroids (Supplementary Material 2). In conclusion, *Salmonella*-derived LPS treatment of chicken 2D and 3D enteroids resulted in differential innate immune responses, with 2D enteroids having a more pronounced response compared to 3D enteroids.

3.4. 2D and 3D enteroids have differing temporally responses to *Salmonella* infection

Next, the statistically significant DEGs (fold change ≥ 1.5, $P < 0.05$ compared to their respective time-matched controls) was analyzed in 2D and 3D enteroids infected with WT STm at 4 and

10.3389/fmicb.2023.1258796

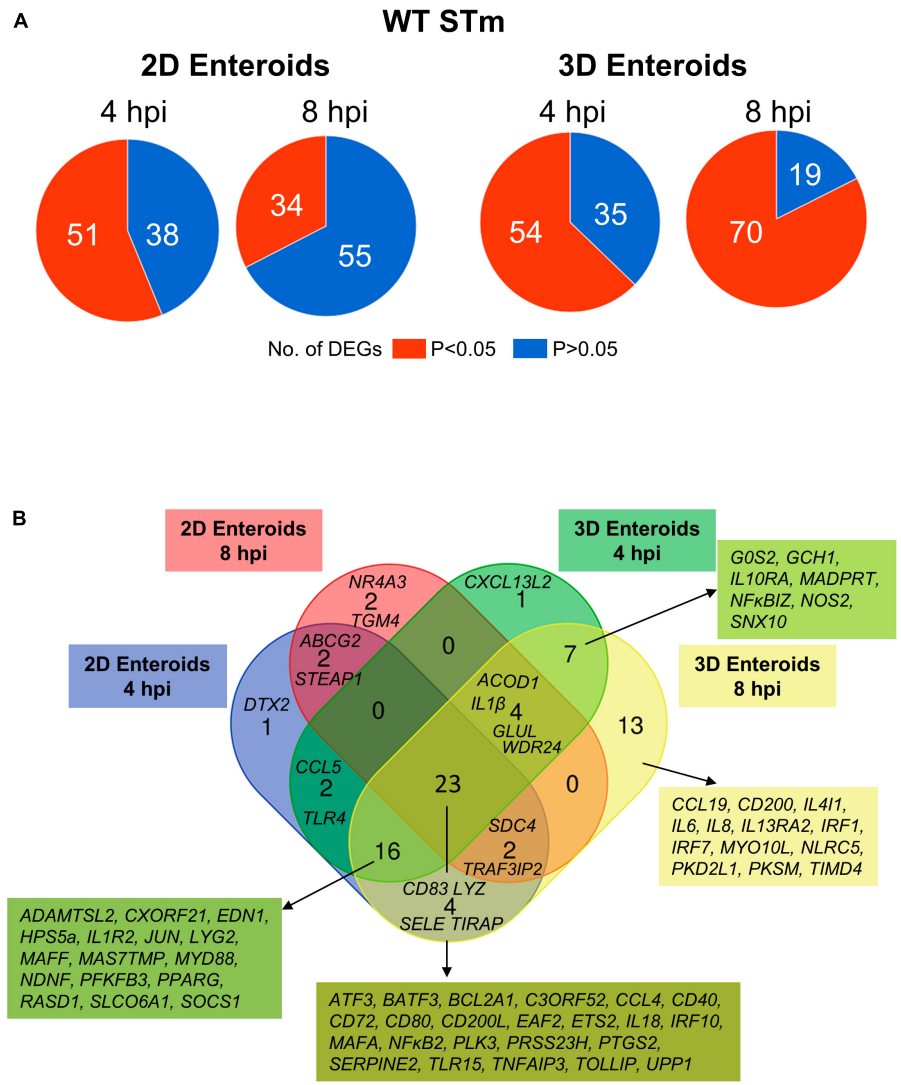

FIGURE 7
Innate immune response increase with time in WT STm infected 3D enteroids. **(A)** Pie charts indicating number of statistically significant, ($P < 0.05$) and non-significant ($P > 0.05$) DEGs in WT STm infected 2D enteroids ($n = 3$) and 3D enteroids ($n = 5$) at 4 hpi and 8 hpi compared to their time-matched, respective controls. DEGs with a significant difference ($P < 0.05$) and a fold change of ≥ 1.5 were identified. **(B)** Venn diagram showing common and unique DEGs across each enteroid model and timepoint.

8 hpi. STm infected 2D enteroids differentially expressed 51 genes at 4 hpi, decreasing to 34 genes by 8 hpi (Figure 7A). In contrast, the number of DEGs in WT STm infected 3D enteroids was 54 at 4 hpi rising to 70 at 8 hpi (Figure 7A). There were 23 DEGs in common between 2D and 3D enteroids at both time-points (Figure 7B). This core set of genes are involved in the regulation of immune responses, *ATF3*, *BATF3*, *ETS2*, *IRF10*, *PTGS2*, *MAFA*, *NFκB2*, *TNFAIP3*, effector functions, *CCL4*, *CD200L*, *CD40*, *CD72*, *CD80*, *IL18*, and TLR signaling, *EAF2*, *TLR15*, *TOLLIP*. The second largest set of common genes (16 DEGs) was shared between 2D enteroids at 4 hpi and 3D enteroids at 4 and 8 hpi. These genes are involved in regulating immune responses (*JUN*, *MAFF*, *PPARG*, *RASD1*, *SOCS1*), TLR/IL1β signaling (*MyD88*, *IL1R2*), and effector functions (*LYG2*, *TLR4*) while *TLR4* and the chemokine, *CCL5*, were differentially expressed at 4 hpi in both models.

The number of DEGs that were uniquely expressed in one or the other model differed substantially, with the 2D enteroids expressing 5 unique genes; specifically, those encoding a regulator of Notch signaling (*DTX2*), a membrane transporter (*ABCG2*), a metalloreductase (*STEAP1*), a nuclear receptor (*NR4A3*), and transglutaminase (*TGM4*). In contrast, the 3D enteroids uniquely expressed 21 genes upon STm infection with a majority associated with immune cell functions. The seven genes shared between 4 and 8 hpi are involved in regulating inflammation (*IL10RA*, *IL13RA2*, *NFκBIZ*), bactericidal activity (*GCH1*, *NOS2*), membrane trafficking in endosomes (*SNX10*), and apoptosis (*GOS2*). By 8 hpi, genes involved in the regulation of interferon (IFN) and IFN-inducible genes (*IRF1*, *IRF7*, *NLRC5*) and macrophage and DC activities (*CCL19*, *CD200*, *IL4IL*, *TIMD4*) were found to be differentially expressed.

The temporal changes in the fold change levels of the 23 common DEGs demonstrates that the vast majority were expressed at higher levels in the 2D enteroids compared to the 3D enteroids at 4 hpi (Figure 8A and Supplementary Material 2). In contrast,

10.3389/fmicb.2023.1258796

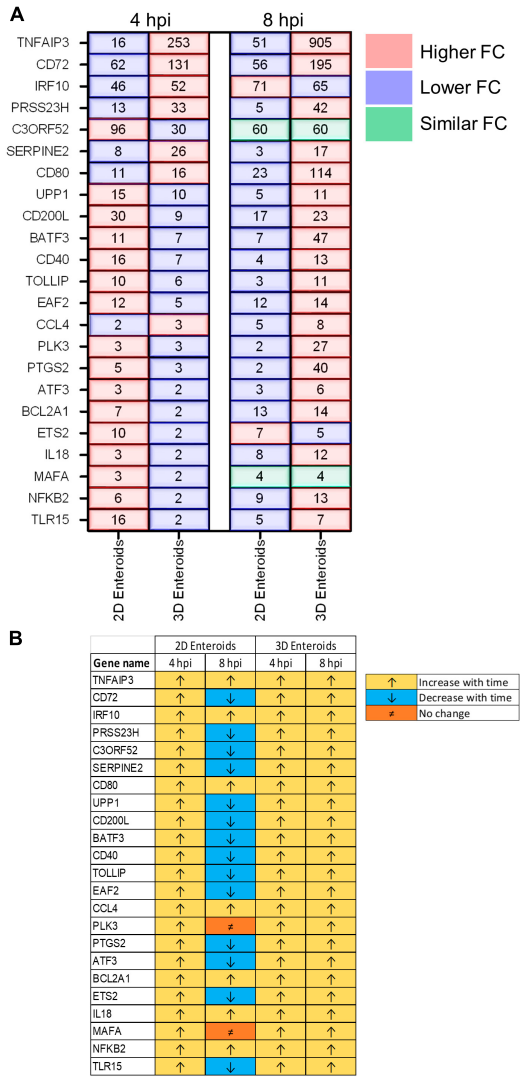

FIGURE 8
Lamina propria cells temporally govern the response to WT STm infection. **(A)** A comparison of the fold change levels of the common DEGs between the enteroid models demonstrates increased expression levels in 2D enteroids compared to 3D enteroids at 4 hpi. At 8 hpi, the expression levels of the common DEG are higher in 3D enteroids compared to 2D enteroids. **(B)** The expression levels of a majority of the common DEGs decrease with time in WT STm infected 2D enteroids and increase with time in 3D enteroids. Fold change values represent the mean of 3 (2D) or 5 (3D) independent experiments, relative to their time-matched respective controls.

at 8 hpi the majority of the common genes had higher fold change levels in the 3D enteroids compared to 2D enteroids. The magnitude of the fold change for DEGs in 2D enteroids did not exceed 96 (*C3ORF52*), whereas in 3D enteroids three common DEGs, possibly involved in inhibiting inflammatory responses, were expressed at a fold change ranging from 114 to 905 (*CD72, CD80, TNFAIP3*). In addition, the magnitude of the fold change of all 23 common genes increased with time in 3D enteroids whereas 13 of the common genes decrease with time in 2D enteroids (Figure 8B). Overall, the data suggests that 2D and 3D enteroids have differing temporal responses to STm infection.

3.5. Chicken enteroids mount an innate immune response to non-invasive *Salmonella*

To characterize the effects of a non-invasive STm strain on innate immune responses, 2D and 3D enteroids were infected with the isogenic Δ*prgH* mutant of STm strain 4/74. At 4 and 8 hpi, 56 and 39 genes were differentially expressed in 2D enteroids at *P*-values < 0.05, fold change of ≥ 1.5, respectively (Figure 9A). In 3D enteroids, infections with the Δ*prgH* STm strain differentially affected 52 genes at 4 hpi at fold change of > 2 and *P*-values < 0.05, increasing to 68 genes by 8 hpi (Figure 9A). Analysis of the DEGs across the models and time-points indicated a core set of 28 common genes (Figure 9B). Similar to WT STm infection, genes involved in the regulation of immune responses (*ATF3*, *BATF3*, *ETS2*, *IRF9*, *NFκB2, MAFA, TNFAIP3*), effector functions, (*CCL4*, *CD200L*, *CD40*, *CD72*, *CD80*, *IL18)* and TLR signaling, (*EAF2, TLR15, TRAF3IP2, TOLLIP*) were upregulated after Δ*prgH* STm infection in both models (Supplementary Material 2). An additional four genes were upregulated in Δ*prgH* STm infection and were involved in the regulation of glycolysis (*PFKFB3*) and cytokine signaling (*SOCS3*), and intracellular signaling (*RASD1*, *TRAF3IP2*). When disentangling the innate responses between the models, 8 and 20 genes were differentially expressed only in 2D and 3D enteroids, respectively. Similar to the response to WT STm infection, Δ*prgH* STm infected 2D enteroids regulated *CCL5* and *DTX2* at 4 hpi and genes involved in the regulation of antigen presentation (*CD83*), and inhibition of NFκB activation (*NFAIP2*). At both time-points, a gene involved in cell-cell junctions (*STEAP1*) and a serine protease (*PRSS23*) were upregulated and by 8 hpi, only one DEG, *TIMD4*, encoding a phosphatidylserine receptor for apoptotic cells, was specifically regulated in 2D enteroids. The shared genes in 3D enteroids were involved in nitric oxide synthesis (*GCH1, NOS2*), negative regulation of inflammation (*NFκBIZ*, *SOCS1*), the mTOR signaling pathway (*WDR24*), and membrane trafficking in endosomes (*SNX10*).

Fold change comparisons of the common genes demonstrates the expression levels for most genes were higher in 2D enteroids compared to 3D enteroids at 4 hpi (Figure 10A). However, by 8 hpi the expression levels for 15 out 28 common genes were higher in 2D enteroids compared to 3D enteroids. In contrast to infection with WT STm, when a differential response was detected between 2D and 3D enteroids over time, treatment with the invasive deficient Δ*prgH* STm strain resulted in the downregulation of almost half of the common DEGs in both 2D and 3D enteroids (Figure 10B). The data indicates that bacterial invasion is not required for 2D and 3D enteroids to mount an early response to STm, but invasion is required in 3D enteroids to increase the responses over-time.

3.6. Transcriptional regulation of innate immune genes remain unaffected by bacterial invasion

When comparing the innate immune responses between 2D and 3D enteroids, a majority of the DEGs were common to both models when infected with the invasive WT or non-invasive Δ*prgH* STm. We next analyzed the contribution of the bacterial load to

10.3389/fmicb.2023.1258796

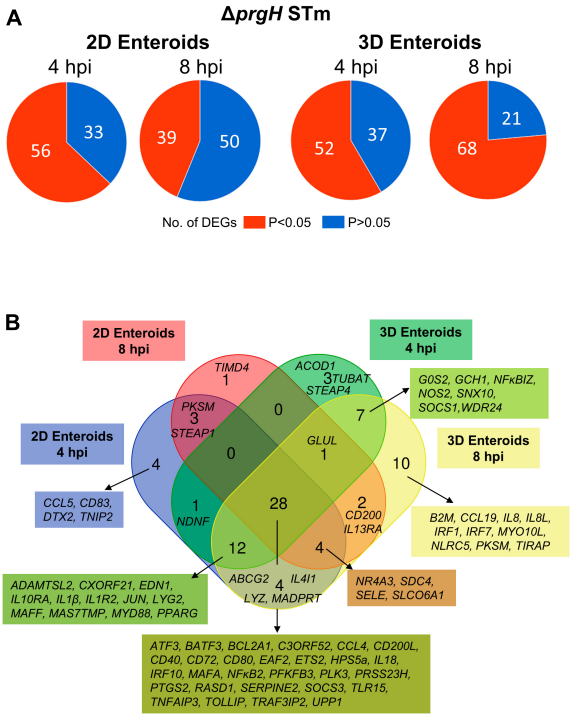

FIGURE 9
Chicken enteroids mount an innate immune response to non-invasive STm. **(A)** Pie charts indicating the number of statistically significant ($P < 0.05$) and non-significant ($P > 0.05$) DEGs in STm infected 2D enteroids ($n = 3$) and 3D enteroids ($n = 5$) at 4 hpi and 8 hpi, compared to their time-matched, respective controls. DEGs with a significant difference ($P < 0.05$) and a fold change of ≥ 1.5 were identified. **(B)** Venn diagram showing common and unique DEGs across each enteroid model and timepoint.

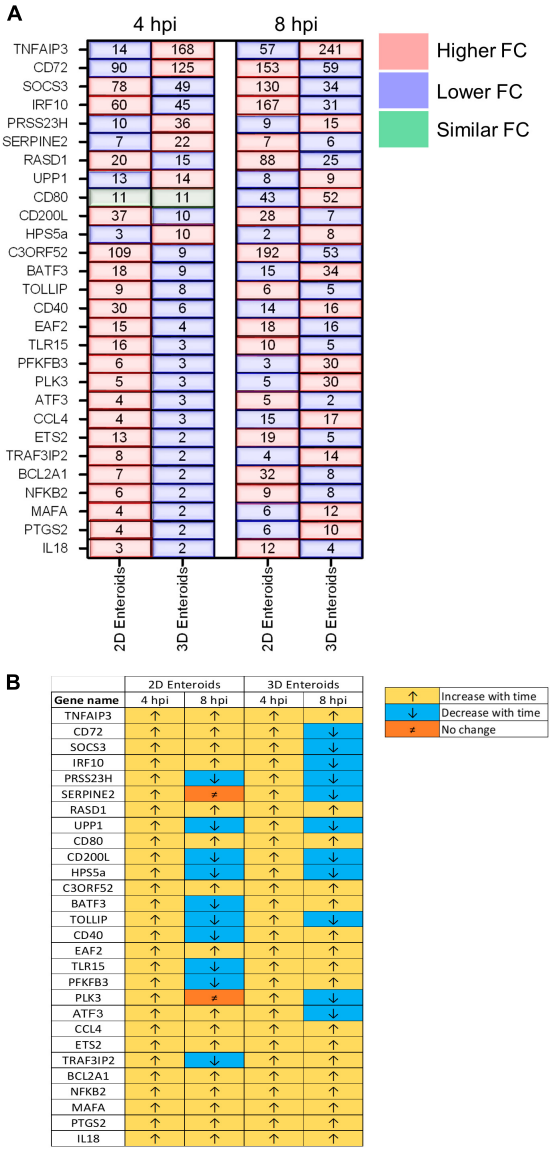

FIGURE 10
Δ*prgH* STm induces a rapid but brief innate immune response in chicken enteroids. **(A)** Fold change difference in the common DEGs in Δ*prgH* STm infected 2D and 3D enteroids at 4 hpi and 8 hpi. **(B)** The innate immune responses decrease with time in Δ*prgH* STm infected 2D and 3D enteroids. Fold change values represent the mean of 3 (2D) or 5 (3D) independent experiments, relative to their time-matched respective controls.

innate responses by comparing the DEGs (fold change of ≥ 1.5 and $P < 0.05$) in WT and Δ*prgH* STm infected enteroids at the late stage of infection, 8 hpi, when we observed numerous cells infected with WT STm in both models. Irrespective of STm strain, 26 DEGs were common across each model demonstrating the transcriptional regulation of these genes is independent of bacterial invasion (Figure 11). Few DEGs were uniquely upregulated by either WT or Δ*prgH* STm, independent of the enteroid model. WT and Δ*prgH* STm infected 2D enteroids shared 1 common gene (*STEAP1*) while each strain regulated 1 specific gene each, *TGM4* and *TLR4*. WT and Δ*prgH* STm infection of 3D enteroids shared 27 common genes while WT STm infection regulated 4 genes, (*CD83, IL6, NDNF, PKD2L1*) and Δ*prgH* STm regulated 3 genes (*ABCG2, B2M, IL8L*). STRING analysis reveals that the common DEGs at 8 hpi are linked to KEGG pathways involved in the intestinal immune network for IgA production and C-type lectin receptors signaling pathways (Supplementary Figure 3). To examine the contributions of lamina propria cells to signaling pathways, STRING analysis was carried out using the common DEGs across each model along with the common genes shared between WT and Δ*prgH* STm infected 3D enteroids at 8 hpi (Supplementary Figure 3). Key KEGG pathways such as Toll-like and NOD-like receptor signaling pathways, Cytosolic DNA-sensing pathway and Cytokine-cytokine receptor interaction were regulated in 3D enteroids.

To determine the effects of bacterial burden on the innate immune responses of lamina propria cells, we infected 3D enteroids with 1,000, 500 and 250 CFU of WT STm for 3 h and analyzed the mRNA expression levels using Fluidigm Biomark high-throughput qPCR. Few genes were significantly differentially regulated, with a fold change of ≥ 1.5 and *P*-values < 0.05, between the different doses of WT STm (Figure 11B). Moreover, the fold change of these DEGs was low. This demonstrates that the burden of bacteria does not significantly alter the transcriptional regulation of innate immune genes in chicken 3D enteroids and further supports the role lamina propria cells have on the regulation of responses to *Salmonella*.

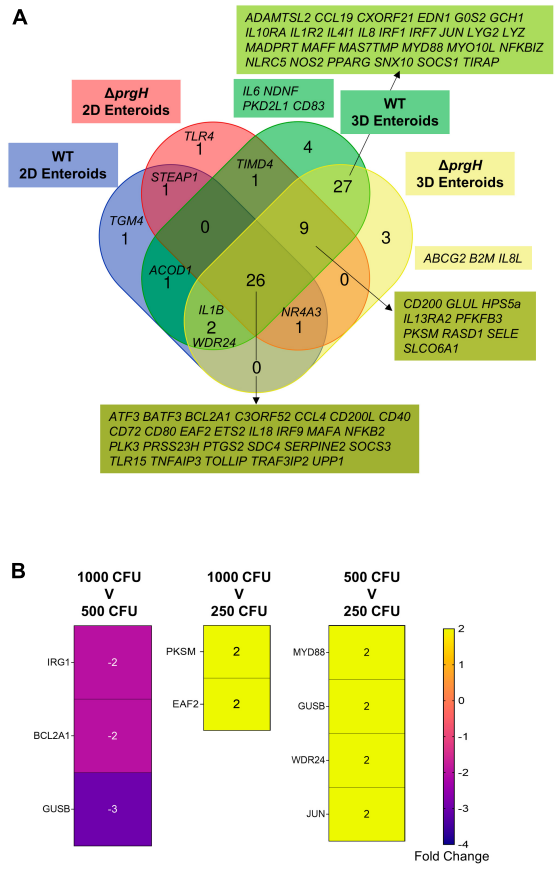

FIGURE 11
Transcriptional regulation of innate immune responses does not require bacterial invasion in chicken enteroids. **(A)** Venn diagram showing the DEGs that are altered by WT or Δ*prgH* STm infected 2D and 3D enteroids at 4 hpi and 8 hpi. **(B)** Heat maps of the fold change difference in the DEGs (Fold change ≥ 1.5, $P < 0.05$) between 1,000, 500, and 250 CFU of WT STm infected 3D enteroids demonstrates that the transcriptional regulation of innate immune genes is not significantly affected by bacterial burden. Fold change values represent the mean of 3 independent experiments.

4. Discussion

Currently, intestinal enteroids represent the gold standard *in vitro* models for studying host-pathogen interactions. In contrast to mammalian enteroids, the inner core of chicken 3D enteroids is solid and contains all cells that are present in the lamina propria because the isolated intact villi become enclosed to develop into 3D structures. In contrast, our 2D model contains all subsets of epithelial cells, few IELs and a layer of mesenchymal cells representing the lamina basalis. Chicken 2D and 3D enteroids offer valuable model systems in which to disentangle the interplay between epithelial/mesenchymal cells (2D) and epithelial/mesenchymal/lamina propria cells (3D) to reveal the cellular interplay that highly affects the overall response to danger signals including STm.

Previously, we demonstrated that WT STm can adhere and enter 3D enteroids in a manner associated with actin remodeling (Nash et al., 2021). In the current study, we used the same invasive WT STm and an isogenic invasion deficient Δ*prgH* mutant strain and demonstrated that the latter was adherent and immunogenic but did not invade chicken 2D and 3D enteroids. We observed that WT STm remodeled F-actin and disrupted tight junctions based on altered localization of ZO-1, whereas these phenotypes were not seen with the Δ*prgH* STm strain or after treatment with *Salmonella* LPS. ZO-1 associates with tight junction proteins, claudins and occludins, required to maintain cellular polarity and the paracellular barrier that allows selective passage of certain components (Odenwald et al., 2017). By altering ZO-1 expression, *Salmonella* increases the permeability of the epithelial layer which in turn enables invasive and otherwise non-invasive bacteria to enter the host tissue (Boyle et al., 2006). This process is known to be dependent on Type 3 secretion system-1 (T3SS-1) and a number of the effector proteins it injects, including SopB, SopE, SopE2, and SipA (Boyle et al., 2006). As the Δ*prgH* mutation abolishes the function of T3SS-1, the absence of disruption of ZO-1 localization upon infection with this strain is consistent with expectations. Much of the research on this topic has relied on mammalian cell lines and models and further work is required to understand the permeability properties of tight junctions in chickens and consequences of disruption of these by STm. Overall, our data are consistent with the known role of T3SS-1 and its effector proteins in *Salmonella* interactions with mammalian intestinal epithelial cells *in vitro* and *in vivo* (Jepson et al., 2000; Boyle et al., 2006; Lhocine et al., 2015).

The chicken 2D and 3D enteroids represent promising and versatile models to study host-pathogen interactions. In this study, we examine the response of 2D and 3D enteroids to LPS and STm infection using Fluidigm qPCR array to measure the mRNA expression levels of 89 innate immune related genes. These genes were selected based on their shared expression after infection of chickens or immune cells with *Salmonella*, *Campylobacter* and *Eimeria* or constituents thereof (Borowska et al., 2019). In contrast to 3D enteroids, 2D enteroids express more genes post-LPS treatment. Comparisons between the models found that after STm infection, a set of common genes was expressed in a temporal fashion in each model. For instance, in WT STm infected enteroids, the expression levels of 60% of the common genes increased with time in 3D enteroids but these genes decreased in 2D enteroids. In Δ*prgH* infected enteroids, 42% of the common genes decreased with time in both models. As the microbiota produce copious amounts of LPS, and to prevent unwanted stimulation and maintain homeostasis, TLR4 expression is restricted to the basal region of mammalian epithelial cells (Price et al., 2018). In this study, we cultured 2D enteroids on plastic plates and in contrast to 2D enteroids grown on Matrigel coated transwell inserts, epithelial barrier integrity could not be measured (Orr et al., 2021). The 2D conformation may not be completely tight and some leakage of LPS to the basolateral sides of the cells may have occurred. Furthermore, the chicken 3D enteroid resembles the natural conformation of the epithelium and prevents access of LPS to the basolateral sides of the cells similar to the *in vivo* situation. This would make the TLRs inaccessible. Therefore, we would recommend to either grow the 2D enteroids on a transwell insert and measure epithelial barrier integrity prior to LPS exposure or use the 3D conformation. Although in the current study, intracellular bacterial replication was not quantified, we demonstrated that varying the size of the bacterial inoculum induced no significant changes in gene expression levels and therefore the differences in temporal gene

expression may be related to the presence of lamina propria cells in 3D enteroids and the structural differences between the models. Future studies involving use of fluorescence dilution may allow replication of *Salmonella* to be measured at the single cell level, including to understand the fate of STm in different types of infected cells. Overall, the differences in temporal gene expression may be related to the presence of lamina propria cells in 3D enteroids and the structural differences between the models.

Interestingly, the invasion deficient Δ*prgH* STm strain was found in close contact with the apical surface of epithelial cells in both models and induced an early immune response at a magnitude similar to WT STm treatment. The close physical association is likely mediated by bacterial adhesins such as fimbriae, flagella and outer membrane proteins (Stones and Krachler, 2016). In addition, day-old chicks are highly susceptible to *Salmonella* infection, usually leading to death (Withanage et al., 2005). In this study, we utilized the small intestines from ED18 embryos, therefore taken together both these attributes may be driving an immune response independent of bacterial invasion. Further research is necessary to examine the differences in the immune response between enteroids-derived from older chickens and how different STm virulence factors affect immune responses.

In vitro and *in vivo* chicken studies have illuminated how the immune system in tissues and cells respond to *Salmonella.* We also found similarities between our models and these studies. In 3D enteroids, the phagocyte chemoattractant genes, *IL8* (*CXCLi1*) and *IL8L* (*CXCLi2*) and transcription factors, *IRF1* and *IRF7*, were induced by STm infection (Poh et al., 2008; Setta et al., 2012). *IRF1* and *IRF7* are upregulated in chicken heterophils stimulated with *S.* Enteritidis leading to the induction of IFNs (Chiang et al., 2008; Kogut et al., 2012). *IL4l1,* a putative anti-inflammatory gene expressed by myeloid cells was upregulated in 3D enteroids (Marquet et al., 2010). IL4IL was the most inducible gene found in chicken cecum post-*S.* Enteritidis infection (Elsheimer-Matulova et al., 2020). Genes upregulated in 2D and/or 3D enteroids, such as *IL6*, *IL1β*, *IL10RA*, *IL18*, *MyD88*, were found to be upregulated in the spleen and caecum of STm infected chickens (Dar et al., 2019, 2022; Ahmad et al., 2023). Genes such as *RASD1, SOSC3, TOLLIP,* that are involved in the negative regulation of downstream TLR4 signaling, NFκB activation and cytokine activities, were upregulated across all models. In contrast both *TOLLIP* and *RASD1* were found to be downregulated in *S.* Enteritidis challenged chickens (Tsai et al., 2010; Sun et al., 2019). This discrepancy can be caused by the model or by the strain of *Salmonella* used. DEGs in both 2D and 3D enteroids are linked to pathways associated with Toll-like receptor signaling, intestinal immune network IgA production, Cytosolic DNA sensing, and Cytokine-receptor interaction. These pathways are similarly regulated in chicken intestines after STm infection (Wang et al., 2019; Khan and Chousalkar, 2020; Dar et al., 2022). Overall, most key features of the immune response against STm *in vivo* could be replicated in 2D and 3D enteroids. Future single-cell RNA sequencing studies will help to fully resolve the contributions and cross-talk between the different epithelial, mesenchymal and immune cells to STm in 2D and 3D enteroids.

Nitric oxide (NO) production is a vital host-defense mechanism against microbial pathogens in mononuclear phagocytes. *NOS2*, was downregulated in 3D enteroids irrespective of the STm strain. *S.* Enteritidis suppresses *NOS2* expression in HD11 cells and experimentally infected chickens (He et al., 2012, 2018; Cazals et al., 2022). In a recent immunometabolic kinome peptide array analysis, *S.* Enteritidis but not *S.* Heidelberg or *S.* Senftenberg infected HD11 cells inhibited NO production and reduced glycolysis which together indicate macrophage polarization from pro-inflammatory, M1, to anti-inflammatory, M2, state (He et al., 2023). Our data indicates that chicken 3D enteroids provide a suitable *ex vivo* intestinal model to examine the relationship between macrophage polarization and immuno-metabolism during infection with different *Salmonella* strains.

5. Conclusion

In conclusion, the chicken 2D and 3D enteroids allowed for the first time a description of the distinct innate immune responses exhibited by epithelial cells and lamina propria cells. The enteroid models replicated several observations demonstrated after *in vivo* infection of chickens with *Salmonella*, including the alteration of tight junctions and the induction of inflammatory responses. The chicken enteroid models offers many advantages over other models to reduce animal use in the study of host-pathogen interactions.

Data availability statement

The original contributions presented in this study are included in the article/**Supplementary material**, further inquiries can be directed to the corresponding authors.

Ethics statement

The animal study was approved by The Roslin Institute's Animal Welfare and Ethical Review Board. The study was conducted in accordance with the local legislation and institutional requirements.

Author contributions

KS, TN, and LV conceptualized the study. LV secured funding to undertake the work and supervised the project. KS, TN, SS, DB, and JM performed the experiments and analyzed the data with support of PV, MS, and LV. KS wrote the manuscript supported by SS, PV, MS, and LV. All authors read and approved the final manuscript.

Funding

The author(s) declare financial support was received for the research, authorship, and/or publication of this article. This work was supported by the Biotechnology and Biological Sciences Research Council Institute Strategic Program Grant funding (BB/X010937/1, BBS/E/D/10002071, BBS/E/D/10002073, and BBS/E/D/20002174) and an iCase doctoral studentship to TN (BB/MO14819).

Acknowledgments

We wish to thank the animal caretakers of the National Avian Research Facility for the supply of eggs and for helpful advice from staff at the Roslin Institute's Bio-imaging Facility. For the purpose of open access, the author has applied a Creative Commons Attribution (CC BY) license to any Authors Accepted Manuscript version arising from this submission.

Conflict of interest

The authors declare that the research was conducted in the absence of any commercial or financial relationships that could be construed as a potential conflict of interest.

Publisher's note

Supplementary material

The Supplementary Material for this article can be found online at: https://www.frontiersin.org/articles/10.3389/fmicb.2023.1258796/full#supplementary-material

References

Ahmad, S. M., Bhat, S. S., Shafi, S., Dar, M. A., Saleem, A., Haq, Z., et al. (2023). Identification of key transcription factors and their functional role involved in *Salmonella* typhimurium infection in chicken using integrated transcriptome analysis and bioinformatics approach. *BMC Genomics* 24:214. doi: 10.1186/s12864-023-09315-3

Balic, A., Chintoan-Uta, C., Vohra, P., Sutton, K. M., Cassady-Cain, R. L., Hu, T., et al. (2019). Antigen sampling CSF1R-expressing epithelial cells are the functional equivalents of mammalian m cells in the avian follicle-associated epithelium. *Front. Immunol.* 10:2495. doi: 10.3389/fimmu.2019.02495

Barrow, P. A., Huggins, M. B., Lovell, M. A., and Simpson, J. M. (1987). Observations on the pathogenesis of experimental *Salmonella* typhimurium infection in chickens. *Res. Vet. Sci.* 42, 194–199.

Bescucci, D. M., Montina, T., Boras, V. F., and Inglis, G. D. (2022). Infection by *Salmonella enterica* serovar typhimurium DT104 modulates immune responses, the metabolome, and the function of the enteric microbiota in neonatal broiler chickens. *Pathogens* 11:1257. doi: 10.3390/pathogens11111257

Blake, R., Jensen, K., Mabbott, N., Hope, J., and Stevens, J. (2022). The development of 3D bovine intestinal organoid derived models to investigate *Mycobacterium avium* ssp paratuberculosis pathogenesis. *Front. Vet. Sci.* 9:921160. doi: 10.3389/fvets.2022.921160

Borowska, D., Kuo, R., Bailey, R. A., Watson, K. A., Kaiser, P., Vervelde, L., et al. (2019). Highly multiplexed quantitative PCR-based platform for evaluation of chicken immune responses. *PLoS One* 14:e0225658. doi: 10.1371/journal.pone.0225658

Boyle, E. C., Brown, N. F., and Finlay, B. B. (2006). *Salmonella enterica* serovar Typhimurium effectors SopB, SopE, SopE2, and SipA disrupt tight junction structure and function. *Cell Microbiol* 8, 1946–1957. doi: 10.1111/j.1462-5822.2006.00762.x

Bryson, K. J., Sives, S., Lee, H. M., Borowska, D., Smith, J., Digard, P., et al. (2023). Comparative analysis of different inbred chicken lines highlights how a hereditary inflammatory state affects susceptibility to avian influenza virus. *Viruses* 15:591. doi: 10.3390/v15030591

Cazals, A., Rau, A., Estelle, J., Bruneau, N., Coville, J. L., Menanteau, P., et al. (2022). Comparative analysis of the caecal tonsil transcriptome in two chicken lines experimentally infected with *Salmonella* Enteritidis. *PLoS One* 17:e0270012. doi: 10.1371/journal.pone.0270012

Chaudhuri, R. R., Morgan, E., Peters, S. E., Pleasance, S. J., Hudson, D. L., Davies, H. M., et al. (2013). Comprehensive assignment of roles for *Salmonella* typhimurium genes in intestinal colonization of food-producing animals. *PLoS Genet.* 9:e1003456. doi: 10.1371/journal.pgen.1003456

Chiang, H. I., Swaggerty, C. L., Kogut, M. H., Dowd, S. E., Li, X., Pevzner, I. Y., et al. (2008). Gene expression profiling in chicken heterophils with *Salmonella* enteritidis stimulation using a chicken 44 K Agilent microarray. *BMC Genomics* 9:526. doi: 10.1186/1471-2164-9-526

Co, J. Y., Margalef-Catala, M., Monack, D. M., and Amieva, M. R. (2021). Controlling the polarity of human gastrointestinal organoids to investigate epithelial biology and infectious diseases. *Nat. Protoc.* 16, 5171–5192. doi: 10.1038/s41596-021-00607-0

Dar, M. A., Ahmad, S. M., Bhat, B. A., Dar, T. A., Haq, Z. U., Wani, B. A., et al. (2022). Comparative RNA-Seq analysis reveals insights in *Salmonella* disease resistance of chicken; and database development as resource for gene expression in poultry. *Genomics* 114:110475. doi: 10.1016/j.ygeno.2022.110475

Dar, M. A., Urwat, U., Ahmad, S. M., Ahmad, R., Kashoo, Z. A., Dar, T. A., et al. (2019). Gene expression and antibody response in chicken against *Salmonella* typhimurium challenge. *Poult. Sci.* 98, 2008–2013. doi: 10.3382/ps/pey560

Derricott, H., Luu, L., Fong, W. Y., Hartley, C. S., Johnston, L. J., Armstrong, S. D., et al. (2019). Developing a 3D intestinal epithelium model for livestock species. *Cell Tissue Res.* 375, 409–424.

Elsheimer-Matulova, M., Polansky, O., Seidlerova, Z., Varmuzova, K., Stepanova, H., Fedr, R., et al. (2020). Interleukin 4 inducible 1 gene (IL4I1) is induced in chicken phagocytes by *Salmonella* Enteritidis infection. *Vet. Res.* 51:67. doi: 10.1186/s13567-020-00792-y

Fasina, Y. O., Holt, P. S., Moran, E. T., Moore, R. W., Conner, D. E., and Mckee, S. R. (2008). Intestinal cytokine response of commercial source broiler chicks to *Salmonella* typhimurium infection. *Poult. Sci.* 87, 1335–1346. doi: 10.3382/ps.2007-00526

Forbester, J. L., Goulding, D., Vallier, L., Hannan, N., Hale, C., Pickard, D., et al. (2015). Interaction of *Salmonella enterica* serovar typhimurium with intestinal organoids derived from human induced pluripotent stem cells. *Infect. Immun.* 83, 2926–2934. doi: 10.1128/IAI.00161-15

He, H., Arsenault, R. J., Genovese, K. J., Johnson, C., and Kogut, M. H. (2018). Chicken macrophages infected with *Salmonella* (S.) Enteritidis or S. Heidelberg produce differential responses in immune and metabolic signaling pathways. *Vet. Immunol. Immunopathol.* 195, 46–55.

He, H., Genovese, K. J., Arsenault, R. J., Swaggerty, C. L., Johnson, C. N., Byrd, J. A., et al. (2023). M2 polarization and inhibition of host cell glycolysis contributes intracellular survival of *Salmonella* strains in chicken macrophage HD-11 cells. *Microorganisms* 11:1838. doi: 10.3390/microorganisms11071838

He, H., Genovese, K. J., Swaggerty, C. L., Nisbet, D. J., and Kogut, M. H. (2012). A comparative study on invasion, survival, modulation of oxidative burst, and nitric oxide responses of macrophages (HD11), and systemic infection in chickens by prevalent poultry *Salmonella* serovars. *Foodborne Pathog. Dis.* 9, 1104–1110. doi: 10.1089/fpd.2012.1233

Iqbal, M., Philbin, V. J., Withanage, G. S., Wigley, P., Beal, R. K., Goodchild, M. J., et al. (2005). Identification and functional characterization of chicken toll-like receptor 5 reveals a fundamental role in the biology of infection with *Salmonella enterica* serovar typhimurium. *Infect. Immun.* 73, 2344–2350. doi: 10.1128/IAI.73.4.2344-2350.2005

Jepson, M. A., Schlecht, H. B., and Collares-Buzato, C. B. (2000). Localization of dysfunctional tight junctions in *Salmonella enterica* serovar typhimurium-infected epithelial layers. *Infect. Immun.* 68, 7202–7208. doi: 10.1128/IAI.68.12.7202-7208.2000

Joo, S. S., Gu, B. H., Park, Y. J., Rim, C. Y., Kim, M. J., Kim, S. H., et al. (2022). Porcine intestinal apical-out organoid model for gut function study. *Animals* 12:372. doi: 10.3390/ani12030372

Khan, S., and Chousalkar, K. K. (2020). Transcriptome profiling analysis of caeca in chicks challenged with *Salmonella* Typhimurium reveals differential expression of genes involved in host mucosal immune response. *Appl. Microbiol. Biotechnol.* 104, 9327–9342. doi: 10.1007/s00253-020-10887-3

Klein, J. R., Fahlen, T. F., and Jones, B. D. (2000). Transcriptional organization and function of invasion genes within *Salmonella enterica* serovar typhimurium pathogenicity island 1, including the prgH, prgI, prgJ, prgK, orgA, orgB, and orgC genes. *Infect. Immun.* 68, 3368–3376. doi: 10.1128/IAI.68.6.3368-3376.2000

Kogut, M., Chiang, H.-I., Swaggerty, C., and Zhou, H. (2012). Gene expression analysis of toll-like receptor pathways in heterophils from genetic chicken lines that differ in their susceptibility to *Salmonella enteritidis*. *Front. Genet.* 3:121. doi: 10.3389/fgene.2012.00121

Lhocine, N., Arena, E. T., Bomme, P., Ubelmann, F., Prevost, M. C., Robine, S., et al. (2015). Apical invasion of intestinal epithelial cells by *Salmonella* typhimurium requires villin to remodel the brush border actin cytoskeleton. *Cell Host Microbe* 17, 164–177. doi: 10.1016/j.chom.2014.12.003

Livak, K. J., and Schmittgen, T. D. (2001). Analysis of relative gene expression data using real-time quantitative PCR and the 2(-Delta Delta C(T)) method. *Methods* 25, 402–408.

Marquet, J., Lasoudris, F., Cousin, C., Puiffe, M. L., Martin-Garcia, N., Baud, V., et al. (2010). Dichotomy between factors inducing the immunosuppressive enzyme IL-4-induced gene 1 (IL4I1) in B lymphocytes and mononuclear phagocytes. *Eur. J. Immunol.* 40, 2557–2568. doi: 10.1002/eji.201040428

Mills, D. M., Bajaj, V., and Lee, C. A. (1995). A 40 kb chromosomal fragment encoding *Salmonella* typhimurium invasion genes is absent from the corresponding region of the *Escherichia coli* K-12 chromosome. *Mol. Microbiol.* 15, 749–759. doi: 10.1111/j.1365-2958.1995.tb02382.x

Nash, T. J., Morris, K. M., Mabbott, N. A., and Vervelde, L. (2021). Inside-out chicken enteroids with leukocyte component as a model to study host-pathogen interactions. *Commun. Biol.* 4:377. doi: 10.1038/s42003-021-01901-z

Nash, T. J., Morris, K. M., Mabbott, N. A., and Vervelde, L. (2023). Temporal transcriptome profiling of floating apical out chicken enteroids suggest stability and reproducibility. *Vet. Res.* 54:12. doi: 10.1186/s13567-023-01144-2

Noel, G., Baetz, N. W., Staab, J. F., Donowitz, M., Kovbasnjuk, O., Pasetti, M. F., et al. (2017). A primary human macrophage-enteroid co-culture model to investigate mucosal gut physiology and host-pathogen interactions. *Sci. Rep.* 7:45270.

Odenwald, M. A., Choi, W., Buckley, A., Shashikanth, N., Joseph, N. E., Wang, Y., et al. (2017). ZO-1 interactions with F-actin and occludin direct epithelial polarization and single lumen specification in 3D culture. *J. Cell Sci.* 130, 243–259. doi: 10.1242/jcs.188185

Orr, B., Sutton, K., Christian, S., Nash, T., Niemann, H., Hansen, L. L., et al. (2021). Novel chicken two-dimensional intestinal model comprising all key epithelial cell types and a mesenchymal sub-layer. *Vet. Res.* 52:142. doi: 10.1186/s13567-021-01010-z

Poh, T. Y., Pease, J., Young, J. R., Bumstead, N., and Kaiser, P. (2008). Re-evaluation of chicken CXCR1 determines the true gene structure: CXCLi1 (K60) and CXCLi2 (CAF/interleukin-8) are ligands for this receptor. *J. Biol. Chem.* 283, 16408–16415. doi: 10.1074/jbc.M800998200

Price, A. E., Shamardani, K., Lugo, K. A., Deguine, J., Roberts, A. W., Lee, B. L., et al. (2018). A map of toll-like receptor expression in the intestinal epithelium reveals distinct spatial, cell type-specific, and temporal patterns. *Immunity* 49, 560–575 e6. doi: 10.1016/j.immuni.2018.07.016

Raffatellu, M., Wilson, R. P., Chessa, D., Andrews-Polymenis, H., Tran, Q. T., Lawhon, S., et al. (2005). SipA, SopA, SopB, SopD, and SopE2 contribute to *Salmonella enterica* serotype typhimurium invasion of epithelial cells. *Infect. Immun.* 73, 146–154. doi: 10.1128/IAI.73.1.146-154.2005

Sato, T., Vries, R. G., Snippert, H. J., Van De Wetering, M., Barker, N., Stange, D. E., et al. (2009). Single Lgr5 stem cells build crypt-villus structures in vitro without a mesenchymal niche. *Nature* 459, 262–265. doi: 10.1038/nature07935

Setta, A. M., Barrow, P. A., Kaiser, P., and Jones, M. A. (2012). Early immune dynamics following infection with *Salmonella enterica* serovars Enteritidis, Infantis, Pullorum, and Gallinarum: Cytokine and chemokine gene expression profile and cellular changes of chicken cecal tonsils. *Comp. Immunol. Microbiol. Infect. Dis.* 35, 397–410. doi: 10.1016/j.cimid.2012.03.004

Smith, D., Price, D. R. G., Burrells, A., Faber, M. N., Hildersley, K. A., Chintoan-Uta, C., et al. (2021). The development of ovine gastric and intestinal organoids for studying ruminant host-pathogen interactions. *Front. Cell. Infect. Microbiol.* 11:733811. doi: 10.3389/fcimb.2021.733811

Staab, J. F., Lemme-Dumit, J. M., Latanich, R., Pasetti, M. F., and Zachos, N. C. (2020). Co-culture system of human enteroids/colonoids with innate immune cells. *Curr. Protoc. Immunol.* 131:e113. doi: 10.1002/cpim.113

Stones, D. H., and Krachler, A. M. (2016). Against the tide: The role of bacterial adhesion in host colonization. *Biochem. Soc. Trans.* 44, 1571–1580. doi: 10.1042/BST20160186

Sun, W., Liu, R., Li, P., Li, Q., Cui, H., Zheng, M., et al. (2019). Chicken gga-miR-1306-5p targets Tollip and plays an important role in host response against *Salmonella* enteritidis infection. *J. Anim. Sci. Biotechnol.* 10:59. doi: 10.1186/s40104-019-0365-2

Tsai, H.-J., Chiu, C.-H., Wang, C.-L., and Chou, C.-H. (2010). A time-course study of gene responses of chicken granulosa cells to *Salmonella* Enteritidis infection. *Vet. Microbiol.* 144, 325–333. doi: 10.1016/j.vetmic.2010.01.004

Valdivia, R. H., and Falkow, S. (1996). Bacterial genetics by flow cytometry: Rapid isolation of *Salmonella* typhimurium acid-inducible promoters by differential fluorescence induction. *Mol. Microbiol.* 22, 367–378. doi: 10.1046/j.1365-2958.1996.00120.x

Vohra, P., Vrettou, C., Hope, J. C., Hopkins, J., and Stevens, M. P. (2019). Nature and consequences of interactions between *Salmonella enterica* serovar Dublin and host cells in cattle. *Vet. Res.* 50:99. doi: 10.1186/s13567-019-0720-5

Wang, F., Zhang, J., Zhu, B., Wang, J., Wang, Q., Zheng, M., et al. (2019). Transcriptome analysis of the cecal tonsil of Jingxing yellow chickens revealed the mechanism of differential resistance to *Salmonella*. *Genes* 10:979. doi: 10.3390/genes10120979

Withanage, G. S., Kaiser, P., Wigley, P., Powers, C., Mastroeni, P., Brooks, H., et al. (2004). Rapid expression of chemokines and proinflammatory cytokines in newly hatched chickens infected with *Salmonella enterica* serovar typhimurium. *Infect. Immun.* 72, 2152–2159. doi: 10.1128/IAI.72.4.2152-2159.2004

Withanage, G. S., Wigley, P., Kaiser, P., Mastroeni, P., Brooks, H., Powers, C., et al. (2005). Cytokine and chemokine responses associated with clearance of a primary *Salmonella enterica* serovar typhimurium infection in the chicken and in protective immunity to rechallenge. *Infect. Immun.* 73, 5173–5182. doi: 10.1128/IAI.73.8.5173-5182.2005

Zhang, Y.-G., Wu, S., Xia, Y., and Sun, J. (2014). *Salmonella*-infected crypt-derived intestinal organoid culture system for host–bacterial interactions. *Physiol. Rep.* 2:e12147. doi: 10.14814/phy2.12147

frontiers | Frontiers in Microbiology

TYPE Original Research
PUBLISHED 12 October 2023
DOI 10.3389/fmicb.2023.1241961

OPEN ACCESS

EDITED BY
Sébastien Holbert,
INRA Centre Val de Loire, France

REVIEWED BY
Jonathan Gray Frye,
Agricultural Research Service (USDA), United States
Peter Johnston,
University of Liverpool, United Kingdom

*CORRESPONDENCE
Dadi Falay
falaydadi@gmail.com

RECEIVED 18 June 2023
ACCEPTED 18 September 2023
PUBLISHED 12 October 2023

CITATION
Falay D, Hardy L, Bonebe E, Mattheus W, Ngbonda D, Lunguya O and Jacobs J (2023) Intestinal carriage of invasive non-typhoidal *Salmonella* among household members of children with *Salmonella* bloodstream infection, Kisangani, DR Congo. *Front. Microbiol.* 14:1241961. doi: 10.3389/fmicb.2023.1241961

Intestinal carriage of invasive non-typhoidal *Salmonella* among household members of children with *Salmonella* bloodstream infection, Kisangani, DR Congo

Dadi Falay[1,2,3]*, Liselotte Hardy[3], Edmonde Bonebe[4], Wesley Mattheus[5], Dauly Ngbonda[1], Octavie Lunguya[4,6] and Jan Jacobs[2,3]

[1]Department of Pediatrics, University Hospital of Kisangani, Kisangani, Democratic Republic of Congo, [2]Department of Clinical Sciences, Institute of Tropical Medicine, Antwerp, Belgium, [3]Department of Microbiology, Immunology and Transplantation, KU Leuven, Leuven, Belgium, [4]Department of Microbiology, National Institute for Biomedical Research, Kinshasa, Democratic Republic of Congo, [5]Division of Human Bacterial Diseases, Sciensano, Uccle, Belgium, [6]Department of Microbiology, University Teaching Hospital of Kinshasa, Kinshasa, Democratic Republic of Congo

Introduction: Invasive non-typhoidal *Salmonella* (iNTS), mainly *Salmonella* Typhimurium and *Salmonella* Enteritidis, causes a severe burden in sub-Saharan Africa; however, its reservoir (animal or environmental) is unclear. The present study assessed healthy household members of index patients for intestinal carriage of *Salmonella*.

Methods: Index patients were admitted to the University Hospital of Kisangani (DR Congo), and *Salmonella* was grown from blood cultures. Household members were asked to provide three stool samples for culture for *Salmonella*. *Salmonella* Typhimurium and *S.* Enteritidis isolates from index patients, and household members were assessed for genetic relatedness using the multiple-locus variable number of tandem repeat analysis (MLVA), and the multilocus sequence type (ST) was determined by whole genome sequencing.

Results: Between May 2016 and January 2020, 22 households were visited. The index patient serotypes were Typhimurium, Enteritidis, Typhi, and Paratyphi C; II:42:r:-; and I:7:y:- (n = 8, 7, 5, and each 1, respectively). The median (range) delay between the index patient and household sampling was 25 days (2 days to 7.3 months); 203 household members provided at least one stool sample. In all, 15 (7.3%) *Salmonella* carriers were found in nine of 22 households. For one index patient, the household comprised *S.* Typhimurium in four household members, including the index patient, sampled 27 days after bloodstream infection; the MLVA types of these five isolates were similar. They belonged to ST313 lineage 2 and were closely related [0–1 allelic distance (AD) among the stool isolates and eight AD with the blood culture isolate]. In another household, the stool culture of the index patient (obtained 67 days after bloodstream infection) grew *S.* Enteritidis of the same MLVA type; both isolates belonged to the ST11 Central/Eastern African clade and were closely related (three AD).

Discussion: The present study provides evidence of household clustering of *S.* Typhimurium ST313 and intestinal carriage of iNTS several weeks after bloodstream infection.

KEYWORDS

invasive non-typhoidal *Salmonella*, *Salmonella* carriage, sub-Saharan Africa, *Salmonella* bloodstream infection, households

Background

Infections caused by non-typhoidal *Salmonella* spp. occur worldwide. In high-income countries, non-typhoidal *Salmonella* serotypes cause self-limiting enterocolitis, but in low-resource settings, they cause bloodstream infections and are currently labeled as "invasive non-typhoidal *Salmonella*" (iNTS) (Feasey et al., 2012; Stanaway et al., 2019). iNTS accounts for ~535,000 invasive bloodstream infections per year, mostly occurring in children under 5 years of age, and is confined to sub-Saharan Africa, where it has a case fatality rate of 17.1% (Stanaway et al., 2019; Marchello et al., 2022). In addition to young age, host risk factors include *Plasmodium falciparum* infection (severe as well as chronic), malnutrition, and anemia (Feasey et al., 2012; Crump et al., 2015; Stanaway et al., 2019). Over 90% of iNTS infections are caused by particular clades of the *Salmonella enterica* subspecies *enterica* serovars Typhimurium and Enteritidis, such as multilocus sequence type (ST) ST313 lineage 1 and multidrug-resistant lineage 2 and ST11 Central/East African and West African clades, respectively (Feasey et al., 2016; Van Puyvelde et al., 2019; Pulford et al., 2021).

In addition to their evolution toward invasive infections, these clades are genetically adapted to human hosts (Feasey et al., 2016; Van Puyvelde et al., 2019; Pulford et al., 2021). This suggests a more restricted host specificity and, as is the case for *Salmonella* Typhi, healthy human carriers as reservoirs for iNTS. In contrast, non-typhoidal *Salmonella* causes enterocolitis and has a broad zoonotic reservoir (Sirinavin et al., 1999; Feasey et al., 2015). Evidence supporting the hypothesis of a human reservoir for iNTS has been provided by studies that compared iNTS isolates from infected patients to *Salmonella* isolates obtained from stool cultures of humans and livestock or other environmental samples close to the infected index patients. Using pulsed-field gel electrophoresis, these studies showed genetic relatedness between the index iNTS isolates and *Salmonella* isolates obtained from stool cultures of healthy humans, whereas they were unrelated to animal or environmental isolates (Kariuki et al., 2002, 2006; Dione et al., 2011; Dekker et al., 2018).

Molecular tools, such as multilocus variable number tandem repeat analysis (MLVA) and whole genome sequencing (WGS), have provided new and more powerful tools for assessing the genetic relatedness of *Salmonella* isolates. Therefore, we conceived an index patient-household study design to provide additional evidence of the human reservoir of the iNTS. Although not conceived as a dual-site study, the design was applied to two iNTS-endemic settings: rural Burkina Faso (Post et al., 2019) and Kisangani, as described in this manuscript. The methods were similar, except that only a single stool sample was sampled in the Burkina Faso study, and livestock and household water were assessed.

The primary objectives of this study were (i) to assess the proportion (frequency) and serotype distribution of *Salmonella* intestinal carriers among household members of index patients with iNTS bloodstream infection; (ii) to assess the genetic relatedness of *S.* Typhimurium and *S.* Enteritidis stool and blood culture isolates; and (iii) to determine the iNTS ST of the *S.* Typhimurium and *S.* Enteritidis isolates. The secondary objective was to assess the antimicrobial resistance profiles of the index patient and household *Salmonella* isolates.

Methods

Study site, microbiological surveillance, and index patient blood culture isolates

Kisangani is the capital city of Tshopo Province, located in the northeast of the Democratic Republic of the Congo (DR Congo), with ~1.3 million inhabitants in 2021 [Central Intelligence Agency (CIA), 2023]. Most inhabitants live below the poverty line (data Gouvernement de la Province Orientale, RD Congo). It has a tropical rainforest climate, and *P. falciparum* malaria is holoendemic with perennial transmission (Falay et al., 2016). Similar to other provinces in DR Congo (Tack et al., 2021), iNTS is endemic in Tshopo Province, and recently, a *P. falciparum* outbreak complicated by iNTS infection occurred (Falay et al., 2016).

Since 2008, the University Hospital of Kisangani (UNIKIS) has participated in a national bloodstream infection surveillance network organized by the National Institute for Biomedical Research (INRB, Kinshasa) in collaboration with the Institute of Tropical Medicine (ITM, Antwerp, Belgium). This network provides a free blood culture service integrated into patient care. The purpose of this network is to monitor bacteria involved in bloodstream infections and their antibiotic resistance profiles (Falay et al., 2016, 2022). For the indications, sampling, and workup [identification and antibiotic susceptibility testing (AST)] of blood cultures, we refer to the article by Tack et al. (2021). As part of the surveillance study, blood culture isolates were shipped to the INRB and ITM for reference testing (confirmation, serotyping, and AST) and stored at −80°C for further analysis (Falay et al., 2016, 2022).

Study design, index patients, and study period

The field study assessed the fecal carriage of iNTS among household members of patients with culture-confirmed iNTS bloodstream infections (index patients). At UNIKIS, children (28 days to 15 years) with *Salmonella* growing from blood cultures were selected as index patients. The head of the household to which the index patient belonged was contacted for recruitment in the *Salmonella* carrier study, which consisted of collecting and culture of *Salmonella* from stool samples for three consecutive days. The study was conducted from March 2016 to March 2020, when it was stopped because of the COVID-19 lockdown decreed in DR Congo.

Salmonella Typhimurium and *S.* Enteritidis isolates from blood and stool cultures were compared for genetic relatedness by MLVA. Isolates from households with index patients (household members with matching MLVA types) were assessed using WGS to assess their ST and genetic relatedness expressed in allelic differences (AD). All *Salmonella* isolates were tested for antibiotic susceptibility.

Household visits, stool sampling, and transport

Upon confirmation of *S. enterica* from blood cultures, the index patient's household address was located. The investigation team visited the household, contacted the household head to explain the study, and invited the household to participate. After obtaining consent, a list of household members was created, and a sampling date was agreed upon. The investigator visited the households the day before sampling. He/she provided a polystyrene container identified by the name, sex, and age of each household member and explained how to collect the stool sample, preferring a morning stool sample. The following morning, the investigator collected the samples between 6 and 8 a.m. and transported them in a cool box to the UNIKIS microbiology laboratory. He/she also provided a container to household members for the next day's sample. The procedure was repeated daily.

Salmonella stool culture

Laboratory processing for stool samples was performed as described previously (Mbuyi-Kalonji et al., 2020). After the reception of samples at the laboratory, ~1 g of each stool sample was suspended in 10 ml of selenite broth (BD Difco, Becton Dickinson and Company, Franklin Lakes, New Jersey) and incubated at 35°C for 12–18 h. Thereafter, 10 µl was inoculated on two *Salmonella-Shigella* (SS) agar plates (Lab M Limited, Lancashire, UK) and incubated at 35°C for 18–24 h and read afterward. In case of no growth, the plates were evaluated after another 18–24 h of incubation at 35°C. In case of growth, up to five colonies suspected to be *Salmonella* were transferred to Kligler Iron Agar (KIA) tubes (Lab M Limited) and incubated for 18–24 h at 35°C. Bacteria grown in the KIA tube and displaying a profile suggestive of *Salmonella* were biochemically confirmed by a panel of disk-based biochemical tests (DiaTabs, Rosco, Taastrup, Denmark). Isolates with a reaction pattern compatible with *Salmonella* were stored in 2 ml tubes of Trypticase Soy Agar (Oxoid, Basingstoke, UK) and shipped to the Institute of Tropical Medicine (ITM, Antwerp, Belgium) for serotyping and AST.

Salmonella serotyping and AST of blood and stool culture isolates

Serotyping of blood and stool culture isolates was performed using commercial antisera (Vison, Pro-Lab Diagnostics Inc., Richmond Hill, Ontario, Canada). AST was done by disk diffusion (Neo-Sensitabs, Rosco, Taastrup, Denmark) and, in the case of azithromycin and ciprofloxacin, by the ETEST macro-method (bioMérieux, Marcy Étoile, France) to assess the minimal inhibitory concentration values (MIC-values) (Tack et al., 2020a). Results were interpreted according to the Clinical and Laboratory Standards Institute (CLSI) M100-S31 criteria (Clinical and Laboratory Standards Institute, 2021). Multidrug resistance (MDR) was defined as combined resistance to amoxicillin, trimethoprim-sulfamethoxazole, and chloramphenicol (Tack et al., 2020b).

Genetic relatedness between *Salmonella* isolates from index cases and household members

Genetic relatedness between *S.* Typhimurium and *S.* Enteritidis isolates was determined at Sciensano (Brussels, Belgium) by MLVA, as previously described (Falay et al., 2016, 2022). For *S.* Typhimurium, profiles were attributed based on the number of tandem repeats at five loci (STTR9-, STTR5-, STTR6-, STTR10-, and STTR3-). For *S.* Enteritidis, these loci were SENTR7-, SENTR5-, SENTR6-, SENTR4-, and SE3-). Identical MLVA clusters for *S.* Typhimurium were defined as isolates with MLVA types with no or one variation in the rapidly changing loci (STTR5, STTR6, and STTR10) but no variation in the stable loci (STTR3 and STTR9) (Dimovski et al., 2014). For *S.* Enteritidis, a cluster was defined as isolates with variation in none or one of the five loci (Bertrand et al., 2015).

Whole genome sequencing

Salmonella Typhimurium and *S.* Enteritidis isolates from the index patient-household member MLVA clusters were selected for WGS. WGS, including DNA extraction, purification, library preparation, and sequencing (Illumina, San Diego, CA, USA), was performed by Eurofins Genomics (Konstanz, Germany), generating 150 bp paired-end reads. Short reads were assembled *de novo* using SPAdes version 3.6.0.23. Tools integrated into EnteroBase[1] were used (Falay et al., 2022). Multilocus sequence typing (MLST) was performed using the 7-gene MLST scheme based on the sequences of seven housekeeping genes: *aroC*, *dnaN*, *hemD*, *hisD*, *purE*, *sucA*, and *thrA* (Kidgell et al., 2002; Achtman et al., 2012). Hierarchical clustering of cgMLST (HierCC) was performed based on 3,002 locus sequences for *Salmonella* (Zhou et al., 2021; Falay et al., 2022).

Ethical issues

The study was approved by the ethics committee of the Public Health School of Kinshasa (Comité d'Éthique de l'École de Santé Publique de Université de Kinshasa, ESP/CE/002/2017) and the Institutional Review Board of the ITM (IRB/AB/ac/038, March, 02 2016). Written informed consent was obtained from the heads of households. Oral consent was obtained from all household members. An independent witness was present in cases of illiteracy.

Data and definitions

For the definition of *Salmonella* index patients and MLVA clusters, refer to earlier paragraphs. A *Salmonella* carrier was defined as a household member who had *Salmonella* growth in at least one of the three stool samples. *Salmonella* isolates with identical serotypes obtained from index patients and corresponding

1 https://enterobase.warwick.ac.uk/ (accessed March 21, 2023).

10.3389/fmicb.2023.1241961

TABLE 1 Serotype distribution and demographic data of patients with blood culture confirmed *Salmonella* infection (index patients).

	All index patients ($n = 43$)	Index patients for whom households were visited ($n = 22$)
Salmonella Typhimurium	19	8
Salmonella Enteritidis	13	7
Salmonella Typhi	8	4
Salmonella Paratyphi C	1	1
Salmonella II:42:r:-	1	1
Salmonella I:7:y:-	1	1
M/F ratio	1.2	1.75
Median (range) age	30 months (3 days to 27 years)	19 months (5 months to 14 years)

household members were defined as matching isolates or matching pairs. For *S.* Typhimurium and *S.* Enteritidis carriers, an identical or similar MLVA profile was added as a criterion. Household *Salmonella* clusters were defined as ≥2 carriers living in the same household and for whom the same *Salmonella* serotype was isolated from at least one stool sample.

Results

Demographic information and serotype distribution of the index patients

During the study period, 43 patients with *Salmonella*-confirmed blood cultures (index patients) were obtained (Table 1). Of these, 22 (51.2%) were obtained from household visits. The reasons for exclusion were unclear addresses and refusal to participate. The median age (range) of the included index patients was 19 months (5 months to 14 years); the oldest children were infected with *Salmonella* Typhi, and 14 (63.6%) were male children. Involved *Salmonella* serotypes were Typhimurium ($n = 8$), Enteritidis ($n = 7$), Typhi ($n = 4$), Paratyphi C, II:42:r:-, and I:7:y:- (one isolate each). Compared to the entire group of index patients, male children were overrepresented, and *S.* Typhimurium infection was slightly underrepresented (eight of 19 index patients; Table 1).

Household member sampling

The 22 included households (Table 2) comprised 243 household members, of whom 203 (83.5%) committed to participate and provided the first stool sample; 163 and 81 participants (80.3% and 39.9% of those providing the first sample, respectively) provided a second and third stool sample. The median (range) delay between the blood culture sampling of the index patient and the date of the first stool sampling in the corresponding household was 25 days (range, 2 days to 7.3 months); long delays occurred mostly during the start of the study.

Intestinal carriers among household members

Analysis of the first, second, and third stool samples from household members revealed five, nine, and two carriers, respectively. One carrier had *Salmonella* growth from two consecutive stool cultures, resulting in a total of 15 carriers. These 15 *Salmonella* carriers represented 7.3% of the 203 household members in nine of 22 (40.9%) households. Their median age was 7 years (15–38 years); 13 of 15 and five of 15 carriers were <15 and 5 years old, respectively; 14 (63.6%) were male individuals. The most prevalent serotype was *S.* Typhimurium (nine household members in five households). *Salmonella* serotypes Mikawasima, II:42:r:-, and Enteritidis were found in three, two, and one household members, respectively (Table 2).

Index patients and corresponding household members with matching MLVA types

In two households, one from an index patient with *S.* Enteritidis and another from an index patient with *S.* Typhimurium, the MLVA types of the *Salmonella* from the index patient's blood culture matched the MLVA types of at least one stool sample in the corresponding household (Table 2, household numbers 7 and 15, respectively).

In the case of *S.* Enteritidis, the household member was the index case; the MLVA types of the blood and stool isolates were identical, and no other household members carried *Salmonella*. WGS showed that both the blood and stool isolates belonged to ST11 of the Central/Eastern African clade (HierBAPS clade 9, HC50_12675), as described by Feasey et al. (2016), and were closely related (three AD). Stool samples were obtained 61 days after the blood culture.

In the case of *S.* Typhimurium, the index patient and three other household members carried *S.* Typhimurium. The isolates from the stool cultures shared the same MLVA type, which differed in one rapidly changing locus (i.e., STTR-6) from the MLVA type of the blood culture isolate. Stool samples were obtained 27 days after the blood culture. WGS revealed that the blood culture isolates, as well as the four stool culture isolates, belonged to ST313 lineage 2, as described by Pulford et al. (2021), and were closely related (0–1 AD among the stool isolates and eight AD with the blood culture isolate; Figure 1). All four *S.* Typhimurium carriers and one *S.* Enteritidis carrier were <10 years old.

The MLVA types of the two households with matching blood and stool culture isolates of *S.* Typhimurium and *S.* Enteritidis (household numbers 7 and 15, respectively) were also observed in other index patients and households (Table 2). *Salmonella* Typhimurium MLVA-type 2-5-9-8-210 from household 15 also occurred in households 14 and 16. The three households were sampled over 2 weeks but were

TABLE 2 Data of the households ($n = 22$) assessed for *Salmonella* carriers.

Index patient					Days between index case and household visit	Household member carriers of *Salmonella*			
Household	Age/sex	Serotype	MLVA type	Date of sampling		Household identifier	Age/sex	Serotype	MLVA type
HH1	18 months, F	Typhimurium	2-6-11-8-0210	26/05/2016	221	HH01	–	–	–
HH2	10 months, F	Enteritidis	2-13-3-3-NA	01/07/2016	208	HH02_11_II	7 years M	Typhimurium	2-7-10-8-0210
HH3	14 years, M	Typhi	–	28/09/2016	162	HH03	–	–	–
HH4	11 months, F	Typhimurium	2-5-8-8-0210	28/10/2016	131	HH04	–	–	–
HH5	5 years, M	Typhimurium	2-10-13-7-210	05/11/2016	123	HH05	–	–	–
HH6	5 months, M	Enteritidis	2-13-3-3-NA	07/11/2016	122	HH06_12	5 years F	II:42:r:-	–
HH7	**3.5 years, F**	**Enteritidis**	**2-13-4-3-NA**	**08/11/2016**	**61**	**HH07_23***	**3 years F**	**Enteritidis**	**2-13-4-3-NA**
						HH07_11	24 years M	Mikawasima	
HH8	4 years, M	Enteritidis	2-13-4-3-NA	15/11/2016	69	HH08_10	24 months M	Typhimurium	2-7-10-8-0210
HH9	10 months, M	Paratyphi C	–	06/06/2018	13	HH09	–	–	–
HH10	8 months, F	Enteritidis	2-13-4-3-NA	09/06/2018	5	HH10	–	–	–
HH11	11 months, M	Typhimurium	2-10-12-7-0210	02/07/2018	43	HH11	–	–	–
HH13	2.5 years, M	I 7 y:-	–	08/07/2018	11	HH13	–	–	–
HH14	6 years, M	Typhimurium	2-10-12-7-210	03/08/2018	32	HH14_02	11 years F	Typhimurium	2-5-9-8-0210
						HH14_03	11,5 years F	Typhimurium	2-5-9-8-0210
HH15	**15 months, F**	**Typhimurium**	**2-5-11-8-0210**	**07/08/2018**	**27**	**HH15_01***	**15 months F**	**Typhimurium**	**2-5-9-8-0210**
						HH15_02	**3 years F**	**Typhimurium**	**2-5-9-8-0210**
						HH15_08	**9 years F**	**Typhimurium**	**2-5-9-8-0210**
						HH15_11	**6 years F**	**Typhimurium**	**2-5-9-8-0210**
HH16	15 months, F	Enteritidis	2-13-4-3-NA	11/08/2018	23	HH16_01	15 months F	Typhimurium	2-5-9-8-0210
HH17	3 years, F	Typhi	–	09/12/2018	2	HH17	–	–	–
HH18	4 years, M	II:42:r:-	–	13/06/2019	20	HH18_11	7 years F	II:42:r:-	–
HH19	4 years, M	Typhimurium	2-NA-12-7-0210	14/06/2019	11	HH19	–	–	–
HH21	2.5 years, M	Enteritidis	2-14-4-3-NA	23/07/2019	4	HH21	–	–	–
HH22	19 months, M	Typhimurium	2-10-13-7-0210	24/12/2019	10	HH22	–	–	–
HH23	7 years, M	Typhi	–	15/01/2020	6	HH23_01	38 years F	Mikawasima	–
						HH23_05	9 years F	Mikawasima	–
HH24	9 months, M	Typhi	–	20/01/2020	12	HH24	–	–	–

Index patients with matching MLVA types among household members are indicated in bold. For index patients 5,568/4 and 6,284/4, the matching household member marked with * was the index patient who had recovered from bloodstream infection.

10.3389/fmicb.2023.1241961

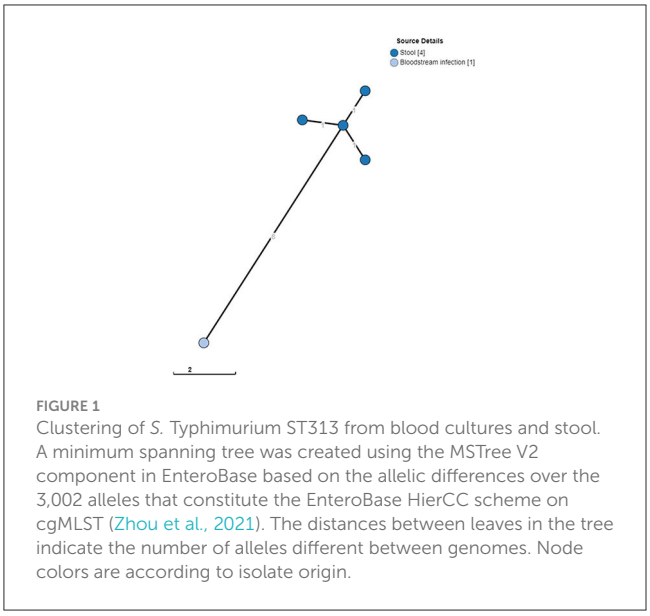

FIGURE 1
Clustering of *S.* Typhimurium ST313 from blood cultures and stool. A minimum spanning tree was created using the MSTree V2 component in EnteroBase based on the allelic differences over the 3,002 alleles that constitute the EnteroBase HierCC scheme on cgMLST (Zhou et al., 2021). The distances between leaves in the tree indicate the number of alleles different between genomes. Node colors are according to isolate origin.

located at a considerable distance (4.1 km) from each other. Similarly, *S.* Enteritidis MLVA type 2-13-4-3-NA also occurred in the index patients from households 8 and 16, sampled over 1 week.

Among the other non-typhoidal *Salmonella* serotypes, one index patient with *Salmonella* II:42:r:- was matched with a 7-year-old sibling from the corresponding household. In none of the four index patients with *Salmonella* Typhi, *Salmonella* was recovered from household members. In three households (household numbers 2, 8, and 16), the index patient was infected with *S.* Enteritidis, whereas the corresponding household member carried *S.* Typhimurium (Table 2).

Antimicrobial resistance profiles

All *S.* Typhimurium ($n = 9$) and *S.* Enteritidis ($n = 1$) isolates from stool cultures were multidrug-resistant. This was in line with the results for the blood cultures of *S.* Typhimurium and *S.* Enteritidis isolates recovered during the study period [68.4% (13/19) and 76.9% (10/13) were multidrug resistant], but in contrast with the other *Salmonella* serotypes from stool cultures, which were all five pan-susceptible, i.e., susceptible to all antibiotics tested (Table 3).

Discussion

Summary of findings

The present index patient-household member carriage study, conducted in an area endemic for iNTS infections, showed *S.* Typhimurium MLVA clusters in one household (including the infected index patient) and intestinal carriage of an identical *S.* Enteritidis MLVA type in the index patient of another household. Delays between blood and stool cultures were 27 and 61 days, respectively, and all carriers were <10 years of age. The matched blood and stool culture isolates belonged to the invasive ST313 lineage 2 (*S.* Typhimurium) and ST11 Central/Eastern African clade (*S.* Enteritidis).

Limitations and strengths

The main limitations of this study are logistics and recruitment. In particular, at the start of the study, delays in communication of the microbiology report occurred, and the addresses of households in informal suburban settlements were unclear. In addition, the locations of the households were dispersed over a large area, precluding sensitization of the local community through communication with local leaders and health workers, as was done in a previous carrier study conducted in DR Congo (Mbuyi-Kalonji et al., 2020). The refusal ratio was also relatively high ($n = 5$ households), which may in part be related to the serious life-threatening condition of children, as observed previously in a hospital-based carrier study in DR Congo (Phoba et al., 2020).

Furthermore, because the research team comprised clinical and laboratory staff, preparing and mobilizing the teams for household visits took time. Consequently, only half of the eligible households were included, and the delays between blood culture sampling and household visits were twice as long as those in the aforementioned index patient-household study in Burkina Faso (median 13 days vs. 25 days in the present study) (Post et al., 2019). Furthermore, we did not include livestock in the present study. The main reason for this choice was the low number of livestock in the suburban slums, in contrast to a study in rural Burkina Faso (Post et al., 2019).

The strengths, sample transport, and laboratory work-up were validated (Post et al., 2019; Mbuyi-Kalonji et al., 2020) and managed for consistent quality. In addition, 3-day sampling (despite moderate participant compliance) substantially increased the cumulative proportion of carriers, as observed in a recent index patient-household study from Malawi (Koolman et al., 2022). As only 80.3 and 39.9% of the participants provided a second and third sample, respectively, it may be expected that the actual proportion of *Salmonella* carriers among household members would have been slightly higher than the actual 7.3%.

Cumulative evidence of healthy human carriers as a potential reservoir of ints

The present study adds to the cumulative evidence that healthy human carriers are potential reservoirs of iNTS, particularly *S.* Typhimurium ST313. Previous index patient-household studies from Burkina Faso (rural areas) and Malawi (urban slums) also found matching index patient-household member pairs of *S.* Typhimurium ST313 and ST3257 (an ST type closely related to ST313), whereas animal and environmental sources did not reveal ST313 (Post et al., 2019; Koolman et al., 2022). For *S.* Enteritidis, so far no evidence of index patient-household control studies has

TABLE 3 Antimicrobial resistance profiles of *Salmonella* serotype isolates recovered from index patients and their household members.

	Index patients				Household members		
	Salmonella Typhimurium ($n = 19$)	*Salmonella* Enteritidis ($n = 13$)	*Salmonella* Typhi + Paratyphi C ($n = 8 + 1$)	Other *Salmonella* ($n = 2$)	*Salmonella* Typhimurium ($n = 9$)	*Salmonella* Enteritidis ($n = 1$)	Other *Salmonella* ($n = 5$)
Ampicillin	19 (100)	10 (76.9)	7 (77.7)	1	9 (100)	1	0
Trimethoprim-sulfamethoxazole	18 (94.7)	10 (76.9)	7 (77.7)	1	9 (100)	1	0
Chloramphenicol	13 (68.4)	10 (76.9)	6 (66.6)	0	9 (100)	1	0
Multidrug resistant (MDR)	13 (68.4)	10 (76.9)	5 (55.5)	0	9 (100)	1	0
Ceftriaxone	6 (31.5)	0	0	1	0	0	0
Azithromycin	2 (10.5)	0	0	1	0	0	0
Fluoroquinolone non-susceptible	6 (31.5)	0	6 (66.6)	1	0	0	0
MDR + fluoroquinolone non-susceptible	1 (5.2)	0	4 (44.4)	0	0	0	0

Data represent numbers (%) of intermediate susceptible and resistant isolates.

been provided; this may partly be explained by the lower frequency of the *S.* Enteritidis serotype in the aforementioned studies.

Other evidence of healthy human carriers as potential reservoirs of iNTS was provided by a *Schistosoma–Salmonella* carrier study in a rural area in the Kongo Central province of DR Congo. In this study, four carriers of *S.* Typhimurium and *S.* Enteritidis had MLVA types similar to those of blood cultures at a nearby hospital (Mbuyi-Kalonji et al., 2020). Furthermore, healthy carriers of *Salmonella* Typhimurium ST313 were also reported in a large case-control diarrhea study in sub-Saharan Africa (Kasumba et al., 2021) and in blood–stool culture case-control studies in informal urban settlements in Kenya (both *S.* Typhimurium ST313 and *S.* Enteritidis ST11) (Kariuki et al., 2019, 2020). Paired blood–stool isolates of *S.* Typhimurium ST313 have been reported in 13 patients from the Central African Republic, but detailed information is lacking (Breurec et al., 2019).

Long delay between stool and blood culture isolates in the index patients

In the present study, stool cultures were positive in two index patients infected with iNTS: *S.* Typhimurium and *S.* Enteritidis. The long delay between stool and blood cultures (27 and 61 days, respectively) supports the hypothesis of long-term carriage after systemic iNTS infection. A similar finding was observed in a hospital-based carrier study in the Kongo Central province of DR Congo (Phoba et al., 2020): stool cultures were performed in 299 children admitted with iNTS bloodstream infection; in nearly 30% of them, paired blood-stool isolates for *S.* Typhimurium ST313 and *S.* Enteritidis ST11 were found, of which two ST313 pairs with identical MLVA types had delays of 16 and 43 days, respectively (Phoba et al., 2020).

However, the above observations were anecdotical. Moreover, both studies were retrospective and provided information only at a single time point. Furthermore, given the long lag time between the index patient's blood cultures and household visits in the present study, the frequency of early convalescent shedding may have been missed. In the case of the household of the *S.* Typhimurium-infected index patients, stool samples, including that of the index patient, differed by eight AD from the blood culture sample, whereas the four stool cultures differed from each other by only one AD (Figure 1). This could raise the hypothesis that the index patient's isolate evolved slightly during the 27-day interval or may have evolved during exchanges between household members. Finally, the possibility of re-infection from a common source within a household cannot be excluded.

The potentially long duration of iNTS carriage contrasts with the short duration of fecal shedding demonstrated for diarrhea-causing non-typhoidal *Salmonella* (Gal-Mor, 2019) and raises the possibility of a "typhoid fever scenario," with silent chronic iNTS carriers as reservoirs and sources of transmission (Kariuki et al., 2020; Phoba et al., 2020). However, this hypothesis should be further explored in longitudinal studies assessing carriage duration (Phoba et al., 2020). Furthermore, the incremental evidence of a human reservoir of the iNTS (Kariuki et al., 2019, 2020; Post et al., 2019; Kasumba et al., 2021; Koolman et al., 2022) and the absence of evidence for a major environmental reservoir (Crump et al., 2015, 2021) do not preclude co-existent environmental reservoirs and transmission routes of the iNTS (Kariuki et al., 2019; Mbae et al., 2020; Tack et al., 2021; Falay et al., 2022).

Future research

Longitudinal cohort studies should assess the duration of iNTS carriage, patient age, and associated factors.

Salmonella Typhimurium carriers in the present study were all children aged <15 years, and two household clusters of *S.* Typhimurium were noted. In the Burkina Faso study, an adult female household member carried ST313, and the other two index patients were siblings. Furthermore, household clusters (including clusters comprising human, livestock, and environmental isolates) of non-invasive non-typhoidal serotypes have been observed in Burkina Faso and Malawi studies (Post et al., 2019; Koolman et al., 2022), and this clustering could be addressed in future community-based studies.

In the present study, six of 22 households contained iNTS carriers, and the 10 iNTS carriers represented 4.9% of household members, with *S.* Typhimurium outnumbering *S.* Enteritidis (nine vs. one carrier). As no negative control households (i.e., households without index patients) were enrolled, we could not provide evidence of iNTS frequency among the entire population. Therefore, cross-sectional studies are required to further assess the population-based frequency of iNTS carriers. Finally, the retrospective study design did not allow for transmission assessment. Prospective, cohort-based field studies can provide such information but require a demographic health surveillance system and accessible microbiological diagnosis across the study area.

Regarding antimicrobial resistance, it is striking that MDR was confined to iNTS, which is a well-known phenomenon in sub-Saharan Africa and DR Congo (Tack et al., 2020a,b), whereas isolates belonging to the other serotypes were mostly pan-susceptible. This observation was previously made during a rat carrier study in Kisangani and may indicate distinct exposure to antibiotics among the iNTS and zoonotic *Salmonella* clades (Falay et al., 2022). To date, pan-susceptible *S.* Typhimurium ST313 lineage 3, which emerged in Malawi in 2016 (Pulford et al., 2021), has not been detected in DR Congo.

Conclusion

The present study adds to the evidence of human carriers as reservoirs of the invasive *Salmonella* Typhimurium ST313 lineage 2 and *S.* Enteritidis ST11 Central/Eastern African clade. It demonstrated the household clustering of *S.* Typhimurium and the intestinal carriage of *S.* Typhimurium and *S.* Enteritidis in index patients several weeks after bloodstream infection.

Data availability statement

Due to the sensitive nature of the data, the authors are unable to share the data directly. Requests to access the data can be made to ITM's contact point for data access (ITMresearchdataaccess@itg.be). All whole genome data are available at the ENA repository under project number PRJEB63268.

Ethics statement

The studies involving humans were approved by Comité d'Éthique de l'École de Santé Publique de Université de Kinshasa Institutional review board of the ITM. The studies were conducted in accordance with the local legislation and institutional requirements. Written informed consent for participation in this study was provided by the participants' legal guardians/next of kin. Written informed consent was obtained from the individual(s), and minor(s)' legal guardian/next of kin, for the publication of any potentially identifiable images or data included in this article.

Author contributions

Conceptualization: DF, DN, and JJ. Data curation: DF, LH, EB, and JJ. Formal analysis, investigation, and visualization: DF, LH, WM, and JJ. Funding acquisition: DN and JJ. Project administration: DF and JJ. Supervision: LH, OL, and DN. Writing—original draft: DF, LH, and JJ. Writing—review and editing: OL, EB, WM, and DN. All authors contributed to the article and approved the submitted version.

Funding

This study was supported by the Belgian Directorate-General for Development Cooperation and Humanitarian Aid (DGD) and the Marc Vervenne Foundation, KU Leuven.

Acknowledgments

The authors thank Michel Lwanzo, David Beango, and colleagues of the microbiological laboratory of the University Hospital of Kisangani for their assistance with field and laboratory work and Editage (www.editage.com) for English language editing.

Conflict of interest

The authors declare that the research was conducted in the absence of any commercial or financial relationships that could be construed as a potential conflict of interest.

Publisher's note

References

Achtman, M., Wain, J., Weill, F. X., Nair, S., Zhou, Z., Sangal, V., et al. (2012). Multilocus sequence typing as a replacement for serotyping in *Salmonella enterica*. *PLOS Pathog.* 8, e1002776. doi: 10.1371/journal.ppat.1002776

Bertrand, S., De Lamine De Bex, G., Wildemauwe, C., Lunguya, O., Phoba, M. F., Ley, B., et al. (2015). Multi locus variable-number tandem repeat (MLVA) typing tools improved the surveillance of *Salmonella* Enteritidis: a 6 years retrospective study. *PLOS ONE* 10, e0117950. doi: 10.1371/journal.pone.0117950

Breurec, S., Reynaud, Y., Frank, T., Farra, A., Costilhes, G., Weill, F. X., et al. (2019). Serotype distribution and antimicrobial resistance of human *Salmonella enterica* in Bangui, Central African Republic, from 2004 to 2013. *PLOS Negl. Trop. Dis.* 13, e0007917. doi: 10.1371/journal.pntd.0007917

Central Intelligence Agency (CIA) (2023). *Factbook*. Available online at: https://www.cia.gov/the-world-factbook/countries/congo-democratic-republic-of-the/ (accessed March 12, 2023).

Clinical and Laboratory Standards Institute (CLSI) (2021). *Performance Standards for Antimicrobial Susceptibility Testing*. 31st ed. Clinical and Laboratory Standards Institute.

Crump, J. A., Sjölund-Karlsson, M., Gordon, M. A., Parry, C. M. (2015). Epidemiology, clinical presentation, laboratory diagnosis, antimicrobial resistance, and antimicrobial management of invasive *Salmonella* infections. *Clin. Microbiol. Rev.* 28, 901–937. doi: 10.1128/CMR.00002-15

Crump, J. A., Thomas, K. M., Benschop, J., Knox, M. A., Wilkinson, D. A., Midwinter, A. C., et al. (2021). Investigating the meat pathway as a source of human nontyphoidal *Salmonella* bloodstream infections and diarrhea in East Africa. *Clin. Infect. Dis.* 73, e1570–e1578. doi: 10.1093/cid/ciaa1153

Dekker, D., Krumkamp, R., Eibach, D., Sarpong, N., Boahen, K. G., Frimpong, M., et al. (2018). Characterization of *Salmonella enterica* from invasive bloodstream infections and water sources in rural Ghana. *BMC Infect. Dis.* 18, 47. doi: 10.1186/s12879-018-2957-4

Dimovski, K., Cao, H., Wijburg, O. L. C., Strugnell, R. A., Mantena, R. K., Whipp, M., et al. (2014). Analysis of *Salmonella enterica* serovar Typhimurium variable-number tandem-repeat data for public health investigation based on measured mutation rates and whole-genome sequence comparisons. *J. Bacteriol.* 196, 3036–3044. doi: 10.1128/JB.01820-14

Dione, M. M., Ikumapayi, U. N., Saha, D., Mohammed, N. I., Geerts, S., Ieven, M., et al. (2011). Clonal differences between non-typhoidal *Salmonella* (NTS) recovered from children and animals living in close contact in the Gambia. *PLOS Negl. Trop. Dis.* 5, e1148. doi: 10.1371/journal.pntd.0001148

Falay, D., Hardy, L., Tanzito, J., Lunguya, O., Bonebe, E., Peeters, M., et al. (2022). Urban rats as carriers of invasive *Salmonella* Typhimurium sequence type 313, Kisangani, Democratic Republic of Congo. *PLOS Negl. Trop. Dis.* 16, e0010740. doi: 10.1371/journal.pntd.0010740

Falay, D., Kuijpers, L. M. F., Phoba, M. F., De Boeck, H., Lunguya, O., Vakaniaki, E., et al. (2016). Microbiological, clinical and molecular findings of non-typhoidal *Salmonella* bloodstream infections associated with malaria, Oriental Province, Democratic Republic of the Congo. *BMC Infect. Dis.* 16, 271. doi: 10.1186/s12879-016-1604-1

Feasey, N. A., Dougan, G., Kingsley, R. A., Heyderman, R. S., Gordon, M. A. (2012). Invasive non-typhoidal *Salmonella* disease: an emerging and neglected tropical disease in Africa. *Lancet* 379, 2489–2499. doi: 10.1016/S0140-6736(11)61752-2

Feasey, N. A., Hadfield, J., Keddy, K. H., Dallman, T. J., Jacobs, J., Deng, X., et al. (2016). Distinct *Salmonella* enteritidis lineages associated with enterocolitis in high-income settings and invasive disease in low-income settings. *Nat. Genet.* 48, 1211–1217. doi: 10.1038/ng.3644

Feasey, N. A., Masesa, C., Jassi, C., Faragher, E. B., Mallewa, J., Mallewa, M., et al. (2015). Three epidemics of invasive multidrug-resistant *Salmonella* bloodstream infection in Blantyre, Malawi, 1998–2014. *Clin. Infect. Dis.* 61(Supplement 4), S363–S371. doi: 10.1093/cid/civ691

Gal-Mor, O. (2019). Persistent infection and long-term carriage of typhoidal and nontyphoidal *Salmonellae*. *Clin. Microbiol. Rev.* 32, e00088-18. doi: 10.1128/CMR.00088-18

Kariuki, S., Mbae, C., Onsare, R., Kavai, S. M., Wairimu, C., Ngetich, R., et al. (2019). Multidrug-resistant nontyphoidal *Salmonella* hotspots as targets for vaccine use in management of infections in endemic settings. *Clin. Infect. Dis.* 68(Supplement 1), S10–S15. doi: 10.1093/cid/ciy898

Kariuki, S., Mbae, C., Van Puyvelde, S., Onsare, R., Kavai, S., Wairimu, C., et al. (2020). High relatedness of invasive multi-drug resistant non-typhoidal *Salmonella* genotypes among patients and asymptomatic carriers in endemic informal settlements in Kenya. *PLOS Negl. Trop. Dis.* 14, e0008440. doi: 10.1371/journal.pntd.0008440

Kariuki, S., Revathi, G., Gakuya, F., Yamo, V., Muyodi, J., Hart, C. A. (2002). Lack of clonal relationship between non-typhi *Salmonella* strain types from humans and those isolated from animals living in close contact. *FEMS Immunol. Med. Microbiol.* 33, 165–171. doi: 10.1111/j.1574-695X.2002.tb00587.x

Kariuki, S., Revathi, G., Kariuki, N., Kiiru, J., Mwituria, J., Muyodi, J., et al. (2006). Invasive multidrug-resistant non-typhoidal *Salmonella* infections in Africa: zoonotic or anthroponotic transmission? *J. Med. Microbiol.* 55, 585–591. doi: 10.1099/jmm.0.46375-0

Kasumba, I. N., Pulford, C. V., Perez-Sepulveda, B. M., Sen, S., Sayed, N., Permala-Booth, J., et al. (2021). Characteristics of *Salmonella* recovered from stools of children enrolled in the global enteric multicenter study. *Clin. Infect. Dis.* 73, 631–641. doi: 10.1093/cid/ciab051

Kidgell, C., Pickard, D., Wain, J., James, K., Diem Nga, L. T., Diep, T. S., et al. (2002). Characterisation and distribution of a cryptic *Salmonella* typhi plasmid pHCM2. *Plasmid* 47, 159–171. doi: 10.1016/S0147-619X(02)00013-6

Koolman, L., Prakash, R., Diness, Y., Msefula, C., Nyirenda, T. S., Olgemoeller, F., et al. (2022). Case-control investigation of invasive *Salmonella* disease in Malawi reveals no evidence of environmental or animal transmission of invasive strains, and supports human to human transmission. *PLOS Negl. Trop. Dis.* 16, e0010982. doi: 10.1371/journal.pntd.0010982

Marchello, C. S., Birkhold, M., Crump, Vacc-iNTS consortium collaborators (2022). Complications and mortality of non-typhoidal *salmonella* invasive disease: a global systematic review and meta-analysis. *Lancet Infect. Dis.* 22, 692–705. doi: 10.1016/S1473-3099(21)00615-0

Mbae, C., Mwangi, M., Gitau, N., Irungu, T., Muendo, F., Wakio, Z., et al. (2020). Factors associated with occurrence of salmonellosis among children living in Mukuru slum, an urban informal settlement in Kenya. *BMC Infect. Dis.* 20, 422. doi: 10.1186/s12879-020-05134-z

Mbuyi-Kalonji, L., Barbé, B., Nkoji, G., Madinga, J., Roucher, C., Linsuke, S., et al. (2020). Non-typhoidal *Salmonella* intestinal carriage in a *Schistosoma mansoni* endemic community in a rural area of the Democratic Republic of Congo. *PLOS Negl. Trop. Dis.* 14, e0007875. doi: 10.1371/journal.pntd.0007875

Phoba, M. F., Barbé, B., Ley, B., Van Puyvelde, S., Post, A., Mattheus, W., et al. (2020). High genetic similarity between non-typhoidal *Salmonella* isolated from paired blood and stool samples of children in the Democratic Republic of the Congo. *PLOS Negl. Trop. Dis.* 14, e0008377. doi: 10.1371/journal.pntd.0008377

Post, A. S., Diallo, S. N., Guiraud, I., Lompo, P., Tahita, M. C., Maltha, J., et al. (2019). Supporting evidence for a human reservoir of invasive non-typhoidal *Salmonella* from household samples in Burkina Faso. *PLOS Negl. Trop. Dis.* 13, e0007782. doi: 10.1371/journal.pntd.0007782

Pulford, C. V., Perez-Sepulveda, B. M., Canals, R., Bevington, J. A., Bengtsson, R. J., Wenner, N., et al. (2021). Stepwise evolution of *Salmonella* Typhimurium ST313 causing bloodstream infection in Africa. *Nat. Microbiol.* 6, 327–338. doi: 10.1038/s41564-020-00836-1

Sirinavin, S., Jayanetra, P., Thakkinstian, A. (1999). Clinical and prognostic categorization of extraintestinal nontyphoidal *Salmonella* infections in infants and children. *Clin. Infect. Dis.* 29, 1151–1156. doi: 10.1086/313469

Stanaway, J. D., Parisi, A., Sarkar, K., Blacker, B. F., Reiner, R. C., Hay, S. I. (2019). The global burden of non-typhoidal *Salmonella* invasive disease: a systematic analysis for the Global Burden of Disease Study 2017. *Lancet Infect. Dis.* 19, 1312–1324. doi: 10.1016/S1473-3099(19)30418-9

Tack, B., Phoba, M. F., Barbé, B., Kalonji, L. M., Hardy, L., Van Puyvelde, S., et al. (2020a). Non-typhoidal *Salmonella* bloodstream infections in Kisantu, DR Congo: emergence of O5-negative *Salmonella* Typhimurium and extensive drug resistance. *PLOS Negl. Trop. Dis.* 14, e0008121. doi: 10.1371/journal.pntd.0008121

Tack, B., Vanaenrode, J., Verbakel, J. Y., Toelen, J., Jacobs, J. (2020b). Invasive non-typhoidal *Salmonella* infections in sub-Saharan Africa: a systematic review on antimicrobial resistance and treatment. *BMC Med.* 18, 212. doi: 10.1186/s12916-020-01652-4

Tack, B., Vita, D., Phoba, M. F., Mbuyi-Kalonji, L., Hardy, L., Barbé, B., et al. (2021). Direct association between rainfall and non-typhoidal *Salmonella* bloodstream infections in hospital-admitted children in the Democratic Republic of Congo. *Sci. Rep.* 11, 21617. doi: 10.1038/s41598-021-01030-x

Van Puyvelde, S., Pickard, D., Vandelannoote, K., Heinz, E., Barbé, B., de Block, T., et al. (2019). An African *Salmonella* Typhimurium ST313 sublineage with extensive drug-resistance and signatures of host adaptation. *Nat. Commun.* 10, 4280. doi: 10.1038/s41467-019-11844-z

Zhou, Z., Charlesworth, J., Achtman, M. (2021). HierCC: a multi-level clustering scheme for population assignments based on core genome MLST. *Bioinformatics* 37, 3645–3646. doi: 10.1093/bioinformatics/btab234

frontiers | Frontiers in Microbiology

TYPE Original Research
PUBLISHED 20 October 2023
DOI 10.3389/fmicb.2023.1282832

OPEN ACCESS

EDITED BY
Sébastien Holbert,
INRA Centre Val de Loire, France

REVIEWED BY
Jie Zheng,
United States Food and Drug Administration, United States
Dhrubajyoti Nag,
City College of New York (CUNY), United States

*CORRESPONDENCE
Shawn M. D. Bearson
✉ Shawn.Bearson@usda.gov

RECEIVED 24 August 2023
ACCEPTED 02 October 2023
PUBLISHED 20 October 2023

CITATION
Burciaga S, Trachsel JM, Sockett D, Aulik N, Monson MS, Anderson CL and Bearson SMD (2023) Genomic and phenotypic comparison of two variants of multidrug-resistant *Salmonella enterica* serovar Heidelberg isolated during the 2015–2017 multi-state outbreak in cattle. *Front. Microbiol.* 14:1282832. doi: 10.3389/fmicb.2023.1282832

Genomic and phenotypic comparison of two variants of multidrug-resistant *Salmonella enterica* serovar Heidelberg isolated during the 2015–2017 multi-state outbreak in cattle

Selma Burciaga[1,2], Julian M. Trachsel[1], Donald Sockett[3], Nicole Aulik[3], Melissa S. Monson[1], Christopher L. Anderson[1] and Shawn M. D. Bearson[1]*

[1]United States Department of Agriculture, Agriculture Research Services, National Animal Disease Center, Ames, IA, United States, [2]Oak Ridge Institute for Science and Education (ORISE), ARS Research Participation Program, Oak Ridge, TN, United States, [3]Wisconsin Veterinary Diagnostic Laboratory, University of Wisconsin, Madison, WI, United States

Salmonella enterica subspecies *enterica* serovar Heidelberg (*Salmonella* Heidelberg) has caused several multistate foodborne outbreaks in the United States, largely associated with the consumption of poultry. However, a 2015–2017 multidrug-resistant (MDR) *Salmonella* Heidelberg outbreak was linked to contact with dairy beef calves. Traceback investigations revealed calves infected with outbreak strains of *Salmonella* Heidelberg exhibited symptoms of disease frequently followed by death from septicemia. To investigate virulence characteristics of *Salmonella* Heidelberg as a pathogen in bovine, two variants with distinct pulse-field gel electrophoresis (PFGE) patterns that differed in morbidity and mortality during the multistate outbreak were genotypically and phenotypically characterized and compared. Strain SX 245 with PFGE pattern JF6X01.0523 was identified as a dominant and highly pathogenic variant causing high morbidity and mortality in affected calves, whereas strain SX 244 with PFGE pattern JF6X01.0590 was classified as a low pathogenic variant causing less morbidity and mortality. Comparison of whole-genome sequences determined that SX 245 lacked ~200 genes present in SX 244, including genes associated with the IncI1 plasmid and phages; SX 244 lacked eight genes present in SX 245 including a second YdiV Anti-FlhC(2)FlhD(4) factor, a lysin motif domain containing protein, and a pentapeptide repeat protein. RNA-sequencing revealed fimbriae-related, flagella-related, and chemotaxis genes had increased expression in SX 245 compared to SX 244. Furthermore, SX 245 displayed higher invasion of human and bovine epithelial cells than SX 244. These data suggest that the presence and up-regulation of genes involved in type 1 fimbriae production, flagellar regulation and biogenesis, and chemotaxis may play a role in the increased pathogenicity and host range expansion of the *Salmonella* Heidelberg isolates involved in the bovine-related outbreak.

KEYWORDS

***Salmonella*, outbreak, pathogenicity, virulence, dairy beef calves, Heidelberg**

1. Introduction

Non-typhoidal *Salmonella* is one of the top five foodborne pathogens and one of the leading causes of bacterial foodborne illness in humans in the United States (U.S.) and worldwide (Scallan et al., 2013; Havelaar et al., 2015). *Salmonella enterica* subspecies *enterica* serovar Heidelberg (*Salmonella* Heidelberg) is primarily isolated from poultry, although it can colonize other hosts and cause salmonellosis in humans (CDC, 2013; Clothier and Byrne, 2016). Like other *Salmonella* serovars, *Salmonella* Heidelberg is typically transmitted from animals to humans *via* contaminated food sources. Also similar to other *Salmonella* serovars, *Salmonella* Heidelberg usually colonizes animals without resulting in clinical disease, but frequently causes gastroenteritis in humans. Over the last decade, six multistate outbreaks of *Salmonella* Heidelberg occurred in the U.S., and five of the outbreaks were associated with consumption of contaminated chicken-or turkey-related products (Antony et al., 2018). The most recent *Salmonella* Heidelberg outbreak was linked to direct contact with dairy beef calves (defined as an intact male dairy calf) from January 2015 through November 2017. Fifty-six people reported infections with multidrug-resistant (MDR) *Salmonella* Heidelberg across 15 states, the majority from Wisconsin. During the course of the outbreak, 54 people were interviewed with 34 (63%) reporting contact with dairy beef calves which were later shown to be infected with MDR *Salmonella* Heidelberg (CDC, 2017). Some of the calves infected with outbreak strains of MDR *Salmonella* Heidelberg displayed signs of disease such as diarrhea and fever, frequently followed by death from generalized bacteremia/septicemia (Sockett et al., 2017). Pulse-field gel electrophoresis (PFGE) and whole-genome sequencing (WGS) conducted on outbreak-associated isolates from sick calves revealed that human-and bovine-origin *Salmonella* Heidelberg isolates were closely related (Nichols et al., 2022). Furthermore, two main variants of *Salmonella* Heidelberg were identified in the cattle population by PFGE (Nichols et al., 2022). One of the variants was dominant and highly pathogenic causing 25–65% of the deaths in dairy beef calves, while the other variant was less pathogenic causing considerably fewer deaths (Sockett et al., 2017; Nichols et al., 2022).

In the current study, two outbreak isolates with varying virulence in calves were genotypically and phenotypically compared to identify factors that may have contributed to the emergence and pathogenic variation of *Salmonella* Heidelberg in the bovine species. Gene content was compared based on whole genome sequencing (WGS), differences in gene expression patterns were revealed through RNA-seq between the isolates when grown in culture, and phenotypic comparisons assessed their invasion of human and bovine epithelial cells.

2. Materials and methods

2.1. *Salmonella* isolates and growth conditions

Salmonella was isolated and identified from bovine cases submitted to the Wisconsin Veterinary Diagnostic Laboratory (WVDL) at the University of Wisconsin-Madison during the 2015–2017 multistate outbreak as previously described by Nichols et al. (2022). Two bovine-origin *Salmonella* Heidelberg isolates were received from the WVDL and referred to hereafter as SX 244 and SX 245; WVDL determined the PFGE patterns for SX 244 (JF6X01.0590) and SX245 (JF6X01.0523). Bacteria were streaked from the frozen glycerol stock solution onto Luria-Bertani (LB; Lennox) agar (Invitrogen, Waltham, MA) and incubated at 37°C overnight. Individual colonies were selected and inoculated into 3 mL of LB broth (Invitrogen) at 37°C overnight with shaking for further analysis.

2.2. DNA isolation, whole-genome sequencing, and analysis

Overnight *Salmonella* cultures were centrifuged for 20 min at 3000 × g. Supernatants were removed and cell pellets resuspended in 400 µL of phosphate buffered saline. DNA isolation was performed on 100 µL of the resuspension using the High Pure PCR Template Preparation Kit (Roche Applied Science, Indianapolis, IN) per manufacturer's instructions. The quality and quantity of DNA were measured on the Qubit 4 Fluorometer using the Qubit™ dsDNA Broad Range Assay Kit (Invitrogen). WGS libraries were generated using the Nextera DNA Flex Library Prep and indices kits (Illumina, San Diego, CA) and sequenced using the MiSeq reagent kit v3 (600-cycle) yielding 2 × 300-bp paired-end reads on the Illumina MiSeq platform (Illumina).

FastQC v0.11.6 was used to evaluate the quality of raw Illumina reads and determine the total number of reads (Andrews and Fast, 2014). Sequencing adapters and artifacts were removed from the short reads using BBtools v38.30 (Bushnell, 2018). Genome assemblies were generated using the *de novo* assembler SPAdes v3.11.1 (Bankevich et al., 2012), and the quality of the assemblies were assessed using QUAST v4.6.3 (Gurevich et al., 2013). SX 244 and SX 245 genomes were annotated with prokka v1.14.6 (Seemann, 2014) using proteins from *Salmonella enterica* serovar Heidelberg strain SL476 (accession GCA_000020705.1) as a first priority for the annotation. Gene ontology (GO) terms were assigned to genes in the SX 244 and SX 245 genomes with interproscan v5.35–74.0 (Jones et al., 2014), and PPanGGOLiN v1.0.1 (Gautreau et al., 2020) was used to identify genes that were shared (core genes) or unique to each genome.

2.3. RNA extraction, RNA sequencing, and transcriptional analysis

Overnight *Salmonella* cultures were diluted 1:200 in LB broth and grown to $OD_{600} = 0.3$ (early log phase growth) *via* shaking at 37°C. An 0.5 mL aliquot of each culture was placed in RNAprotect™ Bacteria Reagent (Qiagen, Germantown, MD) and processed per manufacturer's instructions to provide immediate stabilization of RNA. Cultures and RNA isolations were repeated three times per isolate (three biological replicates). RNA was extracted using the RNeasy Mini Kit (Qiagen), followed by treatment with TURBO™ DNase (Ambion, Austin, TX, USA) to remove genomic DNA. A 2100 Bioanalyzer (Agilent Technologies, Santa Clara, CA) and Agilent RNA 6000 Nano kit (Agilent Technologies) were used to evaluate the quality of total RNA. Bacterial ribosomal RNA (rRNA) sequences were depleted using the Ribo-Zero Plus rRNA Depletion Kit (Illumina), and the quality of the rRNA depleted RNA was assessed using the 2100 Bioanalyzer. RNA libraries were constructed using the NEBNext®

Ultra™ II Directional RNA Library Prep Kit (New England BioLabs®, Ipswich, MA) and sequenced at the Iowa State University DNA Facility on an Illumina Hiseq 3000 (150 cycles, single-end reads; Illumina).

Quality of raw RNA sequencing data was assessed using FastQC v0.11.6. BBtools v38.30 was used to remove sequencing adapters and artifacts and to quality trim (average quality scores <10) the raw Illumina reads. RNA-seq reads of SX 244 and SX 245 were aligned to the genome sequence of SX 244 using BBtools v38.30 with default parameters, and read counts (the number of reads that aligned to a specific gene) were quantified using HTseq v0.11.0 (nonunique reads mapped to all) (Anders et al., 2015). Read counts were normalized and gene expression compared (by Wald test) between the two strains using DESeq2 v.1.34.0 (Love et al., 2014); $\log_2$ fold change (Log_2FC) shrinkage was performed using apeglm v1.16.0 (Zhu et al., 2019). Principal component analysis (PCA) was performed to ascertain expression outliers based on variance stabilized gene expression counts for the top 200 most variable genes using DESeq2 v1.34.0 and pcaExplorer v2.27.1 (Marini and Binder, 2019). Final *p*-value for differential gene expression were adjusted with a Benjamini–Hochberg procedure (false discovery rate; FDR), with an FDR adjusted *p*-value <0.05 and $|\text{Log}_2\text{FC}| \geq 0.50$ considered as significant. Based on the GO terms assigned by interproscan v5.35–74.0, a GO term enrichment analysis (Ashburner et al., 2000) was conducted to predict functional consequences of the differentially expressed genes using a Fisher's exact test in topGO v2.46.0 (Alexa and Rahnenfuhrer, 2021). The topGO analysis ("elimination" algorithm with a minimum node size of 5 genes) was conducted for all three major GO aspects: "biological process," "molecular function," and "cellular component" and any term with a *p*-value <0.05 was considered significantly enriched.

2.4. Invasion cell culture assays

For each biological experiment, an overnight culture was diluted 1:100 in fresh LB broth and grown with shaking for 1.5 h at 37°C to early-log phase ($OD_{600} = 0.3$) for the invasion assays. The human epithelial-like tumor cell line HEp-2 (ATCC: CCL-23) was grown and maintained in Gibco RPMI 1640 medium (Thermo Fisher Scientific, Waltham, MA) with Gibco 10% heat-inactivated fetal bovine serum (FBS) in an atmosphere of 5% CO_2 at 37°C. Madin-Darby bovine kidney epithelial cells (MDBK; ATCC 6071) were grown and maintained in Gibco MEM (Thermo Fisher Scientific) supplemented with Gibco 10% heat-inactivated FBS, Gibco Antibiotic-Antimycotic (Anti:Anti), and Gibco L-glutamine.

For the invasion assays, HEp-2 and MDBK cells were seeded in 24-well cell culture plates (BD Falcon, BD Biosciences, San Jose, CA) at 1.3×10^5 and 2×10^5 cells, respectively, and incubated overnight at 37°C with 5% CO_2 until >95% confluent. Invasion assays were performed with three technical replicates for each biological replicate using a gentamicin protection assay in HEp-2 and MDBK cells with a multiplicity of infection (MOI) ratio of 50:1 as previously described (Elsinghorst, 1994). Three biological replicates were performed for HEp-2 invasion assays and five for MDBK invasion assays. Percent invasion was calculated by dividing colony forming units (CFU) of bacteria recovered by CFU of bacteria added to the cells and multiplying by 100. The significant differences between SX 244 and SX 245 invasion were determined by unpaired Student's *t-test* using GraphPad Prism 9 (Birhanu et al., 2018; Mechesso et al., 2021). *p*-values less than 0.05 were considered significant.

2.5. Antimicrobial susceptibility testing

Antimicrobial susceptibility (AST) of the two *Salmonella* Heidelberg strains was assessed using the Sensititre™ National Antimicrobial Resistance Monitoring System (NARMS) Gram Negative CMV4AGNF AST plate by the National Veterinary Services Laboratories. The CMV4AGNF plate contained 14 antimicrobials in different antibiotic classes including aminoglycosides (gentamicin and streptomycin), penicillin (ampicillin), beta-lactam combinations (amoxicillin/clavulanic acid), cephalosporins (ceftriaxone and cefoxitin), carbapenems (meropenem), macrolides (azithromycin), quinolones/fluoroquinolones (ciprofloxacin and nalidixic acid), phenicol (chloramphenicol), folate pathway antagonists (sulfisoxazole and trimethoprim/sulphamethoxazole), and tetracyclines (tetracycline). The strains were classified as susceptible, intermediate, or resistant as defined by the Clinical and Laboratory Standards Institute (CLSI, 2023), when available. Otherwise, NARMS consensus breakpoints were used. Multidrug resistance (MDR) was defined as resistant to three or more antimicrobial classes and decreased susceptibility to ciprofloxacin (DSC, MIC ≥0.12 μg/mL) was defined by NARMS.

3. Results and discussion

3.1. *Salmonella* Heidelberg genomes

During the 2015–2017 multistate outbreak of MDR *Salmonella* Heidelberg linked to dairy beef calf exposure, SX 245 was identified as a dominant and highly pathogenic variant causing 25–65% of the deaths in dairy beef calves, while SX 244 was a less pathogenic variant causing considerably fewer deaths (Sockett et al., 2017; Nichols et al., 2022). To identify potential pathogenic characteristics of bovine-origin MDR *Salmonella* Heidelberg strains from this outbreak, genome sequencing and analysis of the two *Salmonella* Heidelberg strains were performed and identified 4,960 features in SX 244 and 4,761 in SX 245 (Table 1). After filtering to exclude

TABLE 1 Genomic content of *Salmonella* Heidelberg SX 244 and SX 245 strains.

Feature type		SX 244 (Low pathogenicity)	SX 245 (High pathogenicity)
Protein-coding genes (CDS)	Shared	4,670	4,670
	Unique	204	8
	Total	4,874	4,678
Ribosomal RNAs (rRNAs)		9	9
Transfer messenger RNAs (tmRNAs)		1	1
Transfer RNAs (tRNAs)		76	73
Total		4,960	4,761

non-protein-coding sequences, genomic comparisons revealed 4,670 protein-coding genes shared between both strains. SX 245 lacked 204 genes that were present in SX 244 (Supplementary Table S1). Approximately half (52%) of the 204 genes were hypothetical proteins with unknown function. The remaining genes included several genes associated with the IncI1 plasmid such as conjugal transfer proteins and plasmid thin pilus genes, as well as genes associated with bacteriophages involved in recombination and replication. In contrast, SX 244 lacked 8 genes that were present in SX 245, five of which were unknown hypothetical proteins (Supplementary Table S1). The remaining three genes encode a YdiV Anti-FlhC(2)FlhD(4) factor (*ydiV*), a peptidoglycan DD-metalloendopeptidase family protein with a lysin motif (LysM) domain, and a pentapeptide repeat protein. The genome of SX 244 contained a single *ydiV* gene, while SX 245 contained two copies of this gene. YdiV suppresses the activity of $FlhD_4C_2$, a master regulator of flagellar gene expression, by binding to the FlhD region of the complex further inhibiting transcription of the class II gene *fliA* required for advancing flagella biosynthesis (Wada et al., 2011). Repression of flagellar genes can be beneficial to *Salmonella* during its pathogenesis. For example, YdiV represses flagellar genes in response to nutritional cues, such as poor nutrient conditions inside macrophages (Stewart et al., 2011; Wada et al., 2011). Additionally, YdiV represses flagellar genes in systemic tissues, which protects *Salmonella* from caspase-1-mediated bacterial clearance (Lara-Tejero et al., 2006; Miao et al., 2006; Stewart et al., 2011). The regulation of *Salmonella* flagellar expression reflects the importance of reducing flagella in specific environments for survival. The LysM domain is associated with peptidoglycan binding and is found in various enzymes involved in bacterial cell wall degradation (Joris et al., 1992), comparable to those in peptidoglycan hydrolases (Buist et al., 2008). LysM is reported to enhance survival in macrophages and is needed for systemic infection and pathogenicity in *Salmonella* Enteritidis (Silva et al., 2012).

The presence of a second *ydiV* gene and an additional gene encoding an enzyme with a LysM domain could potentially provide SX 245 with a fitness advantage over SX 244 in the host. Furthermore, the deletion of over 200 genes may benefit SX 245 because maintenance of superfluous genes can be a liability (Ehrenberg and Kurland, 1984; Waters et al., 2022). Deletion of these genes could enhance *Salmonella* fitness as more resources are available for allocation to other rate-limiting processes (Koskiniemi et al., 2012), suggesting the selection and expression of *Salmonella* Heidelberg with a reduced genome may be a driver in the evolution of adaptation and virulence to the bovine host.

3.2. Bacterial transcriptome

RNA-Seq was performed to compare gene expression patterns between the high and low pathogenic *Salmonella* Heidelberg strains in broth culture. Mapping reads to SX 244 as the reference genome provided evidence for expression of 99% of these genes in SX 244 (4,948 genes on average) and 97% of these genes in SX 245 (4,796 genes on average). PCA on the 200 genes with the highest variability between datasets revealed that strain is the main factor driving these transcriptomes, accounting for nearly 95% of the variation in expression (Figure 1). Differential gene expression ($|Log_2FC \geq 0.50|$, $FDR < 0.05$) was observed for 246 genes; however, 194 were unique

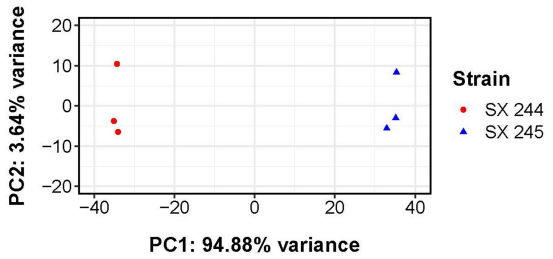

FIGURE 1
Principal component analysis of transcriptomes from *Salmonella* Heidelberg strains SX 244 and SX 245. Variance-stabilized read counts for the 200 most variable genes were used for this analysis. Principal component 1 (PC1) and principal component 2 (PC2) are shown for each strain (indicated by color and shape).

genes that were not present in SX 245 and another five were transfer RNAs (tRNAs), which were not compared across genomes (Supplementary Table S2). Of the 47 differentially expressed genes that were in common between both genomes, 35 genes (74%) had higher expression in SX 245 than SX 244. Twenty-nine of the genes upregulated in the highly pathogenic strain SX 245 were annotatable by prokka and/or interproscan, identifying virulence genes such as fimbriae-related genes (*fimA, fimI, fimC, fimH, fimF*, and a fimbrial biogenesis usher protein), flagella-related genes (*fliA, fliC*, and another flagellin FliC/FljB family member), and genes involved in chemotaxis (*cheW, cheV*) (Figure 2A; Supplementary Table S2). GO enrichment analysis confirmed that genes with higher expression in SX 245 had overrepresented biological functions such as "chemotaxis," "DNA transposition," "bacterial-type flagellar cell motility," and "cell projection organization" (Figure 2A; Supplementary Table S3). Among the genes upregulated in SX 245, eleven genes that lacked associations with GO Biological Process terms (classified as "none" (gray circles) in Figure 2A) as well as one DNA methyltransferase gene appeared to be associated with bacteriophage composition and function based on homology identified with interproscan (Supplementary Table S2). Six genes upregulated in SX 245 were hypothetical proteins of unknown function. Twelve differentially expressed genes (shared by both genomes) had higher expression in SX 244 compared to SX 245, of which six were annotatable and four had GO term associations (Figure 2B; Supplementary Table S2).

The *fim* genes exhibited some of the greatest increases in expression in SX 245 compared to SX 244 ($|Log2FC \geq 0.5|$, $FDR < 0.05$). *FimA*, *fimI*, *fimC*, *fimH*, and *fimF* are structural genes necessary for type 1 fimbriae (T1F) production and are expressed in a single operon under the control of the *fimA* promoter region (Purcell et al., 1987; Rossolini et al., 1993). *Salmonella* contains several fimbriae across their surface which play a vital role in adhesion and invasion to establish colonization as well as maintain infection (van der Velden et al., 1998). T1F are important for *Salmonella* entry into epithelial cells and intestinal colonization of several hosts (Darekar and Duguid, 1972; Duguid et al., 1976; Ernst et al., 1990; Dibb-Fuller and Woodward, 2000; Wilson et al., 2000). Prior studies investigating the role of T1F in *Salmonella* pathogenesis in animal models show that *Salmonella* Enteritidis expressing T1F are more infectious and virulent than non-fimbriated strains in mouse infection models (Darekar and Duguid, 1972; Duguid et al., 1976). Similarly, wildtype

10.3389/fmicb.2023.1282832

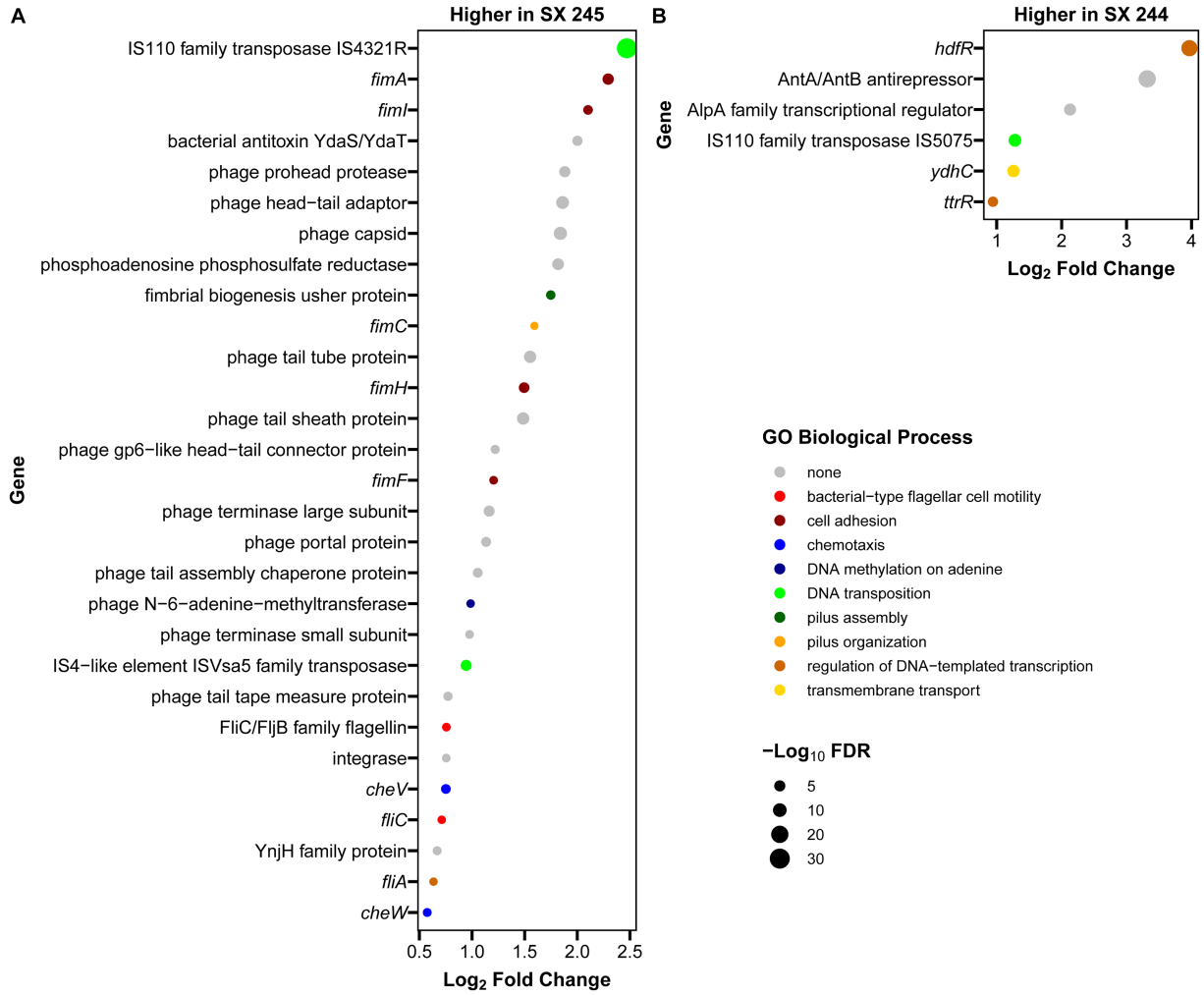

FIGURE 2
Annotated genes with differential expression between *Salmonella* Heidelberg strains SX 244 and SX 245. Log_2 fold changes were filtered for significant differential expression ($|log_2$ fold change$| \geq 0.5$, FDR < 0.05,) and for genes that were annotatable (prokka and interproscan) and present in both the SX 244 and SX 245 genomes. Genes with higher expression in SX 245 **(A)** and in SX 244 **(B)** are shown, along with functions predicted by associated GO Biological Process terms.

Salmonella Enteritidis colonizes the spleen, liver, and ceca of 1-day old chicks in significantly greater loads than a mutant strain unable to express T1F (Dibb-Fuller and Woodward, 2000). Wilson et al. (2000) demonstrated that *Salmonella* serovars Pullorum and Gallinarum expressing Typhimurium T1F display an increased ability to adhere (10-to 20-fold) and invade (20-to 60-fold) the human epithelial HEp-2 cell line. In addition to the highly expressed *fim* operon observed in SX 245, other fimbrial operons were identified in the genomes of SX 244 and SX 245. Genomic comparisons of 617 publicly available *Salmonella* Heidelberg isolates from the National Center for Biotechnology and 17 *Salmonella* Heidelberg isolates from cases submitted to the Animal Disease Research and Diagnostic Laboratory, South Dakota State University and WVDL identified the *saf* operon as the defining feature of outbreak-associated human/bovine isolates (Antony et al., 2018). *Salmonella* atypical fimbriae (Saf) is also important for pathogenesis, particularly in *Salmonella* associated with human disease (Folkesson et al., 1999; Sheikh et al., 2010; Bhuiyan et al., 2014). Therefore, the up-regulation of the *fim* operon along with the presence of the *saf* operon may have contributed to the disease severity of these outbreak-associated *Salmonella* Heidelberg strains in bovine.

Flagella are an important virulence factor of *Salmonella* that allow for motility and chemotaxis to reach sites of infection and evade host, immune responses (Josenhans and Suerbaum, 2002; Duan et al., 2013). Flagella are also required for efficient replication and colonization in the lumen of an inflamed intestine (Stecher et al., 2004, 2008). Along with an unspecified flagellin family member, the flagella-related genes *fliA* and *fliC* had increased expression in SX 245, and these two genes encode the flagella-specific sigma factor (σ^{28}) and phase 1 flagellin (FliC) in *Salmonella*, respectively. Previous studies indicate that FliA positively regulates all class III promoters involved in flagellar biosynthesis controlling the expression of genes responsible for the major subunits of flagella (*fliC*, *fljB*), motility (*motAB*) and chemotaxis (*cheAW*) (Ohnishi et al., 1990; Chilcott and Hughes, 2000; Erhardt et al., 2014). *Salmonella* expressing FliC-flagella have an advantage in motility dependent invasion and target-site selection during swimming in gut colonization in murine gastroenteritis infection models (Bogomolnaya et al., 2014; Horstmann et al., 2017).

Salmonella has an arsenal of virulence mechanisms used to establish infection; higher expression of these virulence genes may play a role in the pathogenicity of outbreak-associated *Salmonella* Heidelberg in dairy beef calves.

3.3. Invasion of epithelial cells

Salmonella invasion of epithelial cells (a first line of defense against intestinal pathogens) is an important phenotype associated with virulence (Wallis Timothy and Barrow, 2005; Gal-Mor et al., 2014; Cheng et al., 2019). Because differential expression of genes involved in invasion was detected, invasion assays were conducted to compare the invasiveness of the high (SX 245) and low (SX 244) pathogenic *Salmonella* Heidelberg strains in human (HEp-2) and bovine (MDBK) epithelial cells. SX 245 (1.35%) had a significantly higher invasion rate (>2-fold) than SX 244 (0.58%) of human epithelial cells (Figure 3A; p-value <0.05). The percent invasion of MDBK by SX 245 (12.12%) was also significantly higher (>7-fold) compared to SX 244 (1.73%) (Figure 3B; p-value <0.05). The results of this study indicate SX 245 has greater invasive ability than SX 244 in bovine and human epithelial cells, which may be influenced by the increased expression of genes involved in T1F production, flagella regulation and biogenesis, and chemotaxis in SX 245.

While extensive cell invasion studies have been performed for *Salmonella* Typhimurium and *Salmonella* Enteritidis, limited studies are available for other serovars such as *Salmonella* Heidelberg (Ernst et al., 1990; Horiuchi et al., 1992; Bäumler et al., 1996; Brackelsberg et al., 1997; Wilson et al., 2000; Ledeboer et al., 2006; Kolenda et al., 2018; Campioni et al., 2021). *Salmonella* Typhimurium and *Salmonella* Braenderup with T1F are known to adhere and invade human cervical cancer (HeLa) cells with greater numbers than non-fimbriated strains (Horiuchi et al., 1992; Bäumler et al., 1996). Hancox et al. (1997) also observed greater adhesion to HEp-2 and HeLa cells of wildtype *Salmonella* Typhimurium than isogenic *fimH* mutants lacking T1F. Along with the current study, these results suggest T1F plays a role in enhancing cellular invasion of *Salmonella*. In contrast, other investigators used *fimH* mutants to report that T1F does not contribute to *Salmonella* Typhimurium adhesion or invasion of HEp-2 cells (Bäumler et al., 1996; Kolenda et al., 2018). These conflicting results may be due to the variability in experimental design such as differences in MOI, incubation times or the use of different *Salmonella* serovars or strains.

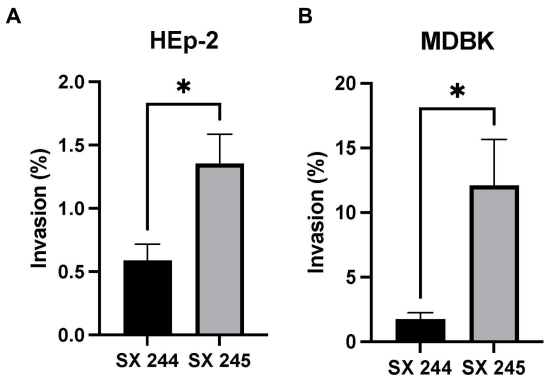

FIGURE 3
Percent invasion of *Salmonella* Heidelberg strains SX 244 and SX 245. Invasion assays were performed on SX 244 and SX 245 in **(A)** HEp-2 human epithelial cells (p-value = 0.0446) and **(B)** MDBK bovine epithelial cells (p-value = 0.0197).

Two studies of *Salmonella* invasion in MDBK epithelial cells compared bovine-adapted *Salmonella* Dublin to host-generalist *Salmonella* Typhimurium and poultry-adapted *Salmonella* Enteritidis (Brackelsberg et al., 1997; Campioni et al., 2021). One reported that *Salmonella* Dublin has greater capability for invasion of MDBK cells than *Salmonella* Typhimurium, which may explain the association of *Salmonella* Dublin with severe forms of salmonellosis in cattle (Brackelsberg et al., 1997). The second study described similar MDBK invasion rates for host-adapted serovars *Salmonella* Enteritidis and *Salmonella* Dublin (Campioni et al., 2021). Invasion rates of these serovars are higher than the *Salmonella* Heidelberg strains in this study, at 75 and 73%, respectively. Brackelsberg et al. (1997) and Campioni et al. (2021) additionally compared strains within the same serovar and described varying rates of invasion of MDBK cells, which is congruent with other studies reporting *Salmonella* invasion being strain dependent (Betancor et al., 2009; Shah et al., 2011). Similarly, this study describes two *Salmonella* Heidelberg strains from the same outbreak with significantly different invasion rates for both MDBK and HEp-2 epithelial cells.

In summary, *Salmonella* can be transmitted from animals to humans directly through contact or indirectly through the food chain, resulting in zoonotic disease (Marshall and Levy, 2011). Thus, *Salmonella* is an animal and human health concern. *Salmonella* Heidelberg is primarily a poultry-associated serovar., linked to human illness *via* consumption of contaminated poultry products (Antony et al., 2018). However, this 2015–2017 multistate outbreak was unique because the *Salmonella* Heidelberg isolates associated with human disease were also associated with septicemia in dairy beef calves, which frequently led to calf death (Sockett et al., 2017; Nichols et al., 2022). Food animals typically harbor *Salmonella* as commensals and are usually subclinical (Stevens et al., 2009; Silva et al., 2014); therefore, the reason for the increased pathogenicity and disease severity of cattle-associated *Salmonella* Heidelberg is of particular interest. Two dominant variants of *Salmonella* Heidelberg were isolated during the outbreak that were similar in their genotypic MDR pattern but differed in their PFGE patterns (Nichols et al., 2022). Because greater morbidity and mortality in calves was associated with one variant (SX 245) compared to the other (SX 244), the present study compared virulence-related characteristics of the *Salmonella* Heidelberg isolates to explore their contrasting disease severity. Highly pathogenic SX 245 had elevated expression of virulence genes and greater invasion of human and bovine epithelial cells, potentially supporting the enhanced severity of *Salmonella* Heidelberg infection in dairy beef calves and eventual salmonellosis in humans (Supplementary Table S4). Altogether, comparison of the two strains suggests that genes involved in fimbriae production and flagellar biosynthesis may contribute to the increased pathogenicity and ecological success of *Salmonella* Heidelberg in the bovine species.

Data availability statement

The genomic and transcriptomic datasets generated for this study are publicly available. The data can be found through NCBI BioProject

PRJNA999325: https://www.ncbi.nlm.nih.gov/bioproject/999325. The raw data supporting the conclusions of the invasion assays will be made available by the authors upon request.

Ethics statement

Ethical approval was not required for the studies on humans and animals in accordance with the local legislation and institutional requirements because only commercially available established cell lines were used.

Author contributions

SB: Data curation, Formal analysis, Investigation, Methodology, Project administration, Software, Validation, Visualization, Writing – original draft, Writing – review & editing. JT: Data curation, Formal analysis, Investigation, Methodology, Software, Supervision, Validation, Writing – review & editing. DS: Conceptualization, Resources, Writing – review & editing. NA: Conceptualization, Resources, Writing – review & editing. MM: Data curation, Formal analysis, Methodology, Software, Validation, Visualization, Writing – original draft, Writing – review & editing. CA: Data curation, Methodology, Writing – review & editing. SMDB: Conceptualization, Data curation, Formal analysis, Investigation, Methodology, Project administration, Resources, Software, Supervision, Validation, Visualization, Writing – original draft, Writing – review & editing.

Funding

The author(s) declare that no financial support was received for the research, authorship, and/or publication of this article. This research used resources provided by the SCINet project of the USDA Agricultural Research Service, ARS project number 0500-00093-001-00-D. This research was supported by appropriated funds from USDA-ARS CRIS project 5030-3200-227-00D and an appointment to the Agricultural Research Service (ARS) Research Participation Program administered by the Oak Ridge Institute for Science and Education (ORISE) through an interagency agreement between the U.S. Department of Energy (DOE) and the U.S. Department of Agriculture (USDA). ORISE is managed by ORAU under DOE contract number DE-SC0014664.

Acknowledgments

The authors greatly appreciate the outstanding technical support of Briony Atkinson and Margaret Walker. The MDBK cells were kindly provided by Kathryn Bickel and Eduardo Casas at the USDA, ARS – Ruminant Diseases and Immunology Research, National Animal Disease Center, Ames, IA, USA. Mention of trade names or commercial products in this article is solely for the purpose of providing specific information and does not imply recommendations or endorsement by the U.S. Department of Agriculture. The U.S. Department of Agriculture is an equal opportunity provider and employer.

Conflict of interest

The authors declare that the research was conducted in the absence of any commercial or financial relationships that could be construed as a potential conflict of interest.

Publisher's note

Supplementary material

The Supplementary material for this article can be found online at: https://www.frontiersin.org/articles/10.3389/fmicb.2023.1282832/full#supplementary-material

References

Alexa, A., and Rahnenfuhrer, J. (2021) topGO: Enrichment analysis for gene ontology 2020 [R package version 2.40.0]. Available at: https://rdrr.io/bioc/topGO/

Anders, S., Pyl, P. T., and Huber, W. (2015). HTSeq--a Python framework to work with high-throughput sequencing data. *Bioinformatics* 31, 166–169. doi: 10.1093/bioinformatics/btu638

Andrews, S., and Fast, Q. C. (2014). *A quality control tool for high throughput sequence data*. Available at: https://www.bioinformatics.babraham.ac.uk/projects/fastqc/

Antony, L., Behr, M., Sockett, D., Miskimins, D., Aulik, N., Christopher-Hennings, J., et al. (2018). Genome divergence and increased virulence of outbreak associated *Salmonella enterica* subspecies enterica serovar Heidelberg. *Gut Pathogens.* 10:53. doi: 10.1186/s13099-018-0279-0

Ashburner, M., Ball, C. A., Blake, J. A., Botstein, D., Butler, H., Cherry, J. M., et al. (2000). Gene ontology: tool for the unification of biology. The Gene Ontology Consortium. *Nat. Genet.* 25, 25–29. doi: 10.1038/75556

Bankevich, A., Nurk, S., Antipov, D., Gurevich, A. A., Dvorkin, M., Kulikov, A. S., et al. (2012). SPAdes: a new genome assembly algorithm and its applications to single-cell sequencing. *J. Comput. Biol.* 19, 455–477. doi: 10.1089/cmb.2012.0021

Bäumler, A. J., Tsolis, R. M., and Heffron, F. (1996). Contribution of fimbrial operons to attachment to and invasion of epithelial cell lines by *Salmonella typhimurium*. *Infect. Immun.* 64, 1862–1865. doi: 10.1128/iai.64.5.1862-1865.1996

Betancor, L., Yim, L., Fookes, M., Martinez, A., Thomson, N. R., Ivens, A., et al. (2009). Genomic and phenotypic variation in epidemic-spanning *Salmonella enterica* serovar Enteritidis isolates. *BMC Microbiol.* 9:237. doi: 10.1186/1471-2180-9-237

Bhuiyan, S., Sayeed, A., Khanam, F., Leung, D. T., Rahman Bhuiyan, T., Sheikh, A., et al. (2014). Cellular and cytokine responses to *Salmonella enterica* serotype Typhi proteins in patients with typhoid fever in Bangladesh. *Am. J. Trop. Med. Hyg.* 90, 1024–1030. doi: 10.4269/ajtmh.13-0261

Birhanu, B. T., Park, N.-H., Lee, S.-J., Hossain, M. A., and Park, S.-C. (2018). Inhibition of *Salmonella Typhimurium* adhesion, invasion, and intracellular survival via treatment with methyl gallate alone and in combination with marbofloxacin. *Vet. Res.* 49:101. doi: 10.1186/s13567-018-0597-8

Bogomolnaya, L. M., Aldrich, L., Ragoza, Y., Talamantes, M., Andrews, K. D., McClelland, M., et al. (2014). Identification of novel factors involved in modulating motility of *Salmonella enterica* serotype typhimurium. *PLoS One* 9:e111513. doi: 10.1371/journal.pone.0111513

Brackelsberg, C. A., Nolan, L. K., and Brown, J. (1997). Characterization of *Salmonella* Dublin and *Salmonella Typhimurium* (Copenhagen) isolates from cattle. *Vet. Res. Commun.* 21, 409–420. doi: 10.1023/A:1005803301827

Buist, G., Steen, A., Kok, J., and Kuipers, O. P. (2008). Lys M, a widely distributed protein motif for binding to (peptido)glycans. *Mol. Microbiol.* 68, 838–847. doi: 10.1111/j.1365-2958.2008.06211.x

Bushnell, B. (2018). BBMap [package version 38.30]. Available at: sourceforge.net/projects/bbmap/

Campioni, F., Gomes, C. N., Bergamini, A. M. M., Rodrigues, D. P., Tiba-Casas, M. R., and Falcão, J. P. (2021). Comparison of cell invasion, macrophage survival and inflammatory cytokines profiles between *Salmonella enterica* serovars Enteritidis and Dublin from Brazil. *J. Appl. Microbiol.* 130, 2123–2131. doi: 10.1111/jam.14924

CDC. *CfDCaP. Atlas of Salmonella in the United States, 1968–2011*. Atlanta, GA: U.S. Department of Health & human services, CDC. (2013).

CDC. *CfDCaP. Multistate outbreak of multidrug-resistant Salmonella Heidelberg infections linked to contact with dairy calves*. Atlanta, GA: U.S. Department of Health & human services, CDC. (2017).

Cheng, R. A., Eade, C. R., and Wiedmann, M. (2019). Embracing diversity: differences in virulence mechanisms, disease severity, and host adaptations contribute to the success of Nontyphoidal *Salmonella* as a foodborne pathogen. *Front. Microbiol.* 10:1368. doi: 10.3389/fmicb.2019.01368

Chilcott, G. S., and Hughes, K. T. (2000). Coupling of flagellar gene expression to flagellar assembly in *Salmonella enterica* serovar typhimurium and *Escherichia coli*. *Microbiol. Mol. Biol. Rev.* 64, 694–708. doi: 10.1128/MMBR.64.4.694-708.2000

Clothier, K. A., and Byrne, B. A. (2016). Phenotypic and genotypic characterization of animal-source *Salmonella* Heidelberg isolates. *J. Vet. Med.* 2016:6380890. doi: 10.1155/2016/6380890

CLSI. (2023). *Performance standards for antimicrobial susceptibility testing. 33rd Edn*. CLSI Supplement M100. Wayne, PA: Clinical Laboratory and Standards Institute.

Darekar, M. R., and Duguid, J. *The influence of fimbriation on the infectivity of Salmonella typhimurium. Proceedings of the Indian Academy of Sciences-section B*. (1972). New Delhi: Springer India.

Dibb-Fuller, M. P., and Woodward, M. J. (2000). Contribution of fimbriae and flagella of *Salmonella enteritidis* to colonization and invasion of chicks. *Avian Pathol.* 29, 295–304. doi: 10.1080/03079450050118412

Duan, Q., Zhou, M., Zhu, L., and Zhu, G. (2013). Flagella and bacterial pathogenicity. *J. Basic Microbiol.* 53, 1–8. doi: 10.1002/jobm.201100335

Duguid, J. P., Darekar, M. R., and Wheater, D. W. (1976). Fimbriae and infectivity in *Salmonella typhimurium*. *J. Med. Microbiol.* 9, 459–473. doi: 10.1099/00222615-9-4-459

Ehrenberg, M., and Kurland, C. G. (1984). Costs of accuracy determined by a maximal growth rate constraint. *Q. Rev. Biophys.* 17, 45–82. doi: 10.1017/S0033583500005254

Elsinghorst, E. A. (1994). Measurement of invasion by gentamicin resistance. *Methods Enzymol.* 236, 405–420. doi: 10.1016/0076-6879(94)36030-8

Erhardt, M., Mertens, M. E., Fabiani, F. D., and Hughes, K. T. (2014). ATPase-independent type-III protein secretion in *Salmonella enterica*. *PLoS Genet.* 10:e1004800. doi: 10.1371/journal.pgen.1004800

Ernst, R. K., Dombroski, D. M., and Merrick, J. M. (1990). Anaerobiosis, type 1 fimbriae, and growth phase are factors that affect invasion of HEp-2 cells by *Salmonella typhimurium*. *Infect. Immun.* 58, 2014–2016. doi: 10.1128/iai.58.6.2014-2016.1990

Folkesson, A., Advani, A., Sukupolvi, S., Pfeifer, J. D., Normark, S., and Löfdahl, S. (1999). Multiple insertions of fimbrial operons correlate with the evolution of *Salmonella* serovars responsible for human disease. *Mol. Microbiol.* 33, 612–622. doi: 10.1046/j.1365-2958.1999.01508.x

Gal-Mor, O., Boyle, E. C., and Grassl, G. A. (2014). Same species, different diseases: how and why typhoidal and non-typhoidal *Salmonella enterica* serovars differ. *Front. Microbiol.* 5:391. doi: 10.3389/fmicb.2014.00391

Gautreau, G., Bazin, A., Gachet, M., Planel, R., Burlot, L., Dubois, M., et al. (2020). PPanGGOLiN: depicting microbial diversity via a partitioned pangenome graph. *PLoS Comput. Biol.* 16:e1007732. doi: 10.1371/journal.pcbi.1007732

Gurevich, A., Saveliev, V., Vyahhi, N., and Tesler, G. (2013). QUAST: quality assessment tool for genome assemblies. *Bioinformatics* 29, 1072–1075. doi: 10.1093/bioinformatics/btt086

Hancox, L. S., Yeh, K.-S., and Clegg, S. (1997). Construction and characterization of type 1 non-fimbriate and non-adhesive mutants of *Salmonella typhimurium*. *FEMS Immunol. Med. Microbiol.* 19, 289–296. doi: 10.1111/j.1574-695X.1997.tb01099.x

Havelaar, A. H., Kirk, M. D., Torgerson, P. R., Gibb, H. J., Hald, T., Lake, R. J., et al. (2015). World Health Organization global estimates and regional comparisons of the burden of foodborne disease in 2010. *PLoS Med.* 12:e1001923. doi: 10.1371/journal.pmed.1001923

Horiuchi, S., Inagaki, Y., Okamura, N., Nakaya, R., and Yamamoto, N. (1992). Type 1 pili enhance the invasion of *Salmonella* braenderup and *Salmonella typhimurium* to HeLa cells. *Microbiol. Immunol.* 36, 593–602. doi: 10.1111/j.1348-0421.1992.tb02059.x

Horstmann, J. A., Zschieschang, E., Truschel, T., de Diego, J., Lunelli, M., Rohde, M., et al. (2017). Flagellin phase-dependent swimming on epithelial cell surfaces contributes to productive *Salmonella* gut colonisation. *Cell. Microbiol.* 19:e12739. doi: 10.1111/cmi.12739

Jones, P., Binns, D., Chang, H. Y., Fraser, M., Li, W., McAnulla, C., et al. (2014). InterProScan 5: genome-scale protein function classification. *Bioinformatics* 30, 1236–1240. doi: 10.1093/bioinformatics/btu031

Joris, B., Englebert, S., Chu, C. P., Kariyama, R., Daneo-Moore, L., Shockman, G. D., et al. (1992). Modular design of the *Enterococcus hirae* muramidase-2 and *Streptococcus faecalis* autolysin. *FEMS Microbiol. Lett.* 70, 257–264. doi: 10.1111/j.1574-6968.1992.tb05218.x

Josenhans, C., and Suerbaum, S. (2002). The role of motility as a virulence factor in bacteria. *Int. J. Med. Microbiol.* 291, 605–614. doi: 10.1078/1438-4221-00173

Kolenda, R., Burdukiewicz, M., Schiebel, J., Rödiger, S., Sauer, L., Szabo, I., et al. (2018). Adhesion of *Salmonella* to pancreatic secretory granule membrane major glycoprotein GP2 of human and porcine origin depends on FimH sequence variation. *Front. Microbiol.* 9:1905. doi: 10.3389/fmicb.2018.01905

Koskiniemi, S., Sun, S., Berg, O. G., and Andersson, D. I. (2012). Selection-driven gene loss in bacteria. *PLoS Genet.* 8:e1002787. doi: 10.1371/journal.pgen.1002787

Lara-Tejero, M., Sutterwala, F. S., Ogura, Y., Grant, E. P., Bertin, J., Coyle, A. J., et al. (2006). Role of the caspase-1 inflammasome in *Salmonella typhimurium* pathogenesis. *J. Exp. Med.* 203, 1407–1412. doi: 10.1084/jem.20060206

Ledeboer, N. A., Frye, J. G., McClelland, M., and Jones, B. D. (2006). *Salmonella enterica* serovar typhimurium requires the Lpf, Pef, and Tafi fimbriae for biofilm formation on HEp-2 tissue culture cells and chicken intestinal epithelium. *Infect. Immun.* 74, 3156–3169. doi: 10.1128/IAI.01428-05

Love, M. I., Huber, W., and Anders, S. (2014). Moderated estimation of fold change and dispersion for RNA-seq data with DESeq2. *Genome Biol.* 15:550. doi: 10.1186/s13059-014-0550-8

Marini, F., and Binder, H. (2019). pcaExplorer: an R/Bioconductor package for interacting with RNA-seq principal components. *BMC Bioinformat.* 20:331. doi: 10.1186/s12859-019-2879-1

Marshall, B. M., and Levy, S. B. (2011). Food animals and antimicrobials: impacts on human health. *Clin. Microbiol. Rev.* 24, 718–733. doi: 10.1128/CMR.00002-11

Mechesso, A. F., Quah, Y., and Park, S. C. (2021). Ginsenoside Rg3 reduces the adhesion, invasion, and intracellular survival of *Salmonella enterica* serovar typhimurium. *J. Ginseng Res.* 45, 75–85. doi: 10.1016/j.jgr.2019.09.002

Miao, E. A., Alpuche-Aranda, C. M., Dors, M., Clark, A. E., Bader, M. W., Miller, S. I., et al. (2006). Cytoplasmic flagellin activates caspase-1 and secretion of interleukin 1beta via Ipaf. *Nat. Immunol.* 7, 569–575. doi: 10.1038/ni1344

Nichols, M., Gollarza, L., Sockett, D., Aulik, N., Patton, E., Francois Watkins, L. K., et al. (2022). Outbreak of multidrug-resistant *Salmonella* Heidelberg infections linked to dairy calf exposure, United States, 2015-2018. *Foodborne Pathog. Dis.* 19, 199–208. doi: 10.1089/fpd.2021.0077

Ohnishi, K., Kutsukake, K., Suzuki, H., and Iino, T. (1990). Gene fliA encodes an alternative sigma factor specific for flagellar operons in *Salmonella typhimurium*. *Mol. Gen. Genet.* 221, 139–147. doi: 10.1007/BF00261713

Purcell, B. K., Pruckler, J., and Clegg, S. (1987). Nucleotide sequences of the genes encoding type 1 fimbrial subunits of Klebsiella pneumoniae and *Salmonella typhimurium*. *J. Bacteriol.* 169, 5831–5834. doi: 10.1128/jb.169.12.5831-5834.1987

Rossolini, G. M., Muscas, P., Chiesurin, A., and Satta, G. (1993). Analysis of the *Salmonella* fim gene cluster: identification of a new gene (fimI) encoding a fimbrin-like protein and located downstream from the fim a gene. *FEMS Microbiol. Lett.* 114, 259–265. doi: 10.1111/j.1574-6968.1993.tb06583.x

Scallan, E., Mahon, B. E., Hoekstra, R. M., and Griffin, P. M. (2013). Estimates of illnesses, hospitalizations and deaths caused by major bacterial enteric pathogens in young children in the United States. *Pediatr. Infect. Dis. J.* 32, 217–221. doi: 10.1097/INF.0b013e31827ca763

Seemann, T. (2014). Prokka: rapid prokaryotic genome annotation. *Bioinformatics* 30, 2068–2069. doi: 10.1093/bioinformatics/btu153

Shah, D. H., Zhou, X., Addwebi, T., Davis, M. A., and Call, D. R. (2011). *In vitro* and *in vivo* pathogenicity of *Salmonella enteritidis* clinical strains isolated from North America. *Arch. Microbiol.* 193, 811–821. doi: 10.1007/s00203-011-0719-4

Sheikh, A., Charles, R. C., Rollins, S. M., Harris, J. B., Bhuiyan, M. S., Khanam, F., et al. (2010). Analysis of *Salmonella enterica* serotype paratyphi a gene expression in the blood of bacteremic patients in Bangladesh. *PLoS Negl. Trop. Dis.* 4:e908. doi: 10.1371/journal.pntd.0000908

Silva, C. A., Blondel, C. J., Quezada, C. P., Porwollik, S., Andrews-Polymenis, H. L., Toro, C. S., et al. (2012). Infection of mice by *Salmonella enterica* serovar Enteritidis involves additional genes that are absent in the genome of serovar typhimurium. *Infect. Immun.* 80, 839–849. doi: 10.1128/IAI.05497-11

Silva, C., Calva, E., and Maloy, S. (2014). One health and food-borne disease: *Salmonella* transmission between humans, animals, and plants. *Microbiol Spectr.* 2:Oh-0020-2013. doi: 10.1128/microbiolspec.OH-0020-2013

Sockett, D. C., Aulik, N. A., Deering, K. M., Klos, R. F., and Valley, A. M. *Salmonella Heidelberg: An emerging problem in the dairy industry. American Association of bovine practitioners*. (2017) 14–16; Omaha, Nebraska: VM Publishing Company.

Stecher, B., Barthel, M., Schlumberger, M. C., Haberli, L., Rabsch, W., Kremer, M., et al. (2008). Motility allows *S. typhimurium* to benefit from the mucosal defence. *Cell. Microbiol.* 10, 1166–1180. doi: 10.1111/j.1462-5822.2008.01118.x

Stecher, B., Hapfelmeier, S., Müller, C., Kremer, M., Stallmach, T., and Hardt, W. D. (2004). Flagella and chemotaxis are required for efficient induction of *Salmonella*

enterica serovar typhimurium colitis in streptomycin-pretreated mice. *Infect. Immun.* 72, 4138–4150. doi: 10.1128/IAI.72.7.4138-4150.2004

Stevens, M. P., Humphrey, T. J., and Maskell, D. J. (2009). Molecular insights into farm animal and zoonotic *Salmonella* infections. *Philos. Trans. Royal Soc. B Biol. Sci.* 364, 2709–2723. doi: 10.1098/rstb.2009.0094

Stewart, M. K., Cummings, L. A., Johnson, M. L., Berezow, A. B., and Cookson, B. T. (2011). Regulation of phenotypic heterogeneity permits *Salmonella* evasion of the host caspase-1 inflammatory response. *Proc. Natl. Acad. Sci. U. S. A.* 108, 20742–20747. doi: 10.1073/pnas.1108963108

van der Velden, A. W., Bäumler, A. J., Tsolis, R. M., and Heffron, F. (1998). Multiple fimbrial adhesins are required for full virulence of *Salmonella typhimurium* in mice. *Infect. Immun.* 66, 2803–2808. doi: 10.1128/IAI.66.6.2803-2808.1998

Wada, T., Morizane, T., Abo, T., Tominaga, A., Inoue-Tanaka, K., and Kutsukake, K. (2011). EAL domain protein YdiV acts as an anti-FlhD4C2 factor responsible for nutritional control of the flagellar regulon in *Salmonella enterica* Serovar typhimurium. *J. Bacteriol.* 193, 1600–1611. doi: 10.1128/JB.01494-10

Wallis Timothy, S., and Barrow, P. A. (2005). *Salmonella* epidemiology and pathogenesis in food-producing animals. *EcoSal Plus* 1. doi: 10.1128/ecosalplus.8.6.2.1

Waters, E. V., Tucker, L. A., Ahmed, J. K., Wain, J., and Langridge, G. C. (2022). Impact of *Salmonella* genome rearrangement on gene expression. *Evol. Lett.* 6, 426–437. doi: 10.1002/evl3.305

Wilson, R. L., Elthon, J., Clegg, S., and Jones, B. D. (2000). *Salmonella enterica* serovars gallinarum and pullorum expressing *Salmonella enterica* serovar typhimurium type 1 fimbriae exhibit increased invasiveness for mammalian cells. *Infect. Immun.* 68, 4782–4785. doi: 10.1128/IAI.68.8.4782-4785.2000

Zhu, A., Ibrahim, J. G., and Love, M. I. (2019). Heavy-tailed prior distributions for sequence count data: removing the noise and preserving large differences. *Bioinformatics* 35, 2084–2092. doi: 10.1093/bioinformatics/bty895

frontiers | Frontiers in Microbiology

TYPE Original Research
PUBLISHED 03 November 2023
DOI 10.3389/fmicb.2023.1301478

OPEN ACCESS

EDITED BY
George Grant,
University of Aberdeen, United Kingdom

REVIEWED BY
France Daigle,
University of Montreal, Canada
Timothy James Wells,
The University of Queensland, Australia
Derek Pickard,
University of Cambridge, United Kingdom

*CORRESPONDENCE
Ashraf Hussain
✉ axh1224@miami.edu
Eugene Boon Beng Ong
✉ eugene@usm.my

†PRESENT ADDRESS
Ashraf Hussain,
John P. Hussman Institute for Human Genomics, University of Miami Miller School of Medicine, Miami, FL, United States

RECEIVED 25 September 2023
ACCEPTED 20 October 2023
PUBLISHED 03 November 2023

CITATION
Hussain A, Ong EBB, Balaram P, Ismail A and Kien PK (2023) Deletion of *Salmonella enterica* serovar Typhi *tolC* reduces bacterial adhesion and invasion toward host cells. *Front. Microbiol.* 14:1301478. doi: 10.3389/fmicb.2023.1301478

Deletion of *Salmonella enterica* serovar Typhi *tolC* reduces bacterial adhesion and invasion toward host cells

Ashraf Hussain*†, Eugene Boon Beng Ong*, Prabha Balaram, Asma Ismail and Phua Kia Kien

Institute for Research in Molecular Medicine (INFORMM), University Sains Malaysia, Penang, Malaysia

Background: *S*. Typhi is a Gram-negative bacterium that causes typhoid fever in humans. Its virulence depends on the TolC outer membrane pump, which expels toxic compounds and antibiotics. However, the role of TolC in the host cell adhesion and invasion by *S*. Typhi is unclear.

Objective: We aimed to investigate how deleting the *tolC* affects the adhesion and invasion of HT-29 epithelial and THP-1 macrophage cells by *S*. Typhi *in vitro*.

Methods: We compared the adhesion and invasion rates of the wild-type and the *tolC* mutant strains of *S*. Typhi using in vitro adhesion and invasion assays. We also measured the expression levels of SPI-1 genes (*invF, sipA*, *sipC*, and *sipD*) using quantitative PCR.

Results: We found that the *tolC* mutant showed a significant reduction in adhesion and invasion compared to the wild-type strain in both cell types. We also observed that the expression of SPI-1 genes was downregulated in the *tolC* mutant.

Discussion: Our results suggest that TolC modulates the expression of SPI-1 genes and facilitates the adhesion and invasion of host cells by *S*. Typhi. Our study provides new insights into the molecular mechanisms of *S*. Typhi pathogenesis and antibiotic resistance. However, our study is limited by the use of *in vitro* models and does not reflect the complex interactions between *S*. Typhi and host cells *in vivo*.

KEYWORDS

***Salmonella* Typhi, TolC, Salmonella pathogenicity island 1, invasion, efflux pump protein, adhesion, pathogenesis, antibiotic resistance**

1. Introduction

Efflux pumps are present in all major pathogenic bacterial species lineages (Piddock, 2006a,b). In Gram-negative bacteria, this active efflux mainly contributes to the intrinsic resistance to several classes of antibiotics, dyes, and detergents (Li and Nikaido, 2004; Piddock, 2006a,b; Sun et al., 2014). In Gram-negative bacterial pathogens, TolC is an outer membrane efflux pump protein that facilitates efflux and contributes to virulence and pathogenesis (Piddock, 2006a,b). The expression of efflux pumps was observed along with the infection process of Gram-negative pathogens (Fernando and Kumar, 2013). Outer membrane efflux pump proteins (OMPs) have essential functions in the physiology of bacteria, such as adhesion and invasion of the host cell, resistance to host serum, maintenance of the membrane integrity, and passive and active transfer of substances (Tokuda, 2009). Although the biological functions of TolC homologs in several Gram-negative bacteria have already been reported, the role of TolC in *Salmonella enterica* serovar Typhi has not been investigated, especially its role in host cell adhesion and invasion. *S*. Typhi is a human-restricted pathogen that causes typhoid fever.

In this study, the role of *S.* Typhi TolC in the adhesion and invasion of host cells were first investigated using a *tolC* mutant. As the expression of Salmonella pathogenicity island 1 (SPI-1) genes for invasion (*sipA, sipC, sipD*, and *invF*) is required for penetration into host cells (Darwin and Miller, 1999a,b), we also investigated the expression of the invasion genes under SPI-1-inducing conditions.

2. Materials and methods

2.1. Bacterial strains and plasmids

A *Salmonella enterica* serovar Typhi (*S.* Typhi) strain (a clinical isolate from an acute typhoid fever patient), denoted as ST-WT was used as the wild-type strain in this study.

This study was conducted in accordance with the ethical principles of the Declaration of Helsinki and the EEC directive of 1986. The *Salmonella enterica* serovar Typhi strain was obtained from patients with acute typhoid fever subjects in Hospital Universiti Sains Malaysia (HUSM). The strain was deposited in the Bank of the Institute for Research in Molecular Medicine (INFORMM), Kubang Kerian, Kelantan, Malaysia. The collection and use of the strain were approved by the Committee for Human Ethical Clearance of Universiti Sains Malaysia, Kubang Kerian, Malaysia under ethical clearance number USMKK/PPP/JEPeM [229.3. (03)]. All participants gave their informed consent before enrollment in the study. Bacterial strains and plasmids used in this study are summarized in Table 1. All strains were routinely grown in Luria-Bertani (LB) agar and broth (Hi-media) at 37°C with antibiotics for selection when required.

2.2. Construction of *tolC* mutant

A *tolC* deletion mutant (ST-Δ*tolC*) was constructed using the one-step inactivation of the chromosomal gene method (Baba et al., 2006). The *tolC* gene of ST-WT strain was replaced by inserting the kanamycin resistance gene *aph* (3′)-II genes that confers kanamycin resistance to generate strain ST-Δ*tolC*. A complementation mutant (ST-Δ*tolC*+) was also constructed by cloning the *tolC* gene, including its native promoter, into the pKK223-3 plasmid and transformed into ST-Δ*tolC*. Primers for construction of *tolC* mutant summarized in Table 2.

2.3. Growth of *Salmonella enterica* serovar Typhi strains

The growth of all *S.* Typhi strains was determined by measuring the optical density (OD 595 nm) of bacterial culture using LB broth in a microtiter plate at 37°C as previously described (Sheridan et al., 2013). The sample was placed in a microtiter plate, and bacterial growth was recorded at 2-h time intervals (Multiskan Spectrum, Thermo Scientific). All growth experiments were performed three times, and results were analyzed by plotting average values for each strain on a logarithmic graph with calculated standard deviations to use as error bars. Generation times were also calculated using the logarithmic growth phase of the line graph by the following equation;

$$g = T \ln 2 / \ln\left(OD\ end / OD\ start\right)$$

(Where g is generation [doubling] time and T is time, ln is Natural log of given value). Values which appeared different to the parent strain were evaluated for significance at defined time points using a student's '*t*' test. OD end is the optical density at the end of the exponential growth phase, OD start is the optical density at the start of the exponential growth phase.

2.4. Efflux activity assay

Efflux activity was evaluated with the ethidium bromide agar screening method (Martins et al., 2006). Overnight cultures of all strains were swabbed onto LB agar plates containing 0.5 and 1 mg/L of ethidium bromide. The plates were incubated at 37°C for 16 h, and the fluorescence intensity associated with efflux pump function in the bacterial mass was photographed.

2.5. Adhesion and invasion assays

The adhesion and invasion of the *S.* Typhi strains were tested using *in vitro* adhesion and invasion assays with THP-1-derived human macrophages and HT-29 human epithelial cells according to the methods of Dibb-Fuller et al. (1999) and Buckley et al. (2006) with some modification. *S.* Typhi cells were grown overnight in 10 mL LB broth at

TABLE 1 Strains and plasmids used in this study.

	Description	Resistance phenotype	Source or reference
Strains			
ST-WT	*S.* Typhi clinical isolate which served as wild type in this study.	None	This study
ST-Δ*tolC*	*S.* Typhi TolC mutant, Δ*tolC*::kanR.	KanR	This study
ST-Δ*tolC*+	ST-Δ*tolC* carrying pKK-tolC.	KanR, AmpR	This study
DH5α	*Escherichia coli* strain for gene cloning and plasmid propagation.		This study
Plasmids			
pKD13	A kanamycin marker-DNA template vector for gene disruption.	KanR	Datsenko and Wanner (2000)
pKD46	Red helper plasmid encoding the λ red recombination system for homologous recombination.	AmpR	Datsenko and Wanner (2000)
pKK-tolC	A plasmid containing *S.* Typhi *tolC* including its native promoter. For complementation in ST-Δ*tolC*.	AmpR	This study

TABLE 2 Primers used in this study to the construction of *tolC* deletion mutant of *S*. Typhi.

Primers set	Primers	Sequence	Description	Reference
1	ST_TolC_Del_Fwd	5′–TTACAAATTGATCAGCGCTAAATAC TGCTTCACAACAAGGAATGCAAATGATT CCGGGGATCCGTCGACC–3′	Forward primer for amplification of deletion fragment	This study
	ST_TolC_Del_Rev	5′–CTGATAAACGCAGCGCCAGCGAATAAC TTATCAATGCCGGAATGGATTGCTGTAGGC TGGAGCTGCTTCG –3′	Reverse primer for amplification of deletion fragment	
2	1a	5′–GCGACCATCTCCAGCAGC–3′	Upstream check	This study
	1b	5′ – TGCTCTTCGTCCAGATCATC–3′	Internal *Kan*^{r} forward check	
3	2a	5′ – GCGAGCACGTACTCGGATGG–3′	Internal *Kan*^{r} reverse check	This study
	2b	5′ – ATGCGGCGGAATAGCAGGAT–3′	Downstream check	
4	H_Fwd	5′ –ACTCAGGCTTCCCGTAACGC–3′	*Salmonella* specific	(Levy et al., 2008)
	H_Red	5′ – GGCTAGTATTGTCCTTATCGG–3′		
5	4a	5′–TTAATGGATCCAGAGAACCTGATGCAAGTT–3′	Internal *tolC* check forward	This study
	4b	5′–GACGGCTCGAGTCAACCGTTCGCATCGCGATA–3′	Internal *tolC* check reverse	
6	*tolC*_F	5′-TTAATGAATTCTTACGCATTGTGCTGCCC	*tolC* complementation forward	This study
	*tolC*_R	5′-GACGGAAGCTTTCAATGCCGGAATGGATT	*tolC* complementation reverse	

37°C. Cell monolayers were grown to confluence in 6-well plates, and the cells were then infected for 2 h at an infection multiplicity of 50. For the adhesion assay, cells were gently washed six times with phosphate-buffered saline (PBS) (pH 7.3) and then disrupted with 1 mL distilled water (Roche et al., 2005). First, all viable bacteria (intra- and extracellular) were counted as colony-forming units after plating serial dilutions with PBS. Then, the entry of *S*. Typhi into HT-29 cells and THP-1 macrophages was quantified by the invasion assay (also called gentamicin protection assay) as previously described (Amy et al., 2004) to quantify intracellular bacteria. All the bacterial strains tested have similar gentamicin susceptibility (data not shown). To calculate the bacterial adhesion, we subtracted the cfu/ml of the invaded bacteria from the cfu/ml of the total viable bacteria that were either adherent to the cell surface or inside the cell after washing step. Results are expressed as cfu/ml of adherent and invasive bacteria compared to the ST-WT strain.

All quantitative invasion assays were performed separately for each strain in triplicates. ST-Δ*tolC* and ST-Δ*tolC*+ were compared with the ST-WT reference strain using Student's *t*-test. Each strain's overall mean cfu/ml was calculated for each biological replicate.

2.6. Reverse transcription PCR of SPI-1 gene expression

Reverse transcription polymerase chain reaction (RT-PCR) was performed to measure the transcription of the invasion-related genes of *S*. Typhi, according to the study of Webber et al. (2009). Bacteria were grown in LB broth until the mid-log phase (OD_{600} of 0.6) containing 0.3 M NaCl for SPI-1-inducing conditions (Arricau et al., 1998). Total bacterial RNA was obtained from the bacteria by using the RNeasy mini kit (Qiagen) according to the manufacturer's recommendation. Possible DNA contamination was removed by treating with DNase I (Sigma). The absence of DNA contamination was tested by PCR amplification using total RNA as a template and primers specific for the *recA* housekeeping gene (Wong et al., 2013). The purity and concentration of RNA were determined by measuring the optical density at 230, 260, and 280 nm before use (A260/280 ranged from 1.8 to 2.0). The quality of the RNA was assessed by gel electrophoresis and ethidium bromide staining.

Real-time RT-PCR was performed to measure the transcriptional level of the *invF, sipA, sipC,* and *sipD*, and the housekeeping gene *recA* was used as a control (Wong et al., 2013). Specific primer sequences were designed for each gene using the Primer3 software program (Table 3). First, 1 μg of DNase-treated total RNA from at least three independent cultures were reverse transcribed using random hexamers and Superscript III 1st Strand Kit (Invitrogen, Cat #18080-051). Then, the amplification was performed using the QuantiFast SYBR Green PCR Kit (Qiagen) on an Applied Biosystems™ 7500 Real-Time PCR System according to the manufacturer's instructions. The amplification of *recA* for target gene expression normalization was conducted simultaneously with the amplification of targeted genes. Fold-change of expression level for a target gene was determined using the comparative Ct approach, whereby the Ct value of the target gene in each sample was normalized to *recA*, and the relative expression level of the target gene and the fold-change in gene expression were calculated (Livak and Schmittgen, 2001). The expression of a target gene was presented as the fold change relative to the ST-WT strain. Data were obtained in three separate experiments with three technical replicates. All results were analyzed by the Student's *t*-test, and *p* values of <0.05 indicate significance.

3. Results

3.1. The growth of the *tolC* mutant was defective

To evaluate the fitness of the strains, we observed the growth of the strains by OD measurement. The ST-WT and ST-Δ*tolC* had similar doubling times of 112 and 116 min ($p = 0.55$), respectively (Figure 1A), while the ST-Δ*tolC*+ had a shorter doubling time of ~80 min ($p = 0.004$). The ST-Δ*tolC* and ST-Δ*tolC*+ strains arrived at the stationary stage at

TABLE 3 Oligonucleotide sequences for the amplification of selected SPI-1 genes in RT-PCR.

Target genes	Oligonucleotide sequence		Amplicon size
sipA	Forward	5′-CGCGTGTGGATTCGACTACG-3′	127 bp
	Reverse	5′-GAGTTGGTCACAGCCTCTGC-3′	
sipC	Forward	5′-CAGTGACCTGGGGTTGAGTC-3′	135 bp
	Reverse	5′-GCCAGGGCATTCAAATCCTG-3′	
sipD	Forward	5′-TTCTCCTCATCCGGGGATCG-3′	100 bp
	Reverse	5′-GCCGCGATGTTCTGTGGTAG-3′	
invF	Forward	5′-GTCGTTTGTGCAGCAGAGC-3′	107 bp
	Reverse	5′-GGTGATGTTCTCGTGGCCTT-3′	
recA	Forward	5′-CAGGCCGAGTTCCAGATCCT-3′	120 bp
	Reverse	5′-CTCGCCGTTGTAGCTGTACC-3′	

8 h; however, ST-WT continued growing at a slower rate with an OD595 reading of ~0.63, ~0.70, and ~ 0.55, respectively. The growth of the bacteria reached a stationary phase after 18 h of incubation. The OD595 of the ST-WT and the ST-Δ*tolC*+ strain was similar, with mean values of ~ 0.76 and ~ 0.74, respectively ($p = 0.20$). However, the OD595 of the ST-Δ*tolC* strain was significantly lower, with a mean value of ~0.56 ($p < 0.05$). Based on the growth curves (Figure 1A), it is deduced that the ST-Δ*tolC* cell growth defect may be due to the lack of the TolC efflux pump. In contrast, the growth defect of the mutant was rescued by the presence of the plasmid carrying *tolC* (ST-Δ*tolC*+) complement strain.

3.2. The efflux activity of the *tolC* mutant was impaired

To evaluate the efflux activity of the ST-Δ*tolC* strain, all strains (ST-WT and ST-Δ*tolC*+ as controls) were streaked on media containing ethidium bromide. After incubation, the plates were observed under UV light. The ST-WT appeared to fluoresce the least, followed by ST-Δ*tolC*+ and ST-Δ*tolC* (Figure 1B). Fluorescence intensity from the cells is inversely proportional to efflux pump function, indicating pump functionality in ST-WT and impairment in ST-Δ*tolC* (at both lower and higher ethidium bromide concentrations). Even though ST-Δ*tolC*+ was expected to have efflux activity similar to ST-WT, the strain's efflux activity was affected (Figure 1B), suggesting that the TolC expressed from the plasmid could be different from the chromosome expressed protein in ST-WT.

3.3. The adhesion and invasion of *tolC* mutant were reduced

To investigate the adhesion and invasion abilities of the strains, the bacterial cells were added to the human intestine epithelial HT-29 and macrophage THP-1 cells. Declines in the adhesion and invasion abilities of ST-Δ*tolC* were observed when the bacterial cell interacted with both host cell types *in vitro* (Figure 1C). The adhesion efficiency of ST-Δ*tolC* was reduced by ~55% in both host cell types compared to ST-WT. The significant loss of invasion is most likely due to the loss of adhesion capability in ST-Δ*tolC* because adhesion is a crucial step preceding invasion. Interestingly, the ST-Δ*tolC*+ strain showed increased adhesion and invasion in both host cell types. We speculate that the presence of multiple copies of *tolC* on the plasmids likely contributed to this phenomenon.

3.4. Invasion-related genes were downregulated in the *tolC* mutant

To evaluate the direct efflux function of TolC and the indirect role of the presence of *tolC* on the expression of SPI-1 TTSS-1 genes, we cultured the strains in the SPI-1-inducing condition (0.3 M NaCl). We performed RT-PCR to quantify relative gene expression. The mRNA expression of invasion-related genes such as *sipA, sipC, sipD,* and *invF* was significantly reduced in ST-Δ*tolC* when compared with the ST-WT reference strain that was used as control; indeed, the transcripts of these genes revealed that transcriptions of *invF, sipA, sipC,* and *sipD* genes were decreased, 15–fold, 1.6–fold, 9.6–fold, and 2.5–fold, respectively, in the ST-Δ*tolC* when compared with the ST-WT reference strain. Although the complementation ST-Δ*tolC*+ strain significantly increased the transcriptions of these genes, *sipA* (2.8-fold), *invF* (2.4-fold), *sipC* (1.2 -fold), and *sipD* (1.8-fold), when compared with ST-WT (Figure 2).

4. Discussion

The molecular mechanisms of *Salmonella* host cell entry and its intracellular survival have been widely investigated in the past few decades, and key bacterial invasion factors (e.g., SPI-1 TTSS-1) have been identified (Kaufmann et al., 2001; Ribet and Cossart, 2015). While previous studies have reported TolC-related functions in *S.* Typhimurium virulence (i.e., colonization, persistence, adhesion, and invasion) (Buckley et al., 2006; Nishino et al., 2006), no studies have been reported for the role of TolC in *S.* Typhi. In this study, we hypothesized that the *S.* Typhi TolC would similarly play an essential role in bacterial adhesion and invasion during the infection of human cells and also investigated whether the lack of TolC will affect SPI-1 gene expression known to be upregulated during the bacterial invasion.

We first constructed a *tolC* mutant, and the analysis of its growth showed that during the log phase, the growth profiles of ST-Δ*tolC*

10.3389/fmicb.2023.1301478

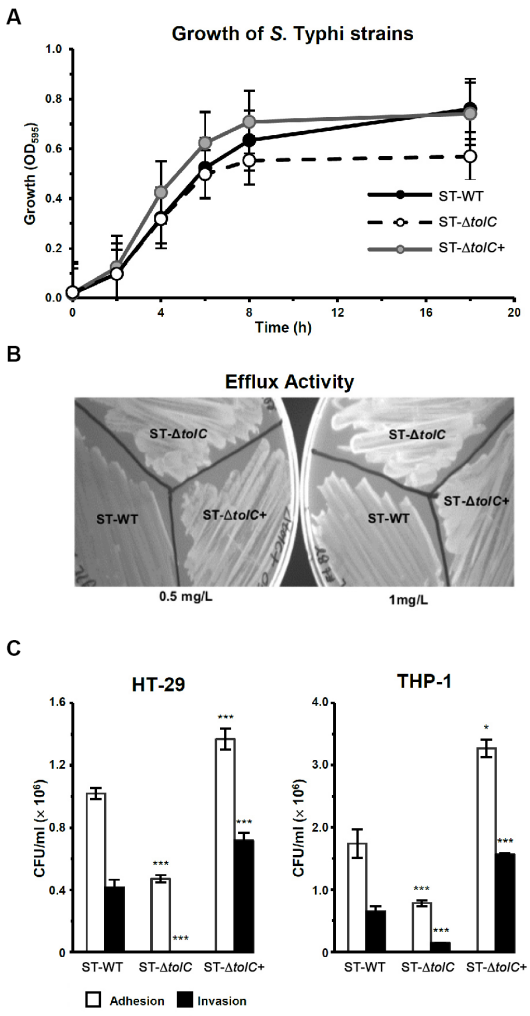

FIGURE 1
Deletion of *S.* Typhi *tolc* affects bacterial growth, efflux, adhesion, and invasion. **(A)** *S.* Typhi strains ST-WT, ST-Δ*tolC*, and ST-Δ*tolC+* were grown at 37°C, and their OD was recorded for up to 18 h. **(B)** Evaluation of the efflux activity of *S.* Typhi strains. Strains were cultured on an LB plate containing 0.5 and 1.0 mg/L ethidium bromide overnight at 37°C and observed under UV light. **(C)** Evaluation of the adhesion and invasion activity of *S.* Typhi strains on HT-29 and THP-1 cells. Data are displayed as the mean of at least three separate experiments performed in triplicate ± standard deviation. Values returning a *p* value of ≤0.001 from a Student's *t*-test comparing ST-Δ*tolC* and ST-Δ*tolC+* strains to the ST-WT strain. The asterisks above the bars represent the significance of the *t*-test, *** < 0.001.

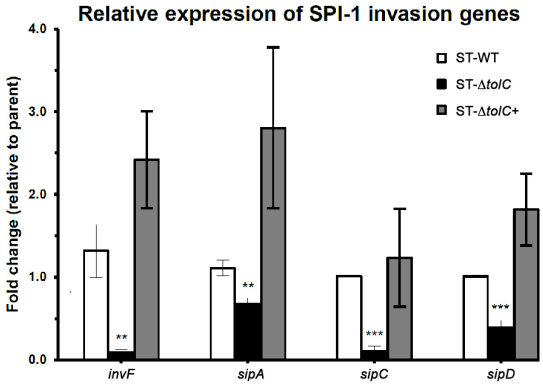

FIGURE 2
The relative expression of selected invasion-related SPI-1 genes in *S.* Typhi strains. The strains were cultured in SPI-1-inducing condition (0.3 M NaCl), and RT-PCR was performed to quantify relative gene expression. The expression of a target gene was presented as the fold change relative to the ST-WT strain used as a control in this study. White bars indicate ST-WT, black bars ST-Δ*tolC*, and gray bars for ST-Δ*tolC+*. Bars indicate the messenger RNA fold-changes observed in ST-Δ*tolC*, and ST-Δ*tolC+* compared to their ST-WT reference strain with +/− standard deviation and the mean of three independent experiments. The asterisks above bars represent significance from a Student's *t*-test, ** < 0.01, *** < 0.001.

were similar to the ST-WT strain; however, it reached the stationary phase earlier and at a lower OD (Figure 1A). One plausible explanation is that intracellular waste and metabolites accumulated due to impaired efflux, and this internal toxicity affects cell viability, thus leading to an earlier stationary phase and lower cell density. Alternatively, it may be due to the altered expression of genes involved in stress response, virulence, or metabolism that are regulated by *tolC* or its associated operons. Further studies are needed to elucidate the molecular mechanisms underlying the growth defect of ST-Δ*tolC* in the stationary phase and its implications for pathogenesis.

Our results are consistent with some previous reports on *tolC* mutants of other bacterial species. For example, Virlogeux-Payant et al. (2008) showed that a *tolC* mutant of *Salmonella Typhimurium* had a comparable growth rate to the wild-type strain based on the growth curve, but they did not report the growth characteristics of the mutant in the stationary phase. Webber et al. (2009) reported that a *tolC* mutant of *Salmonella Typhimurium* did not show a growth defect in the log phase compared to the wild-type strain. However, Santos et al. (2010) reported that a *tolC* mutant of *Sinorhizobium meliloti* had a similar growth rate to the wild-type strain for the first 8 h of growth, but then showed a reduced growth rate and decreased biomass formation (Santos et al., 2010). Similarly, in our study, ST-Δ*tolC* had reduced growth after 8 h compared to ST-WT.

The ST-Δ*tolC* also showed hyper-susceptibility to detergents and antibiotics (results shown in Supplementary material) as demonstrated by its weaker ability to efflux ethidium bromide, unlike the ST-WT strain (Figure 1B).

In the cell adhesion and invasion assay, the ST-Δ*tolC* was significantly less invasive than the ST-WT reference strain in both the epithelium (HT-29) and macrophage (THP-1) cells. The invasion of ST-Δ*tolC* was removed entirely in HT-29 cells and was approximately 20% in THP-1 cells, possibly due to the phagocytic activity of the macrophages. As predicted, the adhesion and invasion activity were restored to a higher level in the ST-Δ*tolC+* strain in both HT-29 and THP-1 (Figure 1C). These findings are consistent with the study on an *S.* Typhimurium *tolC* mutant where it was also reported to be less adherent to epithelial cells than its WT parent and that TolC is crucial for virulence-related phenotypes such as adhesion and invasion to the host cells (Buckley et al., 2006; Virlogeux-Payant et al., 2008).

The growth curves and invasion assays resulting from this report are consistent with our previous preliminary study that was done with other *S.* Typhi strains (Hussain et al., 2016).

Next, we wanted to see if the suppressed invasion activity of ST-Δ*tolC* was also linked to the TTSS-1 system, which is primarily associated with invasion (Galan, 2001). Using RT-PCR, we found lower expression of invasion-related genes of the TTSS-1 (*invF*, *sipA*, *sipC*, and *sipD*) (Figure 2). The transcription of *invF*, a transcriptional regulator which activates the transcription of other SPI-1 genes (Darwin and Miller, 1999a,b), was downregulated by fifteen-fold in the ST-Δ*tolC* compared to the ST-WT. When the *tolC* was complemented, the expressions of the SPI-1 genes in the ST-Δ*tolC*+ strain were higher than ST-WT. The higher gene expression levels of ST-Δ*tolC*+ also reflect the strain's higher adhesion and invasion activities (Figure 1C). In *S.* Typhimurium, deletion of another gene *invH*, located downstream of *invF*, was shown to partially impair the secretion of Sip effector proteins (SipABCD) (Pati et al., 2013).

The reduced expressions of the invasion-related genes are likely mediated by the lowered expression of *invF* in the ST-Δ*tolC*. This downregulation is in agreement with the observation in *S.* Typhimurium (*tolC::aph*), where the *invF* was significantly downregulated in the *tolC* mutant (Webber et al., 2009). The *invF* is a positive regulator of SPI-1 that has been confirmed to be essential for the expression of several SPI-1 genes (Darwin and Miller, 1999a,b).

5. Conclusion

In this study, we demonstrated that TolC-dependent efflux systems play a vital role in the adhesion and invasion of *S.* Typhi to host cells, which are key steps in the pathogenesis of typhoid fever. We also revealed that TolC influences the expression of SPI-1 genes, which encode the type III secretion system (TTSS-1) that mediates the invasion process. Our findings suggest that TolC is a multifunctional protein that modulates both the efflux activity and the virulence gene expression of *S.* Typhi. However, the exact mechanism by which TolC regulates SPI-1 genes remains unknown and requires further investigation. Moreover, the potential of TolC as a target for developing novel anti-virulence strategies against *S.* Typhi needs to be explored in future studies.

Data availability statement

The original contributions presented in the study are included in the article/Supplementary material, further inquiries can be directed to the corresponding authors.

Ethics statement

The studies involving humans were approved by ethical clearance number USMKK/PPP/JEPeM [229.3. (03)]. The studies were conducted in accordance with the local legislation and institutional requirements. Written informed consent for participation in this study was provided by the participants' legal guardians/next of kin.

Author contributions

AH: Conceptualization, Data curation, Formal analysis, Investigation, Writing – original draft, Writing – review & editing. EO: Funding acquisition, Project administration, Resources, Supervision, Validation, Visualization, Writing – review & editing. PB: Conceptualization, Formal analysis, Funding acquisition, Project administration, Resources, Supervision, Validation, Visualization, Writing – review & editing. AI: Funding acquisition, Project administration, Resources, Supervision, Writing – review & editing. PK: Funding acquisition, Project administration, Resources, Supervision, Validation, Visualization, Writing – review & editing.

Funding

The author(s) declare financial support was received for the research, authorship, and/or publication of this article. This study was supported by the University Sains Malaysia Enteric Diseases Research Cluster Grants (1001/PSKBP/8630011 and PSKBP/86300111) and Postgraduate Research Grant (1001/CIPPM/846046). AH was financially supported by the USM Fellowship during his study.

Conflict of interest

The authors declare that the research was conducted in the absence of any commercial or financial relationships that could be construed as a potential conflict of interest.

Publisher's note

Supplementary material

The Supplementary material for this article can be found online at: https://www.frontiersin.org/articles/10.3389/fmicb.2023.1301478/full#supplementary-material

References

Amy, M., Velge, P., Senocq, D., Bottreau, E., Mompart, F., and Virlogeux-Payant, I. (2004). Identification of a new *Salmonella enterica* serovar Enteritidis locus involved in cell invasion and in the colonisation of chicks. *Res. Microbiol.* 155, 543–552. doi: 10.1016/j.resmic.2004.03.005

Arricau, N., Hermant, D., Waxin, H., Ecobichon, C., Duffey, P. S., and Popoff, M. Y. (1998). The RcsB-RcsC regulatory system of *Salmonella typhi* differentially modulates the expression of invasion proteins, flagellin and Vi antigen in response to osmolarity. *Mol. Microbiol.* 29, 835–850. doi: 10.1046/j.1365-2958.1998.00976.x

Baba, T., Ara, T., Hasegawa, M., Takai, Y., Okumura, Y., Baba, M., et al. (2006). Construction of *Escherichia coli* K-12 in-frame, single-gene knockout mutants: the Keio collection. *Mol. Syst. Biol.* 2:2006.0008. doi: 10.1038/msb4100050

Buckley, A. M., Webber, M. A., Cooles, S., Randall, L. P., La Ragione, R. M., Woodward, M. J., et al. (2006). The AcrAB-TolC efflux system of *Salmonella enterica* serovar Typhimurium plays a role in pathogenesis. *Cell. Microbiol.* 8, 847–856. doi: 10.1111/j.1462-5822.2005.00671.x

Darwin, K. H., and Miller, V. L. (1999a). InvF is required for expression of genes encoding proteins secreted by the SPI1 type III secretion apparatus in *Salmonella typhi*murium. *J. Bacteriol.* 181, 4949–4954. doi: 10.1128/JB.181.16.4949-4954.1999

Darwin, K. H., and Miller, V. L. (1999b). Molecular basis of the interaction of Salmonella with the intestinal mucosa. *Clin. Microbiol. Rev.* 12, 405–428. doi: 10.1128/CMR.12.3.405

Datsenko, K. A., and Wanner, B. L. (2000). One-step inactivation of chromosomal genes in Escherichia coli K-12 using PCR products. *Proc. Natl. Acad. Sci. U S A*, 97, 640–6645. doi: 10.1073/pnas.120163297

Dibb-Fuller, M. P., Allen-Vercoe, E., Thorns, C. J., and Woodward, M. J. (1999). Fimbriae- and flagella-mediated association with and invasion of cultured epithelial cells by *Salmonella enteritidis*. *Microbiology* 145, 1023–1031.

Fernando, D. M., and Kumar, A. (2013). Resistance-nodulation-division multidrug efflux pumps in gram-negative bacteria: role in virulence. *Antibiotics* 2, 163–181. doi: 10.3390/antibiotics2010163

Galan, J. E. (2001). Salmonella interactions with host cells: type III secretion at work. *Annu. Rev. Cell Dev. Biol.* 17, 53–86. doi: 10.1146/annurev.cellbio.17.1.53

Hussain, A., Ong, E. B. B., Phei, P. S. C., Hossain, K., Balaram, P., Ismail, A., et al. (2016). Role of TolC in virulence of salmonella enterica serovar Typhi. *J. Pure Appl. Microbiol.*10:887.

Kaufmann, S. H., Raupach, B., and Finlay, B. B. (2001). Introduction: microbiology and immunology: lessons learned from Salmonella. *Microbes Infect.* 3, 1177–1181. doi: 10.1016/S1286-4579(01)01498-8

Levy, H., Diallo, S., Tennant, S. M., Livio, S., Sow, S. O., Tapia, M., et al. (2008). PCR method to identify Salmonella enterica serovars Typhi, Paratyphi A, and Paratyphi B among Salmonella Isolates from the blood of patients with clinical enteric fever. *J. Clin. Microbiol.* 46, 1861–1866. doi: 10.1128/jcm.00109-08

Li, X. Z., and Nikaido, H. (2004). Efflux-mediated drug resistance in bacteria. *Drugs* 64, 159–204. doi: 10.2165/00003495-200464020-00004

Livak, K. J., and Schmittgen, T. D. (2001). Analysis of relative gene expression data using real-time quantitative PCR and the 2(-Delta Delta C(T)) method. *Methods* 25, 402–408. doi: 10.1006/meth.2001.1262

Martins, M., Santos, B., Martins, A., Viveiros, M., Couto, I., Cruz, A., et al. (2006). An instrument-free method for the demonstration of efflux pump activity of bacteria. *In Vivo* 20, 657–664.

Nishino, K., Latifi, T., and Groisman, E. A. (2006). Virulence and drug resistance roles of multidrug efflux systems of *Salmonella enterica* serovar Typhimurium. *Mol. Microbiol.* 59, 126–141. doi: 10.1111/j.1365-2958.2005.04940.x

Pati, N. B., Vishwakarma, V., Jaiswal, S., Periaswamy, B., Hardt, W. D., and Suar, M. (2013). Deletion of invH gene in *Salmonella enterica* serovar Typhimurium limits the secretion of Sip effector proteins. *Microbes Infect.* 15, 66–73. doi: 10.1016/j.micinf.2012.10.014

Piddock, L. J. (2006a). Clinically relevant chromosomally encoded multidrug resistance efflux pumps in bacteria. *Clin. Microbiol. Rev.* 19, 382–402. doi: 10.1128/CMR.19.2.382-402.2006

Piddock, L. J. (2006b). Multidrug-resistance efflux pumps - not just for resistance. *Nat. Rev. Microbiol.* 4, 629–636. doi: 10.1038/nrmicro1464

Ribet, D., and Cossart, P. (2015). How bacterial pathogens colonize their hosts and invade deeper tissues. *Microbes Infect.* 17, 173–183. doi: 10.1016/j.micinf.2015.01.004

Roche, S. M., Gracieux, P., Milohanic, E., Albert, I., Virlogeux-Payant, I., Temoin, S., et al. (2005). Investigation of specific substitutions in virulence genes characterizing phenotypic groups of low-virulence field strains of *Listeria monocytogenes*. *Appl. Environ. Microbiol.* 71, 6039–6048. doi: 10.1128/AEM.71.10.6039-6048.2005

Santos, M. R., Cosme, A. M., Becker, J. D., Medeiros, J. M., Mata, M. F., and Moreira, L. M. (2010). Absence of functional TolC protein causes increased stress response gene expression in *Sinorhizobium meliloti*. *BMC Microbiol.* 10:180. doi: 10.1186/1471-2180-10-180

Sheridan, A., Lenahan, M., Condell, O., Bonilla-Santiago, R., Sergeant, K., Renaut, J., et al. (2013). Proteomic and phenotypic analysis of triclosan tolerant verocytotoxigenic *Escherichia coli* O157: H19. *J. Proteome* 80, 78–90. doi: 10.1016/j.jprot.2012.12.025

Sun, J., Deng, Z., and Yan, A. (2014). Bacterial multidrug efflux pumps: mechanisms, physiology and pharmacological exploitations. *Biochem. Biophys. Res. Commun.* 453, 254–267. doi: 10.1016/j.bbrc.2014.05.090

Tokuda, H. (2009). Biogenesis of outer membranes in gram-negative bacteria. *Biosci. Biotechnol. Biochem.* 73, 465–473. doi: 10.1271/bbb.80778

Virlogeux-Payant, I., Baucheron, S., Pelet, J., Trotereau, J., Bottreau, E., Velge, P., et al. (2008). TolC, but not AcrB, is involved in the invasiveness of multidrug-resistant *Salmonella enterica* serovar typhimurium by increasing type III secretion system-1 expression. *Int. J. Med. Microbiol.* 298, 561–569. doi: 10.1016/j.ijmm.2007.12.006

Webber, M. A., Bailey, A. M., Blair, J. M. A., Morgan, E., Stevens, M. P., Hinton, J. C. D., et al. (2009). The global consequence of disruption of the AcrAB-TolC efflux pump in *Salmonella enterica* includes reduced expression of SPI-1 and other attributes required to infect the host. *J. Bacteriol.* 191, 4276–4285. doi: 10.1128/JB.00363-09

Wong, V. K., Pickard, D. J., Barquist, L., Sivaraman, K., Page, A. J., Hart, P. J., et al. (2013). Characterization of the yehUT two-component regulatory system of *Salmonella enterica* Serovar Typhi and Typhimurium. *PLoS One* 8:e84567. doi: 10.1371/journal.pone.0084567

frontiers | Frontiers in Microbiology

TYPE Original Research
PUBLISHED 16 November 2023
DOI 10.3389/fmicb.2023.1285421

OPEN ACCESS

EDITED BY
Sébastien Holbert,
INRA Centre Val de Loire, France

REVIEWED BY
Arnaud Bridier,
Agence Nationale de Sécurité Sanitaire de l'Alimentation, de l'Environnement et du Travail (ANSES), France
Ahmed Ghamry Abdelhamid,
The Ohio State University, United States

*CORRESPONDENCE
Lynne McLandsborough
✉ lm@foodsci.umass.edu

RECEIVED 29 August 2023
ACCEPTED 16 October 2023
PUBLISHED 16 November 2023

CITATION
Ghoshal M, Bechtel TD, Gibbons JG and McLandsborough L (2023) Adaptive laboratory evolution of *Salmonella enterica* in acid stress.
Front. Microbiol. 14:1285421.
doi: 10.3389/fmicb.2023.1285421

Adaptive laboratory evolution of *Salmonella enterica* in acid stress

Mrinalini Ghoshal[1,2], Tyler D. Bechtel[2], John G. Gibbons[2] and Lynne McLandsborough[2]*

[1]Department of Microbiology, University of Massachusetts, Amherst, MA, United States, [2]Department of Food Science, University of Massachusetts, Amherst, MA, United States

Introduction: Adaptive laboratory evolution (ALE) studies play a crucial role in understanding the adaptation and evolution of different bacterial species. In this study, we have investigated the adaptation and evolution of *Salmonella enterica* serovar Enteritidis to acetic acid using ALE.

Materials and methods: Acetic acid concentrations below the minimum inhibitory concentration (sub-MIC) were used. Four evolutionary lineages (EL), namely, EL1, EL2, EL3, and EL4, of *S.* Enteritidis were developed, each demonstrating varying levels of resistance to acetic acid.

Results: The acetic acid MIC of EL1 remained constant at 27 mM throughout 70 days, while the MIC of EL2, EL3, and EL4 increased throughout the 70 days. EL4 was adapted to the highest concentration of acetic acid (30 mM) and demonstrated the highest increase in its MIC against acetic acid throughout the study, reaching an MIC of 35 mM on day 70. The growth rates of the evolved lineages increased over time and were dependent on the concentration of acetic acid used during the evolutionary process. EL4 had the greatest increase in growth rate, reaching 0.33 (h^{-1}) after 70 days in the presence of 30 mM acetic acid as compared to EL1, which had a growth rate of 0.2 (h^{-1}) after 70 days with no exposure to acetic acid. Long-term exposure to acetic acid led to an increased MIC of human antibiotics such as ciprofloxacin and meropenem against the *S. enterica* evolutionary lineages. The MIC of ciprofloxacin for EL1 stayed constant at 0.016 throughout the 70 days while that of EL4 increased to 0.047. Bacterial whole genome sequencing revealed single-nucleotide polymorphisms in the ELs in various genes known to be involved in *S. enterica* virulence, pathogenesis, and stress response including *phoP, phoQ*, and *fhuA*. We also observed genome deletions in some of the ELs as compared to the wild-type *S.* Enteritidis which may have contributed to the bacterial acid adaptation.

Discussion: This study highlights the potential for bacterial adaptation and evolution under environmental stress and underscores the importance of understanding the development of cross resistance to antibiotics in *S. enterica* populations. This study serves to enhance our understanding of the pathogenicity and survival strategies of *S. enterica* under acetic acid stress.

KEYWORDS

***Salmonella enterica*, adaptive laboratory evolution (ALE), acetic acid stress adaptation, minimum inhibitory concentration (MIC), bacterial whole genome sequencing, missense mutations**

1. Introduction

Adaptive laboratory evolution (ALE) is a technique used to study the evolution of organisms in response to selective pressures over time. In laboratory settings, ALE is typically performed with organisms possessing a short generation time such as bacteria. Through ALE, bacteria are subjected to increasingly harsh conditions over several generations, allowing them to adapt and evolve in response to stress (Dragosits and Mattanovich, 2013). The technique of ALE has proven to be highly effective in providing a deeper understanding of the genetic mechanisms and processes involved in bacterial adaptation, as well as in facilitating research on the evolution of bacterial populations over time (Gresham and Dunham, 2014; LaCroix et al., 2017; Sandberg et al., 2019).

Salmonella enterica is a pathogenic bacterium that can cause serious foodborne illnesses in humans (Spector and Kenyon, 2012; Ren et al., 2015). It frequently encounters acidic conditions in the external environment and inside hosts, and has evolved strategies to survive and adapt to acid stress (Álvarez-Ordóñez et al., 2012). The use of organic acids for fermentation and flavoring in the food industry provides opportunities for contaminating *S. enterica* to become acid-adapted (Coban, 2020). Additionally, the use of acidified solutions for cleaning and sanitization in households and industries creates environments conducive to the development of acid adaptation and acid tolerance response in surviving *S. enterica* (Wang et al., 2019). In this study, we have used an evolutionary approach to understand the adaptation of *S. enterica* to acid stress by subjecting it to sub-inhibitory concentrations of acetic acid over more than 1,000 bacterial generations. Subsequently, we were able to analyze the bacterial genome and identify the genetic mutations resulting from growth under acidic conditions.

Adaptive laboratory evolution of *S. enterica* in environmental stresses is a relatively unexplored field, making our study pioneering and essential. The results of the study have implications for food safety since understanding the evolution of *Salmonella* populations with reduced acid susceptibility can impact the efficacy of food preservation methods that rely on acidification. Moreover, prior adaptation to acid stress has been reported to provide cross-protection against multiple other forms of stresses that are frequently encountered by the pathogen in industrial settings (Xu et al., 2008). In this study, we evaluate whether continued exposure to acetic acid provides cross-resistance in *S. enterica* populations against human antibiotics. Understanding the relationship between acetic acid exposure and antibiotic resistance is crucial in combating the global issue of antibiotic resistance. Analyzing the acid-adaptive capabilities of *S. enterica* will contribute to our knowledge of the dynamics of bacterial evolution in response to stress. Overall, this study emphasizes the importance of understanding the genetic basis of bacterial adaptation to acid stress which will help in the development of effective preventative strategies.

2. Materials and methods

2.1. Bacterial isolates and growth media

The bacterial isolate used in this study is *Salmonella enterica* subsp. enterica serovar Enteritidis (ATCC BAA-1045, phage type 30). This bacterial strain was originally isolated from a salmonellosis outbreak in raw almonds (Brandl et al., 2008). It has been reported to survive long-term desiccation and nutrient starvation stress, which makes it an interesting target to study its adaptation to acid stress (Deng et al., 2012). The bacterial strain was maintained as frozen stocks in a −80°C freezer in trypticase soy broth (TSB; Sigma-Aldrich) supplemented with 15% glycerol. Frozen cultures of *S. enterica* were revived by streaking on tryptic soy agar (TSA; Sigma-Aldrich) and incubated at 37°C for 18 to 20 h to create a bacterial lawn. The bacteria were further streaked on trypticase soy agar (TSA, Sigma-Aldrich). Single colonies of bacteria were then inoculated in tryptic soy broth (TSB, BD diagnostic systems) overnight for 18 h.

2.2. Quantification of MIC (minimum inhibitory concentration) of acetic acid

The MIC of acetic acid against the evolutionary lineages of *S.* Enteritidis was determined using the broth dilution method (Wiegand et al., 2008) with minor modifications. In brief, in 50 mL tubes, a bacterial inoculum of 10^7–10^8 CFU/ml was added in 20 mL TSB containing acetic acid concentrations from 24 to 34 mM. The acetic acid concentration in each tube was incremented by 1 mM. The tubes were incubated under shaking conditions at 37°C for ∼18 h. TSB with 200 mM acetic acid and TSB without any acetic acid were also inoculated with the bacteria and served as negative and positive controls, respectively. The OD_{600} was quantified after 20 h, and $OD_{600} \leq 0.1$ was considered an inhibition of growth. To determine the MIC or minimum bactericidal concentration (MBC) of acetic acid, inoculum was taken from the tubes with $OD_{600} \leq 0.1$ and plated on TSA plates. Recovery of growth was an indication that the acetic acid concentration was MIC. This experiment was repeated in triplicates for each of the replicates of all the evolutionary lineages. The minimum inhibitory concentration of acetic acid of the evolutionary lineages was determined every 5 days after the initiation of the ALE study.

2.3. Adaptive laboratory evolution of *S.* Enteritidis in acetic acid

At the beginning of the adaptive evolutionary study, *Salmonella enterica* subsp. enterica serovar Enteritidis (referred to as WT) was grown in TSB overnight. The overnight *S.* Enteritidis culture was used to quantify the MIC of acetic acid [explained in section 2.2. Quantification of MIC (minimum inhibitory concentration) of acetic acid]. The MIC of WT *S.* Enteritidis was quantified to be 27 mM. The WT culture was grown overnight and after 20 h, the bacterial optical density of the overnight culture was adjusted, and inoculum of 10^7–10^8 CFU/mL was added to three 50 mL conical tubes containing 20 mL of TSB. These tubes were labeled as EL1a, EL1b, and EL1c. Here, EL stands for evolutionary lineage. Inoculum from the WT was also added to three tubes containing 26 mM acetic acid in TSB that were labeled EL2a, EL2b, and EL2c. EL1 served as our control evolutionary lineage, and EL2 served as our first evolutionary lineage that was grown and adapted to sub-MIC of acetic acid. The six tubes were incubated at 37°C for 18–20 h. Following that, the OD_{600} of the six tubes

was measured and recorded. An inoculum of 10^6 CFU/ml from each tube was collected and added to six new tubes for day 2. This process was repeated throughout the ALE study, and a similar inoculum was transferred to fresh tubes for each of the EL daily. The MIC of the six tubes was quantified every 5 days, and on day 20, the MIC of EL2 (all three replicates) increased to 29 mM. Hence, on day 20, inoculum from EL2a-EL2c was also added to three tubes containing 28 mM acetic acid (sub-MIC acetic acid) in TSB and labeled EL3a-EL3c. On day 30, the MIC of EL3 increased to 31 mM, and inoculum from EL3a-EL3c was added to three tubes containing 30 mM acetic acid in TSB and labeled EL4a-EL4c. The OD_{600} for each of the tubes was measured after growing them for 20 h at 37°C under shaking conditions. Samples from the previous day were stored at −80°C over the course of the evolutionary process. The number of bacterial generations 'n' was calculated using the following equation (Lee et al., 2011):

$$n = log(N/N_0)/log(2).$$

where N is the final number of cells in the conical tube after 20 h at the time of passage to the next day's tubes. N_0 is the initial number of cells that are transferred to each conical tube at the beginning of ALE for that day. The initial and final numbers of cells were estimated daily by measuring the OD_{600} using a spectrophotometer and using plate counts. The generation number calculation assumes that each cell is viable, the death rate is negligible, the cells are growing exponentially throughout the ALE experiment, and the cells are dividing by binary fission.

2.4. Quantification of growth rate of the *S.* Enteritidis evolutionary lineages

The growth rate of the bacterial lineages was quantified using previously established methods (Herring et al., 2006; Hall et al., 2013) with some modifications. After 20 h of growth of the evolutionary lineages at 37°C, the inoculum was adjusted to approximately 10^4CFU/ml and added inside the wells of a 96-well microtiter plate (Thermo Fisher Scientific, Waltham, MA, USA, model number 266120). Bacterial cultures collected at the end of day 2 and day 70 from the ELs were used to generate the growth curves inside the oCelloScope. For WT *S.* Enteritidis, EL1 and EL2, along with the bacterial inoculum, the wells also contained TSB with 26 mM acetic acid. For EL3 and EL4, the wells in the microtiter plate contained 28 mM and 30 mM acetic acid in TSB, respectively. The concentration of acetic acid added to the wells for each EL was 1 mM less than their MIC (sub-MIC acetic acid). The microtiter plates were placed inside the oCelloScope for 24 h to monitor the progression of bacterial growth. The exponential growth rate of all three replicates of each of the evolutionary lineages was measured. The background corrected absorption (BCA) algorithm and the BCA normalized algorithm of the software UniExplorer (version 10.1) were used to quantify the kinetics of bacterial growth. The kinetics of growth of the WT *S.* Enteritidis and all the evolutionary lineages in TSB without acetic acid stress were also monitored using the oCelloScope.

2.5. Quantification of MIC of antibiotics against the *S.* Enteritidis evolutionary lineages

The MIC of the following antibiotics: vancomycin, meropenem, ciprofloxacin, gentamycin, and streptomycin, were determined using MTS strips (MIC test strips, Liofilchem) (Matuschek et al., 2018; van den Bijllaardt et al., 2018). Antibiotics with different mechanisms of action were chosen to gain a thorough understanding of their effects on the evolutionary lineages. Vancomycin and meropenem inhibit bacterial cell wall biosynthesis (Yarlagadda et al., 2018), ciprofloxacin inhibits bacterial DNA synthesis, and gentamycin and streptomycin are known to inhibit bacterial protein synthesis (Athamneh et al., 2014).

The test strips for each antibiotic had a concentration range from 0.016 to 256 μg/ml. Overnight cultures of the evolutionary lineages were grown in their corresponding acetic acid concentrations, and the next day, the OD_{600} was adjusted to 10^7 CFU/mL in TSB. Cotton swab applicators were dipped in the bacterial cultures and streaked on TSA to create bacterial lawns. The MTS test strips were carefully positioned at the center of the TSA plates using sterile forceps. The plates were incubated for 18–20 h at 37°C, following which the zones of inhibition around the test strips were recorded. The minimum concentration of the antibiotic, which caused inhibition of bacterial growth, was denoted as the MIC. This experiment was repeated in triplicates for each of the replicates of all the evolutionary lineages. MTS test strips have been used successfully for determining the MIC of antibiotics against different pathogens, and the strips have been reported to provide MIC values similar to those obtained using broth microdilution methods (Hakvoort et al., 2020; Koeth et al., 2022).

2.6. Bacterial whole-genome sequencing

The WT strain of *S.* Enteritidis and evolved lineages after day 70 of the ALE study were streaked on TSA and incubated overnight at 37°C. Genomic DNA extraction and sequencing were performed at SeqCenter (Pittsburgh, PA, USA). For the evolved lineages, after 70 days, the liquid cultures were plated on TSA, and colonies were randomly chosen for sequencing. DNA extraction was performed using Zymo DNA Miniprep (bead-beating lysis). For the WT strain, sample libraries were generated using the Illumina DNA Prep kit and IDT 10bp UDI indices. Sequencing was performed on a NextSeq 2000 sequencer, producing 151-bp paired-end reads. Low-quality reads were trimmed, and adapter sequences were removed from Illumina sequences using bcl-convert version 3.9.3. Oxford Nanopore Technologies (ONT) PCR-free ligation library preparation was also used to generate long sequence reads. ONT reads were adapted and quality-trimmed using porechop33 version 0.2.3_seqan2.1.1 (RRID:SCR_016967). Unicycler version 0.4.8 was used to produce a hybrid assembly from the Illumina and ONT reads. Assembly quality was assessed using QUAST version 5.0.2 (Gurevich et al., 2013). The NCBI Nucleotide BLAST database was then used to characterize the complete genome assembly and identify plasmid sequences. Gene models were predicted with functional annotations using Prokka

version 1.14.5 with default parameters + '–rfam' (Tatusova et al., 2016; Haft et al., 2018). Culturing and DNA extraction of the evolved lineages were performed using the same procedure as the WT, but 151-bp paired-end libraries were generated using only Illumina sequencing as described above.

2.7. Genome assembly and identification of polymorphisms

All software mentioned below was used with default parameters unless specified otherwise. BWA version 0.7.15 (RRID:SCR_010910) was used to map the evolved lineages resequencing data against the ancestral reference genome (Li, 2013). Samtools (v 1.14) (RRID:SCR_002105) was used to index the sorted BAM files. Bamaddrg was used to add read groups to the indexed and sorted BAM files (Danecek et al., 2021). Joint genotyping of the evolved strains was then performed using Freebayes (v 1.3.1) (RRID:SCR_010761) (Garrison and Marth, 2012). GATK (v. 4.0.6) (RRID:SCR_001876) was used to convert the resulting VCF files into a table format (McKenna et al., 2010). A SnpEff database was built for the *S.* Enteritidis BAA-1045 WT reference genome, and SNP annotation prediction was performed in the evolved strains using SnpEff (v. 4.1) (Cingolani et al., 2012). A second variant calling software, Breseq (v. 0.35.4) (RRID:SCR_010810), was used by SeqCenter to align and compare evolved lineage sequence reads to the ancestor (Deatherage and Barrick, 2014). Assemblies were generated from the Illumina reads of each evolved lineage using SPAdes (v. 3.13.1) (RRID:SCR_000131) with the parameters, "-k 21,33,55 –careful" (Anton Bankevich et al., 2012). Large-Scale Blast Score Ratio (LS-BSR) was used to investigate gene presence/absence mutations using default parameters, along with additional parameters "-b blastn -c cdhit" (Sahl et al., 2014). Read-depth analysis was performed using Samtools (v. 1.14).

2.8. Statistical analyses

All bacterial growth measurements were biologically triplicated, and their differences were examined by a two-tailed *t*- test assuming unequal variance (Welch's *t*- test). GraphPad Prism was used to generate all the graphs in this project. Statistical significance was calculated with GraphPad Prism using two-way ANOVA. A *p*-value of ≤ 0.05 was considered statistically significant.

3. Results

3.1. Experimental design of the ALE study

Salmonella Enteritidis was adapted in different concentrations of acetic acid in TSB over 70 days. **Figure 1** outlines the evolution of four lines of *S. enterica* in acetic acid, which we are calling "evolutionary lineages" (EL). The MIC of acetic acid for wild-type (WT) *S.* Enteritidis was 27 mM at the beginning of the experiment (**Figure 2**). On day 0, two ELs were developed from WT *S.* Enteritidis. In the first EL, EL1, *S.* Enteritidis was grown in TSB without any acid stress, and in the second EL, EL2, *S.* Enteritidis was grown in 26 mM acetic acid (sub-MIC) in TSB. Each EL was grown in triplicates at 37°C for 18 h daily before they were transferred into fresh media as described in the section "2. Materials and methods". The MIC of acetic acid of EL1 and EL2 was measured every 5 days, and the OD_{600} was monitored daily before transfer. After 20 ALE days, the MIC of acetic acid for EL2 rose to 29 mM, and a new lineage, EL3, was created from EL2 (**Figure 1**). An inoculum of 10^8CFU/ml was transferred from the three replicates of EL2 to generate three replicates of EL3. EL3 was grown in 28 mM acetic acid for the remainder of the experiment. Here, ALE days refer to the number of days that have passed since the initiation of the ALE study. After 30 ALE days, the MIC of EL3 increased to 31 mM, and a new EL, EL4, was initiated (**Figure 1**). EL4 was grown in 30 mM acetic acid in TSB with daily transfers in fresh media. The number of generations for each EL was quantified from OD_{600} values and is shown in **Figure 1**. After 70 days, the adaptive evolution process was halted, and all the ELs were frozen at −80°C. The MIC of acetic acid of EL2–EL4 was found to increase over time throughout the duration of the ALE study (**Figure 2**). The MIC of acetic acid in EL1 remained constant throughout the study, and the highest increase in the MIC of acetic acid was observed in EL4.

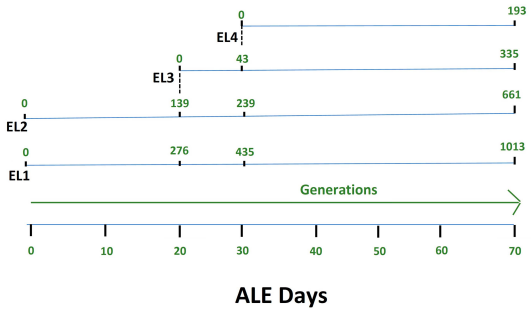

FIGURE 1
Adaptive evolution of *S.* Enteritidis evolutionary lineages (EL) with daily transfers in acetic acid. The MIC of acetic acid of wild-type *S.* Enteritidis was quantified to be 27 mM, and hence, EL2 was grown in 26 mM acetic acid (sub-MIC) while EL1 was grown in no acid stress (control group). The MIC of EL1 and EL2 was quantified every 5 days. On day 20, the MIC of EL2 increased to 29 mM. So, we started EL3 from EL2, and it was grown in 28 mM acetic acid with daily transfers for the remainder of the ALE study. On day 30, the MIC of EL3 went up to 31 mM; hence, we started EL4 from EL3, and EL4 was grown in 30 mM acetic acid with daily transfers until day 70 of the ALE study. The OD_{600} for each of the EL was quantified every day before and after daily transfers, and the values were used to quantify the number of generations. The number of generations of each of the ELs has been shown in green.

3.2. Effect of ALE on the growth rate of the adapted evolutionary lineages

The exponential growth rate of the adapted ELs was evaluated in the presence and absence of acetic acid using the oCelloScope (**Figure 3** and **Table 1**). The oCelloScope has previously been used to study changes in growth rates after treatment with antimicrobial

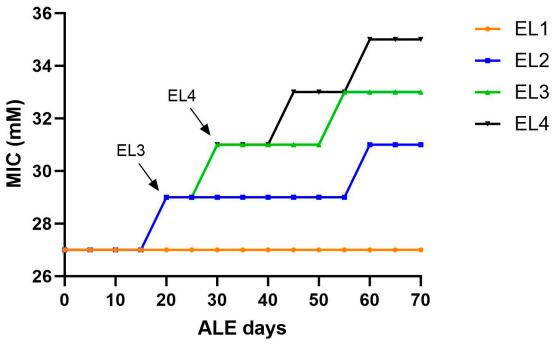

FIGURE 2
Change in acetic acid MIC of the ELs of *S.* Enteritidis. The MIC of acetic acid of the evolutionary lineages was measured every 5 days until day 70 of the ALE study. Bacterial cultures (1 mL) were collected from the three replicates of EL1–EL4 every 5 days to quantify the MIC of acetic acid. The arrows indicate the initiation of EL3 and EL4 from EL2 and EL3, respectively. The evolutionary lineage EL3 was initiated from EL2 (on ALE day 20) when the acetic acid MIC of EL2 increased for the first time and a similar process was used for the initiation of EL4 (on ALE day 30).

compounds (Fredborg et al., 2013; Canali et al., 2018; Ghoshal et al., 2022b). The growth rates were quantified on ALE days 2 for EL1 and EL2 and for ALE days 22 and 32 for EL3 and EL4, respectively. ALE days 22 and 32 were 2 days after the initial transfer of EL3 and EL4, respectively. Growth rates of all ELs were calculated from the exponential growth phase of the growth curves. The growth curves of EL1 and EL4 generated using the oCelloScope are shown in **Supplementary Figure 1**.

No significant differences were observed in the growth rate after days 2 and 70 for EL1 ($p > 0.05$) (**Figure 3A**), while for EL4, the growth rate in 30 mM acetic acid on day 70 was significantly higher than that on day 32 ($p < 0.001$) (**Figure 3B**). However, no significant differences in growth rates in the absence of acetic acid were observed in either EL1 after days 2 and 70 or in EL4 after days 32 and 70 ($p > 0.05$). Additionally, the exponential growth rates of EL2 and EL3 have been represented graphically in **Supplementary Figure 2**. The exponential growth rate of all the ELs 2 days after their initiation and after 70 ALE days in the presence and absence of acetic acid is shown in **Table 1**. The results indicate that the growth rates on ALE day 70 were significantly higher than those on days 2, 22, and 32 for EL2 ($p < 0.01$), EL3 ($p < 0.01$), and EL4 ($p < 0.001$), respectively. On day 70, EL4 had the highest growth rate in 30 mM acetic acid followed by EL3 in 28 mM acetic acid and EL2 in 26 mM acetic acid. The lowest growth rate was observed for EL1 in the presence of 26 mM acetic acid after day 2, and no change in its growth rate was observed after day 70 ($p > 0.05$).

3.3. Effect of ALE on the MIC of human antibiotics in the evolutionary lineages

The MIC of ciprofloxacin, gentamycin, meropenem, streptomycin, and vancomycin was quantified in all the ELs using MTS (MIC test strips). MIC values of the antibiotics were quantified every 10 days starting from 2 days after the initiation of the ELs and ending after ALE day 70. The MIC of the antibiotics tested against EL1 and EL4 is shown in **Figure 4**. There were no significant differences in the MIC values of the antibiotics against EL1 between days 2 and 70. However, there was a significant difference in the MIC of ciprofloxacin ($p < 0.05$), gentamycin ($p < 0.01$), and meropenem ($p < 0.001$) against EL4 between days 32 and 70. Significant differences were also observed in EL3 against ciprofloxacin ($p < 0.001$) between ALE day 22 (2 days after the initiation of the evolutionary lineage) and day 70 of the ALE study. The MIC values of antibiotics against all the ELs are reported in **Supplementary Table 1**.

3.4. Comparative genomic analysis of acetic acid-evolved lineages

Genomic analysis of the evolutionary lineages was conducted after 70 ALE days to investigate the genetic determinants of the increased MIC against acetic acid and the human antibiotics tested. We generated a complete genome assembly of the WT *S.* Enteritidis using Illumina and Oxford Nanopore Technologies (ONT) sequencing. WT *S.* Enteritidis strain BAA-1045 whole-genome Illumina and Oxford Nanopore Technologies sequencing

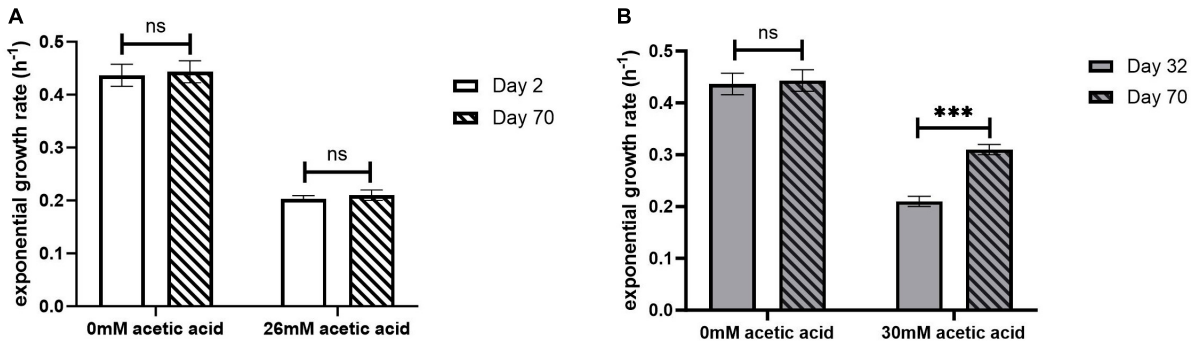

FIGURE 3
Exponential growth rate of EL1 **(A)** quantified on ALE days 2 and 70 and EL4 **(B)** quantified on ALE days 32 and 70 of *S.* Enteritidis evolutionary lines. ALE day 32 was the second day after the initiation of EL4 from EL3. *p*-value of 0.05 was considered to be statistically significant using two-tailed *t*-test. (***$p < 0.001$, ns, non-significant, = $p > 0.05$).

TABLE 1 Growth rates of adapted evolutionary lines.

Acetic acid used during ALE study	Acetic acid used for growth rate determination	Evolutionary lineages	Growth rate without acetic acid (h^{-1})		Growth rate with acetic acid (h^{-1})	
			Day 2	**Day 70**	**Day 2**	**Day 70**
0 mM	26 mM	EL1a	0.40	0.40	0.20	0.22
		EL1b	0.44	0.41	0.21	0.21
		EL1c	0.42	0.41	0.19	0.20
			Day 2	**Day 70**	**Day 2**	**Day 70****
26 mM	26 mM	EL2a	0.43	0.43	0.21	0.23
		EL2b	0.41	0.43	0.20	0.23
		EL2c	0.43	0.43	0.20	0.24
			Day 22	**Day 70**	**Day 22**	**Day 70****
28 mM	28 mM	EL3a	0.45	0.42	0.21	0.26
		EL3b	0.42	0.42	0.22	0.28
		EL3c	0.44	0.43	0.20	0.28
			Day 32	**Day 70**	**Day 32**	**Day 70*****
30 mM	30 mM	EL4a	0.47	0.45	0.21	0.31
		EL4b	0.46	0.47	0.20	0.32
		EL4c	0.45	0.47	0.20	0.33

Growth rates of the evolutionary lineages were quantified using the oCelloScope. Growth rates have been compared between ALE days 2 and 70 for EL1 and EL2, ALE days 22 and 70 for EL3, and ALE days 32 and 70 for EL4 in the presence and absence of acetic acid. For EL3 (a–c) and EL4 (a–c), days 22 and 32 were 2 days after the start of the evolutionary lines, respectively. For quantification of statistical significance, growth rates on day 2 for EL1 and EL2, day 22 for EL3, and day 32 for EL4 have been used as controls. Growth rates of the controls have been compared to that on ALE day 70 for EL1–EL4 in the presence and absence of acetic acid. Although EL1 was not adapted to acetic acid during the evolutionary process, for determination of growth rate using the oCelloScope, EL1 (a–c) and WT were treated with 26 mM acetic acid. For WT, the growth rates with and without 26 mM acetic acid were 0.21 (h^{-1}) and 0.40 (h^{-1}), respectively. Growth rates of all three replicates of EL1, EL2, EL3, and EL4 on ALE day 70 in the absence of acetic acid were found to be statistically non-significant ($p > 0.05$) as compared to the controls. Growth rates of all three replicates of EL1 between days 2 and 70 in the presence of 26 mM acetic acid were also found to be statistically non-significant ($p > 0.05$). However, the growth rates of EL2, EL3, and EL4 on ALE day 70 in the presence of 26, 28, and 30 mM acetic acid, respectively, were found to be statistically significant as compared to their control growth rates. Asterisks (*) in the table indicate significant differences in growth rates in comparison with the controls (**$p < 0.01$ and ***$p < 0.001$).

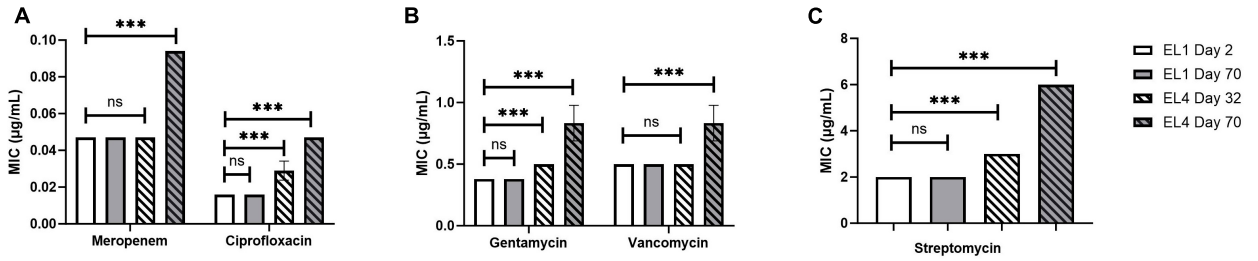

FIGURE 4
Change in MIC of human antibiotics against the *S.* Enteritidis evolutionary lineages EL1 (quantified on ALE days 2 and 70) and EL4 (quantified on ALE days 32 and 70). The antibiotics tested are meropenem and ciprofloxacin **(A)**, gentamycin and vancomycin **(B)**, and streptomycin **(C)**. EL1 was grown and adapted in TSB without stress throughout the ALE study, and EL4 was adapted in 30 mM acetic acid with initial transfer from EL3 on ALE day 30. *p*-value of 0.05 was considered to be statistically significant using two-tailed *t*-test. (***$p < 0.001$, ns, non-significant, = $p > 0.05$).

data are available for wild-type and evolved lineages (Illumina only) under the NCBI BioProject PRJNA1007881. The genome was assembled into four contigs consisting of the circular genome (~4.67 Mb) and three plasmids with approximate sizes of 60 kb (*S.* Enteritidis strain RM2968 plasmid pRM2968-2), 56 kb (*S.* Enteritidis strain 56-3991 plasmid pSE56-3991), and 6.2 kb (*E. coli* strain RHB18-C20 plasmid pRHB18-C20_4) based on the best hits (*e*-value < 0.01, query coverage >99%, and percent identity >99.9%) against the NCBI Nucleotide Collection (nt) database (Johnson et al., 2008).

This high-quality genome assembly and annotation was used as a reference to map Illumina whole-genome sequencing data for each EL. The mutations observed within each evolved lineage are detailed in Table 2. We identified 8, 10, 3, and 5 base substitutions in EL1, EL2, EL3, and EL4, respectively. Base substitutions were observed in a total of 15 different genes (10 missense; 3 synonymous; 2 frameshift). Notably, missense mutations were observed in the histidine kinase gene, *phoQ*, among lineages EL2, EL3, and EL4. Moreover, missense mutations were observed in EL2 within *phoP*, which is the regulatory protein of *phoQ*. For

TABLE 2 Mutations in evolutionary lines after adaptation in acetic acid for 70 ALE days identified using genomic analysis.

Position	Gene	Mutation	Ancestor allele	Evolved allele	Protein product	EL1	EL2	EL3	EL4
869465	*ptsP*	Missense	T	C	Phosphoenolpyruvate-dependent phosphotransferase system	R3: p.Tyr290His	R2: p.Tyr290His	X	x
2024345	*nimT*	Synonymous	C	T	2-nitroimidazole transporter	R1: p.Leu151Leu R2: p.Leu151Leu R3: p.Leu151Leu	R2: p.Leu151Leu	x	x
923432	*barA*	Missense	T	G	Signal transduction histidine-protein kinase BarA	x	R2: p.Thr268Pro	x	x
1061536	*alaS*	Missense	C	T	Alanine—tRNA ligase	x	R2: p.Gly272Gly	x	x
1973318	*phoQ*	Missense	T	G	Virulence sensor histidine kinase PhoQ	x	R2: p.Thr271Pro	x	x
1974384	*phoP*	Missense	C	T	Virulence transcriptional regulatory protein PhoP	x	R1: p.Arg140Gln R3: p.Arg140Gln	x	x
2015140	*zinT*	Frameshift	TAT	TAAT	Metal-binding protein ZinT	x	R2: p.Tyr200fs	x	x
3402681	*ybaY*	Frameshift	GTTTCA	GTTCA	putative lipoprotein YbaY	x	R1: p.Lys135fs	x	x
3675976	*fhuA*	Missense	G	T	Ferrichrome outer membrane transporter/phage receptor	x	R1: p.Ser318Arg R3: p.Ser318Arg	x	x
4348457	*rpoB*	Missense	A	C	DNA-directed RNA polymerase subunit beta	x	R1: p.Ser662Ala R3: p.Ser662Ala	x	x
1745485	*rfbE*	Missense	A	T	CDP-paratose 2-epimerase	x	x	R1: p.Asn220Tyr R2: p.Asn220Tyr R3: p.Asn220Tyr	R1: p.Asn220Tyr R2: p.Asn220Tyr R3: p.Asn220Tyr
1972868	*phoQ*	Missense	T	G	Virulence sensor histidine kinase PhoQ	x	x	R1: p.Ile421Leu R2: p.Ile421Leu R3: p.Ile421Leu	R1: p.Ile421Leu R2: p.Ile421Leu R3: p.Ile421Leu
3776974	*thiB*	Missense	AACGGTG ACGGTGA	AACGGTGACG GTGACGGTGA	Thiamine-binding periplasmic protein	x	x	R1: p.Val193_Thr194dup R2: p.Val193_Thr194dup R3: p.Val193_Thr194dup	R1: p.Val193_Thr194dup R2: p.Val193_Thr194dup R3: p.Val193_Thr194dup
4,39,516	*tuf1*	Synonymous	C	T	Elongation factor Tu 1	x	x	x	R3: p. His320His
5,18,130	*oadB*	Synonymous	T	C	Oxaloacetate decarboxylase beta chain	x	x	x	R3: p. Leu85Leu
14,77,186	*[ackA]–[hxpA]*	Deletion	Δ2,207βπ	x	Acetate kinase-Hexitol phosphatase	x	x	R1: Δ2,207 bp R2: Δ2,207 bp	R1: Δ2,207 bp R2: Δ2,207 bp R3: Δ2,207 bp

All the evolutionary lineages were mapped to the parent genome of *Salmonella enterica* serovar Enteritidis BAA-1045. R1, R2, and R3 refer to the three replicates in each evolutionary lineage. "X" refers to the absence of the specific mutation in that evolutionary lineage.

10.3389/fmicb.2023.1285421

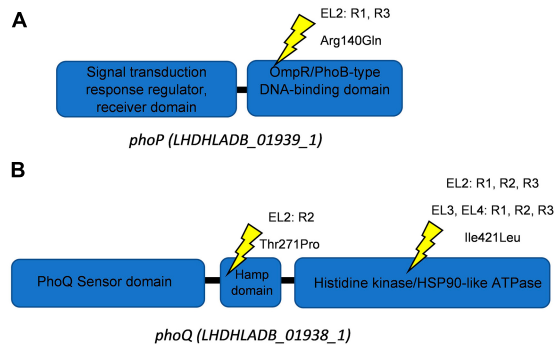

FIGURE 5
Schematics of PhoQ and PhoP proteins. Ellipses show protein domains with their respective Interpro identifiers for PhoP **(A)** and PhoQ **(B)**. Yellow symbols represent locations of missense mutations. The EL (evolutionary lineage), replicate (each EL had three replicates namely R1-R3), and amino acid substitution are provided for each site.

the PhoP protein, mutations were observed in the DNA-binding domain, while in the PhoQ protein, mutations occurred in the HAMP domain and the histidine kinase domain (**Figure 5**).

We used the Large-Scale Blast Ratio (LS-BSR) pipeline (Sahl et al., 2014) to compare the genetic changes in the acid-adapted evolutionary lineages after 70 days. This helped us investigate the potential gain or loss of entire coding sequences in the evolved lineages (**Figure 7**). Additionally, a 2,207 bp deletion was observed in replicate 1 and replicate 2 of EL3 and all three replicates of EL4 (**Figure 6**). Read-depth analysis was used to map the deletion of genes between *ackA* and *hxpA* in EL4 and has been compared to WT *S.* Enteritidis as shown in **Figure 6**. This deleted region in the evolved lineage is relative to the ancestral genome as the genomic region is present in the ancestral genome, but no reads map to that region in the evolved lines, although they do map to the flanking regions.

The BLASTX and InterPro analysis suggests that there were two hypothetical proteins within the deleted range that are homologous to genes *yfbV* and *yfbU*. The read-depth analysis shows that a fraction of *ackA* and *hxpA* has been deleted, while the two hypothetical proteins *yfbV* and *yfbU* have been deleted entirely in EL4 as compared to the WT. The gene yfbV is a cytoplasmic protein that is predicted to be involved in chromosome segregation in *E. coli* (Miyakoshi et al., 2019), and the *yfbU* gene is known to play a role in DNA damage response in *E. coli* (Amitai et al., 2009). Studying the boundaries of the deleted region in EL4 indicates that by examining the extent of the reduction in read depth, it is also possible to estimate the size or length of the deleted region. This information is crucial for understanding the impact of the deletion on the affected genes. In our study, since only a fraction of *ackA* and *hxpA* is deleted, it is possible that a truncated version of the proteins is being expressed.

4. Discussion

This study describes the adaptation and evolution of *Salmonella* Enteritidis to different concentrations of acetic acid in TSB using adaptive laboratory evolution (ALE). The increase in MIC values of EL2, EL3, and EL4 over time suggests that *S.* Enteritidis can adapt to sub-inhibitory concentrations of acetic acid during prolonged acid exposure.

The oCelloScope is a valuable tool for studying the effects of antimicrobial compounds on bacterial growth kinetics and can be used to investigate the adaptation of bacteria to various stress conditions (Fredborg et al., 2013, 2015; McLaughlin et al., 2017). We used it to study the effects of acetic acid stress on the exponential hourly growth rate of the evolved lineages and compared them to the growth rate of WT *S.* Enteritidis. Our results indicate that the growth rates of the evolved lineages in the presence of acetic acid were dependent on the concentration of acid used during the evolutionary process (**Figure 3**, **Table 1** and **Supplementary Figure 2**). Since EL1 was adapted without any acid stress throughout the ALE study, there were no significant differences in the exponential growth rate of its three replicates between ALE days 2 and 70 after exposure to 26 mM acetic acid in the oCelloScope. The exponential growth rates of EL1 recovered from days 2 and 70 in the presence and absence of 26 mM acetic acid were 0.2 (h^{-1}) and 0.4 (h^{-1}), respectively. These values were similar to the exponential growth rate of WT *S.* Enteritidis in the presence and absence of 26 mM acetic acid as monitored using the oCelloScope. The growth rates of EL2–EL4 on ALE day 70 were significantly higher than the values 2 days after the initiation of the corresponding evolutionary lineages ($p < 0.01$). Other researchers have demonstrated that adaptation in stress environments caused an increase in the growth rate of *E. coli* during ALE studies (Fong et al., 2005; Cheng et al., 2014; LaCroix et al., 2015).

Next, we aimed to investigate whether long-term exposure to acetic acid in the evolutionary lineages led to cross-resistance against human antibiotics (**Figure 4**). The different classes of antibiotics used in this study against *S. enterica* have been tested in earlier studies (Georgnaras and von Holy, 2001; Jones et al., 2002; Muhammad et al., 2010; Chang et al., 2021). Studies in *E. coli* have found that resistance against antibiotics changes over the course of ALE studies (Maeda et al., 2020; Marciano et al., 2022). *E. coli* strains sensitive to carbapenem were found to develop resistance against carbapenems by the 15th generation in another ALE study (Geng et al., 2022). Ciprofloxacin has historically been used as the first line of defense against *S. enterica* infections, especially against many multidrug-resistant (MDR) strains (Askoura and Hegazy, 2020). Carbapenems (meropenem) have also been used successfully for the treatment of *S. enterica* infections, especially the ones that are resistant to cefotaxime and ciprofloxacin (Jean et al., 2005). Using antibiotics with distinct mechanisms of action provides us with a more comprehensive understanding of the evolution of resistance in evolved populations.

We did not observe significant changes in the MIC of the antibiotics tested against EL1 between days 2 and 70, likely due to the lack of any selective pressure on EL1 in the ALE study. In contrast, significant increases in the MIC values of ciprofloxacin, gentamycin, and meropenem against EL 4 ($p < 0.05$) (**Figure 4** and **Supplementary Table 1**) were observed after day 70. This highlights that exposure to acid stress provides cross-adaptation against antibiotic stress in *S. enterica* acid-evolved populations. This result is in line with previous studies demonstrating that exposure to low concentrations of stress over time in *S. enterica*

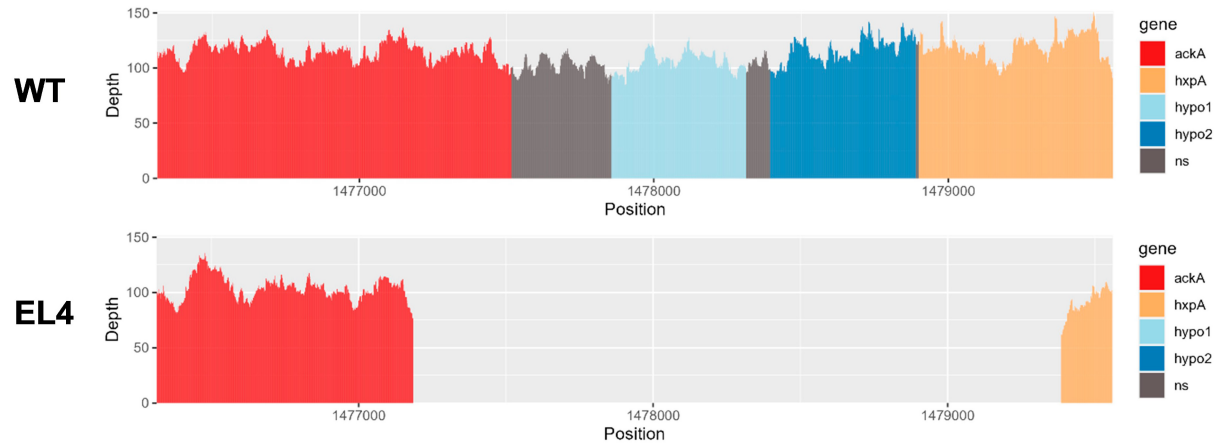

FIGURE 6
Read-depth analysis of the deletion observed between the genes *ackA* and *hxp2* in EL4. The read depth of EL4 has been compared to the wild-type (WT) strain of *S. enterica* serovar Enteritidis BAA-1045. Genes *ackA* and *hxpA* encode for acetate kinase and hexitol phosphatase in *S.* Enteritidis, respectively, and hypo1 and hypo2 stand for hypothetical protein 1 and hypothetical protein 2, respectively.

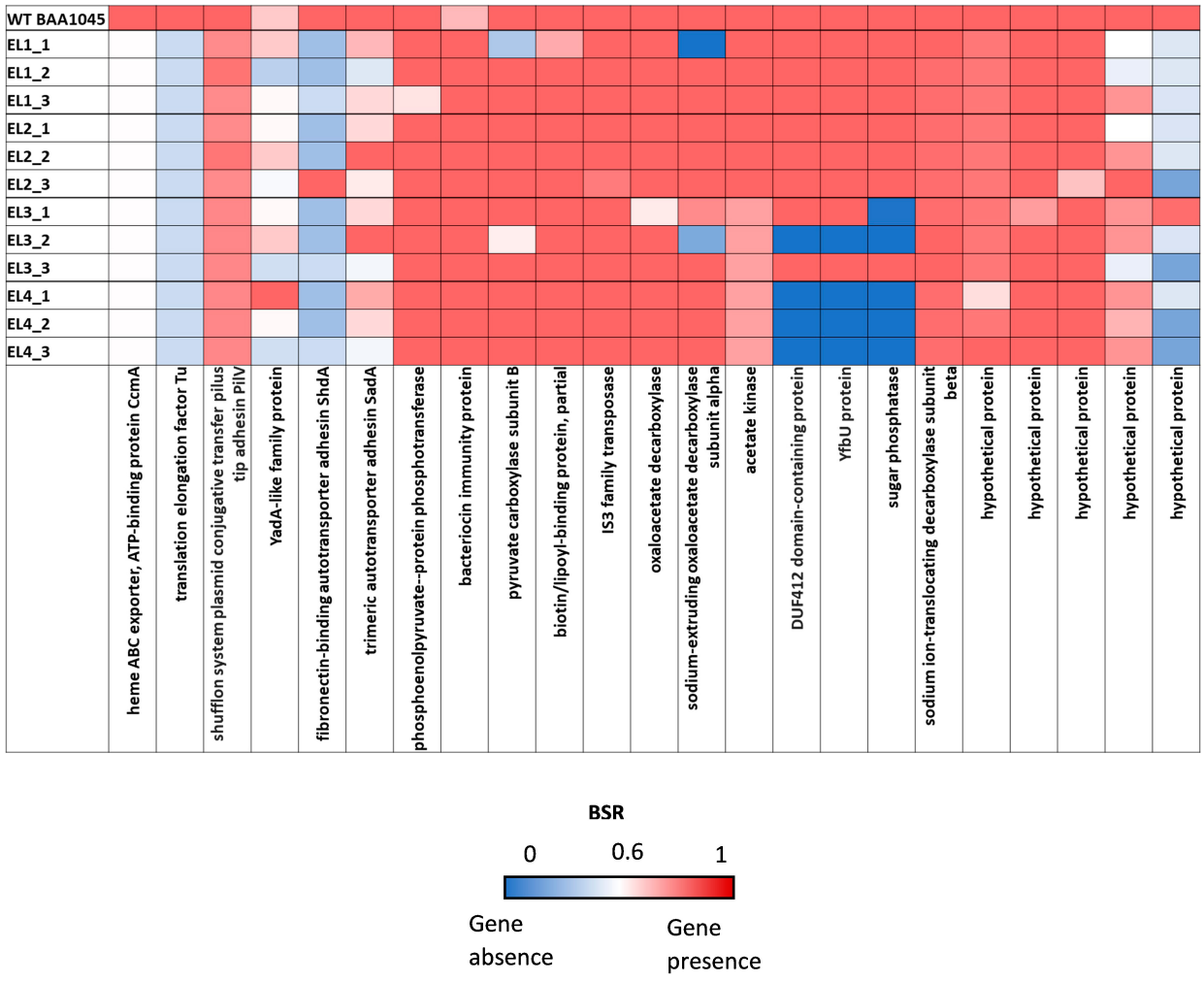

FIGURE 7
Large-Scale Blast Score Ratio (LS-BSR) heatmap of the three replicates of the evolutionary lineages EL1-EL4 after 70 ALE days.

leads to increased MIC against antibiotics (Gullberg et al., 2011; Wistrand-Yuen et al., 2018).

Even though the MIC against the various antibiotics, especially, ciprofloxacin, gentamycin, and meropenem, was found to significantly increase after 70 ALE days, their resultant MIC values still fell within the susceptible range as defined by established clinical breakpoints (FDA, 2023). Despite this, there remains a pertinent cause for concern regarding the increase in MIC values as this suggests that the ELs exposed to acid stress displayed a reduced susceptibility to the antibiotics over time. The rise in MIC values, albeit within the susceptible range, potentially signifies the presence of underlying mechanisms that contribute to reduced antibiotic effectiveness. Such alterations in MIC values hint at adaptive responses in *S. enterica* under acid stress, which could subsequently impact the overall efficacy of antibiotic treatment strategies. This finding also raises concerns about the potential for acidic conditions, such as those encountered during food processing, which may inadvertently contribute to the development of antibiotic-resistant bacterial populations.

The observed differences in growth rate and increase in MIC of acetic acid and antibiotics over time suggest the presence of genetic changes enabling the ELs to adapt to the selective pressure of acid. Long-term exposures to acid stress have been reported to be associated with mutations at the genomic level in *E. coli* (Du et al., 2020; Zeng et al., 2021), which can alter the bacterial cell structure, physiology, and metabolism leading to multidrug resistance (MDR). However, when the ELs from day 70 were desiccated on the surface of stainless-steel coupons for 18 h and subsequently exposed to 100 mM acetic acid using previously established methods (Ghoshal et al., 2022a), no significant differences between the log reduction of the ELs and WT *S.* Enteritidis were observed (**Supplementary Figure 3**). This could be due to the fact that bacterial adaptation to a specific stressor often involves the optimization of cellular mechanisms and regulatory pathways to withstand the stress within a limited concentration range (Mongold et al., 1999). In the case of acetic acid, the acid-adapted bacteria may have undergone genotypic and phenotypic changes such as alterations in membrane permeability, efflux pump activity, intracellular pH regulation, and activation of stress response systems that enable them to survive and proliferate in the presence of lower concentrations of acetic acid. However, when exposed to significantly higher concentrations, the stress exceeds the threshold of their adaptive response, leading to a loss of viability and growth inhibition.

Mutations in the outer membrane lipoproteins and membrane transporters are known to alter the binding properties of bacterial membranes which increase resistance against various antibiotics such as vancomycin and meropenem (Langsrud et al., 2004; Maldonado et al., 2016). We observed mutations in the outer membrane lipoprotein *ybaY* as well as mutations in the outer membrane transporter *fhuA* in the acid-adapted *S.* Enteritidis lineages, and it is possible that these mutations rendered the outer membrane less susceptible to antibiotics. Additionally, periplasmic binding proteins help gram-negative pathogens sense their environment, regulate the uptake of small molecules, and even provide antibiotic resistance in *S. enterica* (Blair et al., 2009). Mutations observed in the thiamine-binding periplasmic protein in EL3 and EL4 as well as in the metal-binding protein *zinT* in EL2 could have possibly played a role in providing antibiotic cross-resistance after acid adaptation.

In *E. coli*, exposure to antimicrobial compounds such as benzalkonium chloride (BAC) has been reported to induce cross-resistance against other antimicrobial compounds and antibiotics (Chapman, 2003; Langsrud et al., 2004). The acquisition of antibiotic resistance in these studies was mainly attributed to the differential expression of bacterial efflux pumps and several outer membrane proteins. Changes in the expression of efflux pumps promote resistance against several classes of antibiotics (Jibril et al., 2021; Dawan et al., 2022). A variety of *Salmonella* strains also differentially express enzymes that can modify and inactivate antibiotics such as streptomycin (Mengistu et al., 2020). Upregulation in the expression of several transcription factors, which are global regulators of stress, is also known to trigger multidrug resistance in *E. coli* (Duval and Lister, 2013). Future RNA sequencing studies on the acid-adapted lineages of *S.* Enteritidis will help to determine the influence of efflux pumps, membrane proteins, and transcription factors in providing cross-resistance against antibiotics. The two-component signal transduction system *PhoP/Q* is reported to provide general cellular defense against stressful conditions and antibiotic resistance in *E. coli* and *S.* Enteritidis (Lázár et al., 2014; Hu et al., 2023). A hypothesis is that the mutations observed in *phoP* and *phoQ* observed in our study played an important role in triggering cross-adaptation against antibiotics in the acid-evolved *S. enterica* lineages.

Additionally, the phenomenon of persistence is triggered in bacteria after exposure to various stressful environments which renders them resistant to future stressors such as exposure to antibiotics (Pacios et al., 2020). Persistence is known to provide *E. coli* with tolerance and resistance against several antibiotics (Li and Zhang, 2007), and short-term exposure to acid stress is reported to trigger persistence in *S. enterica* (Leyer and Johnson, 1992). We hypothesize that reduced susceptibility to the antibiotics could be in part due to the presence of persister cells in the subpopulation of the acid-evolved *S. enterica* lineages. It is also possible that cross-resistance to antibiotics in *S.* Enteritidis acid-evolved lineages is due to a combination of the factors described above.

Genomic analysis of the acetic acid-evolved ELs revealed base substitutions in 15 different genes (**Table 2**), including missense mutations in multiple ELs in *phoQ* and *phoP*. The PhoQ protein is known to control the transcription of a large class of genes (Prost et al., 2007), and the PhoP/Q system is triggered under conditions of low pH and in the presence of antimicrobial and cationic peptides in *S. enterica* (Bearson et al., 1998; Prost et al., 2007; Yuan et al., 2017). Activation of this system is known to regulate *S. enterica* virulence and pathogenesis (Prost et al., 2007). In addition, the PhoP/Q protein system has been reported to be involved in stress resistance and antibiotic resistance and in the regulation of envelope composition in *S. enterica* (Yuan et al., 2017; Shprung et al., 2021; Dawan and Ahn, 2022).

The presence of mutations in the *phoP/Q* genes in all three replicates of EL2, EL3, and EL4 and its absence in EL1 indicate that these mutations are a result of the adaptation to acetic acid stress. One of the mutations observed in *phoQ* in EL2 was in the HAMP domain of the protein (**Figure 5**), which is thought to play an important role in transmitting signal to the catalytic domain of the protein (Lemmin et al., 2013). Base substitutions

in the protein PhoQ Asn255Ileu have been reported where an amino acid with a neutral polar R group was replaced by a neutral non-polar R group under stress conditions (Matamouros et al., 2015) which is similar to our case (Thr271Pro). Researchers found that the Asn255Ileu substitution significantly increased the activity of the PhoQ protein (over 10-fold increase in activity) and that the mutant protein was found to spend more time in the activation state than the wild-type protein (Matamouros et al., 2015). It is possible that the mutation in our system also led to a similar increase in the activity of the PhoP protein. We also observed base substitutions in the sensor histidine kinase domain of *phoQ* in EL3 and EL4, which serves as the catalytic domain and regulates/activates the phosphoryl-state of the protein (Lemmin et al., 2013). Additionally, we observed a mutation in EL2 in the OmpR/PhoB-type DNA-binding domain of *phoP* (**Figure 5**). In this case, arginine, which is a basic amino acid, was replaced by glutamine, which is polar in nature, and at low pH, such amino acids acquire an overall positive charge. This positively charged amino acid in DNA-binding domains of proteins aids in more effective binding with negatively charged DNA (Cherstvy, 2009), and such modifications in response regulators are often associated with differential changes in gene expression of downstream genes (Rhee et al., 2008). It is possible that the mutations in *phoP/Q* among the ELs contributed to the reduced susceptibility against the antibiotics causing a differential expression of stress and acid adaptation genes. Mutations in the *phoPQ* system are associated with increased resistance against antibiotics in other gram-negative pathogens such as *Pseudomonas aeruginosa* (Miller et al., 2011). In our study, we have chosen to prioritize the investigation of missense mutations within the *phoP/Q* genes as a primary focus, while avoiding gene deletion studies. This strategic decision is grounded in several considerations. First, the existing body of literature provides substantial evidence suggesting that missense mutations in *phoP/Q* genes play a pivotal role in bacterial adaptations to stress conditions, including acid stress (Prost et al., 2007; Matamouros et al., 2015; Pitt et al., 2018). Moreover, planned RNA sequencing studies in future will offer valuable insights into the dynamic changes in the expression of *phoP/Q* genes in response to acid stress. These findings will complement our observations of missense mutations and help establish a multifaceted understanding of the molecular mechanisms underlying the adaptation process. By focusing on missense mutations in conjunction with transcriptomic analysis, we aim to provide a comprehensive perspective on the significance of *phoP/Q* genes in stress adaptation without resorting to gene deletions. This will help minimize potential disruptions to the overall cellular machinery and preserve the ecological relevance of our study.

In EL2, we found a mutation in the *fhuA* gene which encodes for the ferrichrome outer membrane transporter. This mutation was present in all three replicates of EL2, suggesting that it was not random and probably associated with the adaptive evolution in acetic acid. The gene *fhuA* is involved in the transport of antibiotics such as albomycin and rifamycin, and bacteriophages and toxins such as colicin M inside *E. coli* cells (Braun et al., 2002). Mutations in this gene have been reported in *E. coli* and *S. enterica* under stress conditions, which enable the bacteria to escape from future attacks of antibiotics while maintaining its siderophore uptake activity that is essential for the survival of the bacteria (Wang et al., 2018). Additionally, two of the three replicates of EL2 showed mutations in the *rpoB* gene, which is usually targeted by antibiotics such as rifampicin in *E. coli* and *S. enterica* (Björkman et al., 1998). Several studies have shown that mutations in the *rpoB* gene lead to resistance against rifampicin and other similar antibiotics in *E. coli* and *S. enterica* (Björkman et al., 1998; Garibyan et al., 2003; Rodríguez-Verdugo et al., 2013). Mutations in *rpoB* are also known to be triggered during stress conditions in antibiotic-free environments (Rodríguez-Verdugo et al., 2013). This is similar to our study, where mutations in *rpoB* gene were triggered during adaptation to acid stress in the absence of antibiotics. Another gene that was mutated in all three replicates of EL3 and EL4 is *rfbE*, which is involved in the synthesis of the O-antigen in *E. coli* and the *rbf* gene cluster is known to be involved in the synthesis of the O-antigen of cell wall LPS in *S. enterica* and other gram-negative Enterobacteriaceae (Iguchi et al., 2011; Cota et al., 2015). The O-antigen is involved in the pathogenesis and virulence of *S. enterica* (Murray et al., 2003). Mutations in the O-antigen in the cell wall LPS are likely to affect the conformation and function of various surface proteins. The composition of the O-antigen affects bacterial surface charge, which is known to alter membrane permeability under changing pH conditions (Lerouge and Vanderleyden, 2002). We measured the surface charge of the ELs after 70 ALE days in acid stress and compared them to the surface charge of WT *S.* Enteritidis to study whether acid adaptation caused any changes in the surface charge. No significant differences in the surface charge of the ELs were observed as compared to the WT *S.* Enteritidis after 70 ALE days ($p > 0.05$) (**Supplementary Table 2**). Furthermore, the gene *thiB* that encodes for the thiamine-binding periplasmic protein was found to be mutated in the three replicates of EL3 and EL4. The presence of environmental stresses has been reported to cause mutations in genes involved in thiamine biosynthesis and transport in yeast cells (Kartal et al., 2018).

Finally, the deletion of 2207 bp of the genome in two replicates of EL3 and all three replicates of EL4 was observed. There were two major genes in this region, namely, *ackA*, which encodes for acetate kinase, and *hxpA*, which encodes for hexitol phosphatase. The gene *ackA* encodes for acetate kinase that is involved in the production of acetate from acetyl phosphate (Kumari et al., 2000). Deletion of this gene could be attributed to the presence of large amounts of acetate available during acetic acid stress, and hence, the need for this enzyme was significantly reduced in the ELs. Even though the *ackA* gene is also involved in the conversion of acetate to acetyl phosphate, which is a precursor to acetyl-CoA, there is an alternative pathway for the synthesis of acetyl-CoA from acetate (Kumari et al., 1995). This pathway is catalyzed by the enzyme acetyl-CoA synthase, and it is commonly used by cells during stressful conditions such as nutrient limitation, low oxygen pressure (De Mets et al., 2019), and, possibly, acid stress.

Since EL2 is the primary ancestor of the evolutionary lineages EL3 and EL4, we studied the genomes of EL2–EL4 to look for any common mutations that may have occurred before ALE day 20 and subsequently passed on to EL3 and EL4. We did not observe any common mutations in EL2–EL4 suggesting that most of the mutations observed in EL2 happened after ALE day 20 when EL3 diverged from EL2. Even though replicate 2 of EL2 and all three

replicates of EL3 and EL4 had mutations in the *phoQ* gene, the positions of this mutation in EL3 and EL4 were different from EL2, indicating these occurred after ALE day 20. Missense mutations in *rfbE*, *phoQ*, and *thiB* were identical between EL3 and EL4, which suggests that these mutations occurred between ALE day 20 (after the split of EL3 from EL2) and ALE day 30 (before the initiation of EL4 from EL3). SNPs in certain genes such as *tuf1* and *oadB* were observed in EL4 alone, indicating these mutations occurred after ALE day 30 when EL4 was split from EL3. EL3 and EL4 demonstrated a 2207 base pair mutation between genes *ackA* and *hxpA*. In EL3 and EL4, this mutation was observed in replicates 1 and 2, which possibly indicates that they were carried from EL3 to EL4.

Although our study is one of the first of its kind to study acid adaptation in *S. enterica*, prior studies have revealed the effects of acid adaptation in *E. coli*, which is a related gram-negative pathogen. Harden et al. (2015) documented that *E. coli* K12 lineages exposed to acid conditions exhibit enhanced growth rates and improved fitness. The same phenomenon was replicated in our investigation, where we observed an increase in growth rates among acid-evolved *S. enterica* lineages when subjected to acidic conditions. Other researchers have also independently corroborated these findings by demonstrating increased growth rates and enhanced survival in acid-evolved *E. coli* lineages exposed to acidic environments (He et al., 2017; Du et al., 2020). These researchers also reported that the acid-evolved *E. coli* lineages had mutations in the RNA polymerase subunits. Our study supports these findings as we also observed mutations in the RNA polymerase subunit beta in EL2. These findings suggest that RNA polymerases play an important role in acid stress adaptation in many gram-negative pathogens. Mutations in the RNA polymerase can lead to changes in gene expression, which could affect the production of acid-resistant proteins, the transport of protons out of the cell, or other cellular processes that are important for acid survival.

The results of this study highlight that adaptation to acetic acid stress is associated with genotypic and phenotypic changes in *S. enterica*. Similar genetic and phenotypic changes in *Salmonella* are expected if other organic acids with similar chain lengths and mechanisms of action against *S. enterica* were used during the adaptive process. The increased MIC of the ELs against both acetic acid and human antibiotics raises concerns regarding the development of cross-resistance and the potential emergence of multidrug-resistant *S. enterica*. Although the specific mechanisms associated with the cross-resistance remain to be elucidated, it is plausible that the mutations identified in the *phoPQ* system and other stress-related genes along with the gene deletions contribute to a broader adaptive response, leading to increased resistance against multiple stressors, including antibiotics.

5. Conclusion

Understanding the genetic mechanisms associated with acid stress adaptation can lead to targeted interventions and therapies to combat antimicrobial resistance. The uniqueness of our study lies in the fact that it is the first of its kind (to the best of our knowledge) to apply adaptive laboratory evolution for studying the adaptation of *S. enterica* under acid stress. The findings of this study have implications for food safety and demonstrate the utility of the ALE approach in studying the evolution and adaptation of foodborne pathogens to environmental stresses, particularly acid stress. Organic acids, especially acetic acid, are often used as additives for flavoring and preserving different foods and for cleaning and sanitization (Mani-López et al., 2012; Coban, 2020). It is possible that *S. enterica*, present as a contaminant in the food industry, is exposed to sub-lethal levels of acetic acid. The results of this study highlight that under such conditions, *S. enterica* will be able to adapt and evolve in acid stress. This might lead to enhanced persistence and survival of the bacteria, leading to a higher risk of contamination of food products during processing. The increase in MIC against human antibiotics in the acid-adapted *S. enterica* strains can also pose a significant public health risk. The results of this ALE study emphasize the need for continuous evaluation and optimization of sanitization protocols to ensure their efficacy against emerging antibiotic-resistant pathogens. Finally, this study underscores the need for comprehensive approaches to combat antimicrobial resistance, including the prudent use of acid-based antimicrobials and the development of alternative antimicrobial strategies.

Data availability statement

The datasets presented in this study can be found in online repositories. The names of the repository/repositories and accession number(s) can be found in the article/**Supplementary material**.

Author contributions

MG: Conceptualization, Data curation, Investigation, Methodology, Writing – original draft, Writing – review and editing. TB: Formal analysis, Methodology, Writing – original draft. JG: Conceptualization, Software, Supervision, Visualization, Writing – review and editing. LM: Conceptualization, Funding acquisition, Methodology, Project administration, Resources, Supervision, Writing – review and editing.

Funding

The author(s) declare financial support was received for the research, authorship, and/or publication of this article. This work was by a Rapid Research Grant through the University of Massachusetts, Amherst Graduate School (to MG), supported by the National Institute of Food and Agriculture (NIFA), the U.S. Department of Agriculture (USDA), and the Center for Agriculture, Food, and the Environment and the Department of Food Science at the University of Massachusetts-Amherst, under project number MAS00567, with support from the Foundational and Applied Science Program (grant number 2020-67017-30786) (to LM).

Conflict of interest

The authors declare that the research was conducted in the absence of any commercial or financial relationships that could be construed as a potential conflict of interest.

Publisher's note

All claims expressed in this article are solely those of the authors and do not necessarily represent those of their affiliated organizations, or those of the publisher, the editors and the reviewers. Any product that may be evaluated in this article, or claim that may be made by its manufacturer, is not guaranteed or endorsed by the publisher.

Supplementary material

The Supplementary Material for this article can be found online at: https://www.frontiersin.org/articles/10.3389/fmicb.2023.1285421/full#supplementary-material

References

Álvarez-Ordóñez, A., Prieto, M., Bernardo, A., Hill, C., and López, M. (2012). The acid tolerance response of *Salmonella* spp.: An adaptive strategy to survive in stressful environments prevailing in foods and the host. *Food Res. Int.* 45, 482–492.

Amitai, S., Kolodkin-Gal, I., Hananya-Meltabashi, M., Sacher, A., and Engelberg-Kulka, H. (2009). *Escherichia coli* MazF leads to the simultaneous selective synthesis of both "death proteins" and "survival proteins". *PLoS Genet.* 5:e1000390. doi: 10.1371/journal.pgen.1000390

Anton Bankevich, S., Dmitry Antipov, N., Alexey, A., Gurevich, Mikhail Dvorkin, Alexander, S., et al. (2012). SPAdes: A new genome assembly algorithm and its applications to single-cell sequencing. *J. Comput. Biol.* 19, 455–477.

Askoura, M., and Hegazy, W. A. H. (2020). Ciprofloxacin interferes with *Salmonella Typhimurium* intracellular survival and host virulence through repression of *Salmonella* pathogenicity island-2 (SPI-2) genes expression. *Pathog. Dis.* 78:ftaa011. doi: 10.1093/femspd/ftaa011

Athamneh, A. I. M., Alajlouni, R. A., Wallace, R. S., Seleem, M. N., and Senger, R. S. (2014). Phenotypic profiling of antibiotic response signatures in *Escherichia coli* using raman spectroscopy. *Antimicrob. Agents Chemother.* 58, 1302–1314. doi: 10.1128/AAC.02098-13

Bearson, B. L., Wilson, L., and Foster, J. W. (1998). A low pH-inducible, PhoPQ-dependent acid tolerance response protects *Salmonella typhimurium* against inorganic acid stress. *J. Bacteriol.* 180, 2409–2417. doi: 10.1128/JB.180.9.2409-2417.1998

Björkman, J., Hughes, D., and Andersson, D. I. (1998). Virulence of antibiotic-resistant *Salmonella typhimurium*. *Proc. Natl. Acad. Sci. U.S.A.* 95, 3949–3953.

Blair, J. M. A., La Ragione, R. M., Woodward, M. J., and Piddock, L. J. V. (2009). Periplasmic adaptor protein AcrA has a distinct role in the antibiotic resistance and virulence of *Salmonella enterica* serovar Typhimurium. *J. Antimicrob. Chemother.* 64, 965–972. doi: 10.1093/jac/dkp311

Brandl, M. T., Pan, Z., Huynh, S., Zhu, Y., and McHugh, T. H. (2008). Reduction of *Salmonella* enteritidis population sizes on almond kernels with infrared heat. *J. Food Protect.* 71, 897–902. doi: 10.4315/0362-028x-71.5.897

Braun, M., Killmann, H., Maier, E., Benz, R., and Braun, V. (2002). Diffusion through channel derivatives of the *Escherichia coli* FhuA transport protein. *Eur. J. Biochem.* 269, 4948–4959. doi: 10.1046/j.1432-1033.2002.03195.x

Canali, C., Spillum, E., Valvik, M., Agersnap, N., and Olesen, T. (2018). Real-time digital bright field technology for rapid antibiotic susceptibility testing. *Methods Mol. Biol.* 1736, 75–84. doi: 10.1007/978-1-4939-7638-6_7

Chang, M.-X., Zhang, J.-F., Sun, Y.-H., Li, R.-S., Lin, X.-L., Yang, L., et al. (2021). Contribution of different mechanisms to ciprofloxacin resistance in *Salmonella* spp. *Front. Microbiol.* 12:663731. doi: 10.3389/fmicb.2021.663731663731

Chapman, J. S. (2003). Disinfectant resistance mechanisms, cross-resistance, and co-resistance. *Int. Biodeteriorat. Biodegradat.* 51, 271–276. doi: 10.1093/jac/49.4.631

Cheng, K.-K., Lee, B.-S., Masuda, T., Ito, T., Ikeda, K., Hirayama, A., et al. (2014). Global metabolic network reorganization by adaptive mutations allows fast growth of *Escherichia coli* on glycerol. *Nat. Commun.* 5:3233. doi: 10.1038/ncomms4233

Cherstvy, A. G. (2009). Positively charged residues in DNA-binding domains of structural proteins follow sequence-specific positions of DNA phosphate groups. *J. Phys. Chem. B* 113, 4242–4247. doi: 10.1021/jp810009s

Cingolani, P., Platts, A., Wang, L. L., Coon, M., Nguyen, T., Wang, L., et al. (2012). A program for annotating and predicting the effects of single nucleotide polymorphisms, SnpEff. *Fly* 6, 80–92. doi: 10.4161/fly.19695

Coban, H. B. (2020). Organic acids as antimicrobial food agents: Applications and microbial productions. *Bioprocess Biosyst. Eng.* 43, 569–591.

Cota, I., Sánchez-Romero, M. A., Hernández, S. B., Pucciarelli, M. G., García-del Portillo, F., and Casadesús, J. (2015). Epigenetic control of *Salmonella enterica* O-Antigen chain length: A tradeoff between virulence and bacteriophage resistance. *PLoS Genet.* 11:e1005667. doi: 10.1371/journal.pgen.1005667

Danecek, P., Bonfield, J. K., Liddle, J., Marshall, J., Ohan, V., Pollard, M. O., et al. (2021). Twelve years of SAMtools and BCFtools. *GigaScience* 10:giab008. doi: 10.1093/gigascience/giab008

Dawan, J., and Ahn, J. (2022). Bacterial stress responses as potential targets in overcoming antibiotic resistance. *Microorganisms* 10:1385.

Dawan, J., Li, Y., Lu, F., He, X., and Ahn, J. (2022). Role of efflux pump-mediated antibiotic resistance in quorum sensing-regulated biofilm formation by *Salmonella* typhimurium. *Pathogens* 11:147. doi: 10.3390/pathogens11020147

De Mets, F., Van Melderen, L., and Gottesman, S. (2019). Regulation of acetate metabolism and coordination with the TCA cycle via a processed small RNA. *Proc. Natl. Acad. Sci. U.S.A.* 116, 1043–1052. doi: 10.1073/pnas.1815288116

Deatherage, D. E., and Barrick, J. E. (2014). Identification of mutations in laboratory-evolved microbes from next-generation sequencing data using breseq. *Methods Mol. Biol.* 1151, 165–188. doi: 10.1007/978-1-4939-0554-6_12

Deng, X., Li, Z., and Zhang, W. (2012). Transcriptome sequencing of *Salmonella enterica* serovar Enteritidis under desiccation and starvation stress in peanut oil. *Food Microbiol.* 30, 311–315. doi: 10.1016/j.fm.2011.11.001

Dragosits, M., and Mattanovich, D. (2013). Adaptive laboratory evolution – principles and applications for biotechnology. *Microb. Cell Fact.* 12:64.

Du, B., Olson, C. A., Sastry, A. V., Fang, X., Phaneuf, P. V., Chen, K., et al. (2020). Adaptive laboratory evolution of *Escherichia coli* under acid stress. *Microbiology* 166, 141–148. doi: 10.1099/mic.0.000867

Duval, V., and Lister, I. M. (2013). MarA, SoxS and Rob of *Escherichia coli* - Global regulators of multidrug resistance, virulence and stress response. *Int. J. Biotechnol. Wellness Ind.* 2, 101–124. doi: 10.6000/1927-3037.2013.02.03.2

FDA, (2023). *Federal NARMS partners.* Available online at: https://www.fda.gov/animal-veterinary/national-antimicrobial-resistance-monitoring-system/resources (accessed August 7, 2023).

Fong, S., Joyce, A., and Palsson, B. (2005). Parallel adaptive evolution cultures of *Escherichia coli* lead to convergent growth phenotypes with different gene expression states. *Genome Res.* 15, 1365–1372. doi: 10.1101/gr.3832305

Fredborg, M., Andersen, K. R., Jørgensen, E., Droce, A., Olesen, T., Jensen, B. B., et al. (2013). Real-time optical antimicrobial susceptibility testing. *J. Clin. Microbiol.* 51, 2047–2053.

Fredborg, M., Rosenvinge, F. S., Spillum, E., Kroghsbo, S., Wang, M., and Sondergaard, T. E. (2015). Rapid antimicrobial susceptibility testing of clinical isolates by digital time-lapse microscopy. *Eur. J. Clin. Microbiol. Infect. Dis.* 34, 2385–2394.

Garibyan, L., Huang, T., Kim, M., Wolff, E., Nguyen, A., Nguyen, T., et al. (2003). Use of the rpoB gene to determine the specificity of base substitution mutations on the *Escherichia coli* chromosome. *DNA Repair* 2, 593–608. doi: 10.1016/s1568-7864(03)00024-7

Garrison, E., and Marth, G. (2012). Haplotype-based variant detection from short-read sequencing. *BioArxiv*. [Preprint]. doi: 10.48550/arXiv.1207.3907

Geng, J., Liu, H., Chen, S., Long, J., Jin, Y., Yang, H., et al. (2022). Comparative genomic analysis of *Escherichia coli* strains obtained from continuous imipenem stress evolution. *FEMS Microbiol. Lett.* 369:fnac015. doi: 10.1093/femsle/fnac015

Geornaras, I., and von Holy, A. (2001). Antimicrobial susceptibilities of isolates of *Staphylococcus aureus*, Listeria species and *Salmonella* serotypes associated with

poultry processing. *Int. J. Food Microbiol.* 70, 29–35. doi: 10.1016/s0168-1605(01)00517-7

Ghoshal, M., Ryu, V., and McLandsborough, L. (2022b). Evaluation of the efficacy of antimicrobials against pathogens on food contact surfaces using a rapid microbial log reduction detection method. *Int. J. Food Microbiol.* 373:109699. doi: 10.1016/j.ijfoodmicro.2022.109699

Ghoshal, M., Chuang, S., Zhang, Y., and McLandsborough, L. (2022a). Efficacy of acidified oils against *Salmonella* in low-moisture environments. *Appl. Environ. Microbiol.* 88:e00935-22. doi: 10.1128/aem.00935-22

Gresham, D., and Dunham, M. J. (2014). The enduring utility of continuous culturing in experimental evolution. *Genomics* 104(6, Part A), 399–405. doi: 10.1016/j.ygeno.2014.09.015

Gullberg, E., Cao, S., Berg, O. G., Ilbäck, C., Sandegren, L., Hughes, D., et al. (2011). Selection of resistant bacteria at very low antibiotic concentrations. *PLoS Pathog.* 7:e1002158. doi: 10.1371/journal.ppat.1002158

Gurevich, A., Saveliev, V., Vyahhi, N., and Tesler, G. (2013). QUAST: Quality assessment tool for genome assemblies. *Bioinformatics* 29, 1072–1075.

Haft, D. H., DiCuccio, M., Badretdin, A., Brover, V., Chetvernin, V., O'Neill, K., et al. (2018). RefSeq: An update on prokaryotic genome annotation and curation. *Nucleic Acids Res.* 46, D851–D860. doi: 10.1093/nar/gkx1068

Hakvoort, H., Bovenkamp, E., Greenwood-Quaintance, K. E., Schmidt-Malan, S. M., Mandrekar, J. N., Schuetz, A. N., et al. (2020). Imipenem-relebactam susceptibility testing of gram-negative bacilli by agar dilution, disk diffusion, and gradient strip methods compared with broth Microdilution. *J. Clin. Microbiol.* 58:e00695-20. doi: 10.1128/JCM.00695-20

Hall, B. G., Acar, H., Nandipati, A., and Barlow, M. (2013). Growth rates made easy. *Mol. Biol. Evol.* 31, 232–238.

Harden, M. M., He, A., Creamer, K., Clark, M. W., Hamdallah, I., Martinez, K. A. II, et al. (2015). Acid-adapted strains of *Escherichia coli* K-12 obtained by experimental evolution. *Appl. Environ. Microbiol.* 81, 1932–1941. doi: 10.1128/AEM.03494-14

He, A., Penix, S. R., Basting, P. J., Griffith, J. M., Creamer, K. E., Camperchioli, D., et al. (2017). Acid evolution of *Escherichia coli* K-12 eliminates amino acid decarboxylases and reregulates catabolism. *Appl. Environ. Microbiol.* 83:e00442-17. doi: 10.1128/AEM.00442-17

Herring, C. D., Raghunathan, A., Honisch, C., Patel, T., Applebee, M. K., Joyce, A. R., et al. (2006). Comparative genome sequencing of *Escherichia coli* allows observation of bacterial evolution on a laboratory timescale. *Nat. Genet.* 38, 1406–1412. doi: 10.1038/ng1906

Higginson, E. E., Ramachandran, G., Hazen, T. H., Kania, D. A., Rasko, D. A., Pasetti, M. F., et al. (2018). Improving our understanding of *Salmonella enterica* serovar paratyphi B through the engineering and testing of a live attenuated vaccine strain. *mSphere* 3:e00474-00418. doi: 10.1128/msphere.00474-00418

Hu, M., Zhang, Y., Huang, X., He, M., Zhu, J., Zhang, Z., et al. (2023). PhoPQ regulates quinolone and cephalosporin resistance formation in *Salmonella* enteritidis at the transcriptional level. *mBio* 14:e0339522. doi: 10.1128/mbio.03395-22

Iguchi, A., Shirai, H., Seto, K., Ooka, T., Ogura, Y., Hayashi, T., et al. (2011). Wide distribution of O157-antigen biosynthesis gene clusters in *Escherichia coli*. *PLoS One* 6:e23250. doi: 10.1371/journal.pone.0023250

Jean, S.-S., Lee, Y.-T., Guo, S.-M., and Hsueh, P.-R. (2005). Recurrent infections caused by cefotaxime- and ciprofloxacin-resistant *Salmonella enterica* serotype choleraesuis treated successfully with imipenem. *J. Infect.* 51, e163–e165. doi: 10.1016/j.jinf.2004.12.011

Jibril, A. H., Okeke, I. N., Dalsgaard, A., Menéndez, V. G., and Olsen, J. E. (2021). Genomic analysis of antimicrobial resistance and resistance plasmids in *Salmonella* Serovars from poultry in nigeria. *Antibiotics* 10:99. doi: 10.3390/antibiotics10020099

Johnson, M., Zaretskaya, I., Raytselis, Y., Merezhuk, Y., McGinnis, S., and Madden, T. L. (2008). NCBI BLAST: A better web interface. *Nucleic Acids Res.* 36(Suppl._2), W5–W9. doi: 10.1093/nar/gkn201

Jones, R. N., Rhomberg, P. R., Varnam, D. J., and Mathai, D. (2002). A comparison of the antimicrobial activity of meropenem and selected broad-spectrum antimicrobials tested against multi-drug resistant gram-negative bacilli including bacteraemic *Salmonella* spp.: Initial studies for the MYSTIC programme in India. *Int. J. Antimicrob. Agents* 20, 426–431. doi: 10.1016/s0924-8579(02)00210-8

Kartal, B., Akçay, A., and Palabiyik, B. (2018). Oxidative stress upregulates the transcription of genes involved in thiamine metabolism. *Turk J. Biol.* 42, 447–452.

Koeth, L. K., DiFranco-Fisher, J. M., Hardy, D. J., Palavecino, E. L., Carretto, E., and Windau, A. (2022). Multilaboratory comparison of Omadacycline MIC test strip to broth microdilution MIC against gram-negative, gram-positive, and fastidious bacteria. *J. Clin. Microbiol.* 60:e0141021. doi: 10.1128/JCM.01410-21

Kumari, S., Beatty, C. M., Browning, D. F., Busby, S. J. W., Simel, E. J., Hovel-Miner, G., et al. (2000). Regulation of acetyl coenzyme A Synthetase in *Escherichia coli*. *J. Bacteriol.* 182, 4173–4179. doi: 10.1128/JB.182.15.4173-4179.2000

Kumari, S., Tishel, R., Eisenbach, M., and Wolfe, A. J. (1995). Cloning, characterization, and functional expression of acs, the gene which encodes acetyl coenzyme A synthetase in *Escherichia coli*. *J. Bacteriol.* 177, 2878–2886. doi: 10.1128/jb.177.10.2878-2886.1995

LaCroix, R. A., Palsson, B. O., and Feist, A. M. (2017). A model for designing adaptive laboratory evolution experiments. *Appl. Environ. Microbiol.* 83:e03115-16. doi: 10.1128/AEM.03115-16

LaCroix, R. A., Sandberg, T. E., O'Brien, E. J., Utrilla, J., Ebrahim, A., Guzman, G. I., et al. (2015). Use of adaptive laboratory evolution to discover key mutations enabling rapid growth of *Escherichia coli* K-12 MG1655 on glucose minimal medium. *Appl. Environ. Microbiol.* 81, 17–30. doi: 10.1128/AEM.02246-14

Langsrud, S., Sundheim, G., and Holck, A. L. (2004). Cross-resistance to antibiotics of *Escherichia coli* adapted to benzalkonium chloride or exposed to stress-inducers. *J. Appl. Microbiol.* 96, 201–208.

Lázár, V., Nagy, I., Spohn, R., Csörgő, B., Györkei, Á, Nyerges, Á, et al. (2014). Genome-wide analysis captures the determinants of the antibiotic cross-resistance interaction network. *Nat. Commun.* 5:4352. doi: 10.1038/ncomms5352

Lee, D. H., Feist, A. M., Barrett, C. L., and Palsson, B. (2011). Cumulative number of cell divisions as a meaningful timescale for adaptive laboratory evolution of *Escherichia coli*. *PLoS One* 6:e26172. doi: 10.1371/journal.pone.0026172

Lemmin, T., Soto, C. S., Clinthorne, G., DeGrado, W. F., and Dal Peraro, M. (2013). Assembly of the Transmembrane domain of *E. coli* PhoQ Histidine Kinase: Implications for signal transduction from molecular simulations. *PLoS Comput. Biol.* 9:e1002878. doi: 10.1371/journal.pcbi.1002878

Lerouge, I., and Vanderleyden, J. (2002). O-antigen structural variation: Mechanisms and possible roles in animal/plant–microbe interactions. *FEMS Microbiol. Rev.* 26, 17–47. doi: 10.1111/j.1574-6976.2002.tb00597.x

Leyer, G. J., and Johnson, E. A. (1992). Acid adaptation promotes survival of *Salmonella* spp. in cheese. *Appl Environ. Microbiol.* 58, 2075–2080. doi: 10.1128/aem.58.6.2075-2080.1992

Li, H. (2013). Aligning sequence reads, clone sequences and assembly contigs with BWA-MEM. *BioArxiv.* [Preprint]. doi: 10.48550/arXiv.1303.3997.

Li, Y., and Zhang, Y. (2007). PhoU is a persistence switch involved in persister formation and tolerance to multiple antibiotics and stresses in *Escherichia coli*. *Antimicrob. Agents Chemother.* 51, 2092–2099. doi: 10.1128/AAC.00052-07

Maeda, T., Iwasawa, J., Kotani, H., Sakata, N., Kawada, M., Horinouchi, T., et al. (2020). High-throughput laboratory evolution reveals evolutionary constraints in *Escherichia coli*. *Nat. Commun.* 11:5970. doi: 10.1038/s41467-020-19713-w

Maldonado, R. F., Sá-Correia, I., and Valvano, M. A. (2016). Lipopolysaccharide modification in Gram-negative bacteria during chronic infection. *FEMS Microbiol. Rev.* 40, 480–493.

Mani-López, E., García, H. S., and ópez-Malo, A. L. (2012). Organic acids as antimicrobials to control *Salmonella* in meat and poultry products. *Food Res. Int.* 45, 713–721.

Marciano, D. C., Wang, C., Hsu, T.-K., Bourquard, T., Atri, B., Nehring, R. B., et al. (2022). Evolutionary action of mutations reveals antimicrobial resistance genes in *Escherichia coli*. *Nat. Commun.* 13:3189. doi: 10.1038/s41467-022-30889-1

Matamouros, S., Hager, K., and Miller, S. (2015). HAMP domain rotation and tilting movements associated with signal transduction in the PhoQ Sensor Kinase. *mBio* 6:e00616-15. doi: 10.1128/mBio.00616-15

Matuschek, E., Åhman, J., Webster, C., and Kahlmeter, G. (2018). Antimicrobial susceptibility testing of colistin – evaluation of seven commercial MIC products against standard broth microdilution for *Escherichia coli*, *Klebsiella pneumoniae*, *Pseudomonas aeruginosa*, and *Acinetobacter* spp. *Clin. Microbiol. Infect.* 24, 865–870. doi: 10.1016/j.cmi.2017.11.020

McKenna, A., Hanna, M., Banks, E., Sivachenko, A., Cibulskis, K., Kernytsky, A., et al. (2010). The genome analysis toolkit: A MapReduce framework for analyzing next-generation DNA sequencing data. *Genome Res.* 20, 1297–1303. doi: 10.1101/gr.107524.110

McLaughlin, H. P., Gargis, A. S., Michel, P., Sue, D., and Weigel, L. M. (2017). Optical screening for rapid antimicrobial susceptibility testing and for observation of phenotypic diversity among strains of the genetically clonal species *Bacillus anthracis*. *J. Clin. Microbiol.* 55, 959–970. doi: 10.1128/JCM.02209-16

Mengistu, G., Dejenu, G., Tesema, C., Arega, B., Awoke, T., Alemu, K., et al. (2020). Epidemiology of streptomycin resistant *Salmonella* from humans and animals in Ethiopia: A systematic review and meta-analysis. *PLoS One* 15:e0244057. doi: 10.1371/journal.pone.0244057

Miller, A. K., Brannon, M. K., Stevens, L., Johansen, H. K., Selgrade, S. E., Miller, S. I., et al. (2011). PhoQ mutations promote lipid A modification and polymyxin resistance of *Pseudomonas aeruginosa* found in colistin-treated cystic fibrosis patients. *Antimicrob. Agents Chemother.* 55, 5761–5769. doi: 10.1128/AAC.05391-11

Miyakoshi, M., Matera, G., Maki, K., Sone, Y., and Vogel, J. (2019). Functional expansion of a TCA cycle operon mRNA by a 3' end-derived small RNA. *Nucleic Acids Res.* 47, 2075–2088. doi: 10.1093/nar/gky1243

Mongold, J. A., Bennett, A. F., and Lenski, R. E. (1999). Evolutionary adaptation to temperature: Extension of the upper thermal limit of *Escherichia coli*. *Evolution* 53, 386–394. doi: 10.1111/j.1558-5646.1999.tb03774.x

Muhammad, M., Muhammad, L. U., Ambali, A.-G., Mani, A. U., Azard, S., and Barco, L. (2010). Prevalence of *Salmonella* associated with chick mortality at hatching and their susceptibility to antimicrobial agents. *Vet. Microbiol.* 140, 131–135. doi: 10.1016/j.vetmic.2009.07.009

Murray, G. L., Attridge, S. R., and Morona, R. (2003). Regulation of *Salmonella typhimurium* lipopolysaccharide O antigen chain length is required for virulence; identification of FepE as a second Wzz. *Mol. Microbiol.* 47, 1395–1406. doi: 10.1046/j.1365-2958.2003.03383.x

Pacios, O., Blasco, L., Bleriot, I., Fernandez-Garcia, L., Ambroa, A., López, M., et al. (2020). (p)ppGpp and Its role in bacterial persistence: New challenges. *Antimicrob. Agents Chemother.* 64:e01283-20.

Pitt, M. E., Elliott, A. G., Cao, M. D., Ganesamoorthy, D., Karaiskos, I., Giamarellou, H., et al. (2018). Multifactorial chromosomal variants regulate polymyxin resistance in extensively drug-resistant *Klebsiella pneumoniae*. *Microb. Genom.* 4:e000158. doi: 10.1099/mgen.0.000158

Prost, L. R., Daley, M. E., Le Sage, V., Bader, M. W., Le Moual, H., Klevit, R. E., et al. (2007). Activation of the bacterial sensor kinase PhoQ by Acidic pH. *Mol. Cell* 26, 165–174.

Ren, J., Sang, Y., Ni, J., Tao, J., Lu, J., Zhao, M., et al. (2015). Acetylation regulates survival of *Salmonella enterica* Serovar typhimurium under acid stress. *Appl. Environ. Microbiol.* 81, 5675–5682. doi: 10.1128/AEM.01009-15

Rhee, J. E., Sheng, W., Morgan, L. K., Nolet, R., Liao, X., and Kenney, L. J. (2008). Amino acids important for DNA recognition by the response regulator OmpR. *J. Biol. Chem.* 283, 8664–8677. doi: 10.1074/jbc.M705550200

Rodríguez-Verdugo, A., Gaut, B. S., and Tenaillon, O. (2013). Evolution of *Escherichia coli* rifampicin resistance in an antibiotic-free environment during thermal stress. *BMC Evol. Biol.* 13:50. doi: 10.1186/1471-2148-13-50

Sahl, J. W., Caporaso, J. G., Rasko, D. A., and Keim, P. (2014). The large-scale blast score ratio (LS-BSR) pipeline: A method to rapidly compare genetic content between bacterial genomes. *PeerJ* 2:e332. doi: 10.7717/peerj.332

Sandberg, T. E., Salazar, M. J., Weng, L. L., Palsson, B. O., and Feist, A. M. (2019). The emergence of adaptive laboratory evolution as an efficient tool for biological discovery and industrial biotechnology. *Metab. Eng.* 56, 1–16. doi: 10.1016/j.ymben.2019.08.004

Shprung, T., Wani, N. A., Wilmes, M., Mangoni, M. L., Bitler, A., Shimoni, E., et al. (2021). Opposing effects of PhoPQ and PmrAB on the properties of *Salmonella enterica* serovar typhimurium: Implications on resistance to antimicrobial peptides. *Biochemistry* 60, 2943–2955. doi: 10.1021/acs.biochem.1c00287

Spector, M. P., and Kenyon, W. J. (2012). Resistance and survival strategies of *Salmonella enterica* to environmental stresses. *Food Res. Int.* 45, 455–481.

Tatusova, T., DiCuccio, M., Badretdin, A., Chetvernin, V., Nawrocki, E. P., Zaslavsky, L., et al. (2016). NCBI prokaryotic genome annotation pipeline. *Nucleic Acids Res.* 44, 6614–6624.

van den Bijllaardt, W., Schijffelen, M. J., Bosboom, R. W., Cohen Stuart, J., Diederen, B., and Kampinga, G. (2018). Susceptibility of ESBL *Escherichia coli* and *Klebsiella pneumoniae* to fosfomycin in the Netherlands and comparison of several testing methods including Etest, MIC test strip, Vitek2, Phoenix and disc diffusion. *J. Antimicrob. Chemother.* 73, 2380–2387. doi: 10.1093/jac/dky214

Wang, J., Sheng, H., Xu, W., Huang, J., Meng, L., Cao, C., et al. (2019). Diversity of serotype, genotype, and antibiotic susceptibility of *Salmonella* prevalent in pickled ready-to-eat meat. *Front. Microbiol.* 10:2577. doi: 10.3389/fmicb.2019.02577

Wang, Y., Chen, X., Hu, Y., Zhu, G., White, A. P., and Köster, W. (2018). Evolution and sequence diversity of FhuA in *Salmonella* and *Escherichia*. *Infect. Immun.* 86:e00573-18. doi: 10.1128/IAI.00573-18

Wiegand, I., Hilpert, K., and Hancock, R. E. W. (2008). Agar and broth dilution methods to determine the minimal inhibitory concentration (MIC) of antimicrobial substances. *Nat. Protoc.* 3, 163–175.

Wistrand-Yuen, E., Knopp, M., Hjort, K., Koskiniemi, S., Berg, O. G., and Andersson, D. I. (2018). Evolution of high-level resistance during low-level antibiotic exposure. *Nat. Commun.* 9:1599.

Xu, H., Lee, H. Y., and Ahn, J. (2008). Cross-protective effect of acid-adapted *Salmonella enterica* on resistance to lethal acid and cold stress conditions. *Lett. Appl. Microbiol.* 47, 290–297. doi: 10.1111/j.1472-765x.2008.02429.x

Yarlagadda, V., Sarkar, P., Samaddar, S., Manjunath, G. B., Mitra, S. D., Paramanandham, K., et al. (2018). Vancomycin analogue restores Meropenem activity against NDM-1 gram-negative pathogens. *ACS Infect. Dis.* 4, 1093–1101. doi: 10.1021/acsinfecdis.8b00011

Yuan, J., Jin, F., Glatter, T., and Sourjik, V. (2017). Osmosensing by the bacterial PhoQ/PhoP two-component system. *Proc. Natl. Acad. Sci. U.S.A.* 114, E10792–E10798. doi: 10.1073/pnas.1717272114

Zeng, J., Wu, L., Liu, Z., Lv, Y., Feng, J., Wang, W., et al. (2021). Gain-of-function mutations in acid stress response (evgS) protect *Escherichia coli* from killing by gallium nitrate, an antimicrobial Candidate. *Antimicrob. Agents Chemother.* 65:e01595-20. doi: 10.1128/AAC.01595-20

frontiers | Frontiers in Microbiology

TYPE Original Research
PUBLISHED 20 November 2023
DOI 10.3389/fmicb.2023.1266977

OPEN ACCESS

EDITED BY
George Grant,
University of Aberdeen, United Kingdom

REVIEWED BY
Samara Paula Mattiello,
University of Tennessee Southern, United States
Marco Larrea-Álvarez,
Espiritu Santo University, Ecuador

*CORRESPONDENCE
Yibing Wang
✉ wangyibing77@163.com
Shouqun Jiang
✉ jiangshouqun@gdaas.cn

RECEIVED 26 July 2023
ACCEPTED 13 October 2023
PUBLISHED 20 November 2023

CITATION
Zhang S, Wang Q, Ye J, Fan Q, Lin X, Gou Z, Azzam MM, Wang Y and Jiang S (2023) Transcriptome and proteome profile of jejunum in chickens challenged with *Salmonella* Typhimurium revealed the effects of dietary bilberry anthocyanin on immune function. *Front. Microbiol.* 14:1266977. doi: 10.3389/fmicb.2023.1266977

Transcriptome and proteome profile of jejunum in chickens challenged with *Salmonella* Typhimurium revealed the effects of dietary bilberry anthocyanin on immune function

Sheng Zhang[1], Qin Wang[1], Jinling Ye[1], Qiuli Fan[1], Xiajing Lin[1], Zhongyong Gou[1], Mahmoud M. Azzam[2], Yibing Wang[1]* and Shouqun Jiang[1]*

[1]State Key Laboratory of Livestock and Poultry Breeding, Key Laboratory of Animal Nutrition and Feed Science in South China, Guangdong Provincial Key Laboratory of Animal Breeding and Nutrition, Ministry of Agriculture and Rural Affairs, Institute of Animal Science, Guangdong Academy of Agricultural Sciences, Guangzhou, Guangdong, China, [2]Department of Animal Production College of Food and Agriculture Sciences, King Saud University, Riyadh, Saudi Arabia

Introduction: The present study investigated the effects of bilberry anthocyanin (BA) on immune function when alleviating *Salmonella* Typhimurium (*S.* Typhimurium) infection in chickens.

Methods: A total of 180 newly hatched yellow-feathered male chicks were assigned to three groups (CON, SI, and SI + BA). Birds in CON and SI were fed a basal diet, and those in SI + BA were supplemented with 100 mg/kg BA for 18 days. Birds in SI and SI + BA received 0.5 ml suspension of *S.* Typhimurium (2×10^9 CFU/ml) by oral gavage at 14 and 16 days of age, and those in CON received equal volumes of sterile PBS.

Results: At day 18, (1) dietary BA alleviated weight loss of chickens caused by *S.* Typhimurium infection ($P < 0.01$). (2) Supplementation with BA reduced the relative weight of the bursa of Fabricius ($P < 0.01$) and jejunal villus height ($P < 0.05$) and increased the number of goblet cells ($P < 0.01$) and the expression of *MUC2* ($P < 0.05$) in jejunal mucosa, compared with birds in SI. (3) Supplementation with BA decreased ($P < 0.05$) the concentration of immunoglobulins and cytokines in plasma (IgA, IL-1β, IL-8, and IFN-β) and jejunal mucosa (IgG, IgM, sIgA, IL-1β, IL-6, IL-8, TNF-α, IFN-β, and IFN-γ) of *S.* Typhimurium-infected chickens. (4) BA regulated a variety of biological processes, especially the defense response to bacteria and humoral immune response, and suppressed cytokine–cytokine receptor interaction and intestinal immune network for IgA production pathways by downregulating 6 immune-related proteins.

Conclusion: In summary, the impaired growth performance and disruption of jejunal morphology caused by *S.* Typhimurium were alleviated by dietary BA by affecting the expression of immune-related genes and proteins, and signaling pathways are related to immune response associated with immune cytokine receptors and production in jejunum.

KEYWORDS

bilberry anthocyanin, *Salmonella* Typhimurium, immune status, transcriptome, proteome, yellow-feathered chicks

1 Introduction

Intensive animal production is increasingly constrained by bacterial diseases such as *Salmonella*, *Escherichia coli*, and *Pasteurella*, among which *Salmonella* is particularly prominent in poultry (Foster et al., 2021). In production settings, poultry is infected with *Salmonella* through ingestion of contaminated feed and water as well as by vertical transmission (Karabasanavar et al., 2020). The immune system of chicks is not fully developed, so they are more susceptible to *Salmonella* infection. Infected chicks suffer from weakness, loss of appetite, diarrhea, poor growth, and even death, causing serious economic losses (Mshelbwala et al., 2019; Abudabos et al., 2020). *Salmonella* colonizes and adheres to the intestinal mucosal epithelium after invading the digestive tract, then damages the intestinal barrier function, unbalances the composition of intestinal microbes, and induces intestinal inflammation. During infection, *Salmonella* causes damage to immune organs, resulting in congestion, bleeding, and inflammatory cell infiltration (Chen et al., 2020; Cheng et al., 2020).

Overuse of antibiotics to obviate *Salmonella* invasive infection leads to the emergence of drug-resistant bacteria and is harmful to the environment and health of animals and humans (Manyi-Loh et al., 2018). Nutrition strategies such as dietary supplementation with plant extracts have been introduced into poultry production as alternative substitutes to antibiotics to alleviate *Salmonella* infection (Wu et al., 2018; Purwanti et al., 2019).

Anthocyanins are flavonoid substances obtained from plants such as flowers, fruits, and tubers, which are characterized by excellent antioxidant, anti-inflammatory, and antibacterial activities (Peng et al., 2020; Moreira et al., 2021). Studies showed that anthocyanins alleviated intestinal inflammatory diseases through various mechanisms. Anthocyanins increased the expression of peroxisome proliferator-activated receptor γ (PPARγ) and inhibited the activation of the downstream NF-κB/MAPK signaling pathway, thereby alleviating colonic inflammation on dextran sulfate sodium-induced inflammatory bowel disease (IBD) in mice (Gao et al., 2021). By inhibiting endoplasmic reticulum stress response, anthocyanins inhibited the activation of NOD-like receptor family protein 3 (NLRP3) and the release of IL-1β and IL-18 in lipopolysaccharide (LPS) and adenosine triphosphate treated BV2 microglia cells (Molagoda et al., 2021). In addition, anthocyanins increased the number of epithelial cells and inhibited the infiltration of inflammatory cells in small intestinal mucosa and submucosa, thus alleviating small intestinal epithelial damage in contaminant-induced rats (Chen et al., 2019). Flavonoid substances reduced the adhesion of *E. coli* and *Salmonella* to IPEC-J2 cells, as well as oxidative stress, inflammation, and barrier damage to intestinal epithelial cells (Kovács et al., 2022). These together indicated the potential value of anthocyanins in the alleviation of intestinal inflammation caused by *Salmonella* infection.

Therefore, the objective of this study was to investigate the effects of dietary supplementation with bilberry anthocyanin (BA) on the intestinal morphology and intestinal inflammatory response of chickens challenged with *Salmonella* Typhimurium (*S.* Typhimurium). In addition, jejunal immune function was examined using genomic and proteomic analyses. The study adds to an understanding of the pathogenic mechanism of *S.* Typhimurium and the further development of nutritional strategies against *Salmonella* infection.

2 Materials and method

2.1 Experimental design and diets

Bilberry anthocyanin (purity >36%) from Tianjin Jianfeng Natural Product R&D Co., Ltd. (Tianjin, China) was used. *S.* Typhimurium (China Center of Industrial Culture Collection 21484, isolated from the pooled heart and liver tissue of 4-week-old chickens), was provided by Professor Weifen Li from Zhejiang University.

A total of 180 Lingnan yellow-feathered male chickens (1 day old, 28.00 ± 0.02 g) were randomly assigned to three treatment groups with six cages per treatment (10 birds per cage). As shown in Figure 1, the controls (CON) and birds infected with *S.* Typhimurium (SI) were fed the basal diet for 18 days. The remaining birds (SI + BA) were supplemented with dietary BA at 100 mg/kg. The diets were formulated referring to Chinese Nutrient Requirements of Yellow broilers (Ministry of Agriculture of the People's Republic of China (PRC), 2020), and the composition and nutrient level of the basal corn-soybean diet are shown in Supplementary Table S1. The birds received 0.5 ml sterile PBS (CON) or *S.* Typhimurium suspension (SI and SI + BA) by oral ingestion with a gavage needle gently at 14 and 16 days of age.

The experimental protocol was approved by the Animal Care Committee of the Institute of Animal Science, Guangdong Academy of Agriculture Science, Guangzhou, P. R. China, with the approval number GAASISA-2021-037. Birds were housed and fed in disease-free cages (100 cm × 50 cm × 50 cm) and had unlimited access to feed and water. During days 1–3, the indoor temperature was maintained at ~34°C along with 24-h artificial light; then, the temperature was gradually reduced by 3°C each week to a final temperature of 26°C, and the illumination was reduced by 2 h each day to 16 h. The body weight (BW) of birds was recorded at 14 and 18 days of age.

2.2 Preparation of *S.* Typhimurium suspension

Salmonella Typhimurium was thawed, streaked on *Salmonella Shigella* agar medium, and placed in a constant temperature incubator at 37°C for 24 h. A single colony was picked and expanded to the exponential phase in Luria–Bertani liquid medium in a shaking incubator (37°C, 180 r/min) for 8 h. The *S.* Typhimurium was washed twice with sterile PBS, quantified by OD_{600}, and adjusted to 2×10^9 CFU/ml for oral gavage.

2.3 Sample collection and calculation of the relative weight of immune organs

On day 18 of the trial, 12 birds (two close to the average BW from each replicate) from each treatment were electrically stunned (head only) at 150 V for 5 s (DMJ, Ningguang Machinery Co., Ltd.,

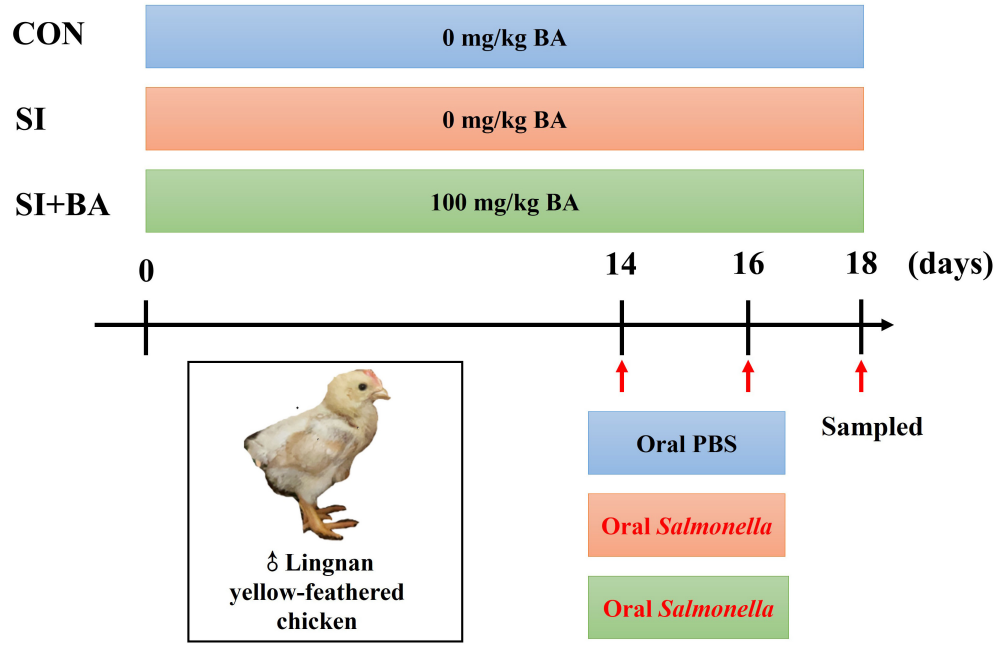

FIGURE 1
Study design for the whole experiment. CON, control group; SI, *S.* Typhimurium infection group; SI + BA, *S.* Typhimurium infection and dietary BA supplementation group; BA, bilberry anthocyanin.

Nanjing, China) and exsanguinated. Blood (5 ml) was collected from the wing vein into anticoagulant (heparin) vacuum tubes and centrifuged at 3,000×*g* for 10 min to obtain plasma. Jejunal segments (~1 cm long) were quickly fixed in 4% paraformaldehyde. The middle part of the jejunum was opened lengthwise and washed in PBS; then, the mucosa was collected by gentle scraping. Mucosa and intact jejunal wall were frozen in liquid nitrogen and stored at −80°C. The whole wall was used for transcriptome and proteome analyses, and mucosa was used for determining the concentration of cytokines. The spleen, thymus, and bursa of Fabricius were cleaned of connective tissue and weighed. The relative weights of immune organs were expressed based on BW.

2.4 Biochemical variables in plasma and jejunal mucosa

Frozen samples of jejunal mucosa were homogenized with ice-cold physiologic saline (1:10, *w*/*v*) and centrifuged at 3,000×g for 10 min to obtain clarified homogenates. The concentrations of secretory immunoglobulin A (sIgA), IgG, IgM, interleukin (IL)-1β, IL-6, IL-8, tumor necrosis factor-α (TNF-α), interferon (IFN)-β, and IFN-γ in plasma and jejunal mucosa were determined by appropriate ELISA kits (Jiangsu Meimian Industrial Co., Ltd., Jiangsu, China).

2.5 Morphology of jejunum

After fixation in 4% paraformaldehyde for 48 h, jejunal segments were trimmed, dehydrated, embedded in paraffin, and sectioned at 5 μm. After mounting and dewaxing, sections were stained with hematoxylin–eosin (H&E) for analysis of morphology and periodic acid–Schiff (PAS) for the observation of goblet cells. The villus height (VH) of five intact intestinal villi in each section and the adjacent crypt depth (CD) were measured, and the number of goblet cells on the villus was counted by scanning browsing software (CaseViewer2.4, 3DHISTECH, Budapest, Hungary) and image analysis software (Image-Pro Plus 6.0). The average of VH and CD and the ratio of villus height to crypt depth (VH/CD) were calculated. In addition, the number of goblet cells on villi was expressed per unit length of the villus.

2.6 Quantitative real-time PCR

Total RNA from jejunal samples was extracted using TRIzol® reagent (Invitrogen, Carlsbad, CA). The concentration and purity of the RNA were assessed spectrophotometrically. The RNA integrity number (RIN) was assessed (Agilent 2100 Bioanalyzer, Agilent Technologies, Palo Alto, CA). The RNA was reverse-transcribed with RNAiso Plus and PrimeScriptTMII 1st Strand cDNA Synthesis Kits (6210A, Takara, Tokyo, JP). The real-time PCR was performed using SYBR Premix Ex Taq II (RR820A, Takara) on the CFX96 RT-PCR Detection System (Bio-Rad, Hercules, CA). The primers used are shown in Supplementary Table S2. The abundance of target transcripts was expressed relative to the housekeeping gene (*β-actin*) by the $2^{-\Delta\Delta Ct}$ method and further normalized, relative to data from the CON animals.

2.7 Transcriptome analysis

The samples were processed as recommended and then analyzed by Majorbio Bio-pharm Technology Co., Ltd (Shanghai, China) Company, and Majorbio Cloud was used for transcriptome and proteomic analyses (Ren et al., 2022).

The transcriptome library was prepared using 1 μg of total RNA without removing ribosomal RNA. mRNA was isolated from total RNA by A-T base pairing with polyA at the 3′ end of eukaryotic mRNA using magnetic beads with oligo (dT). The extracted mRNA was randomly fragmented by fragmentation buffer, and fragments of ~300 bp were isolated by magnetic bead screening. Then, mRNA was used as the template for reverse transcription into double-stranded DNA. The End Repair Mix was added to patch the end of the double-strand and "A" base to the 3′ end for joining the Y-shaped joint, respectively. After amplification and quantification of PCR, the sequencing was carried out via Illumina NovaSeq6000 sequencer platforms (San Diego, CA). Finally, high-quality sequencing data were selected from the raw sequencing data using fastp (https://github.com/OpenGene/fastp) with default parameters, and the gene expression levels were quantified.

2.8 Proteome analysis

Total protein was extracted from the jejunal samples by urea lysis buffer with protease inhibitor, and the concentration of protein was quantified using the Pierce BCA kit (Thermo Scientific Pierce, Rockford, IL). Protein was digested according to the standard procedure, and the resulting peptide mixture was labeled using the 10-plex TMT reagent (90111, Thermo Fisher, Waltham, MA). After desalting with a C18 solid-phase extraction, peptides were used for Nano Liquid Chromatography (EASY-nLC^{TM} 1200, Thermo Scientific)–Mass Spectrometry/Mass Spectrometry (LC-MS/MS) analysis, as previously described (Luo et al., 2019).

2.9 Statistical analysis

Shapiro–Wilk test was used to assess the normality of data, and Levene's test was used to assess whether the assumption of homogeneity of variance was fulfilled. The data of growth performance, the relative weight of immune organs, jejunal morphological structure, and concentration of cytokines were analyzed by one-way analysis of variance (ANOVA) followed by Duncan's multiple range tests to compare the individual means in SPSS v20.0 for Windows (SPSS, Chicago, IL). The results are presented as the mean ± SEM. Differences between means were considered to be statistically significant when a P-value of < 0.05. For body weight and other variables, values are means of six replicate cages; for transcriptome and proteome analysis, values are the results of three randomly selected samples from each group.

According to the transcripts per million (TPM) reads method, the expression level of each gene was calculated. RSEM (http://deweylab.biostat.wisc.edu/rsem) was used to quantify gene abundance. Differentially expressed genes (DEGs) were identified with $|\log_2$ fold change (FC)$| \geq 1$ and a P-value of ≤ 0.05. The proteomics RAW data files were analyzed using Proteome Discoverer v2.2 (Thermo Scientific). The false discovery rate (FDR) of peptide identification was set as FDR ≤ 0.01. The thresholds of FC (≥ 1.2 or ≤ 0.83) and P-value ≤ 0.05 were used to identify differentially expressed proteins (DEPs). In addition, functional-enrichment analyses including Gene Ontology (GO, http://www.geneontology.org) and Kyoto Encyclopedia of Genes and Genomes (KEGG, http://www.genome.jp/kegg) pathways were performed to identify which DEG and DEP were significantly enriched in GO terms and metabolic pathways at a P-value of ≤ 0.05.

3 Results

3.1 Growth performance and relative weights of immune organs

As shown in Figure 2A, no significant difference in the total animal BW of chickens at day 14 was observed among the three treatment groups ($P > 0.05$). By contrast, BW at day 18 was significantly reduced in infected birds (SI) compared with the CON ($P < 0.01$), and this suppression of growth was completely relieved in birds given BA ($P < 0.01$).

For the relative weight of immune organs, *S.* Typhimurium infection significantly increased ($P < 0.01$) that of the spleen (Figure 2B) and decreased ($P < 0.01$) that of the bursa of Fabricius (Figure 2D) compared with the CON, and these alterations were significantly offset by BA supplementation ($P < 0.01$). There was no significant ($P > 0.05$) difference in relative thymic weight (Figure 2C).

3.2 Morphology of jejunum

Representative images of H&E- and PAS-stained jejunum are shown in Figures 3A, B. Compared with the CON, jejunal VH and VH/CD of birds were decreased ($P < 0.05$) when chickens were challenged with *S.* Typhimurium (Figures 3C, D). Compared with the SI, BA supplementation increased ($P < 0.01$) the VH and VH/CD of birds. No significant ($P > 0.05$) difference in CD existed among the three treatment groups (Figure 3E). In addition, no significant ($P > 0.05$) difference in the number of jejunal goblet cells was noted between birds in the CON and the SI, but that variable was increased ($P < 0.01$) in the SI + BA compared with both SI and CON (Figure 3F). BA supplementation (SI + BA) increased ($P < 0.01$) *MUC2* transcripts compared with those in SI (Figure 3G).

3.3 mRNA expression and the concentration of cytokines in plasma and jejunal mucosa

As shown in Figures 4A, B, compared with CON, plasma concentrations of IFN-β IL-8 ($P < 0.01$), IgG, IgA, IL-1β, TNF-α, and IFN-γ ($P < 0.05$) increased following *Salmonella* infection (SI). Compared with the SI, BA supplementation (BA + SI)

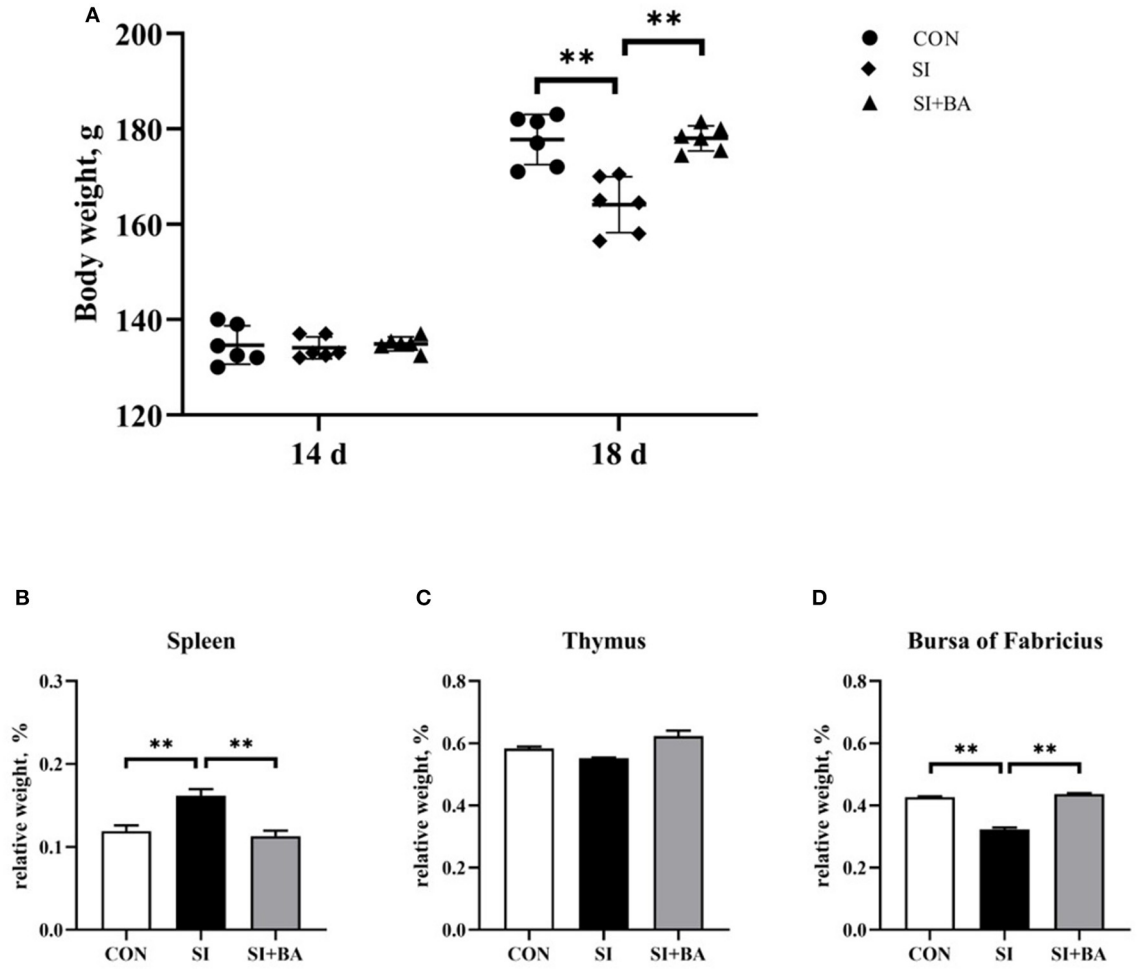

FIGURE 2
Effect of supplementation with bilberry anthocyanin on the body weight and relative weight of immune organs in chickens challenged with *S.* Typhimurium. **(A)** Body weight. The relative weight of **(B)** spleen, **(C)** thymus, and **(D)** bursa of Fabricius. CON, control group; SI, *S.* Typhimurium infection group; SI + BA, *S.* Typhimurium infection and dietary BA supplementation group. The data are means ± SEM, $n = 6$ ($^{**}P < 0.01$).

significantly decreased plasma concentrations of IgA ($P < 0.05$), IL-β ($P < 0.01$), IL-8 ($P < 0.05$), IFN-β ($P < 0.05$), and IFN-γ ($P < 0.01$), without affecting ($P > 0.05$) concentrations of IgG, IgM, IL-6, and TNF-α. In addition, *S.* Typhimurium infection increased ($P < 0.01$) jejunal mucosal concentrations of TNF-α, and the concentration of IgG ($P < 0.01$), IgM ($P < 0.05$), sIgA ($P < 0.01$), IL-1β ($P < 0.01$), IL-6 ($P < 0.01$), IL-8 ($P < 0.01$), TNF-α ($P < 0.01$), IFN-β ($P < 0.05$), and IFN-γ ($P < 0.01$) in the jejunal mucosa (Figures 4C, D) of *Salmonella*-infected chickens was significantly decreased by BA supplementation.

Jejunal mucosal transcripts of pro-inflammatory cytokines (*IL-1β*, *IL-6*, *TNF-α*, and *IFN-γ*) are shown in Figure 4E. Compared with controls, *S.* Typhimurium infection stimulated the expression of *IL-6* ($P < 0.01$), and BA supplementation significantly reduced the expression of *IFN-γ* ($P < 0.01$) and reduced ($P < 0.05$) the expression of *IL-6* in *Salmonella*-infected chickens.

3.4 Identification of immune-relevant mRNA modules

As shown in Figure 5A, a total of 13,660 genes were identified and 12,565 genes were shared among the treatments. Principal component analysis (PCA) of the samples was clustered, based on gene expression levels (Figure 5B). Three samples in each treatment group were closely correlated with each other. Furthermore, samples in CON and SI + BA were separated from those in SI, respectively. In addition, the volcano maps (Figures 5C, D) presented a clear visual of the relationship between the FDR and FC for all genes. Of these, 344 genes were differentially regulated (193 up and 151 down) in infected chickens compared with CON, and 550 genes were differentially regulated (175 up and 375 down) in BA-supplemented chickens (SI + BA) compared with those only infected (SI).

As shown in Figure 6A, BA supplementation significantly suppressed the upregulation of nine DEG, *viz. MHCY8*, *MCHY9*,

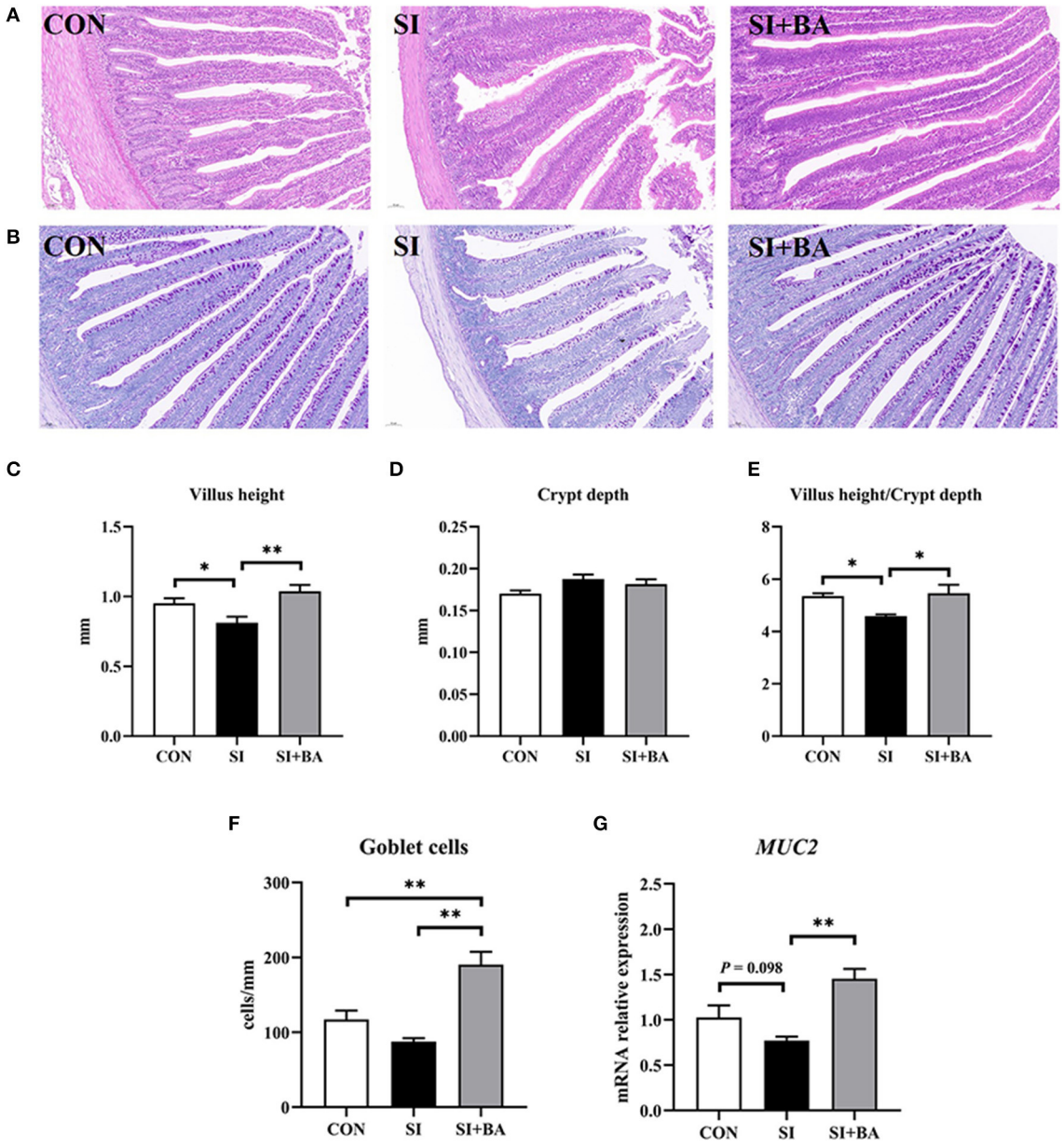

FIGURE 3
Effect of bilberry anthocyanin on jejunal morphology of chickens challenged with *S.* Typhimurium. Representative images of **(A)** H&E-stained and **(B)** PAS-stained jejunal sections (scale bar at 100 μm). **(C)** Villus height, **(D)** crypt depth, and **(E)** villus height/crypt depth in the jejunum of chickens. **(F)** The number of goblet cells and **(G)** the mRNA expression of *MUC2* in the jejunum of chickens. CON, control group; SI, *S.* Typhimurium infection group; SI + BA, *S.* Typhimurium infection and dietary BA supplementation group; *MUC2*, *mucin* 2. The data are means ± SEM, $n = 6$ ($^{*}P < 0.05$, $^{**}P < 0.01$).

*MHCY*11, *COCH*, *CCR*10, *TIFA*, *LOC*776018, *LOC*112531088, and *LOC*121106918, related to immune regulation triggered by *S.* Typhimurium infection. GO enrichment analysis (Figure 6B) and KEGG pathway enrichment analysis (Figure 6C) were performed for these DEG. GO term at level 2 showed that biological processes such as immune response (GO:0006955), defense response to other organisms (GO:0098542), immune system process (GO:0002376), defense response to a bacterium (GO:0042742), and humoral immune response (GO:0006959) were significantly enriched. The results of the KEGG pathway enrichment analysis indicated that the top five KEGG pathways associated with the nine immune-related DEG in samples included autoimmune thyroid disease (map05320), allograft rejection (map05330), viral myocarditis (map05416), Epstein–Barr virus infection (map00830), and graft-versus-host disease (map05332).

10.3389/fmicb.2023.1266977

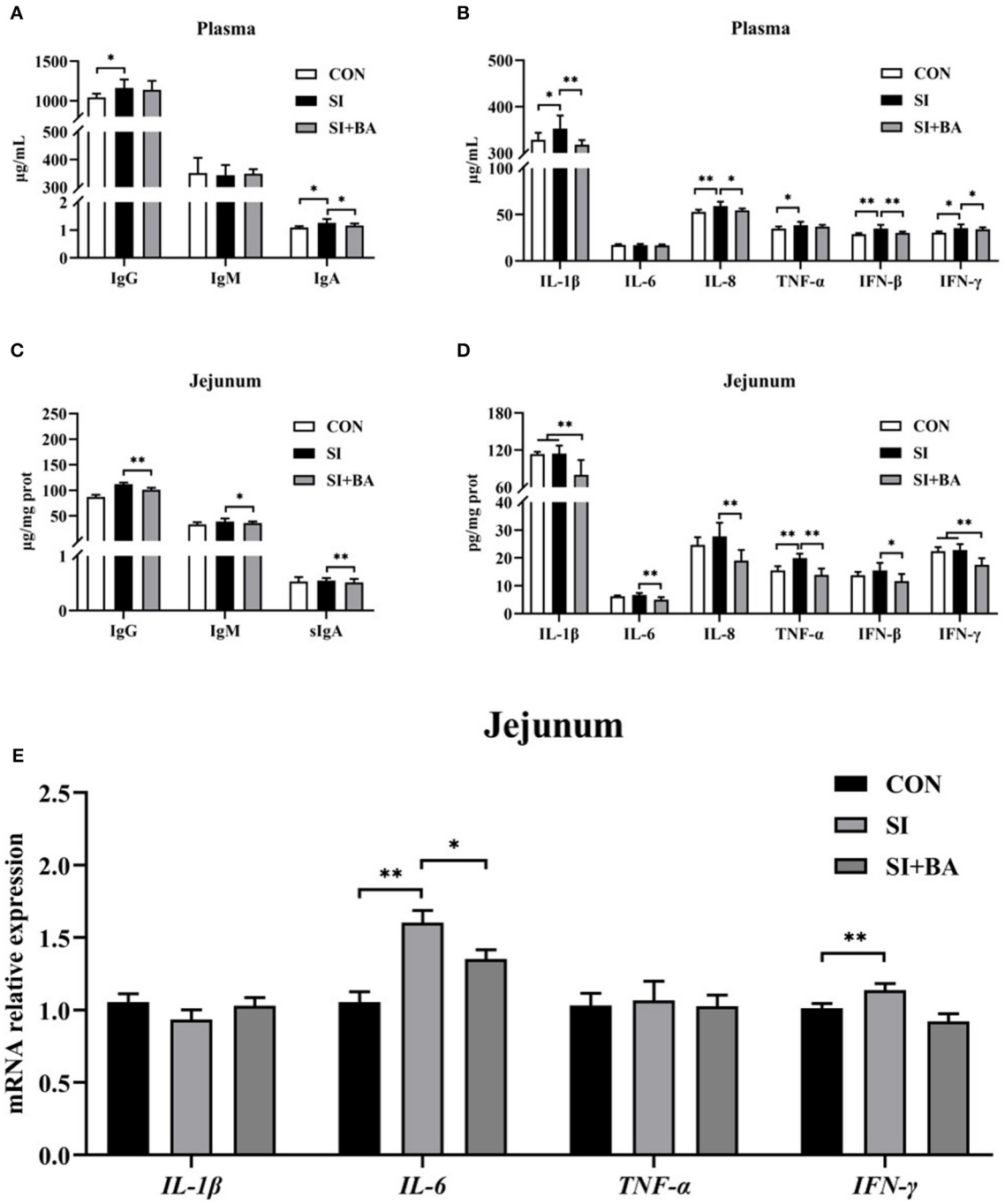

FIGURE 4
Effect of bilberry anthocyanin on plasma and jejunal mucosal concentrations of cytokines in plasma and cytokine gene expression in jejunal mucosa of chickens challenged with *S.* Typhimurium. **(A)** Plasma immunoglobulins, **(B)** plasma inflammatory cytokines, **(C)** jejunal mucosal immunoglobulins, and **(D)** jejunal mucosal inflammatory cytokines. **(E)** Inflammatory cytokine transcripts in jejunal mucosa: CON, controls; SI, chickens infected with *S.* Typhimurium; SI + BA, chickens supplemented with dietary BA and infected with *S.* Typhimurium; IgG, immunoglobulin G; IgM, immunoglobulin M; IgA, immunoglobulin A; IL-1β, interleukin-1β; IL-6, interleukin-6; IL-8, interleukin-8; TNF-α, tumor necrosis factor-α; IFN-β, interferon-β; IFN-γ, interferon-γ. The data are means ± SEM, $n = 6$ ($^{*}P < 0.05$, $^{**}P < 0.01$).

3.5 Identification of immune-relevant protein modules

In the present study, a total of 7,292 protein groups were identified (Figure 7A) in the jejunum. Based on protein expression levels, PCA (Figure 7B) was performed on samples from the three treatments. The SI showed an obvious separation from the CON and SI + BA. Compared with CON, 147 proteins were differentially expressed (105 were increased and 42 decreased) in *S.* Typhimurium-infected chickens (Figure 7C). In addition, 137

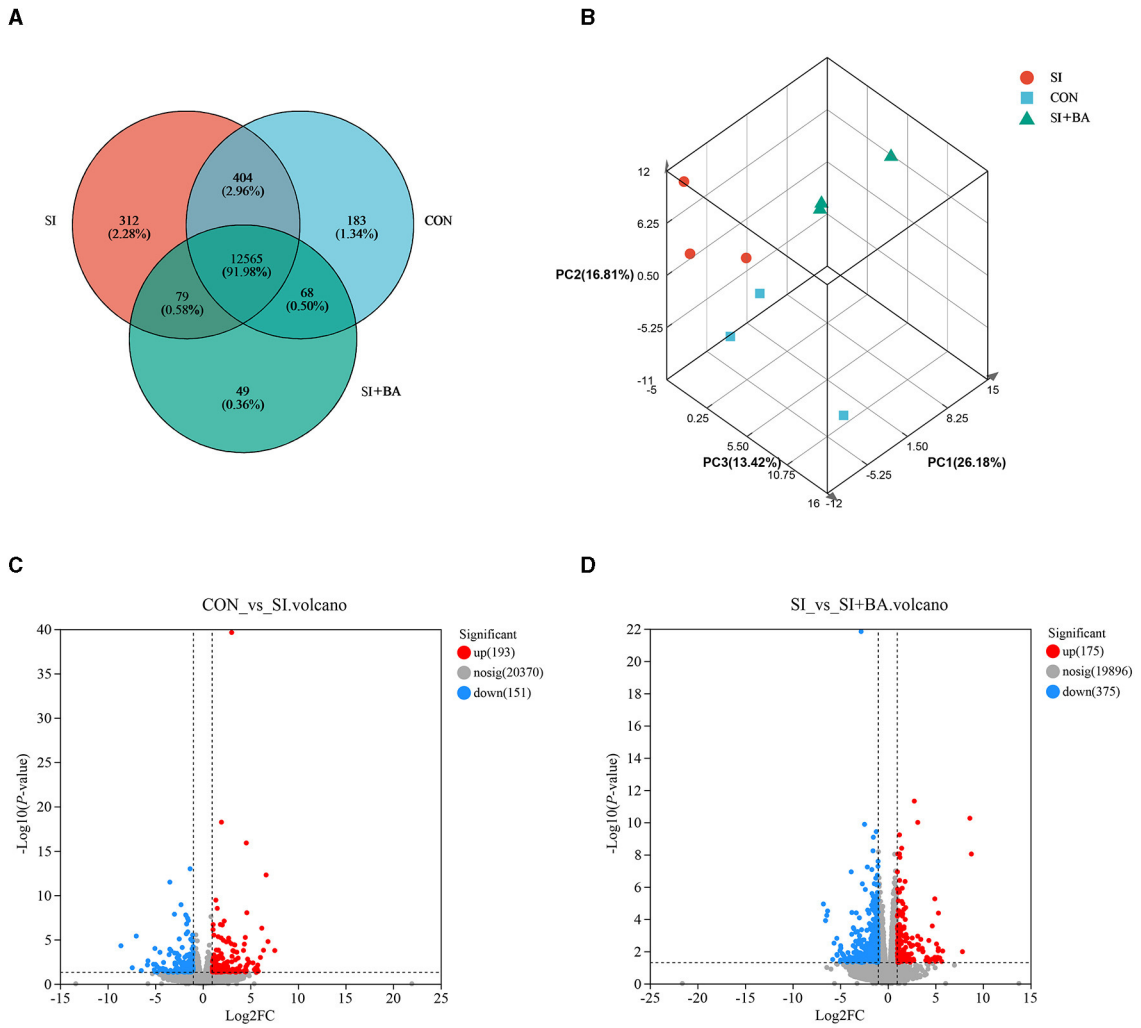

FIGURE 5
Effect of bilberry anthocyanin on the jejunal global gene expression pattern of chicken challenged with *S.* Typhimurium. **(A)** Venn diagram of the number of genes expressed. **(B)** Principal component analysis (PCA) of each sample on the whole genome. Volcano map of differentially expressed genes about **(C)** CON vs. SI and **(D)** SI vs. SI + BA. CON, controls; SI, chickens infected with *S.* Typhimurium; SI + BA, chickens supplemented with dietary BA and infected with *S.* Typhimurium; PC, principal component; FC, fold change; nosig, no significant change.

proteins differed in chickens of SI + BA compared with SI with 19 increased and 118 decreased (Figure 7D). The volcano maps presented a clear visual of the relationship between the FDR and FC for all proteins.

As shown in Figure 8A, the number of immune-related DEP (CON and SI, SI + BA and SI) was counted. Six immune-related proteins (Table 1), common to all chickens, were upregulated in response to *S.* Typhimurium infection (Figure 8B); these included orosomucoid 1 (ovoglycoprotein) precursor [fold change (FC) = 3.03], complement component C6 isoform X1 (FC = 1.93), complement component C8 beta chain precursor (FC = 1.78), chromogranin-A (FC = 1.25), tyrosine-protein kinase BTK isoform X1 (FC = 1.23), and HLA class II histocompatibility antigen gamma chain (FC = 1.21), and, moreover, these changes in infected birds were reversed by dietary supplementation with BA. To better understand the function of these 6 DEP, GO enrichment analysis (Figure 8C) showed that immune-related DEP associated with biological processes, such as immune response (GO:0006955), immune system process (GO:0002376), regulation of immune system process (GO:0002682), immune effector process (GO:0002252), defense response (GO:0006952), positive regulation of immune response (GO:0050778), and complement activation (GO:0006956), was upregulated in the SI compared with CON. Cellular components, such as membrane attack complex (GO:0005579), pore complex (GO:0046930), and plasma membrane protein complex (GO:0098797), were upregulated as well. KEGG enrichment analysis information and enriched protein symbol ID were performed in Table 2. The results in KEGG enrichment analysis indicated that phagosome (gga04145), cell adhesion molecules (gga04514), mucin-type O-glycan biosynthesis (gga00512), PPAR signaling pathway (gga03320), and ECM–receptor interaction (gga04512) were significantly ($P < 0.05$) enriched in 147 DEP between SI and CON, and intestinal immune network for IgA production (gga004672) had a tendency ($P =$

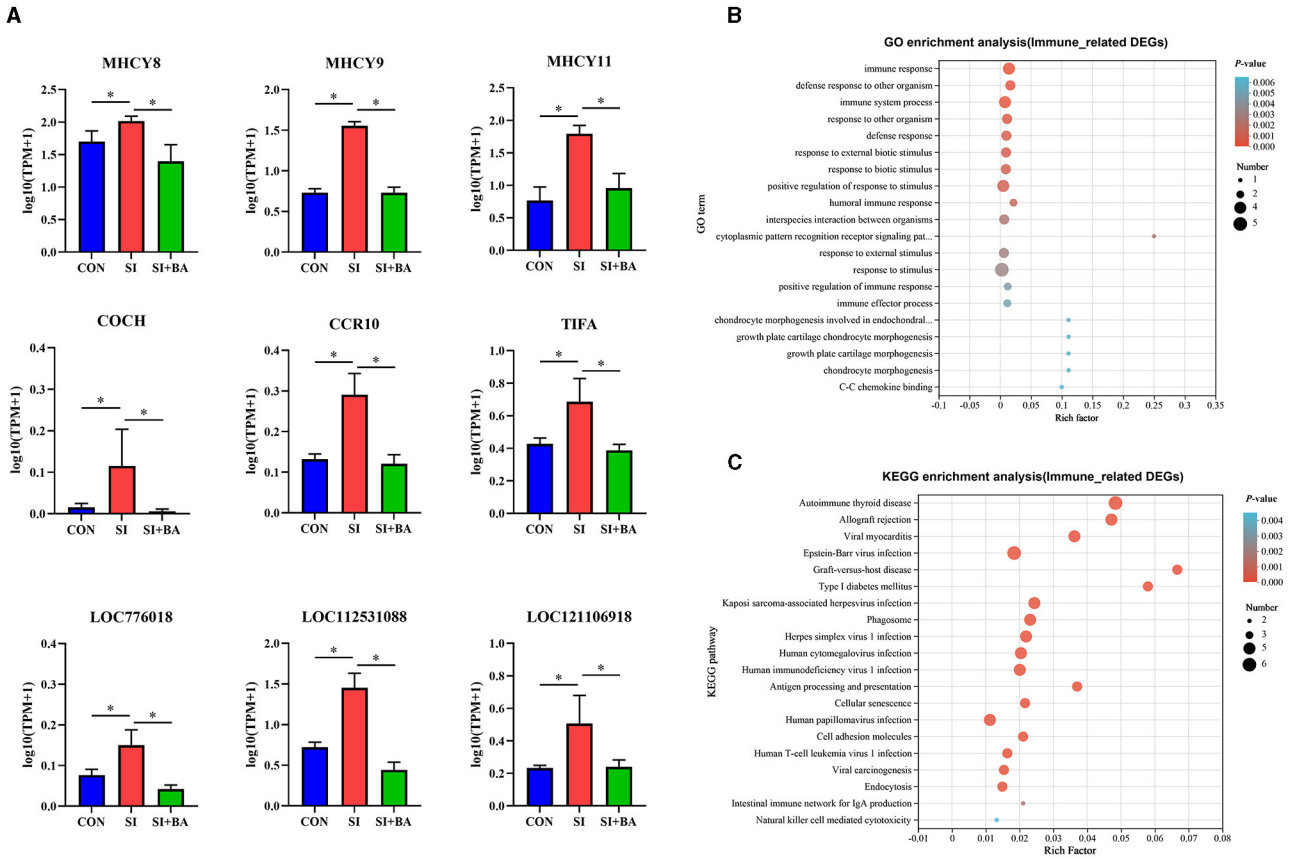

FIGURE 6
Effect of bilberry anthocyanin on the immune-related genes in the jejunum of chickens challenged with *S.* Typhimurium. **(A)** Differential expression of immune-related genes in jejunum. **(B)** Gene Ontology (GO) and **(C)** Kyoto Encyclopedia of Genes and Genomes (KEGG) enrichment analysis of immune-related DEG. CON, controls; SI, chickens infected with *S.* Typhimurium; SI + BA, chickens supplemented with dietary BA and infected with *S.* Typhimurium. The data in A are means ± SEM, $n = 3$ ($^{*}P < 0.05$).

0.05) to enrich (Figure 9A). In addition, lysosome (gga04142), glycosaminoglycan degradation (gga00531), cytokine–cytokine receptor interaction (gga04060), various types of N-glycan biosynthesis (gga00513), porphyrin and chlorophyll metabolism (gga00860), and intestinal immune network for IgA production (gga004672) were significantly ($P < 0.05$) enriched in 137 DEP between SI and SI + BA (Figure 9B).

4 Discussion

4.1 Effect of BA supplementation on growth performance and the relative weight of immune organs in chickens challenged with *S.* Typhimurium

After invading chickens, *Salmonella* transfers from the gut lumen mainly to the spleen and causes intestinal inflammation and systemic infection, resulting in reduced weight gain of chicken (Zhang et al., 2020). *Salmonella* infection also suppresses the development of immune organs, resulting in atrophy and damage of the thymus and bursa of Fabricius (Huang et al., 2016; Ansari et al., 2018). In the present study, *S.* Typhimurium infection significantly reduced the final BW of chickens, similar to previous studies (Wang et al., 2021; Huang et al., 2022). In addition, *S.* Typhimurium infection decreased the relative weight of the bursa of Fabricius and increased that of the spleen. This splenic response was consistent with the report of Wu et al. (2018) and might be related to the transformation and colonization of *Salmonella* into the spleen.

Plants and their extracts such as anthocyanin (Amer et al., 2022), and silymarin (Shanmugam et al., 2022) have been used for the promotion of growth performance and immune status in chickens. Anthocyanins improved growth performance and development of immune organs in mice, including increasing BW and relative weights of thymus and spleen (Yang et al., 2021). Research on DSS-induced colitis in mice showed that dietary anthocyanins restored the BW and feed quantity (Peng et al., 2019). Dietary BA supplementation in *S.* Typhimurium-infected chickens, here, alleviated weight loss and splenomegaly and, similar to Wang et al. (2021), promoted the development of the bursa of Fabricius. These results indicated that BA increased resistance to external pathogens by regulating the state of the immune organs.

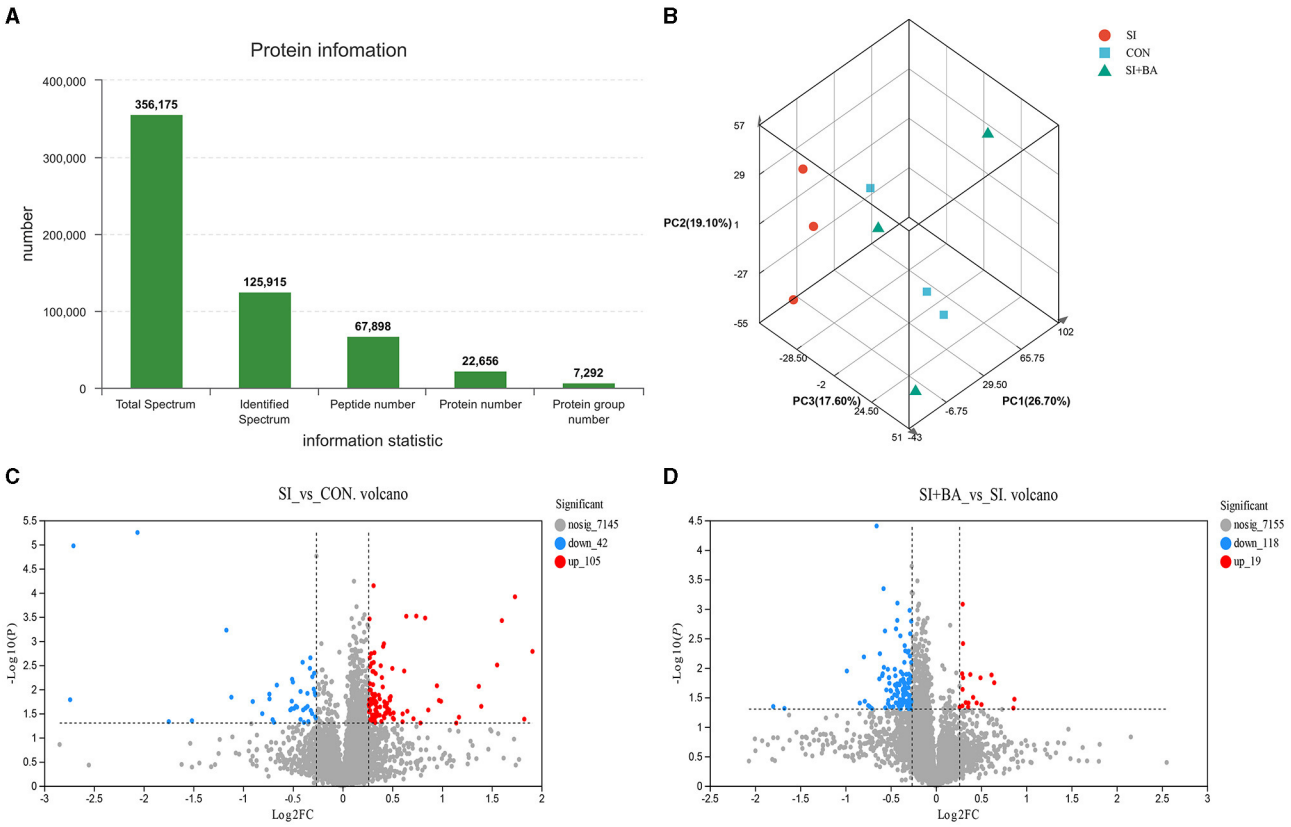

FIGURE 7
Effect of bilberry anthocyanin on the jejunal global protein expression pattern of chickens challenged with *S.* Typhimurium. **(A)** Histogram of protein information statistics. **(B)** Principal component analysis (PCA) of each sample. Volcano map of differentially expressed proteins about **(C)** SI vs. CON and **(D)** SI + BA vs. SI. CON, controls; SI, chickens infected with *S.* Typhimurium; SI + BA, chickens supplemented with dietary BA and infected with *S.* Typhimurium; PC, principal component; FC, fold change; nosig, no significant change.

4.2 Effect of BA supplementation on jejunal morphology and the expression of *mucin* in chickens challenged with *S.* Typhimurium

The intestinal physical barrier and immune functional barrier play an important role in preventing the invasion of pathogens, toxins, and other harmful substances and the diffusion of pro-inflammatory cytokines into the circulatory system (Cornick et al., 2019; Tian et al., 2021). The intestinal tract of chicks lacks an innate immune system; thus, *Salmonella* causes intestinal villus breakage and structural deterioration in chicks more easily and induces intestinal inflammation by damaging intestinal mucosal tolerance after colonization (Zhang et al., 2022). In the present study, *Salmonella* infection decreased VH in the jejunum but BA maintained the integrity and VH of the jejunal villi. Similarly, anthocyanins had an ameliorative effect on intestinal barrier damage from increased intestinal VH with high-fat diet (HFD)-induced colitis in mice (Wang H. et al., 2020) and LPS-induced intestinal inflammation in chickens (Csernus et al., 2020).

Salmonella infection reduced the number of goblet cells in the jejunum of chicks by activating the Notch signaling pathway (Xie et al., 2021). Loss of goblet cells regenerates the mucosal layer of intestinal tissue, decreases the secretion of MUC2, and increases intestinal permeability (Ibrahim et al., 2020; He et al., 2021). Mucins, as the first line of defense of intestinal immunity, help to prevent the invasion of pathogens and toxins (Murai et al., 2018; He et al., 2021). In the present study, the number of goblet cells in the jejunum tended to decrease after *S.* Typhimurium infection, while BA supplementation significantly increased the number of goblet cells and upregulated jejunal expression of the *MUC2* gene. Anthocyanins had previously shown to increase the number of goblet cells in the ileum and colon of HFD-induced mice (Lee et al., 2018; Wang H. et al., 2020) and increased colonic *MUC2* expression in mice (Tian et al., 2019; Wang H. et al., 2020). These are consistent with BA here ameliorating the negative effects of *Salmonella* infection on the number of goblet cells and expression of the *mucin* gene.

4.3 Effect of BA supplementation on jejunal inflammatory cytokines in chickens challenged with *S.* Typhimurium

Immunoglobulins and inflammatory cytokines are key molecules in mediating host cell reactions to *Salmonella* infection.

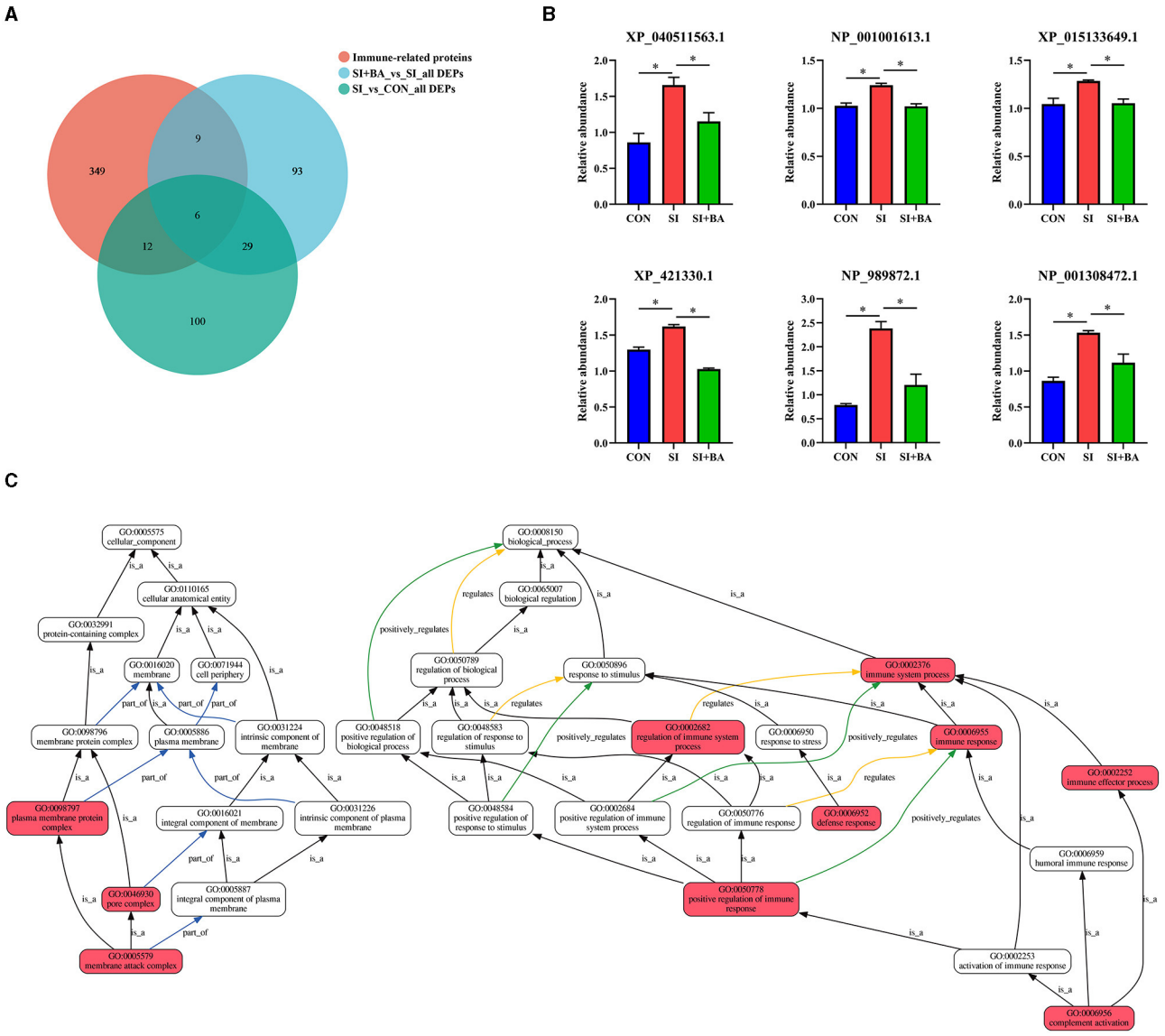

FIGURE 8
Effect of bilberry anthocyanin on the immune-related proteins in the jejunum of chickens challenged with *S.* Typhimurium. In all parts, CON indicates controls; SI are chickens infected with *S.* Typhimurium; SI + BA are chickens supplemented with BA and infected with *S.* Typhimurium; data in B are means ± SEM, $n = 3$ ($^{*}P < 0.05$). **(A)** Venn diagram of the number of immune-related proteins expressed and those that are differentially expressed. **(B)** Differential expression of immune-related proteins. **(C)** Gene Ontology (GO) enrichment analysis of immune-related DEG. Each box represents a GO term (level 2), and the line indicates the relationship between the two GO terms; the closer it is to red, the more significant it is.

IgG, IgM, and IgA are the most common immunoglobulins that are activated during *Salmonella* invasion and released to participate in the elimination of infection (Meijerink et al., 2021). Cytokines (IL-1β, IL-6, IL-8, TNF-α, IFN-β, IFN-γ, etc.), mainly derived from mononuclear phagocytes and other antigen-presenting cells, play important roles in defending against pathogen infection and in promoting infiltration of inflammatory cells in tissues. *S.* Typhimurium infection always results in a strong inflammatory response, accompanied by the secretion of pro-inflammatory cytokines, causing intestinal damage and metabolic abnormalities. *Salmonella* infection in chickens increases the serum concentrations of IgG and IgA (Dar et al., 2019; Song et al., 2020) and IL-1β, IL-6, and TNF-α (Wang G. et al., 2020). *Salmonella* infection increased the expression of *IL-1β*, *IL-6*, and *TNF-α* in the jejunal and ileal mucosa of broilers (Hu et al., 2015; Wu et al., 2018). In the current study, the concentrations of plasma IL-8, TNF-α, IFN-β, IFN-γ, and jejunal TNF-α and IgG were increased in chickens challenged with *S.* Typhimurium. Furthermore, the jejunal expression of *IL-6* increased, similar to the finding of Song et al. (2020).

Anthocyanins show powerful anti-inflammatory activity and immune regulation function. Wu et al. (2017) found that anthocyanins reduced the concentration of inflammatory cytokines (IFN-γ, L-1β, IL-2, IL-4, IL-6, and IL-10) in the serum of chickens. Furthermore, the anti-inflammatory effect of anthocyanins was also demonstrated by inhibiting the levels of IL-1β, IL-6, TNF-α, and

10.3389/fmicb.2023.1266977

TABLE 1 Immune-related DEP information in the jejunum of chickens challenged with *S.* Typhimurium.

Accession	Description	MW, kDa	calc.pI
XP_040511563.1	Complement component C6 isoform X1	104.7	6.92
NP_001308472.1	Complement component C8 beta chain precursor	65.3	7.97
NP_001001613.1	HLA class II histocompatibility antigen gamma chain	31.7	8.31
XP_015133649.1	Tyrosine-protein kinase BTK isoform X1	80.3	7.84
XP_421330.1	Chromogranin-A	53.2	4.49
NP_989872.1	Orosomucoid 1 (ovoglycoprotein) precursor	22.3	5.25

IFN-γ in silica-induced lung tissue injury of mice (Zhao J. et al., 2020), reducing mRNA expression of *IL*-1β, *IL*-6, and *IL*-8 in LPS-induced inflammation in hepatic stellate cell (Lee et al., 2017) and downregulating splenic *IL*-1*β* mRNA expression in chickens (Csernus et al., 2020). Our previous research found that BA supplementation reduced the levels of plasma IgG and IgM in 63-day-old chickens (Wang et al., 2021). This reduction also occurred here, at day 18, where BA reduced plasma IgA and jejunal IgG, IgM, and sIgA in chicks challenged with *S.* Typhimurium. In addition, BA supplementation decreased the content of pro-inflammatory cytokines, such as IL-1β, IL-6, IL-8, TNF-α, IFN-β, and IFN-γ in jejunum and IL-1β, IL-8, and IFN-β in plasma. These results together indicated that BA mainly alleviated the intestinal stress response to *S.* Typhimurium infection, reduced the intestinal pro-inflammatory cytokines, and improved the intestinal environment, thereby alleviating jejunal inflammatory damage, otherwise caused by *S.* Typhimurium infection.

4.4 Effect of BA supplementation on the jejunal transcriptome of chickens challenged with *S.* Typhimurium

In this study, the expression of *MCHY*8, *MCHY*9, *MCHY*11, *TIFA*, and *CCR*10 genes was upregulated by *S.* Typhimurium infection. In addition to classical major histocompatibility complex (MHC), *MHCY* is the second region of polymorphic MHC-like genes associated with bacterial intestinal infection, immune response, and disease incidence (Zhang J. et al., 2021; Goto et al., 2022), the expression of which has a positive correlation with antibody production (Zhang J. B. et al., 2021). In the present study, dietary BA supplementation reduced the expression of *MHCY*, which might be the main reason for suppressing the response to immune challenges and regulating the ability of an individual chicken to respond to *S.* Typhimurium infection.

Activation and oligomerization of TRAF-interacting protein with a forkhead-associated domain (TIFA) were induced by LPS and metabolites produced by Gram-negative bacteria (Gaudet et al.,

TABLE 2 Kyoto Encyclopedia of Genes and Genomes (KEGG) information in the jejunum of chickens challenged with *S.* Typhimurium.

KEGG pathway ID	KEGG description	Associated proteins enriched (symbol ID)	*P*-value
SI vs. CON			
gga04145	Phagosome	C3, C5, CD36, MHC I, MHC II, NOS3, NOX4, SCARB1, SEC22, SRB1	0.004
gga04514	Cell adhesion molecules	B7H3, B7H4, CES1, PDL1, PTPRF, MHC I, MHC II	0.008
gga00512	Mucin-type O-glycan biosynthesis	GALNT, GCNT2	0.022
gga03320	PPAR signaling pathway	ACBP, CAP, CD36, HMGCS, PCK, SCARB1	0.030
gga04512	ECM–receptor interaction	CD36, LAMA4, LAMB2, LAMC2, SCARB1	0.032
gga00980	Metabolism of xenobiotics by cytochrome P450	AKR7, GST, GSTK1, UGT8	0.034
gga00040	Pentose and glucuronate interconversions	SPR, UGT8, XYLB	0.043
gga05168	Herpes simplex virus 1 infection	C3, C5, CASP7, CD74, HCFC, LZTR1, MHC I, MHC II	0.044
gga00860	Porphyrin and chlorophyll metabolism	HEPH, UGT8, UROS	0.049
gga04672	Intestinal immune network for IgA production	LOC101747454, MHC II	0.060
SI + BA vs. SI			
gga04142	Lysosome	ACP2, AP3B, AP4B1, CTCS, GALC, GUSB, HEXA/B, IDUA, NPC1	0.001
gga00531	Glycosaminoglycan degradation	GUSB, HEXA/B, IDUA	0.001
gga04060	Cytokine–cytokine receptor interaction	CD30, IL1RAPL, IL1RL2, NGFR	0.002
gga00513	Various types of N-glycan biosynthesis	FUT8, HEXA/B, MGAT4C	0.031
gga00860	Porphyrin and chlorophyll metabolism	GUSB, HEPH, UROS	0.035
gga04672	Intestinal immune network for IgA production	PDCD1LG2, MHCII	0.048
gga00983	Drug metabolism - other enzymes	AOX, GUSB, GMPR, NME	0.057
gga00232	Caffeine metabolism	AOX	0.090

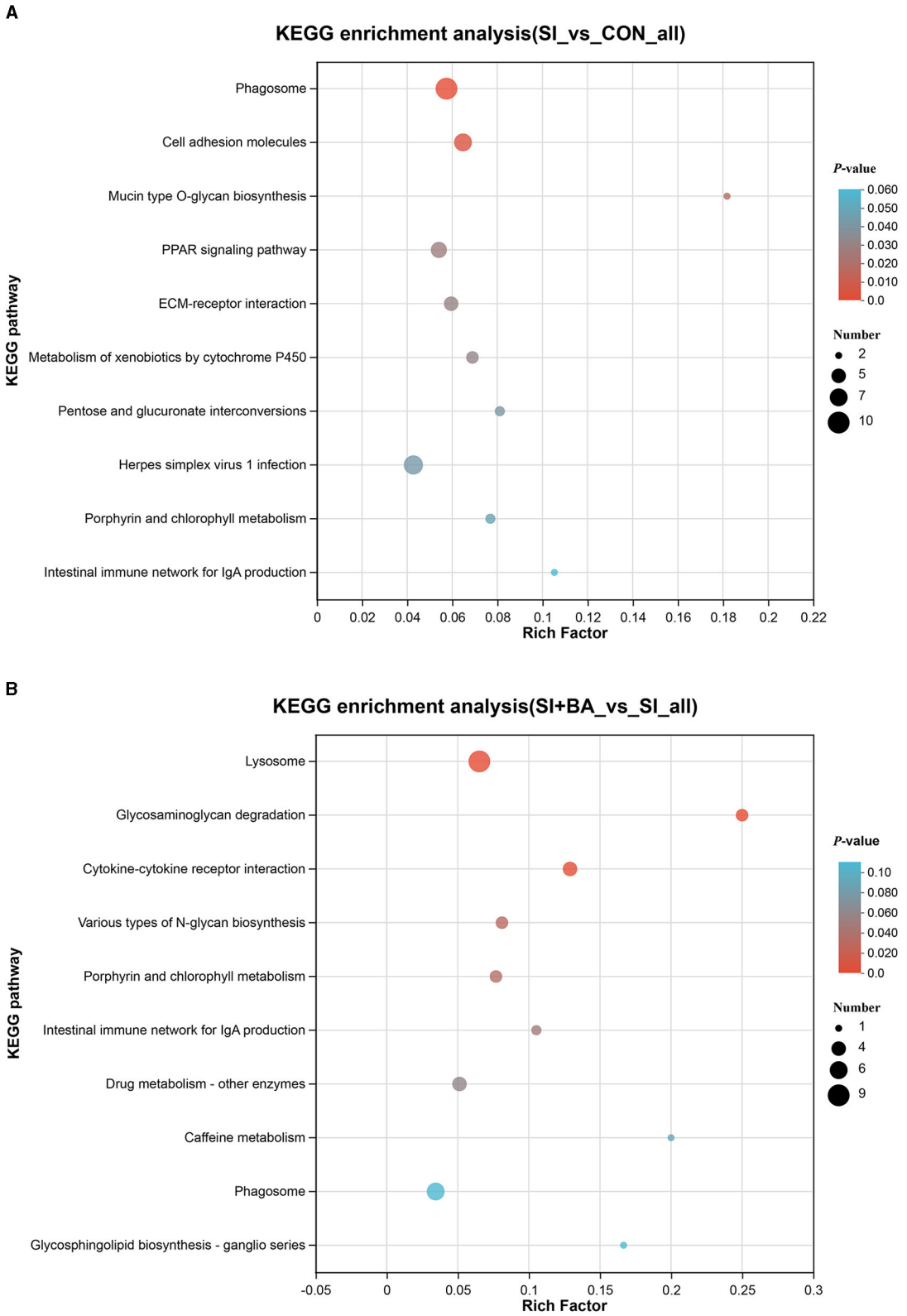

FIGURE 9
Kyoto Encyclopedia of Genes and Genomes (KEGG) analysis of differentially expressed proteins (DEP) in chickens challenged with *S.* Typhimurium. KEGG enrichment analysis of DEP in **(A)** SI vs. CON and **(B)** SI + BA vs. SI. CON, controls; SI, chickens infected with *S.* Typhimurium; SI + BA, chickens supplemented with BA and infected with *S.* Typhimurium.

2017); then, pro-inflammatory cytokines and chemokines were activated via the ALPK1/TIFA signaling axis (Milivojevic et al., 2017; Nasser et al., 2022). In the present study, increased expression of *TIFA* in the jejunum was associated with higher plasma and jejunal contents of TNF-α caused by *S.* Typhimurium infection, similar to the increased phosphorylation and oligomerization of TIFA by TNF-α stimulation (Nakamura et al., 2020). In addition, the increase in plasma IL-8 in the current research was consistent with TIFA-activation promoting IL-8 release (Bauer et al., 2020). As a key regulator of mucosal immune homeostasis, CCR10 is mainly expressed by intestinal IgA^+ plasmablasts and plasma cells (Zhao L. M. et al., 2020; Davila et al., 2022), directing the migration of IgA^+ plasma cells to intestinal epithelium (Seong et al., 2017). Increased *CCR* expression was related to the increased IgA, found here in infected chickens. In *Salmonella*-infected mice, the expression of CCR10 was increased in the inflamed gut and neutrophils (Perez-Lopez et al., 2021). Thus, in the present study, the suppression of *TIFA* and *CCR10* expression with BA supplementation of *S.* Typhimurium-challenged chickens was probably associated with the decreased concentration of immunoglobulins and inflammatory cytokines.

From the GO analysis, nine immune-related DEGs were enriched in the defense response and immune response and increased by *Salmonella* infection. Previous examination of immune markers during the progression of *S.* Typhimurium infection showed that the intestinal defense response was related to the control of inflammation (Bescucci et al., 2020). Research in *Salmonella*-infected chicken showed that humoral immunity, as an effective immune response against *Salmonella* infection, provided effective protection to the host (Wang et al., 2022). In this study, dietary BA supplementation decreased the expression of the above nine immune-related DEGs and the corresponding signaling pathways. Anthocyanin regulated the innate immune system and reduced bacterial systemic dissemination in mice challenged with *Klebsiella pneumoniae* (Dong et al., 2021) and was used as a nutraceutical strategy to modulate stress and immune response in vertebrates (Khan et al., 2023).

Taking these results together, dietary BA supplementation reduced the invasion of *S.* Typhimurium by regulating the immune response and alleviating intestinal inflammatory damage by reducing the production of cytokines.

4.5 Effect of BA supplementation on the jejunal proteome of chicken challenged with *S.* Typhimurium

Complement proteins are the main components of the innate immune system, enhancing the ability of phagocytic cells to disrupt and clear *Salmonella* pathogens. The activation of complement enables the accumulation of membrane attack complexes on the pathogen cell membrane, ultimately leading to the loss of membrane integrity and the death of the pathogen. The complement components C6 and C8 were involved in the process of lysing the cell membrane of pathogens (Meng et al., 2022). The activity of the HLA class II histocompatibility antigen gamma chain was increased in the current study, which was consistent with CD74 being increased in epithelial cells undergoing an inflammatory response (Balasubramanian, 2022). As a chaperone for the correct folding of MHC class II, HLA class II histocompatibility antigen is involved in regulating the antigen presentation pathway of B cells in the immune response (Noer et al., 2021). In addition, the tyrosine-protein kinase *BTK* gene, which plays a key role in the regulation of B-cell receptor signaling, was identified in the *S.* Typhimurium-infected model of mice (Zhang et al., 2018). CgA modulates intestinal barrier permeability and contains unique peptide domains for anti-inflammatory effects (Muntjewerff et al., 2021), and bioactive peptides in the hydrolysates of CgA also have immunomodulatory effects (Muntjewerff et al., 2018). In the present study, two complement proteins (C6 isoform X1 and C8 beta chain precursor), HLA class II histocompatibility antigen gamma chain, and tyrosine-protein kinase BTK isoform X1 and chromogranin-A (CgA) were increased in jejunal mucosa of infected chickens. The secretion of immune-related proteins induced by *S.* Typhimurium infection would cause an adverse response that overactivates the intestinal immune status. These DEPs were associated with the intestinal immune network for IgA production and cytokine–cytokine receptor interaction signaling pathways, consistent with transcriptional findings in the cecal tonsil of chickens challenged with *S.* Typhimurium (Khan and Chousalkar, 2020). The enrichment of the immune-related signaling pathway was involved in the clearance of *S.* Typhimurium in chickens. For example, the cytokine–cytokine receptor interaction signaling pathway was confirmed to be related to the secretion of pro-inflammatory cytokines induced by *S.* Typhimurium infection (Elsharkawy et al., 2022). In addition, the decrease of cytokine responses reduced intestinal inflammation and preserved barrier integrity by *Salmonella*-induced stress of Caco-2 cells (Lépine et al., 2018).

A previous study (Moreira et al., 2021) showed that anthocyanins alleviated LPS-induced stress in mice by suppressing the expression and release of inflammatory cytokines. Consistent with the current study, the expression of the above proteins and the intestinal immune network for the IgA production signaling pathway were downregulated by dietary BA. Secretory IgA is a major immunoglobulin on the mucosal surface against *Salmonella* colonization and invasion (Richards et al., 2021), which protects the intestinal mucosa from infection by binding pathogens and toxins, enhancing the bactericidal activity of monocytes and activating complement production (Adhikari et al., 2019). According to our findings, dietary BA alleviated the immune stimulatory response of *S.* Typhimurium in the jejunum, thus suppressing intestinal inflammatory damage.

5 Conclusion

Dietary supplementation with BA alleviated intestinal inflammatory damage in chickens caused by *S.* Typhimurium infection, as evidenced by the improvement of body weight and the decreased content of inflammatory cytokines in plasma and jejunal mucosal. Furthermore, BA addition decreased the jejunal expression of immune-related genes and proteins, associated

with the defense response to bacteria and the humoral immune response, pathways of cytokine–cytokine receptor interaction, and the intestinal immune network for IgA production. These ensured the healthy immune status and avoided intestinal damage, otherwise caused by an excessive inflammatory response in chickens challenged with *S.* Typhimurium. The current findings provide a new perspective and insight into poultry production in that BA might be used to alleviate *Salmonella* infection.

Data availability statement

The data presented in the study are deposited in the NCBI repository, accession number PRJNA1032740.

Ethics statement

The animal study was approved by Institutional Animal Care and Use Committee, Guangdong Academy of Agricultural Sciences in China (Number: GAASISA-2019-009). The study was conducted in accordance with the local legislation and institutional requirements.

Author contributions

SZ: Conceptualization, Supervision, Writing—original draft, Writing—review & editing. QW: Investigation, Methodology, Writing—review & editing. JY: Investigation, Methodology, Writing—review & editing. QF: Data curation, Formal analysis, Writing—review & editing. XL: Data curation, Formal analysis, Writing—review & editing. ZG: Resources, Writing—review & editing. MA: Resources, Writing—review & editing. YW: Conceptualization, Methodology, Resources, Supervision, Writing—review & editing. SJ: Data curation, Investigation, Resources, Supervision, Visualization, Writing—review & editing.

Funding

The author(s) declare financial support was received for the research, authorship, and/or publication of this article. This study was financially supported by the Natural Science Foundation from Guangdong Province (2021A1515010830), China Agriculture Research System of MOF and MARA (CARS-41), the National Key R&D Project (2021YFD1300404), the Key Realm R&D Program of Guangdong Province (2020B0202090004), the National Natural Science Foundation of China (31802104), the Science and Technology Program of Guangdong Academy of Agricultural Sciences (202106TD and R2019PY-QF008), Introduction of Talents Program from Guangdong Academy of Agricultural Sciences (R2021YJ-YB3012), and Guiding Agreement of Young Scholar from Guangdong Academy of Agricultural Sciences (R2021QD-024), P. R. China. The acknowledgment was extended to the Researchers Supporting Project (RSPD2023R731), King Saud University (Riyadh, Saudi Arabia).

Acknowledgments

W. Bruce Currie (Emeritus Professor, Cornell University) made suggestions for the presentation. The authors thank all workers of the study for their participation.

Conflict of interest

The authors declare that the research was conducted in the absence of any commercial or financial relationships that could be construed as a potential conflict of interest.

Publisher's note

Supplementary material

The Supplementary Material for this article can be found online at: https://www.frontiersin.org/articles/10.3389/fmicb.2023.1266977/full#supplementary-material

References

Abudabos, A. M., Aljumaah, M. R., Alkhulaifi, M. M., Alabdullatif, A., Suliman, G. M., Sulaiman, A. R. A., et al. (2020). Comparative effects of *Bacillus subtilis* and *Bacillus licheniformis* on live performance, blood metabolites and intestinal features in broiler inoculated with *Salmonella* infection during the finisher phase. *Microb. Pathogenesis* 139, 103870. doi: 10.1016/j.micpath.2019.103870

Adhikari, P., Lee, C. H., Cosby, D. E., Cox, N. A., and Kim, W. K. (2019). Effect of probiotics on fecal excretion, colonization in internal organs and immune gene expression in the ileum of laying hens challenged with *Salmonella enteritidis*. *Poultry Sci.* 98, 1235–1242. doi: 10.3382/ps/pey443

Amer, S. A., Al-Khalaifah, H. S., Gouda, A., Osman, A., Goda, N. I., Mohammed, H. A., et al. (2022). Potential effects of anthocyanin-rich roselle (*Hibiscus sabdariffa* L.) extract on the growth, intestinal histomorphology, blood biochemical parameters, and the immune status of broiler chickens. *Antioxidants* 11, 544. doi: 10.3390/antiox11030544

Ansari, A. R., Arshad, M., Masood, S., Huang, H. B., Zhao, X., Li, N. Y., et al. (2018). *Salmonella* infection may alter the expression of toll like receptor 4 and immune related cells in chicken bursa of *Fabricius*. *Microb. Pathogenesis* 121, 59–64. doi: 10.1016/j.micpath.2018.05.019

Balasubramanian, I. (2022). *Paneth Cell-Microbiota Crosstalk Orchestrates Intestinal Homeostasis* [Doctoral dissertation]. Newark, NJ: Rutgers University-Graduate School-Newark.

Bauer, M., Nascakova, Z., Mihai, A. I., Cheng, P. F., Levesque, M. P., Lampart, S., et al. (2020). The ALPK1/TIFA/NF-κB axis links a bacterial carcinogen to R-loop-induced replication stress. *Nat. Commun*. 11, 5117. doi: 10.1038/s41467-020-18857-z

Bescucci, D. M., Moote, P. E., Ortega, P. R., Uwiera, R. R. E., and Inglis, G. D. (2020). *Salmonella enterica* serovar Typhimurium temporally modulates the enteric microbiota and host responses to overcome colonization resistance in swine. *Appl. Environ. Microb*. 86, e01569–20. doi: 10.1128/AEM.01569-20

Chen, C. C., Li, J. Y., Zhang, H. X., Xie, Y. H., Xiong, L. X., Liu, H., et al. (2020). Effects of a probiotic on the growth performance, intestinal flora, and immune function of chicks infected with *Salmonella pullorum*. *Poultry Sci*. 99, 5316–5323. doi: 10.1016/j.psj.2020.07.017

Chen, G. W., Wang, G., Zhu, C. J., Jiang, X. W., Sun, J. X., Tian, L. M., et al. (2019). Effects of cyanidin-3-O-glucoside on 3-chloro-1,2-propanediol induced intestinal microbiota dysbiosis in rats. *Food Chem. Toxicol*. 133, 110767. doi: 10.1016/j.fct.2019.110767

Cheng, Y. L., Zhang, S. H., Lu, Q., Zhang, W. T., Wen, G. Y., Luo, Q. P., et al. (2020). Evaluation of young chickens challenged with aerosolized *Salmonella* Pullorum. *Avian Pathol*. 49, 507–514. doi: 10.1080/03079457.2020.1783433

Cornick, S., Kumar, M., Moreau, F., Gaisano, H., and Chadee, K. (2019). VAMP8-mediated MUC2 mucin exocytosis from colonic goblet cells maintains innate intestinal homeostasis. *Nat. Commun*. 10, 4306. doi: 10.1038/s41467-019-11811-8

Csernus, B., Biró, S., Babinszky, L., Komlósi, I., Jávor, A., Stündl, L., et al. (2020). Effect of carotenoids, oligosaccharides and anthocyanins on growth performance, immunological parameters and intestinal morphology in broiler chickens challenged with *Escherichia coli* lipopolysaccharide. *Animals* 10, 347. doi: 10.3390/ani10020347

Dar, M. A., Urwat, U., Ahmad, S. M., Ahmad, R., Kashoo, Z. A., Dar, T. A., et al. (2019). Gene expression and antibody response in chicken against *Salmonella* Typhimurium challenge. *Poultry Sci*. 98, 2008–2013. doi: 10.3382/ps/pey560

Davila, M. L., Xu, M., Huang, C. Y., Gaddes, E. R., Winter, L., Cantorna, M. T., et al. (2022). CCL27 is a crucial regulator of immune homeostasis of the skin and mucosal tissues. *iScience* 25, 104426. doi: 10.1016/j.isci.2022.104426

Dong, G. K., Xu, N. N., Wang, M., Zhao, Y. Y., Jiang, F., Bu, H. M., et al. (2021). Anthocyanin extract from purple sweet potato exacerbate mitophagy to ameliorate pyroptosis in *Klebsiella pneumoniae* infection. *Int. J. Mol. Sci*. 22, 11422. doi: 10.3390/ijms222111422

Elsharkawy, M. S., Wang, H. L., Ding, J. Q., Madkour, M., Wang, Q., Zhang, Q., et al. (2022). Transcriptomic analysis of the spleen of different chicken breeds revealed the differential resistance of *Salmonella* Typhimurium. *Genes* 13, 811. doi: 10.3390/genes13050811

Foster, N., Kyriazakis, I., and Barrow, P. (Eds). (2021). *Advancements and Technologies in Pig and Poultry Bacterial Disease Control*. Cambridge, MA: Academic Press.

Gao, J., Yu, W. C., Zhang, C. J., Liu, H. W., Fan, J. G., Wei, J., et al. (2021). The protective effect and mechanism of *Aornia melanocarpa* Elliot anthocyanins on IBD model mice. *Food Biosci*. 41, 2212–4292. doi: 10.1016/j.fbio.2021.101075

Gaudet, R. G., Guo, C. X., Molinaro, R., Kottwitz, H., Rohde, J. R., Dangeard, A. S., et al. (2017). Innate recognition of intracellular bacterial growth is driven by the TIFA-dependent cytosolic surveillance pathway. *Cell Rep*. 19, 1418–1430. doi: 10.1016/j.celrep.2017.04.063

Goto, R. M., Warden, C. D., Shiina, T., Hosomichi, K., Zhang, J., Kang, T. H., et al. (2022). The *Gallus gallus* RJF reference genome reveals an MHCY haplotype organized in gene blocks that contain 107 loci including 45 specialized, polymorphic MHC class I loci, 41 C-type lectin-like loci, and other loci amid hundreds of transposable elements. *G3* 11, jkac218. doi: 10.1093/g3journal/jkac218

He, Y., Ayansola, H., Hou, Q. H., Liao, C. Y., Lei, J. Q., Lai, Y. J., et al. (2021). Genistein inhibits colonic goblet cell loss and colorectal inflammation induced by *Salmonella* Typhimurium infection. *Mol. Nutr. Food Res*. 65, 2100209. doi: 10.1002/mnfr.202100209

Hu, J. L., Yu, H., Kulkarni, R. R., Sharif, S., Cui, S. W., Xie, M. Y., et al. (2015). Modulation of cytokine gene expression by selected *Lactobacillus* isolates in the ileum, caecal tonsils and spleen of *Salmonella*-challenged broilers. *Avian Pathol*. 44, 463–469. doi: 10.1080/03079457.2015.1086725

Huang, H. B., Liu, A., Wu, H., Ansari, A. R., Wang, J. X., Huang, X. Y., et al. (2016). Transcriptome analysis indicated that *Salmonella* lipopolysaccharide-induced thymocyte death and thymic atrophy were related to TLR4-FOS/JUN pathway in chicks. *BMC Genomics* 17, 1–11. doi: 10.1186/s12864-016-2674-6

Huang, J. Q., Liang, L., Cui, K. T., Li, P. Y., Hao, G. J., Sun, S. H., et al. (2022). *Salmonella* phage CKT1 significantly relieves the body weight loss of chicks by normalizing the abnormal intestinal microbiome caused by hypervirulent *Salmonella* Pullorum. *Poultry Sci*. 101, 101668. doi: 10.1016/j.psj.2021.101668

Ibrahim, D., Sewid, A. H., Arisha, A. H., Abd El-Fattah, A. H., Abdelaziz, A. M., Al-Jabr, O., et al. (2020). Influence of *glycyrrhiza glabra* extract on growth, gene expression of gut integrity, and *campylobacter jejuni* colonization in broiler chickens. *Front. Vet. Sci*. 7, 612063. doi: 10.3389/fvets.2020.612063

Karabasanavar, S. N., Madhavaprasad, B. C., Gopalakrishna, A. S., Hiremath, J., Shivanagowda, Patil, G., and Barbuddhe, S. B. (2020). Prevalence of *Salmonella* serotypes *S. Enteritidis* and *S.* Typhimurium in poultry and poultry products. *J. Food Safety* 40, e12852. doi: 10.1111/jfs.12852

Khan, M., Mortuza, A., Blumenthal, E., and Mustafa, A. (2023). Role of elderberry (*Sambucus nigra*) on the modulation of stress and immune response of Nile tilapia, *Oreochromis niloticus*. *J. Appl. Aquacult*. 35, 765–787. doi: 10.1080/10454438.2022.2026269

Khan, S., and Chousalkar, K. K. (2020). Transcriptome profiling analysis of caeca in chicks challenged with *Salmonella* Typhimurium reveals differential expression of genes involved in host mucosal immune response. *Appl. Microbiol. Biotechnol*. 104, 9327–9342. doi: 10.1007/s00253-020-10887-3

Kovács, D., Palkovicsné Pézsa, N., Jerzsele, Á., Süth, M., and Farkas, O. (2022). Protective effects of grape seed oligomeric proanthocyanidins in IPEC-J2–*Escherichia coli*/*Salmonella* Typhimurium Co-Culture. *Antibiotics* 11, 110. doi: 10.3390/antibiotics11010110

Lee, J. W., Kim, Y. I., Kim, Y., Choi, M., Min, S., Joo, Y. H>, et al. (2017). Grape seed proanthocyanidin inhibits inflammatory responses in hepatic stellate cells by modulating the MAPK, Akt and NF-κB signaling pathways. *Int. J. Mol. Med*. 40, 226–234. doi: 10.3892/ijmm.2017.2997

Lee, S., Keirsey, K. I., Kirkland, R., Grunewald, Z. I., Fischer, J. G., La, D. e., et al. (2018). Blueberry supplementation influences the gut microbiota, inflammation, and insulin resistance in high-fat-diet–fed rats. *J. Nutr*. 148, 209–219. doi: 10.1093/jn/nxx027

Lépine, A. F. P., de Wit, N., Oosterink, E., Wichers, H., Mes, J., and de Vos, P. (2018). *Lactobacillus acidophilus* attenuates *Salmonella*-induced stress of epithelial cells by modulating tight-junction genes and cytokine responses. *Front. Microbiol*. 9, 1439. doi: 10.3389/fmicb.2018.01439

Luo, G., Zhao, L. M., Xu, X. J., Qin, Y. X., Huang, L. X., Su, Y. Q., et al. (2019). Integrated dual RNA-seq and dual iTRAQ of infected tissue reveals the functions of a diguanylate cyclase gene of *Pseudomonas plecoglossicida* in host-pathogen interactions with *Epinephelus coioides*. *Fish Shellfish Immun*. 95, 481–490. doi: 10.1016/j.fsi.2019.11.008

Manyi-Loh, C., Mamphweli, S., Meyer, E., and Okoh, A. (2018). Antibiotic use in agriculture and its consequential resistance in environmental sources: potential public health implications. *Molecules* 23, 795. doi: 10.3390/molecules23040795

Meijerink, N., van den Biggelaar, R. H. G. A., van Haarlem, D. A., Stegeman, J. A., Rutten, V. P. M. G., and Jansen, C. A. (2021). Contribution of innate and adaptive immune cells to the elimination of *Salmonella enterica* serotype *Enteritidis* infection in young broiler chickens. *Cold Spring Harb. Lab*. 29, 428771. doi: 10.1101/2021.01.29.428771

Meng, Y. Q., Chen, D., Qiu, N., Mine, Y., Keast, R., Meng, S. C., et al. (2022). Comparative N-glycoproteomic analysis of Tibetan and lowland chicken fertilized eggs: implications on proteins biofunction and species evolution. *J. Food Biochem*. 46, e14006. doi: 10.1111/jfbc.14006

Milivojevic, M., Dangeard, A. S., Kasper, C. A., Tschon, T., Emmenlauer, M., Pique, C., et al. (2017). ALPK1 controls TIFA/TRAF6-dependent innate immunity against heptose-1,7-bisphosphate of gram-negative bacteria. *Plos Pathog*. 13, e1006224. doi: 10.1371/journal.ppat.1006224

Ministry of Agriculture of the People's Republic of China (PRC) (2020). *Nutrient Requirements of Yellow Chicken*. Beijing: China Agricultural Press.

Molagoda, I. M. N., Lee, K. T., Choi, Y. H., Jayasingha, J. A. C. C., and Kim, G. Y. (2021). Anthocyanins from *Hibiscus syriacus* L. inhibit NLRP3 inflammasome in BV2 microglia cells by alleviating NF-κB- and ER stress-induced Ca^{2+} accumulation and mitochondrial ROS production. *Oxid. Med. Cell Longev*. 4, 1246491. doi: 10.1155/2021/1246491

Moreira, V., Stanquevis, R., Amaral, E. P., Lajolo, F. M., and Hassimotto, N. M. A. (2021). Anthocyanins from purple maize (*Zea mays L.*) downregulate lipopolysaccharide-induced peritonitis in mice by modulating the MyD88 signaling pathway. *PharmaNutrition* 16, 100265. doi: 10.1016/j.phanu.2021.100265

Mshelbwala, F. M., Ibrahim, N. D. G., Saidu, S. N., Kadiri, A. K. F., and Kwanashie, C. N. (2019). Comparison of the clinical signs, pathological and immuohistochemical findings in visceral organs of chickens experimentally infected with *Salmonella Zega* through three routes. *Acta Trop*. 200, 105123. doi: 10.1016/j.actatropica.2019.105123

Muntjewerff, E. M., Dunkel, G., Nicolasen, M. J. T., Mahata, S. K., and van den Bogaart, G. (2018). Catestatin as a target for treatment of inflammatory diseases. *Front. Immunol*. 9, 2199. doi: 10.3389/fimmu.2018.02199

Muntjewerff, E. M., Tang, K., Lutter, L., Christoffersson, G., Nicolasen, M. J. T., Gao, H., et al. (2021). Chromogranin A regulates gut permeability via the antagonistic actions of its proteolytic peptides. *Acta Physiol.* 232, e13655. doi: 10.1111/apha.13655

Murai, A., Kitahara, K., Terada, H., Ueno, A., Ohmori, Y., Kobayashi, M., et al. (2018). Ingestion of paddy rice increases intestinal mucin secretion and goblet cell number and prevents dextran sodium sulfate-induced intestinal barrier defect in chickens. *Poultry Sci*. 97, 3577–3586. doi: 10.3382/ps/pey202

Nakamura, T., Hashikawa, C., Okabe, K., Yokote, Y., Chirifu, M., Toma-Fukai, S., et al. (2020). Structural analysis of tifA: insight into tifA-dependent signal transduction in innate immunity. *Sci. Rep*. 10, 5152. doi: 10.1038/s41598-020-61972-6

Nasser, A., Mosadegh, M., Azimi, T., and Shariati, A. (2022). Molecular mechanisms of *Shigella* effector proteins: a common pathogen among diarrheic pediatric population. *Mol. Cell. Pediatr*. 9, 1–21. doi: 10.1186/s40348-022-00145-z

Noer, J. B., Talman, M. L. M., and Moreira, J. M. A. (2021). HLA class II histocompatibility antigen γ chain (CD74) expression is associated with immune cell infiltration and favorable outcome in breast cancer. *Cancers* 13, 6179. doi: 10.3390/cancers13246179

Peng, Y. J., Yan, Y. M., Wan, P., Chen, D., Ding, Y., Ran, L. W., et al. (2019). Gut microbiota modulation and anti-inflammatory properties of anthocyanins from the fruits of *Lycium ruthenicum* Murray in dextran sodium sulfate-induced colitis in mice. *Free Radic. Biol. Med*. 136, 96–108. doi: 10.1016/j.freeradbiomed.2019.04.005

Peng, Y. J., Yan, Y. M., Wan, P., Dong, W., Huang, K. Y., Ran, L. W., et al. (2020). Effects of long-term intake of anthocyanins from *Lycium ruthenicum* murray on the organism health and gut microbiota in *vivo*. *Food Res. Int*. 130, 108952. doi: 10.1016/j.foodres.2019.108952

Perez-Lopez, A., Silva, S., Dillon, N., Brandt, S. L., Gerner, R. R., Melchior, K., et al. (2021). CCL28 modulates neutrophil responses during infection with mucosal pathogens. *Cold Spring Harb. Lab*. 19, 436197. doi: 10.1101/2021.03.19.436197

Purwanti, S., Agustina, L., Jamilah, Syamsu, J. A., and Putra, R. D. (2019). Histology of the liver and small intestine broiler using phytobiotic in the ration infected *Salmonella pullorum*. *IOP Conf. Ser.: Earth Environ. Sci*. 247, 012054. doi: 10.1088/1755-1315/247/1/012054

Ren, Y., Yu, G., Shi, C., Liu, L. M., Guo, Q., Han, C., et al. (2022). Majorbio Cloud: A one-stop, comprehensive bioinformatic platform for multiomics analyses. *IMeta* 1, e12. doi: 10.1002/imt2.12

Richards, A. F., Baranova, D. E., Pizzuto, M. S., Jaconi, S., Willsey, G. G., Torres-Velez, F. J., et al. (2021). Recombinant human secretory iga induces *Salmonella* typhimurium agglutination and limits bacterial invasion into gut-associated lymphoid tissues. *ACS Infect. Dis*. 7, 1221–1235. doi: 10.1021/acsinfecdis.0c00842

Seong, Y., Lazarus, N. H., Sutherland, L., Habtezion, A., Abramson, T., He, X. S., et al. (2017). Trafficking receptor signatures define blood plasmablasts responding to tissue-specific immune challenge. *JCI Insight* 2, e90233. doi: 10.1172/jci.insight.90233

Shanmugam, S., Park, J. H., Cho, S., and Kim, I. H. (2022). Silymarin seed extract supplementation enhances the growth performance, meat quality, and nutrients digestibility, and reduces gas emission in broilers. *Anim. Biosci.* 35, 1215. doi: 10.5713/ab.21.0539

Song, J., Li, Q. H., Everaert, N., Liu, R. R., Zheng, M. Q., Zhao, G. P., et al. (2020). Effects of inulin supplementation on intestinal barrier function and immunity in specific pathogen-free chickens with *Salmonella* infection. *J. Anim. Sci*. 98, skz396. doi: 10.1093/jas/skz396

Tian, B. M., Zhao, J. H., An, W., Zhang, J. W., Cao, X., Mi, J. L., et al. (2019). *Lycium ruthenicum* diet alters the gut microbiota and partially enhances gut barrier function in male C57BL/6 mice. *J. Funct. Foods* 52, 516–528. doi: 10.1016/j.jff.2018.11.034

Tian, B. M., Zhao, J. H., Zhang, M., Chen, Z. F., Ma, Q. Y., Liu, H. C., et al. (2021). *Lycium ruthenicum* anthocyanins attenuate high-fat diet-induced colonic barrier dysfunction and inflammation in mice by modulating the gut microbiota. *Mol. Nutr. Food Res.* 65, 2000745. doi: 10.1002/mnfr.202000745

Wang, G., Song, Q. L., Huang, S., Wang, Y. M., Cai, S., Yu, H. T., et al. (2020). Effect of antimicrobial peptide microcin J25 on growth performance, immune regulation, and intestinal microbiota in broiler chickens challenged with *Escherichia coli* and *Salmonella*. *Animals* 10, 345. doi: 10.3390/ani10020345

Wang, H., Liu, D., Ji, Y. L., Liu, Y. J., Xu, L., Guo, Y. T., et al. (2020). Dietary supplementation of black rice anthocyanin extract regulates cholesterol metabolism and improves gut microbiota dysbiosis in C57BL/6J mice fed a high-fat and cholesterol diet. *Mol. Nutr. Food Res.* 64, 1900876. doi: 10.1002/mnfr.201900876

Wang, X. W., Kang, X. L., Pan, M. X., Wang, M., Zhang, J. Y., Song, H. Q., et al. (2022). Evaluation of the protective immune response induced by an *rfbG*-deficient *Salmonella enterica* serovar enteritidis strain as a live attenuated DIVA (differentiation of infected and vaccinated animals) vaccine in chickens. *Microbiol. Spectr*. 15, 01574–22. doi: 10.1128/spectrum.01574-22

Wang, Y. M., Li, J. Y., Xie, Y. H., Zhang, H. X., Jin, J. H., Xiong, L. X., et al. (2021). Effects of a probiotic-fermented herbal blend on the growth performance, intestinal flora and immune function of chicks infected with *Salmonella pullorum*. *Poultry Sci.* 100, 101196. doi: 10.1016/j.psj.2021.101196

Wu, Q. J., Wang, Y. Q., and Qi, Y. X. (2017). Influence of procyanidin supplementation on the immune responses of broilers challenged with lipopolysaccharide. *Anim. Sci. J.* 88, 983–990. doi: 10.1111/asj.12729

Wu, Q. J., Zheng, X. C., Wang, T., and Zhang, T. Y. (2018). Effects of oridonin on immune cells, Th1/Th2 balance and the expression of BLys in the spleens of broiler chickens challenged with *Salmonella pullorum*. *Res. Vet. Sci*. 119, 262–267. doi: 10.1016/j.rvsc.2018.07.008

Xie, S., Zhang, H., Matjeke, R. S., Zhao, J. Y., and Yu, Q. H. (2021). *Bacillus coagulans* protect against *Salmonella enteritidis*-induced intestinal mucosal damage in young chickens by inducing the differentiation of goblet cells. *Poultry Sci*. 101, 101639. doi: 10.1016/j.psj.2021.101639

Yang, S., Wang, C., Li, X. Y., Wu, C. E., Liu, C., Xue, Z. H., et al. (2021). Investigation on the biological activity of anthocyanins and polyphenols in blueberry. *J. Food Sci*. 86, 614–627. doi: 10.1111/1750-3841.15598

Zhang, H. Y., Pan, S. Q., Zhang, K. Y., Michiels, J., Zeng, Q. F., Ding, X. M., et al. (2020). Impact of dietary manganese on intestinal barrier and inflammatory response in broilers challenged with *Salmonella* typhimurium. *Microorganisms* 8, 757. doi: 10.3390/microorganisms8050757

Zhang, J., Goto, R. M., Psifidi, A., Stevens, M. P., Taylor, R. L., Miller, M. M., et al. (2021). Research note: MHCY haplotype impacts *Campylobacter jejuni* colonization in a backcross [(Line 6(1) x Line N) x Line N] population. *Poultry Sci*. 101, 101654. doi: 10.1016/j.psj.2021.101654

Zhang, J., Malo, D., Mott, R., Panthier, J. J., Montagutelli, X., Jaubert, J., et al. (2018). Identification of new loci involved in the host susceptibility to *Salmonella* Typhimurium in collaborative cross mice. *BMC Genomics* 19, 303. doi: 10.1186/s12864-018-4667-0

Zhang, J. B., Goto, R. M., Honaker, C. F., Siegel, P. B., Taylor, R. L., Parmentier, H. K., et al. (2021). Association of MHCY genotypes in lines of chickens divergently selected for high or low antibody response to sheep red blood cells. *Poultry Sci*. 101, 101621. doi: 10.1016/j.psj.2021.101621

Zhang, X. S., Song, M. Z., Lv, P. H., Hao, G. J., and Sun, S. H. (2022). Effects of *Clostridium butyricum* on intestinal environment and gut microbiome under *Salmonella* infection. *Poultry Sci*. 101, 102077. doi: 10.1016/j.psj.2022.102077

Zhao, J., Ma, J. X., Zhang, Q., Tian, J. L., Wang, Y. H., Meng, X. J., et al. (2020). Cyanidin-3-glucoside attenuates silica-induced pulmonary inflammatory responses by modulating T cell immune responses and STAT1/STAT3 signaling. *J. Funct. Foods* 68, 103911. doi: 10.1016/j.jff.2020.103911

Zhao, L. M., Hu, S. M., Davila, M. L., Yang, J., Lin, Y. D., Albanese, J. M., et al. (2020). Coordinated co-migration of CCR10+ antibody-producing B cells with helper T cells for colonic homeostatic regulation. *Mucosal Immunol*. 14, 420–430. doi: 10.1038/s41385-020-0333-3

frontiers | Frontiers in Microbiology

TYPE Original Research
PUBLISHED 24 November 2023
DOI 10.3389/fmicb.2023.1282894

OPEN ACCESS

EDITED BY
Patrick J. Naughton,
Ulster University, United Kingdom

REVIEWED BY
Babak Pakbin,
Technical University of Munich, Germany
Peter Johnston,
University of Liverpool, United Kingdom

*CORRESPONDENCE
Lisette Mbuyi-Kalonji
✉ lisettekalonji@gmail.com

†These authors have contributed equally to this work and share last authorship

RECEIVED 25 August 2023
ACCEPTED 17 October 2023
PUBLISHED 24 November 2023

CITATION
Mbuyi-Kalonji L, Hardy L, Mbuyamba J, Phoba M-F, Nkoji G, Mattheus W, Im J, Marks F, Jeon HJ, Jacobs J and Lunguya O (2023) Invasive non-typhoidal *Salmonella* from stool samples of healthy human carriers are genetically similar to blood culture isolates: a report from the Democratic Republic of the Congo. *Front. Microbiol.* 14:1282894. doi: 10.3389/fmicb.2023.1282894

Invasive non-typhoidal *Salmonella* from stool samples of healthy human carriers are genetically similar to blood culture isolates: a report from the Democratic Republic of the Congo

Lisette Mbuyi-Kalonji[1,2,3,4]*, Liselotte Hardy[3], Jules Mbuyamba[1,2], Marie-France Phoba[1,2], Gaëlle Nkoji[1,2], Wesley Mattheus[5], Justin Im[6], Florian Marks[6,7,8,9], Hyon Jin Jeon[6,7,9], Jan Jacobs[3,4†] and Octavie Lunguya[1,2†]

[1]Department of Microbiology, National Institute for Biomedical Research, Kinshasa, Democratic Republic of Congo, [2]Department of Microbiology, University Teaching Hospital of Kinshasa, Kinshasa, Democratic Republic of Congo, [3]Department of Clinical Sciences, Institute of Tropical Medicine, Antwerp, Belgium, [4]Department of Microbiology, Immunology and Transplantation, KU Leuven, Leuven, Belgium, [5]Department of Human Bacterial Diseases, Sciensano, Brussels, Belgium, [6]International Vaccine Institute, Seoul, Republic of Korea, [7]Cambridge Institute of Therapeutic Immunology and Infectious Disease, University of Cambridge School of Clinical Medicine, Cambridge Biomedical Campus, Cambridge, United Kingdom, [8]Heidelberg Institute of Global Health, University of Heidelberg, Heidelberg, Germany, [9]Madagascar Institute for Vaccine Research, University of Antananarivo, Antananarivo, Madagascar

Invasive non-typhoidal *Salmonella* (iNTS) (serotypes Typhimurium and Enteritidis) are major causes of bloodstream infections in sub-Saharan Africa, but their reservoir is unknown. Aiming to demonstrate human carriers as a reservoir, we assessed an iNTS disease endemic rural community (Kikonka health area, Democratic Republic of the Congo) for intestinal carriage of iNTS. After a census, healthy subjects from randomly selected households provided three successive stool samples for *Salmonella* culture. We next compared the stool isolates for genetic relatedness with time and health area-matched blood culture isolates obtained from hospitalized patients by multiple locus variable-number tandem repeat analysis (MLVA) and performed whole genome sequencing (WGS) on a subset of stool and blood isolates. Among 2,354 eligible subjects, 2,234 (94.9%) consented and provided at least one stool sample, and 2,219 (94.3%) provided three stool samples. The cumulative proportion of *Salmonella* carriers after 3 days was 4.4% (n = 98). *S.* Typhimurium and Enteritidis were found in 26 and 3 carriers, respectively, representing 1.3% (29 out of 2,234) of participants living in 6.0% (26 out of 482) of households. MLVA types of all 26 *S.* Typhimurium stool isolates matched with the corresponding MLVA types of blood isolates. The MLVA type of one out of three Enteritidis stool isolates matched the single MLVA type of the five Enteritidis blood isolates. WGS analysis of *S.* Typhimurium (n = 20) and *S.* Enteritidis (n = 4) isolates revealed Typhimurium multilocus sequence type (ST)313 Lineage 2 and Enteritidis ST11 Central/Eastern African and Outlier clades and confirmed the MLVA clustering. More than three-quarters of Typhimurium isolates showed combined multidrug resistance, ceftriaxone resistance, and fluoroquinolone non-susceptibility. In conclusion, the present

study demonstrated iNTS carriage among healthy community members, with stool isolates that were genetically similar to blood culture isolates obtained in patients from the same community. These findings contribute to the evidence of a human reservoir of iNTS.

KEYWORDS

***Salmonella Typhimurium* ST313, *Salmonella Enteritidis* ST11, human carriers, reservoir, Africa, DR Congo**

Introduction

Non-typhoidal *Salmonella* are a major cause of invasive infections in sub-Saharan Africa, particularly among children younger than 5 years old with *Plasmodium falciparum* malaria or malnutrition and HIV-infected adults (Feasey et al., 2012; Crump and Heyderman, 2015; Gilchrist and MacLennan, 2019). For the year 2017, the burden of invasive non-typhoidal *Salmonella* (iNTS) infections in sub-Saharan Africa was estimated to be 421,600 cases (95% confidence interval (C.I.) 316,000 to 574,100) resulting in 66,520 deaths (40,130 to 105,500) (Stanaway et al., 2019). The most frequent iNTS serotypes are *Salmonella enterica* subspecies *enterica* serotype Typhimurium and Enteritidis, respectively (further shortly referred to as *S.* Typhimurium and *S.* Enteritidis). Typical clades in sub-Saharan Africa are *S.* Typhimurium multilocus sequence type (ST) 313 (in particular the multidrug-resistant Lineage 2) and the Central/East-African and West-African subclades of *S.* Enteritidis ST11 (Feasey et al., 2016; Van Puyvelde et al., 2019; Park et al., 2021; Pulford et al., 2021).

Salmonella Typhi and Paratyphi (causing enteric fever) are human-specific, and human intestinal carriers (*i.e.,* convalescent or healthy subjects shedding *S.* Typhi/Paratyphi in their stools) have been identified as the reservoir; transmission occurs through contaminated water or food (Crump and Heyderman, 2015). Conversely, the reservoir and transmission of iNTS are not fully understood. Given their broad host range, *S.* Typhimurium and *S.* Enteritidis are categorized as "generalist" serovars and their reservoir is assumed to be zoonotic (Feasey et al., 2012; Crump and Heyderman, 2015), but invasive *S.* Typhimurium and *S.* Enteritidis underwent genome degradations such as pseudogenes and deletions, which could be consistent with adaptation to human host (Feasey et al., 2016; Pulford et al., 2021) and consistent arguments for a human reservoir have been provided (Kariukiet al., 2006; Dione, 2010; Post et al., 2019; Phoba et al., 2020).

In the Democratic Republic of the Congo (DRC), the National Institute of Biomedical Research (INRB, Kinshasa) in partnership with the Institute of Tropical Medicine (ITM, Belgium) has a microbiological surveillance network in place since 2007. Laboratories of sentinel hospitals across DRC process free-of-charge blood cultures implemented in routine patient care. Kisantu General Referral Hospital Saint Luc (further referred to as Kisantu Hospital) in the Province of Kongo Central is the main sampling site. Over the years 2015–2017, iNTS accounted for >70% of blood culture pathogens recovered in children younger than 5 years old admitted to Kisantu Hospital, representing nearly 300 patients per year (Tack et al., 2020a). From October 2017 to March 2020, Kisantu Hospital was the DRC study site of the Severe Typhoid in Africa (SETA) program coordinated by the International Vaccine Institute (IVI, Republic of Korea). The SETA program conducted enhanced surveillance for febrile illnesses in sites of six sub-Saharan African countries (Hyon Jin Jeon submitted).

Recently, we assessed non-typhoidal *Salmonella* intestinal carriage in healthy subjects living in a *Schistosoma*-endemic area in the Kongo Central Province of DRC, at a distance of 66 km from Kisantu. Among 38 *Salmonella* isolates (overall prevalence of 3.4%), there were 4 and 5 Typhimurium and Enteritidis isolates, respectively (Mbuyi-Kalonji et al., 2020). Most of these isolates were genetically similar to Typhimurium and Enteritidis isolates obtained from blood cultures in Kisantu Hospital. Furthermore, previous studies (Burkina Faso, DRC) showed among non-typhoidal *Salmonella* a tendency toward household clustering (Im et al., 2016; Post et al., 2019; Falay et al., 2023). We hypothesized that sampling a larger community closer to Kisantu Hospital would allow for a better study of the concordance between blood and stool culture iNTS isolates and their occurrence in households. We therefore conducted a household-level randomized stool culture in a community close to Kisantu Hospital. The objectives were to assess (i) the proportion, age, and gender distribution of human *Salmonella* intestinal carriers (in particular iNTS); (ii) the serotype distribution and antimicrobial resistance (AMR) pattern of the isolates; and (iii) the genetic relatedness between iNTS stool and blood culture isolates obtained from Kisantu Hospital. Secondary objectives were to assess the incremental yield of three consecutive stool samples for the detection of NTS carriers and the potential clustering of *Salmonella* carriers among household members.

Methods

Ethics statement

This study was approved by the Institutional Review Board of the Institute of Tropical Medicine (Reference 1263/18), the Ethical Committee of the University of Antwerp (Reference 18/47/535), and the Ethical Committee of Public Health School in Kinshasa, Democratic Republic of the Congo (ESP/EC/070/2019). Adults were included after written informed consent was provided. All children younger than 18 years old were included after written informed consent from their parents or their legal guardians. Additionally, for adolescents between 12 and 18 years of age, a written assent was obtained. Ethical approval for the blood culture surveillance study was granted by the Institutional Review Board of the Institute of Tropical Medicine (Reference 08 17 12 613) and the Ethics Committee of Public Health School in Kinshasa (version 1:

ESP/CE/073/2015 and version 2: ESP/CE/074/2015). For the SETA study, ethical approvals were granted by the International Vaccine Institute Institutional Review Board (IRB No. 2015-006) and the Ethics Committee of Public Health School in Kinshasa (version 1.1: ESP/CE/011/2017, version 1.2: ESP/CE/011B/2017, and version 1.3: ESP/CE/037/2018 and ESP/CE/037B/2019). Compensation for participation in the study was provided to the participating community, and it was used to procure a plot of land on which a new and large health center for Kikonka area will be built.

Study design

The study design consisted of a cross-sectional community-based study, with a census-based randomized selection of households of which healthy members (participants) were assessed for *Salmonella* intestinal carriage by microbiological culture of three consecutive stool samples. *Salmonella* Typhimurium and Enteritidis stool isolates were compared for genetic relatedness with blood culture isolates obtained from patients of the same community who were hospitalized during the study period.

Study site

The study was conducted in the Province of Kongo Central (western DRC), in Kikonka health area (further referred to as "Kikonka"), located at a distance of 7 km from Kisantu Hospital. Details about the health and population indicators of Kisantu health zone are presented in reference (Tack et al., 2020a). A census was conducted for the preparation of this study.

Households, study participants, and study period

Households were defined as subjects (mostly family members), sharing the same kitchen and sanitation and recognizing the authority of a household head. All residents of Kikonka who were >29 days old had provided consent, were healthy, and were eligible for participation. Healthy status was defined as the absence of a recent history of fever (≤14 days), diarrhea (24 h before enrollment), and antibiotic treatment (≤48 h before enrollment) (Mbuyi-Kalonji et al., 2020). A participant was defined as an eligible household member after consenting to the participation in the study and providing at least one stool sample. The study period extended from September 2019 to March 2020 during the rainy season.

Sample size and selection of households

Based on our previous study in Kongo-Central DRC, a minimum of 60 non-typhoidal *Salmonella* stool culture isolates were targeted to obtain reliable data on serotype distribution, AMR profiles, and genetic relatedness with blood culture isolates. Given the prevalence of *Salmonella* carriage (3%) observed during that study (Mbuyi-Kalonji et al., 2020), the target sample size was calculated to be 2,000 participants. Estimating that 20% (n = 400) of participants would not submit second and third stool samples, the sample size was increased to 2,400 participants. Based on an anticipated household size of four to five members per household, 450 households were foreseen. Each seventh household in the list of all households of Kikonka (n = 3,128, counted by the census) was selected. Selected households were representative of the geographical distribution of the population.

Recruitment, sample collection, and interviews

After the approval of the study by the local health and community authorities, sensitization of the Kikonka population was performed through local television and radio stations and door-to-door visits by community health workers. For recruitment, study teams visited the selected households early in the morning. After consenting, participants were asked to provide three consecutive stool samples within 1 week. Age, gender, and household location by GPS coordinates were recorded, and participants (or their caretakers) were interviewed about demographics and health status. After the first round of recruitment, a second round was organized to catch up with the sample size for subjects who were not available at the first visit or who had consented but not yet provided a stool sample.

Stool culture for *Salmonella*

The day after the study visit, stool samples were collected by community health workers. Within 2–8 h after production, the samples were transported to the Kikonka Health Center using cool boxes (2–8°C). At Kikonka Health Center, ~1 g of each stool sample was inoculated into 10 ml of Selenite broth (BD Difco, Becton Dickinson and Company, NJ, US). Selenite broth samples were transported to the laboratory of the Kisantu Hospital where they were incubated at 36°C. After 18 to 24 h of incubation, 10 µl of Selenite was subcultured on two plates of CHROMagar™ *Salmonella* (CHROMagar™, Paris, France, a selective medium for color-based detection of *Salmonella*). After incubation (18–24 h at 36°C), purple colonies (*i.e.,* indicative of *Salmonella*) were subcultured on Kligler Iron Agar (KIA) (Oxoid Ltd., Basingstoke, Hampshire, England) with a maximum of four colonies per plate. If present, different colony types were subcultured (two colonies per type). When no purple colonies were observed, the plates were incubated for another 24 h and read after 48 h of incubation.

Identification, serotyping, and antibiotic susceptibility testing

Isolates indicative of *Salmonella* were tested biochemically (DiaTabs, Rosco, Taastrup, Denmark) (Mbuyi-Kalonji et al., 2020) and, if confirmed, stored in tubes with Tryptone Soya

Agar (TSA, Oxoid) and shipped to INRB and ITM for serotyping (Pro-lab Diagnostics Inc., Richmond Hill, Ontario, Canada) and antibiotic susceptibility testing. Antibiotic susceptibility testing was performed by the disk diffusion method (Neo-Sensitabs, Rosco) (CLSI, 2022b), in addition to the assessment of ciprofloxacin and azithromycin minimal inhibitory concentration (MIC) values by the E-test macromethod (bioMérieux, Marcy L'Etoile, France). The CLSI breakpoint of azithromycin susceptibility testing for *Salmonella* Typhi was used for NTS isolates (Tack et al., 2022). Multidrug resistance (MDR) was defined as co-resistance to ampicillin, chloramphenicol, and trimethoprim-sulfamethoxazole. Decreased ciprofloxacin susceptibility (DCS, equivalent to the CLSI intermediate susceptibility category) was defined as ciprofloxacin MIC values of $> 0.064\,\mu g/ml$ and $< 1\,\mu g/ml$, ciprofloxacin resistance was defined as MIC-values of $\geq 1\,\mu g/ml$. Fluoroquinolone non-susceptibility (FQNS) comprises both DCS and ciprofloxacin resistance (Tack et al., 2020b). MIC_{50} (MIC required to inhibit 50% of tested isolates) was used to describe differences between ciprofloxacin MIC values of different serotypes (CLSI, 2022a).

Comparison between stool culture isolates and blood culture isolates

Blood culture iNTS isolates obtained between September 2019 and March 2020 from patients living in Kikonka were retrieved [for indications and laboratory work-up, see reference (Tack et al., 2020a)]. Comparison with stool cultures was carried out by multiple locus variable-number of tandem repeat analysis (MLVA) as described previously (Mbuyi-Kalonji et al., 2020). For *S.* Typhimurium, MLVA clusters were defined as isolates with none or one variation in one of the non-stable loci (STTR5, STTR6, and STTR10) and no variation in the stable loci (STTR3 and STTR9) (Dimovski et al., 2014). For *S.* Enteritidis, MLVA clusters were defined as isolates with none or one variation in one of the five loci (Hopkins al., 2011).

For assessing ST lineages, a subset of isolates was selected according to representativity (stool vs. blood culture isolates) and the different MLVA clusters. WGS was performed by the commercial genomic platform of Eurofins Genomics (Konstanz, Germany). DNA extraction and purification from bacterial isolates were performed by Eurofins, as well as library preparation and sequencing (Illumina, San Diego, CA, USA), generating 150 bp paired-end reads. The short reads were assembled *de novo* with SPAdes version 3.6.0.23. Various tools integrated into EnteroBase (REF in footnote)[1] were used for sequence analysis, as described previously (Zhou et al., 2021; Falay et al., 2022). A minimum spanning (MS) tree (MStree V2 using GrapeTree) based on the EnteroBase 3002 loci "cgMLST V2 + HierCC V1" scheme was produced for each serotype to estimate the allelic distances between isolates from this study and the genomes from references (Feasey et al., 2016; Pulford et al., 2021).

1 https://enterobase.warwick.ac.uk/

Definitions, data collection, and analysis

The definition of participants is mentioned above. *Salmonella* carriers were defined as participants with growth of *Salmonella* from at least one stool sample. Household *Salmonella* clusters were defined as ≥ 2 carriers living in the same household, for whom the same *Salmonella* serotype was isolated from at least one stool sample; in the case of *S.* Typhimurium and Enteritidis, an identical or similar MLVA profile was added as a criterium.

Data from paper-based interviews and laboratory data were encoded in and analyzed by Excel 2301 (Microsoft, Richmond, VA, US). Serotyping and MLVA typing were performed on all subsequent *Salmonella* isolates per participant. Data (assessed in Excel) were described by ratios with 95% C.I. and medians with ranges. Differences between proportions were assessed for statistical significance (defined as p-value < 0.05) using chi-square or Fisher exact tests.

Results

Study population and representativeness participation rates

The census revealed 16,503 inhabitants living in 3,218 households, with a population density of 82.5 inhabitants/km^2. A total of 571 households comprising 2,867 eligible subjects were visited, of whom, 513 were not available (Figure 1). Among 2,354 eligible subjects asked for participation, 2.2% refused and another 2.9% consented but did not provide a stool sample, resulting in 94.9% ($n = 2{,}234$) participants who provided at least one stool sample. Their median age was 16 years (30 days—91 years); the male-to-female ratio was 1:1.08. Households comprised a median of 5 (1 – 12) members. These data were representative of the total Kikonka population and similar to those of eligible subjects who were not available during the study visits (Supplementary Tables 1–3). Nearly all participants (99.3%, 2219 out of 2234) provided three samples; 93.4% (2072/2219) of participants submitted three stool samples within 1 week. Two (0.09%) participants reported the use of antibiotics within 48 h prior to inclusion, and one (0.04%) participant reported a history of diarrhea.

Proportions and demographics of *Salmonella* carriers

A total of 98 out of 2,234 (4.4% 95% CI: 3.6–5.4%) *Salmonella* intestinal carriers were detected, living in 61 out of 482 (12.6%) households (Figure 1). Their median age was 13 years (4 months—75 years) with a male-to-female ratio of 1:0.92. The proportion of *Salmonella* carriers among children of < 15 years old (5.0%, 52/1,033; 95% CI: 3.9–6.5) was higher compared with adults (3.8%, 46/1,201; 95% CI: 2.9–5.1), but this difference did not reach statistical significance ($p = 0.166$) (Table 1). *Salmonella* carriers tended to be slightly more frequent among male subjects (51 out of 1,072) (4.8%, 95% CI: 3.6–6.2) than among female subjects (47 out of 1162) (4.0%, 95% CI: 3.0 – 5.3) ($p = 0.411$).

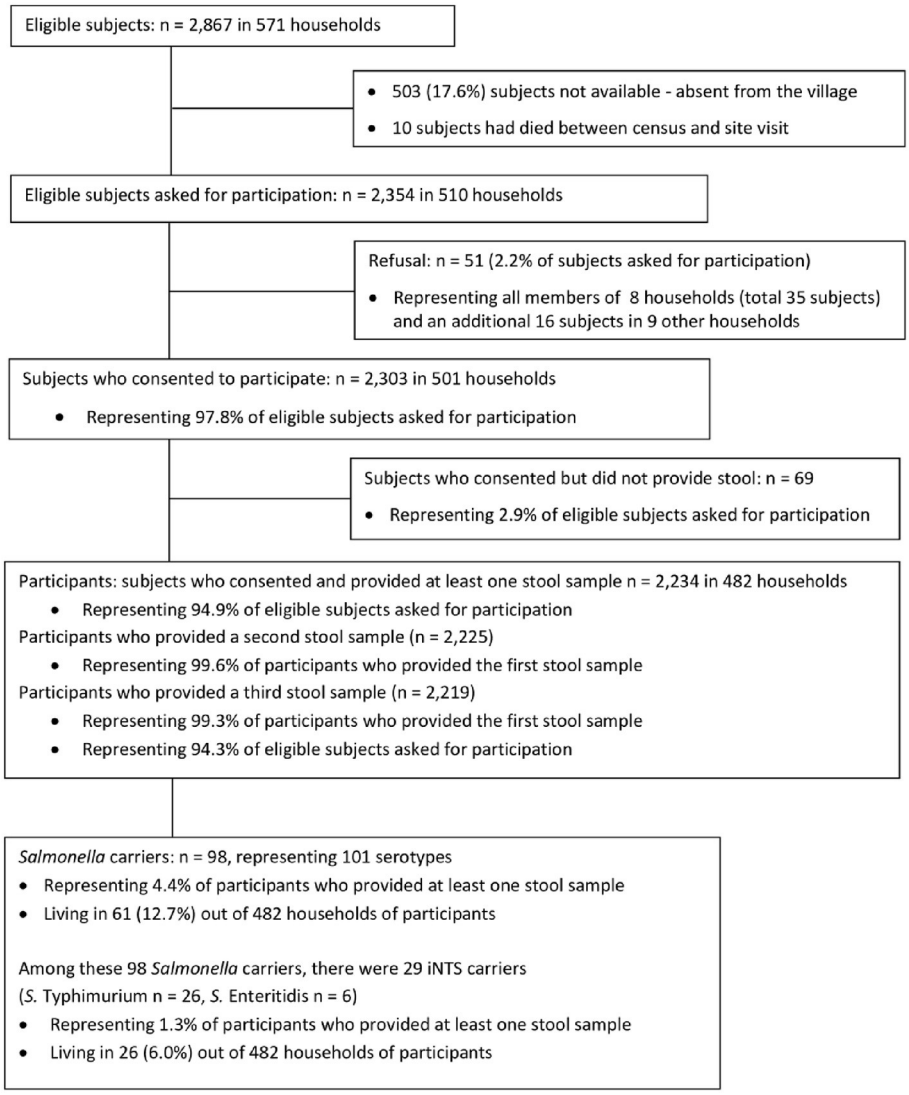

FIGURE 1
Breakdown of the study population (Testing Rounds 1 and 2 combined).

Serotype distribution of *Salmonella* intestinal isolates

The 98 *Salmonella* carriers comprised 101 non-duplicate isolates, as 3 out of 98 carriers had two distinct serotypes. *Salmonella* Kentucky and *S.* Typhimurium were found in half (49 out of 98, 50.0%) and a quarter (26 out of 98, 26.5%) of *Salmonella* carriers (Table 2). Four Typhimurium isolates belonged to the variant Copenhagen (*i.e.*, antigen O5-negative). *Salmonella* II 42:r:- (*Salmonella enterica* subspecies *salamae*) was found in 15.3% (15 out of 98) of *Salmonella* carriers, and the other serotypes included Urbana ($n = 5$ carriers), Enteritidis ($n = 3$), Tempe, Typhi, and *Salmonella* I 11:-:1,2 ($n = 1$ each). Apart from *Salmonella* II 42:r:-, for which 10 out of 15 isolates were found among adults, there was no particular association between age group and serotype (Table 1).

Antibiotic susceptibility profile of *Salmonella* stool culture isolates

All but one (25 out of 26, 96.2%) *S.* Typhimurium intestinal isolates were MDR. Most (80.8%, 21 out of 26) displayed FQNS; their MIC50 (MIC value at which 50% of isolates were inhibited) for ciprofloxacin was 1 (range 0.75–1.5) μg/ml); 3 and 18 of them showed decreased ciprofloxacin susceptibility and ciprofloxacin resistance. Furthermore, they were FQNS, MDR, and resistance to third-generation cephalosporins (Table 3). In total, 1 out of 3 *S.* Enteritidis was MDR; the single *S.* Typhi isolate was resistant to trimethoprim-sulfamethoxazole. Nearly all (48 out of 49, 97.9%) *S.* Kentucky isolates were resistant to trimethoprim-sulfamethoxazole, chloramphenicol, and ciprofloxacin; MIC50 value for ciprofloxacin was 8 (4–24) μg/ml. The remaining *Salmonella* serotype isolates did not display AMR.

10.3389/fmicb.2023.1282894

TABLE 1 Distribution of serotypes among *Salmonella* carriers and numbers of isolates per age group.

Age groups (n)/ *Salmonella* serotypes within the age group	Numbers of *Salmonella* carriers	Numbers of isolates	Proportions of *Salmonella* carriers within the age groups
Children < 5 years ($n = 355$)	20	21	5.6%
Salmonella Enteritidis		2	
Salmonella Kentucky		6	
Salmonella Typhimurium		9	
Salmonella Urbana		2	
Salmonella II 42:r:-		2	
Children 5–<15 years ($n = 678$)	32	34	4.7%
Salmonella Kentucky		20	
Salmonella Typhimurium		9	
Salmonella Urbana		2	
Salmonella II 42:r:-		3	
Adults ≥ 15 years ($n = 1,201$)	46	46	3.8%
Salmonella Enteritidis		1	
Salmonella Kentucky		23	
Salmonella Typhimurium		8	
Salmonella Typhi		1	
Salmonella Urbana		1	
Salmonella II 42:r:-		10	
Salmonella Tempe		1	
Salmonella I 11:-:1,2		1	
Total number of participants ($n = 2234$)	98	101	4.4%

Invasive non-typhoidal *Salmonella* from blood cultures

Blood culture isolates used for comparison included 52 *S.* Typhimurium and 5 *S.* Enteritidis isolates obtained in 56 patients, most of whom ($n = 54$, 96.4%) were younger than 5 years old. *S.* Typhimurium isolates displayed similar proportions of AMR as the stool culture isolates, with 76.9% (40/52) isolates combining MDR, third-generation cephalosporin resistance, and FQNS, the latter mostly ciprofloxacin resistance (Table 3).

TABLE 2 Numbers of serotypes isolated from *Salmonella* carriers.

Serotypes	Numbers of carriers	Number of households per serotype	Numbers of isolates (% of total)
Salmonella Kentucky	49	25	49 (48.5)
Salmonella Typhimurium	26	19	26 (25.7)*
Salmonella II 42:r:-	14	12	15 (14.9)
Salmonella Urbana	3	4	5 (4.9)
Salmonella Enteritidis	3	3	3 (2.9)
Salmonella Tempe	1	1	1 (0.9)
Salmonella Typhi	1	1	1 (0.9)
Salmonella I 11:-:1,2	1	1	1 (0.9)
Total	98	61	101 (100.0)

*Including four isolates of variant Copenhagen.

Genetic relatedness between stool and blood culture iNTS isolates and sequence types

S. Typhimurium isolates from stool and blood cultures comprised 7 and 16 MLVA types, respectively (Table 4). The MLVA types of all 26 *S.* Typhimurium stool culture isolates matched with the corresponding MLVA types from blood culture isolates. MLVA type 2-9-12-7-0210 represented 15 out of 26 stool isolates and 29 out of 52 blood culture isolates, respectively, and occurred throughout the study period, whereas other MLVA types were more time-bound. The stool and blood culture isolates with time-bound MLVA types 2-5-15-8-0210, 2-NA-12-7-0210, and 2-NA-16-8-0210 were coinciding in time and these isolates belonged to the *S.* Typhimurium variant Copenhagen.

S. Enteritidis stool ($n = 3$) and blood culture ($n = 5$) isolates belonged to 3 and 1 MLVA types, respectively. The blood culture MLVA type 2-15-3-3-NA occurred throughout the study period, and one stool culture isolate shared this MLVA type which was MDR. The other three MLVA types from Enteritidis stool cultures were clearly distinct and were susceptible to all antibiotics tested (Table 5).

The iNTS isolates selected for WGS included 20 *S.* Typhimurium and 4 *S.* Enteritidis isolates obtained from blood and stool cultures ($n = 11$ and 13, respectively), representing all MLVA clusters (Tables 4, 5). WGS revealed that all *S.* Typhimurium isolates belonged to ST313 Lineage 2 as described by Pulford et al. (2021). Isolates with the most frequently observed MLVA type 2-9/10-12/13-7-0210 formed a tight cluster [0–7 allelic differences (AD)] of seven stool culture and seven blood culture isolates. The three other Typhimurium stool culture isolates clustered with the selected blood culture isolates of the same MLVA type (Figure 2). Two of the Enteritidis isolates (one blood culture and one stool) belonged to ST11 of the Central/Eastern African clade (HierBAPS clade 9, HC50_12675) as described by Feasey et al. (2016) and

10.3389/fmicb.2023.1282894

TABLE 3 Antibiotic resistance profiles of the non-typhoidal *Salmonella* from stool and blood culture isolates.

Antibiotics	Stool culture isolates ($n = 101$)				Blood culture isolates($n = 57$)	
	Salmonella Kentucky ($n = 49$)	*Salmonella* Typhimurium ($n = 26$*)	*Salmonella* Enteritidis ($n = 3$)	Other serotypes ($n = 23$**)	*Salmonella* Typhimurium ($n = 52$***)	*Salmonella* Enteritidis ($n = 5$)
Ampicillin	0	26	1	0	51	5
Trimethoprim-sulfamethoxazole	48	25	1	1**	48	5
Chloramphenicol	48	25	1	0	48	5
Ciprofloxacin (DCS/Cip-R)	48	3/18	0	0	3/39	0
Ceftriaxone (C3G-R)	0	21	0	0	44	0
Azithromycin	0	0	0	0	0	0
Meropenem	0	0	0	0	0	0
Gentamicin	0	23	0	0	44	0
MDR	0	25	1	0	47	5
FQNS	48	21	0	0	42	0
MDR + FQNS	0	21	0	0	40	0
MDR + C3G-R	0	21	0	0	42	0
MDR + C3G-R + FQNS	0	21	0	0	40	0

Numbers express the numbers of intermediate-susceptible and resistant isolates combined. Abbreviations and definitions: C3G-R: resistance to third-generation cephalosporins; DCS: decreased ciprofloxacin susceptibility, equivalent to intermediate susceptibility (Minimal Inhibitory Concentration (MIC) values: >0.064 and <1 μg/ml), Cip-R, resistance to ciprofloxacin (MIC values: ≥ 1 μg/ml); FQNS, fluoroquinolone non-susceptibility (comprised both DCS and Cip-R); C3G-R, Resistant to third-generation cephalosporins; MDR, multidrug-resistant, i.e., co-resistant to ampicillin, trimethoprim-sulfamethoxazole, and chloramphenicol.
*Including *Salmonella* Typhimurium variant Copenhagen (n = 4).
**Including *Salmonella* Typhi (n = 1).
***Including *Salmonella* Typhimurium var Copenhagen (n = 5).

clustered with 13 AD, whereas the two other stool isolates belonged to ST11 of the outlier clade [previously described by Kariuki et al. (2020)] and were non-related (>200 AD).

Frequency, age, and gender distribution of iNTS carriers

Overall, iNTS carriers represented 29 (1.3%) of participants in 6.0% (26 out of 482) of households. Their median age was 8 years (4 months−64 years), with a male-to-female ratio of 1:0.61. Of all 29 carriers, 11 were younger than 5 years old, 9 were between 5 and 15 years old, and 10 were adults (Table 1).

Clustering and geographic distribution of *Salmonella* carriers

Among the 61 households with *Salmonella* carriers, approximately one-third ($n = 20$, 32.8%) had clusters of two or more carriers of the same serotype, comprising more than half (55 out of 98, 56.1%) of carriers (Table 6). The median number of *Salmonella* carriers per cluster was 2 (2–7); 14 clusters comprised *S.* Kentucky carriers (the largest composed of 5 carriers) and 2 clusters comprised *S.* Typhimurium carriers (the largest included all 7 household members belonging to MLVA type 2-9-12-7-0210). Participating households including those with *Salmonella* carriers were mostly concentrated around the National Road N°1, which canalizes the traffic between the Matadi seaport and the capital, but no particular geographic pattern was observed for any of the serotypes (Figure 3).

Incremental yield of three consecutive stool samples and use of the CHROMagar™ *Salmonella* medium

Among the 98 *Salmonella* carriers, 97 had three consecutive stool samples. The proportions of growth for each of the 3 days were similar, but cumulative carrier ratios increased from 1.8% ($n = 40$) on day 1 to 3.2% ($n = 70$) on day 2, and 4.4% ($n = 98$) on day 3, respectively (Figure 4, Supplementary Table 4). Most (82 out of 98, 83.7%) carriers had only a single sample grown with *Salmonella*, 11.2% (11 out of 98) and 5.2% (5 out of 97) had, respectively, 2 and 3 successive stool samples grown with *Salmonella*. Supplementary Document 1 summarizes the validation and user's experience of The CHROMagarTM *Salmonella* medium.

10.3389/fmicb.2023.1282894

TABLE 4 Multi-locus variable-number tandem repeat analysis (MLVA) types of *Salmonella* Typhimurium isolates from stool cultures (n = 26 carriers, upper panel) vs. isolates from blood cultures (n = 52 hospital admitted patients, lower panel) along the study period.

	October 2019	November 2019	December 2019	January 2020	February 2020	March 2020	Total
MLVA stool culture isolates							
2-5-15-8-0210		2*W	1*	0			3
2-9-12-7-0210	1W	7 W	1	0	2W	4W	15
2-9-12-8-0210	1			0			1
2-10-12-7-0210			2W(2)	0			2
2-10-13-7-0210		1W	2	0			3
2-NA-12-7-0210		1*W		0			1
2-NA-16-8-0210			1*W	0			1
Total	2	11	7	0	2	4	26
MLVA blood culture isolates							
2-4-12-7-0210			1*				1
2-5-10-7-0210					1		1
2-5-15-8-0210			1*W			1*	2
2-8-12-8-0210		1					1
2-9-11-7-0210					1		1
2-9-12-7-0210	7W	5W(2)	6W	5	6W	2W	31
2-9-12-8-0210		1			1		2
2-9-13-7-0210			1				1
2-9-NA-7-0210			1				1
2-10-12-7-0210	1		1				2
2-10-12-NA-0210				1			1
2-10-13-7-0210				1W	3	1	5
2-10-13-8-0210		1					1
2-NA-12-7-0210		1*W					1
2-NA-16-8-0210			1*W				1
Total	8	9	12	7	12	4	52

The shade of colors indicates clusters of MLVA types.
* *Salmonella* Typhimurium variant Copenhagen.
W *Salmonella* isolates selected for whole-genome sequencing analysis (n = 20).

Discussion

Summary of findings

In an area endemic for iNTS infections, 4.4% of healthy residents were *Salmonella* carriers. Invasive iNTS (*S.* Typhimurium ST313 and Enteritidis ST11) accounted for 26 and 3 carriers, respectively, representing together 1.3% of residents living in 6.0% of households assessed. All Typhimurium and 1 out of three Enteritidis stool culture isolates had MLVA types that matched with those of blood cultures obtained in the same period from patients living in the same area. iNTS carriers were observed among all age groups. Over three-quarters of stool and blood culture isolates showed MDR, third-generation cephalosporin resistance, and fluoroquinolone non-susceptibility.

Comparison with proportions of iNTS carriers in sub-Saharan Africa: population-based studies

Recent studies (since 2000) assessing non-typhoidal *Salmonella* carriers in sub-Saharan Africa are rare. Most of them addressed risk groups such as food handlers (Feglo et al., 2004; Smith et al., 2008; Addis et al., 2011; Misganaw and Williams, 2013; Bradbury et al., 2015), *Schistosoma*-infected individuals (Mohager et al., 2014; Salem et al., 2015; Mbuyi-Kalonji et al., 2020), or convalescent patients (Nkuo-Akenji et al., 2001), and none of them assessed sequence type or relatedness with clinical isolates.

The Typhoid Fever Surveillance in Africa Program (TSAP) found in urban populations in Guinea-Bissau and Senegal respectively 2.4% and 1.0% healthy *Salmonella* carriers, equally

TABLE 5 Multi-locus variable-number tandem repeat analysis (MLVA) types of *Salmonella* Enteritidis isolates from stool culture ($n = 3$ carriers, upper panel) vs. isolates from blood cultures ($n = 5$ hospital admitted patients, lower panel) along the study period.

	October 2019	November 2019	December 2019	January 2020	February 2020	March 2020	Total
MLVA stool culture isolates							
2-12-4-6-1	1[W]						1
2-15-3-3-NA		1[W]					1
2-9-7-3-2					1[W]		1
Total	1	1	0	0	1	0	3
MLVA blood culture isolates							
2-15-3-3-NA	1[W]			3		1	5
Total	1	0	0	3	0	1	5

[W] Salmonella isolates selected for whole-genome sequencing analysis.
The shade of colors indicates clusters of MLVA types.

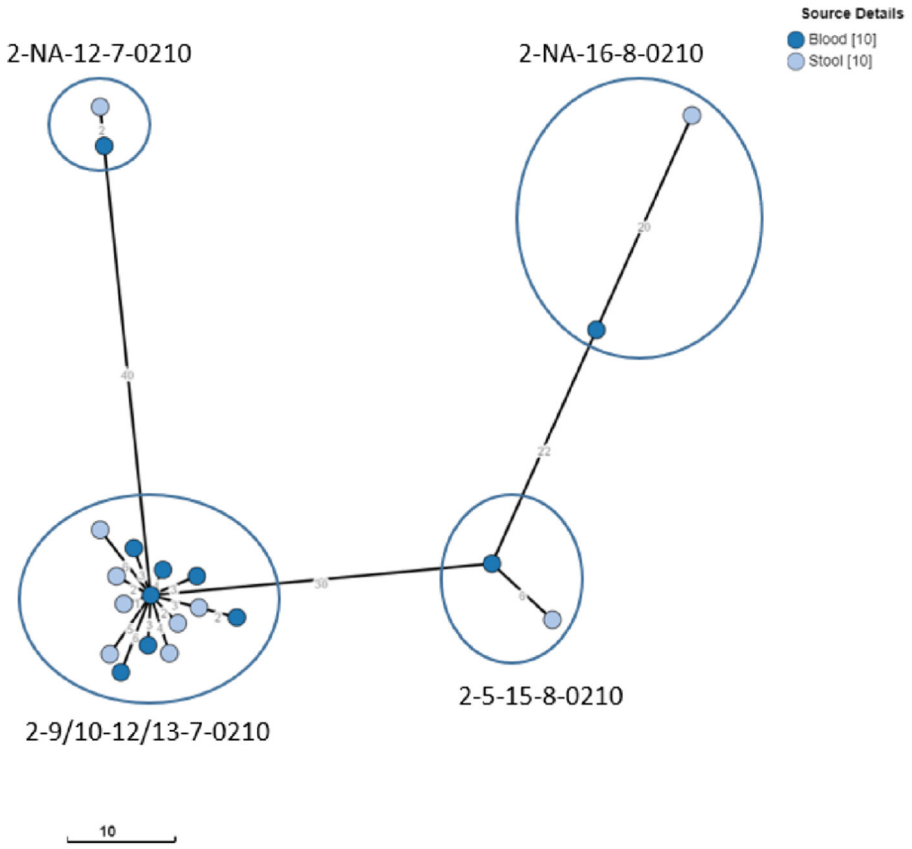

FIGURE 2
Clustering of S. Typhimurium ST313 from blood and stool cultures. Minimum spanning tree created using the MSTree V2 component in EnteroBase, based on the allelic differences over the 3,002 alleles that constitute the EnteroBase HierCC scheme on cgMLST (Zhou et al., 2021). The distances between leaves in the tree indicate the number of alleles which are different between genomes. Node colors are according to isolate origin. Isolates with the same MLVA type are circled.

distributed among sex and age groups except for a higher proportion (4.2%) among the 5 – 14 years olds in Guinea-Bissau (Im et al., 2016). In contrast to the present study, no iNTS serotypes were detected, which is in line with the low incidence ratios of iNTS infections demonstrated in these countries by the TSAP study (Marks et al., 2017).

The aforementioned *Salmonella* carrier study in a *Schistosoma*-endemic area in rural DRC sampled two consecutive stool samples. It revealed that 3.4% of *Salmonella* carriers comprised 9 out of 38 (23.7%) iNTS carriers ($n = 5$ and 4 for Enteritidis and Typhimurium, respectively), most of which had MLVA types matching with those of corresponding serotypes in blood cultures

TABLE 6 Household clusters ($n = 20$) in which more than one *Salmonella* carrier with an identical serotype was detected for 55 *Salmonella* carriers in the Kikonka health area.

Households clusters ($n = 20$)	Serotypes	Number of *Salmonella* carriers ($n = 55$)	Date(s) of sampling
Household KIK0165	*Salmonella* Typhimurium	7	11/11/2019
Household KIK1870	*Salmonella* II 42:r:-	2	02/12/2019
Household KIK2118	*Salmonella* II 42:r:-	2	09/12/2019
Household KIK1036	*Salmonella* Urbana	2	23/12/2019
Household KIK1316	*Salmonella* Kentucky	2	06/01/2020
Household KIK1387	*Salmonella* Kentucky	2	13/01/2020
Household KIK2180	*Salmonella* Kentucky	3	13/01/2020
Household KIK2487	*Salmonella* Kentucky	4	13/01/2020
Household KIK2493	*Salmonella* Kentucky	5	13/01/2020
Household KIK1335	*Salmonella* Kentucky	2	13 - 15/01/2020
Household KIK2499	*Salmonella* Kentucky	3	13 - 16/01/2020
Household KIK2557	*Salmonella* Kentucky	2	20/01/2020
Household KIK2657	*Salmonella* Kentucky	3	20/01/2020
Household KIK2683	*Salmonella* Kentucky	2	20/01/2020
Household KIK2811	*Salmonella* Kentucky	2	20/01/2020
Household KIK2543	*Salmonella* Kentucky	2	20 - 21/01/2020
Household KIK2663	*Salmonella* Kentucky	3	20 - 21/01/2020
Household KIK2671	*Salmonella* Kentucky	3	21/01/2020
Household KIK2626	*Salmonella* II 42:r:-	2	27/01/2020
Household KIK0322	*Salmonella* Typhimurium	2	16 - 17/03/2020

The first column refers to the code number of the household. Clusters are chronologically ranked.

obtained at Kisantu Hospital (Mbuyi-Kalonji et al., 2020). The results of the present study were similar (3.2% of *Salmonella* carriers at day 2; iNTS carriers were observed in 29.6% of carriers) but showed a higher concordance between stool and blood culture isolates (including a larger proportion of Typhimurium isolates) probably because of the neighborhood of Kisantu Hospital and by the fact that blood culture isolates were obtained from the patients living in the same health area as the study participants.

Comparison between iNTS in stool cultures and data from other studies

Recent studies from sub-Saharan Africa provided further evidence of the presence of iNTS in stool samples, both in healthy carriers and in patients with diarrhea. In a hospital-based study in Kisantu, DRC, Phoba and coworkers found paired (same serotype and MLVA-type, closely related to WGS results) stool-blood culture iNTS isolates in 27.4% out of 299 children with iNTS bloodstream infections. Among the control group (children admitted with no febrile illness), the proportion of Salmonella carriers was comparable to that of the present study, *i.e.*, 2.1% (1.6% and 0.5% for Typhimurium and Enteritidis respectively). Further, the MLVA types in the control group were identical to those from blood cultures, which was also observed in the present study.

In suburban slums in Nairobi, Kenya, Kariuki and co-workers assessed the so-called "hot spots" of iNTS bloodstream infections and found Typhimurium and Enteritidis serotypes in stool cultures from patients and healthy controls (Kariuki et al., 2019, 2020). Furthermore, in a population-based cohort study in rural Kenya, *Salmonella* Typhimurium ST313 and Enteritidis ST11 were found in stool samples of patients with diarrhea but in a lower proportion compared with blood cultures (Akullian et al., 2018).

Two studies [one in rural Burkina Faso and another in a Blantyre informal settlement (Malawi)] assessed *Salmonella* carriage in household members and livestock of index patients with *Salmonella* bloodstream infection. Both studies found matching index patient–household member pairs of *S.* Typhimurium ST313 and related ST3257, whereas livestock stool samples grew other (non-iNTS) *Salmonella* serotypes. In a study by Burkina Faso, the three Typhimurium ST313 carriers represented 1.0% out of 293 household members sampled, which is in line with the present findings (Post et al., 2019; Koolman et al., 2022).

Recent genetic analysis of *Salmonella* isolates obtained during the Global Enteric Multicenter Study (GEMS, 2007-10) confirmed widespread asymptomatic carriage of *S.* Typhimurium ST313 in children from sub-Saharan Africa (Gambia, Mali, Mozambique, and Kenya) (Kasumba et al., 2021). Finally, a retrospective analysis of *Salmonella* isolates obtained in Bangy, Central African Republic showed that in 13 patients, *S.* Typhimurium ST313 was obtained from both blood and stool isolates (Breurec et al., 2019).

Interpretation of findings: arguments for a human reservoir of iNTS but questions remain

The present study corroborates the findings of the above cited studies pointing to a human reservoir of iNTS. To the best of our knowledge, it is the first population-based study to demonstrate the widespread occurrence of iNTS carriers, *i.e.,* 1.3% of the population, largely outnumbering the *S.* Typhi carriers. The strength of attribution of healthy humans as a reservoir for iNTS is high, given the matches between MLVA profiles and WGS clustering of stool and blood isolates. Additional evidence contributing to the human reservoir of iNTS are the similar ratios of iNTS Typhimurium versus Enteritidis among the stool and

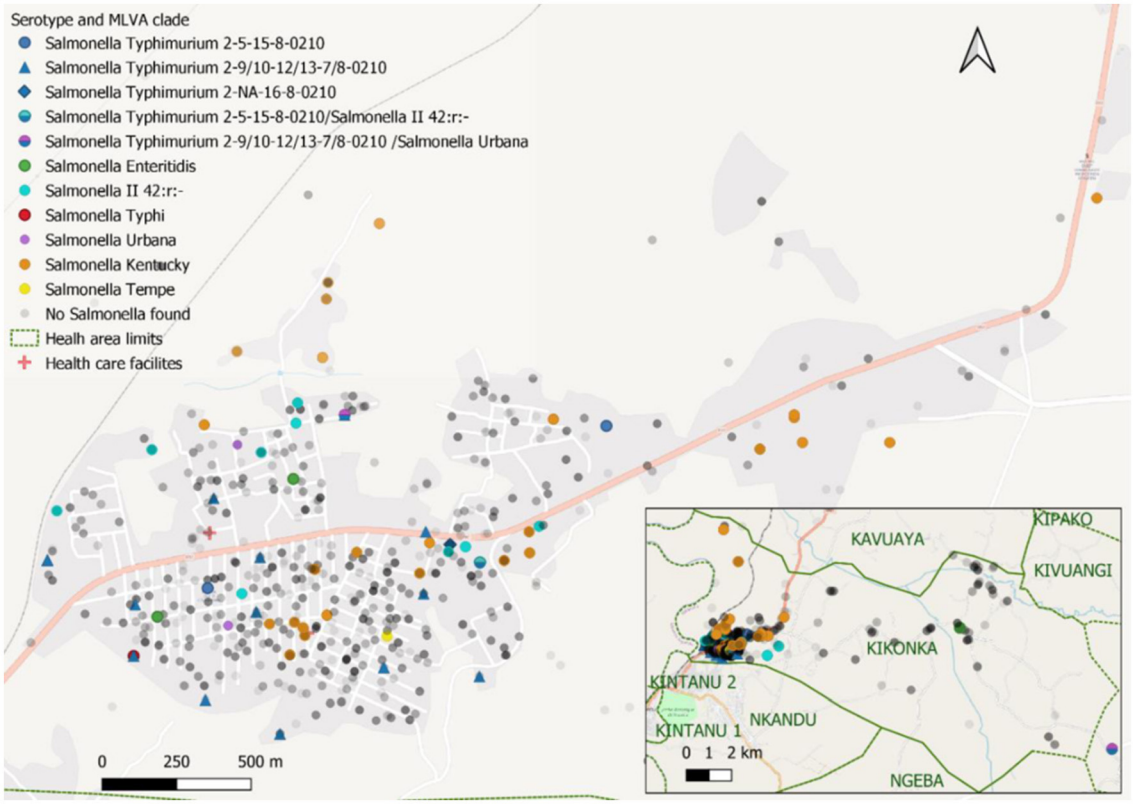

FIGURE 3
Distribution of study participants and *Salmonella* cases in the Kikonka health area. The pink line represents the main road across the Kikonka health area (National Road N°1, between the Atlantic coast and Kinshasa). Gray dots represent the households that participated in the study, with the intensity of gray corresponding to the number of households at a given place. *Salmonella* serovars are displayed using dots with different colors. Dots containing two colors represent *Salmonella* carriers with multiple isolates/serotypes.

blood culture isolates and the coincidence in time between stool and blood culture isolates of the time bound MLVA types.

However, there are questions remaining about the carriage, such as the duration of shedding, factors affecting persistence (*e.g.,* hepatobiliary and urogenital tract lesions), the existence and frequency of chronic carriers, the pattern of excretion (bacterial load and intermittent excretion), and infectious dose of iNTS in vulnerable populations (Im et al., 2016; Mbuyi-Kalonji et al., 2020; Phoba et al., 2020). The few data available are data about the duration of fecal shedding obtained for diarrheagenic (non-iNTS) *Salmonella* serotypes and convalescent shedders: duration of shedding is short, with less than 2.2% of convalescent carriers excreting *Salmonella* beyond 30 days (Haeusler and Curtis, 2013; Ohad Gal-Mor, 2019). The occurrence of iNTS carriers across all ages (as presently observed) also raises the possibility of sub-clinical and unapparent iNTS infections in adults, as in the case of typhoid fever (Parry et al., 2002).

Furthermore, despite index patient–household studies and recent food chain studies in Tanzania and Kenya failed to demonstrate iNTS isolates in animal and environmental samples (Kariukiet al., 2006; Dione et al., 2011; Post et al., 2019; Wilson et al., 2020; Crump et al., 2021; Koolman et al., 2022), most authors concluded that an environmental reservoir for iNTS is not yet excluded (Mather et al., 2015; Post et al., 2019; Crump et al., 2021; Kasumba et al., 2021; Koolman et al., 2022). A recent study from Kisangani (DRC) showed that urban rats harbored ST313 isolates which genetically matched with blood culture isolates (Falay et al., 2022), and another study in Kisantu found a direct and short-cycle type association between rainfall and iNTS (independent from *P. falciparum* malaria), suggesting flooding of water and food by contaminated surface water as an option of transmission (Tack et al., 2021). Other indirect evidence of environmental risk factors—observed in Kenya and Burkina Faso—included the vicinity of unimproved water sources, water vending points, and sewage systems, as well as consumption of street food (Kariuki et al., 2019; Mbae et al., 2020; Nikiema et al., 2021).

Relevance and generalizability of findings

The evidence of a human reservoir and the relatively high (1.3%) proportion of iNTS carriers in the community may orient and prioritize control measures such as vaccines (Im et al., 2016; Kariuki et al., 2019). The present study was conducted in a setting with high NTS but low HIV burden and in an area with a moderate population density but close to a major national road. DRC is one of the few countries in sub-Saharan

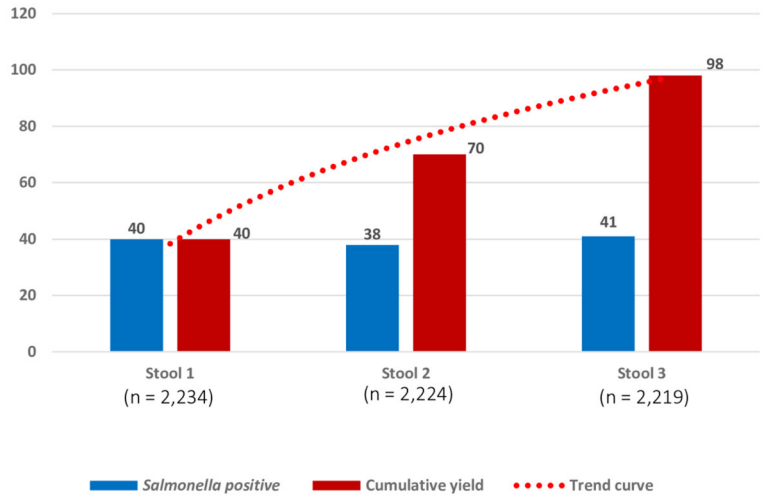

FIGURE 4
Numbers of successive stool samples grown with Salmonella for 2,219 participants who provided three consecutive stool samples. Numbers (Y-axis) represent samples with the growth of *Salmonella* on the day of sampling (three successive samples scheduled on 3 days in 1 week). The blue bar represents the numbers of *Salmonella* carriers detected, respectively, from stool samples on day 1 (40 of 2234; 1.8% (95% confidence interval (C.I.): 1.3–2.4), stool sample on day 2 (38 of 2224; 1.7% C.I.: 1.3–2.3), and stool sample on day 3 (41 of 2219; 1.8% C.I.: 0.9–1.8). The red bar represents the cumulative numbers of *Salmonella* carriers detected: for stool sample 2, $n = 70$ represents 40 *Salmonella* carriers detected in stool sample 1 + 30 additional *Salmonella* carriers detected in stool sample 2; for stool sample 3, $n = 98$ represents 70 *Salmonella* carriers detected in stool sample 1 and stool sample 2 + 28 additional *Salmonella* carriers detected in stool sample 3. Cumulative percentages of growth expressed for 2,219 participants were as follows: stool sample 1(40 of 2219; 1.8% C.I.: 1.3–2.4%), stool sample 2(70/2219; 3.2% C.I.: 2.5–3.9%), and stool sample 3(98/2219; 4.4% C.I.: 3.6–5.4%).

Africa that did not experience a decline in the *P. falciparum* malaria burden (World Health Organization, 2022). Therefore, the present findings are probably not generalizable to other settings and carriers; reservoir and transmission studies should be conducted in settings with different iNTS burdens and associated risk factors.

Antimicrobial resistance profile

Invasive iNTS are known for their association with antimicrobial resistance (Tack et al., 2020b). In the present study, the most worrying was the combination of MDR, resistance to third-generation cephalosporins, and FQNS in *S.* Typhimurium, which can be categorized as extensive drug resistance and leaves few therapeutic options (Tack et al., 2020b). It contrasts with the pan-susceptible *S.* Typhimurium lineage 3 which emerged in Malawi in 2016 (Pulford et al., 2021). Very recently, the World Health Organization listed efficacious and safe antibiotic treatment regimens for drug-resistant *Salmonella* among the 40 priorities on the Global Research Agenda for Antimicrobial Resistance in Human Health, thereby explicitly referring to fluoroquinolone and third-generation cephalosporin resistance (World Health Organization, 2023).

The very low to absent resistance among most of the non-iNTS *Salmonella* serotypes (excluding *S.* Kentucky, see below) has also been observed in the aforementioned rat carrier study from Kisangani (Falay et al., 2022). These observations add to the probability of the human-confined habitat of ST 313 Typhimurium.

Other findings (secondary objectives)

Culturing three consecutive stool samples provided a 2.5 times higher yield than culturing a single sample (4.4 vs. 1.8%, respectively). This practice of three consecutive stool samples is based on a small-scale study detecting chronic carriers of typhoid fever (Anderson et al., 1961) and, to our knowledge, has not been validated before. In the present study, if only the first stool sample per participant was cultured, 59.2% (58 out of 98) of *Salmonella* carriers including 76.9% (20 out of 26) of *S.* Typhimurium would have been missed (Supplementary Table 4). As to laboratory work-up, the CHROMagar™ *Salmonella* proved to be reliable and user-friendly.

In line with other anecdotal observations (Im et al., 2016; Post et al., 2019; Koolman et al., 2022), *Salmonella* isolates (including *S.* Typhimurium) tended to cluster in households. These observations highlight the transmissibility of non-typhoidal *Salmonella* including iNTS and may provide support to the "hot spot" concept of iNTS transmission as a priority for the implementation of iNTS vaccines (Kariuki et al., 2019). In the present study, the spectrum of *Salmonella* serotypes other than iNTS differed from the earlier *Schistosoma-Salmonella* study in the same province in DRC (Mbuyi-Kalonji et al., 2020) and may reflect local or over-time evolutions. The preponderance of *Salmonella* Kentucky is striking; MDR *S.* Kentucky ST198 has spread worldwide through human traveling and poultry trade (Hello et al., 2013; Dieye et al., 2022) but was previously not reported from DRC. The ciprofloxacin MIC values of *S.* Kentucky were strikingly high, suggesting the accumulation of resistance genes and a food chain-related reservoir.

Limitations and strengths

Limitations inherent to the study design are the "snapshot" design, which precludes interpretation of transmission. The study was conducted during the rainy season, which is associated with an increase in iNTS infections (Tack et al., 2021). However, in the aforementioned hospital-based iNTS carrier study in Kisantu, the proportions of stool cultures grown with iNTS were similar across the rainy and dry seasons (Phoba et al., 2020). Furthermore, there were risks of bias by the non-availability of working-age adult men, but, in anticipation of this risk, household visits were conducted early morning, and the included participants had similar demographic profiles as the total population of Kikonka. Finally, to assess household clustering of *Salmonella* carriers, the sample selection was based on households and not on individuals. Household clustering may have increased the number of detected carriers, but, in turn, this risk may be mitigated by the high number of households enrolled.

Strengths of the present study included the recent census (guiding selection of households), the large sample size, and the representation of participants for the total Kikonka population and geography of the area. In addition, the participation ratio was as high as 94.9%, compared to 82.9% and 72.7% previously reported in Guinea-Bissau and Senegal (Im et al., 2016). Further, the compliance with 3-day sampling was excellent and much higher compared to 85.0% for a 2-day sampling previously (Mbuyi-Kalonji et al., 2020). Furthermore, different colony types were assessed (allowing to detect mixed infections) and quality indicators were monitored. The high consistency of proportions across visit rounds and days of sampling illustrated the robustness of procedures (Koolman et al., 2022).

Conclusion

In conclusion, the present study demonstrated iNTS (Typhimurium ST313 and in a lower proportion Enteritidis ST11) carriage among healthy community members in an iNTS endemic area. The stool iNTS isolates were genetically similar to blood culture isolates from patients obtained in the same place and time frame. The present findings complement the growing evidence of humans as the reservoir of iNTS, but further studies are needed to understand transmission and explore co-existent animal or environmental reservoirs.

Data availability statement

The data presented in the study are deposited in the European Nucleotide Archive (ENA) repository, accession number PRJEB64271.

Ethics statement

The studies involving humans were approved by The Institutional Review Board of the Institute of Tropical Medicine (Reference 1263/18). The Ethical Committee of the University of Antwerp (Reference 18/47/535). The Ethical Committee of Public Health School in Kinshasa, Democratic Republic of the Congo (ESP/EC/070/2019). Ethical approval for the blood culture surveillance study was granted by the Institutional Review Board of the Institute of Tropical Medicine (Reference 08 17 12 613) and the Ethics Committee of Public Health school in Kinshasa (version 1: ESP/CE/073/2015 and version 2: ESP/CE/074/2015). For the SETA study, ethical approvals were granted by the International Vaccine Institute Institutional Review Board (IRB No. 2015-006) and the Ethics Committee of Public Health school in Kinshasa (version 1.1: ESP/CE/011/2017, version 1.2: ESP/CE/011B/2017 and version 1.3: ESP/CE/037/2018 and ESP/CE/037B/2019). The studies were conducted in accordance with the local legislation and institutional requirements. Written informed consent for participation in this study was provided by the participants' legal guardians/next of kin. Written informed consent was obtained from the individual(s), and minor(s)' legal guardian/next of kin, for the publication of any potentially identifiable images or data included in this article.

Author contributions

LM-K: Conceptualization, Data curation, Formal analysis, Investigation, Methodology, Software, Visualization, Writing—original draft, Writing—review & editing. LH: Data curation, Formal analysis, Investigation, Methodology, Resources, Validation, Writing—original draft, Writing—review & editing. JM: Investigation, Resources, Writing—review & editing. M-FP: Conceptualization, Investigation, Methodology, Project administration, Resources, Supervision, Validation, Writing—review & editing. GN: Investigation, Resources, Writing—review & editing. WM: Data curation, Formal analysis, Investigation, Methodology, Resources, Writing—original draft, Writing—review & editing. JI: Funding acquisition, Project administration, Resources, Writing—review & editing. FM: Funding acquisition, Project administration, Resources, Supervision, Writing—review & editing. HJ: Funding acquisition, Resources, Writing—review & editing. JJ: Conceptualization, Formal analysis, Funding acquisition, Methodology, Project administration, Resources, Software, Supervision, Validation, Visualization, Writing—original draft, Writing—review & editing. OL: Conceptualization, Funding acquisition, Methodology, Project administration, Resources, Supervision, Validation, Writing—review & editing.

Funding

The author(s) declare financial support was received for the research, authorship, and/or publication of this article. This work was funded by the Belgian Directorate of Development Cooperation and humanitarian aid (DGD) through the 5th Framework Agreement between the Institute of Tropical Medicine (ITM) in Belgium, Antwerp, Belgium and the National Institute for Biomedical Research, Kinshasa, Democratic Republic of the Congo (BE-BCE_KBO-0410057701-prg2022-1-CD), as

well as by the Bill and Melinda Gates Foundation project OPP1127988 funded to International Vaccine Institute. LM-K holds a PhD scholarship from the Belgian DGD funded to ITM. The funders had no role in study design, data collection and analysis, decision to publish, or preparation of the manuscript.

Acknowledgments

The authors would like to thank the Medical Doctor Head of the Kisantu Health Zone and the entire team of the central office of the Health Zone for their participation in the mass sensitization of the Kikonka health area inhabitants. The authors are grateful to the medical doctors and community health workers of the Kikonka health area for their participation in the study field activities. The authors further thank the laboratory team of the Saint Luc Hospital of Kisantu for their dedicated work for the bacteriological analysis during field activities as well as the bacteriology teams of the National Institute for Biomedical Research and the Institute of Tropical Medicine for reference analyses.

Conflict of interest

The authors declare that the research was conducted in the absence of any commercial or financial relationships that could be construed as a potential conflict of interest.

Publisher's note

All claims expressed in this article are solely those of the authors and do not necessarily represent those of their affiliated organizations, or those of the publisher, the editors and the reviewers. Any product that may be evaluated in this article, or claim that may be made by its manufacturer, is not guaranteed or endorsed by the publisher.

Supplementary material

The Supplementary Material for this article can be found online at: https://www.frontiersin.org/articles/10.3389/fmicb.2023.1282894/full#supplementary-material

References

Addis, Z., Kebede, N., Worku, Z., Gezahegn, H., Yirsaw, A., and Kassa, T. (2011). Prevalence and antimicrobial resistance of Salmonella isolated from lactating cows and in contact humans in dairy farms of Addis Ababa: a cross sectional study, *BMC Infect. Dis.* 11, 254. doi: 10.1186/1471-2334-11-222

Akullian, A., Montgomery, J. M., John-Stewart, G., Miller, S. I., Hayden, H. S., Radey, M. C., et al. (2018). Multi-drug resistant non-typhoidal *Salmonella* associated with invasive disease in western Kenya. *PLoS Neglect. Tropic. Dis.* 12, 156. doi: 10.1371/journal.pntd.0006156

Anderson, E. S., Kwantes, W., Bemstein, A., Gray, R. D., Henderson, R. J., Hobbs, B. C., et al. (1961). The detection of the typhoid carrier state. *J. Hygiene* 59, 231–247. doi: 10.1017/S0022172400038882

Bradbury, R. S., Barbé, B., Jacobs, J., Jallow, A. T., Camara, K. C., Colley, M., et al. (2015). Enteric pathogens of food sellers in rural Gambia with incidental finding of *Myxobolus* species (Protozoa: Myxozoa). *Transact. Roy. Soc. Tropic. Med. Hygiene* 109, 334–339. doi: 10.1093/trstmh/trv020

Breurec, S., Reynaud, Y., Frank, T., Farra, A., Costilhes, G., Weill, F.-X., et al. (2019). Serotype distribution and antimicrobial resistance of human *Salmonella enterica* in Bangui, Central African Republic, from 2004 to 2013. *PLoS Neglect. Tropic. Dis.* 13, 1–13. doi: 10.1371/journal.pntd.0007917

CLSI (2022a). "Analysis and presentation of cumulative antimicrobial susceptibility test data," in *CLSI Guideline M39. 5th ed.* Clinical and Laboratory Standards Institute.

CLSI (2022b). "Performance Standards for Antimicrobial susceptibility testing," in *CLSI supplement M100.* 32nd ed. Clinical and Laboratory Standards Institute.

Crump, J. A., and Heyderman, R. S. (2015). A perspective on invasive *Salmonella* disease in Africa. *Clinic. Infect. Dis.* 61, 709. doi: 10.1093/cid/civ709

Crump, J. A., Thomas, K. M., Benschop, J., Knox, M. A., Wilkinson, D. A., Midwinter, A. C., et al. (2021). Investigating the meat pathway as a source of human non-typhoidal *Salmonella* bloodstream infections and diarrhea in East Africa. *Clinic. Infect. Dis.* 73, E1570–E1578. doi: 10.1093/cid/ciaa1153

Dieye, Y., Hull, D. M., Wane, A. A., Harden, L., Fall, C., Sambe-Ba, B., et al. (2022). Genomics of human and chicken *Salmonella* isolates in Senegal: broilers as a source of antimicrobial resistance and potentially invasive non-typhoidal salmonellosis infections, *PLoS ONE* 17, 266065. doi: 10.1371/journal.pone.0266025

Dimovski, K., Cao, H., Wijburg, O. L. C., Strugnell, R. A., Mantena, R. K., Whipp, M., et al. (2014). Analysis of *Salmonella enterica* serovar Typhimurium variable-number tandem-repeat data for public health investigation based on measured mutation rates and whole-genome sequence comparisons. *J. Bacteriol.* 196, 3036–3044. doi: 10.1128/JB.01820-14

Dione, M. (2010). Epidemiology of non-typhoidal *Salmonella* (NTS) in humans and animals in the Gambia and Senegal. *Tropicultura* 253–254. Available online at: https://search.ebscohost.com/login.aspx?direct=trueandAuthType=cookieipshibanddb$=$awnandAN$=$DJ2012058563andsite$=$ehost-live

Dione, M. M., Ikumapayi, U. N., Saha, D., Mohammed, N. I., Geerts, S., Ieven, M., et al. (2011). Clonal differences between non-typhoidal *Salmonella* (NTS) recovered from children and animals living in close contact in the Gambia. *PLoS Neglect. Tropic. Dis.* 5, 1–7. doi: 10.1371/journal.pntd.0001148

Falay, D., Hardy, L., Bonebe, E., Mattheus, W., Ngbonda, D., Lunguya, O., et al. (2023). Intestinal carriage of invasive non-typhoidal *Salmonella* among household members of children with Salmonella bloodstream infection, Kisangani, DR Congo. *Front. Microbiol.* 14, 1961. doi: 10.3389/fmicb.2023.1241961

Falay, D., Hardy, L., Tanzito, J., Lunguya, O., Bonebe, E., Peeters, M., et al. (2022). Urban rats as carriers of invasive *Salmonella* Typhimurium sequence type 313, Kisangani, Democratic Republic of Congo. *PLoS Neglect. Tropic. Dis.* 16, 1–21. doi: 10.1371/journal.pntd.0010740

Feasey, N. A., Dougan, G., Kingsley, R. A., Heyderman, R. S., and Gordon, M. A. (2012). Invasive non-typhoidal *Salmonella* disease: an emerging and neglected tropical disease in Africa. *The Lancet* 379, 2489–2499. doi: 10.1016/S0140-6736(11)61752-2

Feasey, N. A., Hadfield, J., Keddy, K. H., Dallman, T. J., Jacobs, J., Deng, X., et al. (2016). Distinct *Salmonella* Enteritidis lineages associated with enterocolitis in high-income settings and invasive disease in low-income settings. *Nat. Genet.* 48, 10. doi: 10.1038/ng.3644

Feglo, P. K., Frimpong, E. H., and Essel-Ahun, M. (2004). *Salmonellae* carrier status of food vendors in Kumasi, Ghana. *East Afric. Med. J.* 81, 358–361. doi: 10.4314/eamj.v81i7.9191

Gilchrist, J. J., and MacLennan, C. A. (2019). Invasive non-typhoidal *Salmonella* disease in Africa. *EcoSal Plus* 8, 2. doi: 10.1128/ecosalplus.ESP-0007-2018

Haeusler, G. M., and Curtis, N. (2013). Non-typhoidal *Salmonella* in children: microbiology, epidemiology and treatment. *Adv. Experiment. Med. Biol.* 764, 13–26. doi: 10.1007/978-1-4614-4726-9_2

Hello, S. L., Bekhit, A., Granier, S. A., Barua, H., Beutlich, J., Zajac, M., et al. (2013). The global establishment of a highly-fluoroquinolone resistant *Salmonella enterica* serotype Kentucky ST198 strain. *Front. Microbiol.* 4, 395. doi: 10.3389/fmicb.2013.00395

Hopkins, K. L., Peters, T. M., De Pinna, E., and Wain, J. (2011). Standardisation of multilocus variable-number tandem repeat analysis (MLVA) for subtyping of *Salmonella enterica* serovar Enteritidis. *Euro. J. infect. Dis. Epidemiol. Prevent. Contr.* 16, 32. doi: 10.2807/ese.16.32.19942-en

Im, J., Nichols, C., Bjerregaard-Andersen, M., Sow, A. G., Løfberg, S., Tall, A., et al. (2016). Prevalence of *Salmonella* excretion in stool: a community survey in 2 sites, Guinea-Bissau and Senegal. *Clinic. Infect. Dis.* 62, 789. doi: 10.1093/cid/civ789

Kariuki, S., Mbae, C., Onsare, R., Kavai, S. M., Wairimu, C., Ngetich, R., et al. (2019). Multidrug-resistant non-typhoidal *Salmonella* hotspots as targets for vaccine use in management of infections in endemic settings. *Clinic. Infect. Dis.* 68, S10–S15. doi: 10.1093/cid/ciy898

Kariuki, S., Mbae, C., Van Puyvelde, S., Onsare, R., Kavai, S., Wairimu, C., et al. (2020). High relatedness of invasive multi-drug resistant non-typhoidal *Salmonella* genotypes among patients and asymptomatic carriers in endemic informal settlements in Kenya. *PLoS Neglect. Tropic. Dis.* 14, 1–14. doi: 10.1371/journal.pntd.0008440

Kariuki, S., Revathi, G., Kariuki, N., Kiiru, J., Mwituria, J., Muyodi, J., et al. (2006). Invasive multidrug-resistant non-typhoidal *Salmonella* infections in Africa: zoonotic or anthroponotic transmission? *J. Med. Microbiol.* 55, 585–591. doi: 10.1099/jmm.0.46375-0

Kasumba, I. N., Pulford, C. V., Perez-Sepulveda, B. M., Sen, S., Sayed, N., Permala-Booth, J., et al. (2021). Characteristics of *Salmonella* recovered from stools of children enrolled in the Global Enteric Multicenter Study, *Clinical Infectious Diseases*, 73(4), 631–641. doi: 10.1093/cid/ciab051

Koolman, L., Prakash, R., Diness, Y., Msefula, C., Nyirenda, T. S., Olgemoeller, F., et al. (2022). Case-control investigation of invasive *Salmonella* disease in Malawi reveals no evidence of environmental or animal transmission of invasive strains, and supports human to human transmission. *PLoS Neglect. Tropic. Dis.* 16, 1–17. doi: 10.1371/journal.pntd.0010982

Marks, F., von Kalckreuth, V., Aaby, P., Adu-Sarkodie, Y., Tayeb, M. A. E., Ali, M., et al. (2017). Incidence of invasive *Salmonella* disease in sub-Saharan Africa: a multicentre population-based surveillance study. *Lancet Glob. Health* 5, e310–e323. doi: 10.1016/S2214-109X(17)30022-0

Mather, A. E., Vaughan, T. G., and French, N. P. (2015). Molecular approaches to understanding transmission and source attribution in non-typhoidal *Salmonella* and their application in Africa. *Clinic. Infect. Dis.* 61, S259–S265. doi: 10.1093/cid/civ727

Mbae, C., Mwangi, M., Gitau, N., Irungu, T., Muendo, F., Wakio, Z., et al. (2020). Factors associated with occurrence of salmonellosis among children living in Mukuru slum, an urban informal settlement in Kenya. *BMC Infect. Dis.* 20, 1–12. doi: 10.1186/s12879-020-05134-z

Mbuyi-Kalonji, L., Barbé, B., Nkoji, G., Madinga, J., Roucher, C., Linsuke, S., et al. (2020). Non-typhoidal *Salmonella* intestinal carriage in a *Schistosoma mansoni* endemic community in a rural area of the Democratic Republic of Congo. *PLoS Neglect. Tropic. Dis.* 14, 1–15. doi: 10.1371/journal.pntd.0007875

Misganaw, B., and Williams, D. (2013). A Study of *Salmonella* carriage among asymptomatic food-handlers in Southern Ethiopia. *Int. J. Nutri. Food Sci.* 2, 243. doi: 10.11648/j.ijnfs.20130205.15

Mohager, M. O., Mohager, S. O., and Kaddam, L. A. (2014). The association between schistosomiasis and enteric fever in a single *Schistosoma* endemic area in Sudan. *Int. J. Pharmaceutic. Sci. Res.* 5, 2181–2184. doi: 10.1108/ET-04-2013-0062

Nikiema, M. E. M., Gandara, M. P., d, Compaore, K. A. M., Ba, A. K., Soro, K. D., Nikiema, P. A., et al. (2021). Contamination of street food with multi-drug resistant *Salmonella*, in Ouagadougou, Burkina Faso. *PLoS ONE* 16, 1–13. doi: 10.1371/journal.pone.0253312

Nkuo-Akenji, N., Ntemgwa, M. L., and Ndip, R. N. (2001). Asymptomatic salmonellosis in Buea District, Cameroon. *Cent Afr. J. Med.* 47, 254–257. doi: 10.4314/cajm.v47i11.8626

Ohad Gal-Mor (2019). Persistent infection and long-term carriage of typhoidal and non-typhoidal *Salmonellae*. *Clinic. Microbiol. Rev.* 32, 1–31. doi: 10.1128/CMR.00088-18

Park, S. E., Pham, D. T., Pak, G. D., Panzner, U., Espinoza, L. M. C., von Kalckreuth, V., et al. (2021). The genomic epidemiology of multi-drug resistant invasive non-typhoidal *Salmonella* in selected sub-Saharan African countries. *BMJ Global Health* 6, 1–14. doi: 10.1136/bmjgh-2021-005659

Parry, C. M., Hien, T. T., Dougan, G., White, N. J., and Farrar, J. J. (2002). Typhoid fever. *New Engl. J. Med.* 2, 201. doi: 10.1056/NEJMra020201

Phoba, M.-F., Barbé, B., Ley, B., Van Puyvelde, S., Post, A., Mattheus, W., et al. (2020). High genetic similarity between non-typhoidal *Salmonella* isolated from paired blood and stool samples of children in the Democratic Republic of the Congo. *PLoS Neglect. Tropic. Dis.* 14, 1–15. doi: 10.1371/journal.pntd.0008377

Post, A. S., Diallo, S. N., Guiraud, I., Lompo, P., Tahita, M. C., Maltha, J., et al. (2019). Supporting evidence for a human reservoir of invasive non-typhoidal *Salmonella* from household samples in Burkina Faso. *PLoS Neglect. Tropic. Dis.* 13, 10. doi: 10.1371/journal.pntd.0007782

Pulford, C. V., Perez-Sepulveda, B. M., Canals, R., Bevington, J. A., Bengtsson, R. J., Wenner, N., et al. (2021). Stepwise evolution of *Salmonella* Typhimurium ST313 causing bloodstream infection in Africa. *Nat. Microbiol.* 6, 327–338. doi: 10.1038/s41564-020-00836-1

Salem, A. K., Bilal, N. E., and Ibrahim, M. E. (2015). Frequent carriage of invasive *Salmonellae* amongst patients infected with schistosomiasis in Sudan. *Afric. J. Microbiol. Res.* 9, 543–548. doi: 10.5897/AJMR2014.7210

Smith, S. I., Alao, F., Goodluck, H. T., Fowora, M., Bamidele, M., Omonigbehin, E., et al. (2008). Prevalence of *Salmonella* Typhi among food handlers from Bukkas in Nigeria, *Br. J. Biomed. Sci.* 65, 158–160. doi: 10.1080/09674845.2008.11978119

Stanaway, J. D., Parisi, A., Sarkar, K., Blacker, B. F., Reiner Jr, R. C., Hay, S. I., et al. (2019). The global burden of non-typhoidal *Salmonella* invasive disease: a systematic analysis for the Global Burden of Disease Study 2017. *Lancet Infect. Dis.* 19, 1312–1324. doi: 10.1016/S1473-3099(19)30418-9

Tack, B., Phoba, M.-F., Barbé, B., Kalonji, L. M., Hardy, L., Van Puyvelde, S., et al. (2020a). Non-typhoidal *Salmonella* bloodstream infections in Kisantu, DR Congo: Emergence of O5-negative *Salmonella* Typhimurium and extensive drug resistance. *PLoS Neglect. Tropic. Dis.* 14, 1–22. doi: 10.1371/journal.pntd.0008121

Tack, B., Phoba, M.-F., Thong, P., Lompo, P., Hupko, C., Desmet, S., et al. (2022). Epidemiological cut-off value and antibiotic susceptibility test methods for azithromycin in a collection of multi-country invasive non-typhoidal *Salmonella*. *Clinic. Microbiol. Infect.* 28, 1615–1623. doi: 10.1016/j.cmi.2022.06.009

Tack, B., Vanaenrode, J., Verbakel, J. Y., Toelen, J., and Jacobs, J. (2020b). Invasive non-typhoidal *Salmonella* infections in sub-Saharan Africa: a systematic review on antimicrobial resistance and treatment. *BMC Med.* 18, 1–22. doi: 10.1186/s12916-020-01652-4

Tack, B., Vita, D., Phoba, M.-F., Mbuyi-Kalonji, L., Hardy, L., Barbé, B., et al. (2021). Direct association between rainfall and non-typhoidal *Salmonella* bloodstream infections in hospital-admitted children in the Democratic Republic of Congo. *Scientific Rep.* 11, 1–14. doi: 10.1038/s41598-021-01030-x

Van Puyvelde, S., Pickard, D., Vandelannoote, K., Heinz, E., Barbé, B., de Block, T., et al. (2019). An African *Salmonella* Typhimurium ST313 sublineage with extensive drug-resistance and signatures of host adaptation, *Nat. Commun.* 10, 1–12. doi: 10.1038/s41467-019-11844-z

Wilson, C. N., Pulford, C. V., Akoko, J., Sepulveda, B. P., Predeus, A. V., Bevington, J., et al. (2020). *Salmonella* identified in pigs in Kenya and Malawi reveals the potential for zoonotic transmission in emerging pork markets. *PLoS Neglect. Tropic. Dis.* 14, 1–16. doi: 10.1371/journal.pntd.0008796

World Health Organization (2022). *World malaria report*. Geneva. Available online at: https://www.who.int/teams/global-malaria-programme/reports/world-malaria-report-2022 (accessed October 17, 2023).

World Health Organization (2023). *Global Research Agenda for Antimicrobial Resistance in Human Health*. Available online at: https://www.who.int/publications/m/item/global-research-agenda-for-antimicrobial-resistance-in-human-health (accessed October 17, 2023).

Zhou, Z., Charlesworth, J., and Achtman, M. (2021). HierCC: a multi-level clustering scheme for population assignments based on core genome MLST, *Bioinformatics*, 37(20), 3645–3646. doi: 10.1093/bioinformatics/btab234

frontiers | Frontiers in Microbiology

TYPE Review
PUBLISHED 04 January 2024
DOI 10.3389/fmicb.2023.1333500

OPEN ACCESS

EDITED BY
Sébastien Holbert,
INRA Centre Val de Loire, France

REVIEWED BY
Qiuhe Lu,
Cleveland Clinic, United States
Che-Hsin Lee,
National Sun Yat-sen University, Taiwan

*CORRESPONDENCE
Qi Xu
✉ xuqi@yzu.edu.cn
Lizhi Lu
✉ lulizhibox@163.com

RECEIVED 06 November 2023
ACCEPTED 12 December 2023
PUBLISHED 04 January 2024

CITATION
Zhang Y, Xu M, Guo Y, Chen L, Vongsangnak W, Xu Q and Lu L (2024) Programmed cell death and *Salmonella* pathogenesis: an interactive overview. *Front. Microbiol.* 14:1333500. doi: 10.3389/fmicb.2023.1333500

Programmed cell death and *Salmonella* pathogenesis: an interactive overview

Yu Zhang[1,2], Maodou Xu[2], Yujiao Guo[2], Li Chen[1], Wanwipa Vongsangnak[3], Qi Xu[2]* and Lizhi Lu[1]*

[1]State Key Laboratory for Managing Biotic and Chemical Threats to the Quality and Safety of Agro-Products, Zhejiang Academy of Agricultural Sciences, Hangzhou, Zhejiang, China, [2]College of Animal Science and Technology, Yangzhou University, Yangzhou, Jiangsu, China, [3]Department of Zoology, Faculty of Science, Kasetsart University, Bangkok, Thailand

Programmed cell death (PCD) is the collective term for the intrinsically regulated death of cells. Various types of cell death are triggered by their own programmed regulation during the growth and development of organisms, as well as in response to environmental and disease stresses. PCD encompasses apoptosis, pyroptosis, necroptosis, autophagy, and other forms. PCD plays a crucial role not only in the growth and development of organisms but also in serving as a component of the host innate immune defense and as a bacterial virulence strategy employed by pathogens during invasion. The zoonotic pathogen *Salmonella* has the ability to modulate multiple forms of PCD, including apoptosis, pyroptosis, necroptosis, and autophagy, within the host organism. This modulation subsequently impacts the bacterial infection process. This review aims to consolidate recent findings regarding the mechanisms by which *Salmonella* initiates and controls cell death signaling, the ways in which various forms of cell death can impede or restrict bacterial proliferation, and the interplay between cell death and innate immune pathways that can counteract *Salmonella*-induced suppression of host cell death. Ultimately, these insights may contribute novel perspectives for the diagnosis and treatment of clinical *Salmonella*-related diseases.

KEYWORDS

programmed cell death, salmonella, apoptosis, pyroptosis, necroptosis, autophagy

1 Introduction

Programmed cell death (PCD) is a pervasive phenomenon in the growth and development of organisms, characterized by a genetically regulated process of active and organized cell death. Specifically, PCD involves the initiation of a protective mechanism in response to cytokine stimulation from either the internal or external environment. This mechanism entails the activation of gene coding and protein metabolism. Initially, apoptosis was acknowledged as the prevailing form of cell death in the early stages of PCD research, while necrosis was predominantly viewed as an incidental consequence of external stimuli leading to cell death. Necrosis is commonly defined as the uncontrolled death of a cell, typically occurring after a significant injury, leading to the release of cellular contents into neighboring tissues and subsequent harm (D'Arcy, 2019). As investigations into this genetically regulated, self-contained, and organized form of cell death progress, an increasing number of cell death modalities have been unveiled. In the context of pathogenic bacterial infections, these cell deaths are commonly classified into various prevalent forms of PCD, such as apoptosis, pyroptosis, necroptosis, autophagy, and ferroptosis, based on discernible morphological alterations, essential biochemical factors, immune pathway components, and effector proteins (Table 1).

Host cell death is a prevalent characteristic observed in numerous bacterial infections, serving as a means to restrict bacterial replication. Conversely, bacteria employ a diverse range of virulence factors or effector proteins to counteract or manipulate the signaling pathways associated with cell death, thereby evading or impeding cell death induction. For instance, the T3SS effectors of *Salmonella* Typhimurium have been identified to interact with apoptotic, necroptotic, and pyroptotic cell death cascades, thereby impeding the efficient elimination of the bacteria and the recruitment of neutrophils or dendritic cells to the site of infection (LaRock et al., 2015). PCD is widely recognized as an integral component of the innate immune defense in host organisms. *Salmonella*, a zoonotic pathogen, is a facultative intracellular pathogen that poses a significant threat to both global human and animal health, resulting in substantial economic burdens. This pathogen consistently influences the progression and resolution of infections by stimulating the production of cytokines with potent immunomodulatory properties and the secretion of various virulence effector proteins via the bacterial type III secretion system (T3SS), which governs the regulation of PCD (Wemyss and Pearson, 2019). However, the type of cell death induced during a bacterial infection is contingent upon various factors, including the infecting pathogen, its virulence factors, the specific tissues and cell types affected, and the host's inflammatory response. This review aims to provide a comprehensive overview of the molecular mechanisms governing PCD in *Salmonella* infections, with a particular emphasis on apoptosis, pyroptosis, necroptosis, and autophagy, as well as their interplay in the containment or eradication of *Salmonella* during infections. The insights presented herein offer novel targets and ideas for the treatment of diseases associated with *Salmonella* infection.

2 Apoptosis induced by activation of caspases by *Salmonella* infection

Apoptosis is a regulated process of cellular death, wherein the activation of Caspases serves as the principal mechanism (Stringer et al., 2023). It is triggered in cells that have been subjected to either internal or external signaling cascades due to damage or stress. The initiation of apoptosis is contingent upon the activation of apoptotic Caspases and is marked by various cellular changes, including the formation of apoptotic vesicles, cell membrane blebbing, cell shrinkage, DNA fragmentation, and nucleoplasmic condensation (Guiney, 2005). The pathways of Caspase dependency encompass both the extrinsic death pathway mediated by death receptors and the intrinsic death pathway mediated by mitochondria. The extrinsic death pathway is triggered when ligands or cytokines bind to transmembrane death receptors located on the cell surface, thereby regulating apoptosis through the activation of the death-inducing signaling complex (DISC) and Caspases-8. Specifically, the death receptor Fas binds to the ligand FasL and interacts with the Death domain (DD) on the protein, leading to the recruitment of the Fas-associated death domain protein (FADD). FADD possesses a Death effector domain (DED) that facilitates the interaction between FADD and other DED-containing proteins, such as Caspase-8. FADD undergoes aggregation with Caspase-8 to form the DISC. Upon activation, Caspase-8 undergoes a conformational change from a single-stranded zymogen to a biologically active double-stranded protein. This activated Caspase-8 then further activates Caspase-3, initiating the extrinsic death pathway (Grassme et al., 2001). On the other hand, the intrinsic death pathway is triggered by the release of apoptotic proteins due to internal stimulation. Various factors such as microbial infection, DNA damage, cytotoxic stimulation, and other influences lead to the oligomerization of B cell lymphoma 2 (Bcl-2) family proteins Bax and Bak (Stringer et al., 2023). This oligomerization increases the permeability of the mitochondrial membrane, resulting in the formation of annular lipid pores in the intermembrane space of the mitochondria. Cytochrome C (CytC) and other pro-apoptotic factors are released into the cytoplasm via perforated mitochondria. In the presence of dATP, CytC and apoptotic protease-activating factor 1 (Apaf-1) with CARD domain bind to Caspase-9, forming an apoptotic complex. This complex can activate Caspase-9, which in turn triggers the hydrolysis and processing activation of apoptosis execution proteins Caspase-3 and Caspase-7 into their mature forms. Ultimately, this cascade leads to intrinsic cell death (Ketelut-Carneiro and Fitzgerald, 2022) (Figure 1).

The foodborne pathogen *Salmonella* is acquired through the ingestion of contaminated food and subsequently enters the digestive tract. During the initial phase of *Salmonella* infection, the pathogen infiltrates intestinal epithelial cells by employing SPI-1 effectors, which induce alterations in intestinal folds and actin structures. This process facilitates the uptake of *Salmonella* by non-phagocytic cells. Alternatively, *Salmonella* may traverse M cells that cover the Peyer's patches, allowing entry into the lymphoid follicles and lamina propria, where they are captured by phagocytes such as dendritic cells and macrophages. Upon internalization by host cells and residing within specialized membrane-bound blebs known as *Salmonella*-containing vacuoles (SCVs), the expression of SPI-1 T3SS and its associated effectors is down-regulated, while SPI-2 is up-regulated (LaRock et al., 2015; Wemyss and Pearson, 2019). This regulatory shift promotes the formation of SCVs and facilitates the replication of *Salmonella* (Figure 2). Within these vacuoles, the bacteria employ the T3SS to deliver various effector proteins into the cytoplasm of phagocytes, thereby triggering Caspase-1 activation and subsequent cell death. The release of SipB leads to rapid cell death, exhibiting characteristics of both necrosis and apoptosis, along with the release of the proinflammatory cytokines IL-1β and IL-18 (Boise and Collins, 2001). The second mechanism primarily involves the activation of Toll-like receptor 4 (TLR4) by *Salmonella* through various components such as lipopolysaccharide (LPS) in the cell wall, intracellular TLR4 adapter proteins, and kinase pathways. This activation initiates a complex cascade of signal transduction, leading to the induction of both pro- and anti-apoptotic factors. Specifically, IKK and JNK activate the transcription factors NF-κB and AP-1, which are pivotal in the stimulation of pro-inflammatory cytokine genes, including TNF-α. Additionally, p38-MAPK and AKT play crucial roles in the induction of anti-apoptotic proteins (Guiney, 2005). On the other hand, the kinase PKR plays a role in facilitating *Salmonella*-induced apoptosis through its ability to impede protein synthesis via eIF2a phosphorylation. Additionally, PKR and type I interferons

TABLE 1 Comparison of apoptosis, pyroptosis, necroptosis, and autophagy.

PCD form	Morphological characteristics	Biochemical characteristics	Immunological characteristics	Key effector proteins
Apoptosis	Reduced cell and nuclear volume, chromatin condensation, nuclear fragmentation, apoptotic vesicle formation, and cytoskeletal disintegration	Caspase activation, DNA degradation fragmentation	Usually does not elicit an inflammatory response, anti-inflammatory, and in some cases elicits an immune response through exposure and release of DAMPs	Caspase, Bcl-2, Bax, P53, Fas
Pyroptosis	Plasma membrane rupture, release of cell contents and pro-inflammatory cytokines	Caspase1 and Caspase11 activation, generation of active IL-1β, and IL-I8, GSDMD protein hydrolysis activation	Release of DAMPs, pro-inflammatory	GSDM protein family, Caspase-1/3/4/5/8/11, Inflammasomes
Necroptosis	Swelling of cells and organelles, moderate condensation of chromatin, rupture of cell membranes, and spillage of cellular components	Decreased levels of ATP. RIP1, RIP3, and MLKL activation	Usually releases DAMPs pro-inflammatory and in some cases anti-inflammatory	RIP1 and RIP3
Autophagy	Massive autophagic vesicle formation	LC3-I to LC3-I1, Self-substrate (e.g., p62) degradation	Usually inhibits the activation of inflammasomes to act as an anti-inflammatory, and in some cases pro-inflammatory	ATG5, ATG7, LC3, Beclin-1, DRAM3, and TFEB
Ferroptosis	Reduced mitochondrial volume, increased density of bilayer membranes, reduction or disappearance of mitochondrial cristae, and rupture of the outer mitochondrial membrane	Iron accumulation and lipid peroxidation	Release of DAMPs and pro-inflammatory	GPX4, TFR1, ferritin, SLC7A11, NRF2, P53, ACSL4, and FSP1

stimulate the activation of interferon response factor 3 (IRF3), which further triggers the production of pro-apoptotic factors within phagocytes (Hsu et al., 2004). The equilibrium between these apoptotic regulators ultimately dictates the fate of a cell, determining whether it will endure or undergo PCD. Notably, Caspase-3 assumes a pivotal role as the principal executor of these distinctive apoptotic alterations. However, *Salmonella* is known to produce several effector proteins that have the potential to influence the apoptotic pathway. Specifically, the SPI-1 T3SS facilitates the secretion of SptP, AvrA, and SspH1 (also secreted by SPI-2), which in turn promote apoptosis by inhibiting NF-κB, down-regulating MAPK signaling, or facilitating the secretion of SigD (SopB) to activate the AKT effect and delay apoptosis. Additionally, the SPI-2 T3SS mediates the secretion of SpvB, which leads to the depolymerization of the actin cytoskeleton in macrophages, thereby contributing to SPI-2-dependent apoptosis (Schleker et al., 2012; Wemyss and Pearson, 2019) (Figure 1).

3 *Salmonella* induces inflammasome-mediated pyroptosis

Pyroptotic cell death is characterized by the progressive enlargement of cells until the rupture of the plasma membrane, leading to the formation of a pore. This pore allows for the release of intracellular contents, including the cytokines IL-1β and IL-18, resulting in a robust inflammatory response (Ketelut-Carneiro and Fitzgerald, 2022). The classical pathway of pyroptosis is regulated by Caspase-1, which undergoes processing and activation within the inflammasomes. These inflammasomes are supramolecular complexes that consist of NLRs, typically featuring C-terminal leucine-rich repeat sequences (LRRs), and are responsible for sensing signals from bacteria (Frank and Vince, 2019). Furthermore, nucleotide-binding domain and leucine-rich repeat containing receptors (NLRs) possess a variable N-terminal region housing the pyrin structural domain (PYD). Upon stimulation of the host by signals emanating from bacterial infection, inducible pattern recognition receptors (PRRs) engage with pathogen-associated molecular patterns (PAMPs) and assemble an inflammasome alongside the pyroptosis adapter protein ASC. This assembly catalyzes the activation of Caspase-1, which subsequently cleaves the precursors of IL-1β and IL-18, resulting in the formation of biologically active inflammatory cytokines (Fink and Cookson, 2007). IL-1β is an endogenous pyrogen that elicits fever, stimulates the expression of cytokines and chemokines, and facilitates the migration of leukocytes. Additionally, IL-18 triggers the production of IFN-γ, which plays a crucial role in the activation of T cells and macrophages (Guiney, 2005). Furthermore, the activation of the inflammasome-associated Caspase-1 can cleave Gasdermin D (GSDMD), leading to the formation of structural domain proteins containing the active fragment of GSDMD-N (Fink and Cookson, 2007). This active fragment induces the perforation and rupture of the cell membrane, resulting in the rapid release of IL-1β and IL-18 into the extracellular environment, thereby instigating inflammatory responses and pyroptosis (Brokatzky and Mostowy, 2022) (Figure 3).

Pyroptosis serves as a vital innate immune response against *Salmonella*, influencing the progression of bacterial infection by inducing pyroptosis in both immune and non-immune cells. The activation of distinct inflammasomes in *Salmonella*-induced pyroptosis is contingent upon the virulence of the *Salmonella* strain and the response of the infected cell. During the *Salmonella* Typhimurium infection, the activation of host cell NLR family

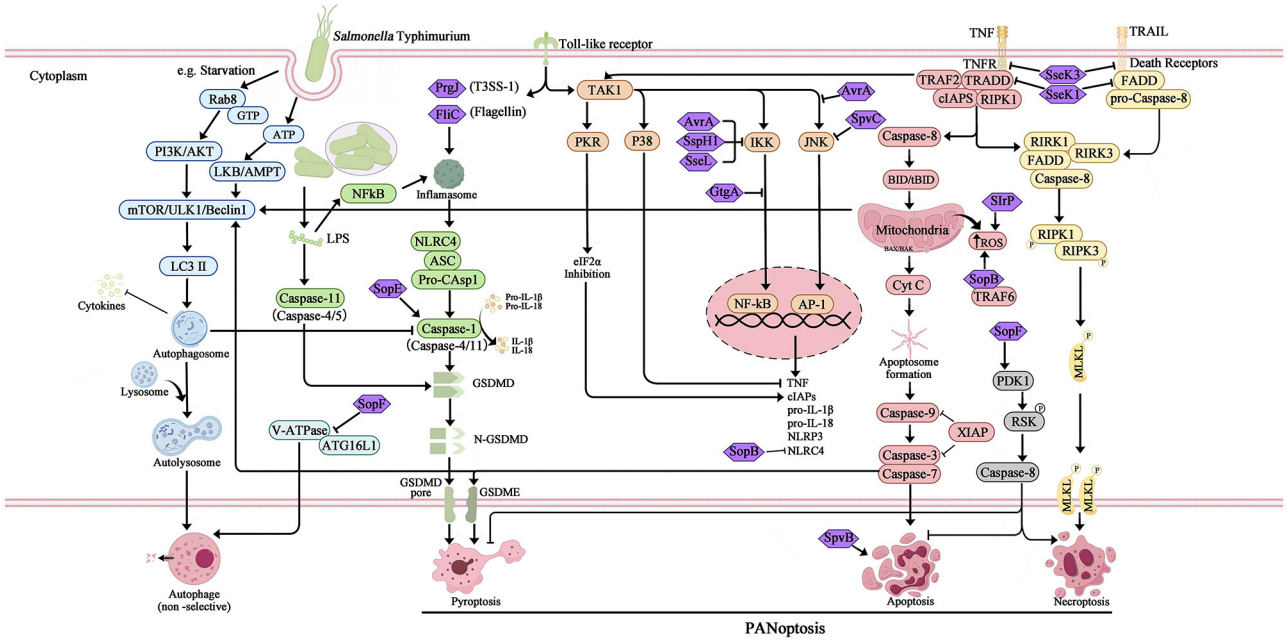

FIGURE 1
Overview of the different type of programmed cell death and the interference of T3SS effector proteins during *Salmonella* Typhimurium infection. The activation and inhibition of apoptosis, pyroptosis, necroptosis, and canonical autophagy are mediated by the SPI-1 and SPI-2 T3SS effector proteins, which interact with host innate immune pathways during *Salmonella* Typhimurium infection. The extensive overlap between apoptosis, pyroptosis, and necroptosis results in a phenomenon known as PANoptosis was also induced during *Salmonella* Typhimurium infection.

apoptosis inhibitory proteins (NAIP) occurs upon sensing of flagellin (FliC and FljB) or PrgJ (an SPI-1 secreted protein). These proteins subsequently interact with protein 4 (NLRC4), which possesses the NLR family Caspase recruitment domain (CARD), resulting in the formation of a complex with ASC. This complex then catalyzes the hydrolytic activation of Caspase-1, thereby mediating cellular pyroptosis (Fink and Cookson, 2007; Wemyss and Pearson, 2019). Additionally, NLRP3 (which detects increased ROS or K^+ efflux) and pyrin (which senses inhibition of RhoA GTPase activity) can also induce pyroptosis through ASC Caspase-1 inflammasomes (Wemyss and Pearson, 2019). Both NLRC4 and NLRP3 are involved in the maturation of IL-1β and IL-18, as well as the induction of pyroptosis, in macrophages infected with *Salmonella* Typhimurium (Vladimer et al., 2013). In the non-classical pathway of pyroptosis, the LPS from *Salmonella* directly interacts with Caspase-4/5/11 in macrophages, leading to the activation of Caspase-4/5/11 (Knodler et al., 2014). This activated Caspase then cleaves GSDMD protein, triggering the activation of NLRP3 inflammasomes and subsequent activation of Caspase-1. This cascade ultimately results in the release of IL-1β, IL-18, and the occurrence of pyroptosis (Ma et al., 2021). Additionally, NLRC4 and the activation of non-classical inflammasomes are implicated in the response of epithelial cells to *Salmonella* infection, potentially contributing to the containment of bacterial dissemination within the intestinal mucosa.

Salmonella is known to generate various effector proteins that have the potential to impact the pyroptosis pathway. In the case of *Salmonella* Typhimurium-infected HeLa and RAW264.7 cells, as well as *in vivo* infection of mouse enterocytes, the *Salmonella* Typhimurium type III effector protein (SopE) was observed to stimulate the activation of host cell Rac1, which is a subunit of the Rho GTPase. This activation subsequently induces Caspase-1 activation and the secretion of IL-1β (Müller et al., 2009; Hoffmann et al., 2010). SopB has been found to be linked with the downregulation of NLRC4 in *Salmonella* Typhimurium-infected macrophages and B cells (Hu et al., 2017). The absence of NLRC4, a crucial inflammasome, hinders the pyroptosis response to *Salmonella* Typhimurium infection, thereby providing bacteria with an enhanced opportunity for replication prior to evading the host cell (García-Gil et al., 2018). SipB which interacts with SipC to form a translocon pore, facilitating SPI-1 effector translocation into the host cell is reportedly sufficient to induce Caspase-1-mediated "apoptosis" and IL-18 maturation in SipB transfected or *Salmonella* Typhimurium-infected (Hersh et al., 1999; van der Velden et al., 2003). Overall, *Salmonella* infection process is capable of activating different inflammasomes, causing cellular focalization and enhancing bacterial invasion and immune escape from the host cell.

4 *Salmonella* infection induces necroptosis dependent on the classical pathway TNF signaling

Necrosis is characterized as a passive and unregulated form of cell death, whereas necroptosis adheres to intracellular signaling regulation, exhibiting Caspase activity-independent characteristics. Necroptosis is visually manifested through cell swelling, mitochondrial dysfunction, plasma rupture, and

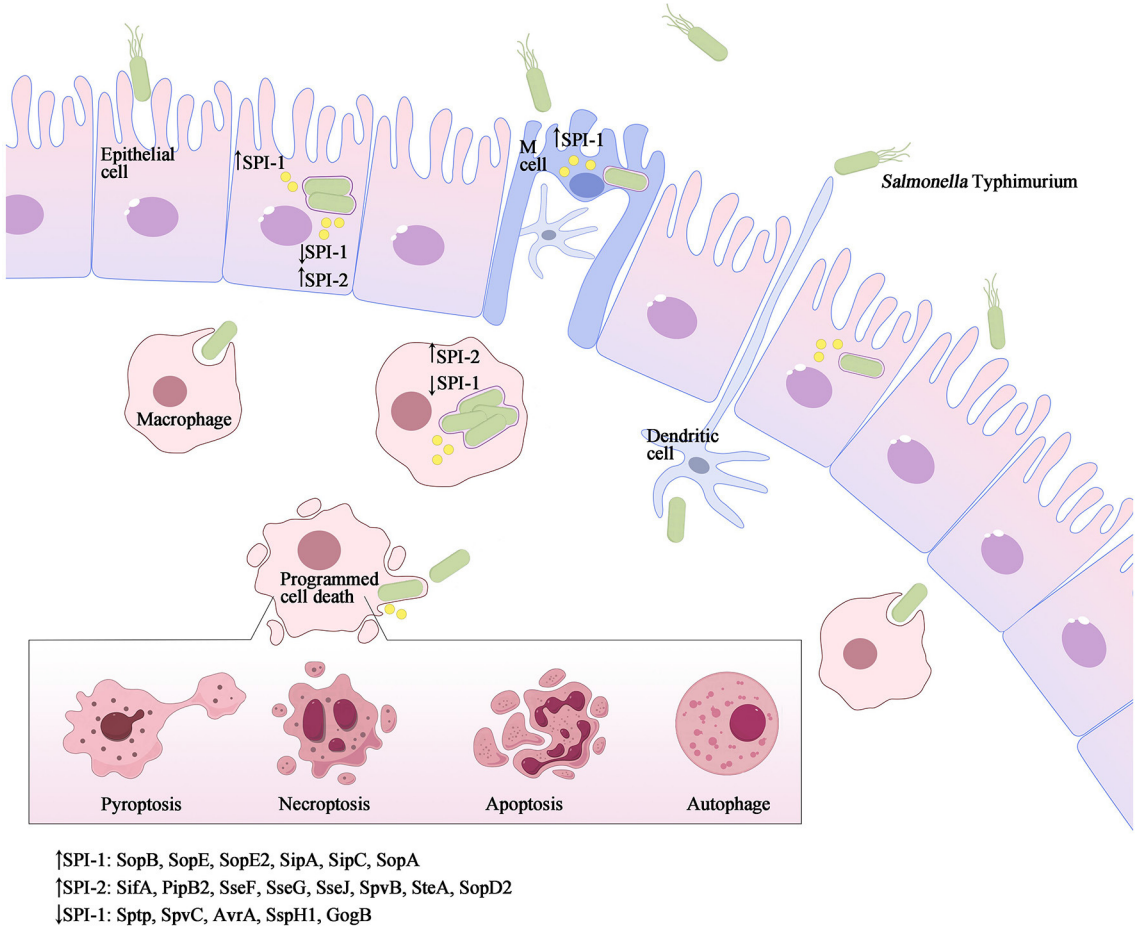

FIGURE 2
Salmonella Typhimurium invasion elicits various forms of programmed cell death. As a facultative intracellular pathogen, *Salmonella* Typhimurium can infect a range of cell types such as macrophages, dendritic cells, and epithelial cells. *Salmonella* Typhimurium accomplishes intestinal epithelium traversal by invading M-cells located above Peyer's patches, and it can also be captured by phagocytic cells such as dendritic cells or macrophages from the intestinal lumen. Once internalized, the SPI-1 T3SS and its effectors are downregulated, while SPI-2 is upregulated to promote the formation of *Salmonella*-containing vacuoles (SCVs) and facilitate *Salmonella* replication. Throughout the infection process, both SPI-1 and SPI-2 effector proteins interact with host innate immune pathways, either activating or inhibiting inflammatory responses and inducing different types of programmed cell death, such as apoptosis, pyroptosis, necroptosis, autophagy and others.

subsequent release of intracellular contents, which incites an inflammatory response in the surrounding tissue (Blériot and Lecuit, 2016). The canonical pathway of necroptosis, known as the tumor necrosis factor (TNF) signaling pathway, necessitates the participation of various kinases, including receptor-interacting serine/threonine protein kinase 1/3 (RIPK1/RIPK3)and mixed-lineage kinase domain-like protein (MLKL). Furthermore, the process of necroptosis necessitates the involvement of specialized receptors and ligands located on the plasma membrane, primarily mediated by tumor necrosis factor-α (TNF-α) and tumor necrosis factor receptor 1 (TNFR1). Upon ligation of TNF-α and TNFR1, RIPK1 and TNFR1-associated death domain protein (TRADD) are recruited, leading to the formation of a multimeric complex 1. This multimeric complex I comprises not only RIPK1 and TRADD, but also cellular inhibitors of apoptosis 1/2 (cIAP1/2), tumor necrosis factor receptor-associated factor 2/5 (TRAF2/5). Additionally, cIAP1/2 is capable of inducing the ubiquitination of RIPK1 and facilitating the up-regulation of anti-apoptotic genes. When the deubiquitinase CYLD deubiquitinates RIPK1, it results in a reduction in the stability of multimeric complex I. This reduction leads to the formation of a multimeric complex consisting of RIPK1, FADD, TRADD, RIPK3, and Caspase-8. The activation of multimeric complex II triggers the downstream signaling pathway of apoptosis. Caspase-8 then cleaves and inactivates RIPK1 and RIPK3, initiating the Caspase cascade reaction, ultimately resulting in cell apoptosis (Hu and Zhao, 2013; Wemyss and Pearson, 2019). However, bacterial pathogens hinder the activity of Caspase-8, preventing the cleavage and inactivation of RIPK1 and RIPK3 by Caspase-8. RIPK1 and RIPK3 form a complex and initiate phosphorylation, leading to the recruitment of the downstream necrosis execution protein MLKL and the subsequent formation of necrosomes (Hu and Zhao, 2013). Within these bodies, RIPK3 phosphorylates MLKL, resulting in the oligomerization and translocation of phosphorylated MLKL to the plasma membrane. At the plasma membrane, phosphorylated MLKL interacts with phosphatidylinositol phosphate (PIP), thereby increasing the

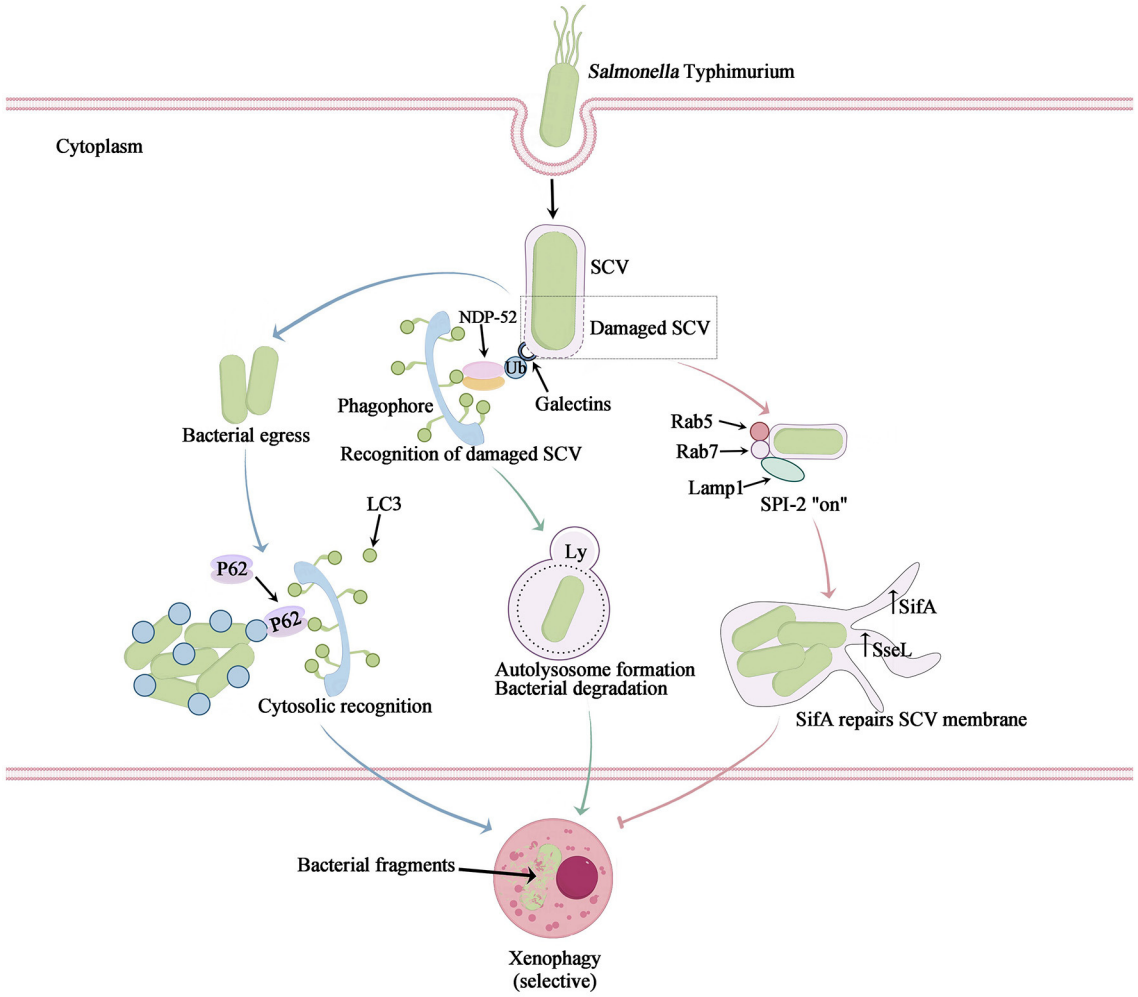

FIGURE 3
The mechanism of intracellular *Salmonella* Typhimurium-induced xenophagy. *Salmonella* Typhimurium infection not only causes cell nutrient deprivation or stimulation leading to non-selective autophagy, but also triggers selective autophagy to clear bacteria, also known as xenophagy. After their escape from a *Salmonella*-containing vacuole (SCV), *Salmonella* bacteria are marked with ubiquitin. Autophagy adaptors then bind to the ubiquitylated bacteria and link them to LC3-II on the initial autophagosome membrane (blue arrow). The SCV is damaged by T3SS-1, leading to the recruitment of galectin-8 to bind ubiquitin and the recruitment of NDP52, which connects LC3 and promotes autophagosome maturation. This process exposes internal proteins of the SCV membrane to the cytosol and causes sharp changes in ion concentration, potentially resulting in the formation of an ubiquitinated SCV membrane. The autophagic machinery recognizes this ubiquitinated membrane (green arrow). Autophagy facilitates the restoration of the SCV membrane damaged by T3SS-1 and subsequently induces acidification to generate SIFs, thereby enabling bacterial survival and replication within (pink arrow).

permeability of the cytoplasmic membrane and facilitating the release of highly inflammatory damage-associated molecular patterns (DAMPs) into the extracellular space (Frank and Vince, 2019). This process ultimately leads to cell rupture and the induction of cell necroptosis (Figure 1).

During *Salmonella* Typhimurium infection, virulence effector proteins are involved in facilitating the host necroptotic response. Specifically, *Salmonella* secretes effector proteins SseK1 and SseK3, which glycosylate TNFR superfamily members and TRADD or FADD. This glycosylation process inhibits TNF-mediated NF-κB signaling and prevents cell death through apoptosis or necroptosis. Mass spectrometry analysis has identified TNFR1 and TRAIL-R as the glycosylation targets of SseK3, while TRADD is the preferred binding target of SseK1 (Günster et al., 2017; Xue et al., 2020). In addition, SopF was found could activate phosphoinositide-dependent protein kinase-1 (PDK1) to phosphorylate p90 ribosomal S6 kinase (RSK) which down-regulated Caspase-8 activation, resulting in inhibition of pyroptosis and apoptosis, but promotion of necroptosis (Yuan et al., 2023).

5 Bidirectional regulation of autophagy induced by *Salmonella* infection

Both apoptosis and autophagy are activated in response to metabolic stress. Growth factor deprivation, limitation of nutrients

TABLE 2 *Salmonella* effectors intervention in programmed cell death.

PCD form	Effector protein	T3SS	Cells affected	Mechanism	References
Apoptosis	SlrP	1/2	HeLa	SPI-1 and SPI-2 translocated E3 ubiquitin ligases that interact with thioredoxin-1 (Trx1) and ER chaperone protein ERdj3	Bernal-Bayard et al., 2010; Zouhir et al., 2014
Apoptosis	SpvB	2	HMDM CHO HT-29	Making ADP-ribosylated actin and disrupting the cytoskeleton of eukaryotic cells	Lesnick et al., 2001; Browne et al., 2002; Paesold et al., 2002
Apoptosis	SopB (SigD)	1	MEFs Henle407	Inhibits production of mitochondrial superoxide ROS Activates MAPK and NF-κB signaling through stimulation of Rho-family GTPases	Ruan et al., 2014, 2016
Apoptosis	AvrA	1	HeLa HCT116 HEK293T	Inhibits NF-κB and JNK pro-inflammatory pathways	Collier-Hyams et al., 2002; Ye et al., 2007; Jones et al., 2008
Apoptosis	SseK3	2	HeLa, HEK293	SseK3 Binds TRIM32 and modulates the host's NF-κB signaling activity	Yang et al., 2015
Necroptosis	SseK1	1/2	RAW264.7	Arginine glycosylation of FADD inhibits TNF-induced NF-κB signaling	Günster et al., 2017
Necroptosis	SseK3	2	RAW264.7	Arginine glycosylation of TRADD inhibits TNF-induced NF-κB signaling	Günster et al., 2017
Necroptosis	SopF	1	IECs	PDK1 to phosphorylate RSK which down-regulated Caspase-8 activation	Yuan et al., 2023
Pyroptosis	PrgJ	1	BMMs	Activates caspase-1 through NLRC4	Rayamajhi et al., 2013
Pyroptosis	SlrP	1/2	IECs	Inhibition of IL-1β activation	Rao et al., 2017
Pyroptosis	SipB	1	RAW264.7 DC	SipB induces macrophage apoptosis by binding to caspase-1 SipB induces IL-18 activation and release in human dendritic cells	Hersh et al., 1999; van der Velden et al., 2003
Pyroptosis	SopE	1	HeLa RAW264.7	SopE-driven Rho GTPase-mediated caspase-1 activation	Müller et al., 2009; Hoffmann et al., 2010
Pyroptosis	SopB (SigD)	1	BMDM B Cells	SopB inhibits IL-1β secretion and caspase-1 activation. SopB triggers the PI3K-Akt-YAP pathway to inhibit the NLRC4 inflammasomes	Hu et al., 2017; García-Gil et al., 2018
Autophagy	SopB (SigD)	1	B Cells	SopB activates mTORC1 and inhibits autophagy by phosphorylating ULK1 at its Ser757	Luis et al., 2022
Autophagy	SopF	1	HeLa	SopF specifically modifies V-ATPase to inhibit the autophagic recognition	Xu et al., 2022
Autophagy	SseL	2	HeLa	SseL inhibits selective autophagy of cytosolic aggregates	Mesquita et al., 2012
Autophagy	SopA	1	HeLa HEK293T	Interacting with Human RMA1 Promote the escape of *Salmonella* from the SCVs Stimulates inflammation targeting TRIM56 and TRIM65	Zhang et al., 2006; Kamanova et al., 2016
Autophagy	SseF	2	HeLa	Interacts with the small GTPase Rab1A in host cells to impair autophagy initiation	Feng et al., 2018
Autophagy	SseG	2	HeLa	Interacts with the small GTPase Rab1A in host cells to impair autophagy initiation	Feng et al., 2018
Autophagy	AvrA	1	HCT116	Suppression of autophagy by reducing Beclin-1 expression through the JNK pathway	Jiao et al., 2020
Autophagy	SrrB	2	BMDMs	Targeting Sirt1/LKB1/AMPK for lysosomal degradation, which enables sustained mTOR-activation and inhibition of autophagy	Ganesan et al., 2017
Autophagy	SifA	2	HeLa	Inhibiting retrograde trafficking of M6PR and lysosome function	McGourty et al., 2012

and energy metabolism, activate the mTOR/ULK1/Beclin1 pathway, the multiple effects of some key proteins such as Caspase-3, Beclin1, and p53 lead to the complex interplay between these two pathways (Nikoletopoulou et al., 2013). However, *Salmonella* infection not only causes cell nutrient deprivation or stimulation leading to non-selective autophagy, but also triggers

selective autophagy to clear bacteria, also known as xenophagy. *Salmonella* infection elicits non-selective autophagy, primarily triggered by amino acid deficiency, resulting in the suppression of the cell growth regulator mTOR. The PI3K-Akt-mTOR signaling pathway plays a pivotal role in this process (Miller et al., 2020) (Figure 1). Furthermore, xenophagy which is the activation of selective autophagy, is widely recognized as a promising strategy to combat bacterial infections. Xenophagy exerts its influence on *Salmonella* infection through three distinct pathways, two of which function as antibacterial defense mechanisms, effectively targeting invading *Salmonella*, eradicating pathogens, and subsequently safeguarding host cells. Additionally, *Salmonella*-infected cells employ an alternative pathway that not only facilitates the restoration of the damaged SCV, but also fosters an environment conducive to the replication and survival of the pathogen itself (Owen and Casanova, 2015; Zheng et al., 2022) (Figure 3). In the initial route, a portion of *Salmonella* bacteria possess the ability to evade this vacuole. Once these bacteria infiltrate the cytoplasm, they become tagged with unbound ubiquitin and undergo selective autophagy. Adapter proteins, namely SLRs (such as SQSTM1/p62, NDP52, and OPTN proteins), are recognized for their capacity to bind to ubiquitin-labeled bacteria. Additionally, these adapter proteins function as autophagy substrates, binding to LC3 in order to facilitate the mediation of autophagosomes. Specifically, it accomplishes this by means of the ubiquitin-binding domain and ubiquitin-labeled bacteria. It establishes a bond with characterized bacteria and engages with the autophagosome molecular marker Atg8/LC3 as well as the autophagy substrate SQSTM1/p62, thereby facilitating its association with the developing autophagosome. Consequently, it encapsulates *Salmonella* within the autophagosome and subsequently breaks down the bacteria. Another mechanism by which cells defend against *Salmonella* autophagy involves the recognition of damage to the SCV membrane caused by the pinhole apparatus of SPI-1 T3SS (Mostowy, 2013). In this scenario, *Salmonella* is found within the damaged SCV. The perforation of the SCV membrane, induced by SPI-1 T3SS, attracts various cytosolic components, including galectin-8. Galectin-8 serves as a marker protein for intact membrane structure and also acts as an inducer of autophagy. The galectin-8-labeled SCV then recruits LC3 and NDP52 to the cell membrane, thereby promoting the generation of autophagy signals. Consequently, this process leads to the autophagic capture and degradation of *Salmonella* (Wu et al., 2020).

Salmonella, being a parthenogenetic intracellular bacterium, has the ability to enhance its own survival through the induction of cellular autophagy. Unlike autophagy, which serves as a natural cellular immune defense mechanism, *Salmonella* can secrete certain effector proteins to evade fusion with lysosomes during autophagy, allowing for persistent proliferation within the SCV (Wang et al., 2018). For instance, *Salmonella* Typhimurium possesses a virulence plasmid that encompasses a conserved region of approximately 8 kb, which plays a crucial role in bacterial serum resistance, adhesion, and colonization. The spv region of the *Salmonella* plasmid virulence gene encompasses three genes associated with virulence, namely the transcriptional regulator spvR, as well as the structural genes spvB and spvC. Among these, spvB plays a crucial role in determining the extent of *Salmonella* proliferation within macrophages, while also inducing late apoptosis in host cells during *Salmonella* infection. The SPV proteins are essential for ADP-ribosyltransferase activity, which serves as an endotoxin and covalently modifies monomeric actin, thereby creating a favorable growth environment for *Salmonella* infection (Shintani and Klionsky, 2004; Xie et al., 2020). The upregulation of the autophagosome molecular marker Atg8/LC3 facilitates the repair and maturation of the SCV membrane. This process is accompanied by the recruitment of essential membrane-loading molecules Rab5 and Rab7, which ensure cellular maturation and enable the expression of the SPI-2 T3SS. Consequently, the effector protein filamentous body SifA is produced to maintain the integrity of the SCV membrane, further promoting SCV maturation and facilitating the replication of *Salmonella* within the host cell, thereby enhancing its survival (Birmingham and Brumell, 2006). During this temporal phase, the SPI-1 T3SS-mediated damage to the SCV leads to the liberation of ubiquitin and galectin-8 signaling molecules, thereby facilitating the internalization of crucial antimicrobial autophagic constituents (Owen and Casanova, 2015; Xie et al., 2020). Concurrently, the SPI-2 T3SS effector protein, SseL, is activated, culminating in the fulfillment of intracellular *Salmonella* replication through the reduction of autophagic fluxes. Consequently, this reduction instigates apoptosis in macrophages (Mesquita et al., 2012) (Figure 3).

In the initial stages of autophagic activation, the bacteria secrete effector proteins to impede the recognition of PAMPs, thereby evading cellular autophagy (Wang et al., 2018). During the process of autophagy, *Salmonella* fluid releases multiple effector proteins through either simulation or direct covalent modification of host proteins, thus facilitating their escape mechanisms (Table 2). Furthermore, *Salmonella* Typhimurium counteracts host SLRs and releases the effector protein SopA, which promotes the ubiquitination and subsequent degradation of TRIM56 and TRIM65, thereby suppressing IFN-γ-driven autophagy (Zhang et al., 2006). *Salmonella* Typhimurium has developed the membrane proteinase IcsP as a means of evading recognition by the C3 complement system and escaping cell-autonomous autophagy (Sorbara et al., 2018). The effector protein SrrB plays a role in disrupting the activation of the AMPK pathway, leading to the degradation of the AMPK/Sirt1/LBK1 complex. This disruption by SrrB results in an increase in mTOR levels and the inhibition of ULK complex formation (Ganesan et al., 2017). Recent studies have revealed that *Salmonella* effector proteins SseF and SseG disrupt the interaction between the guanine nucleotide exchange factor of GTPase Rab1A and transporter protein particle III, impede the assembly of the ULK1 complex, and reduce the synthesis of PI3P. These actions ultimately inhibit the nucleation of autophagosomes and membrane elongation. Additionally, it has been discovered that the *Salmonella* effector protein SopF can specifically modify V-ATPase, a crucial protein involved in sensing bacterial infection and recruiting autophagy protein ATG16L1 to initiate xenophagy. This alteration inhibits the V-ATPase-ATG16L1 pathway, thereby promoting the proliferation and spread of *Salmonella* within the host (Xu et al., 2019, 2022). In a typical physiological state, mannose-6-phosphate receptors

(M6PR) facilitate the transportation of synthetic hydrolases from the trans-Golgi network (TGN) to endocytic lysosomes. However, the *Salmonella*-secreted effector SifA, in conjunction with the small guanosine triphosphatase Rab9, obstructs M6PR transport and reduces hydrolase activity (McGourty et al., 2012). Consequently, this enhances bacterial survival within the host cell.

6 Crosstalk between cell death programs

Furthermore, the interplay between *Salmonella* effector proteins and the phenomenon of cross-regulation among different cell death pathways gives rise to the manifestation of hybrid forms of PCD. The interconnectedness of apoptosis and necroptosis pathways is primarily facilitated by the involvement of Caspase-8, whereby the activation of extrinsic death receptors mediated by the RIPK1/FADD/Caspase-8 complex can yield diverse signaling outcomes. In the absence of inhibition of RIPK or Caspase, the dominant mechanism of cell survival was through the activation of anti-apoptotic programs mediated by NF-κB. Suppression of RIPK resulted in the initiation of extrinsic apoptosis through Caspase-8 homodimerization. Conversely, inhibition of Caspase-8 facilitated necroptosis by promoting the oligomerization of RIPK1 and RIPK3 (Demarco et al., 2020). Necroptosis interacts with focal death signaling pathways via the effector protein MLKL. Additionally, the activation of cytoplasmic ZBP1 leads to the phosphorylation of MLKL, which in turn forms a pore in cellular membranes, including the plasma membrane. The activation of the NLRP3 inflammasome, triggered by subsequent K^+ efflux mediated by MLKL, leads to the assembly of inflammasomes and cleavage of Caspase-1, resulting in the formation of GSDM-D pores and the release of IL-1β and IL-18 (Frank and Vince, 2019). Similarly, both apoptosis and pyroptosis involve the activation of Caspase proteases, which may have common evolutionary origins. As a result, these processes can interact at various levels. For example, the pyroptotic Caspase-1 protease can cleave the Bcl-2 family member Bid, leading to mitochondrial outer membrane permeabilization (MOMP) and subsequent activation of apoptotic signaling (Bock and Tait, 2020). Apoptosis-induced Caspase-8 has the capability to interact with ASC, resulting in Caspase-8-dependent pyroptotic activation (Fink and Cookson, 2007). Additionally, the transcription of NLRC4 and NLRP3 inflammasomes driven by apoptosis can facilitate Caspase-1 activation, leading to the hydrolysis of the pyroptotic execution protein GSDMD and subsequent formation of gasdermin pores, thereby inducing morphological characteristics associated with pyroptosis (Wemyss and Pearson, 2019). Emerging evidence indicates that autophagy and apoptosis can also engage in interactions, exhibiting antagonistic or cooperative effects, thereby exerting distinct influences on cellular destiny. Regulators involved in the interplay between autophagy and apoptosis have been identified, including the Bcl-2 protein family, Caspases, Beclin1, NF-κB, and certain microRNAs. These regulators exhibit dual coordinated roles at the transcriptional level. Additionally, kinase signaling pathways such as JNK and PI3K/Akt/mTOR have been demonstrated to play a significant role in mediating the interaction between autophagy and apoptosis (Wemyss and Pearson, 2019; Snyder and Oberst, 2021). Notably, recent research has revealed a significant finding that *Salmonella* infection has the capability to induce PANoptosis, a complex interplay involving apoptosis, pyroptosis, and necroptosis. Moreover, it has been discovered that the *Salmonella* effector SopF plays a crucial role in regulating the PANoptosis of intestinal epithelial cells, thereby exacerbating systemic infection (Christgen et al., 2020; Yuan et al., 2023). The intricate molecular network and the pleiotropic nature displayed by these regulators are expected to be influenced by the cellular milieu and diverse downstream targets. Alternatively, inhibition of specific proteins in the pathway may activate multiple PCD pathways, thereby enabling the organism to accomplish its defense objectives through alternative mechanisms.

7 Conclusions and future prospects

During *Salmonella* infection, bacteria manipulate PCD in immune and non-immune cells through multiple mechanisms, including interference with cell signaling pathways and regulation of cellular metabolism. The interaction between these pathways of cell death implies that, similar to numerous immune pathways, cell death signals have undergone evolutionary adaptation and diversification in response to the selective pressure imposed by *Salmonella* infection. The flexible utilization and interconnectedness of various cell death pathways serve as a defense mechanism against intracellular infection. Through extensive research on the mechanism of action of *Salmonella* and PCD, our understanding of the intricate complexity and diverse nature of *Salmonella* and cell programmed has significantly advanced. However, numerous unanswered questions persist. For instance, which PCD pathway is predominantly activated during *Salmonella* infection? How do the multiple virulence factors produced by *Salmonella* synchronize and regulate these PCD mechanisms? What are the principal regulatory effector proteins implicated in these processes? Do effector proteins possess comparable sites for bulk activation or inhibition, facilitating precise regulation of PCD processes through ubiquitination modification? Furthermore, what is the safety profile of clinical drugs targeting PCD in the treatment of *Salmonella* infections, considering the escalating issue of antibiotic resistance? In an era of increasing antibiotic resistance, it is imperative to comprehend the significance of PCD within the innate immune system, as well as to unravel the intricate molecular mechanisms employed by bacteria to evade and exploit PCD. This comprehension is of utmost importance in the regulation of bacterial infections through PCD, the identification of novel drug targets for intracellular bacterial infections, and the formulation of innovative strategies for the prevention and control of bacterial proliferation.

Author contributions

YZ: Supervision, Writing—original draft. MX: Investigation, Writing—original draft. YG: Visualization, Writing—review

& editing. LC: Writing—review & editing. WV: Supervision, Writing—review & editing. QX: Conceptualization, Writing—review & editing. LL: Formal analysis, Investigation, Writing—review & editing.

Funding

The author(s) declare financial support was received for the research, authorship, and/or publication of this article. This work was supported by the National Natural Science Funds of China (32372863), Jiangsu Province Agricultural Science and Technology Independent Innovation Fund Project (CX (22) 3033), and State Key Laboratory for Managing Biotic and Chemical Threats to the Quality and Safety of Agro-products (2021DG700024-KF202KF202319).

Conflict of interest

The authors declare that the research was conducted in the absence of any commercial or financial relationships that could be construed as a potential conflict of interest.

Publisher's note

References

Bernal-Bayard, J., Cardenal-Munoz, E., and Ramos-Morales, F. (2010). The *Salmonella* type III secretion effector, *Salmonella* leucine-rich repeat protein (SlrP), targets the human chaperone ERdj3. *J. Bio. Chem.* 285, 16360–16368. doi: 10.1074/jbc.M110.100669

Birmingham, C. L., and Brumell, J. H. (2006). Autophagy recognizes intracellular *Salmonella* enterica serovar Typhimurium in damaged vacuoles. *Autophagy* 2, 156–158. doi: 10.4161/auto.2825

Blériot, C., and Lecuit, M. (2016). The interplay between regulated necrosis and bacterial infection. *Cell. Mol. Life Sci.* 73, 2369–2378. doi: 10.1007/s00018-016-2206-1

Bock, F. J., and Tait, S. W. G. (2020). Mitochondria as multifaceted regulators of cell death. *Nat. Rev. Mol. Cell Biol.* 21, 85–100. doi: 10.1038/s41580-019-0173-8

Boise, L. H., and Collins, C. M. (2001). *Salmonella*-induced cell death: apoptosis, necrosis or programmed cell death? *Trends Microbiol.* 9, 64–67. doi: 10.1016/S0966-842X(00)01937-5

Brokatzky, D., and Mostowy, S. (2022). Pyroptosis in host defence against bacterial infection. *Dis. Model. Mech.* 15, 414. doi: 10.1242/dmm.049414

Browne, S. H., Lesnick, M. L., and Guiney, D. G. (2002). Genetic requirements for *Salmonella*-induced cytopathology in human monocyte-derived macrophages. *Infect. Immun.* 70, 7126–7135. doi: 10.1128/IAI.70.12.7126-7135.2002

Christgen, S., Zheng, M., Kesavardhana, S., Karki, R., Malireddi, R. K. S., Banoth, B., et al. (2020). Identification of the PANoptosome: a molecular platform triggering pyroptosis, apoptosis, and necroptosis (PANoptosis). *Front. Cell. Infect. Microbiol.* 10, 237. doi: 10.3389/fcimb.2020.00237

Collier-Hyams, L. S., Zeng, H., Sun, J., Tomlinson, A. D., Bao, Z. Q., Chen, H., et al. (2002). Cutting edge: *Salmonella* AvrA effector inhibits the key proinflammatory, anti-apoptotic NF-κB pathway. *J. Immunol.* 169, 2846–2850. doi: 10.4049/jimmunol.169.6.2846

D'Arcy, M. S. (2019). Cell death: a review of the major forms of apoptosis, necrosis and autophagy. *Cell Biol. Int.* 43, 582–592. doi: 10.1002/cbin.11137

Demarco, B., Chen, K. W., and Broz, P. (2020). Cross talk between intracellular pathogens and cell death. *Immunol. Rev.* 297, 174–193. doi: 10.1111/imr.12892

Feng, Z. Z., Jiang, A. J., Mao, A. W., Feng, Y. H., Wang, W. N., Li, J. J., et al. (2018). The *Salmonella* effectors SseF and SseG inhibit Rab1A-mediated autophagy to facilitate intracellular bacterial survival and replication. *J. Biol. Chem.* 293, 9662–9673. doi: 10.1074/jbc.M117.811737

Fink, S. L., and Cookson, B. T. (2007). Pyroptosis and host cell death responses during *Salmonella* infection. *Cell Microbiol.* 9, 2562–2570. doi: 10.1111/j.1462-5822.2007.01036.x

Frank, D., and Vince, J. E. (2019). Pyroptosis versus necroptosis: similarities, differences, and crosstalk. *Cell Death Differ.* 26, 99–114. doi: 10.1038/s41418-018-0212-6

Ganesan, R., Hos, N. J., Gutierrez, S., Fischer, J., Stepek, J. M., Daglidu, E., et al. (2017). *Salmonella typhimurium* disrupts Sirt1/AMPK checkpoint control of mTOR to impair autophagy. *PLoS Pathog.* 13, e1006227. doi: 10.1371/journal.ppat.1006227

García-Gil, A., Galán-Enríquez, C. S., Pérez-López, A., Nava, P., Alpuche-Aranda, C., Ortiz-Navarrete, V., et al. (2018). SopB activates the Akt-YAP pathway to promote *Salmonella* survival within B cells. *Virulence* 9, 1390–1402. doi: 10.1080/21505594.2018.1509664

Grassme, H., Jendrossek, V., and Gulbins, E. (2001). Molecular mechanisms of bacteria induced apoptosis. *Apoptosis* 6, 441–445. doi: 10.1023/A:1012485506972

Guiney, D. G. (2005). The role of host cell death in *Salmonella* infections. *Curr. Top Microbiol. Immunol.* 289, 131–150. doi: 10.1007/3-540-27320-4_6

Günster, R. A., Matthews, S. A., Holden, D. W., and Thurston, T. L. M. (2017). SseK1 and SseK3 type III secretion system effectors inhibit NF-κB signaling and necroptotic cell death in *Salmonella*-infected macrophages. *Infect. Immun.* 85, e00010–17. doi: 10.1128/IAI.00010-17

Hersh, D., Monack, D. M., Smith, M. R., Ghori, N., Falkow, S., Zychlinsky, A., et al. (1999). The *Salmonella* invasin SipB induces macrophage apoptosis by binding to Caspase-1. *Proc. Natl. Acad. Sci. U.S.A.* 96, 2396–2401. doi: 10.1073/pnas.96.5.2396

Hoffmann, C., Galle, M., Dilling, S., Käppeli, R., Müller, A. J., Songhet, P., et al. (2010). In macrophages, Caspase-1 activation by SopE and the type III secretion system-1 of S. Typhimurium can proceed in the absence of flagellin. *PLoS ONE* 5, e12477. doi: 10.1371/journal.pone.0012477

Hsu, L. C., Park, J. M., Zhang, K. Z., Luo, J. L., Maeda, S., Kaufman, R. J., et al. (2004). The protein kinase PKR is required for macrophage apoptosis after activation of Toll-like receptor 4. *Nature* 428, 341–345. doi: 10.1038/nature02405

Hu, G. Q., Song, P. X., Chen, W., Qi, S., Yu, S. X., Du, C. T., et al. (2017). Cirtical role for *Salmonella* effector SopB in regulating inflammasome activation. *Mol. Immunol.* 90, 280–286. doi: 10.1016/j.molimm.2017.07.011

Hu, Z. Q., and Zhao, W. H. (2013). Type 1 interferon-associated necroptosis: a novel mechanism for *Salmonella* enterica Typhimurium to induce macrophage death. *Cell. Mol. Immunol.* 10, 10–12. doi: 10.1038/cmi.2012.54

Jiao, Y., Zhang, Y. G., Lin, Z. J., Lu, R., Xia, Y. L., Meng, C., et al. (2020). *Salmonella* Enteritidis effector AvrA suppresses autophagy by reducing Beclin-1 protein. *Front. Immunol.* 11, 686. doi: 10.3389/fimmu.2020.00686

Jones, R. M., Wu, H. X., Wentworth, C., Luo, L. P., Collier-Hyams, L., Neish, A. S., et al. (2008). *Salmonella* AvrA coordinates suppression of host immune and apoptotic defenses via JNK pathway blockade. *Cell Host Microbe.* 3, 233–244. doi: 10.1016/j.chom.2008.02.016

Kamanova, J., Sun, H., Lara-Tejero, M., and Galán, J. E. (2016). The *Salmonella* effector protein SopA modulates innate immune responses by targeting TRIM E3 ligase family members. *PLoS Pathog.* 12, e1005552. doi: 10.1371/journal.ppat.1005552

Ketelut-Carneiro, N., and Fitzgerald, K. A. (2022). Apoptosis, pyroptosis, and necroptosis-oh my! The many ways a cell can die. *J Mol Biol.* 434, 167378. doi: 10.1016/j.jmb.2021.167378

Knodler, L.eigh A., Crowley, S.hauna M., Sham, H.o P., Yang, H., Wrande, M., Ma, C., et al. (2014). Noncanonical inflammasome activation of caspase-4/caspase-11 mediates epithelial defenses against enteric bacterial pathogens. *Cell Host Microbe.* 16, 249–256. doi: 10.1016/j.chom.2014.07.002

LaRock, D. L., Chaudhary, A., and Miller, S. I. (2015). *Salmonella*e interactions with host processes. *Nat. Rev. Microbiol.* 13, 191–205. doi: 10.1038/nrmicro3420

Lesnick, M. L., Reiner, N. E., Fierer, J., and Guiney, D. G. (2001). The *Salmonella* spvB virulence gene encodes an enzyme that ADP-ribosylates actin and destabilizes the cytoskeleton of eukaryotic cells. *Mol. Microbiol.* 39, 1464–1470. doi: 10.1046/j.1365-2958.2001.02360.x

Luis, L. B., Ana, G. T., Carlos, G. E., Abraham, G. G., Iris, E. G., Martha, M. L., et al. (2022). *Salmonella* promotes its own survival in B cells by inhibiting autophagy. *Cells* 11, 2061. doi: 10.3390/cells11132061

Ma, X. Y., Li, Y. J., Shen, W. X., Oladejo, A. O., Yang, J., Jiang, W., et al. (2021). LPS mediates bovine endometrial epithelial cell pyroptosis directly through both NLRP3 classical and non-classical inflammasome pathways. *Front. Immunol.* 12, 676088. doi: 10.3389/fimmu.2021.676088

McGourty, K., Thurston, T. L., Matthews, S. A., Pinaud, L., Mota, L. J., Holden, D. W., et al. (2012). *Salmonella* inhibits retrograde trafficking of mannose-6-phosphate receptors and lysosome function. *Science* 338, 963–967. doi: 10.1126/science.1227037

Mesquita, F. S., Thomas, M., Sachse, M., Santos, A. J. M., Figueira, R., Holden, D. W., et al. (2012). The *Salmonella* deubiquitinase SseL inhibits selective autophagy of cytosolic aggregates. *PLoS Pathog.* 8, e1002743. doi: 10.1371/journal.ppat.1002743

Miller, D. R., Cramer, S. D., and Thorburn, A. (2020). The interplay of autophagy and non-apoptotic cell death pathways. *Cell Death Dis.* 352, 159–187. doi: 10.1016/bs.ircmb.2019.12.004

Mostowy, S. (2013). Autophagy and bacterial clearance: a not so clear picture. *Cell Microbiol.* 15, 395–402. doi: 10.1111/cmi.12063

Müller, A. J., Hoffmann, C., Galle, M., Van Den Broeke, A., Heikenwalder, M., Falter, L., et al. (2009). The *S. typhimurium* effector SopE induces Caspase-1 activation in stromal cells to initiate gut inflammation. *Cell Host Microbe* 6, 125–136. doi: 10.1016/j.chom.2009.07.007

Nikoletopoulou, V., Markaki, M., Palikaras, K., and Tavernarakis, N. (2013). Crosstalk between apoptosis, necrosis and autophagy. *Biochim. Biophys. Acta.* 1833, 3448–3459. doi: 10.1016/j.bbamcr.2013.06.001

Owen, K. A., and Casanova, J. E. (2015). *Salmonella* manipulates autophagy to "serve and protect". *Cell Host Microbe.* 18, 517–519. doi: 10.1016/j.chom.2015.10.020

Paesold, G., Guiney, D. G., Eckmann, L., and Kagnoff, M. F. (2002). Genes in the *Salmonella* pathogenicity island 2 and the *Salmonella* virulence plasmid are essential for *Salmonella*-induced apoptosis in intestinal epithelial cells. *Cell. Microbiol.* 4, 771–781. doi: 10.1046/j.1462-5822.2002.00233.x

Rao, S., Schieber, A. M. P., O'Connor, C. P., Leblanc, M., Michel, D., Ayres, J. S., et al. (2017). Pathogen-mediated inhibition of anorexia promotes host survival and transmission. *Cell* 168, 503–516. doi: 10.1016/j.cell.2017.01.006

Rayamajhi, M., Zak, D. E., Chavarria-Smith, J., Vance, R. E., and Miao, E. A. (2013). Cutting edge: mouse NAIP1 detects the type III secretion system needle protein. *J. Immunol.* 191, 3986–3989. doi: 10.4049/jimmunol.1301549

Ruan, H. H., Li, Y., Zhang, X. X., Liu, Q., Ken, H., Zhang, K. S., et al. (2014). Identification of TRAF6 as a ubiquitin ligase engaged in the ubiquitination of SopB, a virulence effector protein secreted by *Salmonella typhimurium*. *Biochem. Biophys. Res. Commun.* 447, 172–177. doi: 10.1016/j.bbrc.2014.03.126

Ruan, H. H., Zhang, Z., Tian, L., Wang, S. Y., Hu, S. Y., Qiao, J. J., et al. (2016). The *Salmonella* effector SopB prevents ROS-induced apoptosis of epithelial cells by retarding TRAF6 recruitment to mitochondria. *Biochem. Biophys. Res. Commun.* 478, 618–623. doi: 10.1016/j.bbrc.2016.07.116

Schleker, S., Sun, J., Raghavan, B., Srnec, M., Muller, N., Koepfinger, M., et al. (2012). The current *Salmonella*-host interactome. *Proteomics Clin Appl* 6, 117–133. doi: 10.1002/prca.201100083

Shintani, T., and Klionsky, D. J. (2004). Autophagy in health and disease: a double-edged sword. *Science* 306, 990–995. doi: 10.1126/science.1099993

Snyder, A. G., and Oberst, A. (2021). The antisocial network: cross talk between cell death programs in host defense. *Annu. Rev. Immunol.* 39, 77–101. doi: 10.1146/annurev-immunol-112019-072301

Sorbara, M. T., Foerster, E. G., Tsalikis, J., Abdel-Nour, M., Mangiapane, J., Sirluck-Schroeder, I., et al. (2018). Complement C3 drives autophagy-dependent restriction of cyto-invasive bacteria. *Cell Host Microbe* 23, 644–652. doi: 10.1016/j.chom.2018.04.008

Stringer, J. M., Alesi, L. R., Winship, A. L., and Hutt, K. J. (2023). Beyond apoptosis: evidence of other regulated cell death pathways in the ovary throughout development and life. *Hum Reprod. Update* 29, 434–456. doi: 10.1093/humupd/dmad005

van der Velden, A. W. M., Velasquez, M., and Starnbach, M. N. (2003). *Salmonella* rapidly kill dendritic cells via a Caspase-1-dependent mechanism. *J. Immunol.* 171, 6742–6749. doi: 10.4049/jimmunol.171.12.6742

Vladimer, G. I., Marty-Roix, R., Ghosh, S., Weng, D., and Lien, E. (2013). Inflammasomes and host defenses against bacterial infections. *Curr. Opin. Microbiol.* 16, 23–31. doi: 10.1016/j.mib.2012.11.008

Wang, L. D., Yan, J., Niu, H., Huang, R., and Wu, S. Y. (2018). Autophagy and ubiquitination in *Salmonella* infection and the related inflammatory responses. *Front. Cell. Infect. Microbiol.* 8, 78. doi: 10.3389/fcimb.2018.00078

Wemyss, M. A., and Pearson, J. S. (2019). Host cell death responses to non-typhoidal *Salmonella* infection. *Front. Immunol.* 10, 1758. doi: 10.3389/fimmu.2019.01758

Wu, S., Shen, Y. R., Zhang, S., Xiao, Y. Q., and Shi, S. R. (2020). *Salmonella* interacts with autophagy to offense or defense. *Front. Microbiol.* 11, 721. doi: 10.3389/fmicb.2020.00721

Xie, Z., Zhang, Y., and Huang, X. (2020). Evidence and speculation: the response of *Salmonella* confronted by autophagy in macrophages. *Future Microbiol.* 15, 1277–1286. doi: 10.2217/fmb-2020-0125

Xu, Y., Cheng, S., Zeng, H., Zhou, P., Ma, Y., Li, L., et al. (2022). ARF GTPases activate *Salmonella* effector SopF to ADP-ribosylate host V-ATPase and inhibit endomembrane damage-induced autophagy. *Nat. Struct. Mol. Biol.* 29, 67–77. doi: 10.1038/s41594-021-00710-6

Xu, Y., Zhou, P., Cheng, S., Lu, Q., Nowak, K., Hopp, A. K., et al. (2019). A bacterial effector reveals the V-ATPase-ATG16L1 axis that initiates xenophagy. Cell 178, 552–566.e520. doi: 10.1016/j.cell.2019.06.007

Xue, J., Hu, S., Huang, Y., Zhang, Q., Yi, X., Pan, X., et al. (2020). Arg-GlcNAcylation on TRADD by NleB and SseK1 is crucial for bacterial pathogenesis. *Front. Cell Dev. Biol.* 8, 641. doi: 10.3389/fcell.2020.00641

Yang, Z., Soderholm, A., Lung, T. W. F., Giogha, C., Hill, M. M., Brown, N. F., et al. (2015). SseK3 is a *Salmonella* effector that binds TRIM32 and modulates the host's NF-κB signalling activity. *PLoS ONE* 10, e0138529. doi: 10.1371/journal.pone.0138529

Ye, Z. D., Petrof, E. O., Boone, D., Claud, E. C., and Sun, J. (2007). *Salmonella* effector AvrA regulation of colonic epithelial cell inflammation by deubiquitination. *Am. J. Pathol.* 171, 882–892. doi: 10.2353/ajpath.2007.070220

Yuan, H. B., Zhou, L. T., Chen, Y. L., You, J. Y., Hu, H. Y., Li, Y. Y., et al. (2023). *Salmonella* effector SopF regulates PANoptosis of intestinal epithelial cells to aggravate systemic infection. *Gut Microbes* 15, 2180315. doi: 10.1080/19490976.2023.2180315

Zhang, Y., Higashide, W. M., McCormick, B. A., Chen, J., and Zhou, D. G. (2006). The inflammation-associated *Salmonella* SopA is a HECT-like E3 ubiquitin ligase. Mol. *Microbiol.* 62, 786–793. doi: 10.1111/j.1365-2958.2006.05407.x

Zheng, L., Wei, F., and Li, G. L. (2022). The crosstalk between bacteria and host autophagy: host defense or bacteria offense. *J. Microbiol.* 60, 451–460. doi: 10.1007/s12275-022-2009-z

Zouhir, S., Bernal-Bayard, J., Cordero-Alba, M., Cardenal-Muñoz, E., Guimaraes, B., Lazar, N., et al. (2014). The structure of the Slrp-Trx1 complex sheds light on the autoinhibition mechanism of the type III secretion system effectors of the NEL family. *Biochem. J.* 464, 135–144. doi: 10.1042/BJ20140587

frontiers | Frontiers in Microbiology

TYPE Original Research
PUBLISHED 05 January 2024
DOI 10.3389/fmicb.2023.1340143

OPEN ACCESS

EDITED BY
George Grant,
University of Aberdeen, United Kingdom

REVIEWED BY
Yuanyuan Li,
Soochow University, China
Etienne Giraud,
Institut National de Recherche Pour L'agriculture, L'alimentation et L'environnement (INRAE), France
Changyong Cheng,
Zhejiang A&F University, China

*CORRESPONDENCE
Krzysztof Grzymajlo
krzysztof.grzymajlo@upwr.edu.pl

RECEIVED 17 November 2023
ACCEPTED 11 December 2023
PUBLISHED 05 January 2024

CITATION
Aleksandrowicz A, Kolenda R, Baraniewicz K, Thurston TLM, Suchański J and Grzymajlo K (2024) Membrane properties modulation by SanA: implications for xenobiotic resistance in *Salmonella* Typhimurium.
Front. Microbiol. 14:1340143.
doi: 10.3389/fmicb.2023.1340143

Membrane properties modulation by SanA: implications for xenobiotic resistance in *Salmonella* Typhimurium

Adrianna Aleksandrowicz[1], Rafał Kolenda[1], Karolina Baraniewicz[1], Teresa L. M. Thurston[2], Jarosław Suchański[1] and Krzysztof Grzymajlo[1]*

[1]Department of Biochemistry and Molecular Biology, Faculty of Veterinary Medicine, Wrocław University of Environmental and Life Sciences, Wrocław, Poland, [2]Department of Infectious Disease, Centre for Bacterial Resistance Biology, Imperial College London, London, United Kingdom

Introduction: Multidrug resistance in bacteria is a pressing concern, particularly among clinical isolates. Gram-negative bacteria like *Salmonella* employ various strategies, such as altering membrane properties, to resist treatment. Their two-membrane structure affects susceptibility to antibiotics, whereas specific proteins and the peptidoglycan layer maintain envelope integrity. Disruptions can compromise stability and resistance profile toward xenobiotics. In this study, we investigated the unexplored protein SanA's role in modifying bacterial membranes, impacting antibiotic resistance, and intracellular replication within host cells.

Methods: We generated a *sanA* deletion mutant and complemented it *in trans* to assess its biological function. High-throughput phenotypic profiling with Biolog Phenotype microarrays was conducted using 240 xenobiotics. Membrane properties and permeability were analyzed via cytochrome c binding, hexadecane adhesion, nile red, and ethidium bromide uptake assays, respectively. For intracellular replication analysis, primary bone marrow macrophages served as a host cells model.

Results: Our findings demonstrated that the absence of *sanA* increased membrane permeability, hydrophilicity, and positive charge, resulting in enhanced resistance to certain antibiotics that target peptidoglycan synthesis. Furthermore, the *sanA* deletion mutant demonstrated enhanced replication rates within primary macrophages, highlighting its ability to evade the bactericidal effects of the immune system. Taking together, we provide valuable insights into a poorly known SanA protein, highlighting the complex interplay among bacterial genetics, membrane physiology, and antibiotic resistance, underscoring its significance in understanding *Salmonella* pathogenicity.

KEYWORDS

antibiotics, *Salmonella*, inner membrane proteins, membrane permeability, SanA

Introduction

Salmonellosis is a major intestinal foodborne disease, globally affecting approximately 200 million people and causing 60,000 fatalities annually (Havelaar et al., 2015). Thus, it is an epidemiological threat and an impediment to socio-economic development worldwide. Considering the ability of *Salmonella* to survive in various conditions, adapt to new environments, and facultatively survive and replicate inside cells, the prevention and treatment of salmonellosis become quite challenging. This often results in an over-reliance on antibiotic therapy, particularly in developing countries (Ayukekbong et al., 2017). Predictive models suggest that by 2050, antimicrobial resistance (AMR) may result in 10 million annual fatalities worldwide (O'Neil, 2016). Hence, non-typhoidal *Salmonella* and *Salmonella ser.* Typhi have been categorized by the Center for Disease Control as "Serious Threats," alongside other pathogens such as multidrug-resistant *Pseudomonas aeruginosa* and methicillin-resistant *Staphylococcus aureus* (Centers for Disease Control and Prevention, 2019).

Primarily, pathogenic bacteria have developed various defense mechanisms to withstand different environmental challenges, including exposure to xenobiotics. These mechanisms include (I) efflux pumps, which eliminate drugs from bacterial cells, thus reducing their concentration to non-toxic levels and causing loss of potency; (II) antibiotic inactivation by bacterial enzymes that alter or degrade antibiotic structures; (III) target site modification by spontaneous mutation and changing the chemical structure of their molecular targets; and (IV) preventing drug entry by altering bacterial membrane compositions (Alenazy, 2022). In all these processes the cell envelope, consisting of two lipid bilayers—inner membrane (IM) and outer membrane (OM) plays a critical role in protecting microorganisms from environmental stresses, as well as in cell viability and growth (Silhavy et al., 2010). The interdependence between OM and IM proteins is essential for preserving structural integrity of the bacterial cell envelope. Mutations in genes encoding IM proteins, such as *dedA* or *tat* may alter the membrane composition, potentially impacting membrane permeability and consequently resulting in antibiotic resistance (Boughner and Doerrler, 2012).

The outer membrane (OM) is a distinctive feature of gram-negative bacteria (Sun et al., 2022). It consists of an asymmetric lipid bilayer with the outer leaflet made of lipopolysaccharide (LPS) and the inner leaflet made of phospholipids (Nikaido, 2003; Sun et al., 2022). OM proteins can be classified as integral transmembrane β-barrel proteins (OMPs) and lipoproteins anchored in the inner leaflet (Malinverni and Silhavy, 2011). The most common lipoprotein is Lpp, which maintains periplasmic distance (Asmar and Collet, 2018). The OM's essential role is to protect against hydrophobic molecules, and some OMPs act as channels for small or large molecules (Nikaido, 2003). It also provides mechanical strength to compensate for the thin cell wall (Nikaido, 2003). Changes in OM composition can lead to drug resistance, emphasizing its importance in antibiotic sensitivity. They may also influence the efficiency of phagocytosis and the intracellular survival of pathogens within macrophages, as a result of an increased resistance toward antimicrobial activity of these host cells (Matz and Jürgens, 2001; Lei et al., 2019).

In addition to the OM, the bacterial cytoplasm is surrounded by a phospholipid bilayer IM, regulating the movement of nutrients and ions in and out of the cytoplasm. It serves as the site for various metabolic processes such as energy production, lipid and peptidoglycan biosynthesis, protein transport, and translocation (Silhavy et al., 2010). IM proteins vary extensively, from peripheral and integral proteins to lipoproteins attached to the periplasmic side of the IM. Together, they constitute approximately 25% of the bacterial proteome (Papanastasiou et al., 2016). Despite their abundance, the functions of several IM proteins are still unclear. One such IM protein is SanA, which is potentially involved in envelope biogenesis (Rida et al., 1996).

sanA multi-copy expression suppresses the vancomycin sensitivity of *Escherichia coli* K-12 mutant, showing OM permeability defect which was confirmed using compounds such as Sodium Dodecyl Sulfate (SDS), Ethidium Bromide (EB), and the ingredients of MacConkey medium (Rida et al., 1996). The *S.* Typhimurium *sfiX* (*sanA* ortholog) deletion mutant is also vancomycin-sensitive, which suggests that SanA may constitute a barrier that denies antibiotic access to its site of action (Mouslim et al., 1998). Furthermore, our previous study demonstrated the role of SanA in the initial stages of *Salmonella* pathogenicity—invasion and adhesion (Kolenda et al., 2021). Although SanA is hypothesized to be potentially associated with bacterial cell wall synthesis or may function as an efflux pump activated during extreme conditions such as cold/heat shock or bile exposure, these roles lack conclusive establishment. Notably, the subcellular localization of the SanA protein has not been experimentally demonstrated, and prediction tools provide inconsistent results in this context. Furthermore, the influence of SanA on membrane properties remains unexplored, and the correlation between physicochemical changes in the envelope and their subsequent effects on antibiotic resistance has not been investigated.

Considering all these aspects, we hypothesized that *sanA* deletion affects the membrane permeability of *Salmonella* and induces shifts in the membrane's physicochemical properties. These modifications are postulated to alter resistance to multiple antibiotic classes and enhance the bacterium's ability to replicate within primary macrophages.

Materials and methods

Bacteria, plasmids, and growth conditions

All bacterial strains, plasmids, and primers used in this study are listed in Tables 1–3, respectively. All *Salmonella* strains used in this work were derived from the *Salmonella enterica* serovar Typhimurium 4/74. Unless stated otherwise, bacterial cultures were routinely grown at 37°C for 16 h under dynamic or static conditions in Lysogeny Broth (LB) or on agar plates, respectively. According to manufacturer's recommendations, Biolog Universal Growth agar with 5% sheep blood was used to grow bacteria for the Biolog Phenotype Microarray. Mueller Hinton Broth (MHB) was used to measure antimicrobial activity. When necessary, ampicillin (Amp, 100 μg/mL) or kanamycin (Km, 50 μg/mL) was added. For *lac* promoter induction, isopropylthio-β-galactoside was added to a final concentration of 0.5 mM. Cell growth was monitored by measuring the optical density (OD) at 600 nm.

Xenobiotics

The following xenobiotic stock solutions were used: 5,7-dichloro-8-hydroxyquinaldine [55 mg/mL in dimethyl

TABLE 1 Bacterial strains used in this study.

Strain	Relevant feature(s)	References
S. Typhimurium 4/74	Wild type (WT)	Dr Derek Pickard, Cambridge Institute for Therapeutic Immunology and Infectious Disease, University of Cambridge Department of Medicine, Cambridge, United Kingdom
S. Typhimurium 4/74 Δ*sanA*	*S.* Typhimurium 4/74 with *sanA* gene knockout (Δ*sanA*)	This study
S. Typhimurium 4/74 Δ*sanA*-pWSK29	*S.* Typhimurium 4/74 Δ*sanA* with pWSK29 empty plasmid	This study
S. Typhimurium 4/74 Δ*sanA-pWSK29-sanA*	*S.* Typhimurium 4/74 Δ*sanA* complemented with *sanA* carrying pWSK29 plasmid	This study
E. coli XL1-Blue	*recA1 endA1 gyrA96 thi-1 hsdR17 supE44 relA1 lac [F´ proAB lacIq Z¨M15 Tn10 (Tetr)]*	Wroclaw University of Environmental and Life Sciences, Department of Biochemistry and Molecular Biology collection

TABLE 2 Plasmids used in this study.

Plasmid	Relevant feature(s)	References
pKD46	pBAD λ redαβγ ts ori; AmpR	Datsenko and Wanner (2000)
pKD4	template plasmids for FRT-flanked kanamycin cassette	Datsenko and Wanner (2000)
pCP20	Helper plasmid FLP ts *ori*; AmpR, KanR	Cherepanov (1995)
pWSK29	Expression vector under the IPTG-induced lac promoter, AmpR	prof. dr hab. Dariusz Bartosik, Institute of Microbiology, Department of Bacterial Genetics, University of Warsaw
pWSK29-*sanA*	pWSK29 vector with *sanA* sequence insert, AmpR	This study

sulfoxide (DMSO)]; bleomycin (2.56 mg/mL in sterile water); carbenicillin (20.5 mg/mL in sterile water); ceftriaxone (4 mg/mL in sterile water); cetylpyridinium chloride (164 mg/mL in sterile water); chlorhexidine acetate (25.6 mg/mL in ethanol); norfloxacin (0.8 mg/mL in DMSO); phosphomycin (40 mg/mL in sterile water); polymyxin B (1 mg/mL in sterile water); spectinomycin [100 mg/mL in DMSO:water (1:1)]; streptomycin (1 mg/mL in sterile water); sulfamonomethoxine (5 mg/mL in ethanol); thioridazine (16 mg/mL in DMSO); tobramycin (43.2 mg/mL in sterile water); umbelliferone (40 mg/mL in ethanol); and vancomycin (100 mg/mL in sterile water). All xenobiotic solutions were sterilized using 0.22 μm membrane filters and diluted in MHB medium to the appropriate concentration.

Bioinformatic analysis

In the study, a comprehensive array of open-access bioinformatics tools was utilized to investigate the SanA in *S.* Typhimurium 4/74. The nucleotide and protein sequences of SanA (accession number CP002487.1: 2277943-2278662; protein ID: ADX17941.1) were extracted from the NCBI database in a FASTA format for the analyses. Orthologs of the SanA across various taxonomic groups were identified using the EggNOG tool, enabling the generation of a report on the prevalence of SanA in different taxa (Huerta-Cepas et al., 2019).

To compare the sequence similarity of SanA between *Salmonella* and *Escherichia coli*, BLASTN and BLASTP were employed for nucleotide and protein sequence analysis, respectively. Furthermore, the investigation included an in-depth analysis of subcellular protein localization. For this purpose, several tools such as Phobius, SignalP-5.0, PsortB, THMM 2.0, and TMpred were applied (Krogh et al., 2001; Käll et al., 2007; Yu et al., 2010; Petersen et al., 2011; Finn et al., 2014).

Subsequently, Phyre2 was employed to conduct a comparative analysis of SanA against homologous sequences available in the database (Kelley et al., 2015). Additionally, the Panther classification system was utilized to categorize the protein and predict its function, providing insights into its potential biological roles and activities (Thomas et al., 2003).

Bacterial mutant construction

Salmonella Typhimurium 4/74 with *sanA* gene knockout was generated using the protocol described by Datsenko and Wanner (2000), with slight modifications (Datsenko and Wanner, 2000). Initially, electrocompetent cells of the wild-type (WT) strain were transformed with a Red recombinase-carrying plasmid pKD46. The positive clones were further transformed with a kanamycin cassette flanked by FRT sites, which was obtained via polymerase chain reaction (PCR) using primers sanA_del_for and sanA_del_rev on the pKD4 template, and selected on LB agar plates containing kanamycin at 37°C. The FRT flippase present on the pCP20 plasmid was then utilized to eliminate the kanamycin cassette. Colony PCR using locus-specific primer pairs, sanA_upstream_for, sanA_upstream_rev, and sanA_internal_rev was performed to confirm the correct integration and removal of the marker cassette. To determine whether the newly-created strain differed in growth rate or morphology from the parental isolate, growth curves were determined, and acridine orange staining was used to examine them using a fluorescence microscope. Furthermore, the absence of any unintended mutations was confirmed using Next Generation Sequencing.

TABLE 3 Primers used in this study.

Name	Sequence (5′-3′)	References
sanA_del_for	ATGTTAAAGCGCGTGTTTTACAGCCTGTTGGTCCTGGTAGGCTTGCTGCTGTGTAGGCTGGAGCTGCTTC	Datsenko and Wanner (2000) and this study
sanA_del_rev	TCATTTCCCTTTTTTCTTTTCCAGTTCAAGCAATTGTTCCGGCGTAACTGCATATGAATATCCTCCTTAG	Datsenko and Wanner (2000) and this study
sanA_upstream_for	CGATACAAGGGAAATCATGCTG	This study
sanA_downstream_rev	TTCCAGGCCTCACGGAAG	This study
sanA_internal_rev	GCCCTGGATACGATAACGA	This study
O1646 k1	CAGTCATAGCCGAATAGCCT	Datsenko and Wanner (2000)
O1647 k2	CGGTGCCCTGAATGAACTGC	Datsenko and Wanner (2000)
sanA_XbaIpWSK_for	ACATTCTAGAAGGAGGACAGCTATGTTAAAGCGCGTGTTTTAC	This study
sanA_PstIpWSK_rev	ATCTGCAGTCATTTCCCTTTTTTCTTTTCCAG	This study
pWSK_T7_up	CTTCGCTATTACGCCAGCTG	This study

Cloning of *sanA* into pWSK29 plasmid and mutation complementation

The *sanA* from *S.* Typhimurium 4/74 was amplified using sanA_XbaIpWSK_for, sanA_PstIpWSK_rev primers, and Phusion polymerase (Thermo), according to the manufacturer's protocol. The PCR products were purified using the GeneJET PCR purification kit (Thermo) and the plasmid DNA was isolated using the GeneJET Plasmid Miniprep Kit (Thermo). To insert *sanA* into the pWSK29 plasmid, the gene was cloned into the XbaI/PstI digestion sites using the classical ligation method. DNA sequence of the insert was confirmed using colony PCR via the use of a specific primer pair sanA_internal_rev and pWSK_T7_up, and Sanger sequencing. For complementing the deletion mutant, electrocompetent *S.* Typhimurium 4/74 Δ*sanA* was transformed with a plasmid carrying complementing gene as well as pWSK29 vector plasmid alone (without insert) as a control. All clones were analyzed in positive selection on LB agar with ampicillin.

Growth curve determination

To determine the growth curves of *Salmonella* strains, a single bacterial colony of each isolate was inoculated in LB and incubated overnight at 37°C with shaking (180 rpm). The resulting cultures were diluted to $OD_{600} = 0.05$ using LB and incubated until the early logarithmic growth phase ($OD_{600} = 0.5$, 37°C, 220 rpm). Each culture was then centrifuged, washed, and suspended in 0.9% NaCl solution. The OD_{600} values were measured, and the cultures were diluted in LB to obtain 5×10^6 CFU/mL bacterial suspensions. For determining the antimicrobial effect of vancomycin and bile salts, the assay was performed in LB or MHB medium, respectively with 0%–15% bile salts and 0–500 μg/mL vancomycin. The samples were then applied to a polystyrene or polypropylene 96-well plate in triplicate and incubated in a spectrophotometer (Tecan) at 37°C with measurements taken at 15-min intervals for 16 h, with shaking before each reading. The experiment was performed in at least three independent biological replicates, and dilution series on LB agar were prepared to verify initial bacterial concentrations.

Phenotype microarray analysis

The susceptibility of mutant and the parental strain to 240 chemical compounds was determined in three independent experiments using the Phenotype MicroArray (PM) PM11-PM20 (Biolog), as described in a previous study (Shea et al., 2012). Briefly, strains were grown overnight on Biolog Universal Growth agar with 5% sheep blood at 37°C, colonies were then picked using a sterile cotton swab and suspended in 15 mL of 1× inoculation fluid (IF-0a GN/GP Base, Biolog). The cell density was adjusted to 85% transmittance (T) using a Biolog turbidimeter. The inoculation fluid for PM11-20 was prepared by mixing 100 mL of IF-10a GN Base (1.2X; Biolog), 1.2 mL of Biolog Redox Dye A (100X; Biolog), 0.6 mL of cell suspension at 85% T, and sterile water to reach a final volume of 120 mL. The mixture was then inoculated in the PM plates (100 μL per well) and color development was monitored every 15 min for 48 h at 37°C using an Omnilog reader (Biolog). The kinetic curves of both strains were compared using Omnilog-PM software to identify the phenotypes. Raw data were obtained for 10 plates, which included 240 antibiotics arranged as a dilution series across four wells (960 wells in total). Data were recorded in the RA format and filtered using differences of average height with standard thresholds to identify statistically significant differences using Student's t-test (Guard-Bouldin et al., 2007). The reproducibility of our results was ensured by excluding any differences greater than 50 Omnilog units between biological replicates from the analysis (see Supplementary Table S1).

Antimicrobial susceptibility testing

As the manufacturer of PM plates (Biolog) does not disclose the concentrations of compounds in their plates, on the basis of available

10.3389/fmicb.2023.1340143

literature, we selected 8 different concentrations for all compounds by making two-fold dilutions. Polypropylene and polystyrene plates were utilized for cationic and anionic compounds, respectively. Bacterial strains were incubated in LB for 16 h at 37°C, 180 rpm. Further, the OD_{600} was determined, and bacteria were diluted in MHB to get a total density of 10^6 CFU/mL. The suspensions were aliquoted at 50 µL per well into previously prepared 96-well plates and incubated at 37°C. After 16 h, OD_{600} of each well was measured with using the Tecan microplate reader (Spark®). MHB without xenobiotics serves as a positive control of growth. At least three technical and biological repetitions were performed for each strain. All xenobiotics and tested concentration ranges are listed in Table 4. Antibiotic susceptibility testing results determine the fold change of OD_{600} values between the *ΔsanA* and WT strain at concentrations showing a significant difference. The standard error of mean (SEM) was calculated using the standard deviation of the sample and the square root of the sample size.

TABLE 4 Antimicrobial concentration ranges included in the study.

Compound	Concentration range (µg/mL)	Solvent
5,7-Dichloro-8-hydroxyquinaldine	0.100–27.700	DMSO
Bleomycin	0.025–6.400	Water
Carbenicillin	0.400–102.400	Water
Ceftriaxone	0.002–0.4192	Water
Cetylpyridinium chloride	3.250–832	Water
Chlorhexidine acetate	0.250–64	Ethanol
Norfloxacin	0.010–2	DMSO
Phosphomycin	0.200–39.600	Water
Polymyxin B	0.020–5	Water
Spectinomycin	1.953–500	DMSO:water (1:1)
Streptomycin	0.390–100	Water
Sulfamonomethoxine	1–248	Ethanol
Thioridazine	6.250–1,600	DMSO
Tobramycin	0.084–21.600	Water
Umbelliferone	7.810–2000	Ethanol
Vancomycin	1.953–500	Water

Membrane permeability

The OM permeability was investigated by utilizing the influx of either the cationic Ethidium Bromide (EB) or the neutral Nile Red dye (NR; Murata et al., 2007; Viau et al., 2011). Overnight bacterial cultures were diluted to $OD_{600} = 0.05$ using LB, incubated until early stationary growth phase ($OD_{600} = 2.0$, 37°C, 220 rpm) and rinsed twice with assay buffer (50 mM KH_2PO_4, 137 mM NaCl, pH 7.0). To perform dye uptake assays, the proton motive force inhibitor carbonyl cyanide-m-chlorophenylhydrazone (CCCP) was added at a final concentration of 10 µM. Fluorescence was measured for 30 min at 1-min intervals using a Tecan microplate reader (Spark®) immediately upon mixing cells (final $OD_{600} = 0.2$) with EB at a final concentration of 6 µM (with excitation at 545 nm and emission at 600 nm) or NR at a final concentration of 2 µM (with excitation at 540 nm and emission at 630 nm). Membrane permeability was measured in at least three independent experiments. According to Murata et al., the dye uptake rates of different strains varied between experiments, but the pattern of dye uptake remained consistent across repetitions (Murata et al., 2007).

Hexadecane adhesion assay

Bacterial surface hydrophobicity was determined using the hexadecane adhesion assay (Oguri et al., 2016). Overnight bacterial cultures were diluted to $OD_{600} = 0.05$ using LB and incubated until early stationary growth phase ($OD_{600} = 2.0$, 37°C, 220 rpm). Subsequently, the cultures were harvested, washed twice with phosphate buffered saline (PBS), and resuspended in 1 mL of PBS. Following this, 100 µL of cells were diluted 10× in PBS and the OD_{600} was measured (C_0). Next, 900 µL of the cell suspension was mixed with 200 µL of hexadecane (Merck Millipore), vortexed for 1 min, and left undisturbed at room temperature until the phases separated. Cell samples (100 µL) from the lower, aqueous phase were then diluted in 900 µL PBS and OD_{600} was measured (C_H). The percentage of hexadecane adherence was determined in three independent experiments, using the following formula: % hexadecane adherence $= [(C_0 - C_H)/C_0] \times 100$.

Cytochrome c binding assay

The cytochrome c binding assay was performed as described previously, with minor modifications (Kristian et al., 2005). Briefly, overnight bacterial cultures were diluted to $OD_{600} = 0.05$ using LB and incubated until early stationary growth phase ($OD_{600} = 2.0$, 37°C, 220 rpm). Bacteria were then collected, washed twice in 3-(N-morpholino)propanesulfonic acid (MOPS) buffer (20 mM, pH 7.4), and adjusted to a final $OD_{600} = 7.0$ in the same buffer. Next, bacteria were mixed with cytochrome c (Merck Millipore) to a final concentration of 0.5 mg/mL, incubated for 10 min at room temperature, and centrifuged at 18,000 × g for 6 min. Cytochrome c without bacteria in the same buffer was also incubated as a negative control. The cytochrome c contents in the supernatants were measured at the absorption maximum of the prosthetic group (530 nm). The percentage of bound cytochrome c was calculated from three independent experiments, each performed in triplicate.

Bone marrow-derived macrophages derivation and culture

The isolation of primary bone marrow-derived macrophages (pBMDMs) was performed in accordance with a UK Home Office Project License in a Home Office designated facility, as previously described (Thurston et al., 2016; Bailey et al., 2020). Briefly, bone marrow was obtained from 6 to 8 week-old female C57BL/6 mice (Charles River) by flushing the tibias and femurs. The collected cells were then added to non-tissue culture-treated petri plates at a concentration of 3×10^6 cells per plate in 8 mL Dulbecco's modified Eagle's medium (DMEM) with high glucose supplemented with 20% (v/v) L929-MCSF supernatant, 10% (v/v) fetal bovine serum (FBS),

10 mM HEPES, 1 mM sodium pyruvate, 0.05 mM β-mercaptoethanol, and 100 U/mL penicillin/streptomycin. After 3–4 days, 10 mL fresh medium was supplemented and the differentiated BMDMs were harvested on day 7. The macrophages were then seeded into 24-well tissue culture-treated plates at a concentration of 2×10^5 macrophages per well and infected the following day with DMEM media supplemented with the above concentrations of FBS, HEPES, sodium pyruvate, and β-mercaptoethanol but without antibiotics.

Infection assay

The macrophage monolayer was infected with stationary phase bacteria opsonized in mouse serum for 20 min at room temperature at a multiplicity of infection of 10:1. To synchronize the infection, the culture plates were centrifuged for 5 min at 165 × g, followed by a 30-min incubation at 37°C (5% CO_2). Fresh DMEM supplemented with 100 μg/mL gentamicin (Gm) was added to kill extracellular bacteria, and the macrophage monolayers were incubated with added Gm for 90 min (Monack et al., 1996). After washing with DMEM, the monolayers were lysed in 1% Triton X-100 and diluted with PBS. Dilutions of the suspension were then plated on LB agar to quantify the number of viable bacteria. To evaluate intracellular growth, the medium containing 100 μg/mL Gm was replaced with DMEM supplemented with 10 μg/mL Gm, and parallel cell cultures were examined for viable bacteria 24 h following infection (Monack et al., 1996).

Statistical analyses

Statistical analyses were performed using GraphPad Prism (GraphPad Software, Inc., La Jolla, CA, United States). The Shapiro–Wilk normality test was used to determine data distribution. Depending on the data distribution, either Student's *t*-test, two-way ANOVA analysis of variance with Tukey's correction, or the Kruskal–Wallis test with Dunn's multiple comparison post-hoc test was used. For each condition, data were collected from at least three independent experiments. $p \leq 0.05$ was considered statistically significant. The results were presented as mean ± SEM. The symbols $^*p < 0.05$; $^{**}p < 0.01$; $^{***}p < 0.001$; and $^{****}p < 0.0001$ were used to indicate significance levels.

Results

Insights into SanA protein: analysis using bioinformatic tools

According to our analysis of the eggNOG database, we found that the *sanA* is present across a diverse range of bacterial taxa. Specifically, the gene was identified in both, gram-negative and gram-positive bacteria with a prevalence of 44.1% in species classified under *Gammaproteobacteria*, 17.2% of *Bacteroidetes*, 18.9% of *Actinobacteridae*, 5.72% of *Clostridia*, and 3.37% of *Spirochaetia*. Additionally, all SanA homologs have an unknown domain, DUF218. We performed a BLAST comparison and found that SanA in *E. coli* and *Salmonella* share 94% identity, with an estimated 97% amino acids having identical or similar chemical properties, suggesting its high conservative among bacteria.

The predictions for the subcellular localization were inconsistent: Phobius suggested a location outside the cytoplasm, SignalIP-5.0 detected no signal peptide implying a cytoplasmic protein, PsortB indicated a cytoplasmic position, while both THMM 2.0 and TMpred identified a transmembrane domain. Since proteins with similar structures can have similar functions, we elucidated the potential function of SanA by predicting its structure using Phyre2 and comparing it to homologous sequences. Our findings suggested that SanA shares structural similarities with the YdcF protein of *E. coli*, which is involved in binding S-adenosyl-L-methionine; transferases (5-methyltetrahydrofolate homocysteine s-methyltransferase); OmpA like protein; peptide binding protein; membrane protein, and structural protein. Moreover, the Panther classification system revealed that SanA is an IM protein with potential permease activity and is classified into the transporters group.

Impact of *sanA* knockout on resistance profile toward vancomycin and bile salts

As SanA is known as a vancomycin exclusion protein, the first stage of our investigation incorporated analysis of the WT and Δ*sanA* mutant bacteria growth in the presence of vancomycin or bile salts. Surprisingly, the mutant strain showed higher resistance to vancomycin than the WT (Figure 1A). While the WT grew only up to 125 μg/mL vancomycin, *sanA* deletion allowed the strain to grow up to a concentration of 250 μg/mL vancomycin. Moreover, a significant difference in the optical density between the two strains was observed in the presence of 62.5 and 125 μg/mL vancomycin, and the highest contrast was visible in the stationary growth phase—after 10 h (Figure 1A). Additionally, the two strains displayed contrasting growth patterns in the presence of bile salts. The deletion mutant strain demonstrated decreased resistance with growth up to only 3.75% bile salts compared to the WT, which grew up to 7.5% bile salts. Significant growth variations were also noted between the two strains at bile salt concentrations of 0.47%–1.88% (Figure 1B). The phenotypic parallels observed between the strain complemented with *sanA* and the one transformed with the empty pWSK29 plasmid further underscore the function of SanA in these resistance profiles (Supplementary Figure S2).

High-throughput analysis of xenobiotic resistance phenotype

WT and Δ*sanA* were further characterized using Biolog (Biolog®) phenotypic arrays to investigate potential gene knockout-induced changes in resistance profiles. The arrays featured various compounds with some known antimicrobials included on plates PM11a to PM20. Prior to testing, no significant differences in growth kinetics were observed among the strains (Supplementary Figure S1).

Our results revealed distinct resistance patterns for more than 20% (49/240) of the analyzed compounds with different mechanisms of action ($p < 0.05$; Table 5). The Δ*sanA* strain exhibited improved growth in the presence of approximately 35% (17/49) of these 49 agents, grouped mostly as cell wall-and DNA-associated antibiotics.

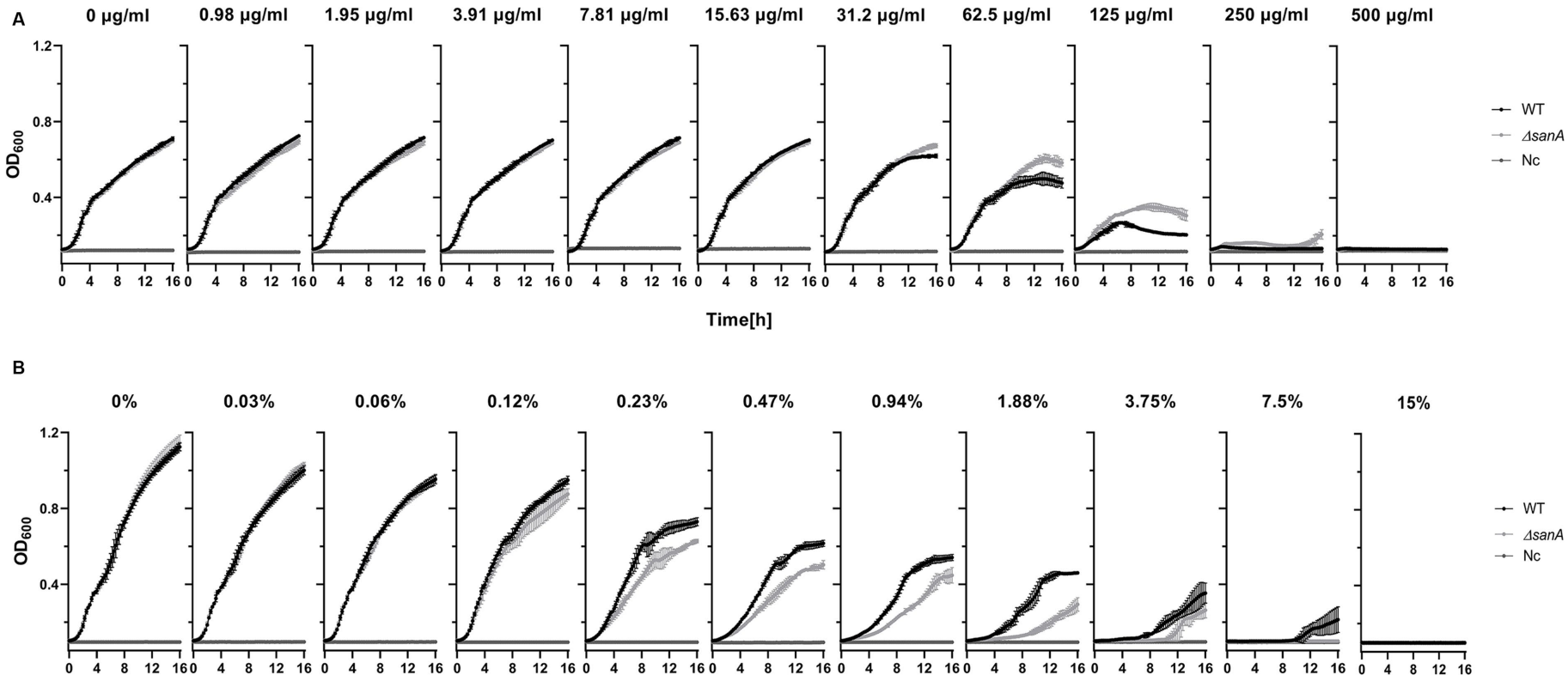

FIGURE 1
Growth curve of *Salmonella* Typhimurium 4/74 and its deletion mutant *ΔsanA* strains in the presence of: **(A)** vancomycin in the concentration range between 0 and 500 µg/mL, **(B)** bile salts in the concentration range between 0% and 15%. The data comprises of median values and median absolute deviation (MAD) of at least three separate experiments in triplicate. Nc represents a negative control: medium containing xenobiotics but lacking bacteria.

10.3389/fmicb.2023.1340143

10.3389/fmicb.2023.1340143

TABLE 5 Schematic representation of statistically significant data obtained from PM (from PM11a to PM20) analyses.

Compound	Difference	Mode of action
PHENOTYPE LOST (lower optical density after sanA knockout) BY Salmonella Typhimurium ΔsanA RELATIVE TO S. Typhimurium WT		
Umbelliferone	**−67.59**	**DNA intercalator**
Thioridazine	**−63.98**	**Membrane, phenothiazine, efflux pump inhibitor, anti-psychotic**
Cetylpyridinium chloride	**−62.62**	**Membrane, detergent, cationic**
Norfloxacin	**−58.49**	**DNA topoisomerase, fluoroquinolone**
DL-Serine hydroxamate	−51.68	tRNA synthetase
Pentachlorophenol	−51.56	Respiration, ionophore, H+
Chlorhexidine diacetate	**−51.28**	**Membrane, electron transport**
5,7-Dichloro-8-hydroxyquinaldine	**−51.18**	**RNA synthesis inhibitor, interference with transcription**
Sulfamonomethoxine	**−50.87**	**Folate antagonist, sulfonamide**
Ethionamide	−50.21	Anti-tuberculosic
Bleomycin	**−43.09**	**Inhibition DNA replication, oxidation, glycopeptide**
Sulfamethazine	−42.3	Folate antagonist, PABA analog, sulfonamide
Fusaric acid	−40.02	chelator, lipophilic
Trifluorothymidine	−35.2	Nucleic acid analog, pyrimidine, DNA synthesis
Sulfadiazine	−34.56	Folate antagonist, PABA analog, sulfonamide
Sulfisoxazole	−33.73	Folate antagonist, PABA analog, sulfonamide
1-Hydroxypyridine-2-thione (pyrithione)	−32.27	Biofilm inhibitor, chelator, anti-fungal
Sorbic acid	−31.04	Respiration, ionophore, H+, preservative
Sulfanilamide	−30.64	Folate antagonist, PABA analog, sulfonamide
Nitrofurantoin	−29.41	Nitro compound, oxidizing agent, DNA damage
Vancomycin	**−29.24**	**Wall, glycopeptide**
Tetraethylthiuram disulfide	−26.81	Nucleic acid inhibitor, purine
trans-Cinnamic acid	−26.7	Respiration, ionophore, H+
Sulfachloropyridazine	−23.02	Folate antagonist, PABA analog, sulfonamide
Phosphomycin	**−22.85**	**Wall, phosphonic**
5-Fluorouracil	−21.73	Nucleic acid analog, pyrimidine
5-Azacytidine	−21.54	DNA methylation, methyltransferase inhibitor
Polymyxin B	**−20.89**	**Membrane, cyclic peptide, polymyxin**
Ruthenium red	−19.28	Respiration, mitochondrial Ca++ porter
Penimepicycline	−15.34	Protein synthesis, 30S ribosomal subunit, tetracycline
Diamide	−11.06	Oxidizes sulfhydryls, depletes glutathione
Captan	−3.28	Fungicide, carbamate
PHENOTYPE GAINED (higher optical density after sanA knockout) BY S. Typhimurium ΔsanA RELATIVE TO S. Typhimurium WT		
Menadione, sodium bisulfite	4.87	Respiration, uncoupler
Spectinomycin	**10.16**	**Protein synthesis, 30S ribosomal subunit, aminoglycoside**
Poly-L-lysine	10.67	Membrane, detergent, cationic
2-Phenylphenol	13.67	DNA intercalator, preservative
Streptomycin	**15.65**	**Protein synthesis, 30S ribosomal subunit, aminoglycoside**
Cytosine-1-beta-D-arabinofuranoside	17.12	Nucleic acid analog, pyrimidine
Chromium (III) chloride	19.38	Toxic cation
Hydroxylamine	20.87	DNA damage, mutagen, antifolate (inhibits thymine and methionine synthesis)
3,5-Diamino-1,2,4-triazole (Guanazole)	22.31	Ribonucleotide DP reductase inhibitor, aromatic amine
Thiosalicylate	22.44	Biofilm inhibitor, anti-capsule agent, chelator, prostaglandin syntetase inhibitor

(Continued)

TABLE 5 (Continued)

Compound	Difference	Mode of action
Phenyl-methylsulfonyl-fluoride (PMSF)	24.9	Protease inhibitor, serine
Chelerythrine chloride	26.82	Protein kinase C inhibitor
Myricetin	28.82	DNA & RNA synthesis, polymerase inhibitor
Cesium chloride	29.38	Toxic cation
Ceftriaxone	**31.69**	**Wall, cephalosporin**
Tobramycin	**35.91**	**Protein synthesis, 30S ribosomal subunit, aminoglycoside**
Carbenicillin	**57.92**	**Wall, lactam**

Data from Omnilog were recorded in the RA format and filtered using differences of average height values between *S.* Typhimurium 4/74 WT and *ΔsanA* to identify statistically significant differences. Phenotype lost indicates lower optical density after *sanA* knockout (negative values in the Table), and gained—higher optical density as a result of mutation (positive values in the Table). The bold text indicates agents which were chosen for further analysis with the use of microbroth dilution assay.

The same strain demonstrated lower resistance to folate antagonists (sulfonamides), membrane-targeting antibiotics, and DNA and protein-associated antibiotics (fluoroquinolones, glycopeptides, nucleic acid analogs; Table 5).

Considering the known adjustments of the PM plates method with MIC measurements, we cross-checked PM results using a microbroth dilution assay. We focused on 16 compounds with the most significant differences between strains, particularly those targeting the membrane and cell wall (Table 5). The results, showing fold changes at OD_{600} between the *ΔsanA* and WT at specific concentrations (Supplementary Figure S3), led to further investigation using complemented strains (Figure 2B).

In the presence of 16 different agents, the *ΔsanA* strain exhibited reduced resistance to ten xenobiotics but displayed increased resistance to six others (Figure 2A). We grouped these agents into the following five categories: (1) membrane, (2) protein synthesis, (3) cell wall and efflux pumps, (4) replication, and (5) transcription (Figure 2A). The *sanA* knockout resulted in compromised growth with certain membrane-associated xenobiotics such as chlorhexidine acetate (2 μg/mL; $p = 0.0003$), cetylpyridinium chloride (6.5 μg/mL; $p = 0.0093$), umbelliferone (500 μg/mL; $p = 0.0465$), and polymyxin B (0.625 μg/mL; $p = 0.0205$). Notably, reintroducing *sanA* restored the resistance pattern on these agents to resemble WT bacteria (Figure 2B).

The *ΔsanA* exhibited lower resistance to agents targeting protein synthesis, such as tobramycin (0.675 μg/mL; $p = 0.0070$), streptomycin (100 μg/mL; $p = 0.0152$), and spectinomycin (31.250 μg/mL; $p = 0.0359$), as well as those targeting transcription, such as norfloxacin (0.010 μg/mL; $p = 0.0052$) and 5,7-dichloro-8-hydroxyquinaldine (3.5 μg/mL; $p = 0.0065$; Figure 2A). Notably, the *ΔsanA* strain showed a different resistance pattern to protein synthesis agents than that suggested by PM. However, when the mutation was complemented, the resistance pattern was mostly attributed to the *sanA* deletion, except for tobramycin (0.675 μg/mL; $p = 0.9998$; Figure 2B).

As anticipated, *sanA* deletion resulted in greater resistance to cell wall and efflux pumps associated compounds, like ceftriaxone (0.002 μg/mL; $p = 0.016$), vancomycin (125 μg/mL; $p = 0.0044$), carbenicillin (3.200 μg/mL; $p = 0.0281$), and thioridazine (1,600 μg/mL; $p = 0.027$). Surprisingly, this strain showed reduced resistance to phosphomycin (9.900 μg/mL; $p = 0.0483$; Figure 2A). Complementation mostly restored WT phenotypes, with the exception of thioridazine (1,600 μg/mL; $p = 0.2196$). In contrast to the PM data, *ΔsanA* demonstrated reduced susceptibility to replication agents, such as bleomycin (0.400 μg/mL; $p = 0.0104$) and sulfamonomethoxine (248 μg/mL; $p = 0.0432$). This phenotype was further validated by complementing *sanA*, highlighting its critical role in this phenotype (Figure 2B).

SanA is responsible for membrane integrity

The impact of *sanA* on resistance to vancomycin along with other antimicrobial agents suggests a general effect on membrane integrity rather than specific vancomycin sensitivity. Thus, OM permeability was determined by measuring influx of the cationic dye, EB or the neutral dye, NR. Dye uptake assays were performed in the presence of CCCP, which enables the inward transport of H^+ across lipid membranes. Therefore, it prevents the efflux of compound by active pumps, so that only passive permeability is measured. In the experiment without CCCP, a minimal increase in dye uptake was noted, suggesting that the increased retention of EtBr in the *ΔsanA* is not due to pump inactivation, but increased membrane permeability (Supplementary Figure S4).

When CCCP was present, the *ΔsanA* bacteria demonstrated a notably higher OM permeability baseline than the WT for both EB and NR, with a remarkably increased rate of dye uptake observed particularly after approximately 10 min of assay initiation (Figure 3; Supplementary Figure S5). Importantly, complementation of the mutation restored the WT phenotype for NR and further reduced the permeability for EB, strongly suggesting that the observed phenotype was primarily due to *sanA* deletion. Moreover, the permeabilities differed between WT and *ΔsanA*, as well as between *ΔsanA*-pWSK29 and its complemented *ΔsanA*-pWSK29-*sanA* counterpart, consistently throughout the assay (Figure 3).

SanA knockout decreases hydrophobicity and negative charge of the bacterial membrane

Considering the distinct resistance phenotype observed for different groups of xenobiotics, we hypothesized that the surface charges and hydrophobicity of bacterial cells could be contributing factors. To investigate potential alterations in the surface properties of the *ΔsanA*, we performed the following two assays: (1) determining

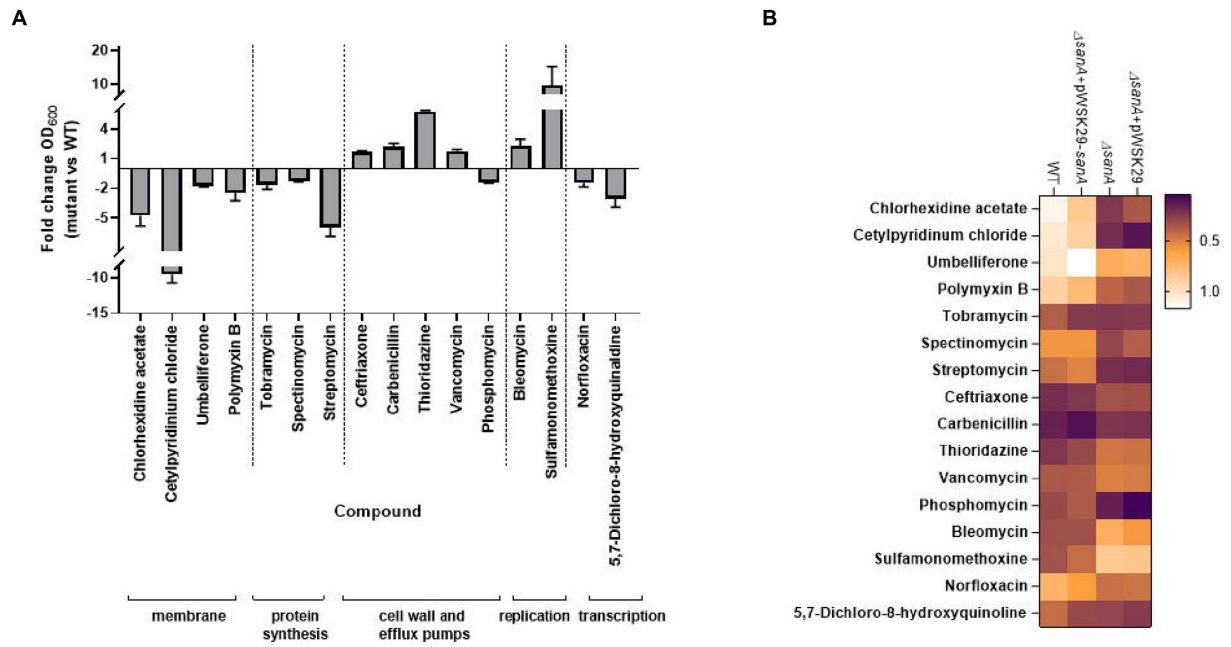

FIGURE 2
Antibiotic susceptibility testing represented by **(A)** bar chart with fold change OD_{600} of *Salmonella* Typhimurium 4/74 deletion mutant *ΔsanA* and WT after 16 h incubation in MHB medium with the presence of indicated agents. Data shown are means and SEM for at least three independent experiments **(B)** heatmap of OD_{600} of *S.* Typhimurium 4/74, its deletion mutant *ΔsanA* and *ΔsanA* transformed with empty pWSK29 plasmid or vector with *sanA* after 16 h incubation in MHB medium with the presence of indicated agents. Brown represents low relative growth in a given condition while white represents high growth.

surface charges by evaluating the binding of the cationic protein cytochrome c to bacterial cells, and (2) determining surface hydrophobicity by measuring the adherence of cells to the hydrophobic solvent hexadecane.

The *ΔsanA* cells displayed significantly lower affinity to cytochrome c (80%) than that of WT cells (90%; $p = 0.0046$; Figure 4A). Additionally, approximately 10% of *ΔsanA* cells adhered to hexadecane, in contrast to approximately 16% of WT cells ($p = 0.0256$; Figure 4B). This suggests a decrease in the negative charge and hydrophobicity on the cell surface of *ΔsanA* mutant, respectively. Moreover, all these changes were attributed entirely to *sanA*, as introduction of *sanA* to the deletion mutant restored the WT phenotype ($p = 0.0199$; $p = 0.005$).

SanA influences the replication of *Salmonella* Typhimurium within primary bone marrow macrophages

Alterations in bacterial membranes significantly influence antimicrobial efficacy and bacterial replication within phagocytes (Ernst et al., 1999). To further investigate this, we monitored *Salmonella* replication in primary BMDMs, which provide a relevant physiological context to examine the interactions between *Salmonella* and host cells. Our results showed that the uptake of *S.* Typhimurium by BMDMs was similar for the WT and *ΔsanA* ($p = 0.0572$; Figure 5A), but the mutant exhibited a significantly increased number of intracellular bacteria 24 h post-infection ($p = 0.0051$; Figure 5B). Furthermore, we observed a marked difference between *ΔsanA* + pWSK29 and *ΔsanA* + pWSK29-*sanA*, whereby expression of *sanA* reduced replication ($p = 0.0351$; Figure 5B).

Discussion

Multidrug resistance among bacteria, including prominent species such as *Salmonella*, *Pseudomonas*, and *Campylobacter*, constitutes a major public health concern (Centers for Disease Control and Prevention, 2019). These bacteria utilize diverse mechanisms, including the creation of enzymatic barriers and altering membrane compositions, to mitigate the impact of surface disinfection or antibiotic therapies (Reygaert, 2018). Gram-negative bacteria exhibit a complex cellular envelope with the OM forming an extra line of defense. Its permeability properties have significant implications for the bacterium's sensitivity to antibiotics (Silhavy et al., 2010). Moreover, although less studied, the IM proteins play a crucial role in coordinating processes pivotal for bacterial survival and resistance to extreme environmental conditions. Mutations in the genes encoding these proteins could increase membrane permeability, thereby promoting antibiotic resistance (Ize et al., 2003; Boughner and Doerrler, 2012).

Our study emphasizes on a lesser-known protein, SanA, and examines its role in altering the physicochemical properties of bacterial membranes, which consequently affect the bacterium's resistance phenotype.

SanA is composed of 239 amino acids and is predicted to primarily localize in the inner membrane, featuring a small N-terminal cytoplasmic domain spanning just six amino acids. It possesses a

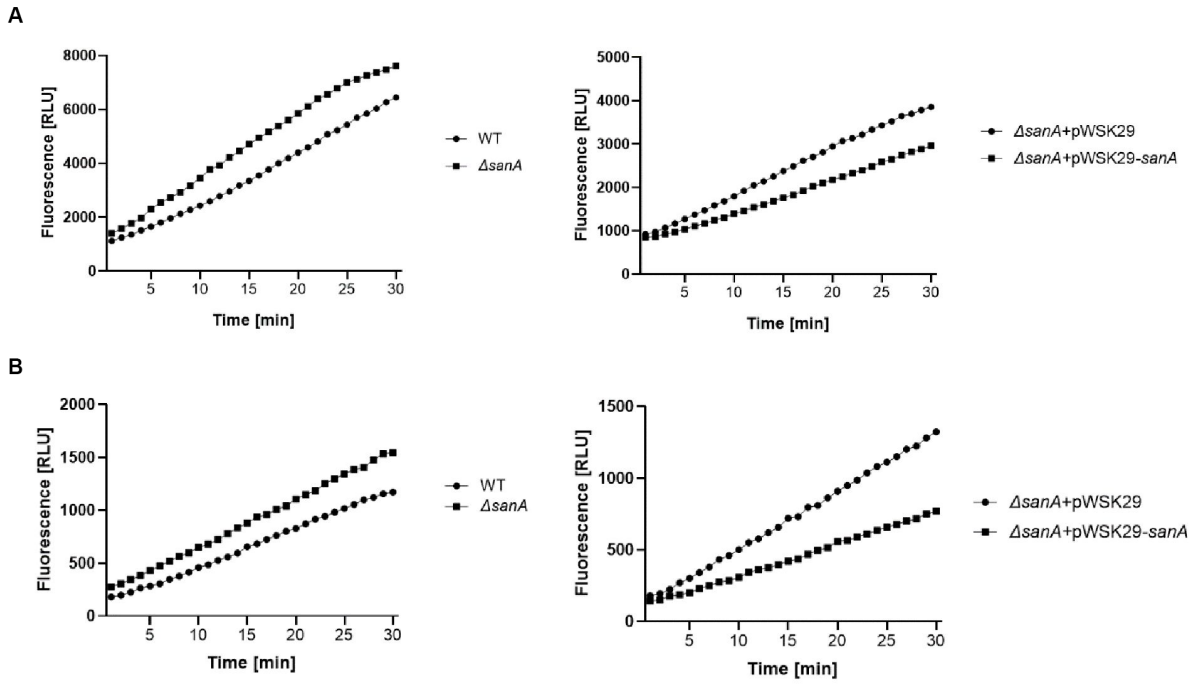

FIGURE 3
Outer membrane permeability of *Salmonella* Typhimurium 4/74, its deletion mutant *ΔsanA* and *ΔsanA* transformed with empty pWSK29 plasmid or vector with *sanA* **(A)** cationic dye Ethidium Bromide or **(B)** neutral dye Nile Red. The assay was conducted in the presence of CCCP to prevent the efflux of compound by active pump to measure only passive permeability. Data shown are representative of at least three independent experiments with similar results.

single transmembrane helix, with the remainder of the protein predominantly situated in the periplasmic space (Krogh et al., 2001; Petersen et al., 2011). Within the periplasmic part, SanA harbors a DUF218 domain designated as a domain of the unknown function (Finn et al., 2014). DUF218 domains contain multiple charged amino acids, implying potential enzymatic activity, and are prevalent across various bacterial species. These domains are primarily associated with proteins whose functions remain elusive (Mitchell et al., 2017). SanA was initially discovered as a multicopy suppressor in response to unknown mutations that affected the OM permeability. This included not only the deletion of the *sanA* gene but also other mutations that were associated with impairments in the OM (Rida et al., 1996). Moreover, in a study on *sanA* ortholog (97% identity of nucleotide sequence), the *S.* Typhimurium *sfiX-strain* failed to grow in the presence of vancomycin in high temperature (Mouslim et al., 1998).

Thus, we initially aimed to determine how *sanA* deletion affects the growth of *S.* Typhimurium 4/74 in the presence of vancomycin and bile salts, a key substrate of McConkey medium at 37°C, what corresponds to the host's physiological temperature. Apparently, our findings aligned with previous outcome, indicating that a *Salmonella* strain carrying a 10-nucleotide deletion in *sanA* displays enhanced vancomycin resistance than that with wild-type *sanA* at the same temperature (Kolenda et al., 2021). It is crucial to highlight that the variance in these findings compared to Rida et al.'s study may arise from various factors, including the higher temperature utilized in their assay and the use of a less well-characterized mutant with additional to *sanA* mutations (Rida et al., 1996). Additionally, it might stem from methodological distinctions, particularly the choice of plate material. The polypropylene plates with a neutral surface aimed to minimize non-specific binding—a critical aspect frequently overlooked in the realm of antibiotic resistance research, to ensure precise measurement of vancomycin activity (Singhal et al., 2018). Furthermore, our demonstration of detectable differences in the stationary growth phase allows us to suggest that SanA expression may occur in stress conditions, such as the late growth phase or elevated temperatures employed in prior studies.

In contrast, we observed an inverse effect with anionic bile salts, wherein the WT demonstrated higher resistance. This observation aligns with that of Langridge et al. (2009) who found that an *S.* Typhimurium *sanA* mutant exhibits increased bile sensitivity (Langridge et al., 2009). It suggests a distinct role of SanA on various chemical compounds, implying that the protein affects barrier function by altering properties of the envelope, rather than the antibiotic's mechanism of action, sequestration, modification, or target blocking (Langridge et al., 2009). Thus, we further explored this phenomenon using the PM, which analyzed the growth of strains in the presence of 240 different agents, simultaneously. The obtained data were then validated using the microbroth dilution assay, since the Biolog phenotype microarray is a screening method and results are not as accurate as using the classical approach (Dunkley et al., 2019). Moreover, the Biolog PM assay indirectly measures bacterial growth through colorimetric signals, which may not directly correlate with the bacterial growth inhibition caused by antibiotics (Dunkley et al., 2019). Our analysis highlighted a decreased resistance trend in the *ΔsanA* to phosphomycin, detergents, and polymyxin B. Additionally, the same strain showed lower resistance to protein synthesis-targeting

10.3389/fmicb.2023.1340143

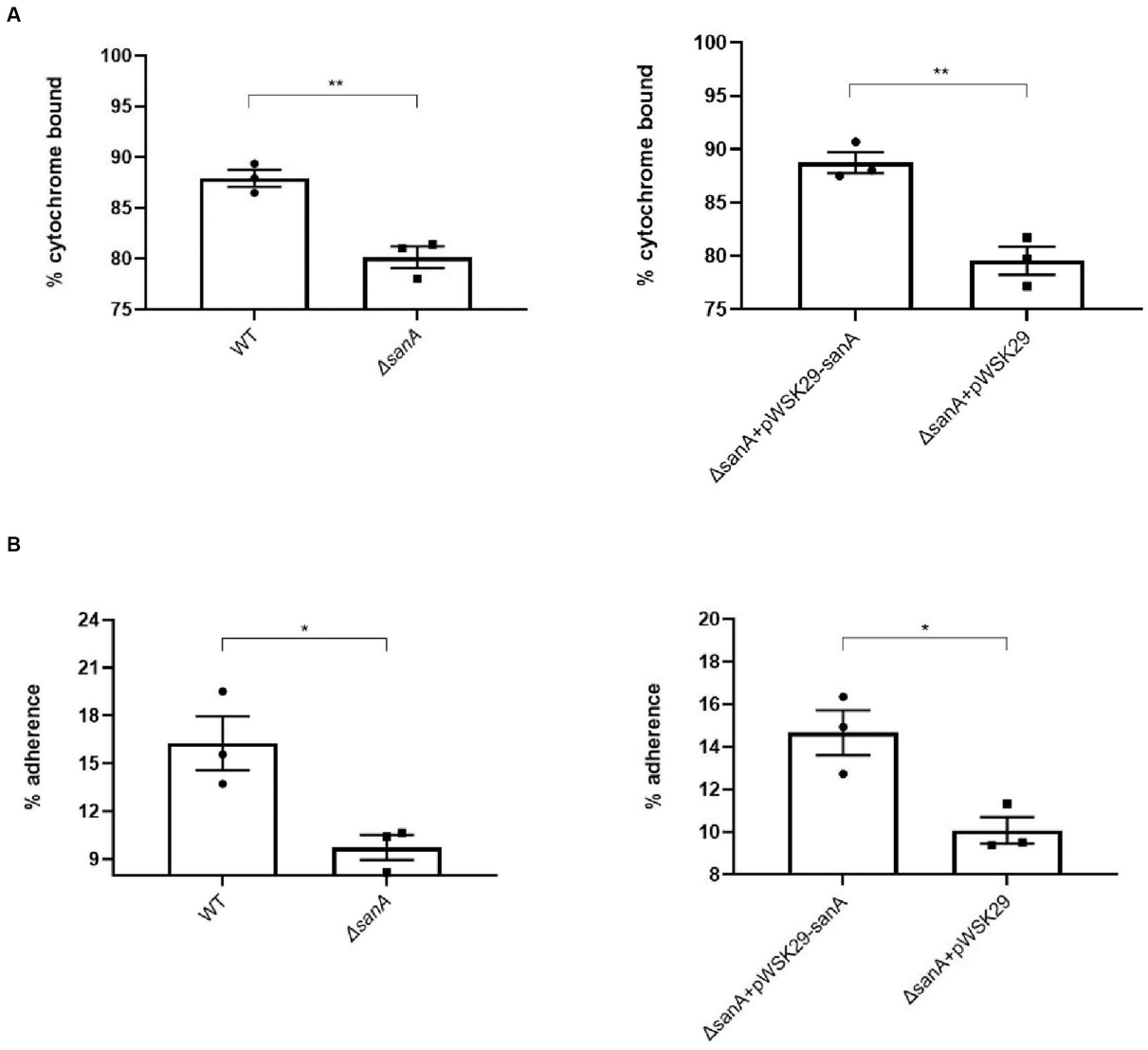

FIGURE 4
Physicochemical properties of the cell surfaces of *Salmonella* Typhimurium 4/74, its deletion mutant *ΔsanA*, and *ΔsanA* transformed with empty pWSK29 plasmid or vector with *sanA* **(A)** Surface charges were examined by a cytochrome c binding assay. **(B)** Hydrophobicities of cell surfaces were examined by a hexadecane adhesion assay. Data shown are means and SEM for at least three independent experiments. Statistical significance was determined by Student's *t* test (*$p < 0.05$; **$p < 0.01$).

antibiotics, such as aminoglycosides and aminocyclitoles, as well as to transcription-related compounds such as fluoroquinolones and quinolines. Conversely, enhanced resistance was noted toward cell wall synthesis and efflux pumps-associated xenobiotics as well as DNA targeting agents, such as glycopeptides and sulfonamides.

Previously published data did not determine the role of *sanA* unequivocally, but has suggested its role in peptidoglycan synthesis (Mouslim et al., 1998). The location of the C-terminus, containing DUF218 domain with charged amino acids in the periplasm, which is the site of the cell wall synthesis, may indicate that it plays a role in blocking the activity of vancomycin at its site of action (Mitchell et al., 2017). In contrast, the hydrophobic nature of the SanA protein, suggests that it participates in the barrier functions of bacterial cell envelopes, affecting the synthesis of murein, which is essential for cell wall function and maintenance. This role was indicated by the dual effect of the *sanA* mutation—induction of vancomycin sensitivity and suppression of cell division inhibition (Rida et al., 1996; Mouslim et al., 1998). Our data revealed that *sanA* deletion resulted in higher resistance to vancomycin as well as different classes of antibiotics associated with the cell wall synthesis—ceftriaxone and carbenicillin. In contrast, the same strain revealed higher susceptibility to phosphomycin, another murein synthesis-targeting antibiotic. Since all these agents hinder bacterial growth by inhibiting peptidoglycan synthesis, each of them targets another stage of this process. Carbenicillin, and ceftriaxone are beta-lactam antibiotics, which function by mimicking the D-alanyl-D-alanine structure and binding to Penicillin-binding proteins; this prevents them from cross-linking the peptidoglycan layers and causing cell death in the final, extracytoplasmic stage of peptidoglycan synthesis (Lima et al., 2020). Unlike beta-lactam antibiotics, vancomycin affects the second stage of creating bacterial cell membranes, by targeting the

10.3389/fmicb.2023.1340143

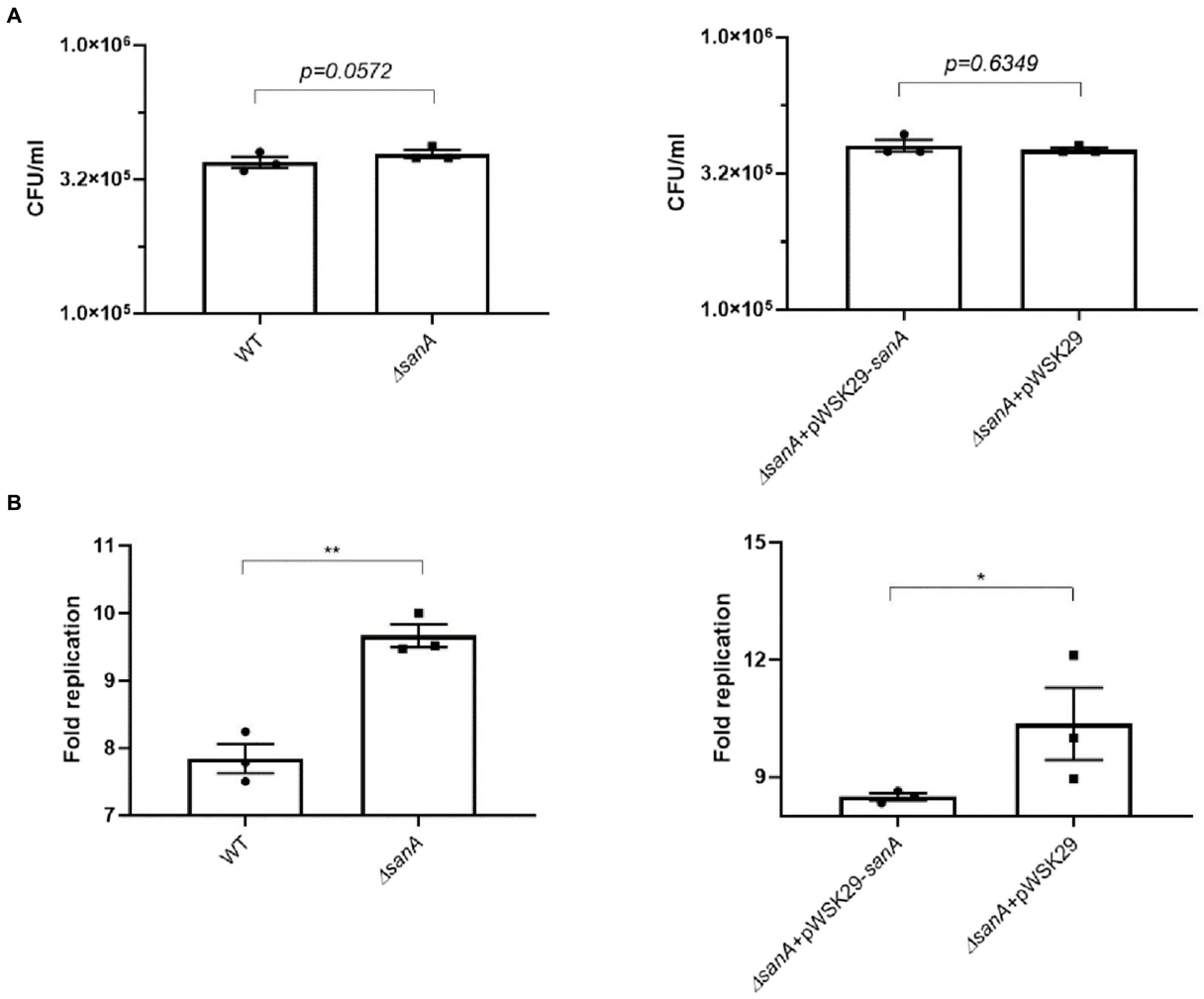

FIGURE 5
Salmonella infection of primary bone marrow macrophages (pBMDM). **(A)** invasion level of BMDM, **(B)** intracellular replication within BMDM isolated from C57BL/6 mice of *S. Typhimurium* 4/74, its deletion mutant *ΔsanA* and *ΔsanA* transformed with empty pWSK29 plasmid or vector with *sanA*. The fold replication was determined by comparing the bacterial population within macrophages after a 24 h incubation period to that after a 2 h initial incubation. The data are shown as mean values and SEM of three separate experiments of intracellular replication. Statistical differences were analyzed by Student's *t* test (*$p < 0.05$; **$p < 0.01$).

d-Ala-d-Ala terminus of peptidoglycan. In turn, phosphomycin has a unique mechanism of action. It inhibits the first step in peptidoglycan synthesis by targeting the enzyme MurA (UDP-N-acetylglucosamine enolpyruvyl transferase). This enzyme catalyzes the conversion of UDP-N-acetylglucosamine to UDP-N-acetylmuramic acid, the first committed step in peptidoglycan synthesis. By inhibiting this enzyme, phosphomycin disrupts the production of peptidoglycan precursors, repressing early cell wall synthesis (Falagas et al., 2016). Thus, the role of SanA in peptidoglycan synthesis, and hence in antibiotic resistance, may be more complex than expected. Based on our *in silico* predictions and considering SanA's putative role as a permease, its function might be similar to that of AmpG, an IM permease responsible for transporting anhydromuropeptides into the bacterial cytoplasm, contributing to peptidoglycan recycling (Jacobs et al., 1994). This would explain why the deletion of *sanA* does not confer resistance to all antibiotics targeting peptidoglycan synthesis, as demonstrated by reduced resistance to phosphomycin. It is worth noting however that the Panther database's classification of SanA as a potential permease may not align with biological reality, given that SanA has only one transmembrane helix (Thomas et al., 2003). The same database assigns a similar classification to YdcF, a cytoplasmic protein containing a DUF218 domain (Thomas et al., 2003).

Any changes in peptidoglycan synthesis can alter the bacterial envelope structure and composition, leading to modified interactions with xenobiotics (Nikolaidis et al., 2014; Yadav et al., 2018). Since peptidoglycan is critical for maintaining the shape and structural integrity of the cell wall, interference at any stage of its synthesis, assembly, or recycling can effectively inhibit cell growth (Typas et al., 2012). It correlates with previously published data demonstrating the role of *sanA* in the cell division of a defective mutant (Mouslim et al., 1998). Additionally, changes to the murein synthesis pathway could impact the overall cell wall structure and stability, bacterial membrane permeability, or transport mechanisms, which could impact the uptake or efflux of antibiotics. The stability of the OM is maintained through tethering of the OM to the sacculus, a process that is

facilitated by both covalent and non-covalent interactions between abundant OM proteins (such as Lpp, Pal, and OmpA) and peptidoglycan (Hantke and Braun, 1973; Parsons et al., 2006). Complex resistance effect, based on increased susceptibility to membrane-bound antibiotics–chlorhexidine acetate, cetylpyridinum chloride, umbelliferone, and polymyxin B confirmed this occurrence, suggesting a correlation between the IM protein, SanA, and OM, responsible for maintaining integrity of the envelope. This situation is reminiscent to that of TolA, wherein a defect in *tolA* leads to detergent sensitivities. This protein, being anchored in the IM by its hydrophobic amino-terminal 21-residue segment similar to SanA, presumably interacts through its carboxyl-terminal domain with components on the inner surface of the OM for maintaining its integrity (Levengood et al., 1991; Levengood-Freyermuth et al., 1993). Our data indicating significantly higher OM permeability of the *sanA* mutant corroborates this hypothesis.

Furthermore, the phenotype of *sanA* mutant correlates with an increased sensitivity for aminoglycosides—streptomycin, tobramycin, and aminocyclitole—spectinomycin, having the same target of action. Aminoglycoside resistance typically involves diminished uptake or decreased cellular permeability, modifications at the ribosomal binding sites, or the generation of aminoglycoside modifying enzymes (Garneau-Tsodikova and Labby, 2016). Thus, enhanced membrane permeability due to *sanA* knockout was the primary reason for the observed shifts in the resistance phenotype. Notably, we observed a reverse phenotype for all the agents tested, except tobramycin, further supporting that the resistance phenotype is more complex than initially assumed. Similarly, we demonstrated decreased resistance of the *ΔsanA* to transcription-associated antibiotics such as fluoroquinolones and quinolines. Nevertheless, the expression of *sanA* from a plasmid did not completely reverse the effects of the mutation, indicating that SanA plays only a partial role in this phenotype. Additionally, the absence of a specific SanA antibody prevents direct comparison of *sanA* expression in its plasmid and chromosomal forms. Therefore, variations in expression levels and regulatory elements could be responsible for the observed incomplete restoration of the phenotype.

Although WT bacteria exhibited resistance to a broader spectrum of xenobiotics, the mutant displayed increased resistance to replication-targeting antibiotics, bleomycin and sulfamonomethoxine. These two antibiotics have similar targets of action, but differ significantly in their physicochemical properties. Bleomycin, like vancomycin, has a notably high molecular weight (1,415 Da) and is classified as a cationic glycopeptide however, bleomycin and vancomycin have distinct mechanisms of action (Hecht, 2000). This finding further suggests that *sanA* is not directly associated with the specific action mechanisms of these xenobiotics. Instead, it seems to be linked, at least partially, with the membrane charge (Davlieva et al., 2013). As *sanA* contributes to a more positive membrane charge, it subsequently increased resistance to cationic antibiotics.

Bacterial resistance to bleomycin and sulfamonomethoxine, a derivative of sulfonamide, is mainly attributed to the Resistance-Nodulation-Division (RND) family of efflux pumps. The SanA structure does not resemble that of an RND transporter, suggesting that its absence, as observed in the mutant, may lead to the overexpression of another efflux pump that compensates for the transport of this antibiotic. Moreover, due to the neutral charge of sulfamonomethoxine, alterations in the phospholipid composition of the IM may hinder the passive diffusion of neutral antibiotics (Kadner, 1996).

Considering the distinct effects of *sanA* deletion on resistance to different classes of antibiotics, we decided to explore whether this genetic modification also affects the intracellular replication of *Salmonella* within macrophages. Macrophages are immune cells essential for host defense against bacterial infections, as they internalize and destroy them using various mechanisms, including the production of reactive oxygen and nitrogen species and antimicrobial peptides (Gordon, 1999). These substances possess bactericidal properties and disrupt bacterial cell envelope integrity and function, similar to antibiotics. Therefore, modifications affecting antibiotic resistance might also influence the bacterium's ability to tolerate the hostile intracellular environment of a macrophage. To further explore this phenomenon, we selected a C57BL/6 primary BMDM model for *Salmonella* replication, which provides a physiologically relevant environment for studying the interactions between *Salmonella* and host cells compared to cell lines As a result, *sanA* deletion resulted in higher replication rates of *Salmonella* within primary macrophages, suggesting that the absence of *sanA* may enhance the ability of the bacterium to resist the bactericidal actions of macrophages. We suggest it is linked to alterations in the bacterial cell envelope associated with *sanA* deletion as our data suggest that *sanA* knockout leads to increased membrane hydrophilicity and positive charge. As the outer layer of bacterial cells possesses an anionic charge, most antimicrobial peptides (AMPs) effective against bacteria are cationic, enabling them to bind to the negatively charged bacterial surface (Lei et al., 2019). Consequently, bacterial resistance to AMPs often involves surface modification to reduce the negative charge, which serves as an initial defense mechanism (Peschel, 2002). Also, previously published data revealed that the efficiency of phagocytosis increases with the hydrophobicity of bacterial cells and that hydrophilic bacteria resist ingestion by phagocytes (Matz and Jürgens, 2001). Surprisingly, we did not observe significant changes in the invasiveness of the analyzed strains in the conditions we used. To better elucidate the role of *sanA* in host-pathogen interactions, it is necessary to investigate changes occurring in the bacterial envelope due to *sanA* knockout. We hypothesize that *sanA* deletion and the subsequent increase in membrane permeability may be linked to an upregulation of SPI-II and/or SPI-I genes, which are responsible for intracellular replication and invasion, respectively. Currently, this hypothesis is under investigation.

In conclusion, our study offers a crucial understanding of the dynamics of antibiotic resistance, underscoring how alterations in membrane properties influence bacterial susceptibility to various xenobiotics. The insights regarding SanA's influence on membrane physicochemical properties shed new light on the role of membrane proteins in *Salmonella*'s resistance to environmental stressors. This highlights the importance of these proteins in comprehending bacterial pathogenicity and survival mechanisms.

Data availability statement

The original contributions presented in the study are included in the article/Supplementary material, further inquiries can be directed to the corresponding author.

Ethics statement

The animal study was approved by UK Home Office Project License in a Home Office designated facility. Imperial College Animal Welfare and Ethical Review Body (AWERB) granted approval for all mouse work. The study was conducted in accordance with the local legislation and institutional requirements.

Author contributions

AA: Conceptualization, Data curation, Investigation, Methodology, Validation, Visualization, Writing – original draft. RK: Conceptualization, Resources, Supervision, Writing – review & editing. KB: Investigation, Writing – review & editing. TLMT: Methodology, Resources, Writing – review & editing. JS: Investigation, Writing – review & editing. KG: Conceptualization, Data curation, Formal analysis, Funding acquisition, Project administration, Resources, Supervision, Writing – review & editing.

Funding

The author(s) declare financial support was received for the research, authorship, and/or publication of this article. AA and KG were supported by the Polish National Science Centre Research Grant PRELUDIUM BIS number 2019/35/O/NZ6/01590. TLMT was funded by a Biotechnology and Biological Sciences Research Council David Phillips Fellowship BB/R011834/1. The APC was co-financed by the Wrocław University of Environmental and Life Sciences.

Acknowledgments

The authors thank dr hab. Krzysztof Matkowski and Department of Plant Protection, Wroclaw University of Environmental and Life Sciences for giving us the access to Biolog Phenotype Microarrays instrument.

Conflict of interest

The authors declare that the research was conducted in the absence of any commercial or financial relationships that could be construed as a potential conflict of interest.

The author(s) declared that they were an editorial board member of Frontiers, at the time of submission. This had no impact on the peer review process and the final decision.

Publisher's note

Supplementary material

The Supplementary material for this article can be found online at: https://www.frontiersin.org/articles/10.3389/fmicb.2023.1340143/full#supplementary-material

References

Alenazy, R. (2022). Antibiotic resistance in Salmonella: targeting multidrug resistance by understanding efflux pumps, regulators and the inhibitors. *J King Saud Univ Sci.* 34:102275. doi: 10.1016/j.jksus.2022.102275

Asmar, A. T., and Collet, J. F. (2018). Lpp, the Braun lipoprotein, turns 50—major achievements and remaining issues. *FEMS Microbiol. Lett.* 365:fny199. doi: 10.1093/femsle/fny199

Ayukekbong, J. A., Ntemgwa, M., and Atabe, A. N. (2017). The threat of antimicrobial resistance in developing countries: causes and control strategies. *Antimicrob. Resist. Infect. Control* 6:47. doi: 10.1186/s13756-017-0208-x

Bailey, J. D., Shaw, A., McNeill, E., Nicol, T., Diotallevi, M., Chuaiphichai, S., et al. (2020). Isolation and culture of murine bone marrow-derived macrophages for nitric oxide and redox biology. *Nitric Oxide* 100-101, 17–29. doi: 10.1016/j.niox.2020.04.005

Boughner, L. A., and Doerrler, W. T. (2012). Multiple deletions reveal the essentiality of the DedA membrane protein family in *Escherichia coli*. *Microbiology* 158, 1162–1171. doi: 10.1099/mic.0.056325-0

Centers for Disease Control and Prevention (2019). *Antibiotic resistance threats in the United States*, Centers for Disease Control and Prevention (United States) 2019

Cherepanov, W. W. (1995). Gene disruption in *Escherichia coli*: Tc R and km R cassettes with the option of Flp-catalyzed excision of the antibiotic-resistance determinant. *Gene* 158, 9–14. doi: 10.1016/0378-1119(95)00193-a

Datsenko, K. A., and Wanner, B. L. (2000). One-step inactivation of chromosomal genes in *Escherichia coli* K-12 using PCR products. *Proc. Natl. Acad. Sci.* 97, 6640–6645. doi: 10.1073/pnas.120163297

Davlieva, M., Zhang, W., Arias, C. A., and Shamoo, Y. (2013). Biochemical characterization of cardiolipin synthase mutations associated with daptomycin resistance in enterococci. *Antimicrob. Agents Chemother.* 57, 289–296. doi: 10.1128/AAC.01743-12

Dunkley, E. J., Chalmers, J. D., Cho, S., Finn, T. J., and Patrick, W. M. (2019). Assessment of phenotype microarray plates for rapid and high-throughput analysis of collateral sensitivity networks. *PloS One* 14:e0219879. doi: 10.1371/journal.pone.0219879

Ernst, R. K., Guina, T., and Miller, S. I. (1999). How Intracellular Bacteria survive: surface modifications that promote resistance to host innate immune responses. *J Infect Dis* 179, S326–S330. doi: 10.1086/513850

Falagas, M. E., Vouloumanou, E. K., Samonis, G., and Vardakasa, K. Z. (2016). Fosfomycin. Clin Microbiol rev. American society for. *Microbiology* 29, 321–347. doi: 10.1128/CMR.00068-15

Finn, R. D., Bateman, A., Clements, J., Coggill, P., Eberhardt, R. Y., Eddy, S. R., et al. (2014). Pfam: the protein families database. *Nucleic Acids Res.* 42, D222–D230. doi: 10.1093/nar/gkt1223

Garneau-Tsodikova, S., and Labby, K. J. (2016). Mechanisms of resistance to aminoglycoside antibiotics: overview and perspectives. *Medchemcomm* 7, 11–27. doi: 10.1039/c5md00344j

Gordon, S. (1999). *Phagocytosis: The host*. Stamford, CT: JAI Press.

Guard-Bouldin, J., Morales, C. A., Frye, J. G., Gast, R. K., and Musgrove, M. (2007). Detection of *Salmonella enterica* subpopulations by phenotype microarray antibiotic resistance patterns. *Appl. Environ. Microbiol.* 73, 7753–7756. doi: 10.1128/AEM.01228-07

Hantke, K., and Braun, V. (1973). Covalent binding of lipid to protein diglyceride and amide-linked fatty acid at the N-terminal end of the Murein-lipoprotein of the *Escherichia coli* outer membrane Eur. *J. Biochem.* 34, 284–296. doi: 10.1111/j.1432-1033.1973.tb02757.x

Havelaar, A. H., Kirk, M. D., Torgerson, P. R., Gibb, H. J., Hald, T., Lake, R. J., et al. (2015). World Health Organization global estimates and regional comparisons of the burden of foodborne disease in 2010. *PLoS Med.* 12:e1001923. doi: 10.1371/journal.pmed.1001923

Hecht, S. M. (2000). Bleomycin: new perspectives on the mechanism of action. *J. Nat. Prod.* 63, 158–168. doi: 10.1021/np990549f

Huerta-Cepas, J., Szklarczyk, D., Heller, D., Hernández-Plaza, A., Forslund, S. K., Cook, H., et al. (2019). Egg NOG 5.0: a hierarchical, functionally and phylogenetically annotated orthology resource based on 5090 organisms and 2502 viruses. *Nucleic Acids Res.* 47, D309–D314. doi: 10.1093/nar/gky1085

Ize, B., Stanley, N. R., Buchanan, G., and Palmer, T. (2003). Role of the *Escherichia coli* tat pathway in outer membrane integrity. *Mol. Microbiol.* 48, 1183–1193. doi: 10.1046/j.1365-2958.2003.03504.x

Jacobs, C., Huang, L.-J., Bartowsky, E., Normark, S., and Park, J. T. (1994). Bacterial cell wall recycling provides cytosolic muropeptides as effectors for-lactamase induction. *EMBO J.* 13, 4684–4694. doi: 10.1002/j.1460-2075.1994.tb06792.x

Kadner, R. J. (1996). Cytoplasmic membrane. *Cell. Mol. Biol.* 1, 58–87.

Käll, L., Krogh, A., and Sonnhammer, E. L. L. (2007). Advantages of combined transmembrane topology and signal peptide prediction-the Phobius web server. *Nucleic Acids Res.* 35, W429–W432. doi: 10.1093/nar/gkm256

Kelley, L. A., Mezulis, S., Yates, C. M., Wass, M. N., and Sternberg, M. J. E. (2015). The Phyre2 web portal for protein modeling, prediction and analysis. *Nat. Protoc.* 10, 845–858. doi: 10.1038/nprot.2015.053

Kolenda, R., Burdukiewicz, M., Wimonc, M., Aleksandrowicz, A., Ali, A., Szabo, I., et al. (2021). Identification of natural mutations responsible for altered infection phenotypes of *Salmonella enterica* clinical isolates by using cell line infection screens. *Appl. Environ. Microbiol.* 87, e02177–e02120. doi: 10.1128/AEM.02177-20

Kristian, S. A., Datta, V., Weidenmaier, C., Kansal, R., Fedtke, I., Peschel, A., et al. (2005). D-alanylation of teichoic acids promotes group a Streptococcus antimicrobial peptide resistance, neutrophil survival, and epithelial cell invasion. *J. Bacteriol.* 187, 6719–6725. doi: 10.1128/JB.187.19.6719-6725.2005

Krogh, A., Larsson, B., Von Heijne, G., and Sonnhammer, E. L. L. (2001). Predicting transmembrane protein topology with a hidden Markov model: application to complete genomes. *J. Mol. Biol.* 305, 567–580. doi: 10.1006/jmbi.2000.4315

Langridge, G. C., Phan, M. D., Turner, D. J., Perkins, T. T., Parts, L., Haase, J., et al. (2009). Simultaneous assay of every *Salmonella Typhi* gene using one million transposon mutants. *Genome Res.* 19, 2308–2316. doi: 10.1101/gr.097097.109

Lei, J., Sun, L., Huang, S., Zhu, C., Li, P., He, J., et al. (2019). The antimicrobial peptides and their potential clinical applications. *Am. J. Transl. Res.* 11, 3919–3931.

Levengood, S. K., Beyer, W. F., and Webster, R. E. (1991). TolA: a membrane protein involved in colicin uptake contains an extended helical region. *Nati. Acad. Sci. USA.* 88, 5939–5943. doi: 10.1073/pnas.88.14.5939

Levengood-Freyermuth, S. K., Click, E. M., and Webster, R. E. (1993). Role of the carboxyl-terminal domain of TolA in protein import and integrity of the outer membrane. *J. Bacteriol.* 175, 222–228. doi: 10.1128/jb.175.1.222-228.1993

Lima, L. M., Silva, B. N. M., Barbosa, G., and Barreiro, E. J. (2020). β-Lactam antibiotics: an overview from a medicinal chemistry perspective. *Eur. J. Med. Chem.* 208:112829. doi: 10.1016/j.ejmech.2020.112829

Malinverni, J. C., and Silhavy, T. J. (2011). Assembly of outer membrane β-barrel proteins: the bam complex. *Eco Sal Plus.* 4, 16–23. doi: 10.1128/ecosalplus.4.3.8

Matz, C., and Jürgens, K. (2001). Effects of hydrophobic and electrostatic cell surface properties of bacteria on feeding rates of heterotrophic nanoflagellates. *Appl. Environ. Microbiol.* 67, 814–820. doi: 10.1128/AEM.67.2.814-820.2001

Mitchell, A. M., Wang, W., and Silhavy, T. J. (2017). Novel RpoS-dependent mechanisms strengthen the envelope permeability barrier during stationary phase. *J. Bacteriol.* 199, e00708–e00716. doi: 10.1128/JB.00708-16

Monack, D. M., Raupach, B., Hromockyj, A. E., and Falkow, S. (1996). *Salmonella typhimurium* invasion induces apoptosis in infected macrophages source. *Proc. Natl. Acad. Sci. U. S. A.* 93, 9833–9838. doi: 10.1073/pnas.93.18.9833

Mouslim, C., Cano, D. A., and Casadesús, J. (1998). The sfiX, rfe and metN genes of Salmonella typhimurium and their involvement in the his (c) pleiotropic response. *Mol. Gen. Genet.* 259, 46–53. doi: 10.1007/s004380050787

Murata, T., Tseng, W., Guina, T., Miller, S. I., and Nikaido, H. (2007). PhoPQ-mediated regulation produces a more robust permeability barrier in the outer membrane of *Salmonella enterica* serovar typhimurium. *J. Bacteriol.* 189, 7213–7222. doi: 10.1128/JB.00973-07

Nikaido, H. (2003). Molecular basis of bacterial outer membrane permeability revisited. *Microbiol. Mol. Biol. Rev.* 67, 593–656. doi: 10.1128/mmbr.67.4.593-656.2003

Nikolaidis, I., Favini-Stabile, S., and Dessen, A. (2014). Resistance to antibiotics targeted to the bacterial cell wall. *Protein Sci.* 23, 243–259. doi: 10.1002/pro.2414

O'Neil, J. (2016). *Antimicrobial resistance: Tackling a crisis for the health and wealth of nations*. London, United Kingdom: Antimicrobial Resistance.

Oguri, T., Yeo, W. S., Bae, T., and Lee, H. (2016). Identification of envC and its cognate amidases as novel determinants of intrinsic resistance to cationic antimicrobial peptides. *Antimicrob. Agents Chemother.* 60, 2222–2231. doi: 10.1128/AAC.02699-15

Papanastasiou, M., Orfanoudaki, G., Kountourakis, N., Koukaki, M., Sardis, M. F., Aivaliotis, M., et al. (2016). Rapid label-free quantitative analysis of the *E. coli* BL21(DE3) inner membrane proteome. *Proteomics* 16, 85–97. doi: 10.1002/pmic.201500304

Parsons, L. M., Lin, F., and Orban, J. (2006). Peptidoglycan recognition by pal, an outer membrane lipoprotein. *Biochemistry* 45, 2122–2128. doi: 10.1021/bi052227i

Peschel, A. (2002). How do bacteria resist human antimicrobial peptides? *Trends Microbiol.* 10, 179–186. doi: 10.1016/s0966-842x(02)02333-8

Petersen, T. N., Brunak, S., Von Heijne, G., and Nielsen, H. (2011). SignalP 4.0: discriminating signal peptides from transmembrane regions. *Nat. Methods* 8, 785–786. doi: 10.1038/nmeth.1701

Reygaert, C. (2018). An overview of the antimicrobial resistance mechanisms of bacteria. *AIMS Microbiol* 4, 482–501. doi: 10.3934/microbiol.2018.3.482

Rida, S., Caillet, J., and Alix, J. H. (1996). Amplification of a novel gene, sanA, abolishes a vancomycin-sensitive defect in *Escherichia coli*. *J. Bacteriol.* 178, 94–102. doi: 10.1128/jb.178.1.94-102.1996

Shea, A., Wolcott, M., Daefler, S., and Rozak, D. A. (2012). Biolog phenotype microarrays. *Methods Mol. Biol.* 881, 331–373. doi: 10.1007/978-1-61779-827-6_12

Silhavy, T. J., Kahne, D., and Walker, S. (2010). The bacterial cell envelope. *Cold Spring Harb. Perspect. Biol.* 2:a000414. doi: 10.1101/cshperspect.a000414

Singhal, L., Sharma, M., Verma, S., Kaur, R., Britto, X. B., Kumar, S. M., et al. (2018). Comparative evaluation of broth microdilution with polystyrene and glass-coated plates, agar dilution, E-test, vitek, and disk diffusion for susceptibility testing of colistin and polymyxin B on carbapenem-resistant clinical isolates of *acinetobacter baumannii*. *Microb. Drug Resist.* 24, 1082–1088. doi: 10.1089/mdr.2017.0251

Sun, J., Rutherford, S. T., Silhavy, T. J., and Huang, K. C. (2022). Physical properties of the bacterial outer membrane. *Nat. Rev. Microbiol.* 20, 236–248. doi: 10.1038/s41579-021-00638-0

Thomas, P. D., Campbell, M. J., Kejariwal, A., Mi, H., Karlak, B., Daverman, R., et al. (2003). PANTHER: a library of protein families and subfamilies indexed by function. *Genome Res.* 13, 2129–2141. doi: 10.1101/gr.772403

Thurston, T. L. M., Matthews, S. A., Jennings, E., Alix, E., Shao, F., Shenoy, A. R., et al. (2016). Growth inhibition of cytosolic Salmonella by caspase-1 and caspase-11 precedes host cell death. *Nat. Commun.* 7:13292. doi: 10.1038/ncomms13292

Typas, A., Banzhaf, M., Gross, C. A., and Vollmer, W. (2012). From the regulation of peptidoglycan synthesis to bacterial growth and morphology. *Nat. Rev. Microbiol.* 10, 123–136. doi: 10.1038/nrmicro2677

Viau, C., Le Sage, V., Ting, D. K., Gross, J., and Le Moual, H. (2011). Absence of PmrAB-mediated phosphoethanolamine modifications of *Citrobacter rodentium* lipopolysaccharide affects outer membrane integrity. *J. Bacteriol.* 193, 2168–2176. doi: 10.1128/JB.01449-10

Yadav, A. K., Espaillat, A., and Cava, F. (2018). Bacterial strategies to preserve cell wall integrity against environmental threats. *Front. Microbiol.* 9:2064. doi: 10.3389/fmicb.2018.02064

Yu, N. Y., Wagner, J. R., Laird, M. R., Melli, G., Rey, S., Lo, R., et al. (2010). PSORTb 3.0: improved protein subcellular localization prediction with refined localization subcategories and predictive capabilities for all prokaryotes. *Bioinformatics* 26, 1608–1615. doi: 10.1093/bioinformatics/btq249

frontiers | Frontiers in Microbiology

TYPE Original Research
PUBLISHED 15 January 2024
DOI 10.3389/fmicb.2023.1327739

OPEN ACCESS

EDITED BY
George Grant,
University of Aberdeen, United Kingdom

REVIEWED BY
Palmy Jesudhasan,
Agricultural Research Service, United States
Kenneth James Genovese,
Agricultural Research Service, United States

*CORRESPONDENCE
Shaun A. Cawthraw
✉ shaun.cawthraw@apha.gov.uk

RECEIVED 25 October 2023
ACCEPTED 27 December 2023
PUBLISHED 15 January 2024

CITATION
Cawthraw SA, Goddard A, Huby T, Ring I, Chiverton L and Mueller-Doblies D (2024) Early vaccination of laying hens with the live bivalent *Salmonella* vaccine AviPro^{TM} Salmonella DUO results in successful vaccine uptake and increased gut colonization.
Front. Microbiol. 14:1327739.
doi: 10.3389/fmicb.2023.1327739

Early vaccination of laying hens with the live bivalent *Salmonella* vaccine AviPro^{TM} Salmonella DUO results in successful vaccine uptake and increased gut colonization

Shaun A. Cawthraw[1]*, Adam Goddard[2], Tom Huby[1], Isaac Ring[1], Louise Chiverton[1] and Doris Mueller-Doblies[3]

[1]Department of Bacteriology, Animal and Plant Health Agency (APHA - Weybridge), New Haw, Surrey, United Kingdom, [2]Elanco Animal Health, Form 2, Bartley Way, Bartley Wood Business Park, Hook, United Kingdom, [3]Elanco Austria GmbH, Quartier Belvedere Central, Vienna, Austria

Introduction: *Salmonella* Enteritidis and *S.* Typhimurium are the two most clinically important zoonotic *Salmonella* serovars and vaccination of breeding and laying hens affords effective *Salmonella* control. The use of live vaccines has proven beneficial for a number of reasons, including ease of application, protection from the first day of life onwards and initiation of a strong local immune response. Live vaccines can be applied in the drinking water from the first day of life onwards, but some rearers choose to wait until the end of the first week to ensure sufficient water consumption. However, this practice leaves the birds unprotected during the crucial first week of life, where they are most susceptible to colonization by field strains. The aim of this study was to determine if successful vaccine uptake is achieved when layer pullets are vaccinated as early as day one.

Methods: Three pullet flocks were vaccinated at 1, 2, 3 or 5 days-of-age with AviPro^{TM} Salmonella DUO, a live vaccine containing attenuated strains of *S.* Enteritidis and *S.* Typhimurium (Elanco Animal Health, Cuxhaven, Germany). The vaccine was administered via the drinking water following manufacturer's instructions. Two days post-vaccination, 10 birds per flock were culled and caecal and liver samples taken, along with two pools of faeces per flock. Levels of vaccine strains were determined by quantitative and qualitative bacteriology.

Results: Vaccine strains were detected in all birds from all age groups indicating successful uptake of the vaccine. Levels of the *S.* Enteritidis vaccine were higher than levels of the *S.* Typhimurium vaccine, with the latter frequently only detectable following enrichment. There was an inverse correlation between age and caecal levels of vaccines, with the highest numbers seen in birds vaccinated at 1-day-of-age. Interestingly, *S.* Enteritidis vaccine strain levels in liver samples were highest when birds were vaccinated at 5 days-of-age.

Discussion: These results show that successful uptake of both vaccine strains was evident in all age groups. The earlier the chicks were vaccinated,

the higher the vaccine levels in caecal contents. We therefore recommend vaccination of pullets as early as practicably possible to ensure protection against exposure to field strains.

KEYWORDS

Salmonella Enteritidis, *Salmonella* Typhimurium, live vaccines, laying hens, vaccination

Introduction

Zoonotic strains of *Salmonella enterica* are some of the most important food-borne pathogens worldwide, causing an estimated 78.7 million illnesses and 59,000 deaths each year (World Health Organization, 2015). More than 2,600 serovars are known, most of which are a public health concern. Although *Salmonella* can be present in a variety of foods of animal and non-animal origin, European data show that the majority of *Salmonella* outbreaks are linked to the poultry sector, in particular to eggs and egg products (European Food Safety Authority, 2022).

The serovar responsible for most egg-related human illness and outbreaks is *S.* Enteritidis, which started to emerge in Europe and in the US in the 1980s and has been the most important serovar in many parts of the world since (O'Brien, 2013; Lane et al., 2014; World Health Organization, 2018). Although significant progress has been made in the control of *S.* Enteritidis in the laying hen sector in Europe, this particular serovar is still causing the highest number of outbreaks and outbreak-related illnesses, most of which can be linked to eggs and egg products (European Food Safety Authority, 2022).

Control of zoonotic *Salmonella* in the poultry sector can only be achieved using a holistic approach, including high biosecurity, adequate pest control and good management practices. An additional helpful tool in the battle against *Salmonella* infection are vaccines, and to date, vaccines offering protection against *S.* Enteritidis and *S.* Typhimurium are widely used in many parts of the world.

Inactivated *Salmonella* vaccines, which are administered through intramuscular injection, first became available in the early 1990s (Lane et al., 2014) and were subsequently used mainly in the breeding sector. However, because of the inconvenience of application, their use in laying hens was limited. Only the introduction of live attenuated vaccines a few years later and their extended use in both the breeding and laying hen sectors led to a significant reduction in human case numbers and laying hen prevalence (Lane et al., 2014). The use of live vaccines proved particularly efficient as they can be applied via drinking water and as early as on the first day of life.

It is acknowledged that live *Salmonella* vaccines generally confer better protection than killed vaccines, because they stimulate both cell-mediated and humoral immunity, including local, mucosal IgA responses (Zhang-Barber et al., 1999; Van Immerseel et al., 2005). When live vaccines are administered orally to young birds (through drinking water application or hatchery spray), they lead to extensive gut colonization and a strong local immune stimulus. Early colonization of newly-hatched chicks with a live vaccine strain leads to the so-called colonization-inhibition effect which prevents the colonization of the gut with other bacteria, thus offering an early protection which goes even beyond the vaccine-specific serovar (Van Immerseel et al., 2005).

Ideally, pullets should be vaccinated as early as possible to protect them during the first weeks of life when they are most susceptible to colonization by *Salmonella* (Shivaprasad et al., 2013). However, the main reason why some pullet-rearers often wait until the end of the first week before administering the first dose is the worry that the water-intake of the pullets may be too low during the first few days, potentially leading to a reduced uptake of the vaccine.

The efficacy of the vaccine used in this trial has been proven over many years ago, both through controlled trials and from experience in the field since the early 1990s. Several studies showed successful protection of birds with the first dose applied at day one (Gantois et al., 2006; Eekhout et al., 2018; Huberman et al., 2019). However, in these trials, the vaccine was administered via oral gavage to ensure the successful vaccination of each individual chick. In commercial poultry production, it is not possible to administer a live vaccine in such a way to individual birds, so application via the drinking water line has been a well-established method for vaccine administration. As there are sufficient data to show that the vaccine is efficacious when applied at an early age, we focused on the question of successful uptake.

The aim of this field study was therefore to analyze and compare the vaccine uptake of pullets which received their first dose of the live, bivalent *Salmonella* vaccine AviPro^{TM} Salmonella DUO (Elanco Animal Health) at 1-, 2, 3- or 5-days-old (d.o.). The results of this study may help pullet rearers in their decision-making process on when to administer the first dose safely and effectively, ensuring that the birds receive an appropriate dose of the vaccinal product in a timely manner.

Materials and methods

On-farm vaccination

Four commercial pullet rearing farms in England with at least three houses each were recruited for the study. Chicks were sourced from a reputable UK hatchery and had been vaccinated against Marek's disease, coccidiosis and Infectious Bronchitis at the hatchery according to standard vaccination protocols. No *Salmonella* was detected in routine National Control Program samples taken from the flocks used in the study. On farm, they were vaccinated with AviPro^{TM} Salmonella DUO, a licensed vaccine consisting of two attenuated live strains: *S.* Enteritidis

strain Sm24/Rif12/Ssq and *S.* Typhimurium strain Nal2/Rif9/Rtt (vSE and vST, respectively). Chicks were vaccinated either at 1-, 2-, 3- or 5-days-old. Vaccines were prepared and administered on farm under the supervision of qualified personnel from the vaccine company. Briefly, freeze-dried vaccine was reconstituted according to manufacturer's instructions using mains water and a water stabilizer (Aviblue, Lohmann Animal Health, Maine, USA). The vaccine was administered via a water proportioner, dosing at 2%. Once the vaccine was reconstituted in stabilized water, the nipple lines were lifted and the lines were primed with vaccine, removing all clear surplus water until the blue dye was present at the end of each nipple line. Once all the nipple lines had been primed, they were lowered to allow the chicks to drink. The early vaccination in the first days of life has always been challenging as the water system holds more water than the chicks would drink over a normal vaccination period of up to 3 h. Key is knowing the capacity of the system (total volume of water) to enable successful vaccination to take place in the first days of life. Vaccines were administered for up to 12 h with the following rates dependant on the birds' age: day one—2.5 ml per chick, day two—4 ml per chick, day three—4.5 ml per chick, day 5—5.5 ml per chick.

Sampling

For each farm on the day of vaccination, vaccine/drinking water samples were taken from two points on the drinker line. Two days post-vaccination, 10 chicks were randomly selected and euthanised and two pools of 10 individual fecal droppings were collected from each flock. Samples and carcases were despatched in chilled containers to the APHA laboratory on the day of collection and processed the same day.

Bacteriology

Upon receipt at APHA, samples of caecal contents and liver tissue were taken from each carcase. Samples were weighed and homogenized in Buffered Peptone Water (1:9, w:v) supplemented with rifampicin (100 μg/ml; Merck, Germany). Homogenized samples and vaccine samples were serially diluted (1/10) in PBS and dilutions spread-plated onto selective agars (200 μl for the starting homogenate, and 100 μl for the subsequent dilutions). For detection of vSE, brilliant green agar (BGA) supplemented with rifampicin (100 μg/ml) and streptomycin (200 μg/ml) was used. For vST detection, xylose lysine deoxycholate agar (XLD) supplemented with rifampicin (100 μg/ml) and nalidixic acid (5 μg/ml) was used. BGA and XLD plates were incubated at 37°C for 24 ± 3 h and 48 ± 3 h, respectively, and colonies enumerated. Representative colonies were tested by slide agglutination (Poly O A-S, Pro-Lab Diagnostics, UK) for confirmation of being *Salmonella*. Both vaccine strains are resistant to rifampicin, and the vSE strain has an additional resistance to streptomycin, while the vST strain has an additional resistance to nalidixic acid. The addition of these antibiotics to media allows positive selection for the vaccine strains and discrimination between the two strains on agar plates. Homogenates were also incubated at 37°C for 20 ± 2 h in order to enrich low levels of vaccines. Where no colonies were detectable from direct plating, enriched samples were plated out for a qualitative result. The limit of detection was 50 cfu/g.

Statistics

Colonization levels for each vaccination age group were analyzed by *t*-tests (GraphPad Prism). Where vaccine strains were recovered only after enrichment, the median value between 0 and the limit of detection (i.e., 25 cfu/g) was assigned.

Results

Vaccine concentrations

Vaccine concentrations were determined in two samples taken from different points along the drinker line in each house on the day of administration. Levels were consistent between each flock and on all occasions. The vSE levels were $3.6 \pm 1.5 \times 10^7$ cfu/ml, and vST levels were $1 \times 10^7 \pm 3.9 \times 10^6$ cfu/ml. These levels were as expected and sufficient to meet the prescribed vaccine uptake given expected water consumption levels.

Vaccine uptake levels

Vaccine concentrations were determined two days post-vaccination in caecal and liver samples from 10 chicks randomly selected from each flock. There was a clear trend for higher levels of vaccines in caecal contents the earlier the birds were vaccinated (**Figure 1**; **Table 1** and **Supplementary Table 1**). In birds vaccinated at 1-d.o. all had detectable levels of vSE, with quantifiable numbers in 29/30 birds. Levels ranged from 50 cfu/g to 10^6 cfu/g (mean 2.9×10^5 cfu/g). Vaccination at 2- and 3-d.o. both resulted in 29/30 birds with detectable vSE, of which 28/30 and 26/30 resp. were quantifiable (means 1.2×10^5 and 1.8×10^4 cf/g resp). In contrast, in birds vaccinated at 5-d.o. only 16/30 birds had detectable vSE (incl 8/30 with quantifiable levels). Statistical analyses (*t*-tests) revealed there were significant decreases between vaccination at 1- and 5-d.o. ($p = 0.039$), 2- and 3-d.o. ($p = 0.032$), 2- and 5-d.o. ($p = 0.011$) and 3- and 5-d.o. ($p = 0.027$).

For vST, 29/30 birds vaccinated at 1-d.o. had detectable levels, with quantifiable numbers in 24/30 birds. Levels ranged from 50 cfu/g to 10^6 cfu/g (mean 1.7×10^5 cfu/g). Vaccination at 2-d.o. resulted in 25/30 birds with detectable vSE, of which 17/30 were quantifiable (mean 6.7×10^3 cf/g). With vaccination at 3-d.o. 29/30 birds with detectable vSE, of which 18/30 were quantifiable (mean 3.4×10^4 cf/g). As seen with vSE, there was a notable decrease in vST recovered from birds vaccinated at 5-d.o.: 16/30 birds had detectable levels, with only 1/30 having quantifiable numbers (10^2 cfu/g). There were significant decreases between vaccination at 1- and 2-d.o. ($p = 0.034$), 1- and 5-d.o. ($p = 0.027$), and 2- and 5-d.o. ($p = 0.012$).

Compared to caecal contents, levels of both vaccines were considerably lower in liver samples (**Table 1** and

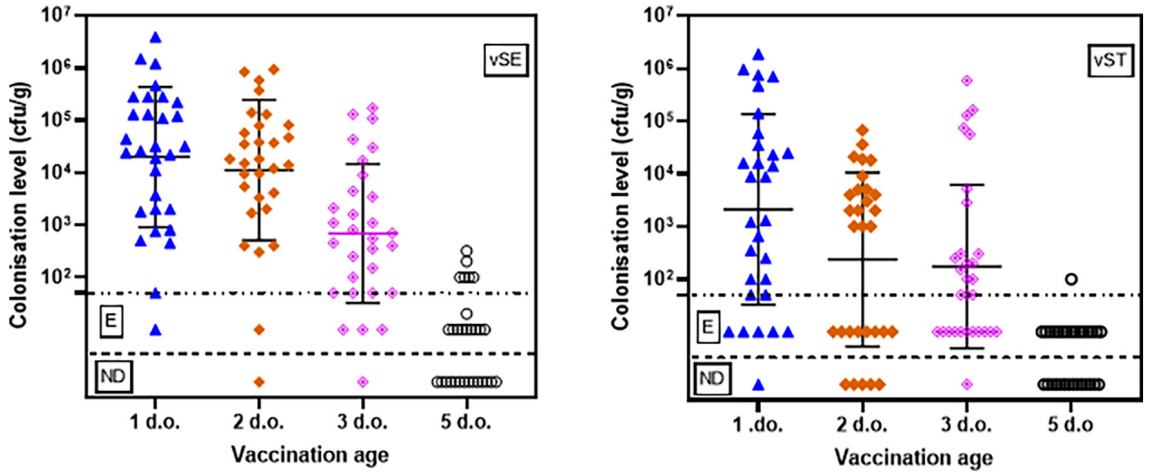

FIGURE 1
Caecal levels (cfu/g) of vSE and vST in chickens vaccinated at 1-, 2-, 3-, and 5-d.o. Samples were taken 2 days post-vaccination. Detection limit = 50 cfu/g. E–positive only after enrichment; ND, none detected.

TABLE 1 Numbers of caecal (C) and liver (L) samples from which vSE and vST were recovered following vaccination of chickens at 1-, 2-, 3-, and 5-d.o (n = 30 per age group).

		1do			2do			3do			5do		
		DQ	E	ND	DQ	E	ND	DQ	E	ND	DQ	E	ND
vSE	C	29	1	0	28	1	1	26	3	1	8	8	14
	L	0	12	18	5	25	0	2	9	19	30	0	0
	C and/or L	30		0	30		0	30		0	30		0
vST	C	24	5	1	17	8	5	18	11	1	1	15	14
	L	4	17	9	1	12	17	0	6	24	1	15	14
	C and/or L	30		0	28		2	29		1	19		11

Samples were taken 2 days post-vaccination. C and/or L—numbers of birds where at least one sample type was positive. DQ, directly quantifiable (≥ 50 cfu/g); E, positive only after enrichment; ND, none detected.

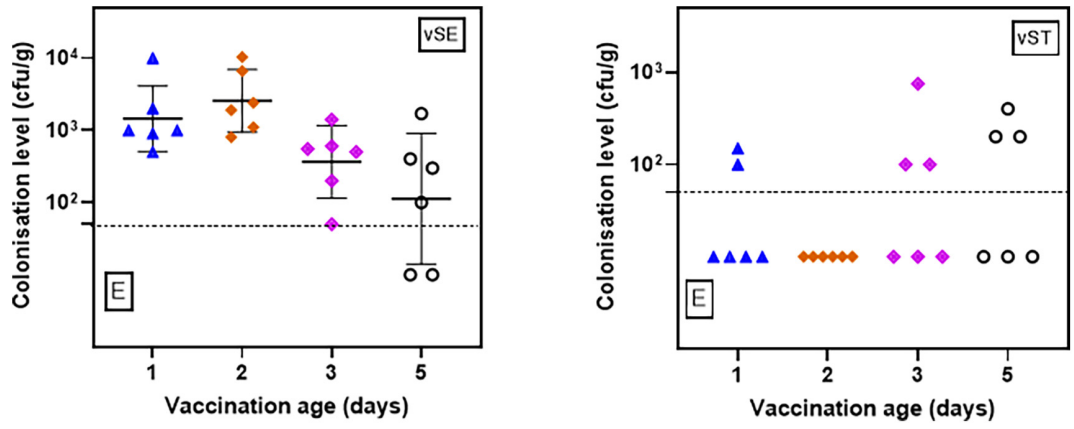

FIGURE 2
Levels (cfu/g) of vSE and vST in pooled fecal samples from chickens vaccinated at 1-, 2-, 3-, and 5-d.o. Samples were collected 2 days post-vaccination. Detection limit = 50 cfu/g. E–positive only after enrichment.

Supplementary Table 1). Where recovered, levels were mostly only detectable after enrichment, and none were detected in many of the birds. The exception to this was for vSE in birds vaccinated at 5-d.o. where all 30 birds had quantifiable levels (mean 2.5 × 10^2 cfu/g). This was significantly higher than in birds vaccinated at 1-, 2- (both $p < 0.001$) and 3-d.o. ($p = 0.003$).

For the pooled feces, both vaccines were detectable in all samples tested (Figure 2 and Supplementary Table 2). For

vSE, all samples had quantifiable levels (range 50 to 10^4 cfu/g) except 2/6 samples from 5-d.o. vaccinees where enrichment was necessary. Levels of vST were lower and mostly detectable only after enrichment. There were no significant differences ($p > 0.05$) relating to age of vaccination and fecal levels.

Discussion

It is accepted that vaccination of chickens in rear (both future breeding and laying birds) against *Salmonella* is most successful if a live vaccine is used (Van Immerseel et al., 2005; Desin et al., 2013). Colonization of chicks often happens early in life as a result of hatchery contamination or persistent farm contamination, and leads to high levels of environmental contamination and rapid transmission of pathogens via contaminated litter (Van Immerseel et al., 2005). As inactivated vaccines can't be administered before six to eight weeks of age, depending on the product, only live vaccines administered via drinking water can provide adequate early protection. Furthermore, oral administration of live *Salmonella* to the newly hatched chicks not only induces an adaptive immune response, but is also able to confer, within 24 h of application, a high degree of resistance against colonization and tissue invasion by other *Salmonella* strains, through a combination of microbiological and innate immunological phenomena (Van Immerseel et al., 2005). From the literature and from earlier studies (Elanco, data on file), we can deduct that colonization of the caeca happens very rapidly after inoculation with the vaccine strain and that caecal levels gradually start to drop after a few days, to disappear around 21 days after vaccination. Berchieri and Barrow (1990) could show that inoculation of chicks within the first 24 h of placement with 10^8 cfu of an avirulent *Salmonella* strain resulted in 10^8 organisms found per gram of caecal content a day later; this level was maintained for at least 4 days.

Older studies have previously shown that a specific, locally induced (intestinal) IgA response offers protection against intestinal colonisation by *Salmonella* following challenge (Desmidt et al., 1998). The earlier a vaccine can be administered, the earlier the birds will be protected against exposure to field strains. This is the reason why producers of live vaccines recommend administration as early as 1-day-old. However, the small volumes of water drunk during the first days of a chick's life, combined with the long drinking water lines often found in poultry houses, sometimes makes it difficult to apply the necessary amount of vaccine over the course of two to four hours, as recommended by most manufacturers. As a consequence, the first dose of vaccine may not be administered on-farm until the birds are several days old as farmers may be concerned about sufficient uptake. In the study described here, vaccination took place over a much longer period than the recommended two to three hours. This was particularly important for birds vaccinated at 1- or 2-days-of-age, where there were concerns birds would not drink sufficient quantities during the vaccination period to enable uptake of appropriate levels of vaccine. A possible downside to prolonged administration is the potential loss of viability of the attenuated vaccine strains. However, despite the long application time, every single bird consumed sufficient volumes to enable detection of live vaccine strains in individual tissue samples (caecum and/or liver), and in all pooled fecal samples collected. Although the producers of live vaccines usually recommend administration of vaccines in drinking water over a short period of time, typically two to four hours, recent data confirm that AviPro^{TM} Salmonella DUO is stable in drinking water for over 12 h (RHConsultancy, UK, personal communication). This helps explain the good results obtained from birds vaccinated at 1- and 2-days-of-age.

Significantly higher levels of vaccine strains in caecal content were found in birds vaccinated earlier in life compared to birds vaccinated slightly later which is perhaps not unexpected as it is known younger birds are more susceptible to colonization by *Salmonella* than older birds (Shivaprasad et al., 2013). In newly-hatched chicks this may be a reflection of an undeveloped gut microbiome as well as an immature innate immune system (Barnes, 1972; Smith et al., 2008). Furthermore, day-of-hatch birds have been shown to be particularly susceptible to bacterial colonization even when there are potentially protective maternally-derived antibodies present (Cawthraw and Newell, 2010). These observations add weight to the idea of administering a live vaccine as early as possible, for reasons of both need and ease of uptake.

The comparatively high levels of vaccine in liver samples in birds vaccinated at 5-d.o. compared to birds vaccinated at 1-d.o. was unexpected, and it is not clear if this finding has any clinical or immunological relevance. Previous data on liver colonization of vaccinated birds were not gathered at such detail, and different vaccination ages of birds were not compared (Elanco, data on file). However, the fact that every bird had at least one positive tissue sample two days after vaccination shows that vaccine uptake was successful although there were differences in liver colonization patterns between the different age groups of birds.

The survivability of live vaccines in the drinking water line depends greatly on water quality and the cleanliness of the line and is easily compromised through unwanted substances or residues as a result of poor hygiene practices. However, the results obtained from this study show that good quality drinking water and/or the use of a stabilizer such as Aviblue supports the survival of AviPro^{TM} Salmonella DUO live vaccine for at least 12 h—long enough to allow all birds, even very young ones, sufficient time to drink enough for successful vaccine uptake. Diligent analysis of the quality of the drinking water and cleanliness of the lines are important considerations for satisfactory vaccination.

The efficacy of the product used in this trial when administered to one-day-old birds via oral gavage has been shown in several studies, for example (Gantois et al., 2006; Eekhout et al., 2018; Huberman et al., 2019), where the vaccinated birds proved to be protected in a challenge experiment. Hence, it was not deemed necessary to perform a challenge experiment, but to focus on the main question instead, which was the successful survival of the vaccine strains in the drinking water line over several hours and the successful uptake of the vaccine by the birds.

In conclusion, the results of this study show that the product AviPro^{TM} Salmonella DUO can be safely and successfully applied to layer pullets as early as 1-day-of-age, despite the necessity to vaccinate over several hours, as long as the quality of the drinking water is carefully monitored.

Data availability statement

The original contributions presented in this study are included in this article/**Supplementary material**, further inquiries can be directed to the corresponding author.

Ethics statement

Ethical approval was not required for the study involving animals in accordance with the local legislation and institutional requirements because the local Ethical Review board (at APHA) were aware of the work and deemed formal review was not required. No experimental procedures were undertaken. The study was a field trial of a vaccine currently licensed for use within the target host (chickens). Normal vaccinal regimes used by the layer industry were followed. Birds would have been vaccinated regardless of this study.

Author contributions

SC: Conceptualization, Data curation, Formal Analysis, Investigation, Methodology, Supervision, Writing – original draft, Writing – review & editing. AG: Methodology, Supervision, Writing – review & editing. TH: Investigation, Writing – review & editing. IR: Investigation, Writing – review & editing. LC: Investigation, Writing – review & editing. DM-D: Conceptualization, Writing – original draft, Writing – review & editing.

Funding

The authors declare financial support was received for the research, authorship, and/or publication of this article. This work was funded by the Elanco Animal Health.

Conflict of interest

APHA was funded by Elanco Animal Health on a commercial basis to undertake this work investigating one of their products. SC, TH, IR, and LC were employed by APHA. AG and DM-D were employed by Elanco.

Publisher's note

All claims expressed in this article are solely those of the authors and do not necessarily represent those of their affiliated organizations, or those of the publisher, the editors and the reviewers. Any product that may be evaluated in this article, or claim that may be made by its manufacturer, is not guaranteed or endorsed by the publisher.

Supplementary material

The Supplementary Material for this article can be found online at: https://www.frontiersin.org/articles/10.3389/fmicb.2023.1327739/full#supplementary-material

References

Barnes, E. M. (1972). The avian intestinal flora with particular reference to the possible ecological significance of the cecal anaerobic bacteria. *Am. J. Clin. Nutr.* 25, 1475–1479. doi: 10.1093/ajcn/25.12.1475

Berchieri, A., and Barrow, P. A. (1990). Further studies on the inhibition of colonization of the chicken alimentary tract with *Salmonella typhimurium* by pre-colonization with an avirulent mutant. *Epidemiol. Infect.* 104, 427–441. doi: 10.1017/s0950268800047440

Cawthraw, S. A., and Newell, D. G. (2010). Investigation of the presence and protective effects of maternal antibodies against *Campylobacter jejuni* in chickens. *Avian Dis.* 54, 86–93. doi: 10.1637/9004-072709-Reg.1

Desin, T. S., Koster, W., and Potter, A. A. (2013). *Salmonella* vaccines in poultry: Past, present and future. *Expert Rev. Vaccines* 12, 87–96. doi: 10.1586/erv.12.138

Desmidt, M., Ducatelle, R., Mast, J., Goddeeris, B., Kaspers, B., and Haesebrouck, F. (1998). Role of the humoral immune system in *Salmonella enteritidis* phage type four infection in chickens. *Vet. Immunol. Immunopathol.* 63, 355–367. doi: 10.1016/s0165-2427(98)00112-3

Eekhout, V., Haesebrouck, F., Ducatelle, R., and van Immerseel, F. (2018). Oral vaccination with a live *Salmonella enteritidis*/typhimurium bivalent vaccine in layers induces cross-protection against caecal and internal organ colonization by a *Salmonella infantis* strain. *Vet. Microbiol.* 218, 7–12. doi: 10.1016/j.vetmic.2018.03.022

European Food Safety Authority (2022). The European Union One Health 2021 zoonoses report. *EFSA J.* 20:e07666.

Gantois, I., Ducatelle, R., Timbermont, L., Boyen, F., Bohez, L., Haesebrouck, F., et al. (2006). Oral immunisation of laying hens with the live vaccine strains of TAD *Salmonella* vac E and TAD *Salmonella* vac T reduces internal egg contamination with *Salmonella enteritidis*. *Vaccine* 24, 6250–6255. doi: 10.1016/j.vaccine.2006.05.070

Huberman, Y. D., Velilla, A. V., and Terzolo, H. R. (2019). Evaluation of different live *Salmonella enteritidis* vaccine schedules administered during layer hen rearing to reduce excretion, organ colonization, and egg contamination. *Poult. Sci.* 98, 2422–2431. doi: 10.3382/ps/pez003

Lane, C. R., Lebaigue, S., Esan, O. B., Awofisyo, A. A., Adams, N. L., Fisher, I. S., et al. (2014). *Salmonella enterica* serovar enteritidis, England and Wales, 1945–2011. *Emerg. Infect. Dis.* 20:1097. doi: 10.3201/eid2007.121850

O'Brien, S. J. (2013). The "decline and fall" of nontyphoidal *Salmonella* in the United Kingdom. *Clin. Infect. Dis.* 56, 705–710.

Shivaprasad, H. L., Methner, U., and Barrow, P. (2013). "*Salmonella* infections in the domestic fowl," in *Salmonella* in domestic animals, eds P. Barrow and U. Methner, Vol. 2 (United Kingdom: CAB International, University of Nottingham), 162–192. doi: 10.1079/9781845939021.0162

Smith, C. K., AbuOun, M., Cawthraw, S. A., Humphrey, T. J., Rothwell, L., Kaiser, P., et al. (2008). Campylobacter colonization of the chicken induces a proinflammatory response in mucosal tissues. *FEMS Immunol Med Microbiol.* 54, 114–121. doi: 10.1111/j.1574-695X.2008.00458.x

Van Immerseel, F., Methner, U., Rychlik, I., Nagy, B., Velge, P., Martin, G., et al. (2005). Vaccination and early protection against non-host-specific *Salmonella* serotypes in poultry: Exploitation of innate immunity and microbial activity. *Epidemiol. Infect.* 133, 959–978. doi: 10.1017/S0950268805004711

World Health Organization (2015). *WHO estimates of the global burden of foodborne diseases: Foodborne disease burden epidemiology reference group 2007-2015 (World Health Organization)*. Geneva: WHO.

World Health Organization (2018). *Fact sheets: Salmonella* (non-typhoidal), Journal, Vol. 2023. Geneva: WHO.

Zhang-Barber, L., Turner, A. K., and Barrow, P. A. (1999). Vaccination for control of Salmonella in poultry. *Vaccine* 17, 2538–2545.

frontiers | Frontiers in Microbiology

TYPE Perspective
PUBLISHED 12 February 2024
DOI 10.3389/fmicb.2024.1307563

OPEN ACCESS

EDITED BY
Sébastien Holbert,
INRA Centre Val de Loire, France

REVIEWED BY
Nandkishor Bankar,
Datta Meghe Institute of Medical Sciences, India

*CORRESPONDENCE
Dayna M. Harhay
✉ dayna.harhay@usda.gov

RECEIVED 05 October 2023
ACCEPTED 25 January 2024
PUBLISHED 12 February 2024

CITATION
Katz TS, Harhay DM, Schmidt JW and Wheeler TL (2024) Identifying a list of *Salmonella* serotypes of concern to target for reducing risk of salmonellosis. *Front. Microbiol.* 15:1307563. doi: 10.3389/fmicb.2024.1307563

Identifying a list of *Salmonella* serotypes of concern to target for reducing risk of salmonellosis

Tatum S. Katz, Dayna M. Harhay*, John W. Schmidt and Tommy L. Wheeler

U.S. Department of Agriculture, Agricultural Research Service, Roman L. Hruska U.S. Meat Animal Research Center, Clay Center, NE, United States

There is an increasing awareness in the field of *Salmonella* epidemiology that focusing control efforts on those serotypes which cause severe human health outcomes, as opposed to broadly targeting all *Salmonella,* will likely lead to the greatest advances in decreasing the incidence of salmonellosis. Yet, little guidance exists to support validated, scientific selection of target serotypes. The goal of this perspective is to develop an approach to identifying serotypes of greater concern and present a case study using meat- and poultry-attributed outbreaks to examine challenges in developing a standardized framework for defining target serotypes.

KEYWORDS

non-typhoidal salmonellosis, *Salmonella enterica*, serotypes, machine learning, public health, epidemiology

1 Introduction

In the United States, non-typhoidal *Salmonella* (NTS) is the leading cause of bacterial foodborne illness (Centers for Disease Control and Prevention, 2023b) with $4.1 billion lost to NTS illness yearly (United States Department of Agriculture Economic Research Service, 2023). Despite numerous improvements in the control of *Salmonella* cross-contamination in food processing and production environments, NTS illness rates have not decreased in the last 20 years (Centers for Disease Control and Prevention, 2023c). This indicates that scientific understanding of NTS throughout affected food production and processing systems has not reached the level that enables effective control strategies.

A complicating factor in *Salmonella* control is the diversity of the genus. Consisting of two species and seven subspecies, *Salmonella* are further subtyped by serotyping, a phenotyping method which determines agglutination of the bacteria with antisera to identify antigenic variants (Grimont and Weill, 2007). Less than 2% of the >2,600 known serotypes consistently appear in reports on U.S. human infections (Issenhuth-Jeanjean et al., 2014; Centers for Disease Control and Prevention, 2023d). New information on genomic differences among *Salmonella* serotypes (den Bakker et al., 2011; Suez et al., 2013; Cheng et al., 2019; Rakov et al., 2019; Wang et al., 2020) has led to specifically targeting *Salmonella* that pose the greatest risk to human health, rather than broadly managing all *Salmonella* contamination. To this end, industry, academia, and government organizations have begun to focus research efforts on determining which serotypes to target and methods for rapidly identifying those serotypes of greater concern (Cohn et al., 2021; Chen et al., 2022; United States Department of Agriculture Food Safety and Inspection Service, 2022; Centers for Disease Control and Prevention, 2023a).

Analysis of epidemiological data may identify *Salmonella* serotypes with a greater impact on human health. A key original epidemiological analysis determined that there were significant differences among serotypes in their epidemiological outcomes by analysis of 1996 to 2006 FoodNet data (Jones et al., 2008). The Jones study presented a unique and practical approach based on retrospective, epidemiological data, but was limited to data collected from 10 states (representing 10–15% of the US population) over 11 years. Furthermore, FoodNet data consists of sporadic illnesses which are not necessarily part of an identified outbreak, and are not confirmed to be transmitted by food (Centers for Disease Control and Prevention, 2021). Given the evolving *Salmonella* regulatory landscape and the limitations of the Jones study, we have revisited this epidemiological analysis using new data and with a new goal: identification of serotypes to target for management to improve human health outcomes (which we will refer to throughout as "serotypes of concern" or SoC). In our analyses, we focus on salmonellosis outbreaks across the United States with a confirmed food transmission route utilizing the CDC's National Outbreak Reporting System (Centers for Disease Control and Prevention, 2023d). Accordingly, we present two different methods for analyzing CDC *Salmonella* outbreak data collected between 2009–2021 and attributed to meat and poultry (8,524 illnesses across 36 serotypes). During these analyses, we also identified several obstacles that complicate the conclusions made. The goals of this perspective, therefore, are to (1) suggest serotypes of concern associated with meat and poultry; (2) outline some of the obstacles and opportunities in determining SoC using epidemiological data.

2 Statistical approaches using epidemiological data

There is no consensus on what constitutes a SoC. The Jones study, while providing a powerful framework for examining differences across serotypes by epidemiological data, did not produce a definitive list of target serotypes (Jones et al., 2008). The USDA FSIS has identified their most commonly-detected serotypes Infantis, Enteritidis, and Typhimurium as Key Performance Indicators (KPIs), yet these together represented just 4.22% of *Salmonella* positive FSIS samples from 2020 to 2021, and 26% of all-cause sporadic illness isolates in 2020 (United States Department of Agriculture Food Safety and Inspection Service, 2022; Centers for Disease Control and Prevention, 2023a). Furthermore, much of the scientific literature on *Salmonella* virulence and host-pathogen interaction focuses on two of the highest-incidence serotypes (Typhimurium and Enteritidis), with little study devoted to other serotypes that contribute to most human illnesses in the US each year.

To provide an actionable list of SoC, quantitative validation is key. We define two major challenges to achieving this list: first, the list should be complete enough that targeting the serotypes included would result in decreasing salmonellosis to meet the DHHS Healthy People 2030 goals (U. S. Department of Health and Human Services, 2020) but concise enough to be actionable; and second, the determination of which epidemiological variables are critical for reducing outbreaks and illnesses. We have developed two methods for identifying SoC: a machine learning-based approach and a more classical, outlier-based approach. These approaches represent two extremes of statistical approaches to this problem: the machine learning approach is highly flexible and less constrained by researcher input, while the outlier approach brings together researcher input and quantitative validation in a simple decision rule. The results of both approaches were combined to create a priority SoC list that could be targeted for reducing U.S. illnesses attributed to chicken, turkey, pork, and beef.

2.1 Epidemiological data

Data representing all 50 U.S. states and Puerto Rico were downloaded from Centers for Disease Control's National Outbreak Reporting System (NORS) on 1/18/2023 (Centers for Disease Control and Prevention, 2023d). This dataset contained information on the confirmed or suspected food source, categorized following the Integrated Food Safety Analytics Collaboration (IFSAC) Food Categorization Scheme (Richardson et al., 2017), as well as the year of the first illness, the confirmed or suspected *Salmonella* serotype(s) responsible, and information on the outbreak including the number ill, number hospitalized, and number of deaths. We focus on outbreak-associated cases because we seek to identify those serotypes which cause systematic illness (i.e., we can examine source attribution as a variable) compared to serotypes which cause sporadic cases, where the source is generally unknown. Following data cleaning, including removal of observations with missing epidemiological, attribution, or etiology data, 694 out of 3042 outbreaks remained for analysis across all attributed sources (Supplementary material).

2.2 Machine learning approach

Detailed methods for both approaches are available in the Supplementary material, and all data and code generated for this study is available for free download at https://github.com/tatumskatz/serotypesOfConcern. Machine learning methods are especially useful for uncovering previously unnoticed trends and patterns in complex biological data since minimal assumptions have to be made about the data generation process (Bzdok et al., 2018). In this approach, we utilized an agglomerative nesting hierarchical cluster analysis (AGNES) to categorize serotypes as SoC or not (Supplementary material). Hierarchical cluster analysis proceeds by calculating the similarity between observations over multiple variables, and then using those similarity scores to group observations. Each observation starts off alone and is iteratively grouped with others based on distance (Altman and Krzywinski, 2017). After groups are created, the optimal number of groups is determined by assessing how similar the observations in a group are to each other and by maximizing within-group similarity while minimizing between-group similarity (Altman and Krzywinski, 2017). Once the optimal number of groups was determined, we then used expert knowledge to identify the group which contains the SoC so that any serotype in that group is classified as a SoC. By using a flexible, pattern-seeking approach

and allowing the researcher to only provide input at the very end, this method can potentially reveal new insights in this complex dataset.

2.2.1 Machine learning results

SoC were identified for meat overall and each commodity. In all cases, the Ward cluster method outperformed other methods and so was used to generate all clusters. Optimal number of groups ranged from 3 for meat overall, beef, chicken, and turkey to 4 for pork. Decision rules for categorizing serotypes as SoC varied by commodity: for meat overall, beef, chicken, and turkey "more than one outbreak in at least 2 years"; and for pork, "more than one outbreak in at least 2 years, or one outbreak with at least 7 hospitalizations in at least 2 years". The SoC lists also varied by commodity: SoC for the four commodities and meat overall are presented in Table 1. Notably, the list for chicken SoC included only Enteritidis (Supplementary Table 1). Further analysis showed that the large number of Enteritidis outbreaks attributable to chicken products appeared to overwhelm other outbreaks so that no other serotypes are identified. Conversely, commodities with fewer outbreaks overall, and beef especially, revealed unanticipated SoC including Dublin and Uganda. Comparisons of the epidemiological data of these serotypes with established outbreak serotypes such as Enteritidis and Typhimurium revealed similar values for outbreaks, illnesses, and hospitalizations within the beef commodity (Table 1, Figure 1).

2.3 Outlier approach

If the machine learning approach produces a "black box" decision rule, the outlier approach produces a "clear box" decision rule. Outliers have no single mathematical definition, but we can intuitively describe them as observations which are so different from the rest of the data that they seem to be generated by an entirely different process (Hawkins, 1980). To define an outlier, we must have an idea of what "normal" observations are; then, we can identify abnormal observations (Aggarwal, 2017). By allowing for an *a priori* model of a "normal" data generation process (i.e., what a "normal" outbreak looks like), we can incorporate expert knowledge into our SoC definition and still allow quantitative validation by generating a score for how outlied each "abnormal" serotype is. Outlier identification is challenging for a variety of reasons, but we meet a specific challenge for our serotype list: many outlier tests assume only one or two outliers exist (Aggarwal, 2017); yet, we do not want to pre-define the number of outliers. Therefore, we utilized an approach which defines outliers using quartiles. This method avoids specifying a distribution (which is challenging given the nature of the data) or number of outliers and instead calculates how different each observation is from the rest of the data. For our case study, we used the average outbreak size and hospitalization:illness ratio to determine target serotypes. This method is similar, and sometimes identical to, the way one might use a box-and-whisker plot to identify outliers (Aggarwal, 2017).

2.3.1 Outlier results

As with the machine learning method, the outlier method results varied by commodity. Outlier cutoffs for meat overall were an average outbreak size >60.60 individuals and a hospitalization to illness ratio of greater than 0.30; for beef and turkey, any serotype with an average outbreak size and hospitalization to illness ratio >0 were SoC; for chicken, an average outbreak size >14.50 and a ratio of >0; for pork, an average outbreak size >24.50 and a ratio >0.15 were SoC (Supplementary Table 2, Supplementary Figure 2). Serotypes identified as SoC for the four commodities and meat overall are presented in Table 1 and Figure 1.

2.4 Generating the serotypes of concern list

To generate our final list of SoC, any serotype that was identified by either the machine learning approach or the outlier approach was classified as a SoC (Table 1, Figure 1). Additionally, serotypes are marked as SoC for a given commodity if either approach identified it as such for that commodity. Combining the results of both methods results in a more holistic list, in alignment with our goals.

3 Obstacles and opportunities

3.1 Data limitations

Perhaps the most important limitation of our work is that NORS is a dynamic reporting system (reports can be modified, added, or removed at any time), so that future analyses may differ from ours due to the dynamic nature of the database. There are also limitations in the data available at the time of analysis. Outbreaks make up on average 10% of documented illnesses (Scallan et al., 2011; The Interagency Food Safety Analytics Collaboration, 2020), as such, this analysis does not take illnesses attributed to sporadic incidence into account, unlike the Jones study (Jones et al., 2008). Additionally, NORS is a voluntary reporting system and so does not represent all outbreaks in the U.S. Breaking down the data by specific source attribution commodities resulted in low sample sizes for some analyses. Beef and turkey for example, had few outbreak data ($n_{outbreaks} = 37$ and 31, respectively) and accordingly, more serotypes were identified for beef and turkey than chicken ($n_{outbreaks} = 96$) and pork ($n_{outbreaks} = 63$). If these data were parsed at the level of detail required for a business entity wanting to take actions in a specific production system, there are even less data available for analysis. Epidemiological data are naturally imperfect in that they contain information not just about the pathogen, but about the host and the environment as well. For example, Montevideo was identified as a beef SoC, yet the two largest beef-attributed Montevideo outbreaks can be traced back to a single caterer with a backyard chicken flock which may have contributed to the contamination of the beef prepared by the caterer (North Dakota Department of Health - Division of Disease Control, 2009). This final issue is challenging to tackle without parsing all individual outbreak reports, and there is not information at this level of detail for every outbreak. Researchers

TABLE 1 Summary statistics for identified serotypes of concern attributed to meat and poultry from the CDC NORS dataset.

Serotype	Number of outbreaks	Number of illnesses	Number of hospitalizations	Hospitalization to illness ratio	Proportion of total illnesses	Identifying approach	Commodity (ML approach)	Commodity (outlier approach)
Enteritidis	65	1,848	204	0.11	0.22	Both	Meat overall, beef, chicken, pork, turkey	Beef, turkey
Typhimurium	24	864	127	0.15	0.10	Both	Meat overall, beef, pork, turkey	Beef, chicken, turkey
I,4,[5],12:i:-	19	751	138	0.18	0.09	Both	Meat overall, pork, turkey	Beef, chicken, pork
Heidelberg	17	1,380	386	0.27	0.17	Both	Meat overall, turkey	Beef, chicken, turkey
Infantis	9	334	62	0.19	0.04	Both	Meat overall	Beef, chicken, pork
Newport	13	856	224	0.26	0.10	Both	Meat overall, beef	Beef, turkey
Uganda	5	67	11	0.16	0.01	Both	Beef	Beef
Braenderup	8	133	23	0.17	0.02	Outlier		Beef, chicken
Muenchen	4	119	6	0.05	0.01	Outlier		Beef, turkey
Montevideo*	4	441	3	0.01	0.05	Both	Meat overall	Beef, chicken
Javiana	5	113	46	0.41	0.01	Both	Meat overall	Chicken, turkey
Reading	3	375	133	0.35	0.05	Both	Turkey	Meat overall, turkey
Dublin	2	51	16	0.31	0.01	Both	Beef	Beef
Oranienburg	1	18	2	0.11	0.00	Outlier		Beef
Potsdam	1	9	1	0.11	0.00	Outlier		Beef
Thompson	5	166	19	0.11	0.02	Outlier		Chicken
Saintpaul	3	83	16	0.19	0.01	Both	Turkey	Chicken, turkey
Hadar	2	51	12	0.24	0.01	Both	Turkey	Turkey
Schwarzengrund	3	53	0	0.00	0.01	Outier		Pork, turkey
Anatum	2	12	1	0.08	0.00	Outlier		Turkey
Berta	2	65	8	0.12	0.01	Outlier		Pork, turkey
Total	197	7,789	1,216		0.95			

*See additional information in *Data Limitations*. Bolded serotypes were identified by CDC BEAM as moderate to high illness burden SoC for one or more of the four commodities on 08/29/2023.

10.3389/fmicb.2024.1307563

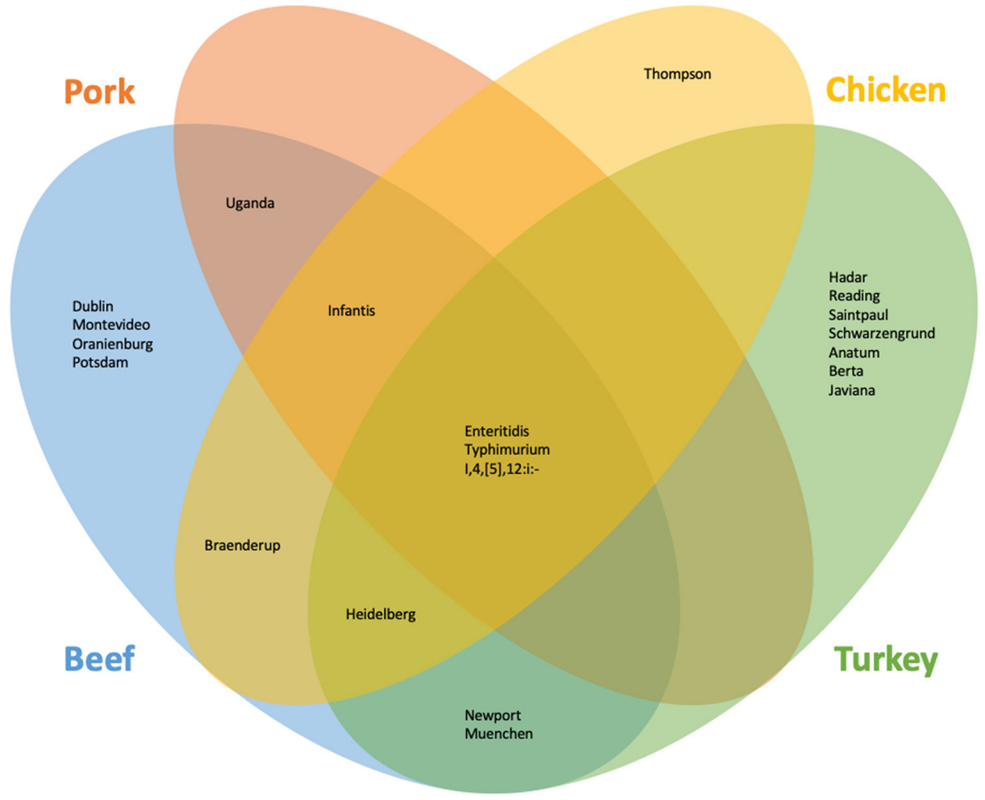

FIGURE 1
Serotypes identified as of concern using the machine learning and outlier approach for beef, chicken, pork, and turkey.

must be careful to be clear about the limits of their data as they identify SoC.

3.2 Machine learning is not a panacea

As expected, this case study did reveal candidate SoC that may have been "hidden" by traditional approaches. Many machine learning methods are rejected as "black boxes." That is, the methods are poorly documented to a degree that no critical analysis can be performed. This can be remedied by clearly and accurately explaining the techniques used that resulted in the final output. Machine learning tools should not be treated as a black box, rather, we must focus on replicability and clear communication of research.

3.3 The outlier approach requires many decisions

Unlike the machine learning approach, the outlier approach required two major decisions to be made: what variables to use and how to define an outlier. While these decisions were made using expert knowledge, we have limited tools to quantitatively validate them. This may be the greatest weakness of the outlier approach, but it is also its strength as we can seamlessly incorporate expert knowledge into our methods.

3.4 Other considerations

In addition to the above obstacles, the issues of what data to include and the role of pathogen evolution must be considered. Incidence alone is not enough for the determination of SoCs because most cases of salmonellosis are self-limiting with at-home care, and to improve human health we need to target the most "dangerous" types of *Salmonella*. Similarly, including death in the SoC definition may also bias results because salmonellosis is usually not the only factor contributing to a death outcome—comorbidities are often present (Cummings et al., 2010). Therefore, we instead propose the inclusion of a measurement of disease severity (i.e., hospitalization to infection ratio) or another metric of pathogenicity other than death in SoC definitions. Furthermore, while this list of SoC represents a snapshot of the current *Salmonella* epidemiological landscape, pathogens are constantly evolving. For example, the Infantis strain containing the pESI plasmid has become a highly successful strain that now dominates the *Salmonella* isolated from poultry at harvest in the U.S. (McMillan et al., 2022). In the earlier 20th century, successful control of serotype Gallinarum likely led to the emergence of Enteritidis as a dominant serotype in poultry (Rabsch et al., 2000). When targeting serotypes, we must be cautious to include

evolutionary models to understand how best to manage them. Increased surveillance and re-visiting SoC definitions periodically will be required to help us stay ahead of *Salmonella* evolution. Finally, while serotyping has historically been instrumental in subtyping and understanding the diversity of *Salmonella*, evidence suggests that there are important differences even within serotypes (Cohn et al., 2021; Chen et al., 2022). As we move away from serotyping as the dominant subtyping method and toward genetics-based subtyping, ensuring "backwards compatibility" of new methods against SoC is key.

4 Conclusions

Defining a list of *Salmonella* serotypes to target to improve public health outcomes is a challenging yet critical task. Current approaches may oversimplify the true complexity of the *Salmonella* problem, leaving us to target only the most common serotypes. Yet, little evidence exists to suggest that control of the premier serotypes, such as Enteritidis or Typhimurium, will achieve the goal of decreasing *Salmonella* infection in humans. We developed frameworks for a quantitative, epidemiological method to define target serotypes for management and control and have produced a list of serotypes of concern (SoC) for the meat and poultry industry. The serotypes identified can be utilized by industry to target specific *Salmonella* and improves upon existing Key Performance Indicators by being epidemiologically validated. The development of rapid testing technologies, which target a suite of *Salmonella* serotypes based on shared features, could use this list as validation to ensure the tool will bring about the desired human health improvements. Further, using the code generated during this study and the CDC National Outbreak Reporting system, researchers and industry alike can tailor this analysis to their specific needs or update the analysis with new data over time.

New approaches to defining SoC must consider the holistic scope of host-pathogen-environment interactions, evolution, and comorbidities in the host while remaining scientifically and statistically supported. By incorporating these factors into new definitions of target serotypes, we believe there is great opportunity for advancing the control of *Salmonella* for the betterment of public health.

Data availability statement

Publicly available datasets were analyzed in this study. These data can be found here: Centers for Disease Control National Outbreak Reporting System and https://github.com/tatumskatz/serotypesOfConcern.

Author contributions

TK: Data curation, Formal analysis, Investigation, Methodology, Software, Visualization, Writing – original draft, Writing – review & editing. DH: Conceptualization, Methodology, Validation, Writing – review & editing. JS: Conceptualization, Writing – review & editing. TW: Conceptualization, Supervision, Writing – review & editing.

Funding

The author(s) declare financial support was received for the research, authorship, and/or publication of this article. This work was supported by funds from U.S. Department of Agriculture, Agricultural Research Service CRIS project 3040-42000-020-00D. This research was supported in part by an appointment to the Agricultural Research Service (ARS) Research Participation Program administered by the Oak Ridge Institute for Science and Education (ORISE) through an interagency agreement between the U.S. Department of Energy (DOE) and the U.S. Department of Agriculture (USDA). ORISE is managed by ORAU under DOE contract number DE-SC0014664.

Acknowledgments

The authors would like to thank Dr. Taylor Eisenstein with the Centers for Disease Control and Prevention, for assistance with accessing NORS data and review of the manuscript draft. We wish to thank Jody Gallagher for administrative support. We also thank the USDA-ARS *Salmonella* Grand Challenge. The use of product and company names is necessary to accurately report the methods and results; however, the United States Department of Agriculture (USDA) neither guarantees nor warrants the standard of the products, and the use of names by the USDA implies no approval of the product to the exclusion of others that may also be suitable. The USDA is an equal opportunity provider and employer.

Conflict of interest

The authors declare that the research was conducted in the absence of any commercial or financial relationships that could be construed as a potential conflict of interest.

Publisher's note

All claims expressed in this article are solely those of the authors and do not necessarily represent those of their affiliated organizations, or those of the publisher, the editors and the reviewers. Any product that may be evaluated in this article, or claim that may be made by its manufacturer, is not guaranteed or endorsed by the publisher.

Author disclaimer

All opinions expressed in this paper are the author's and do not necessarily reflect the policies and views of USDA, DOE, or ORAU/ORISE.

Supplementary material

The Supplementary Material for this article can be found online at: https://www.frontiersin.org/articles/10.3389/fmicb.2024.1307563/full#supplementary-material

References

Aggarwal, C. C. (2017). *Outlier Analysis*. 2nd ed. Yorktown Heights, New York: Springer. doi: 10.1007/978-3-319-47578-3

Altman, N., and Krzywinski, M. (2017). Points of significance: clustering. *Nat. Methods* 14, 545–546. doi: 10.1038/nmeth.4299

Bzdok, D., Altman, N., and Krzywinski, M. (2018). Points of significance: statistics versus machine learning. *Nat. Methods* 15, 233–234. doi: 10.1038/nmeth.4642

Centers for Disease Control and Prevention (2023c). *FoodNet Fast*. Available online at: https://www.cdc.gov/foodnet/foodnet-fast.html (accessed July 31, 2023).

Centers for Disease Control and Prevention (2021). *FoodNet Fast: Pathogen Surveillance Tool FAQ*. Available online at: https://www.cdc.gov/foodnet/foodnet-fast/faq-pathogen-surveillance.html (accessed December 13, 2023).

Centers for Disease Control and Prevention (2023a). *BEAM (Bacteria, Enterics, Amoeba, and Mycotics) Dashboard*. Available online at: https://www.cdc.gov/ncezid/dfwed/BEAM-dashboard.html (accessed August 31, 2023).

Centers for Disease Control and Prevention (2023d). *National Outbreak Reporting System*. Available online at: https://www.cdc.gov/nors/index.html (accessed August 31, 2023).

Centers for Disease Control and Prevention (2023b). *Foodborne Germs and Illnesses*. Available online at: https://www.cdc.gov/foodsafety/foodborne-germs.html (accessed August 31, 2023).

Chen, R., Cheng, R. A., Wiedmann, M., and Orsi, R. H. (2022). Development of a genomics-based approach to identify putative hypervirulent nontyphoidal salmonella isolates: salmonella enterica serovar saintpaul as a model. *mSphere* 7:e00730–21. doi: 10.1128/msphere.00730-21

Cheng, R. A., Eade, C. R., and Wiedmann, M. (2019). Embracing diversity: differences in virulence mechanisms, disease severity, and host adaptations contribute to the success of nontyphoidal salmonella as a foodborne pathogen. *Front. Microbiol.* 10:1368. doi: 10.3389/fmicb.2019.01368

Cohn, A. R., Cheng, R. A., Orsi, R. H., and Wiedmann, M. (2021). Moving past species classifications for risk-based approaches to food safety: salmonella as a case study. *Front. Sustain. Food Syst.* 5:652132. doi: 10.3389/fsufs.2021.652132

Cummings, P. L., Sorvillo, F., and Kuo, T. (2010). Salmonellosis-related mortality in the United States, 1990-2006. *Foodborne Pathog. Dis.* 7, 1393–1399. doi: 10.1089/fpd.2010.0588

den Bakker, H. C., Moreno Switt, A. I., Govoni, G., Cummings, C. A., Ranieri, M. L., Degoricija, L., et al. (2011). Genome sequencing reveals diversification of virulence factor content and possible host adaptation in distinct subpopulations of Salmonella enterica. *BMC Genom.* 12, 1–11. doi: 10.1186/1471-2164-12-425

Grimont, P. A. D., and Weill, F.-X. (2007). "Antigenic formulae of the Salmonella serovars," in *WHO Collaborating Centre for Reference and Research on Salmonella*, 1–166.

Hawkins, D. M. (1980). *Identification of Outliers*. Dordrecht: Springer Netherlands doi: 10.1007/978-94-015-3994-4

Issenhuth-Jeanjean, S., Roggentin, P., Mikoleit, M., Guibourdenche, M., De Pinna, E., Nair, S., et al. (2014). *Supplement 2008-2010 (no. 48) to the White-Kauffmann-Le Minor scheme 2 3 4*. Available online at: http://www.pasteur.fr/sante/clre/cadrecnr/salmoms/WKLM_En.pdf (accessed July 18, 2023).

Jones, T. F., Ingram, L. A., Cieslak, P. R., Vugia, D. J., Tobin-D'Angelo, M., Hurd, S., et al. (2008). Salmonellosis outcomes differ substantially by serotype. *J. Infect. Dis.* 198, 109–114. doi: 10.1086/588823

McMillan, E. A., Weinroth, M. D., and Frye, J. G. (2022). Increased prevalence of salmonella infantis isolated from raw chicken and Turkey products in the united states is due to a single clonal lineage carrying the pESI Plasmid. *Microorganisms* 10:1478. doi: 10.3390/microorganisms10071478

North Dakota Department of Health - Division of Disease Control (2009). *The Pump Handle Archives*. Available online at: https://gcc02.safelinks.protection.outlook.com/?url=http%3A%2F%2Fndhealth.gov%2Fdisease%2FNewsletters%2FPumpHandleArchives%2F06-09.pdfanddata=05%7C01%7CTatum.Katz%40usda.gov%7C2f873ab009eb4b191fff08dbaa5a62f5%7Ced5b36e701ee4ebc867ee03cfa0d4697%7C1%7C0%7C638291077910762205%7CUnknown%7CTWFpbGZsb3d8eyJWIjoiMC4wLjAwMDAiLCJQIjoiV2luMzIiLCJBTiI6Ik1haWwiLCJXVCI6Mn0%3D%7C3000%7C%7C%7Candsdata=loqvhtb1nFkGPuLNQwMiJPHGgUEDsKFRY%2BSwnz7Rwm8%3Dandreserved=0 (accessed August 31, 2023).

Rabsch, W., Hargis, B. M., Tsolis, R. M., Kinglsey, R. A., Hinz, K.-H., Tschäpe, H., et al. (2000). Competitive exclusion of *Salmonella* enteritidis bysalmonella gallinarum in poultry. *Emerg. Infect. Dis.* 6:443. doi: 10.3201/eid0605.000501

Rakov, A. V., Mastriani, E., Liu, S. L., and Schifferli, D. M. (2019). Association of Salmonella virulence factor alleles with intestinal and invasive serovars. *BMC Genom.* 20, 1–14. doi: 10.1186/s12864-019-5809-8

Richardson, L. C., Bazaco, M. C., Parker, C. C., Dewey-Mattia, D., Golden, N., Jones, K., et al. (2017). An updated scheme for categorizing foods implicated in foodborne disease outbreaks: a tri-agency collaboration. *Foodborne Pathog. Dis.* 14, 701–710. doi: 10.1089/fpd.2017.2324

Scallan, E., Hoekstra, R. M., Angulo, F. J., Tauxe, R. V., Widdowson, M.-A., Roy, S. L., et al. (2011). Foodborne illness acquired in the United States—major pathogens. *Emerg. Infect. Dis.* 17, 7–15. doi: 10.3201/eid1701.P11101

Suez, J., Porwollik, S., Dagan, A., Marzel, A., Schorr, Y. I., Desai, P. T., et al. (2013). Virulence gene profiling and pathogenicity characterization of non-typhoidal salmonella accounted for invasive disease in humans. *PLoS ONE* 8:e58449. doi: 10.1371/journal.pone.0058449

The Interagency Food Safety Analytics Collaboration (2020). *Foodborne illness source attribution estimates for 2018 for Salmonella, Escherichia coli O157, Listeria monocytogenes, and Campylobacter using multi-year outbreak surveillance data, United States*. GA and D.C. Available online at: https://www.cdc.gov/foodsafety/ifsac/projects/index.html (accessed July 19, 2023).

United States Department of Agriculture Economic Research Service (2023). *Cost Estimates of Foodborne Illness*. Available online at: https://www.ers.usda.gov/data-products/cost-estimates-of-foodborne-illnesses/ (accessed July 31, 2023).

United States Department of Agriculture Food Safety and Inspection Service (2022). *USDA FY 2022-2026 Food Safety Key Performance Indicator*. Available online at: https://www.fsis.usda.gov/sites/default/files/media_file/2022-06/FY2022-2026_Salmonealla_KPI_One-Pager.pdf (accessed December 19, 2023).

U. S. Department of Health and Human Services (2020). *Reduce infections caused by Salmonella—FS-04*. Heal. People 2030. Available online at: https://health.gov/healthypeople/objectives-and-data/browse-objectives/foodborne-illness/reduce-infections-caused-salmonella-fs-04 (accessed August 29, 2023).

Wang, M., Qazi, I. H., Wang, L., Zhou, G., and Han, H. (2020). Salmonella virulence and immune escape. *Microorganisms* 8:407. doi: 10.3390/microorganisms8030407

frontiers | Frontiers in Microbiology

TYPE Original Research
PUBLISHED 21 March 2024
DOI 10.3389/fmicb.2024.1342887

OPEN ACCESS

EDITED BY
George Grant,
University of Aberdeen, United Kingdom

REVIEWED BY
Na Zhang,
Harbin University of Commerce, China
Sundus Javed,
COMSATS University,
Islamabad Campus, Pakistan

*CORRESPONDENCE
Margie D. Lee
✉ mlee2@vt.edu

RECEIVED 22 November 2023
ACCEPTED 19 February 2024
PUBLISHED 21 March 2024

CITATION
Maurer JJ, Cheng Y, Pedroso A, Thompson KK, Akter S, Kwan T, Morota G, Kinstler S, Porwollik S, McClelland M, Escalante-Semerena JC and Lee MD (2024) Peeling back the many layers of competitive exclusion.
Front. Microbiol. 15:1342887.
doi: 10.3389/fmicb.2024.1342887

Peeling back the many layers of competitive exclusion

John J. Maurer[1], Ying Cheng[2], Adriana Pedroso[2], Kasey K. Thompson[2], Shamima Akter[3], Tiffany Kwan[2], Gota Morota[1], Sydney Kinstler[1], Steffen Porwollik[4], Michael McClelland[4], Jorge C. Escalante-Semerena[5] and Margie D. Lee[3]*

[1]School of Animal Sciences, College of Veterinary Medicine, Virginia Polytechnic Institute and State University, Blacksburg, VA, United States, [2]Department of Population Health, University of Georgia, Athens, GA, United States, [3]Department of Biomedical Sciences and Pathobiology, College of Veterinary Medicine, Virginia Polytechnic Institute and State University, Blacksburg, VA, United States, [4]Department of Microbiology and Molecular Genetics, University of California, Irvine, Irvine, CA, United States, [5]Department of Microbiology, University of Georgia, Athens, GA, United States

Baby chicks administered a fecal transplant from adult chickens are resistant to *Salmonella* colonization by competitive exclusion. A two-pronged approach was used to investigate the mechanism of this process. First, *Salmonella* response to an exclusive (*Salmonella* competitive exclusion product, Aviguard®) or permissive microbial community (chicken cecal contents from colonized birds containing 7.85 Log_{10} *Salmonella* genomes/gram) was assessed *ex vivo* using a *S. typhimurium* reporter strain with fluorescent YFP and CFP gene fusions to *rrn* and *hilA* operon, respectively. Second, cecal transcriptome analysis was used to assess the cecal communities' response to *Salmonella* in chickens with low (≤5.85 Log_{10} genomes/g) or high (≥6.00 Log_{10} genomes/g) *Salmonella* colonization. The *ex vivo* experiment revealed a reduction in *Salmonella* growth and *hilA* expression following co-culture with the exclusive community. The exclusive community also repressed *Salmonella*'s SPI-1 virulence genes and LPS modification, while the anti-virulence/inflammatory gene *avrA* was upregulated. *Salmonella* transcriptome analysis revealed significant metabolic disparities in *Salmonella* grown with the two different communities. Propanediol utilization and vitamin B12 synthesis were central to *Salmonella* metabolism co-cultured with either community, and mutations in propanediol and vitamin B12 metabolism altered *Salmonella* growth in the exclusive community. There were significant differences in the cecal community's stress response to *Salmonella* colonization. Cecal community transcripts indicated that antimicrobials were central to the type of stress response detected in the low *Salmonella* abundance community, suggesting antagonism involved in *Salmonella* exclusion. This study indicates complex community interactions that modulate *Salmonella* metabolism and pathogenic behavior and reduce growth through antagonism may be key to exclusion.

KEYWORDS

pathogen, exclusion, *Salmonella*, antimicrobials, competition, attenuation

Introduction

Day-of-hatch chicks are susceptible to clinical disease in response to *Salmonella* exposure (Gast and Beard, 1989); however, chicks challenged at 2 days of age are easily colonized but do not exhibit clinical disease symptoms (Cheng et al., 2015). Young chicks' intestinal microbiota contains low community diversity, with *Enterobacteriaceae* as a dominant bacterial group, indicating that the community may have a large niche for Gram-negative enterics (Lu et al., 2003; Ballou et al., 2016; Zhou et al., 2021). *Salmonella* colonization and *Enterobacteriaceae* abundance diminish with age as community diversity increases (Pedroso et al., 2021). Firmicutes and Actinomycetota become the abundant Gram-positive bacteria, while the Bacteroidetes, are the dominant Gram-negatives in the chicken intestinal microbiome as it matures (Lu et al., 2003; Xiao et al., 2017; Bhogoju et al., 2018; Khan et al., 2020). In the mature chicken, small intestinal and cecal intestinal compartments contain distinctly different communities (Lu et al., 2003; Choi et al., 2014; Xiao et al., 2017; Khan et al., 2020). This community segregation, however, does not occur until birds are approximately 3 weeks old (Lu et al., 2003), and at this time the abundance of intestinal *Salmonella* begins to decline (Cheng et al., 2015).

Day-of-hatch chicks exposed to a mature intestinal microbiota rapidly develop high community diversity (Pedroso et al., 2016) and are resistant to *Salmonella* infection and colonization (Nurmi and Rantala, 1973). One of the earliest examples of fecal transplants was done in chickens, where cecal bacteria from mature hens were shown to block *Salmonella* colonization in chicks (Nurmi and Rantala, 1973). This phenomenon was later termed competitive exclusion, even though it was not known whether competition (Fujikawa, 2016) was at the heart of the exclusion mechanism. Fecal transplants with the intestinal microbiota from adult chickens have also been shown to dramatically reduce *Salmonella* prevalence in broiler chickens in the field (Wierup et al., 1988; Hirn et al., 1992). Nurmi suggested that competitive exclusion may be attributed to: (1) competition for limiting nutrients; (2) competition for attachment sites on the mucosa; or (3) the production of antibacterial substances, including volatile fatty acids (VFAs) or bacteriocins (Nurmi et al., 1992). Another possibility is that competitive exclusion (4) modulates the virulence of the enteropathogens, reducing their ability to modify the intestinal environment or create a tissue reservoir to enable persistence (Watkins and Miller, 1983).

A great deal of culture-based and molecular studies have focused on identifying potential intestinal community members involved in pathogen exclusion. Most molecular studies have used a 16S census approach to characterize the intestinal microbiota (Stenkamp-Strahm et al., 2018; Pedroso et al., 2021; Valeris-Chacin et al., 2022; Falardeau et al., 2023). Candidate taxons have been identified that positively or negatively correlate with *Salmonella* abundance (Azcarate-Peril et al., 2018; Ding et al., 2021; Pedroso et al., 2021; Pottenger et al., 2023). However, the identified intestinal species have not been repeatedly encountered across studies, suggesting a multifactorial role (Pedroso et al., 2021). The key to pathogen exclusion likely involves a diverse microbial community exhibiting complex metabolic and inhibitory effects (Lone et al., 2013; Stanley et al., 2014; Zhang et al., 2015; Chopyk et al., 2016; Pedroso et al., 2021).

With the success of undefined, diverse intestinal communities in competitive exclusion, efforts led to the development of undefined intestinal communities free of any avian pathogens (Schneitz et al., 1991). Aviguard® is a competitive exclusion product derived from the cecal contents of adult hens that has been shown to be effective at reducing *Salmonella* and other enteropathogens in the intestine of chickens (Hofacre et al., 1998, 2000; Weschka et al., 2021). This competitive exclusion product has also been shown to promote intestinal development in young chicks (Lee et al., 2023a). Undefined intestinal communities used as competitive exclusion products have been limited in their distribution or application by regulatory agencies like the U.S. Food and Drug Administration (Lee et al., 2023b). This has turned emphasis toward the development of single or multiple microbial species formulations capable of excluding an animal pathogen (Khan et al., 2020). These microbes have either been isolated from the intestine (Pascual et al., 1999; Kubasova et al., 2019), chosen based on similarities with intestinal species (Nair et al., 2021), or based on microbial properties of competition or antagonism so as to be detrimental to the pathogen in question (Latorre et al., 2016).

While the chicken small intestine is rich in nutrients, *Salmonella* and other Proteobacteria are a minor population within the bacterial community in this environment (Lu et al., 2003; Wang et al., 2022). In chickens, *Salmonella*'s niche appears to be the cecum (Snoeyenbos et al., 1982). While this compartment, in comparison to the small intestine, is scarce in free sugars (Józefiak et al., 2004), *Salmonella* abundance can reach 10^7 cells per gram of cecal content (Cheng et al., 2015), despite the fact that the cecum expels its content daily. In general, Proteobacteria are not capable of degrading the fibers and mucin polysaccharides that are plentiful in the cecal compartment. They are therefore largely dependent on *Clostridia*, which are primary degraders capable of breaking down complex polysaccharides into free mono- and disaccharides that *Salmonella* and other scavengers can then metabolize. This scavenger activity would be able to occur through cooperation, in that members of the microbiota could provide nutrition for other members. However, the pathogen is in competition with other intestinal species for even these resources. One possible adaptation for this competition would be for *Salmonella* to metabolize fermentation end products produced by the primary degraders through respiration (Shelton et al., 2022). Their metabolism of these waste products would also help maintain an environment favorable to continued metabolism and growth for the primary degraders, illustrating another example of cooperation (Benoit et al., 2020). In ecological terms, intestinal member species can interact with *Salmonella* favorably or unfavorably through cooperation, competition, or antagonism (Hammarlund et al., 2021; Rogers et al., 2021). Some intestinal member species can only compete with *Salmonella* for the same limited resources by producing metabolites that suppress growth or kill their competitor through antagonism (Sibinelli-Sousa et al., 2022). Competitive exclusion therefore works by failing to support pathogen growth either through competition or antagonism, which has been the guiding principle of many groups in developing probiotics (Zhao et al., 2006; Maltby et al., 2013). Competition may only be effective under conditions where primary degraders and other member species stop feeding *Salmonella* nutrients that only it can metabolize, forcing it to compete for other resources equally metabolized by other intestinal community members.

Because the mechanism of competitive exclusion is currently unknown and is likely multifactorial, in this study, an *ex vivo* transcriptomic approach was used to reveal *Salmonella* physiology and behavior in response to permissive or exclusive communities. The

ex vivo approach would allow direct analysis of *Salmonella* transcriptional response even if their growth was inhibited. In addition, chickens were experimentally infected with *Salmonella*, and its abundance was quantified in order to allow *in vivo* analysis of the cecal microbial transcriptomes to identify community metabolism that favors or excludes *Salmonella*. These experiments revealed significant metabolic differences in *Salmonella*'s response to the intestinal community and vice versa; however, failure to metabolize liberated sugars or microbial metabolites did not fully account for the mechanism of exclusion by the *Salmonella* exclusive community. The chicken intestinal community was found to reduce pathogen behavior (attenuation) and metabolism (cooperation/competition) and produce antimicrobials that limit *Salmonella* growth (antagonism), suggesting that the mechanism of competitive exclusion was multifactorial.

Materials and methods

Experimental approach

The mechanism underlying competitive exclusion involves one of the principles of population biology: cooperation, competition, antagonism, or attenuation. Table 1 describes the research approach to identifying the role of each in the competitive exclusion of *Salmonella*. One methodological challenge, addressed by this research approach, was detecting *Salmonella* growth rate and transcriptional signal in low abundance in the cecal microbiota, whose abundance may exceed *Salmonella*'s by 1,000-fold (Cheng et al., 2015). Therefore, a non-culture-based approach was used to determine cecal community metabolism correlating with *Salmonella* abundance *in vivo* in chickens (Figure 1A) and *Salmonella* gene expression and growth *ex vivo*, in response to communities that "permit" or "exclude" *Salmonella* (Figure 1B). The permissive community used in the *ex vivo* experiments was acquired from the *in vivo* chicken experiment and consisted of cecal contents from 35-day-old birds with high *Salmonella* abundance (7.86 Log_{10} *Salmonella* genomes/g cecal content) (Pedroso et al., 2021). The exclusive community used in the *ex vivo* experiments was the commercially competitive exclusion product, Aviguard® (Lallemand Animal Nutrition; Montreal, Canada), which reduces *Salmonella* colonization in chickens by at least 5.0 Log_{10} CFU (Lee et al., 2023b).

The *ex vivo* system was developed to monitor *Salmonella* growth, virulence (SPI-1 expression), and gene expression (microarray) in response to the permissive and exclusive communities. The jellyfish green fluorescent protein variants, yellow fluorescent protein (*yfp*) and cyan fluorescent protein (*cfp*), were fused to *rrn* growth-dependent promoter and *hilA* operon (SPI-1 cell invasion locus), respectively, in *Salmonella*. Fluorescence associated with the YFP and CFP reporters was used to monitor *Salmonella* growth and SPI-1 virulence gene expression in co-culture with cecal communities *ex vivo*. The *Salmonella* reporter strain was grown in dialysis tubing in a simulated cecal medium, *Ex Vivo* Cecal Contents (EVCC), submerged in permissive or exclusive communities to enable collection of *Salmonella* cells for study even if there was poor growth. Initially, the fluorescent reporters were used to empirically determine the earliest time point at which the exclusive community had the most significant impact on *Salmonella* growth or virulence expression relative to the permissive community. Six-hour co-culture of the reporter strain with the communities was determined based on YFP brightness measured by flow cytometry. Cells were then harvested for gene expression (microarray) comparisons, and genes within metabolic pathways that were differentially expressed in permissive vs. exclusive communities were deleted in *Salmonella* using pGLOW, a fluorescent reporter visible in anaerobic conditions. *Salmonella* mutants' growth dynamics when co-cultured with the exclusive community were monitored continuously over 48 h using a fluorescence plate reader.

Table 1 also describes expected outcomes based on the roles of cooperation, competition, antagonism, or attenuation in the mechanism of *Salmonella* competitive exclusion with respect to the *in vivo* and *ex vivo* community transcriptomics and *Salmonella* response. The detailed methodology for each research approach is described in detail below (*in vivo*: "The cecal communities' transcriptome relative to *Salmonella* abundance"; *ex vivo*: "Assessing *Salmonella* growth rate and SPI-1 T3SS expression in an *ex vivo* system with permissive or exclusive communities," "Microarray analysis of *S.* Typhimurium YC 1104 reporter strain growth in permissive or exclusive microbial communities," and "Contribution of metabolic gene(s) to *Salmonella* Typhimurium growth in an exclusive community").

Construction of *Salmonella* reporter strains and mutants

λ Red (Datsenko and Wanner, 2000) was used to construct *rrn* and *iag* (SPI-1) reporters, tagged with jellyfish green fluorescent protein variants: yellow fluorescent protein (YFP) and cyan fluorescent protein (CFP), respectively (Heim and Tsien, 1996; Miyashiro and Goulian, 2007). The growth-dependent *rrn* promoter was cloned upstream of a "promoter-less" *yfp* in tandem with the chloramphenicol resistance marker *cat* (Supplementary Tables S1, S2). The *rrnB* P1 promoter was engineered into the forward primer targeting 5′ *yfp* with its ribosome binding site (RBS) (Supplementary Table S2). The reverse primer was initially designed with a 3′ overlap with *yfp* and the *rrnB*T12 transcriptional terminator, previously cloned downstream of *yfp* in plasmid pMG32 to create pMG32T1T2 (Supplementary Tables S1, S2). These primers, using pMG32T1T2 as template, were used to amplify *yfp*, now with *rrnB* P1 promoter and T1T2 transcriptional terminators. The resulting amplicon was cloned into pCR-XL-TOPO and subsequently subcloned into Π-dependent suicide vector pGP704 (Miller and Mekalanos, 1988) to create pCY01 (Supplementary Figure S1). The *rrnB*T1T1 was replaced with λT0 transcriptional terminator (pCY02), to which *cat* was introduced 3′ from this terminator by cloning amplicons with engineered restriction enzyme sites for directional cloning to generate the final plasmid pCY03 (Supplementary Tables S1, S2). PCR primers were designed to target a P22 insertion site, an intergenic site between *thrW* and STM0324, and contained overlap with the *rrn* promoter and *cat* sequences. These primers were used to amplify the reporter construct using pCY03 as template (Supplementary Figure S1; Supplementary Table S2). λ Red was used to introduce *Salmonella* growth reporter into a P22 integration site with the P22*att-rrnB* P1-*yfb-cat* amplicon (Datsenko and Wanner, 2000).

The *hilA* operon reporter using *cfp* was constructed as follows. Tetracycline resistance gene *tetA* was first introduced into the intergenic region between *iagB* and *sptP*, just 5′ of the transcriptional terminator for the *hilA* operon, using λ Red (Datsenko and Wanner, 2000), with primers described in Supplementary Table S2 and pKD3

TABLE 1 The mechanism underlying competitive exclusion.

Mechanism	*Salmonella* growth *in vivo*	Cecal community activities	Research approach	Expected outcomes
Cooperation	Dependent on community activity to provide nutritional resources	Provides essential resources for *high* *Salmonella* abundance	*Ex vivo* growth system (Figure 1A) 1. Monitor *Salmonella* abundance and virulence expression in the presence of permissive or exclusive communities 2. Monitor *Salmonella* expression by microarray analysis 3. Monitor *Salmonella* mutants' growth rates and growth dynamics *In vivo* chicken cecal colonization (Figure 1B) 1. Monitor *Salmonella* abundance (qPCR) 2. Perform cecal community transcriptomics	1. *Salmonella* growth and abundance will be higher in permissive vs. exclusive communities 2. *Salmonella*'s catabolic gene expression will reflect growth metabolism from nutrients provided by a permissive community vs. starvation response resulting from attempts to replicate in an exclusive community 3. Transcriptomes of cecal communities with high *Salmonella* abundance metabolically correlate with *ex vivo Salmonella* gene expression in the presence of a permissive community
Competition	Dependent on community metabolic activity to provide nutritional resources. However, the community also provides nutritional resources for multiple species of organisms	Provides essential resources but *Salmonella* abundance varies depending on abundance of competing species		1. Same Outcomes 1 and 2 for Cooperation 2. Cecal transcriptomes will differ within birds with differing *Salmonella* abundance 3. *Salmonella* metabolic mutants display growth defects within exclusive community
Antagonism	Dependent on community metabolic activity but abundance independent of nutritional resources	Provides essential resources varied *Salmonella* abundance Inhibitory behavior *low* *Salmonella* abundance		1. Same as Outcome 1 for Cooperation and Competition 2. *Salmonella*'s expression of stress response reveals production of antimicrobials by the exclusive community 3. Cecal communities' transcriptomes contain transcripts for antimicrobial synthesis bacteriocins or other antibacterial mechanisms, for example, Type 6 Secretion System, indicating antimicrobial activity in communities with low *Salmonella* abundance
Attenuation	Dependent on community metabolic activity but invasion provides additional resources	Provides essential resources varied *Salmonella* abundance Oxidative stress *high* *Salmonella* abundance		1. No difference in *Salmonella* growth *ex vivo* with either community 2. SPI-1 (invasion) repressed in *Salmonella* grown *ex vivo* with exclusive community 3. Cecal transcriptome contains transcripts associated with production of attenuating molecules such as butyrate or indole

to generate the amplicon used to transform *S. typhimurium* SL1344. *iagB* is the last gene in the *hilA* operon. The *tetA* was later replaced with a "promoter-less" *cfp* following transformation with the *cfp* amplicon generated with *iagB*, *sptB*, and *cfp* primers (Supplementary Table S2) and selection for fusaric acid resistance. Fusaric-resistant colonies were screened for tetracycline sensitivity (Bochner et al., 1980). P22 was used to move *rrnB* P1-*yfp-cat* into *Salmonella* strain with *hilA* operon-*cfp* reporter to construct the final *S. typhimurium* strain YC1104 with *yfp* growth and *cfp*, *hilA* operon reporters (Provence and Curtiss Iii, 1994).

λ Red was also used to create single and double mutations in metabolic pathways in *Salmonella* (Supplementary Tables S1, S2). P22 generalized transduction was used to introduce λ*red*-generated knockouts with intact antibiotic resistance gene cassettes into *S. typhimurium* SL1344 or SL1344 mutants before removing the antibiotic resistance marker with pCP20. YFP was replaced with pGLOW as a reporter of *Salmonella* growth (evocatal GmbH, Monheim am Rhein, Germany). This reporter was chosen because fluorescence is not oxygen-dependent (Drepper et al., 2007), which allows monitoring of *Salmonella* growth continuously under strictly anaerobic conditions. Electroporation was used to introduce plasmids into *Salmonella* strains (Dower et al., 1988).

Measuring YFP and CFP expression using fluorescence-activated cell sorting

Flow cytometry was conducted with a CyAn ADP Analyzer (Beckman Coulter; Brea, CA) using the software Summit (ver. 4.3, Beckman Coulter). The 468 nm excitation and FL1 530/30 BP filter

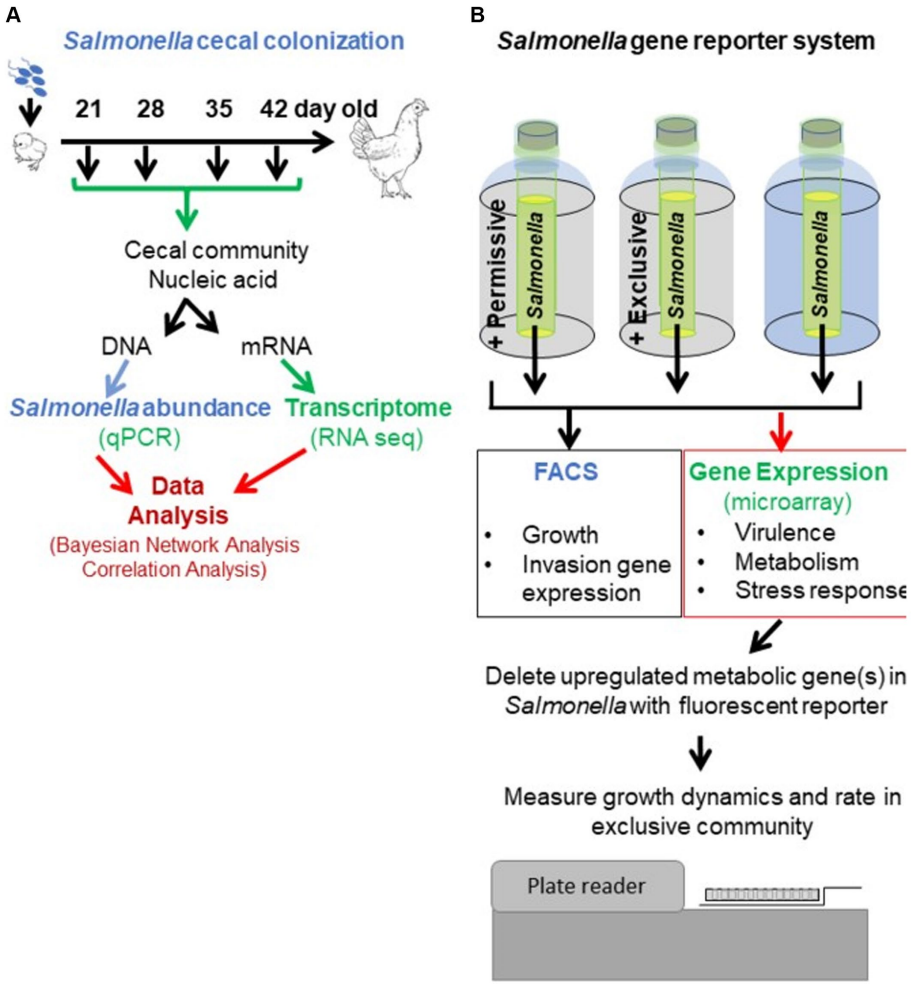

FIGURE 1
Experimental approach to revealing the mechanism of action of competitive exclusion. A two-prong approach involved determining cecal community metabolism relative to *Salmonella* abundance *in vivo* **(A)** and *Salmonella* expression in response to a permissive or exclusive community *ex vivo* **(B)**. In the *in vivo* study, 2-day-old, specific pathogen-free white leghorn chickens were orally administered *Salmonella* Typhimurium SL1344 (1×10^5 CFU). At different ages, chickens were sacrificed, the ceca were aseptically collected from each bird, and nucleic acids were extracted. *Salmonella invA* qPCR was used to determine *Salmonella* abundance in the cecal community samples. The cecal community RNA was sequenced and annotated using the MG-RAST pipeline. The *ex vivo* study focused on *Salmonella* response when grown microaerophilically in a simulated cecal medium, *Ex Vivo* Cecal Contents (EVCC), containing a permissive or exclusive community. A fluorescent *S. typhimurium* SL1344 *rrn* promoter::*yfp*, *hilA* operon::*cfp* reporter strain was placed within dialysis tubing, physically separate from the permissive or exclusive community, enabling the collection of *Salmonella* cells for analysis. Jellyfish green fluorescent protein variants YFP and CFP served as reporters for *Salmonella* growth and SPI-1 invasion gene reporter, respectively. Fluorescence was measured using fluorescence-activated cell sorting. The cecal community from a 35-day-old chicken with high *Salmonella* abundance served as the permissive community, while the exclusive community consisted of the cecal community comprising the competitive exclusion product Aviguard®. *Salmonella* grown in EVCC alone served as a control. Select *Salmonella* metabolic genes, upregulated in either or both communities, were deleted in a *S. typhimurium* SL1344 fluorescent reporter strain, and mutants were compared to the wild-type reporter strain for growth in the exclusive community.

were used for YFP detection. The 409 nm excitation and FL6 450/50 BP filter were used for detecting CFP. For each sample, a total of 20,000 events were collected. In some instances, samples were read multiple times to detect variations between sample collections. The flow cytometer reported fluorescence as median intensity values of arbitrary units. The cytometer flow rate was adjusted to keep the average event rate between 1,000 and 3,000 events per second to avoid coincidental detection of bacterial cells. Data were analyzed using FlowJo software (ver. 9.4, TreeStar, Inc.). Particles that did not fall into the expected size and shape of a bacterial cell were not included in the analyses. Positive (YFP, CFP; *Escherichia coli* with pMG32 or pMG34, respectively) and negative (*S. typhimurium* SL1344, wild-type strain) controls were included with every run.

Assessing *Salmonella* growth and SPI-1 T3SS expression in an *ex vivo* system with permissive or exclusive communities

The *ex vivo* study entailed the growth of *Salmonella* reporter strain YC1104 in the presence of a permissive or exclusive community. The *S. typhimurium* reporter strain has *rrn-yfp* and *hilA* operon-*cfp* chromosomal promoter fusions for monitoring growth and SPI-1 expression, respectively. This approach allowed for growth of *Salmonella* to cell densities and volumes to later harvest sufficient *Salmonella* mRNA for microarray analysis. The reporter strain is a derivative of *S. typhimurium* SL1344, the same wild-type strain used in the *in vivo* study (see below).

A medium was developed to mimic the luminal cecal nutritional environment, based on published literature, and contained porcine gastric mucin, uric acid, six amino acids (arginine, cysteine, isoleucine, lysine, methionine, and threonine), and phytone peptone. All amino acids, except cysteine, were at concentrations previously reported to be found in the chicken cecum (Babinszky et al., 2006). Uric acid was added at a concentration found in the cecal contents of white leghorn chickens (Beck and Chang, 1980). A redox indicator, resazurin, and a reducing agent, cysteine, were also added at concentrations to enhance anaerobiosis (Demain and Solomon, 1986). This *ex vivo* chicken cecal (EVCC) medium formulation is described in Supplementary Table S3. Stock solutions were made for resazurin (1,000×), hemin (1,000×), uric acid (100×, pH 8.8–9.0), and amino acid supplement (10×, pH 7). The pH of the basal medium was adjusted to 6.1 ± 0.1 prior to autoclaving. After the addition of uric acid and amino acid supplements, the final pH of the EVCC medium was approximately 6.5.

All cultures, media preparation, and dilutions were performed in an anaerobic glove box. Media and diluent were sparged with gas to make conditions microaerophilic. Autoclaved, 30-ml-capacity serum bottles (Fisher Scientific) with rubber stoppers served as culture vessels. About 20 mL of EVCC medium (Supplementary Table S3) was added to each vessel in an anaerobic cabinet, to which a *Salmonella* permissive (7.86 Log_{10} *Salmonella* genomes/g cecal contents) or exclusive community was added (Supplementary Figure S2). One culture vessel was left uninoculated (EVCC alone) (Supplementary Figure S2). The lyophilized Aviguard® product was rehydrated in sterile saline according to the manufacturer's recommendation. This product is generally administered to chickens in drinking water and has been shown to reduce *Salmonella* colonization by at least 5 Log_{10} in chickens (Lee et al., 2023b). Direct bacterial cell counts were determined microscopically at 1,000× magnification using a Petroff-Hausser counting chamber. The cell density of the starting material was estimated for both communities at 10^{11} cells/ml. The rehydrated Aviguard viability was determined by a LIVE/DEAD BacLight stain (Molecular Probes; Grand Island, NY). The viability of the commercial lots varied between 30 and 75%. Both communities were diluted 100-fold in sterile saline before adding 2 mL of this cell suspension to EVCC medium to generate a final cell density of 10^8 cells/ml. Spectrum™ (Fisher Scientific) cellulose ester membrane with 100,000 Daltons exclusion limit and 20 mm width served as the internal culture vessel for the *Salmonella* reporter. Approximately 80 mm of dialysis tubing was cut, rehydrated in sterile H_2O, and clamped at one end with a dialysis clip, pre-treated with 70% ethanol. The clamped end was placed in a serum bottle first, and the open dialysis end was pulled over the mouth of the bottle. The *Salmonella* reporter strain was prepared as follows. Strain YC1104 was grown anaerobically on MacConkey agar at 39°C for 48 h. A cell suspension was made from growth on the MacConkey agar plate in sterile saline to 0.2 OD (λ 600 nm) (~10^8 CFU/mL). The cell suspension was diluted 100-fold in sterile saline. Subsequently, 1 mL of the 100-fold dilution was used to inoculate 5 mL of EVCC medium (10^5 CFU/mL final cell density), which was transferred to the dialysis tubing. A rubber stopper and metal crimp were used to seal the vessel. A sterile syringe needle was used to sparge the vessel with a gas mix of 6% CO_2, 6% O_2, 85% N_2, and 3% H_2 or sample the dialysis tubing as depicted (Supplementary Figure S2). The oxygen concentration was chosen based on jellyfish green fluorescent proteins and its variants' requirements for oxygen to fluoresce (Heim et al., 1994) and the likely minimal oxygen tension necessary for supporting the microaerophile *Campylobacter jejuni* (Pennie et al., 1984), an abundant (8 Log_{10} CFU/g) bacterial species in the chicken cecum (Hue et al., 2011). The top was sealed with tape. Culture vessels were placed in an anaerobic jar, flushed with the same gas mix described previously, and incubated at 39°C to simulate the chicken's internal body temperature. This and subsequent samplings (see below) were all done within an anaerobe glove box. The dialysis tubing's exclusion limit allowed free exchange of metabolites, peptides, and proteins between *Salmonella* and the external microbial community. Due to the nature of the cellulose dialysis material and because the cecal anaerobic community may secrete cellulases, the integrity of the membrane during experimentation was determined earlier by incubating tubing containing just dextran blue with a cecal community grown anaerobically in EVCC for 24 h at 39°C. There was no visible leakage of the dextran blue into the external culture, confirming the integrity of the dialysis membrane. Culture vessels were incubated at 39°C. The *Salmonella* reporter strain was periodically sampled over time (3, 6, 9, 12, and 24 h) using a sterile needle and syringe to sample the dialysis tubing, and fluorescence was monitored by fluorescence-activated cell sorting (FACS) to empirically identify the best time point, for harvesting *Salmonella*, where growth or SPI-1 expression was significantly reduced in the exclusive community, compared to the permissive community and the uninoculated, EVCC control. 0.2 mL aliquots were added to cryotubes containing 40 µL of 60% sterile glycerol (12% final concentration) and stored at −80°C for later FACS analysis.

Microarray analysis of *Salmonella typhimurium* YC 1104 strain growth in permissive or exclusive microbial communities

Microarray analysis was used to assess *Salmonella*'s transcriptome response to microbial communities in the *ex vivo* system, as previously described, with the following modifications. *Salmonella* strain YC1104 was grown anaerobically on MacConkey agar at 39°C for 48 h. A cell suspension was made in 5-ml sterile saline from the MacConkey plate, adjusted to a cell density of 0.2 OD (λ 600 nm) (~10^8 CFU/mL). This cell suspension was used to inoculate 5 mL of EVCC medium (10^6 CFU/mL) and incubate anaerobically at 39°C for 12 h. Five milliliter of EVCC was inoculated with a 4-fold dilution of the 12 h culture to 10^7 CFU/mL and transferred to dialysis tubing. The higher cell density per dialysis volume was needed to provide a sufficient amount of *Salmonella* RNA for microarray analysis. This experiment was done in triplicate, where *Salmonella* was grown and harvested after 6-h incubation in EVCC alone or in EVCC with the permissive or exclusive community (Supplementary Figure S2). *Salmonella* grown in culture vessels with EVCC alone served as the comparison control in the microarray analysis. Total RNA was harvested from *Salmonella* grown in the dialysis tubing, and microarray analysis was performed as previously described (Cheng et al., 2015). Briefly, the samples were treated with 0.1 mL volume of 95% ethanol and 5% acidic phenol (pH 4.3), and total RNA was extracted using MasterPure Complete DNA and RNA purification kits (Epicentra; Madison, WI) and High Pure RNA isolation kit (Roche; Indianapolis, IN). The samples were subsequently treated two times with the Turbo DNA-free kit (Ambion; Austin, TX).

Salmonella-specific *hilA* PCR (Cheng et al., 2015) was used to confirm that RNA was free of contaminating DNA, and the quality and integrity of the RNA were evaluated by gel electrophoresis (Sambrook et al., 1989). Genomic *Salmonella* DNA served as a labeling and hybridization reference control. Hybridization and fluorescent labeling of RNA were performed as described by Fink et al. (2007). Microarray chips were scanned with a ScanArray 5,000 laser scanner (GSI Lumonics; Watertown, MA). The data were analyzed using QuantArray v.2.01 software, and background intensity was subtracted from spot boundary signal intensities to derive Cy3 and Cy5 median signal intensities. Differential gene expression and statistical significance were determined with the Significance Analysis of Microarrays software package (Stanford University).[1] The data were analyzed using paired Student's *t*-test, and statistical significance from multiple comparisons was determined by one-way analysis of variance followed by Bonferroni posttest, with statistically significant *p*-values set at <0.001.

Contribution of metabolic gene(s) to *Salmonella* Typhimurium growth in an exclusive community

Mutant or wild-type strains, with the pGLOW reporter, were grown in EVCC + Aviguard. Oxyrase (Sigma-Aldrich; St. Louis, MO) was added to the medium (1:20 final dilution) and overlaid with mineral oil to create low oxygen conditions. *Salmonella* starting cell density was 10^5 CFU/mL. The lyophilized Aviguard was reconstituted as recommended by the manufacturer (Lallemand Animal Nutrition) in sterile saline with Oxyrase and used to inoculate EVCC cecal medium (1:20 dilution) (7.99 Log_{10} viable cells/mL). The viability of the rehydrated Aviguard was determined microscopically using LIVE/DEAD BacLight stain (Molecular Probes). Sterile 96-well, black-walled polystyrene microtiter plates with a clear bottom (Fisher Scientific) were used to monitor *Salmonella* fluorescence with a BioTek Synergy HT 96-well fluorescence microtiter plate reader at 37°C. A filter was added to the BioTek Synergy HT fluorescent plate reader (BioTek; Winooski, VT) to record pGLOW fluorescence based on its excitation frequency (Drepper et al., 2007). Fluorescence was recorded every 30 min. Strains were run in triplicate.

The cecal communities' transcriptome relative to *Salmonella* abundance

The *in vivo* study involved oral administration of *Salmonella* Typhimurium SL1344 (1×10^5 CFU) to 2-day-old, specific pathogen-free (certified *Salmonella*-free), white leghorn chickens (Charles River Laboratories; Wilmington, MA; $n = 100$), dispersed into five HEPA-filtered isolator units with wire mesh floors to reduce re-exposure due to coprophagy. To ensure birds were *Salmonella*-free, day-of-hatch chicks and their isolator environment were also tested for *Salmonella* by enrichment (Pedroso et al., 2021). Chicks and their environment were culture-negative for *Salmonella*. The birds were fed a non-medicated, commercial starter feed *ad libitum*. The bird density per isolator unit was reflective of commercial standards; culling birds was necessary periodically to maintain this stocking density. No probiotic(s), competitive exclusion product, or cocktail of intestinal bacterial species was administered to chickens in this study. One bird from each of five isolator units ($n = 5$) was collected at 21, 28, 35, and 42 days of age, euthanized, and the ceca was aseptically obtained. One bird in isolator 5 died after day 35, and therefore, there were only four subjects for day 42. *Salmonella invA* qPCR was used to enumerate *Salmonella* present in cecal DNA as previously described (Pedroso et al., 2021). Nucleic acid was extracted from cecal bacteria using the Mo Bio Soil DNA extraction kit, vortexing samples with glass beads at maximum speed for 40 min (Lu et al., 2003). Lysate was treated with 0.5% SDS and proteinase K (0.1 mg/mL) at 37°C for 30 min before phenol–chloroform–isoamyl alcohol (25:24:1) extraction. Sample nucleic acid was portioned equally, one being stored at −80°C for RNA purification (see below) and the other treated with DNAse-free RNase for *Salmonella* qPCR.

RNAse-free DNAse was added to nucleic acid (Pedroso et al., 2021) for each sample ($n = 19$) and incubated at 37°C. The quality and quantity of RNA were assessed by agarose gel electrophoresis. PCR, using universal 16S rRNA primers (Supplementary Table S2; Suzuki et al., 2000), assessed and confirmed that the RNA was free of DNA. Nucleic acid preps were repeatedly treated with RNAse-free DNAse until no PCR amplicon was detected to confirm RNA purity. Ribosomal RNA was removed using the MICROBExpress™ Additional rRNA removal was performed until samples were free of the detectable 23S and 16S rRNA bands (2.9 and 1.5 Kb, respectively) on an agarose gel. Finally, the Bacterial mRNA Enrichment Kit (Thermo Fisher Scientific; Waltham, MA) was used to further purify and concentrate cecal community mRNA, as described by the manufacturer's instructions. mRNA was submitted to the Georgia Genomics and Bioinformatics Core for sequencing using RNA-seq (Illumina; San Diego, CA). The resulting sequence reads were uploaded to the MG-RAST server for annotation (Keegan et al., 2016).

Carbohydrate and volatile fatty acid analysis of the chicken cecum

In order to reveal carbohydrates present in the cecal glycome of a permissive community, two samples with high (7.20 Log_{10} *Salmonella* genomes/g) vs. low *Salmonella* abundance (5.85 Log_{10} *Salmonella* genomes/g) were submitted to the University of Georgia Complex Carbohydrate Center for glycome analysis. Glycosyl composition analysis was performed by combined gas chromatography–mass spectrometry (GC–MS) of the per-O-trimethylsilyl (TMS) derivatives of the monosaccharide methyl glycosides produced by acidic methanolysis as previously described (Santander et al., 2013). GC–MS analysis of the resulting TMS methyl glycosides was performed on an Agilent 7890A GC interfaced to a 5975C MSD (Agilent; Santa Clara, CA), using a Supelco Equity-1 fused silica capillary column (30 mm × 0.25 mm, internal diameter).

Because some short-chain fatty acids can attenuate *Salmonella* virulence, inhibit, or promote pathogen growth (Kwon and Ricke, 1999; Zhang S. et al., 2020; Zhang Z.J. et al., 2020), cecal contents were obtained from two birds with high *Salmonella* abundance (7.00 Log_{10}

1 http://statweb.stanford.edu/~tibs/SAM/

Salmonella genomes/g cecal contents, 8.51 Log_{10} *Salmonella* genomes/g cecal contents). VFA analysis was performed by combined gas chromatography–mass spectrometry (GC–MS) of the butyl ester derivatives produced from the samples. The cecal contents were lyophilized and subsequently suspended in hexane, to which octadecane was added as an internal standard. Butyl esters were prepared by adding BF_3-1-butanol to the sample and heating it at 100°C for 2 h in a sealed tube. The reaction was subsequently quenched with 1–2 mL H_2O. The aqueous layer was discarded, and the organic phase was washed once with an equal volume of H_2O. The organic layer was then used for GC–MS analysis, performed using HP 6890 GC (Agilent) interfaced to a 5975b MSD (Agilent) using an All Tech EC-1 fused silica capillary column (30 mm × 0.25 mm) (Fisher Scientific). A mixture containing known concentrations of VFAs and octadecane was treated under the same conditions and served as standards for quantification.

Network and statistical analyses of chicken cecal meta-transcriptomes for cecal communities with high or low *Salmonella* abundance

Chicken cecum transcriptome read counts were normalized as a percentage of total reads for the MG-RAST categories KO metabolism, COG metabolism, virulence, and stress response. Enzymes were mapped and counted in the raw data set for sequence reads through Python version 3.7 (Ekmekci et al., 2016). These counted reads were merged in R through scripting, and then calculated as the percentage of these reads against total reads in Python to create a data set with normalized read counts of all enzymes in all samples. The read count data were edited, transposed, combined with *Salmonella* abundance, associated with individual samples, and filtered according to abundance from highest to lowest. The mean value of *Salmonella* abundance was calculated, and the value above the mean (5.85 Log_{10} *Salmonella* genomes/g cecal contents) was considered high abundance; a value equal to or below the mean was considered low abundance.

For analysis of the fermentation meta-transcriptome, the data set was first limited to 45 enzymes associated with fermentation in the KO data set, listed in Supplementary Table S5. This data set was expanded to 164 enzyme transcripts to include the enzymes listed in Supplementary Table S6. In the analysis of the microbiome's stress response, data were pulled from stress response and virulence data sets and categorized into groups based on function ascribed to the enzyme, for example, DnaK and heat shock, and consolidated into the individual categories. Two hundred thirty-four enzymes extracted from these data sets included those associated with the following categories: heat shock; carbon starvation; extra-cytoplasmic/envelop stress response; regulation; translation and protein export; oxidative stress; osmotic shock; acid tolerance; iron metabolism; antimicrobials; miscellaneous; and polyketide synthesis (Supplementary Table S7).

Bayesian network analysis was performed in R with the bnlearn package (Friedman et al., 2013; Scutari and Denis, 2021). Bayesian network analysis is a probabilistic model in which a graph structure represents a qualitative dependency relationship among random variables and a conditional probability expresses a quantitative link between individual variables. This method is comparable to approaches used to infer gene regulatory networks based on microarray or RNA-seq data and represents a directed edge connecting two genes used to determine a biochemical process such as a reaction, transformation, interaction, activation, or inhibition. The arc or arrows represent the probability of connectivity. A graph structure showing dependency relationships between nodes, obtained from a collection of conditional probabilities, defines the model (Ebana and Furukawa, 2019). The conditional probability with the state of the node close to the arrow propagates through the arrow one after the other. The probability of each node is used to generate the graph structure. The effective final network produced automatically from the data indicates the impact and the association link between the data. The strength of probabilistic links, reflected by the arc of a connection, was measured and presented.

Several different network models were used, including the score-based learning algorithm—Hill-Climbing (HC) (Friedman et al., 2013); constraint-based structure learning algorithms—Max–Min Parents and Children (MMPC) (Lagani and Tsamardinos, 2010); hybrid structure learning algorithms—Max–Min Hill-Climbing (MMHC) (Song et al., 2022), Hybrid Parents and Children (H2PC) (Anonymous, 2021), and General 2-Phase Restricted Maximization (RSMAX2) (Yu et al., 2019) to identify a common network structure for the various enzymes or categories described. Among all these implemented algorithms, HC performed best and produced the highest number of connections with various data sets. Therefore, for model fitting, a network structure was inferred using the Hill-Climbing approach, and the quality of the fit was evaluated using the Bayesian information criterion (BIC). The HC algorithm trains the network in a score-based "greedy search" (Scutari et al., 2019). This algorithm ranks network architectures based on the increase/decrease in BIC score induced by the removal of the arc. The network score was used to build arcs connecting two nodes if there were direct relationships between them. The arc strength value >0.5 was considered reliable. Illogical arcs were "blacklisted" and excluded from analysis to improve model fitting and avoid circular structure in the structure learning process (Ebana and Furukawa, 2019).

A more detailed analysis was performed at the individual enzyme level for those enzymes associated with carbohydrate metabolism, fermentation/respiration, antimicrobials, and stress response (Supplemental Cecal Transcriptome Data Set; $n = 598$). Pearson and Spearman-rank correlations were determined for enzyme transcript abundance compared to *Salmonella* abundance. Significance was given to Pearson or Spearman r or ρ values >0.6999 or < −0.6999 and *p*-values <0.05.

The identity of enzyme transcripts, with network connections or statistically significant correlation with *Salmonella* abundance, was determined by BLAST search at the nucleotide level (Altschul et al., 1990). Species or genus were assigned to the enzyme transcript if there was ≥99% coverage and 98–100% sequence match. Some matches based on these criteria identified *Clostridia* yet to be classified, which were assigned strain name or descriptor of the matching deposited sequence or genome.

Results

Salmonella growth and expression of virulence genes were reduced in the presence of an exclusive community

A fluorescence-reporter system was developed to monitor the *Salmonella* response to permissive and exclusive communities *ex vivo*.

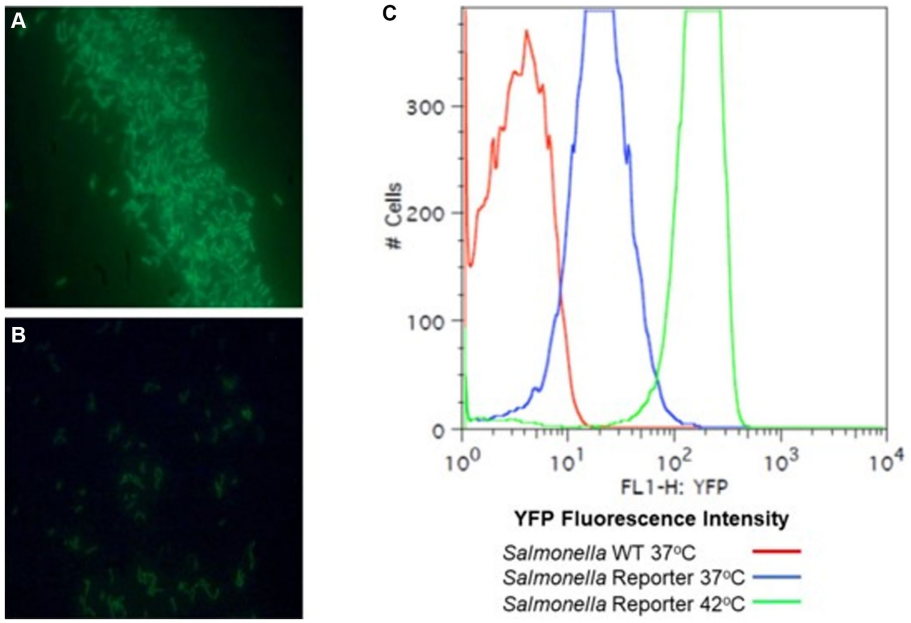

FIGURE 2
A *rrn* promoter jellyfish yellow fluorescent protein (YFP) gene fusion as a reporter for *Salmonella* growth. Lambda red was used to construct *rrn* tagged with YFP. The *rrn* promoter was cloned upstream of a "promoter-less" *yfp* and in tandem with *cat*. PCR primers were designed to overlap with the target insertion site, an intergenic site between *thrW* and STM0324. The λ Red system (Datsenko and Wanner, 2000) was used to introduce this reporter into *S. enterica* Typhimurium SL1344. *S. typhimurium* SL1344 strain YC1104 with the *rrn-yfp* reporter was grown aerobically to OD 1.0, λ 600 nm, in LB broth **(A)** or M9 minimal medium with 0.4% glycerol as a carbon source **(B)** with aeration and observed with a fluorescence microscope. **(C)** Fluorescence-activated cell sorting (FACS) analysis of the *Salmonella rrn-yfp* reporter strain grown aerobically, in LB broth to mid-exponential phase (OD 0.5, λ 600 nm) at 37°C or 42°C to demonstrate fluorescence intensity with a high growth rate.

The growth-dependent promoter for rRNA operon, *rrn* (Bartlett and Gourse, 1994), was fused to the jellyfish fluorescent protein variant YFP and inserted into the P22 prophage integration site within the *Salmonella* chromosome, while CFP was inserted downstream of *iag*, the last gene in SPI-1 *hilA* operon, to monitor expression of the type 3 secretion system (T3SS) cell invasion genes. Both reporter insertions were expected to be neutral, as one was placed within the intragenic site for P22 prophage integration and the other involved insertion behind the last gene of the *hilA* operon *iag*, leaving all genes within this operon intact. The *rrn-yfp* promoter fusion reported was used to monitor *Salmonella* growth. Fluorescence varied depending on growth conditions, with intensive signal observed from cells grown in complex medium (LB vs. minimal medium with glycerol as a carbon/energy source) or at higher growth temperatures in LB broth (37°C vs. 42°C) (Figure 2). *Salmonella* reporter strain's growth dynamics and growth rate were the same as the wild type under these *ex vivo* conditions with regard to doubling time (Dt) and growth rate (μ) at 30°C vs. 37°C (Supplementary Figure S3; Parish, 1985). When *Salmonella* was grown in EVCC medium, its growth was reduced after 6 h in the exclusive community compared to the permissive community (Figure 3). For *Salmonella* grown in the EVCC alone (control), the intensity of YFP fluorescence diminished over time until there was no detectable fluorescence after 24 h. When grown with either cecal community, *Salmonella* YFP fluorescence decreased to undetectable levels after 9 h. Expression of *Salmonella* T3SS invasion *hilA* operon increased over 6 h in the EVCC control, then decreased to undetectable levels by 24 h. Two peaks were observed in the FACS analysis: a major peak that overlapped with the non-fluorescent *Salmonella* negative control and a minor CFP fluorescent peak, indicating that the majority of cells were not expressing *hilA* (Figure 4). The proportion of *Salmonella* expressing CFP was diminished when grown in the presence of either cecal community after 3 h, but after 6 h of growth in the exclusive community, CFP expression was at its lowest compared to the other two conditions (Figure 4). The data indicate that after 6 h with the exclusive community, *Salmonella* growth was reduced and T3SS invasion expression was repressed. This time point was therefore selected to examine the *Salmonella* transcriptome response to growth in the communities.

Microarray transcriptome analysis of *Salmonella* revealed that the exclusive community had a profound effect on the expression of pathogenic behavior, significantly affecting the expression of 52 virulence genes (15.9%), compared to 7 that were altered when *Salmonella* was grown in the presence of the permissive community (Figure 5). The major differences in virulence gene expression in response to these communities were associated with LPS synthesis and *Salmonella* pathogenicity island 1 (Figures 6, 7). Most of the important virulence genes in SPI-1 as well as its ancillary T3SS effectors were repressed when *Salmonella* was grown with the exclusive community, compared to growth in the permissive community or the EVCC control ($p < 0.001$) (Figure 6). AvrA, an anti-inflammatory/anti-virulence factor (Jones et al., 2008), was elevated in *Salmonella* grown with the exclusive community. The only fimbrial operon expressed under these experimental conditions was the type I fimbrial operon, an important adhesin essential to the cell invasion process (Ernst et al., 1990). While the major fimbrial subunit FimA was expressed under all conditions, there was significantly less expression of export apparatus (*fimC,D*) and fimbrial adhesin (*fimF*) ($p < 0.001$). The polymyxin resistance operon *pmr*, responsible for modifying the *Salmonella* LPS (Gunn, 2008), was also repressed by the exclusive community. These results indicate that attenuation is likely involved in the mechanism of competitive exclusion.

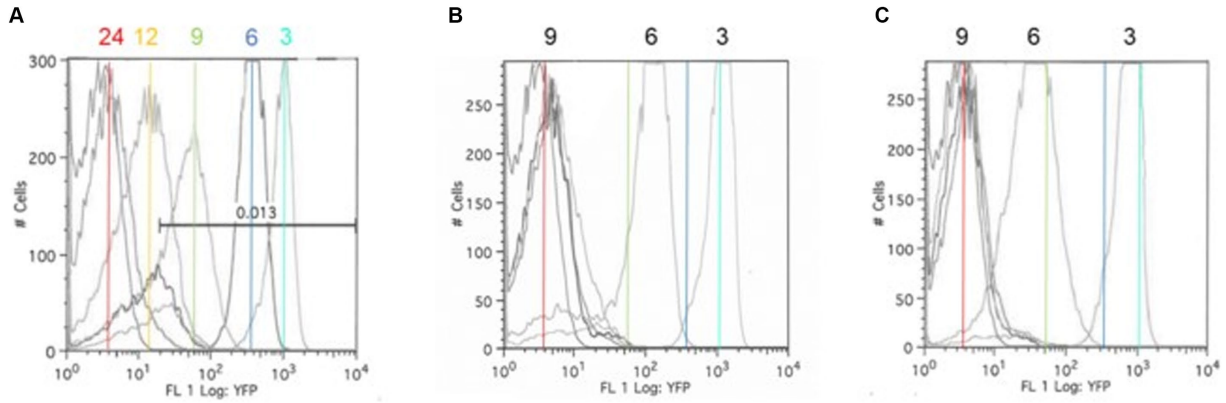

FIGURE 3
The *Salmonella ex vivo* growth in permissive **(B)** or exclusive **(C)** communities. FACS analysis was used to measure the *rrn-yfp* promoter activity in *S. typhimurium* SL1344 grown in simulated cecal medium (EVCC) **(A)** within a permissive or exclusive community. *Salmonella* YFP expression was monitored by FACS analysis at 3, 6, 9, 12, and 24 h using the parental strain as a negative fluorescence control. Cyan (3 h), blue (6 h), green (9 h), and red (24 h) lines mark the peak fluorescence levels of the reporter strain grown alone in EVCC **(A)** in order to demonstrate changes in intensity when grown in a permissive **(B)** or exclusive **(C)** community.

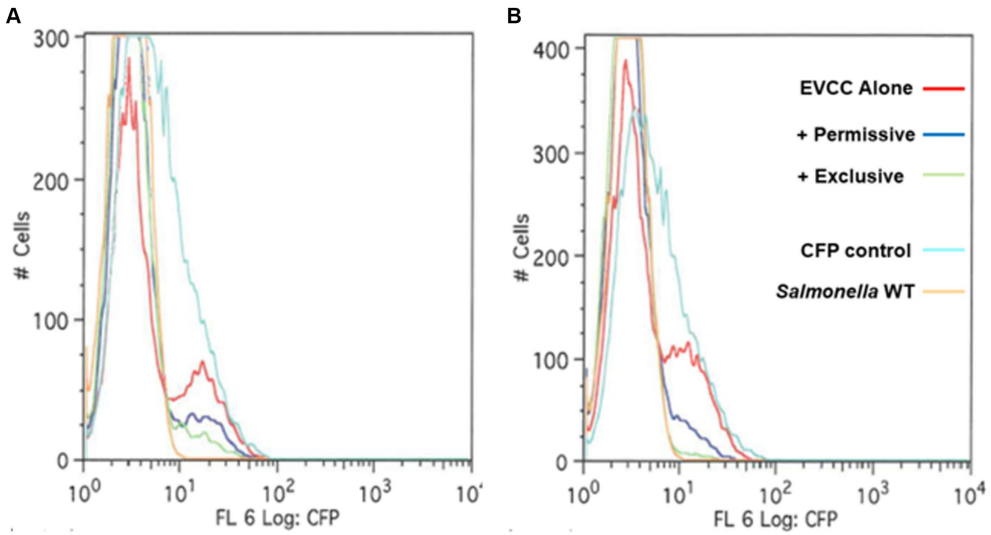

FIGURE 4
A *hilA* operon-*cfp* promoter fusion using jellyfish cyan fluorescent protein (CFP) as a reporter for *Salmonella* pathogenicity. A "promoter-less" *cfp* was placed between *iag* and the transcriptional terminator for the *hilA* operon using λ Red recombineering (Datsenko and Wanner, 2000). The *Salmonella* reporter strain was grown in EVCC medium alone or EVCC medium inoculated with the permissive or exclusive cecal community at **(A)** 3 h or **(B)** 6-h incubation. FACS analysis was used to measure the *hilA* operon-*cfp* promoter fusion in *S. typhimurium* SL1344 grown in EVCC medium alone (red line) or with a permissive (blue line) or exclusive (green line) community. The *S. typhimurium* SL1344 parental strain (orange line) served as a negative fluorescence control in FACS analysis. The CFP plasmid vector, pMG34, was used as a fluorescence-positive control (cyan line) (Miyashiro and Goulian, 2007). While a fluorescent population of cells were detected for *Salmonella* grown in EVCC alone or in a permissive community, an exclusive community repressed the *Salmonella hilA* locus, which is a global regulator of the pathogenicity island 1 (SPI-1) associated type 3 secretion system (T3SS).

Salmonella catabolic and anabolic response to permissive and exclusive communities *ex vivo*

Individual gene transcript levels for salmonellae grown with either permissive or exclusive communities were compared to those of *Salmonella* grown in the EVCC medium alone. Of the 6,069 genes analyzed, 161 were significantly elevated ($p < 0.0001$) in *Salmonella* grown with either community (Figure 8). Thirty-six percent of these transcripts were associated with energy production, and most of these genes (87.5%; $n = 48$) were responsible for propanediol metabolism, the end product of fucose and rhamnose fermentation (Obradors et al., 1988). However, there was low to no expression of transcripts associated with propionate metabolism (*prpB-E*), the end product of propanediol metabolism (Supplemental: *Salmonella* Coculture Data Set). In addition, genes associated with vitamin B12 synthesis (*cbi* operon), a key co-factor involved in both propanediol and ethanolamine metabolism pathways (Jeter, 1990; Brinsmade et al.,

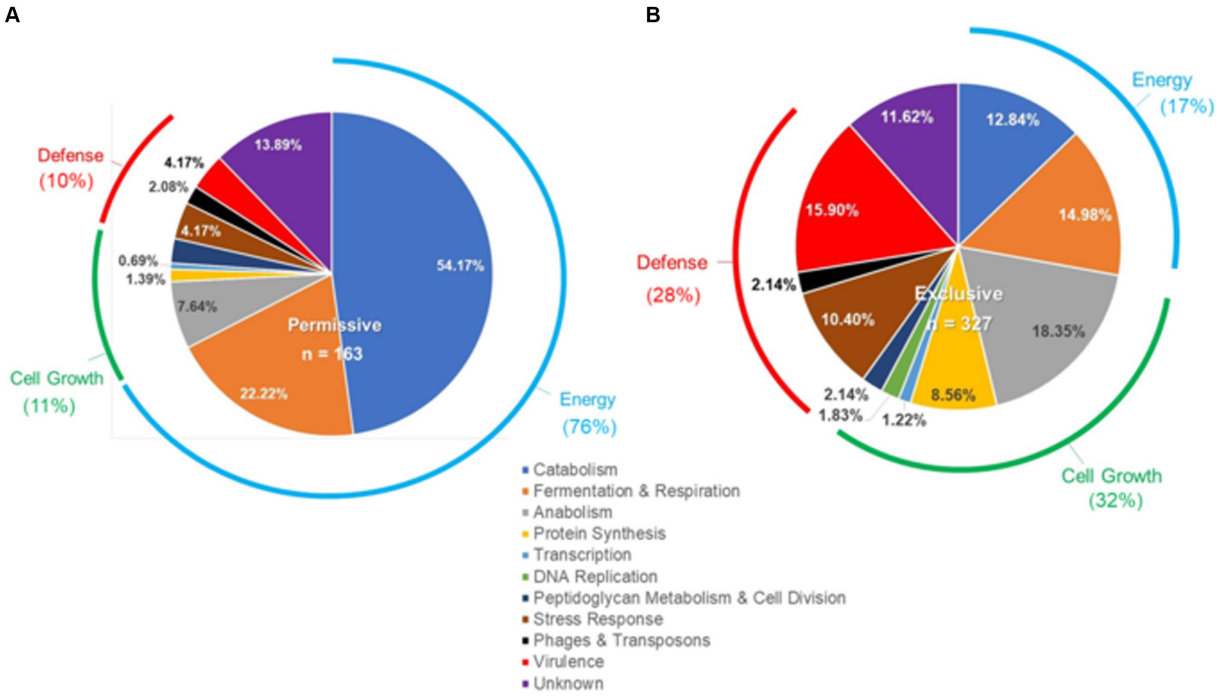

FIGURE 5
Differences in the *Salmonella* response to cecal permissive **(A)** and exclusive **(B)** communities *ex vivo*. The *Salmonella* SL1344 *rrn-yfp*, *hilA* operon-*cfp* reporter strain was grown in EVCC alone or with a permissive or exclusive community. Total RNA was extracted from *Salmonella* after 6-h growth. Genes reported with elevated expression and significant differences in expression ($p < 0.0001$) for growth in the permissive or exclusive community versus the negative community control were categorized based on function.

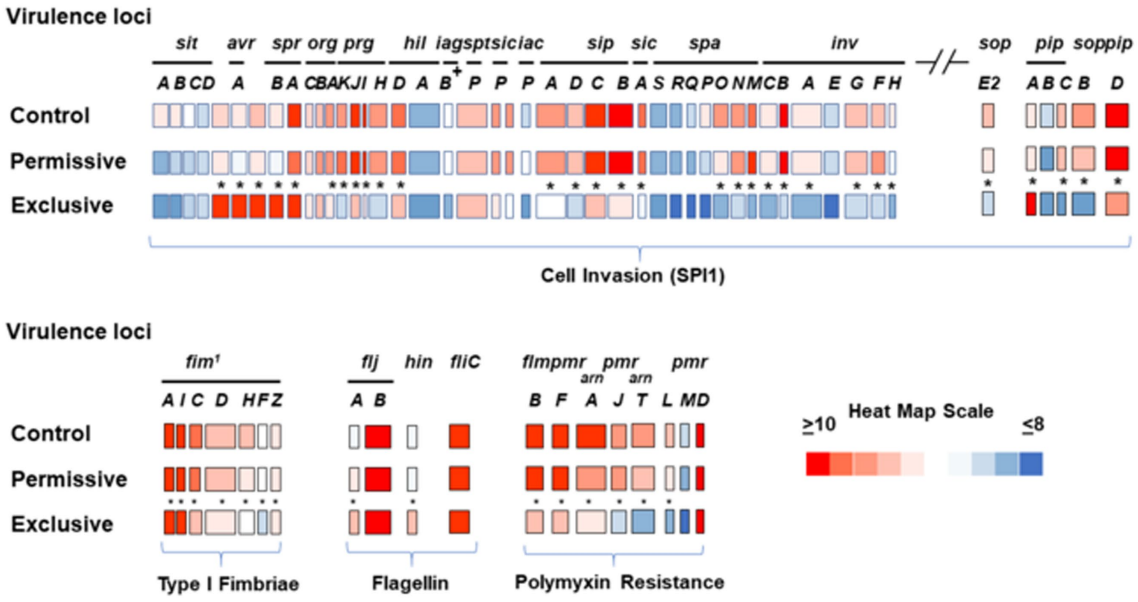

FIGURE 6
Transcriptional analysis of *Salmonella* virulence expression after growth in permissive or exclusive communities. FACS analysis was used to measure the *hilA* operon-*cfp* promoter fusion expression in *S. typhimurium* SL1344 grown in EVCC or with permissive or exclusive communities. Because Cfp expression was diminished in the *Salmonella* reporter strain after 6 h of growth in the exclusive community, the reporter strain was harvested after 6 h for microarray analysis. Significant transcription differences (*$p < 0.0001$) were observed in the SPI-1 locus, its ancillary T3SS effectors *sopE2*, *pipA-D*, and *sopB*, the type I fimbriae operon, flagellin, and polymyxin resistance expression. A heat map scale depicts the magnitude of microarray signal.

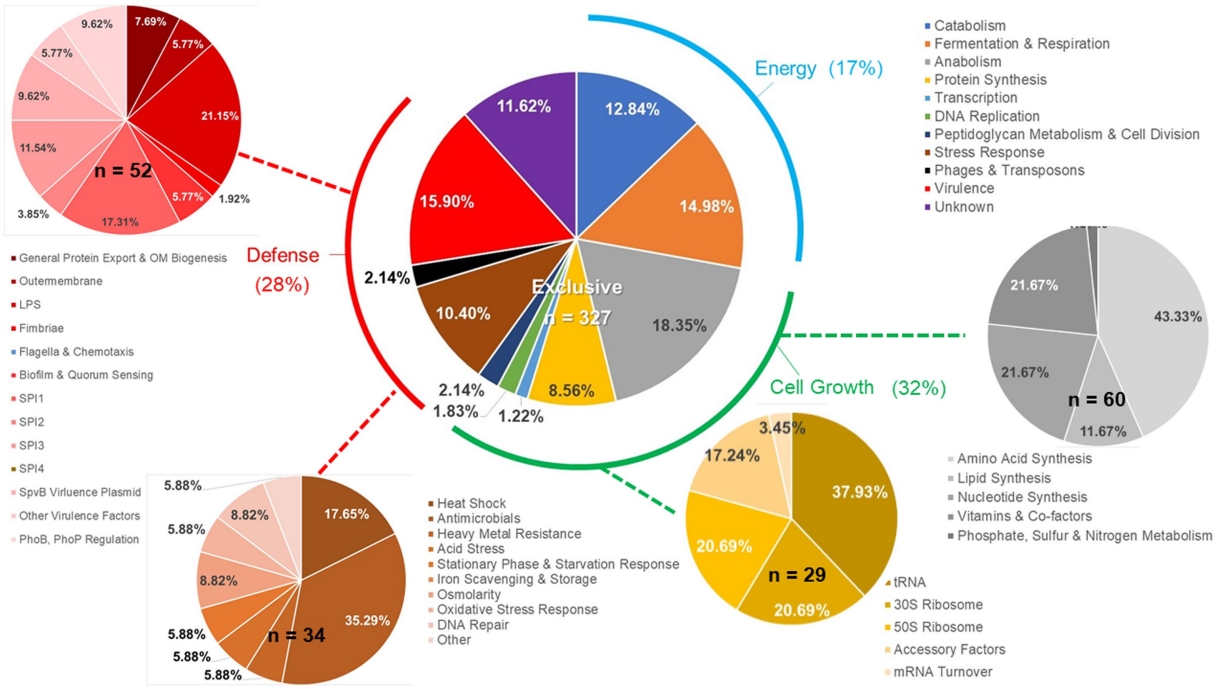

FIGURE 7
Details of *ex vivo Salmonella* transcriptional response to an exclusive community. *Salmonella* SL1344 *rrn-yfp, hilA* operon-*cfp* reporter strain was grown in co-culture in EVCC with an exclusive community or media alone. Total RNA was extracted from *Salmonella* after 6-h growth. Genes reported with significant differences in expression ($p < 0.0001$) versus the medium control were categorized based on function.

2005), were also elevated in *Salmonella* grown with either microbial community, compared to the EVCC control (Table 2). In the presence of the exclusive community, *Salmonella* did not express vitamin B12 transporters (*btuBCD*) compared to EVCC medium alone or with the permissive community. Moreover, ethanolamine utilization transcripts were only expressed in *Salmonella* grown in EVCC alone (Table 2).

There were significant differences in the *Salmonella* global transcriptome response to the microbial communities. Over 75% of 163 elevated gene transcripts from *Salmonella* grown with the permissive community, compared to the control, were dedicated to energy metabolism, whereas this was only the case for 17% of 327 elevated gene transcripts for *Salmonella* grown with the exclusive community (Figure 5). *Salmonella* grown with the permissive community directed fewer resources toward anabolism, as a percentage of upregulated genes (8%) than those grown with the exclusive community, where 18% of the upregulated genes were devoted to anabolism (Figure 5). *Salmonella* metabolic genes associated with the catabolism of arabinose, fructose, fucose, D-glucosaminate, and other amino-sugars were exclusively upregulated in *Salmonella* grown with the permissive community, while maltose was the only sugar utilization pathway expressed by *Salmonella* in co-culture with the exclusive community (Table 2). Several genes annotated as sugar transporters and associated enzymes, whose substrates have yet to be identified, were also expressed in *Salmonella* grown with the permissive community. In addition, *Salmonella* grown in EVCC medium alone or with the permissive community also upregulated genes responsible for sialic acid metabolism (*nanATEK*) and transport of methyl-galactose (*mglCAB, galS*). Catabolite repression may be central to regulating *Salmonella* gene expression in either microbial community, as several of these and other catabolic genes tied to energy generation (i.e., respiration) and a few genes with a role in the anabolic pathways responsible for nucleotide and amino acid metabolism possessed the signature nucleotide sequence recognized by the catabolite repressor protein Crp (Gunasekera et al., 1992). Transcripts for *crp* and the adenylate cyclase *cyaA* were produced in *Salmonella* under all growth conditions. *Ex vivo*, *Salmonella* produced enzymes under all conditions for metabolizing glucose (*ptsG, glk, pfkAB, fdaB, tpiA, pgk, gpmA, eno, pykF*), galactose (*galMKTE*), mannose (*manA, manXYZ*), glucuronate/galacturonate (*kdgT, uxaA, uxaC*), N-acetyl-galactosamine (*gatY*), and N-acetyl-glucosamine (*nag* operon) (Supplemental: *Salmonella* Coculture Data Set). There was greater expression for several of these genes (*ptsG, glk, fdaB, manXYZ*) in *Salmonella* grown with the permissive cecal community versus the exclusive community.

As propanediol is an end product of fucose and rhamnose fermentation, the focus of the *Salmonella* transcriptome analysis was shifted toward metabolism of microbial metabolites, including volatile fatty acids. Several genes tied to acetate (*ackA, pta, poxB*), D-lactate (*dld*), and hydrogen (hydrogenase-1, hydrogenase-2, and hydrogenase-3) metabolism were expressed under all conditions (Supplemental: *Salmonella* Coculture Data Set). However, neither acetate nor lactate was likely to be serving as a resource provided by its microbial community members, as the acetate permeases ActP and YaaH and lactate permease LldP were not elevated in *Salmonella* under any growth conditions. Differential expression was observed for formate (*fdnH*) and aldehyde (*aldB*) dehydrogenases in *Salmonella* grown in the presence of the microbial communities. However, the

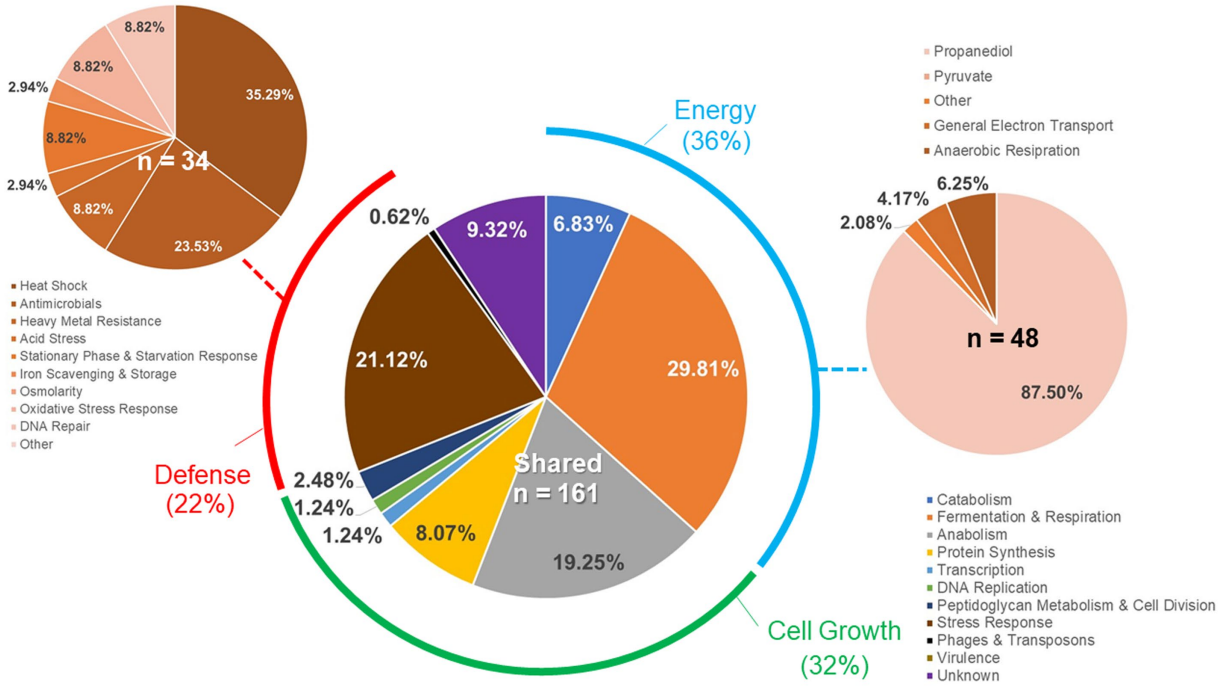

FIGURE 8
Differences in the *Salmonella* response to cecal permissive or exclusive communities *ex vivo*. The *Salmonella* SL1344 *rrn-yfp, hilA* operon-*cfp* reporter strain was grown in EVCC alone or with a permissive or exclusive community. Total RNA was extracted from *Salmonella* after 6-h growth. Genes reported with significant differences in expression ($p < 0.0001$) for both communities versus the negative community control were categorized based on function.

highest transcript levels of these genes were detected in *Salmonella* grown in the absence of either community.

Respiration may be central to *Salmonella* growth in that NAD appeared to be regenerated via electron transport, and NADH dehydrogenase genes (*nuo* operon) were strongly expressed under all growth conditions. In addition, cytochrome d oxidase genes (*cydAB*) were expressed under all growth conditions, whereas there was a significant decrease in cytochrome o oxidase *cyo* operon transcripts in *Salmonella* grown with the exclusive community (Table 2). While aerobic respiration appeared to be involved in *Salmonella* metabolism, several enzymes involved in anaerobic respiration were also differentially transcribed by *Salmonella* grown in EVCC alone (nitrate reductase: *narGHIJ*, *narL*), with the permissive community (nitrate reductases: *napD*; *nrfCDEG*; thiosulfate reductase: *phsABC*) or the exclusive community (nitrite reductase: *nirBD*; anaerobic sulfide reductase: *asrABC*).

Finally, there were substantial differences in the upregulation of anabolic enzyme transcripts between *Salmonella* grown with either community compared to EVCC medium alone (7% vs. 20%, respectively; Figure 5). In *Salmonella* grown in the presence of the exclusive community, a total of 65% of these anabolic enzymes were dedicated to amino acid and nucleotide synthesis. *Salmonella* grown with the exclusive community-expressed enzymes needed to synthesize nucleotides (*STM3473*; *ibrA*; *yicD*), especially purines (*purG*; *purM*; *purDH*; *purKE*; *guaB*) (Table 2). The peptide transporters STM3592 and STM2759 were expressed by *Salmonella* with the permissive community, as well as several enzymes associated with amino acid metabolism for serine (*sdaB*), threonine (*tdcA*), asparagine (asparaginase *ansB*), cysteine (*cysK*, *eamA*), glutamate (*gluD*), and D-alanine (*dadA*). There were significantly fewer transcripts found in the expression of enzymes involved in catabolism of serine/threonine (*sdaA*, *sdaBC*; *tdc* operon) in *Salmonella* grown with the exclusive community (Supplemental: *Salmonella* Coculture Data Set). These catabolic enzymes are subject to catabolite repression by Crp (Table 2). Methionine (*metF*, *metN*), arginine (*carAB*), and asparagine (*asnCA*) anabolism enzyme transcripts were upregulated in *Salmonella* grown with the exclusive community.

Cecal communities in chickens with high *Salmonella* abundance have a volatile fatty acid metabolic network

A Bayesian network analysis was used to analyze the cecal transcriptome pulled from MG-RAST-generated metabolism data sets. Guided by the findings of the *ex vivo* transcriptome, analysis of the cecal transcriptome was focused on enzyme transcripts involved in fermentation. A Hill-Climbing network identified 36 enzymes with 20 total connections (total enzymes, $n = 45$), of which there were seven single connections and five multiple connections with three or more enzymes (Figure 9) for the cecal communities with high *Salmonella* abundance (>5.85 Log_{10} *Salmonella* genomes/g cecal contents). Twelve enzymes associated with propanediol fermentation were identified in this network analysis in cecal communities with high *Salmonella* abundance. Propionate kinase PduW was a major node connected to

TABLE 2 *Salmonella* transcriptome response when co-cultured with cecal communities with high *Salmonella* abundance (permissive), with the competitive exclusion product (exclusive), or in EVCC medium (control).

Function	Genes[1]	Regulation[2]	Control[5]	Permissive[5]	Exclusive[5]
Catabolism					
Arabinose	*ara***C***BAD*; *araE*	*crp*	–	+	–
	yjcB	*crp*	–	+*	+
Fructose	*fruAKF*	*crp*	–	+	–
Fucose	*fuc***R***UKIP*	*crp*	–	+	–
Tagatose	*STM3253-5*		+	–	–
Sialic acid	*nanATEK*	*crp*	+	+	–
D-Glucosaminate	*STM***4534**		+	+	–
	STM45354-38; *STM4540.S**		–	+	–
Amino sugars	*STM1130-32*		+	+	–
	STM1129		–	+	–
Unknown sugars	*STM3780-85*; *STM1128*; *STM4535-8*		–	+	–
	STM3774-75; *STM2289-91*; *STM1613*		+	+	–
	STM3772		–	+	–
Gluconate	*hex**R**; edd*		–	–	+
5-Keto-4-deoxyuronate	*kduDI*		+	+	–
Idonate	*idn***R***TODK*	*crp*	+	+	–
Methyl-galactose	*mglCAB*;**galS**	*crp*	+	+	–
Maltose	*malZ*; *malGF***K**; *malS*	*crp*	–	–	+
Mannitol	*mtl***R**	*crp*	–	–	+
Glucose–phosphate stress	*sgr***R**		–	–	+
Carbon starvation	*cstA_1*		+	+	–
	csiE	*crp*; *rpoS*	+	–	–
	yjjY		–	–	+
C4-Dicarboxylate	*dctA*; *dcuC*	*crp*; *fnr*	+	+	–
	dcuB	*crp*; *fnr*	–	–	+
TCA cycle	*acnA*	*fnr*	+	+	–
Cysteine catabolism	*STM0458*		+	+	–
Ethanolamine utilization	*eut* operon[3]	*fur*; *crp*	+	–	–
Respiration					
Electron transport	*rnfABCD*		–	–	+
Cytochrome oxidase	*cyoABCDE*	*fur*; *fnr*	+	+	–
Nitrate reductase	*narGHJI*;**narL**	*fnr*	+	–	–
	napD	*fnr*	+	+	–
Formate-dependent nitrate reductase	*nrfCDEG*	*fnr*	+	+	–
Nitrite reductase	*nirBD*	*crp*; *fnr*	–	–	+
Anaerobic sulfide reductase	*asrABC*		–	–	+
Thiosulfate reductase	*phsABC*		+	+	–
Fermentation					
Fermentation end products	*fdnH*; *aldB*	*crp*; *fnr*	+	+	–
Propanediol utilization	*pdu* operon[4]		–	+	+
	pduX		–	+	–
Anabolism					
Vitamin B12	*cbiA-E*		–	+	+

(Continued)

10.3389/fmicb.2024.1342887

TABLE 2 (Continued)

Function	Genes[1]	Regulation[2]	Control[5]	Permissive[5]	Exclusive[5]
Vitamin B12 transport	*btuCD*		+	–	–
	btuB		+	+	–
Thiamin biosynthesis	*cof*		+	+	–
Purine synthesis	*purG*; *purM*; *purDH*; *purKE*	*fnr*	–	–	+
	guaB	*crp*; *rpoS*	–	–	+
Allantoin	*gcl*; *gip*; *glxR*; *allPR*; *ybbY*; *glxK*; *allCD*	*rpoS*	+	–	–
Pyrimidine metabolism	*STM2186-7*		+	+	–
Nucleotide metabolism	*ndk*; *cdpB*; *nupG*	*crp*	+	+	–
	STM3473; *ibrA*; *yjcD*	*crp*	–	–	+
Peptide transport	*STM3592*; *STM2759*		+	+	–
Methionine	*metF*; *metN*		–	–	+
Serine	*sdaB*	*crp*	+	+	–
Threonine	*tdcA*	*crp*; *fnr*	+	+	–
Arginine	*carAB*		+*	–	+
Asparagine	*asnCA*		–	–	+
	ansB	*crp*	+	+	–
Cysteine	*cysK*; *eamA*		+	+	–
Glutamate	*gluD*		+	+	–
Alanine	*dadA*	*crp*; *rpoS*	+	+	–
	dadX; *STM1633*	*crp*	+	–	–
Stringent response	*ytfK*		+	+	_
Fatty acid metabolism	*aidB*; *ugpB*; *ucpA*	*crp*	+	+	–
Ferrichrome transport	*fhuA*; *STM0191*	*fur*	+	–	–
Iron	*bfd*; *ryhB*	*fur*; *rpoS*	+	–	–
Protein synthesis	*queA*; *trpS2*; *yadB*		–	–	+
	STM4446		–	+	–
Replication	*tus*		+	–	–
DNA repair	*STM1514*		+	–	–
Regulation					
Transcription factors	*phoH*; *rsd*; *arcZ*	*rpoS*	+	+	–
	STM1001		+	–	–
	adiY		–	+	+
	STM3834		–	+	–
	crp/cyaA; *fnr*; *fur*; *rpoS*		+	+	+
Virulence and stress response					
Quorum sensing (*lsr*)	*STM4071-80*	*crp*	+	+	–
SPI-1	*invFGBJ*; *spaO*; *sicA*; *sipD*; *prgHK*		+	+	–
	sitABC	*fur*	+	–	–
	pipC; *sopB*; *orfX*		+	+	–
	pipA		–	–	+
SPI3	*mgtBC*		–	–	+
Polymyxin resistance	*pmrJ*; *arnT*; *pmrL*; *ybjG*		+	+	–
Other virulence factors	*virK_2*		–	–	+
	rck		–	+	+

(Continued)

TABLE 2 (Continued)

Function	Genes[1]	Regulation[2]	Control[5]	Permissive[5]	Exclusive[5]
Fimbriae	*stcA*		+	+	–
Motility and chemotaxis	*trg*; *flgJ*; *STM3156*; *STM3604*		+	+	–
Outer membrane	*pgtE*		–	–	+
	yhcN; *STM3361-2*		–	+	+
	STM0080		+	–	–
	yhfL		+	+	–
Cell wall	*cidAB*		–	–	+
Oxidative stress	*srgA*		–	–	+
	yciGFE		+	–	–
Osmotic stress	*yehY*		+	+	–
Antimicrobials	*emrD*		–	–	+
	yabI		–	+	–
	ydhE		+	–	
CRISPR	*STM2938-93*; *STM2937-43*		+	+	–
Phage	*STM2740*				
Unknown					
	yeiH		+*	–	+
	STM4441-2	*crp*	–	+	–
	STM0514; *yhhX*		+	–	–
	ybhQ; *ygjR*; *yidE*; *yiiL*; *yjcO*; *ylbA*; *STM0660*; *STM1810*; *STM1933*; *STM2950*; *STM3343*; *STM4503*	*crp*	+	+	–
	ybdH; *yfhL*		–	–	+

[1]Bold-transcription factor. [2]crp-regulated genes (regulon of Crp in *Salmonella* Typhimurium LT2; https://regprecise.lbl.gov/regulon.jsp?regulon_id=10138; accessed 08/02/2023); fur-regulated genes [(Troxell et al., 2011) or Regulon of Fur in *Salmonella* Typhimurium LT2 https://regprecise.lbl.gov/regulon.jsp?regulon_id=10114; accessed 08/02/2023]; fnr-regulated genes (Regulon of Fnr in *Salmonella* Typhimurium LT2; https://regprecise.lbl.gov/regulon.jsp?regulon_id=41958) or rpoS-regulated (Wong et al., 2017). [3]eut**R**AHGJ; eutD; eutS. [4]pduGH; pduKLMOPQSTUV; *Weak expression. +: "on"; –: "off"; crp: catabolite repression; fnr: anaerobic metabolism; and fur: iron-regulated genes; rpoS: stationary phase response. [5]"+": upregulated; "–" downregulated.

enzymes involved in propanediol and acetate metabolism. The network connections for the high *Salmonella* abundance group mirrored their enzymatic positions within their respective metabolic pathways for some enzyme transcripts. Ten enzyme connections involving 18 enzymes were identified from the low *Salmonella* abundance cecal transcriptome. Here, propanediol-associated enzymes: methylglyoxal synthase, glycerol dehydratase, propionyl-CoA carboxylase, propionyl-CoA synthase, and propionaldehyde dehydrogenase were identified. Fourteen enzymes were present in both groups and included: methylglyoxal synthase; glycerol dehydratase; propionyl-CoA carboxylase; propionyl-CoA transferase; glutaconate-CoA transferase; hydroxybutyryl-CoA dehydratase; hydroxybutyryl-CoA dehydrogenase; pyruvate oxidase; acetyl-CoA synthase; acetyl-CoA hydrolase; ethanolamine ammonia-lyase; 4-aminobutyrate aminotransferase; cobalamin (vitamin B12); and cobalamin biosynthesis; although some of these were in different enzyme connections between these two groups.

As these enzymatic pathways are associated with carbohydrate or amino acid fermentation, network analysis was expanded to include metabolic enzyme transcripts (164 total enzymes) with polysaccharide degradation and fucose/rhamnose catabolism responsible for producing the fermentation end product propanediol. Forty-four were identified in single or multiple connections for the two groups, producing 26 and 17 connections from the cecal transcriptomes for the high and low *Salmonella* abundance groups, respectively (Supplementary Figure S4). Propanediol and acetate metabolism remain dominant metabolic pathways in this new network analysis, especially for the high *Salmonella* abundance group, pulling in additional enzymes mostly associated with glucose metabolism and the TCA cycle. In fact, the same 30 fermentation enzymes from the first network analysis were identified in the expanded network analysis, except there were fewer single-enzyme connections for both *Salmonella* abundance groups. As expected, the expanded network analysis identified similar connections in the high *Salmonella* abundance group compared to the original 45-gene analysis (Supplementary Figure S3; Figure 9). Three of 10 enzyme transcripts involved with fermentation ($n = 25$), propionyl-CoA carboxylase, butyryl-CoA dehydrogenase, and pyruvate dehydrogenase, also had a significantly positive correlation with low *Salmonella* abundance (<6.00 Log_{10} *Salmonella* genomes/g cecal contents) (Table 3), while propionyl-CoA synthase and pyruvate oxidase had a significantly negative correlation with *Salmonella* abundance at *Salmonella* levels <6.00 Log_{10} *Salmonella* genomes/g of cecal contents. Other propionate enzyme transcripts (propionaldehyde dehydrogenase and propionate kinase) exhibited a negative correlation ($p < 0.05$) related to the age of the bird (not shown).

Most cecal transcripts identified as propionate kinase, methyl-malonyl CoA mutase, propionyl-CoA synthase,

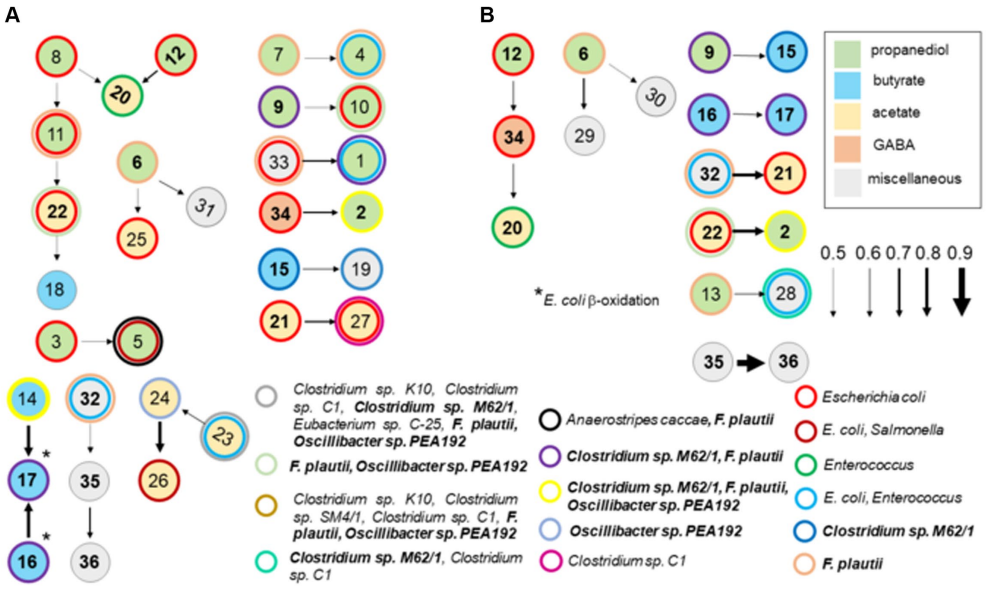

FIGURE 9
A Bayesian network analysis of cecal transcriptome, focused on fermentation, from chickens with high (>5.85 Log_{10} *Salmonella* genomes/g cecal contents) **(A)** or low **(B)** *Salmonella* abundance. The network depicted was identified using the score-based learning algorithm Hill-Climbing. The data were obtained from KO metabolism data sets in MG-RAST. Connections were identified among the 45 enzyme transcripts by network analysis, of which 36 were identified as single or multiple connections, producing 20 and 10 connections from the transcriptomes of cecal communities with high or low *Salmonella* abundance, respectively. Arrows indicate the direction and strength of the connection. Enzymes are color-coded based on their associated propanediol (green), butyrate (blue), or acetate (yellow) fermentation pathways. Enzymes identified in these networks were: methyl-malonyl-CoA decarboxylase (1); methylglyoxal synthase (2); lactaldehyde dehydrogenase (3); hydroxyacylglutathione hydrolase (4); glycerol dehydrogenase (5); glycerol dehydratase (6); propanediol dehydratase (7); propionate kinase (8); propionyl-CoA carboxylase (9); propionate-CoA transferase (10); methyl-malonyl-CoA mutase (11); propionyl-CoA synthase (12); propionaldehyde dehydrogenase (13); butyryl-CoA dehydrogenase (14); glutaconate-CoA transferase (15); hydroxybutyryl-CoA dehydratase (16); hydroxybutyryl-CoA dehydrogenase (17); thiolase (18); ferredoxin hydrogenase (19); pyruvate oxidase (20); acetyl-CoA synthase (21); acetyl-CoA hydrolase (22); acetate kinase (23); pyruvate ferredoxin oxidoreductase (24); acetyl-CoA synthetase (25); aldehyde dehydrogenase (26); phosphotransacetylase (27); lactate dehydrogenase (28); phosphoketolase (29); glutamate synthase (30); methylaspartate ammonia-lyase (31); ethanolamine ammonia-lyase (32); ethanolamine utilization protein (33); 4-aminobutyrate aminotransferase (34); cobalamin (vitamin B12) (35); and cobalamin biosynthesis (36). The following enzymes were not identified in any network analysis: lactaldehyde reductase, butyrate kinase, pyruvate dehydrogenase, citramalate synthase, serine dehydratase, alanine dehydrogenase, formate hydrogenlyase, formate C-acetyltransferase, and glutamate mutase. Numbers in bold are enzymes shared between cecal communities with high and low *Salmonella* abundance. Circles with thick-colored borders are for enzymatic transcripts with 98–100% nucleotide identity and 99–100% coverage by BLAST scores for intestinal species including *Escherichia coli*, *Enterococcus faecium*, and *Flavonifractor plautii*.

acetyl-CoA hydrolase, lactate dehydrogenase, or acetyl-CoA synthetase had 98–100% identity to *Escherichia coli* at the nucleotide level (Supplementary Table S8). The identities of other genera within the Enterobacteriaceae were all <98% nucleotide identities. However, some of these same transcripts had 98–100% identity, at the nucleotide level, to *Enterococcus faecium*, *Flavonifractor plautii*, or *Clostridia*. Some butyryl-CoA dehydrogenase and propionyl-CoA carboxylase enzyme transcripts had >98% nucleotide identity with *Clostridia* yet to be given a genus or species designation. However, there were many enzyme transcripts with little to no homology to any nucleotide sequences in BLAST but contained pfam domains characteristic of these enzymes. Pyruvate oxidase transcripts were primarily from *Enterococcus* or *Lactobacillus* species.

Analysis of the volatile fatty acid profile of the cecal contents of two birds with high *Salmonella* abundance showed variability. One sample had high acetate levels relative to the other VFAs, whereas another had high propionate and butyrate concentrations (Table 4). Therefore, in this small sample set, the volatile fatty acid profile and abundance did not correlate with the community transcriptome associated with fermentation.

Cecal community transcripts that correlate with *Salmonella* abundance *in vivo*

Carbohydrate analysis revealed that arabinose and glucose were the most abundant sugars present in the cecal lipid fraction (Table 5), with varying levels of rhamnose, fucose, xylose, glucuronic acid, galacturonic acid, galactose, N-acetyl galactosamine, and N-acetyl glucosamine in the lipid or precipitate fractions of both groups. However, mannose was present in the cecal contents of birds with high *Salmonella* abundance. The cecal community transcriptome contained many enzyme transcripts associated with liberating the sugars from complex carbohydrates, including transcripts annotated as: α-L-arabinofuranosidase, arabinogalactan endo-β-1,4-galactanase, β-fructofuranosidase, β-fructosidase, α-fucosidase, β-N-acetylhexosaminidase, β-hexosaminidase, α,β-galactosidases, α,β-glucosidases, α-mannosidase, α-glucuronidase, β-xylosidase, glycosidases, endoglucanase, cellulase, chitinase, and xylanases. Sialidase was present as a rare transcript in the cecal transcriptome. The transcriptome also contained various enzyme

TABLE 3 Cecal microbial community enzyme transcripts correlate with *Salmonella* abundance.

Enzyme transcripts[1]	*Salmonella* abundance (Log_{10} genomes/g^2)	Correlation coefficients[3]			
		Pearson		Spearman	
		r =	p =	ρ =	p =
Carbohydrate utilization					
α-Galactosidase	7.00–9.22	0.7965	0.9939	**0.7186**	**0.0340**
	6.79–9.22	0.5445	0.9519	−0.3830	**0.0259**
Galactose-1-phosphate uridyltransferase	2.11–6.89	**−0.7275**	**0.0159**	−0.5952	0.0977
	2.11–5.85	**−0.7628**	**0.0282**	−0.7714	0.0535
Arabinogalactan endo-1,4-β-galactosidase	2.11–5.85	0.7275	0.9609	**0.8286**	**0.0297**
Ribose/xylose/arabinose/galactoside ABC-type transport system	0.00–5.85	0.5329	0.9193	**0.7489**	**0.0243**
β-Fructofuranosidase	0.00–5.85	−0.5082	0.0932	**−0.7553**	**0.0225**
	7.00–9.22	0.6920	0.9766	0.6826	**0.0484**
Phosphofructokinase	7.00–9.22	**−0.7106**	**0.0192**	**−0.7904**	**0.0142**
α-L-Fucosidase	2.11–5.85	**−0.7284**	**0.0388**	−0.5429	0.2219
L-Fuculokinase	7.00–9.22	0.8723	0.9988	**0.8503**	**0.0052**
L-Fucose isomerase and related proteins	7.00–9.22	0.7387	0.9861	**0.8144**	**0.0099**
	2.11–6.89	0.6788	0.9733	**0.8095**	**0.0107**
L-Fucose isomerase	7.00–9.22	0.7387	0.9861	**0.8144**	**0.0099**
	2.11–6.89	0.7387	0.9861	**0.8144**	**0.0099**
Rhamnulokinase	7.00–9.22	0.7123	0.9811	**0.7425**	**0.0262**
N-acetylneuraminate lyase	0.00–5.85	0.6925	0.9767	**0.7085**	**0.0377**
	7.00–9.22	−0.6692	**0.0292**	−0.6707	0.0539
ABC-type maltose transport system	0.00–5.85	0.0596	0.5563	**0.8193**	**0.0092**
Maltose-binding periplasmic proteins	2.11–5.85	**−0.8447**	**0.0098**	**−0.8986**	**0.0102**
β-hexosaminidase	0.00–5.85	0.4909	0.8976	0.6991	**0.0414**
Dehydro-3-deoxyphosphogluconate aldolase	0.00–5.85	0.4909	0.9209	**0.9429**	**0.0032**
Aldose 1-epimerase	2.11–6.89	−0.5501	0.0727	**−0.7381**	**0.0275**
	2.11–5.85	−0.6470	0.0703	**−0.8286**	**0.0297**
α-Glucuronidase	2.11–5.85	**−0.7086**	**0.0457**	−0.3714	0.4216
β-Glucuronidase	0.00–5.85	−0.388	0.4633	**0.7009**	**0.0407**
α-Glucosidase	2.11–6.89	**−0.7193**	**0.0174**	−0.5238	0.1549
Glucose-6-phosphate 1-dehydrogenase	0.00–5.85	−0.0222	0.4790	**−0.7664**	**0.0197**
Phosphoglycerate kinase	7.00–9.22	−0.5926	0.0546	**−0.7785**	**0.0168**
β-Xylosidase	2.11.5.85	**−0.8864**	**0.0043**	**−0.8857**	**0.0130**
Fermentation					
Glycerol dehydratase	0.00–5.85	−0.1834	0.3299	**−0.8131**	**0.0101**
Propionyl-CoA carboxylase	2.11–5.85	0.7350	0.9633	**0.9429**	**0.0032**
Propionyl-CoA synthase	2.11–5.85	**−0.8424**	**0.0102**	−0.6547	0.1249
Butyryl-CoA dehydrogenase	0.00–5.85	0.0013	0.5012	**0.9364**	**0.0004**
Glutaconate-CoA transferase	0.00–5.85	0.4489	0.8733	0.6837	**0.0479**
	7.00–9.82	−0.6112	**0.0476**	−0.4671	0.2117
Pyruvate dehydrogenase	0.00–6.89	0.4684	0.9177	**0.8079**	**0.0034**
	2.11–6.89	0.4946	0.8996	**0.7143**	**0.0356**
	2.11–5.85	0.8899	0.9960	**0.8857**	**0.0130**
Pyruvate oxidase	2.11–6.89	**−0.7811**	**0.0077**	−0.5774	0.1106
	2.11–5.85	**−0.8424**	**0.0102**	−0.6547	0.1249
Acetyl-CoA hydrolase	0.00–5.85	0.4381	0.8666	**0.7131**	**0.0360**
	2.11–8.51	−0.4781	**0.0401**	−0.5919	**0.0244**
Na + −transporting methyl-malonyl-CoA/oxaloacetate decarboxylase	0.00–6.89	**−0.7383**	**0.0057**	−0.6687	**0.0272**
	0.00–5.85	**−0.7084**	**0.0197**	−0.4669	0.2119
N-methylhydantoinase A/acetone carboxylase	0.00–6.89	**−0.7289**	**0.0065**	**−0.7877**	**0.0050**
TCA					
Citrate lyase	0.00–5.85	0.1961	0.6813	**−0.7175**	**0.0344**
Malic enzyme	7.00–9.22	0.8016	0.9944	**0.8982**	**0.0017**

(Continued)

TABLE 3 (Continued)

Enzyme transcripts[1]	*Salmonella* abundance (Log_{10} genomes/g[2])	Correlation coefficients[3]			
		Pearson		Spearman	
		r =	p =	ρ =	p =
Pyruvate/oxaloacetate carboxyltransferase	2.11–5.85	0.7265	0.9605	**0.8286**	**0.0297**
Respiration					
Ubiquinone oxidoreductase	2.11–6.89	−0.3813	0.1709	**−0.7143**	**0.0356**
Cytochrome bd-type quinol oxidase	0.00–6.89	0.6345	0.9787	**0.8024**	**0.0038**
	2.11–6.89	0.6098	0.9519	**0.7619**	**0.0208**
	2.11–5.85	0.7100	0.9548	**0.8286**	**0.0297**
Cytochrome o ubiquinol oxidase	2.11–5.85	**−0.7651**	**0.0275**	**−0.8197**	**0.0329**
Nitrate reductase	2.11–6.89	0.5273	0.9165	**0.8024**	**0.0120**
Nickel-dependent hydrogenase	7.00–9.22	0.6132	0.9531	**0.7545**	**0.0228**
	2.11–6.89	0.7117	0.9810	**0.9048**	**0.0014**
	2.11–5.85	0.7408	0.9652	**0.8286**	**0.0297**
Amino acid/nitrogen metabolism					
Glutamate dehydrogenase	0.00–5.85	0.2271	0.7082	**−0.7175**	**0.0344**
ABC-type histidine transport system	2.11–6.89	−0.6175	**0.0453**	**−0.8810**	**0.0026**
ABC-type polar amino acid transport system	0.00–5.85	−0.5227	0.0858	**0.8217**	**0.0088**
Dipeptidase	2.11–6.89	−0.5522	0.0717	**−0.7319**	**0.0295**
Periplasmic component/domain	0.00–5.85	0.5861	0.9428	**0.7569**	**0.0221**
Histidinol-phosphate/aromatic aminotransferase and cobyric acid decarboxylase	0.00–6.89	−0.5063	0.0639	**−0.7416**	**0.0106**
Isopropylmalate/homocitrate/citramalate synthases	0.00–5.85	−0.5417	0.0765	**0.7413**	**0.0266**
Transglutaminase-like enzyme	7.00–9.22	0.4183	0.8540	**0.7349**	**0.0285**
Tryptophanase	7.00–9.22	0.6833	0.9745	**0.7401**	**0.0269**
Zinc metalloprotease (elastase)	7.00–9.22	0.6567	0.9673	**0.8507**	**0.0052**
	2.11–6.89	**−0.7397**	**0.0137**	−0.3546	0.3544
5-Enolpyruvylshikimate-3-phosphate synthase	0.00–5.85	−0.0925	0.4128	**−0.9157**	**0.0009**
Acetylglutamate kinase	0.00–5.85	0.2930	0.7628	**0.8109**	**0.0105**
Acetylornithine deacetylase/succinyl-diaminopimelate desuccinylase	0.00–5.85	−0.1849	0.3286	**−0.7522**	**0.0234**
	2.11–6.89	0.8070	0.9949	**0.8571**	**0.0046**
Allophanate hydrolase	2.11–5.85	**−0.7979**	**0.0191**	−0.6000	0.1688
	0.00–5.85	**−0.8984**	**0.0005**	0.5747	0.1125
Amino acid permeases	0.00–6.89	0.5764	0.9630	**0.8511**	**0.0013**
	2.11–6.89	0.5355	0.9205	**0.7143**	**0.0356**
Ammonia permease	7.00–9.22	0.7553	0.9888	**0.8144**	**0.0099**
	2.11–6.89	−0.5740	0.0622	**−0.7143**	**0.0356**
Anthranilate phosphoribosyltransferase	7.00–9.22	0.9302	0.9999	**0.8862**	**0.0023**
Anthranilate/para-aminobenzoate synthase	7.00–9.22	0.6953	0.9774	**0.7904**	**0.0142**
Aspartate/tyrosine/aromatic aminotransferase	2.11–6.89	−0.6139	**0.0466**	**−0.7381**	**0.0275**
Aspartate ammonia-lyase	0.00–6.89	−0.6037	**0.0289**	**−0.8207**	**0.0026**
Aspartyl aminopeptidase	2.11–6.89	**−0.7314**	**0.0152**	−0.6190	0.0821
Aspartate-semialdehyde dehydrogenase	0.00–5.85	−0.1194	0.3880	**−0.7396**	**0.0271**
Chorismate synthase	0.00–5.85	0.5157	0.9107	**0.8456**	**0.0057**
	7.00–9.22	**−0.7571**	**0.0109**	**−0.7545**	**0.0228**
Di- and tripeptidases	7.00–9.22	0.8528	0.9980	**0.8503**	**0.0052**
γ-Aminobutyrate permease and related permeases	2.11–6.89	0.7297	0.9845	**0.7857**	**0.0152**
	0.00–6.89	0.7358	0.9941	**0.8875**	**0.0004**
Glutamate 5-kinase	0.00–5.85	0.0364	0.5344	**0.7228**	**0.0325**
Glutaminase	0.00–5.85	**−0.7147**	**0.0184**	0.1199	0.7601
Glutamine amidotransferase	0.00–6.89	−0.6801	**0.0127**	**−0.7356**	**0.0116**
Glutamine synthetase	7.00–9.22	0.7693	0.9908	**0.8503**	**0.0052**
Glycine cleavage system	2.11–8.51	**−0.8150**	**0.0153**	**−0.8286**	**0.0297**
Histidine ammonia-lyase	7.00–9.22	0.5501	0.9274	**0.7186**	**0.0340**

(Continued)

TABLE 3 (Continued)

Enzyme transcripts[1]	*Salmonella* abundance (Log_{10} genomes/g[2])	Correlation coefficients[3]			
		Pearson		Spearman	
		r =	p =	ρ =	p =
Histidinol dehydrogenase	0.00–6.89	**−0.7217**	**0.0073**	**−0.8024**	**0.0038**
Imidazolonepropionase	0.00–5.85	0.3145	0.7798	**−0.8977**	**0.0017**
Arginine lysine ornithine decarboxylases	2.11–5.85	**−0.8961**	**0.0034**	–	–
L-Serine deaminase	0.00–6.89	**−0.7128**	**0.0083**	**−0.7052**	**0.0175**
Threonine efflux protein	2.11–5.85	**−0.8012**	**0.0183**	−0.4286	0.3486
Na+/alanine symporter	2.11–6.89	−0.4081	0.1527	**−0.7143**	**0.0356**
O-Acetylhomoserine sulfhydrylase	0.00–6.89	−0.6020	**0.0294**	**−0.7173**	**0.0149**
Oligoendopeptidase F	0.00–6.89	−0.6813	**0.0125**	**−0.7052**	**0.0175**
Peptidylarginine deiminase	2.11–6.89	−0.4507	0.1256	**−0.8095**	**0.0107**
Phosphoribosylanthranilate isomerase	2.11–5.85	**−0.7429**	**0.0341**	**−0.8286**	**0.0297**
Uncharacterized protein involved in cysteine biosynthesis	2.11–6.89	**−0.7811**	**0.0077**	−0.5774	0.1106
	2.11–5.85	**−0.8424**	**0.0102**	−0.6547	0.1249
Urease	2.11–6.89	−0.6991	**0.0217**	−0.3095	0.4222
Antimicrobials					
Lactacin F ABC transporter	2.11–6.89	−0.1990	0.3161	**−0.7407**	**0.0267**
creA; colicin E2 tolerance	2.11–6.89	0.6291	0.9586	**0.8456**	**0.0057**
creD; colicin E2 tolerance	2.11–5.85	**−0.8424**	**0.0102**	−0.6547	0.1249
Membrane protein involved in colicin uptake	0.00–5.84	0.4838	0.8937	**−0.7154**	**0.0351**
Polyketide synthase module	2.11–5.85	**−0.8333**	**0.0118**	**−0.8804**	**0.0142**
Non-ribosomal peptide synthetase module	0.00–5.85	**−0.8319**	**0.0031**	0.3689	0.3342
	2.11–5.85	**−0.8154**	**0.0152**	−0.2571	0.5839
Thioesterase domains of type I polyketide synthases	0.00–5.85	−0.6147	**0.0464**	**0.8561**	**0.0047**
	2.11–5.85	**−0.8424**	**0.0102**	−0.6547	0.1249
Yersiniabactin non-ribosomal peptide synthetase	2.11–6.89	**−0.7386**	**0.0139**	−0.2790	0.4712
	2.11–5.85	**−0.8638**	**0.0070**	−0.6983	0.0946
Yersiniabactin non-ribosomal peptide/polyketide synthase	0.00–6.89	**−0.7000**	**0.0099**	−0.5854	0.0622
	0.00–5.85	**−0.8408**	**0.0026**	—	—
	2.11–5.85	**−0.9383**	**0.0008**	**−0.9856**	**0.0002**
Yersiniabactin synthetase	2.11–5.85	**−0.8424**	**0.0102**	−0.6547	0.1249
	2.11–6.89	**−0.7811**	**0.0077**	−0.5774	0.1106
	2.11–8.51	−0.6897	**0.0026**	−0.4477	0.1012
Yersiniabactin salicyl-AMP ligase	2.11–6.89	**−0.7811**	**0.0077**	−0.5774	0.1106
	2.11–5.85	**−0.8424**	**0.0102**	−0.6547	0.1249
	2.11–8.51	−0.6897	**0.0026**	−0.4477	0.1012
Mycobactin salicyl-AMP ligase	0.00–5.85	−0.2261	0.2926	**1.0000**	**<0.0001**
	2.11–5.85	**−0.8424**	**0.0102**	−0.6547	0.1249
	2.11–8.51	−0.5132	**0.0286**	0.1061	0.7085
Oligoketide cyclase/lipid transport protein	2.11–5.85	**−0.8424**	**0.0102**	−0.6547	0.1249
Predicted thioesterase involved in non-ribosomal peptide biosynthesis	0.00–6.89	**−0.7430**	**0.0053**	**−0.8078**	**0.0034**
	0.00–5.85	**−0.7511**	**0.0118**	−0.3436	0.3704
	2.11–6.89	**−0.7811**	**0.0077**	−0.5774	0.1106
	2.11–5.85	**−0.8424**	**0.0102**	−0.6547	0.1249
Type 6 secretion system	7.00–9.22	−0.3975	0.1598	**−0.7731**	**0.0180**
Ribosomal RNA small subunit methyltransferase E	2.11–5.85	**−0.7014**	**0.0483**	−0.2571	0.5839
rRNA small subunit methyltransferase I	7.00–9.22	**0.7050**	0.9795	**0.7186**	**0.0340**
Streptomycin 3-*O*-adenylyltransferase	0.00–6.89	−0.6742	**0.0137**	**−0.7853**	**0.0052**
	0.00–5.85	−0.6750	**0.0277**	−0.3305	0.3899
Spectinomycin 9-*O*-adenylyltransferase	7.00–9.22	0.8248	0.9964	**0.7370**	**0.0279**
Translation elongation factor LepA	0.00–5.85	0.1102	0.6036	**0.8518**	**0.0051**
SsrA-binding protein SmpB	2.11–6.89	**−0.7811**	**0.0077**	−0.5774	0.1106
	2.11–5.85	**−0.8424**	**0.0102**	−0.6547	0.1249

(Continued)

TABLE 3 (Continued)

Enzyme transcripts[1]	*Salmonella* abundance (Log_{10} genomes/g[2])	Correlation coefficients[3]			
		Pearson		Spearman	
		r =	p =	ρ =	p =
	2.11–8.51	−0.6897	**0.0026**	−0.4477	0.1012
DedA protein	2.11–6.89	−0.4985	0.0983	**−0.7326**	**0.0293**
Anti-sigma B factor RsbT	0.00–5.85	0.1998	0.6846	**0.7339**	**0.0289**
Transcriptional regulator YkgA	2.11–5.85	**−0.8424**	**0.0102**	−0.6547	0.1249
ABC-type antimicrobial peptide transport system	7.00–9.22	0.7960	0.9939	**0.8264**	**0.0081**
Oxidative Stress					
Rubredoxin-NAD (+) reductase	2.11–6.89	**−0.7811**	**0.0077**	−0.5774	0.1106
	2.11–5.85	**−0.8424**	**0.0102**	−0.6547	0.1249
QorR	2.11–5.85	**−0.8424**	**0.0102**	−0.6547	0.1249
	0.00–5.85	−0.2261	0.2926	**−0.7367**	**0.0280**
Uncharacterized glutathione S-transferase-like protein	6.79–9.22	0.2190	0.0826	0.6208	**0.0034**
Alkyl hydroperoxide reductase	2.11–5.85	**−0.8892**	**0.0041**	−0.5218	0.2432
OT coproporphyrinogen III oxidase	2.11–6.89	**−0.8333**	**0.0031**	−0.6429	0.0682
	2.11–5.85	**−0.9678**	**0.0001**	−0.7143	0.0846
Glutamate-cysteine ligase	2.11–5.85	**−0.8923**	**0.0038**	**−0.9411**	**0.0034**
Paraquat-inducible protein A	0.00–6.89	0.7090	0.9913	**0.7570**	**0.0084**
Glutathionylspermidine amidohydrolase	6.79–9.22	0.2094	0.0881	0.5293	**0.0075**
CoA-disulfide reductase	0.00–5.85	0.7287	0.9843	**0.8429**	**0.0060**
Hydroxyacylglutathione hydrolase	7.00–9.22	0.2236	0.1126	**−0.7186**	**0.0340**
Iron-binding ferritin-like antioxidant protein	0.00–5.85	0.1037	0.7855	**0.9708**	**<0.0001**
Glutaredoxin-related protein	2.11–6.89	−0.5407	0.0770	**−0.7075**	**0.0381**
Oxidoreductase YihU	2.11–5.95	**−0.8424**	**0.0102**	−0.6547	0.1249
GshF	2.11–5.95	**−0.8424**	**0.0102**	−0.6547	0.1249
Hydrogen peroxide-inducible genes activator	7.00–9.22	**−0.7824**	**0.0076**	**−0.8836**	**0.0025**
	6.79–9.22	**−0.7433**	**0.0052**	0.9416	0.2619
Glutathione synthetase	0.00–6.89	0.5343	0.9480	**0.7028**	**0.0180**
	2.11–6.89	0.3819	0.9548	**0.7638**	**0.0203**
Radical SAM family heme chaperone	2.11–6.89	**−0.7811**	**0.0077**	−0.5774	0.1106
	2.11–5.85	**−0.8424**	**0.0102**	−0.6547	0.1249
Xanthosine/inosine triphosphate pyrophosphatase	0.00–6.89	**−0.7243**	**0.0070**	**−0.8081**	**0.0034**
Xanthosine/inosine triphosphate diphosphatase	0.00–6.89	−0.6499	**0.0181**	**−0.7173**	**0.0149**
	2.11–6.89	**−0.9638**	**0.0002**	–	–
Probable peroxiredoxin	2.11–6.89	**−0.7811**	**0.0077**	−0.5474	0.1106
	2.11–5.85	**−0.8424**	**0.0102**	−0.6547	0.1249
Organic hydroperoxide resistance transcriptional regulator	6.79–9.22	−0.3910	0.1286	0.3731	**0.0068**
Thiol:disulfide oxidoreductase	2.11–6.89	**−0.7811**	**0.0077**	−0.5774	0.1106
	2.11–5.85	**−0.8424**	**0.0102**	−0.6547	0.1249
	0.00–5.85	−0.2261	0.2926	**1.0000**	**<0.0001**
Osmotic stress					
Glycine betaine transporter OpuD	2.11–6.89	**−0.7639**	**0.0100**	−0.6001	0.0944
	2.11–5.85	**−0.7038**	**0.0474**	−0.5161	0.2491
Choline ABC transport system	2.11–6.89	**−0.7216**	**0.0170**	−0.6088	0.0886
	2.11–5.85	**−0.7414**	**0.0346**	−0.6983	0.0946
Glycine betaine ABC transport system	2.11–5.85	**−0.8498**	**0.0090**	**−0.8286**	**0.0297**
L-Proline glycine betaine ABC transport system permease	6.79–9.22	−0.3996	0.1229	0.4931	**0.0059**
YehW	2.11–5.85	**−0.8424**	**0.0102**	−0.6547	0.1249
Osmotically inducible protein OsmY	2.11–5.85	**−0.8424**	**0.0102**	−0.6547	0.1249
Glucans biosynthesis protein C	2.11–5.85	**−0.8424**	**0.0102**	−0.6547	0.1249
Glucans biosynthesis glucosyltransferase H	2.11–5.85	**−0.7298**	**0.0383**	−0.6983	0.0946
NdvA	0.00–6.89	−0.0691	0.4347	**0.9324**	**0.0005**

(Continued)

TABLE 3 (Continued)

Enzyme transcripts[1]	*Salmonella* abundance (Log_{10} genomes/g[2])	Correlation coefficients[3]			
		Pearson		Spearman	
		r =	p =	ρ =	p =
Acid tolerance					
Carbonic anhydrous	0.00–5.85	0.3307	0.7922	**0.7350**	**0.0285**
Ornithine aminotransferase	7.00–9.22	**−0.7900**	**0.0067**	**−0.7609**	**0.0211**
Glutamate transport ATP-binding protein	7.00–9.22	0.7719	0.9911	**0.7545**	**0.0228**
Iron acquisition					
Iron chelate uptake ABC transporter family permease	2.11–5.85	**−0.8424**	**0.0102**	−0.6547	0.1249
	2.11–6.89	**−0.7811**	**0.0077**	−0.5774	0.1106
Heat shock					
DnaJ	0.00–5.85	−0.6695	**0.0291**	**0.9767**	**<0.0001**
GrpE	7.00–9.22	0.6085	0.9514	**0.7425**	**0.0262**
HrcA	7.00–9.22	0.7567	0.9890	**0.7665**	**0.0196**
Ribosome-associated heat shock protein	2.11–6.89	−0.5922	0.0547	**−0.7326**	**0.0293**
Carbon starvation					
Adenylate cyclase	0.00–6.89	0.5411	0.9506	**0.7966**	**0.0042**
	0.00–5.85	0.6448	0.9637	**0.7617**	**0.0208**
	2.11–6.89	0.5415	0.9234	**0.7545**	**0.0228**
CRP/FNR family transcriptional regulator	2.11–5.85	**−0.9377**	**0.0008**	**−0.9429**	**0.0032**
Carbon starvation protein A	7.00–9.22	0.7533	0.9885	**0.7904**	**0.0142**
Starvation lipoprotein Slp	2.11–5.85	**−0.8424**	**0.0102**	−0.6547	0.1249
Aldose-ketose isomerase YihS	2.11–5.85	**−0.8424**	**0.0102**	−0.6547	0.1249
Cellobiose phosphorylase	2.11–5.85	**−0.7420**	**0.0344**	−0.0286	0.9521
Outer membrane sugar transport protein YshA	2.11–5.85	**−0.8424**	**0.0102**	−0.6547	0.1249
Transcriptional regulator SgrR	2.11–5.85	**−0.8424**	**0.0102**	−0.6547	0.1249
	0.00–5.85	−0.2261	0.2926	**0.8488**	**0.0054**
Various polyols ABC transporters	2.11–6.89	**−0.7259**	**0.0162**	−0.6429	0.0682
Universal stress response					
Universal stress protein D	0.00–5.85	0.1950	0.6804	**0.8851**	**0.0024**
Universal stress protein G	2.11–5.85	**−0.8424**	**0.0102**	−0.6547	0.1249
Cold shock response					
CspD	6.79–9.22	−0.4641	0.0846	0.5354	**0.0002**
Envelop stress					
Phage shock protein A	2.11–5.85	**−0.8769**	**0.0054**	−0.4638	0.3067
	0.00–5.85	−0.1500	0.3599	**0.7211**	**0.0331**
Psp operon transcriptional activator	2.11–6.89	**−0.7811**	**0.0077**	−0.5774	0.1106
	2.11–5.85	**−0.8424**	**0.0102**	−0.6547	0.1249
Outer membrane stress sensor protease Deg	2.11–6.89	0.7090	0.9804	**0.8539**	**0.0049**
Outer membrane protein H precursor	2.11–6.89	**−0.7811**	**0.0077**	−0.5774	0.1106
	2.11–5.85	**−0.8424**	**0.0102**	−0.6547	0.1249
Sigma factor RpoE-negative regulatory protein RseA	0.00–5.85	0.4320	0.8628	**0.7633**	**0.0203**

[1]Pearson or Spearman correlation analysis was performed for enzyme abundance versus *Salmonella* abundance for 598 enzyme transcripts from MG-RAST KO metabolism, stress, or virulence data sets. Results are organized into metabolism (carbohydrate utilization; fermentation; TCA; respiration; or amino acid/nitrogen metabolism) or stress response (antimicrobials; oxidative stress; osmotic stress; acid tolerance, iron acquisition; heat shock; carbon starvation; universal stress response; cold shock or envelop stress) categories. Of all enzyme transcripts, 171 correlated with *Salmonella* abundance ($p < 0.05$), whereas 52 correlated with chicken age ($p < 0.05$, not shown). [2]qPCR was used to estimate *Salmonella* abundance per gram cecal content (Pedroso et al., 2021). [3]Significant r- or ρ-values > 0.6999 for Pearson or Spearman, respectively, or $p < 0.05$ are bold.

transcripts for transport and channeling of these sugars into central catabolic pathways. Twenty-four enzyme transcripts associated with carbohydrate utilization, out of 70 analyzed, had a significantly positive or negative correlation with *Salmonella* abundance as determined by Pearson or Spearman correlation coefficients ($p < 0.05$), and 5 and 12 of these enzyme transcripts correlated with high or low *Salmonella* abundance, respectively (Table 3). The enzymes α-galactosidase, L-fuculokinase, and rhamnulokinase exhibited a significant ($p < 0.05$) positive correlation with high *Salmonella* abundance (7.00–9.22 Log_{10} *Salmonella* genomes/g cecal contents), while arabinogalactan endo-4,4-β-galactosidase, ribose/xylose/arabinose/galactoside ABC-type transport, ABC-type maltose transport system, β-hexosaminidase, and dehydro-3-deoxyphosphogluconate

10.3389/fmicb.2024.1342887

TABLE 4 Volatile fatty acid composition of cecal contents of chickens colonized with *Salmonella*.

Volatile fatty acid	8.51 Log_{10} genomes/g[1]		7.00 Log_{10} genomes/g[1]	
	Weight (μg)	Mole %	Weight (μg)	Mole %
Acetate	13.6	2.7	146.8	91.0
Propionate	325.3	51.5	5.2	2.6
Butyrate	325.0	43.3	15.0	6.4
Valerate	21.0	2.4	0.0	0.0
Caproate	0.0	0.0	0.0	0.0
Decanoate	0.0	0.0	0.0	0.0
SUM	684.9	100.0	167.1	100.0

[1]*Salmonella* abundance.

TABLE 5 Carbohydrate composition of cecal contents from chickens colonized with *Salmonella*.

Sugar	5.85 Log_{10} genomes/g[1]			7.20 Log_{10} genomes/g[1]		
	Free[2]	Lipid[2]	Precipitate[2]	Free[2]	Lipid[2]	Precipitate[2]
Arabinose	0.0	40.2	24.2	0.0	32.7	32.5
Rhamnose	0.0	3.9	0.0	0.0	8.0	4.3
Fucose	0.0	2.7	2.7	0.0	0.7	2.1
Xylose	0.0	14.8	19.4	0.0	6.0	15.9
Glucuronic acid	0.0	2.0	0.0	0.0	9.3	Trace
Galacturonic acid	0.0	1.0	2.5	0.0	0.3	1.9
Mannose	0.0	1.6	1.7	3.9	2.4	1.7
Galactose	31.0	17.6	11.1	26.2	16.9	29.4
Glucose	69.0	11.9	29.8	62.9	19.4	10.9
N-acetyl galactosamine	0.0	0.0	0.0	0.0	1.6	0.0
N-acetyl glucosamine	0.0	4.2	2.8	0.0	2.7	1.3
N-acetyl mannosamine	0.0	0.0	0.0	0.0	0.0	0.0

[1]*Salmonella* abundance. [2]Fractions.

aldolase were positively correlated with *Salmonella* low abundance (<6.00 Log_{10} *Salmonella* genomes/g cecal contents; $p < 0.05$). There was also a significant positive correlation with fucose isomerase and *Salmonella* abundance (2.11–9.22 Log_{10} *Salmonella* genomes/g, cecal content). Most fuculokinase (*fucK*) transcripts were identified as *E. coli* transcripts, while L-fucose isomerase (*fucI*) transcripts had >98% sequence identity with *Anaerotruncus colihominis* or *Clostridium* sp. *M62/1* (Supplementary Table S8).

Cytochrome bd type quinol oxidase and cytochrome o ubiquinol oxidase had a significant positive and negative correlation, respectively, with *Salmonella* abundance. Nickel-dependent hydrogenase had a positive correlation with *Salmonella* abundance from 2.11 to 9.22 Log_{10} *Salmonella* genomes/g cecal contents ($p < 0.05$) (Table 3). The majority of the enzyme transcripts associated with respiration were from *E. coli*, with a few identified as *Salmonella enterica* (*hybD*, *narI*) (Supplementary Table S8).

Finally, a detailed analysis of the cecal community transcriptome focused on amino acid metabolism and *Salmonella* abundance identified 43 enzyme transcripts associated with amino acid/nitrogen transport or metabolism and *Salmonella* abundance ($p < 0.05$ by Pearson or Spearman) (Table 3). These transcripts were responsible for arginine, aspartate, glutamate, glutamine, glycine, histidine, phenylalanine, threonine, tryptophan, and tyrosine metabolism. Five (ABC-type polar amino acid transport system; periplasmic component/domain involved in amino acid transport; isopropylmalate/homocitrate/citramalate synthases; acetylglutamate kinase; and glutamate 5-kinase) and 10 enzyme transcripts (glutamate dehydrogenase; 5-enolpyruvylshikimate-3-phosphate synthase; allophanate hydrolase; aspartate-semialdehyde dehydrogenase; glutaminase; imidazolonepropionase; arginine/lysine/ornithine decarboxylases; threonine efflux protein; phosphoribosylanthranilate isomerase; and uncharacterized protein involve in cysteine biosynthesis) from cecal transcriptomes with low *Salmonella* levels had positive or negative correlations, respectively, with *Salmonella* abundance ($p < 0.05$), while seven enzyme transcripts (transglutaminase-like enzyme; tryptophanase; anthranilate phos phoribosyltransferase; anthranilate/para-aminobenzoate synthase; di- and tripeptidases; glutamine synthetase; and histidine ammonia-lyase) had a significantly positive correlation with high *Salmonella* abundance. Enzyme transcripts that focused primarily on glutamate metabolism (*glt*, *gadB*, *gadC*, *gabT*, and *gabD*) were from *E. coli*, *Enterococcus*, *Lactobacillus*, *Clostridia*, and unknown organisms (Supplementary Table S8).

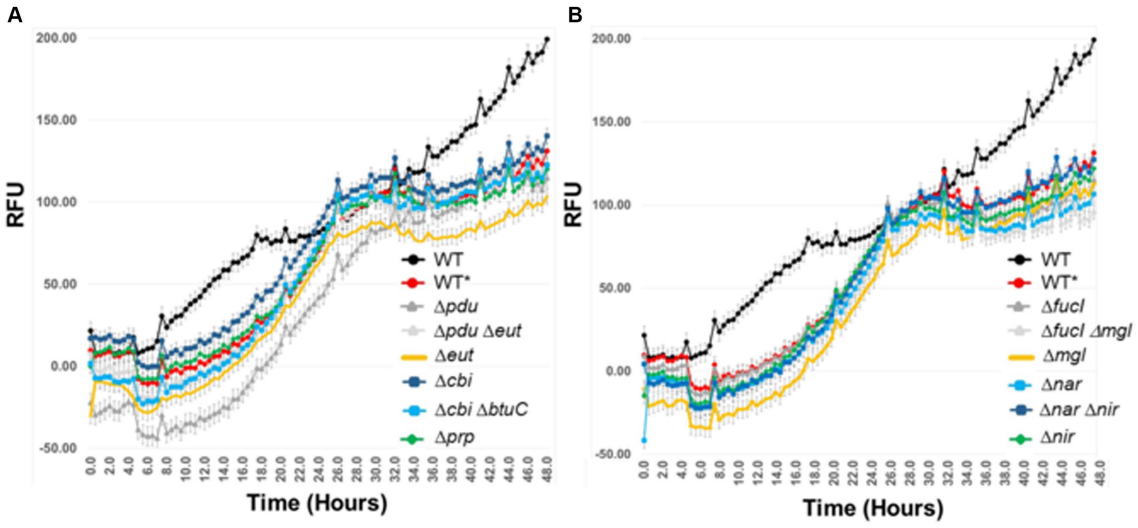

FIGURE 10
The effect of mutations in one or more metabolic pathways involved in *Salmonella* catabolism in an *ex vivo* intestinal environment containing an exclusive community. λ Red was used to create single and double mutations in *Salmonella* SL1344. pGLOW, a fluorescent reporter that fluoresces under aerobic and anaerobic conditions, was used to monitor *Salmonella* growth over 48 h. Mutant and wild-type (WT*) *S. typhimurium* SL1344 strains were grown in EVCC with exclusive community; WT was grown in EVCC alone as a control. Oxyrase (Sigma-Aldrich; St. Louis, MO) was added to the medium and overlaid with mineral oil to create and maintain low oxygen conditions. The selected mutations affect the catabolism of: **(A)** microbial metabolites (*eut*, *pdu*, *prp*), vitamin B12 synthesis (*cbi*), vitamin B12 uptake (*btuC*), or **(B)** sugar utilization (*fucI*, *mgl*) or anaerobic respiration (*nar*, *nir*).

Salmonella exclusion by the intestinal community *ex vivo* was not due to scavenger metabolism and competition

Single and double mutations were examined in *Salmonella* that affected vitamin B12 synthesis (Δ*cbi*) or transport (Δ*btuC*); propanediol (Δ*pdu*) and ethanolamine utilization (Δ*eut*); propionate metabolism (Δ*prp*), fucose (Δ*fucI*) metabolism; anaerobic respiration (Δ*nar* or Δ*nir*), or glucose/galactose (Δ*mgl*) transport (Figure 10). A fluorescent reporter that functions under anaerobic conditions was used to monitor *Salmonella* growth over time. The *Salmonella* wild-type strain had a longer growth lag in co-culture with the exclusive community, and its growth plateaued sooner compared to growth in EVCC medium alone. At 18.5- to 26-h incubation, the exponential phase growth rate, as determined from the slope of the line, was the same for the *Salmonella* wild-type and most metabolic mutants when grown with the exclusive community (m = 4.27 + 0.04; range 4.04–4.57). However, the *Salmonella* Δ*pdu* single and Δ*cbi*, Δ*btuC* double mutants had slower (3.84) or faster (4.76) growth rates, respectively, compared to the wild type (4.23; Student's *t*-test $p < 0.05$), when grown with the exclusive community. Biphasic growth was observed over the 48-h incubation, but *Salmonella* growth was significantly retarded in co-culture with the exclusive community during the last 8 h ($m = 4.27$ vs. 1.35). The biphasic growth exhibited by *Salmonella* wild type in EVCC medium alone exhibited a slower growth rate in the first phase ($m = 2.74$) compared to the second phase ($m = 3.14$). These results using mutants deficient in scavenger metabolism, anaerobic respiration, and multiple carbohydrate utilization indicate that *Salmonella*'s metabolic versatility augments its ability to compete for nutrients with an exclusive community.

The role of antagonism in the mechanism of competitive exclusion

Salmonella ex vivo transcripts in response to both communities were elevated for 34 of the total 161 genes associated with the stress response (Figure 8), compared to their growth in EVCC alone. Approximately 70% of the response was associated with heat shock, acid tolerance, and antimicrobials. There was also a significant difference in the *Salmonella* stress response in the exclusive community, where transcription of 32 genes was increased compared to the permissive community. One-third of these genes were associated with response to antimicrobials (Figure 7). In a network analysis of the cecal community transcriptomes' stress response, a pattern emerged between cecal communities with high versus low *Salmonella* abundance (Figure 11). Oxidative stress appeared to be a major stress response in both cecal communities, but none of these or other stress response transcripts were shared, indicating that the stressors experienced in the communities were different. This contrasts with the results from the fermentation network analysis, where 30 enzyme transcripts were shared between *Salmonella* abundance groups and network analyses. For the high *Salmonella* abundance group, the organic hydroperoxide resistance protein (*ohr*) was the central node linked to various enzymes involved in carbon starvation, cold stress, envelope stress, osmotic stress, and acid tolerance. It also connected with glutamate-1-semialdehyde aminotransferase, an enzyme with a role in antibiotic synthesis. Yersiniabactin non-ribosomal peptide synthase was the major node in the stress response network for the cecal community with low *Salmonella* abundance (Figure 11). Forty-one of the enzyme transcripts from the two cecal communities were identified as *E. coli* or *Enterococcus* transcripts (>98% nucleotide identity with >99% coverage by BLAST) (Figure 11; Supplementary Table S8). There was

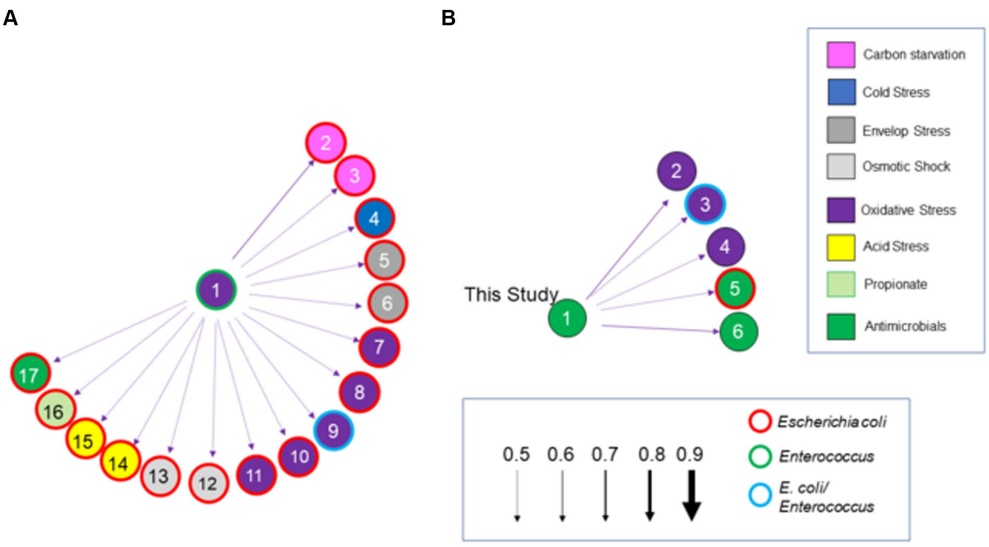

FIGURE 11
A Bayesian network analysis of the cecal transcriptome, focused on stress response, from chickens with high (>5.85 Log_{10} *Salmonella* genomes/g) **(A)** or low **(B)** *Salmonella* abundance. The network depicted was constructed using the score-based learning algorithm Hill-Climbing (arrows with solid line). Arrows indicate the direction and strength of the connection. Enzymes are color-coded based on the stress response. Enzymes or genes identified in the high *Salmonella* abundance community **(A)** are: (1) organic hydroperoxide resistance protein (*ohr*); (2) universal stress protein E (*uspE*); (3) *yciT*; (4) *cspI*; (5) *pspC*; (6) *rseA*; (7) *arcA*; (8) glutaredoxin; (9) *nrd*; (10) *yncG*; (11) *fmrR*; (12) *betI*; (13) *yehZ*; (14) *ybaT*; (15) *hdeA*; (16) propanediol diffusion facilitator; (17) glutamate-1-semialdehyde aminotransferase. Enzymes or genes identified in the low *Salmonella* abundance community **(B)** are: (1) yersiniabactin non-ribosomal peptide synthase; (2) putative bacterial hemoglobin; (3) *gshF*; (4) *hemW*; (5) *tehB*; (6) thioesterase domains of type I polyketides. Circles with thick red, green, or blue borders are for enzymatic transcripts with 98–100% nucleotide identity, by BLAST scores, to *Escherichia coli*, *Enterococcus* spp. or both, respectively.

a significantly negative correlation between transcript and *Salmonella* abundance for 72.5% of the enzyme transcripts associated with cecal transcriptomes' stress response (Table 3). Several of these transcripts were associated with polyketide synthesis and annotated as: polyketide synthase module; thioesterase domains of type I polyketide synthases; Yersiniabactin non-ribosomal peptide synthase, non-ribosomal peptide/polyketide synthase, synthetase, and salicyl-AMP ligase; mycobactin salicyl-AMP ligase; oligoketide cyclase/lipid transport protein; and predicted thioesterase involved in non-ribosomal peptide biosynthesis. For yersiniabactin non-ribosomal peptide synthase, a few transcripts displayed a significant nucleotide identity with *E. coli* and *Klebsiella pneumoniae*. These sequence matches were identified as polyketide synthases *irp* responsible for producing the iron-scavenging yersiniabactin siderophore.

Several of the antimicrobial transcripts with a positive correlation to *Salmonella* abundance were also associated with antimicrobial resistance, such as colicin E2 resistance *creA*; rRNA small subunit methyltransferase I (*rsmI*); spectinomycin 9-O-adenylyltransferase [*ant (9)*]; and translation elongation factor *lepA*. The *creA* transcript was from *E. coli* (≥98% nucleotide identity; ≥99 coverage by BLAST). The aminoglycoside resistance gene *ant (9)* was commonly associated with a variety of diverse bacterial species with near-identical nucleotide sequences, including spectinomycin-resistant *Bacteroides*, *Campylobacter jejuni*, *Lactobacillus crispatus*, *Clostridioides difficile*, and *Clostridium* sp. *C1*. Additionally, the following antimicrobial resistance genes were identified in the chicken cecal transcriptome: *aadA1*, *spw*, *erm(B)*, and *ermG*. The latter two antibiotic resistance genes were from many bacterial species, including those commonly inhabiting the gastrointestinal tract (Supplementary Table S8). The *lepA* and *rsmI* enzyme transcripts had identity to sequences in *E. coli*, *Enterococcus* sp., various *Clostridia*, and unknown bacteria.

These results indicate that many of the members of the intestinal bacterial community were expressing resistance to antimicrobial compounds such as bacteriocins and antibiotics; however, there were no exogenous antimicrobials administered to the birds. The polyketide pathways suggest that some members of the microbiota may have been secreting antimicrobials that modulated the bacterial community, indicating the role of antagonism in competitive exclusion.

Discussion

An exclusive bacterial community attenuates the expression of virulence

These experiments illustrated that the chicken intestinal microbiota can significantly modulate *Salmonella*'s pathogenic behavior, indicating that attenuation may be involved in competitive exclusion. This suppression may be due to microbial metabolites like butyrate (Zhang Z.J. et al., 2020) or indole (Kohli et al., 2018) being shown to repress the SPI-1 T3SS cell invasion locus. Butyrate was not likely the main repressor, as this pathway was expressed in the cecal transcriptome of chickens with low and high *Salmonella* abundance, and there were differences in butyrate levels in chickens with high *Salmonella* abundance. Tryptophanase, the enzyme that liberates indole from tryptophan, was also present in the cecal transcriptome and directly proportional to *Salmonella* levels in the cecum, suggesting indole as a likely modulator of *Salmonella* virulence by the intestinal community.

However, repression of SPI-1 T3SS by the exclusive community may be indirect, as this community also slowed *Salmonella* growth *ex vivo*, and growth rate is important in regulating the cell invasion of T3SS (Lee and Falkow, 1990). In addition, the exclusive community turned on *avrA*, a gene within the SPI-1 locus that lowers inflammation (Jones et al., 2008) and restores intestinal barrier integrity (Liao et al., 2008). It is the combination of SPI-1 T3SS repression and *avrA* activation that is responsible for *Salmonella*'s reduced virulence in the presence of an exclusive community. Others have shown repression of an enteropathogen's virulence by the intestinal community or its member species (Le Bihan et al., 2015; Girinathan et al., 2021; Saenz et al., 2023).

In avian and mammalian species, juveniles are more likely to exhibit disease symptoms than adults when infected with *Salmonella* (Barrow and Methner, 2013). Day-of-hatch chicks may succumb to *Salmonella* infection after challenge (Bythwood et al., 2019), while 2-day-old birds will not. Instead, they shed high levels of *Salmonella* for 2–3 weeks before there is a precipitous drop in *Salmonella* shedding at approximately 3 weeks of age (Cheng et al., 2015; Pedroso et al., 2021). This suggests that the hatchling's intestinal community is not effective in reducing the expression of *Salmonella* pathogenic behavior, but the microbiota rapidly gains this ability or at least counters inflammation induced by the pathogen (Yu et al., 2023). The exclusive community repressed LPS modification by the *pmr* locus in *Salmonella*, which is associated with resistance to cationic antimicrobial peptides (Matamouros and Miller, 2015). The host's intestinal surface expresses β-defensins, a group of cationic antimicrobial peptides toxic to *Salmonella* (Milona et al., 2007). The exclusive community repressed *pmr* and therefore would make *Salmonella* susceptible to these and other defensins. While this early community can reduce the pathogen's virulence early in the chick's life, it's not sufficient to exclude the pathogen from the intestinal luminal environment. The mechanism of competitive exclusion must involve more than suppression of the pathogen's virulence in its mode of action.

Competition did not overcome *Salmonella*'s metabolic versatility

Salmonella appeared to spend less energy toward anabolism when grown in the permissive community compared to the exclusive community. There was a substantial difference in transcript abundance for amino acid metabolism and peptide transport, nucleotide biosynthesis, and vitamin B12 uptake between *Salmonella* grown in these two communities. There were also differences in cecal community transcript abundance in the comparison of enzymes involved in amino acid metabolism. These findings suggest substantial differences in the availability of free amino acids, nucleotides, and vitamins within permissive and exclusive communities. Low availability of these nutrients in an exclusive community should result in *Salmonella*'s slow growth because of the energy cost of *de novo* synthesis (Ushijima and Seto, 1991; Ha et al., 1994; Yang et al., 2016, 2017).

However, the diverse sugars available for *Salmonella* utilization were reflected in the glycome analysis of the cecal contents of birds with high *Salmonella* abundance. In addition, the cecal community transcriptome displayed a diversity of glycosyl hydrolases that would liberate these sugars from complex carbohydrates and glycoproteins. Carbohydrate metabolism appeared to be central to *Salmonella* growth, as revealed by the array of *Salmonella* enzyme transcripts associated with catabolism and the significant number of differentially expressed genes subject to catabolite repression. This concurs with the finding that mutations in *crp* and *cya* attenuate *Salmonella* (Curtiss and Kelly, 1987) and other intestinal pathogens (Peighambari et al., 2002; Sun et al., 2010; Zhou et al., 2020). The *ex vivo* transcriptome revealed that the exclusive community appeared to contain fewer sugars but more fermentation end products, such as propanediol, for *Salmonella* growth. Network connections and cecal community enzyme transcript abundance relative to *Salmonella* levels indicated that propanediol may be linked to *Salmonella* growth through community cooperation. Transcriptional analysis of *Salmonella* grown anaerobically *ex vivo* in the exclusive community showed abundant respiration transcripts, suggesting that it was involved in growth on a poor energy source such as 1,2-propanediol. Propanediol utilization has previously been shown to be a contributor to early *Salmonella* colonization in mice and chickens; however, these studies were done with animals lacking a mature intestinal microbiota (Harvey et al., 2011; Faber et al., 2017). These results suggest that cooperation may be involved in promoting *Salmonella* growth in cecal communities.

Several metabolic genes were identified that were differentially regulated in the cecal communities with high or low *Salmonella* abundance. Single and multiple deletions were introduced into these genes to assess their contribution to *Salmonella* growth in the exclusive community. The genes *pdu*, *cbi*, and vitamin B12 receptors are all necessary for propanediol metabolism, and they were transcribed during the *ex vivo* growth of *Salmonella* with the cecal communities. Only the *Salmonella* Δ*pdu* single mutation significantly reduced *Salmonella* growth rates compared to wild type. There were no significant growth defects between the other mutants and wild type in the presence of the exclusive community. This finding suggests that, when presented with a diverse array of nutrients, *Salmonella* is metabolically versatile and adapts to the changing availability of nutrients in the intestine. Its metabolic versatility is reflected in the different metabolic genes shown to be involved in the colonization of different animal and plant species (Kwan et al., 2018). Therefore, neither cooperation nor competition appears to be the sole mechanism behind competitive exclusion.

Cecal communities may exhibit antagonism via the production of antimicrobials

The network analysis of the cecal stress response revealed that a polyketide synthase was the central node linked to similar enzymes in the cecal community containing low *Salmonella* abundance. With a few exceptions, these enzyme transcripts could not be assigned to known intestinal species in the NCBI database but exhibited similarity to as yet to be identified clostridial species. Most polyketide synthase modules responsible for antibiotic synthesis have been found in aerobic soil microbes because much research has focused on these organisms (Behnken and Hertweck, 2012a). However, recent studies have identified potential antimicrobial polyketides in *Clostridia* (Seedorf et al., 2008; Behnken and Hertweck, 2012b; Li et al., 2020), and polyketide synthases have been identified within the human

intestinal microbiome (Fritz et al., 2018). Clostridial polyketide synthase may also be involved in siderophore synthesis (Singh et al., 2017). There was a negative correlation between transcript abundance for many of these enzymes and *Salmonella* levels in the cecum, as well as other enzyme transcripts associated with antibiotic and colicin resistance. This finding suggests that the exclusive community was likely producing antimicrobial substances. In addition, transcripts annotated as resistance genes with homology to many intestinal species, including *Salmonella* and *E. coli*, were detected, indicating the expression of antibiotic resistance. The chickens used in this study were reared without any antibiotics; therefore, the *in vivo* detection of antimicrobial resistance gene expression was not due to iatrogenic usage. Alternatively, the contact-dependent antibacterial type 6 secretion system (T6SS) (Alteri et al., 2013) might be at play in *Salmonella* exclusion. The *ex vivo* experiment would have precluded the detection of this mechanism. However, *E. coli* T6SS transcripts were present in the cecal transcriptomes, demonstrating the strength of a combined *ex vivo*/*in vivo* approach to unraveling the mechanism of competitive exclusion. While there was a negative correlation between the cecal T6SS transcript and *Salmonella* abundance, this is not the likely mechanism, as this correlation was only observed in chickens with high *Salmonella* colonization.

Early work demonstrated inhibition of *Salmonella* growth by cecal microbiota *in vivo* (Bohnhoff et al., 1964a; Royal and Mutimer, 1972), and pretreatment of mice with streptomycin reduced the inhibitory effect of the cecal microbiota on *Salmonella* colonization (Bohnhoff et al., 1964b). Others have looked at the ability of intestinal species to compete with bacterial pathogens for limiting resources (Barrow et al., 1987; Ushijima and Seto, 1991) or adherence to mucosal surfaces, indicating that competition was accepted as the mechanism of competitive exclusion (Gusils et al., 2003; Collado et al., 2005). However, the inhibitory effect on *Salmonella* growth was hypothesized to be related to volatile fatty acid (VFA) production and the potentiating effect of pH, suggesting that the role of inhibition was also considered (Bohnhoff et al., 1964b; Royal and Mutimer, 1972). This led to bio-prospecting for intestinal bacteria species for their production of inhibitory VFAs (Hinton et al., 1991). Antimicrobial production has also been used to select candidate probiotics; however, most have failed to reduce *Salmonella* colonization (Pan et al., 2008; Grant et al., 2018; Lu et al., 2023). There has also been considerable focus on microbes that produce bacteriocins (Grant et al., 2018; Angelopoulou et al., 2019; Khan et al., 2020). As an example, Wooley *et al.* demonstrated the inhibitory effects of a microcin-producing avian *E. coli* isolate on *Salmonella* colonization in chickens (Wooley et al., 1999). More recently, *Bacillus* spp. have been shown to be quite effective at excluding or controlling some intestinal pathogens in chickens (Grant et al., 2018). The genus *Bacillus* contains many member species containing antimicrobial polyketide synthases (*pks*) (Olishevska et al., 2019). *B. subtilis pks* has been shown to produce substances that inhibit *Salmonella* growth in co-culture (Podnar et al., 2022). It has been long established that prophylactic use of antibiotics, even at sub-therapeutic levels, can adversely affect *Salmonella* colonization in several animal species, including chickens (Sieburth, 1957; Evangelisti et al., 1975; Smith and Tucker, 1975). The logical next step would be to screen, isolate, and characterize presumptive antimicrobials from exclusive communities to demonstrate their effects on colonization.

Conclusion

The mode of action of competitive exclusion in reducing *Salmonella* in chickens appears to involve a combination of competition, attenuation, and antagonism by member species in the cecal community. Studies have demonstrated the importance of microbial community diversity in pathogen exclusion (recently reviewed in Pedroso et al., 2021). There have been many studies seeking to identify one or several intestinal species that inversely correlate with *Salmonella* abundance in the chicken intestine in an effort to describe a defined competitive exclusion formulation. Except for the *Bacillus* commercial products, no single species has been shown to directly affect *Salmonella* abundance in chickens across multiple studies. Even the competitive exclusion product Aviguard® exhibits considerable variability in community composition while retaining product efficacy for reducing *Salmonella* levels in chickens (Lee et al., 2023b). This diversity may reflect the multitude of intestinal species required to collectively affect *Salmonella*'s metabolic versatility and compete for the available resources in the intestine, reduce pathogenic behavior, or produce antimicrobials that inhibit *Salmonella*. Overlap of single functions may occur between different members of the collective community, rendering individual species dispensable. Alternatively, all three functions may be required for pathogen exclusion within the collective community, with a diversity of members necessary to achieve pathogen control.

Data availability statement

The datasets presented in this study can be found in online repositories. The names of the repository/repositories and accession number(s) can be found in the article/Supplementary material.

Ethics statement

The animal study was approved by the University of Georgia Animal Care and Use and Procedures Committee. The study was conducted in accordance with the USDA and institutional requirements.

Author contributions

JM: Conceptualization, Data curation, Formal analysis, Funding acquisition, Investigation, Writing – original draft, Writing – review & editing. YC: Conceptualization, Formal analysis, Investigation, Methodology, Writing – review & editing. AP: Investigation, Methodology, Writing – review & editing. KT: Formal analysis, Investigation, Methodology, Writing – review & editing. SA: Data curation, Formal analysis, Investigation, Methodology, Writing – review & editing. TK: Investigation, Methodology, Writing – review & editing. GM: Formal analysis, Supervision, Writing – review & editing. SK: Data curation, Formal analysis, Writing – review & editing. SP: Data curation, Formal analysis, Investigation, Methodology, Validation, Writing – review & editing. MM: Conceptualization, Data curation,

Formal analysis, Funding acquisition, Investigation, Writing – review & editing. JE-S: Methodology, Writing – review & editing. ML: Conceptualization, Funding acquisition, Investigation, Project administration, Supervision, Writing – review & editing.

Funding

The author(s) declare financial support was received for the research, authorship, and/or publication of this article. This study was supported by grants from the United States Department of Agriculture (2005–01378, 2009–03561, and VA-160130). JE-S was supported by NIH grant R35-GM130399. Carbohydrate analysis was supported by the Chemical Sciences, Geosciences, and Biosciences Division, Office of Basic Energy Sciences, U.S. Department of Energy grant (DE-SC0015662) to Parastoo Azadi at the University of Georgia Complex Carbohydrate Research Center.

Acknowledgments

We wish to thank Beatrice Kolwaski's assistance with measuring the growth rate of the *Salmonella* reporter strain YC1104.

Conflict of interest

The authors declare that the research was conducted in the absence of any commercial or financial relationships that could be construed as a potential conflict of interest.

The author(s) declared that they were an editorial board member of Frontiers, at the time of submission. This had no impact on the peer review process and the final decision.

Publisher's note

Supplementary material

The Supplementary material for this article can be found online at: https://www.frontiersin.org/articles/10.3389/fmicb.2024.1342887/full#supplementary-material

References

Alteri, C. J., Himpsl, S. D., Pickens, S. R., Lindner, J. R., Zora, J. S., Miller, J. E., et al. (2013). Multicellular bacteria deploy the type VI secretion system to preemptively strike neighboring cells. *PLoS Pathog.* 9:e1003608. doi: 10.1371/journal.ppat.1003608

Altschul, S. F., Gish, W., Miller, W., Myers, E. W., and Lipman, D. J. (1990). Basic local alignment search tool. *J. Mol. Biol.* 215, 403–410. doi: 10.1016/S0022-2836(05)80360-2

Angelopoulou, A., Warda, A. K., Hill, C., and Ross, R. P. (2019). Non-antibiotic microbial solutions for bovine mastitis - live biotherapeutics, bacteriophage, and phage lysins. *Crit. Rev. Microbiol.* 45, 564–580. doi: 10.1080/1040841X.2019.1648381

Anonymous (2021). *Salmonella outbreak linked to wild songbirds*. Center for Disease Control and Prevention. Available at: https://www.cdc.gov/salmonella/typhimurium-04-21/index.html (Accessed April 29, 2021).

Azcarate-Peril, M. A., Butz, N., Cadenas, M. B., Koci, M., Ballou, A., Mendoza, M., et al. (2018). An attenuated *Salmonella enterica* Serovar typhimurium strain and Galacto-oligosaccharides accelerate clearance of Salmonella infections in poultry through modifications to the gut microbiome. *Appl. Environ. Microbiol.* 84:e02526-17. doi: 10.1128/AEM.02526-17

Babinszky, I. J., Tossenberger, K. N., and Halas, V. (2006). Determination of amino acid distibility with different methods in birds (a comparative study). *Slovak J. Anim. Sci.* 39, 74–78.

Ballou, A. L., Ali, R. A., Mendoza, M. A., Ellis, J. C., Hassan, H. M., Croom, W. J., et al. (2016). Development of the Chick microbiome: how early exposure influences future microbial diversity. *Front. Vet. Sci.* 3:2. doi: 10.3389/fvets.2016.00002

Barrow, P. A., and Methner, U. (2013). *Salmonella in domestic animals*. Wallingford, United Kingdom: CABI.

Barrow, P. A., Tucker, J. F., and Simpson, J. M. (1987). Inhibition of colonization of the chicken alimentary tract with *Salmonella* Typhimurium gram-negative facultatively anaerobic bacteria. *Epidemiol. Infect.* 98, 311–322. doi: 10.1017/S0950268800062063

Bartlett, M. S., and Gourse, R. L. (1994). Growth rate-dependent control of the rrnB P1 core promoter in *Escherichia coli*. *J. Bacteriol.* 176, 5560–5564. doi: 10.1128/jb.176.17.5560-5564.1994

Beck, J. R., and Chang, T. S. (1980). Measurement of uric acid levels in chicken cecal contents. *Poult. Sci.* 59, 1193–1196. doi: 10.3382/ps.0591193

Behnken, S., and Hertweck, C. (2012a). Anaerobic bacteria as producers of antibiotics. *Appl. Microbiol. Biotechnol.* 96, 61–67. doi: 10.1007/s00253-012-4285-8

Behnken, S., and Hertweck, C. (2012b). Cryptic polyketide synthase genes in non-pathogenic Clostridium SPP. *PLoS One* 7:e29609. doi: 10.1371/journal.pone.0029609

Benoit, S. L., Maier, R. J., Sawers, R. G., and Greening, C. (2020). Molecular hydrogen metabolism: a widespread trait of pathogenic Bacteria and Protists. *Microbiol. Mol. Biol. Rev.* 84:e00092-19. doi: 10.1128/MMBR.00092-19

Bhogoju, S., Nahashon, S., Wang, X., Darris, C., and Kilonzo-Nthenge, A. (2018). A comparative analysis of microbial profile of Guinea fowl and chicken using metagenomic approach. *PLoS One* 13:e0191029. doi: 10.1371/journal.pone.0191029

Bochner, B. R., Huang, H. C., Schieven, G. L., and Ames, B. N. (1980). Positive selection for loss of tetracycline resistance. *J. Bacteriol.* 143, 926–933. doi: 10.1128/jb.143.2.926-933.1980

Bohnhoff, M., Miller, C. P., and Martin, W. R. (1964a). Resistance of the mouse's intestinal tract to experimental Salmonella infection. I. Factors which interfere with the initiation of infection by oral inoculation. *J. Exp. Med.* 120, 805–816. doi: 10.1084/jem.120.5.805

Bohnhoff, M., Miller, C. P., and Martin, W. R. (1964b). Resistance of the mouse's intestinal tract to experimental Salmonella infection. II. Factors responsible for its loss following streptomycin treatment. *J. Exp. Med.* 120, 817–828. doi: 10.1084/jem.120.5.817

Brinsmade, S. R., Paldon, T., and Escalante-Semerena, J. C. (2005). Minimal functions and physiological conditions required for growth of *salmonella enterica* on ethanolamine in the absence of the metabolosome. *J. Bacteriol.* 187, 8039–8046. doi: 10.1128/JB.187.23.8039-8046.2005

Bythwood, T. N., Soni, V., Lyons, K., Hurley-Bacon, A., Lee, M. D., Hofacre, C., et al. (2019). Antimicrobial resistant *Salmonella enterica* typhimurium colonizing chickens: the impact of plasmids, genotype, bacterial communities, and antibiotic administration on resistance. *Front. Sustain. Food Syst.* 3:20. doi: 10.3389/fsufs.2019.00020

Cheng, Y., Pedroso, A. A., Porwollik, S., Mcclelland, M., Lee, M. D., Kwan, T., et al. (2015). rpoS-regulated core genes involved in the competitive fitness of *Salmonella enterica* Serovar Kentucky in the intestines of chickens. *Appl. Environ. Microbiol.* 81, 502–514. doi: 10.1128/AEM.03219-14

Choi, J. H., Kim, G. B., and Cha, C. J. (2014). Spatial heterogeneity and stability of bacterial community in the gastrointestinal tracts of broiler chickens. *Poult. Sci.* 93, 1942–1950. doi: 10.3382/ps.2014-03974

Chopyk, J., Moore, R. M., Dispirito, Z., Stromberg, Z. R., Lewis, G. L., Renter, D. G., et al. (2016). Presence of pathogenic *Escherichia coli* is correlated with bacterial community diversity and composition on pre-harvest cattle hides. *Microbiome* 4, 1–11. doi: 10.1186/s40168-016-0155-4

Collado, M. C., Gueimonde, M., Hernández, M., Sanz, Y., and Salminen, S. (2005). Adhesion of selected Bifidobacterium strains to human intestinal mucus and the role of adhesion in Enteropathogen exclusion. *J. Food Prot.* 68, 2672–2678. doi: 10.4315/0362-028X-68.12.2672

Curtiss, R., and Kelly, S. M. (1987). *Salmonella* Typhimurium deletion mutants lacking adenylate cyclase and cyclic AMP receptor protein are avirulent and immunogenic. *Infect. Immun.* 55, 3035–3043. doi: 10.1128/iai.55.12.3035-3043.1987

Datsenko, K. A., and Wanner, B. L. (2000). One-step inactivation of chromosomal genes in *Escherichia coli* K-12 using PCR products. *Proc. Natl. Acad. Sci. USA* 97, 6640–6645. doi: 10.1073/pnas.120163297

Demain, A. L., and Solomon, N. A. (1986). *Manual of industrial microbiology and biotechnology*. Washington DC, United States: American Society for Microbiology.

Ding, J., Zhou, H., Luo, L., Xiao, L., Yang, K., Yang, L., et al. (2021). Heritable gut microbiome associated with *Salmonella enterica* Serovar Pullorum infection in chickens. *mSystems* 6:e01192-20. doi: 10.1128/mSystems.01192-20

Dower, W. J., Miller, J. F., and Ragsdale, C. W. (1988). High efficiency transformation of *E. coli* by high voltage electroporation. *Nucleic Acids Res.* 16, 6127–6145. doi: 10.1093/nar/16.13.6127

Drepper, T., Eggert, T., Circolone, F., Heck, A., Krauss, U., Guterl, J. K., et al. (2007). Reporter proteins for *in vivo* fluorescence without oxygen. *Nat. Biotechnol.* 25, 443–445. doi: 10.1038/nbt1293

Ebana, Y., and Furukawa, T. (2019). Networking analysis on superior vena cava arrhythmogenicity in atrial fibrillation. *Int J Cardiol Heart Vasc* 22, 150–153. doi: 10.1016/j.ijcha.2019.01.007

Ekmekci, B., Mcanany, C. E., and Mura, C. (2016). An introduction to programming for bioscientists: a Python-based primer. *PLoS Comput. Biol.* 12:e1004867. doi: 10.1371/journal.pcbi.1004867

Ernst, R. K., Dombroski, D. M., and Merrick, J. M. (1990). Anaerobiosis, type 1 fimbriae, and growth phase are factors that affect invasion of HEp-2 cells by *Salmonella* Typhimurium. *Infect. Immun.* 58, 2014–2016. doi: 10.1128/iai.58.6.2014-2016.1990

Evangelisti, D., English, A., Girard, A., Lynch, J., and Solomons, I. (1975). Influence of subtherapeutic levels of oxytetracycline on *Salmonella* Typhimurium in swine, calves, and chickens. *Antimicrob. Agents Chemother.* 8, 664–672. doi: 10.1128/AAC.8.6.664

Faber, F., Thiennimitr, P., Spiga, L., Byndloss, M. X., Litvak, Y., Lawhon, S., et al. (2017). Respiration of microbiota-derived 1,2-propanediol drives Salmonella expansion during colitis. *PLoS Pathog.* 13:e1006129. doi: 10.1371/journal.ppat.1006129

Falardeau, J., Yildiz, E., Yan, Y., Castellarin, S. D., and Wang, S. (2023). Microbiome and physicochemical features associated with differential *Listeria monocytogenes* growth in soft, surface-ripened cheeses. *Appl. Environ. Microbiol.* 89:e0200422. doi: 10.1128/aem.02004-22

Fink, R. C., Evans, M. R., Porwollik, S., Vazquez-Torres, A., Jones-Carson, J., Troxell, B., et al. (2007). FNR is a global regulator of virulence and anaerobic metabolism in *Salmonella enterica* serovar typhimurium (ATCC 14028s). *J. Bacteriol.* 189, 2262–2273. doi: 10.1128/JB.00726-06

Friedman, N., Goldszmidt, M., and Wyner, A. (2013). Data analysis with Bayesian networks: A bootstrap approach. arXiv preprint arXiv:1301.6695.

Fritz, S., Rajaonison, A., Chabrol, O., Raoult, D., Rolain, J. M., and Merhej, V. (2018). Full-length title: NRPPUR database search and *in vitro* analysis identify an NRPS-PKS biosynthetic gene cluster with a potential antibiotic effect. *BMC Bioinform.* 19:463. doi: 10.1186/s12859-018-2479-5

Fujikawa, H. (2016). Prediction of competitive microbial growth. *Biocontrol Sci.* 21, 215–223. doi: 10.4265/bio.21.215

Gast, R. K., and Beard, C. W. (1989). Age-related changes in the persistence and pathogenicity of *Salmonella* Typhimurium in chicks. *Poult. Sci.* 68, 1454–1460. doi: 10.3382/ps.0681454

Girinathan, B. P., Dibenedetto, N., Worley, J. N., Peltier, J., Arrieta-Ortiz, M. L., Immanuel, S. R. C., et al. (2021). *In vivo* commensal control of *Clostridioides difficile* virulence. *Cell Host Microbe* 29, 1693–1708.e1697. doi: 10.1016/j.chom.2021.09.007

Grant, A., Gay, C. G., and Lillehoj, H. S. (2018). *Bacillus* spp. as direct-fed microbial antibiotic alternatives to enhance growth, immunity, and gut health in poultry. *Avian Pathol.* 47, 339–351. doi: 10.1080/03079457.2018.1464117

Gunasekera, A., Ebright, Y. W., and Ebright, R. H. (1992). DNA sequence determinants for binding of the *Escherichia coli* catabolite gene activator protein. *J. Biol. Chem.* 267, 14713–14720. doi: 10.1016/S0021-9258(18)42099-6

Gunn, J. S. (2008). The Salmonella PmrAB regulon: lipopolysaccharide modifications, antimicrobial peptide resistance and more. *Trends Microbiol.* 16, 284–290. doi: 10.1016/j.tim.2008.03.007

Gusils, C., Oppezzo, O., Pizarro, R., and González, S. (2003). Adhesion of probiotic lactobacilli to chick intestinal mucus. *Can. J. Microbiol.* 49, 472–478. doi: 10.1139/w03-055

Ha, S. D., Ricke, S. C., Nisbet, D. J., Corrier, D. E., and Deloach, J. R. (1994). Serine utilization as a potential competition mechanism between Salmonella and a chicken Cecal bacterium. *J. Food Prot.* 57, 1074–1079. doi: 10.4315/0362-028X-57.12.1074

Hammarlund, S. P., Gedeon, T., Carlson, R. P., and Harcombe, W. R. (2021). Limitation by a shared mutualist promotes coexistence of multiple competing partners. *Nat. Commun.* 12:619. doi: 10.1038/s41467-021-20922-0

Harvey, P. C., Watson, M., Hulme, S., Jones, M. A., Lovell, M., Berchieri, A. Jr., et al. (2011). *Salmonella enterica* serovar typhimurium colonizing the lumen of the chicken intestine grows slowly and upregulates a unique set of virulence and metabolism genes. *Infect. Immun.* 79, 4105–4121. doi: 10.1128/IAI.01390-10

Heim, R., Prasher, D. C., and Tsien, R. Y. (1994). Wavelength mutations and posttranslational autoxidation of green fluorescent protein. *Proc. Natl. Acad. Sci. U. S. A.* 91, 12501–12504. doi: 10.1073/pnas.91.26.12501

Heim, R., and Tsien, R. Y. (1996). Engineering green fluorescent protein for improved brightness, longer wavelengths and fluorescence resonance energy transfer. *Curr. Biol.* 6, 178–182. doi: 10.1016/S0960-9822(02)00450-5

Hinton, A., Spates, G. E., Corrier, D. E., Hume, M. E., Deloach, J. R., and Scanlan, C. M. (1991). *In vitro* inhibition of the growth of *Salmonella* Typhimurium and Escherichia coli 0157:H7 by Bacteria isolated from the Cecal contents of adult chickens. *J. Food Prot.* 54, 496–501. doi: 10.4315/0362-028X-54.7.496

Hirn, J., Nurmi, E., Johansson, T., and Nuotio, L. (1992). Long-term experience with competitive exclusion and salmonellas in Finland. *Int. J. Food Microbiol.* 15, 281–285. doi: 10.1016/0168-1605(92)90059-C

Hofacre, C. L., Froyman, R., Gautrias, B., George, B., Goodwin, M. A., and Brown, J. (1998). Use of Aviguard and other intestinal bioproducts in experimental *Clostridium perfringens*-associated necrotizing enteritis in broiler chickens. *Avian Dis.* 42, 579–584. doi: 10.2307/1592685

Hofacre, C. L., Primm, N. D., Vance, K., Goodwin, M. A., and Brown, J. (2000). Comparison of a lyophilized chicken-origin competitive exclusion culture, a lyophilized probiotic, and fresh Turkey Cecal material against Salmonella colonization. *J. Appl. Poult. Res.* 9, 195–203. doi: 10.1093/japr/9.2.195

Hue, O., Allain, V., Laisney, M. J., Le Bouquin, S., Lalande, F., Petetin, I., et al. (2011). Campylobacter contamination of broiler caeca and carcasses at the slaughterhouse and correlation with Salmonella contamination. *Food Microbiol.* 28, 862–868. doi: 10.1016/j.fm.2010.11.003

Jeter, R. M. (1990). Cobalamin-dependent 1,2-propanediol utilization by *Salmonella* Typhimurium. *J. Gen. Microbiol.* 136, 887–896. doi: 10.1099/00221287-136-5-887

Jones, R. M., Wu, H., Wentworth, C., Luo, L., Collier-Hyams, L., and Neish, A. S. (2008). Salmonella AvrA coordinates suppression of host immune and apoptotic defenses via JNK pathway blockade. *Cell Host Microbe* 3, 233–244. doi: 10.1016/j.chom.2008.02.016

Józefiak, D., Rutkowski, A., and Martin, S. (2004). Carbohydrate fermentation in the avian ceca: a review. *Anim. Feed Sci. Technol.* 113, 1–15. doi: 10.1016/j.anifeedsci.2003.09.007

Keegan, K. P., Glass, E. M., and Meyer, F. (2016). MG-RAST, a metagenomics Service for Analysis of microbial community structure and function. *Methods Mol. Biol.* 1399, 207–233. doi: 10.1007/978-1-4939-3369-3_13

Khan, S., Moore, R. J., Stanley, D., and Chousalkar, K. K. (2020). The gut microbiota of laying hens and its manipulation with prebiotics and probiotics to enhance gut health and food safety. *Appl. Environ. Microbiol.* 86:e00600-20. doi: 10.1128/AEM.00600-20

Kohli, N., Crisp, Z., Riordan, R., Li, M., Alaniz, R. C., and Jayaraman, A. (2018). The microbiota metabolite indole inhibits Salmonella virulence: involvement of the PhoPQ two-component system. *PLoS One* 13:e0190613. doi: 10.1371/journal.pone.0190613

Kubasova, T., Kollarcikova, M., Crhanova, M., Karasova, D., Cejkova, D., Sebkova, A., et al. (2019). Gut anaerobes capable of chicken Caecum colonisation. *Microorganisms* 7:597. doi: 10.3390/microorganisms7120597

Kwan, G., Plagenz, B., Cowles, K., Pisithkul, T., Amador-Noguez, D., and Barak, J. D. (2018). Few differences in metabolic network use found between *Salmonella enterica* colonization of plants and Typhoidal mice. *Front. Microbiol.* 9:695. doi: 10.3389/fmicb.2018.00695

Kwon, Y., and Ricke, S. (1999). *Salmonella* Typhimurium poultry isolate growth response to propionic acid and sodium propionate under aerobic and anaerobic conditions. *Int. Biodeterior. Biodegradation* 43, 161–165. doi: 10.1016/S0964-8305(99)00045-1

Lagani, V., and Tsamardinos, I. (2010). Structure-based variable selection for survival data. *Bioinformatics* 26, 1887–1894. doi: 10.1093/bioinformatics/btq261

Latorre, J. D., Hernandez-Velasco, X., Wolfenden, R. E., Vicente, J. L., Wolfenden, A. D., Menconi, A., et al. (2016). Evaluation and selection of Bacillus species based on enzyme production, antimicrobial activity, and biofilm synthesis as direct-fed microbial candidates for poultry. *Front. Vet. Sci.* 3:95. doi: 10.3389/fvets.2016.00095

Le Bihan, G., Jubelin, G., Garneau, P., Bernalier-Donadille, A., Martin, C., Beaudry, F., et al. (2015). Transcriptome analysis of *Escherichia coli* O157:H7 grown *in vitro* in the sterile-filtrated cecal content of human gut microbiota associated rats reveals an adaptive expression of metabolic and virulence genes. *Microbes Infect.* 17, 23–33. doi: 10.1016/j.micinf.2014.09.008

Lee, C. A., and Falkow, S. (1990). The ability of *Salmonella* to enter mammalian cells is affected by bacterial growth state. *Proc. Natl. Acad. Sci. U. S. A.* 87, 4304–4308. doi: 10.1073/pnas.87.11.4304

Lee, M. D., Pedroso, A. A., Lumpkins, B., Cho, Y., and Maurer, J. J. (2023a). Pioneer colonizers: Bacteria that alter the chicken intestinal morphology and development of the microbiota. *Front. Physiol.* 14:1139321. doi: 10.3389/fphys.2023.1139321

Lee, M. D., Pedroso, A. A., and Maurer, J. J. (2023b). Bacterial composition of a competitive exclusion product and its correlation with product efficacy at reducing Salmonella in poultry. *Front. Physiol.* 13:1043383. doi: 10.3389/fphys.2022.1043383

Li, J. S., Barber, C. C., Herman, N. A., Cai, W., Zafrir, E., Du, Y., et al. (2020). Investigation of secondary metabolism in the industrial butanol hyper-producer *Clostridium saccharoperbutylacetonicum* N1-4. *J. Ind. Microbiol. Biotechnol.* 47, 319–328. doi: 10.1007/s10295-020-02266-8

Liao, A. P., Petrof, E. O., Kuppireddi, S., Zhao, Y., Xia, Y., Claud, E. C., et al. (2008). Salmonella type III effector AvrA stabilizes cell tight junctions to inhibit inflammation in intestinal epithelial cells. *PLoS One* 3:e2369. doi: 10.1371/journal.pone.0002369

Lone, A. G., Selinger, L. B., Uwiera, R. R., Xu, Y., and Inglis, G. D. (2013). *Campylobacter jejuni* colonization is associated with a dysbiosis in the cecal microbiota of mice in the absence of prominent inflammation. *PLoS One* 8:e75325. doi: 10.1371/journal.pone.0075325

Lu, J., Idris, U., Harmon, B., Hofacre, C., Maurer, J. J., and Lee, M. D. (2003). Diversity and succession of the intestinal bacterial community of the maturing broiler chicken. *Appl. Environ. Microbiol.* 69, 6816–6824. doi: 10.1128/AEM.69.11.6816-6824.2003

Lu, H., Yang, P., Zhong, M., Bilal, M., Xu, H., Zhang, Q., et al. (2023). Isolation of a potential probiotic strain Bacillus amyloliquefaciensLPB-18 and identification of antimicrobial compounds responsible for inhibition of food-borne pathogens. *Food Sci. Nutr.* 11, 2186–2196. doi: 10.1002/fsn3.3094

Maltby, R., Leatham-Jensen, M. P., Gibson, T., Cohen, P. S., and Conway, T. (2013). Nutritional basis for colonization resistance by human commensal *Escherichia coli* strains HS and Nissle 1917 against *E. coli* O157:H7 in the mouse intestine. *PLoS One* 8:e53957. doi: 10.1371/journal.pone.0053957

Matamouros, S., and Miller, S. I. (2015). *S. typhimurium* strategies to resist killing by cationic antimicrobial peptides. *Biochim. Biophys. Acta* 1848, 3021–3025. doi: 10.1016/j.bbamem.2015.01.013

Miller, V. L., and Mekalanos, J. J. (1988). A novel suicide vector and its use in construction of insertion mutations: osmoregulation of outer membrane proteins and virulence determinants in *Vibrio cholerae* requires toxR. *J. Bacteriol.* 170, 2575–2583. doi: 10.1128/jb.170.6.2575-2583.1988

Milona, P., Townes, C. L., Bevan, R. M., and Hall, J. (2007). The chicken host peptides, gallinacins 4, 7, and 9 have antimicrobial activity against Salmonella serovars. *Biochem. Biophys. Res. Commun.* 356, 169–174. doi: 10.1016/j.bbrc.2007.02.098

Miyashiro, T., and Goulian, M. (2007). Stimulus-dependent differential regulation in the *Escherichia coli* PhoQ PhoP system. *Proc. Natl. Acad. Sci. USA* 104, 16305–16310. doi: 10.1073/pnas.0700025104

Nair, D. V. T., Johnson, T. J., Noll, S. L., and Kollanoor Johny, A. (2021). Effect of supplementation of a dairy-originated probiotic bacterium, *Propionibacterium freudenreichii* subsp. freudenreichii, on the cecal microbiome of turkeys challenged with multidrug-resistant Salmonella Heidelberg. *Poult. Sci.* 100, 283–295. doi: 10.1016/j.psj.2020.09.091

Nurmi, E., Nuotio, L., and Schneitz, C. (1992). The competitive exclusion concept: development and future. *Int. J. Food Microbiol.* 15, 237–240. doi: 10.1016/0168-1605(92)90054-7

Nurmi, E., and Rantala, M. (1973). New aspects of Salmonella infection in broiler production. *Nature* 241, 210–211. doi: 10.1038/241210a0

Obradors, N., Badía, J., Baldomà, L., and Aguilar, J. (1988). Anaerobic metabolism of the L-rhamnose fermentation product 1,2-propanediol in *Salmonella* Typhimurium. *J. Bacteriol.* 170, 2159–2162. doi: 10.1128/jb.170.5.2159-2162.1988

Olishevska, S., Nickzad, A., and Déziel, E. (2019). Bacillus and Paenibacillus secreted polyketides and peptides involved in controlling human and plant pathogens. *Appl. Microbiol. Biotechnol.* 103, 1189–1215. doi: 10.1007/s00253-018-9541-0

Pan, X., Wu, T., Zhang, L., Song, Z., Tang, H., and Zhao, Z. (2008). *In vitro* evaluation on adherence and antimicrobial properties of a candidate probiotic *Clostridium butyricum* CB2 for farmed fish. *J. Appl. Microbiol.* 105, 1623–1629. doi: 10.1111/j.1365-2672.2008.03885.x

Parish, J. H. (1985) in *Biochemistry of bacterial growth*. eds. J. Mandelstam, K. McQuillen and I. Dawes. *3rd* ed (Oxford: Blackwell Scientific Publications)

Pascual, M., Hugas, M., Badiola, J. I., Monfort, J. M., and Garriga, M. (1999). *Lactobacillus salivarius* CTC2197 prevents *Salmonella enteritidis* colonization in chickens. *Appl. Environ. Microbiol.* 65, 4981–4986. doi: 10.1128/AEM.65.11.4981-4986.1999

Pedroso, A. A., Batal, A. B., and Lee, M. D. (2016). Effect of in ovo administration of an adult-derived microbiota on establishment of the intestinal microbiome in chickens. *Am. J. Vet. Res.* 77, 514–526. doi: 10.2460/ajvr.77.5.514

Pedroso, A. A., Lee, M. D., and Maurer, J. J. (2021). Strength lies in diversity: how community diversity limits Salmonella abundance in the chicken intestine. *Front. Microbiol.* 12:694215. doi: 10.3389/fmicb.2021.694215

Peighambari, S. M., Hunter, D. B., Shewen, P. E., and Gyles, C. L. (2002). Safety, immunogenicity, and efficacy of two *Escherichia coli* cya crp mutants as vaccines for broilers. *Avian Dis.* 46, 287–297. doi: 10.1637/0005-2086(2002)046[0287:SIAEOT]2.0.CO;2

Pennie, R. A., Zunino, J. N., Rose, C. E. Jr., and Guerrant, R. L. (1984). Economical, simple method for production of the gaseous environment required for cultivation of *Campylobacter jejuni*. *J. Clin. Microbiol.* 20, 320–322. doi: 10.1128/jcm.20.3.320-322.1984

Podnar, E., Erega, A., Danevčič, T., Kovačec, E., Lories, B., Steenackers, H., et al. (2022). Nutrient availability and biofilm polysaccharide shape the Bacillaene-dependent antagonism of *Bacillus subtilis* against *Salmonella* Typhimurium. *Microbiol. Spectr.* 10:e0183622. doi: 10.1128/spectrum.01836-22

Pottenger, S., Watts, A., Wedley, A., Jopson, S., Darby, A. C., and Wigley, P. (2023). Timing and delivery route effects of cecal microbiome transplants on *Salmonella* Typhimurium infections in chickens: potential for in-hatchery delivery of microbial interventions. *Anim. Microbiome* 5:11. doi: 10.1186/s42523-023-00232-0

Provence, D. L., And Curtiss Iii, R. (1994). *Gene transfer in gram-negative bacteria*. Washington, DC: ASM Press.

Rogers, A. W. L., Tsolis, R. M., and Bäumler, A. J. (2021). Salmonella versus the microbiome. *Microbiol. Mol. Biol. Rev.* 85:e00027-19. doi: 10.1128/MMBR.00027-19

Royal, W. A., and Mutimer, M. D. (1972). Inhibition of *Salmonella* Typhimurium by fowl Caecal cultures. *Res. Vet. Sci.* 13, 184–185. doi: 10.1016/S0034-5288(18)34069-4

Saenz, C., Fang, Q., Gnanasekaran, T., Trammell, S. A. J., Buijink, J. A., Pisano, P., et al. (2023). *Clostridium scindens* secretome suppresses virulence gene expression of *Clostridioides difficile* in a bile acid-independent manner. *Microbiol. Spectr.* 11:e0393322. doi: 10.1128/spectrum.03933-22

Sambrook, J., Fritsch, E. F., and Maniatis, T. (1989). *Molecular cloning: A laboratory manual*. Cold Spring Harbor, NY: Cold Spring Harbor Laboratory Press.

Santander, J., Martin, T., Loh, A., Pohlenz, C., Gatlin, D. M., and Curtiss, R. (2013). Mechanisms of intrinsic resistance to antimicrobial peptides of Edwardsiella ictaluri and its influence on fish gut inflammation and virulence. *Microbiology* 159, 1471–1486. doi: 10.1099/mic.0.066639-0

Schneitz, C., Nuotio, L., Kiiskinen, T., and Nurmi, E. (1991). Pilot-scale testing of the competitive exclusion method in chickens. *Br. Poult. Sci.* 32, 881–884. doi: 10.1080/00071669108417414

Scutari, M., and Denis, J.-B. (2021). *Bayesian networks: with examples in R*. Boca Raton, Florida, United States: CRC Press.

Scutari, M., Vitolo, C., and Tucker, A. (2019). Learning Bayesian networks from big data with greedy search: computational complexity and efficient implementation. *Stat. Comput.* 29, 1095–1108. doi: 10.1007/s11222-019-09857-1

Seedorf, H., Fricke, W. F., Veith, B., Brüggemann, H., Liesegang, H., Strittmatter, A., et al. (2008). The genome of *Clostridium kluyveri*, a strict anaerobe with unique metabolic features. *Proc. Natl. Acad. Sci. U. S. A.* 105, 2128–2133. doi: 10.1073/pnas.0711093105

Shelton, C. D., Yoo, W., Shealy, N. G., Torres, T. P., Zieba, J. K., Calcutt, M. W., et al. (2022). *Salmonella enterica* serovar Typhimurium uses anaerobic respiration to overcome propionate-mediated colonization resistance. *Cell Rep.* 38:110180. doi: 10.1016/j.celrep.2021.110180

Sibinelli-Sousa, S., De Araújo-Silva, A. L., Hespanhol, J. T., and Bayer-Santos, E. (2022). Revisiting the steps of Salmonella gut infection with a focus on antagonistic interbacterial interactions. *FEBS J.* 289, 4192–4211. doi: 10.1111/febs.16211

Sieburth, J. M. (1957). The effect of Furazolidone on the cultural and serological response of *Salmonella typhi*-murium infected chickens. *Avian Dis.* 1, 180–194. doi: 10.2307/1587730

Singh, M., Chaudhary, S., and Sareen, D. (2017). Non-ribosomal peptide synthetases: identifying the cryptic gene clusters and decoding the natural product. *J. Biosci.* 42, 175–187. doi: 10.1007/s12038-017-9663-z

Smith, H. W., and Tucker, J. (1975). The effect of antibiotic therapy on the faecal excretion of *Salmonella* Typhimurium by experimentally infected chickens. *Epidemiol. Infect.* 75, 275–292. doi: 10.1017/S0022172400047306

Snoeyenbos, G. H., Soerjadi, A. S., and Weinack, O. M. (1982). Gastrointestinal colonization by salmonellae and pathogenic *Escherichia coli* in monoxenic and holoxenic chicks and poults. *Avian Dis.* 26, 566–575. doi: 10.2307/1589903

Song, W., Qiu, L., Qing, J., Zhi, W., Zha, Z., Hu, X., et al. (2022). Using Bayesian network model with MMHC algorithm to detect risk factors for stroke. *Math. Biosci. Eng.* 19, 13660–13674. doi: 10.3934/mbe.2022637

Stanley, D., Wu, S. B., Rodgers, N., Swick, R. A., and Moore, R. J. (2014). Differential responses of cecal microbiota to fishmeal, Eimeria and *Clostridium perfringens* in a necrotic enteritis challenge model in chickens. *PLoS One* 9:e104739. doi: 10.1371/journal.pone.0104739

Stenkamp-Strahm, C., Mcconnel, C., Magzamen, S., Abdo, Z., and Reynolds, S. (2018). Associations between *Escherichia coli* O157 shedding and the faecal microbiota of dairy cows. *J. Appl. Microbiol.* 124, 881–898. doi: 10.1111/jam.13679

Sun, W., Roland, K. L., Kuang, X., Branger, C. G., and Curtiss, R. (2010). *Yersinia pestis* with regulated delayed attenuation as a vaccine candidate to induce protective immunity against plague. *Infect. Immun.* 78, 1304–1313. doi: 10.1128/IAI.01122-09

Suzuki, M. T., Taylor, L. T., and Delong, E. F. (2000). Quantitative analysis of small-subunit rRNA genes in mixed microbial populations via 5′-nuclease assays. *Appl. Environ. Microbiol.* 66, 4605–4614. doi: 10.1128/AEM.66.11.4605-4614.2000

Troxell, B., Fink, R. C., Porwollik, S., Mcclelland, M., and Hassan, H. M. (2011). The Fur regulon in anaerobically grown *Salmonella enterica* sv. Typhimurium: identification of new Fur targets. *BMC Microbiol.* 11:236. doi: 10.1186/1471-2180-11-236

Ushijima, T., and Seto, A. (1991). Selected faecal bacteria and nutrients essential for antagonism of *Salmonella* Typhimurium in anaerobic continuous flow cultures. *J. Med. Microbiol.* 35, 111–117. doi: 10.1099/00222615-35-2-111

Valeris-Chacin, R., Weber, B., Johnson, T. J., Pieters, M., and Singer, R. S. (2022). Longitudinal changes in Campylobacter and the litter microbiome throughout the broiler production cycle. *Appl. Environ. Microbiol.* 88:e0066722. doi: 10.1128/aem.00667-22

Wang, M., Hu, J., Yu, H., Li, W., He, G., Dong, J., et al. (2022). *Lactobacillus fermentum* 1.2133 display probiotic potential *in vitro* and protect against *Salmonella* pullorum in chicken of infection. *Lett. Appl. Microbiol.* 76:ovac041. doi: 10.1093/lambio/ovac041

Watkins, B. A., and Miller, B. F. (1983). Competitive gut exclusion of avian pathogens by *Lactobacillus acidophilus* in gnotobiotic chicks. *Poult. Sci.* 62, 1772–1779. doi: 10.3382/ps.0621772

Weschka, D., Mousavi, S., Biesemeier, N., Bereswill, S., and Heimesaat, M. M. (2021). Survey of pathogen-lowering and Immuno-modulatory effects upon treatment of *Campylobacter coli*-infected secondary abiotic IL-10(−/−) mice with the probiotic formulation Aviguard®. *Microorganisms* 9:1127. doi: 10.3390/microorganisms9061127

Wierup, M., Wold-Troell, M., Nurmi, E., and Häkkinen, M. (1988). Epidemiological evaluation of the Salmonella-controlling effect of a Nationwide use of a competitive exclusion culture in poultry. *Poult. Sci.* 67, 1026–1033. doi: 10.3382/ps.0671026

Wong, G. T., Bonocora, R. P., Schep, A. N., Beeler, S. M., Lee Fong, A. J., Shull, L. M., et al. (2017). Genome-wide transcriptional response to varying RpoS levels in *Escherichia coli* K-12. *J. Bacteriol.* 199:e00755-16. doi: 10.1128/JB.00755-16

Wooley, R. E., Gibbs, P. S., and Shotts, E. B. Jr. (1999). Inhibition of *Salmonella* Typhimurium in the chicken intestinal tract by a transformed avirulent avian *Escherichia coli*. *Avian Dis.* 43, 245–250. doi: 10.2307/1592614

Xiao, Y., Xiang, Y., Zhou, W., Chen, J., Li, K., and Yang, H. (2017). Microbial community mapping in intestinal tract of broiler chicken. *Poult. Sci.* 96, 1387–1393. doi: 10.3382/ps/pew372

Yang, H. J., Bogomolnaya, L. M., Elfenbein, J. R., Endicott-Yazdani, T., Reynolds, M. M., Porwollik, S., et al. (2016). Novel two-step hierarchical screening of mutant pools reveals mutants under selection in chicks. *Infect. Immun.* 84, 1226–1238. doi: 10.1128/IAI.01525-15

Yang, H. J., Bogomolnaya, L., Mcclelland, M., and Andrews-Polymenis, H. (2017). De novo pyrimidine synthesis is necessary for intestinal colonization of *Salmonella* Typhimurium in chicks. *PLoS One* 12:e0183751. doi: 10.1371/journal.pone.0189541

Yu, H., Campbell, M. T., Zhang, Q., Walia, H., and Morota, G. (2019). Genomic Bayesian confirmatory factor analysis and Bayesian network to characterize a wide Spectrum of Rice phenotypes. *G3* 9, 1975–1986. doi: 10.1534/g3.119.400154

Yu, Z., Chen, J., Liu, Y., Meng, Q., Liu, H., Yao, Q., et al. (2023). The role of potential probiotic strains *Lactobacillus reuteri* in various intestinal diseases: new roles for an old player. *Front. Microbiol.* 14:1095555. doi: 10.3389/fmicb.2023.1095555

Zhang, S., Dogan, B., Guo, C., Herlekar, D., Stewart, K., Scherl, E. J., et al. (2020). Short chain fatty acids modulate the growth and virulence of Pathosymbiont Escherichia coli and host response. *Antibiotics* 9:462. doi: 10.3390/antibiotics9080462

Zhang, L., Dong, D., Jiang, C., Li, Z., Wang, X., and Peng, Y. (2015). Insight into alteration of gut microbiota in *Clostridium difficile* infection and asymptomatic *C. difficile* colonization. *Anaerobe* 34, 1–7. doi: 10.1016/j.anaerobe.2015.03.008

Zhang, Z. J., Pedicord, V. A., Peng, T., and Hang, H. C. (2020). Site-specific acylation of a bacterial virulence regulator attenuates infection. *Nat. Chem. Biol.* 16, 95–103. doi: 10.1038/s41589-019-0392-5

Zhao, T., Podtburg, T. C., Zhao, P., Schmidt, B. E., Baker, D. A., Cords, B., et al. (2006). Control of Listeria spp. by competitive-exclusion bacteria in floor drains of a poultry processing plant. *Appl. Environ. Microbiol.* 72, 3314–3320. doi: 10.1128/AEM.72.5.3314-3320.2006

Zhou, P., Han, X., Ye, X., Zheng, F., Yan, T., Xie, Q., et al. (2020). Phenotype, virulence and immunogenicity of Edwardsiella piscicida cyclic AMP receptor protein (Crp) mutants in catfish host. *Microorganisms* 8:517. doi: 10.3390/microorganisms8040517

Zhou, Q., Lan, F., Li, X., Yan, W., Sun, C., Li, J., et al. (2021). The spatial and temporal characterization of gut microbiota in broilers. *Front. Vet. Sci.* 8:712226. doi: 10.3389/fvets.2021.712226

frontiers | Frontiers in Microbiology

TYPE Original Research
PUBLISHED 04 June 2024
DOI 10.3389/fmicb.2024.1329798

OPEN ACCESS

EDITED BY
Sébastien Holbert,
INRA Centre Val de Loire, France

REVIEWED BY
Vianney Ortiz-Navarrete,
National Polytechnic Institute of Mexico (CINVESTAV), Mexico
Steven L. Foley,
National Center for Toxicological Research (FDA), United States
Fernando Gil,
Andres Bello University, Chile

*CORRESPONDENCE
Michael Hensel
✉ michael.hensel@uni-osnabrueck.de

†PRESENT ADDRESSES
Alfonso Felipe-López,
Mikrobiologisches Institut, Universitätsklinikum Erlangen, FAU Erlangen-Nürnberg, Erlangen, Germany;
Nicole Hansmeier,
Department of Biology, Luther College at the University of Regina, Regina, SK, Canada

RECEIVED 29 October 2023
ACCEPTED 06 May 2024
PUBLISHED 04 June 2024

CITATION
Felipe-López A, Hansmeier N and Hensel M (2024) Destruction of the brush border by *Salmonella enterica* sv. Typhimurium subverts resorption by polarized epithelial cells. *Front. Microbiol.* 15:1329798. doi: 10.3389/fmicb.2024.1329798

Destruction of the brush border by *Salmonella enterica* sv. Typhimurium subverts resorption by polarized epithelial cells

Alfonso Felipe-López[1†], Nicole Hansmeier[1†] and Michael Hensel[1,2*]

[1]Abt. Mikrobiologie, Universität Osnabrück, Osnabrück, Germany, [2]CellNanOs—Center of Cellular Nanoanalytics Osnabrück, Universität Osnabrück, Osnabrück, Germany

Salmonella enterica serovar Typhimurium is an invasive, facultative intracellular gastrointestinal pathogen that destroys the brush border of polarized epithelial cells (PEC). The brush border is critical for the functions of PEC because it resorbs nutrients from the intestinal lumen and builds a physical barrier to infecting pathogens. The manipuation of PEC during infection by *Salmonella* was investigated by live-cell imaging and ultrastructural analysed of the brush border. We demonstrate that the destruction of the brush border by *Salmonella* significantly reduces the resorption surface of PEC along with the abrogation of endocytosis at the apical side of PEC. Both these changes in the physiology of PEC were associated with the translocation of type III secretion system effector protein SopE. Additionally, the F-actin polymerization rate at the apical side of PEC was highly altered by SopE, indicating that reduced endocytosis observed in infected PEC is related to the manipulation of F-actin polymerization mediated by SopE and, to a lesser extent, by effectors SopE2 or SipA. We further observed that in the absence of SopE, *Salmonella* effaced microvilli and induced reticular F-actin by bacterial accumulation during prolonged infection periods. In contrast to strains translocating SopE, strains lacking SopE did not alter resorption by PEC. Finally, we observed that after engulfment of *Salmonella*, ezrin was lost from the apical side of PEC and found later in early endosomes containing *Salmonella*. Our observations suggest that the destruction of the brush border by *Salmonella* may contribute to the pathogenesis of diarrhea.

KEYWORDS

epithelial cells, brush border, endocytosis, ezrin, invasion

Introduction

The intestine is the main organ of the digestive tract and is responsible for the digestion and resorption of nutrients from the diet. The intestinal tract has evolved a specialized surface formed predominantly by polarized epithelial cells (PEC) to fulfill its function. Extensions of the intestinal epithelium are designated as villi. At the cellular level, each PEC of the epithelial layer develops at its apical surface actin-based membranous protrusions called microvilli (MV). MV are the functional structures of epithelial cells for nutrient resorption. Two morpho-physiological features contribute to this function: (a) MV augment the functional surface for resorption since cells possess a high number of MV (>1,000 MV), and (b) each microvillus contributes to the secretion of digestive enzymes such as disaccharidases and peptidases (McConnell and Tyska, 2007; McConnell et al., 2009; Revenu et al., 2012). The biochemical activity of MV is dependent on the function of structural proteins specifically localized in each microvillus. Loss of actin-coordinating proteins such as epsin, villin, or fimbrin (plastin I) by gene knockout negatively affects the localization and secretion of digestive enzymes (Revenu et al., 2012). Therefore, the

membrane protrusions by MV are only functional if digestive enzymes can be properly secreted to the external milieu (Delacour et al., 2016).

MV also contribute to regulating the microbiota that reside along the intestine. Nevertheless, pathogenic bacteria such as enteropathogenic *Escherichia coli* (EPEC), enterohaemorrhagic *E. coli* (EHEC), enterotoxigenic *E. coli* (ETEC), *Helicobacter pylori,* or *Salmonella enterica* can disturb the integrity and function of the intestinal epithelium. After adhesion to host cells, these pathogens efface MV by translocation of virulence proteins that modify (a) actin, (b) increase the adhesion surface, in the case of EPEC and *H. pylori*, or (c) alter the transporter expression and localization by ribosylating toxins as the labile toxin (LT) of ETEC (Segal et al., 1996; Tan et al., 2009; Wong et al., 2011; Sheikh et al., 2022; Felipe-Lopez et al., 2023).

MV effacement results from the remodeling of actin and leads to the formation of pedestals, a typical feature observed during infection by EPEC or EHEC (Frankel et al., 1998; Wong et al., 2011; Lai et al., 2013). Additionally, brush border destruction is commonly accompanied by the formation of microcolonies at the host cell's apical side (Pedersen et al., 2017). This pathogenic interference leads to a loss of resorption by PEC (Dean et al., 2006) since digestive enzymes and the cotransporter Na^+/Glucose SGLT-1 are also relocated to pedestals. Reduction of the resorption ability of enterocytes is also associated with high doses of infection and with the translocation of effector proteins such as Map, Tir, EspF, and the adhesin Intimin. In all these observations, EPEC formed microcolonies at the apical side of PEC. EPEC effector proteins NleH specifically target EPS8, hindering its function in actin bundling for pedestal formation (Dean et al., 2006). Infections by *H. pylori* alter the uptake of iron by PEC (Tan et al., 2011), as *H. pylori* does not diminish the uptake but increases the resorption of transferrin. Recruitment of the transferrin receptor to microcolonies at host cell apical side was dependent on effector protein CagA. In contrast to EPEC/EHEC and *H. pylori, S. enterica* serovar Typhimurium (STM) is an invasive pathogen that destroys the brush border of PEC *in vivo* and *in vitro* (Takeuchi, 1967; Finlay et al., 1988; Ginocchio et al., 1992; Felipe-Lopez et al., 2023). The SPI1-encoded type III secretion system (SPI1-T3SS) translocates a cocktail of effector proteins into host cells after intimate contact. Collectively, these effector proteins remodel the actin cytoskeleton of host cells, induce MV effacement, and internalize STM. Translocation of effector proteins also induces proinflammatory responses in intestinal PEC [Galan, 2021; reviewed in Fattinger et al. (2021b)].

The invasion of enterocytes by STM is highly cooperative and allows the invasion of multiple bacteria in the same infection foci (Lorkowski et al., 2014; Felipe-Lopez et al., 2023). The invasion concludes with extensive reorganization of the brush border and the formation of a structure called reticular F-actin (RA) at the apical side of PEC. Previous observations of STM-induced alterations of the apical site of PEC and the F-actin cytoskeleton are compiled in Supplementary Figure 1, demonstrating the ultrastructural features of RA. Fine filaments arose from the invasion foci to the periphery of the apical side of the cells once bacteria were internalized (Felipe-Lopez et al., 2023). In this experimental setup, the formation of RA on PEC was dependent upon the translocation of SopE and observed in MDCK and Caco-2 BBe1 cells but not in non-polarized cells, e.g., epithelioid cell line HeLa. RA remained even after bacterial internalization, coinciding with reduced recovery of MV structures as demonstrated by correlative confocal laser-scanning microscopy (CLSM) and atomic force microscopy (AFM) or scanning electron microscopy (SEM) (Kommnick et al., 2019; Felipe-Lopez et al., 2023). The internalization of STM, formation of RA, and disruption of the brush border might, therefore, alter the physiological apical resorption of PEC. Indeed, a recent study revealed that infection by STM altered the expression of ascorbic acid transporters in mice due to the inflammatory response caused by SPI1-T3SS effector proteins. However, no structural modifications of the brush border or enterocytes were mentioned (Teafatiller et al., 2023).

In this study, we investigate the physiological consequences of the translocation of SPI1-T3SS effector proteins. We focused on SopE and SopE2, which act as guanidine exchange factors for Rac1 and Cdc42 in mammalian host cells (Friebel et al., 2001). We show that RA is induced either by an invasion of STM expressing *sopE* or by the accumulation of STM devoid of *sopE* over time. The destruction of brush border architecture also demonstrated that resorption by PEC was disturbed after MV effacement and internalization of STM, which was dependent on SopE. The loss of MV by strains lacking SopE was insufficient to fully abrogate the uptake of fluid tracers by infected cells. We observed that STM invasion was accompanied by delocalization of ezrin from the apical side of host cells. Ezrin links F-actin to the plasma membrane of MV, and the interaction of ezrin with F-actin is controlled by the phosphocycling of ezrin [reviewed in Pelaseyed and Bretscher (2018)]. Therefore, we propose that as a consequence of the delocalization of ezrin and the resulting actin reorganization on the apical side of PEC, endocytosis of PEC is highly altered. The loss of MV and formation of RA during STM invasion thus may contribute to the pathogenesis of diarrhea during Salmonellosis.

Results

Role of STM effector SopE in invasion of polarized epithelial cells, microcolony formation, and induction of reticular actin

Our prior work indicated a key role of SPI1-T3SS effector protein SopE in manipulating the apical side of PEC (Felipe-Lopez et al., 2023). However, the majority of clinical isolates of STM lack SopE, while all strains harbor SopE2 (Mirold et al., 1999). As STM strains lacking SopE also cause self-limited intestinal infections, in this study, we aim to analyze the effects of STM with or without SopE on PEC function and epithelial integrity.

Abbreviations: AFM, atomic force microscopy; Caco-2 BBe1, cancer coli cell line; CLSM, confocal laser-scanning microscopy; EHEC, enterohemorrhagic *E. coli*; EPEC, enteropathogenic *E. coli*; ETEC, enterotoxinogenic *E. coli*; FRAP, fluorescence recovery after photobleaching; LCI, live-cell imaging; LT, labile toxin; MDCK, Madin-Darby canine kidney cells; MIP, maximal intensity projection; MV, Microvilli; PEC, polarized epithelial cells; p.i., post-infection; RA, reticular F-actin; STM, *Salmonella enterica* serovar Typhimurium; SPI, Salmonella pathogenicity island; TEER, transepithelial electrical resistance; TIRF, total internal reflection microscopy; T1SS, type I secretion system; T3SS, type III secretion system; WT, wild type.

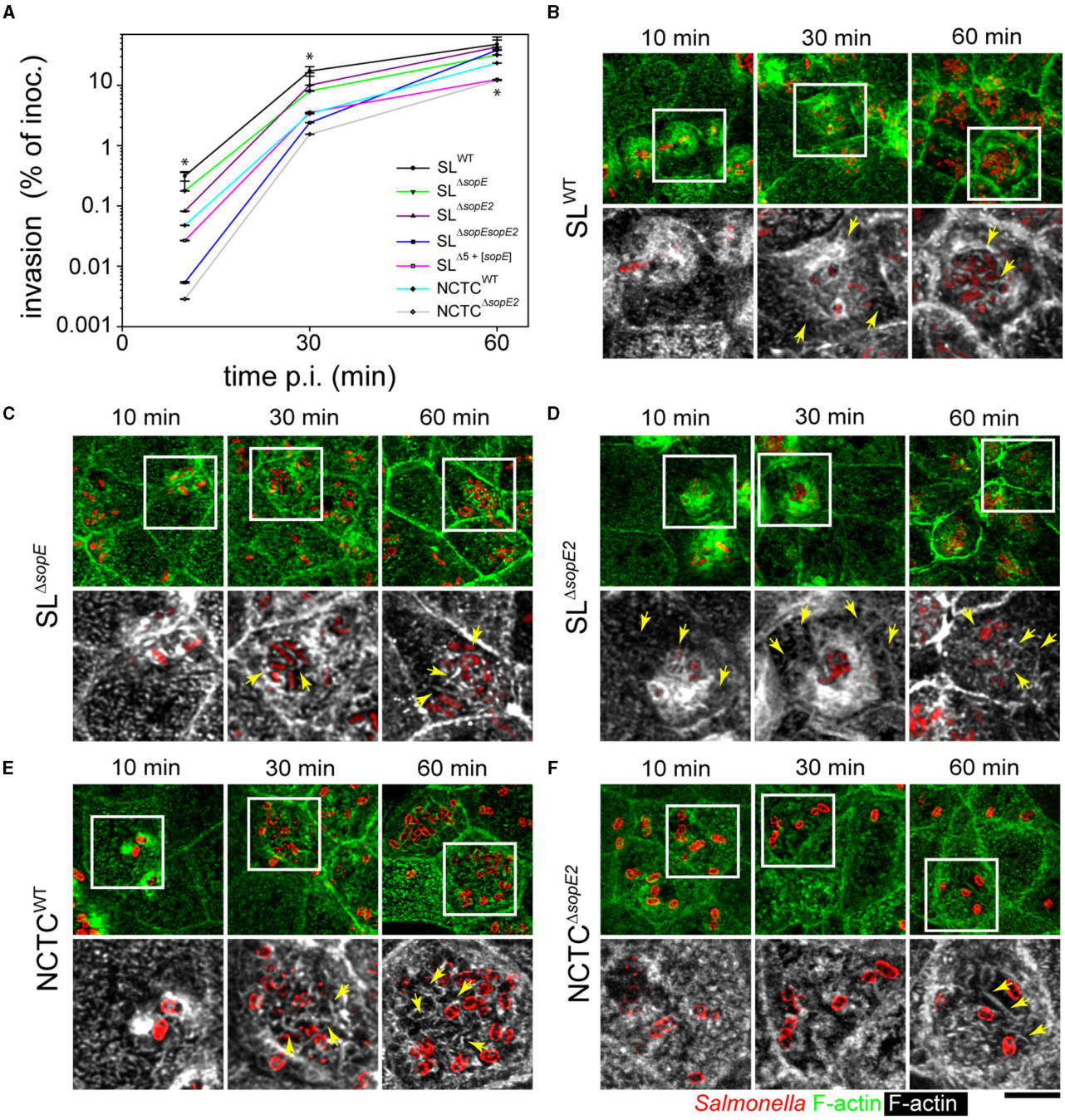

FIGURE 1
Effector proteins SopE and SopE2 are required for the manipulation of apical F-actin of PEC by STM. **(A)** Polarized MDCK monolayers were infected with STM WT and various mutant strains lacking *sopE* or *sopE* for 10, 30, or 60 min as indicated. After washing, non-internalized bacteria were killed by incubation with a medium containing 100 μg × ml^{-1} gentamicin for 1 h. Cells were lysed and internalized STM was quantified by plating serial dilutions of lysates for CFU determination. Invasion is expressed as the percentage of internalized bacteria of the inoculum applied. One-way ANOVA was applied for statistical analysis, and the results are indicated as; $^{*}p < 0.05$. **(B–F)** STM infection leads to MV effacement and formation of microcolonies at the apical side of PEC. MDCK cells were infected with STM wild-type (WT) or mutant strains expressing mTagRFP **(B–D)** as fluorescently labeled, or WT and mutant strains immuno-stained with O-antigen of LPS **(E, F)**. Samples were fixed at 10, 30, or 60 min p.i., labeled with Phalloidin-Alexa488 (green in overview, white in details), and analyzed by confocal laser-scanning microscopy (CLSM). STM SL strains harbored pFPV-mCherry (red) for detection in **(B–D)**, while STM NCTC strains were immunolabeled for O-antigen (red) in **(E, F)**. Micrographs show accumulation of STM and alteration of F-actin at various time points p.i. Yellow arrows indicate RA along the apical side of MDCK cells and adjacent to STM cells. Scale bar, 10 μm (overviews), 5 μm (details).

The cell line Madin-Darby Canine Kidney (MDCK) was used as PEC for infection experiments and to quantify invasion of PEC by wild-type (WT) strains SL1344 harboring both *sopE* and *sopE2* (SL^{WT}) and NCTC12023 harboring only *sopE2* (NCTC^{WT}). Isogenic *sopE*/*sopE2*-deficient or *sopE2*-deficient mutant strains were performed (Figure 1A). At 10 and 30 min p.i., the invasion by SL$^{\Delta sopEE2}$ and NCTC$^{\Delta sopE2}$ strains was about 100- and 10-fold, respectively, lower than that of corresponding WT strains.

Although invasion by STM $SL^{\Delta sopE}$, $SL^{\Delta sopE2}$, or $SL^{\Delta sopE\ sopE2}$ was lower at earlier time points, these strains reached levels similar to SL^{WT} at 60 min p.i. (Figure 1A). Invasion by $SL^{\Delta sopE}$ and $NCTC^{WT}$, which naturally lacks SopE, was slightly but significantly lower than that of SL^{WT}. Using a reductionist approach (Felipe-Lopez et al., 2023) with a strain lacking *sipA sopABEE2* ($SL^{\Delta 5}$) with similar invasion to an *invF* mutant strain, we found that STM $SL^{\Delta 5+[sopE]}$ also showed augmented invasiveness; however, this was still 10-fold less than STM SL^{WT} and was similar to that quantified for STM $NCTC^{\Delta sopE2}$.

We previously demonstrated that MDCK and Caco-2 Bbe1 (C2BBe1) cells form homogeneous monolayers, and with such a model, epithelia infection of the apical side by STM can be analyzed. MDCK cells were infected by adding STM inoculum to the apical reservoir as described before (Hölzer and Hensel, 2012; Felipe-Lopez et al., 2023), and imaging was performed by CLSM. Micrographs of infected MDCK cells registered at the same time points demonstrated that only SL1344 background strains harboring SopE triggered membrane ruffling and MV effacement at 10 min p.i. (Figures 1B, D). Additionally, while MDCK cells infected for 30 min with STM SL^{WT} or $SL^{\Delta sopE2}$ showed RA distributed on the apical side of PEC (Figures 1B, D), STM $SL^{\Delta sopE}$ did not induce large ruffles and bacteria accumulated at the apical side of the cell in microcolonies (Figure 1C). Cells infected by STM $SL^{\Delta sopE}$ showed RA only adjacent to bacteria but not extending further on the apical side (Figure 1B vs. Figure 1C). At 60 min p.i., RA was present only in cells highly infected by any of the strains tested (Figures 1B–D). In contrast to strains with SL1344 background, STM $NCTC^{WT}$ only induced moderate membrane ruffling at 10 min p.i. (Figure 1E). STM $NCTC^{\Delta sopE2}$ triggered a low accumulation of actin around the bacterial cells, but it was not accompanied by membrane extensions (Figure 1F). At 30 min p.i., STM $NCTC^{WT}$ accumulated in microcolonies at the apical side of cells, similar to STM $SL^{\Delta sopE}$ (Figure 1C vs. Figure 1E), and RA surrounded the bacteria, which was not evenly distributed on the cell, compared to SL^{WT} strain (Figure 1B vs. Figure 1E). MDCK cells infected by STM $NCTC^{\Delta sopE2}$ only showed small changes in the actin cytoskeleton (Figure 1F) associated with four to six bacteria, but no bacterial microcolonies were observed for this strain. At 60 min p.i., the STM $NCTC^{WT}$ strain caused a complete loss of the brush border architecture (Figure 1E). Bacteria were grouped in microcolonies, and RA was tightly associated with bacterial cells. Only slight reorganization of the actin cytoskeleton was appreciable in cells infected by $NCTC^{\Delta sopE2}$, but on cells infected by this strain, microcolonies were absent, and only short filaments of actin were observed around invading bacteria (Figure 1F). RA was evenly distributed at the apical side of host cells infected by STM SL^{WT} at early time points (10 min p.i., Figure 1B), whereas in cells infected by STM $NCTC^{WT}$, RA was tightly associated with invading bacteria and only fully visible at 60 min p.i. (Figure 1E).

Role of SPI1-T3SS effector proteins in breaching epithelial barriers

We sought to further characterize the effects of SopE on PEC physiology and deployed the human colonic epithelial cell line C2BBe1. Polarization of these cells leads to epithelial layers with high transepithelial electrical resistance (TEER), and pathogenic manipulation of PEC decreases TEER. The TEER of C2BBe1 polarized monolayers was monitored during infection by STM (Figures 2A, B). As previously reported (Felipe-Lopez et al., 2023), deletion of only *sopE* had no effect on the destruction of the epithelial barrier. On the contrary, deletion of both *sopE* and *sopE2* in SL1344 partially ablated the epithelial damage since at 40 min p.i., the TEER dropped to ca. 70% of the value prior to infection and remained low. Only after 120 min p.i. was a further slight decay observed. Infection by STM $SL^{\Delta 5+[sopE]}$ caused decay of TEER similar to that observed in infection by STM SL^{WT} (Figure 2A).

The TEER of cells infected by $NCTC^{WT}$ dropped slower than that of cells infected by STM SL^{WT} (Figure 2B). At 60 min p.i., STM $NCTC^{WT}$ infection decreased TEER to 85% of TEER prior to infection, while the TEER of SL^{WT}-infected cells decreased to 75% already 20 min p.i. TEER decay of cells infected by STM $NCTC^{\Delta sopE2}$ was slower than for cells infected by $NCTC^{WT}$ (Figure 2A vs. Figure 2B) and decayed in a rather linear manner (Figure 2A). Since the effects observed were associated with effector proteins SopE or SopE2, $NCTC^{\Delta sopE2}$ was complemented with *sopE* from SL1344. This strain caused the rapid decay of TEER identical to the phenotype induced by infection with STM SL^{WT} (Figure 2B).

These data indicate that *Salmonella's* alteration of the epithelial barrier function is primarily dependent on either single translocation of SopE (see $SL^{\Delta 5+[sopE]}$) or the translocation of a group of effector proteins controlling F-actin such as SipA, SopE2 and, to a lesser extent, SopB, when SopE is absent.

F-actin remodeling by STM induces the formation of reticular actin

Our observations from fixed time points suggested that SopE not only enhanced invasiveness but also strongly influenced actin reorganization after the full engulfment of STM and the events after the invasion. The RA already appeared after 10 min in cells infected by STM SL^{WT} but was delayed to 60 min p.i. in infections by STM $SL^{\Delta sopE}$ or STM $NCTC^{WT}$. To investigate the formation of RA by apparently distinct mechanisms, the infection of MDCK LifeAct-eGFP cells by various STM strains was followed by live-cell imaging (LCI). The infection of STM SL^{WT} triggered ruffle formation within 8 min after initial apical adhesion (Figure 3; Supplementary Movie 1), as previously reported (Felipe-Lopez et al., 2023). After full engulfment of STM SL^{WT} and ruffle retraction, thin filaments of actin appeared surrounding the invasion locus on the apical side. These filaments gradually increased over the next 10 min from the periphery to the invasion locus, forming a reticular F-actin structure (Figure 3, SL^{WT}, Supplementary Movie 1). In contrast, STM $SL^{\Delta sopE}$ induced only small ruffles, and changes in brush border architecture were not detected when a single bacterium invaded (Figure 3, $SL^{\Delta sopE}$). However, when the same cell was subsequently invaded by further bacteria, the brush border was lost, and RA appeared between the invading bacteria (yellow arrows). F-actin filaments only emerged close to the invasion foci but not from the periphery, as observed for STM SL^{WT} (Figure 3). Further invasion events increased the formation of RA, which was inter-connected to the previous

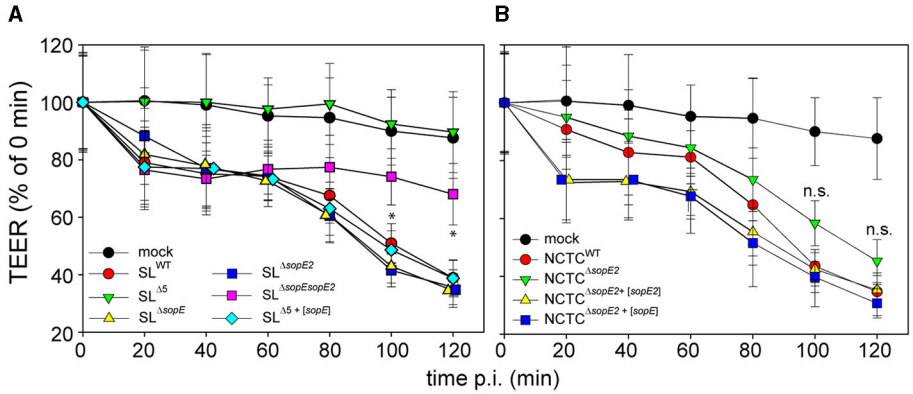

FIGURE 2
Effector proteins SopE and SopE2 are key factors for the disruption of the epithelial barrier function of PEC by STM. C2BBe1 cells were seeded on transwell inserts with polycarbonate filters of 0.4 μm pore size and cultured for 10–15 d to allow the formation of polarized monolayers. Polarization is indicated by the increase of transepithelial electrical resistance (TEER) to 500–700 Ω per well. Polarized monolayers were infected at MOI 25 with STM WT or various mutant strains lacking *sopE, sopE2,* or *sipA sopA sopB sopE sopE2* (strain Δ5), without or with plasmids harboring *sopE* or *sopE2*. Infections were performed with isogenic STM strains in strain background SL1344 **(A)** or NCTC12023 **(B)**. The TEER was scored over a period of 2 h p.i. The TEER is expressed as the percentage of TEER of respective transwells determined immediately prior to infection. Means and standard deviations are shown for TEER quantifications. All experiments were repeated at least three times with two technical replicates. One-way ANOVA was applied for statistical analysis, and the results are indicated as not significant (n.s.); $*p < 0.05$.

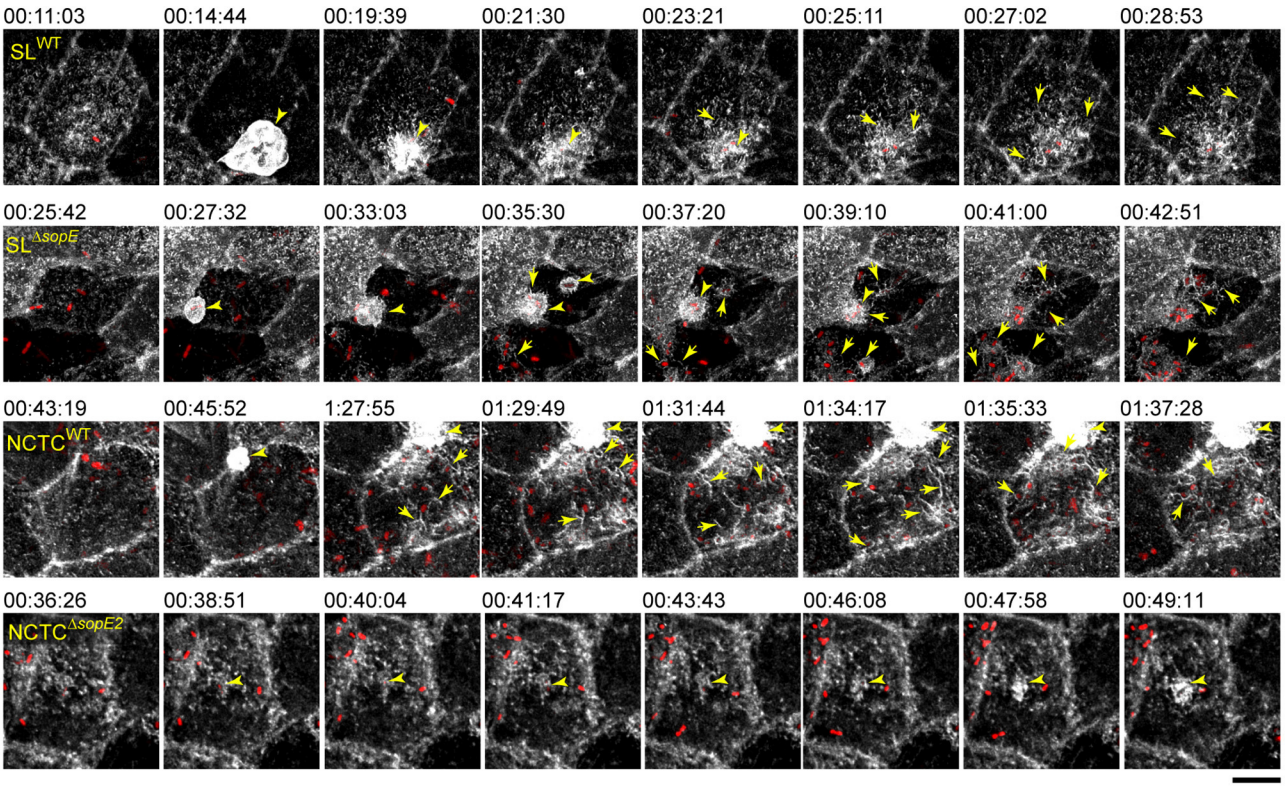

FIGURE 3
Brush border architecture is destroyed by bacterial cells clustering on the apical side of PEC and substituted with RA. MDCK cells expressing Lifeact-eGFP were grown in fluoro dishes for 5 d. Lifeact-eGFP labels F-actin filaments in living cells, which are shown in white. PEC were infected with various STM strains as indicated, and image acquisition by SD with maximal acquisition speed (2–3 frames per min) was started immediately after infection for 120 min of acquisition. Maximum intensity projection (MIP) images show the dynamics of STM accumulation at the apical side of MDCK cells, MV effacement, and formation of RA. Arrowheads indicate F-actin accumulation in membrane ruffles induced by STM. Arrows indicate the formation of RA. Scale bar, 15 μm. Timestamp, h:min:sec. See Supplementary Movie 1 for the time-lapse series.

invasive bacteria. STM SL$^{\Delta sopE2}$ showed similar behavior as STM SL^{WT} (data not shown).

STM NCTC^{WT} induced RA similar to STM SL$^{\Delta sopE}$ (Figure 3, NCTC^{WT} yellow arrows), but this phenotype was delayed. After the first invasion event, other bacteria induced the formation of RA and brush border effacement. These bacteria were surrounded by intense actin signals. Actin filaments were distributed mainly at the periphery and around invading STM. The deletion of *sopE2* in STM NCTC altered the ability of *Salmonella* to induce RA (Figure 3, NCTC$^{\Delta sopE2}$). Cells infected by this strain also formed small clusters and showed further brush border destruction; however, there was no induction of RA even after several bacteria had invaded. Only short and very thin F-actin filaments were locally associated with bacteria.

These results demonstrate that while SopE was sufficient to cause MV effacement and formation of RA by one single bacterial cell, for strains lacking SopE infection over long time periods, the accumulation of multiple bacteria at the apical side was necessary to cause similar alterations to the host cell. Strains lacking both *sopE* and *sopE2* were unable to induce the formation of RA, and we conclude that RA is dependent on SopE and/or SopE2.

Intracellular STM affects brush border regeneration

Our data demonstrate that RA only appeared shortly after the engulfment of *sopE*-harboring STM or after the accumulation of multiple *sopE*-deficient STM. Therefore, we tested if invasion only controls the formation of RA and loss of the brush border or if intracellular *Salmonella* also interferes with the regeneration of the brush border and the disappearance of RA. MDCK cells were infected by various strains lacking SopE or SopE2 in either strain background for 30 min. Infected cells were then washed and treated with gentamicin for 1 h or only rigorously washed and further incubated for 1 h w/o gentamicin addition. Micrographs generated by AFM (Figure 4A) or CLSM (Figure 4B) show that even after gentamicin treatment to kill non-internalized STM, RA was still present in cells infected by STM SL^{WT} and, to a lesser extent, STM NCTC^{WT}. Cells infected by STM NCTC$^{\Delta sopE2}$ or STM SL$^{\Delta sopE}$ showed a slight recovery of brush border after gentamicin treatment (Figures 4A, B). Additionally, F-actin structures were concentrated in clusters of intracellular bacteria (Figure 4B). Cells infected by *sopE*-deficient strains also showed recovery of MV. Interestingly, cells infected by SL$^{\Delta sopE}$ without gentamicin treatment still possessed RA, and as observed for STM SL^{WT}, bacteria were surrounded by actin. Altogether, these results show that STM continues to alter the brush border architecture after internalization.

Reticular actin displaces resorptive areas, and SopE alters actin polymerization at the apical side of host cells

Our results indicate that SopE and SopE2 induce the formation of RA after brush border effacement. Such gross alteration of the F-actin cytoskeleton might change the physiological properties of the brush border. To address this point, we determined the effect of STM invasion on the roughness of the apical side using AFM (Antonio et al., 2012). Compared to non-infected controls, peaks of roughness probability were shifted to lower roughness in STM-infected cells, in line with the observed loss of brush border (Figure 5). The roughness of the apical side of host cells infected by SL^{WT} was highly reduced compared to non-infected cells (Figures 5C, D). The maximal peak observed in SL^{WT}-infected cells was 10 nm less rough than that quantified in non-infected cells (23 vs. 30 nm; Figure 5D). Similarly, STM NCTC^{WT}-infected cells showed, on average, a reduced surface roughness compared to non-infected cells (24 vs. 33 nm). However, in contrast to SL^{WT}-infected cells, NCTC^{WT}-infected cells showed a larger distribution of roughness probabilities. Cells infected by STM SL$^{\Delta sopE}$ or NCTC$^{\Delta sopE2}$ showed no reduced roughness but rather values close to the maximal roughness of non-infected cells (28 vs. 30 nm). Cells infected by STM NCTC^{WT} showed, on average, a reduced surface roughness compared to the non-infected cells (24 vs. 30 nm). However, in contrast to SL^{WT}-infected cells, NCTC^{WT}-infected cells showed a larger distribution of roughness probabilities.

These measurements demonstrate that STM infections fully remodel the apical architecture of PEC, depending on SopE. The reorganization of cells after infection with NCTC background strains naturally lacking SopE was rather moderate, and infected cells also showed high roughness similar to non-infected cells. Based on our LCI results, these cells still contained MV on the apical surface under the experimental conditions applied.

The loss of the absorptive surface of PEC, accompanied by the formation of RA, suggests that actin polymerization at the apical side may also be affected. To quantify the turnover of actin from RA, fluorescence recovery after photobleaching (FRAP) was applied to infected cells showing RA. Data were adjusted to the model proposed by Ishikawa-Ankerhold et al. (2012). After a pulse of 500 ms for photobleaching, RA was recovered (Figures 6A, B) in cells infected by STM SL^{WT}, indicating that RA formation by F-actin polymerization continued even when STM was intracellular (Figures 6A, B). Further quantification of the signal recovery revealed that actin polymerization at the apical side of host cells was increased after infection by STM SL^{WT} or NCTC^{WT} (Figure 6C). The cells infected by either SL$^{\Delta sopE}$ or NCTC$^{\Delta sopE2}$ did not cause any significant reduction of the actin polymerization rate (Figure 6C). Data from this experimental setup confirmed that actin polymerization was altered by STM infection, even when bacteria were located intracellularly, and this exclusively depended on SopE by SL^{WT} and SopE2 in NCTC^{WT}. Furthermore, actin remodeling occurring during STM internalization may not be sufficient to alter the physiological functions of PEC.

SopE disrupts the physiological resorption of polarized epithelial cells

Epithelia of the intestine, kidney, and other organs are responsible for the uptake of nutrients and ions. The loss of the brush border architecture abrogates this function. Given that

10.3389/fmicb.2024.1329798

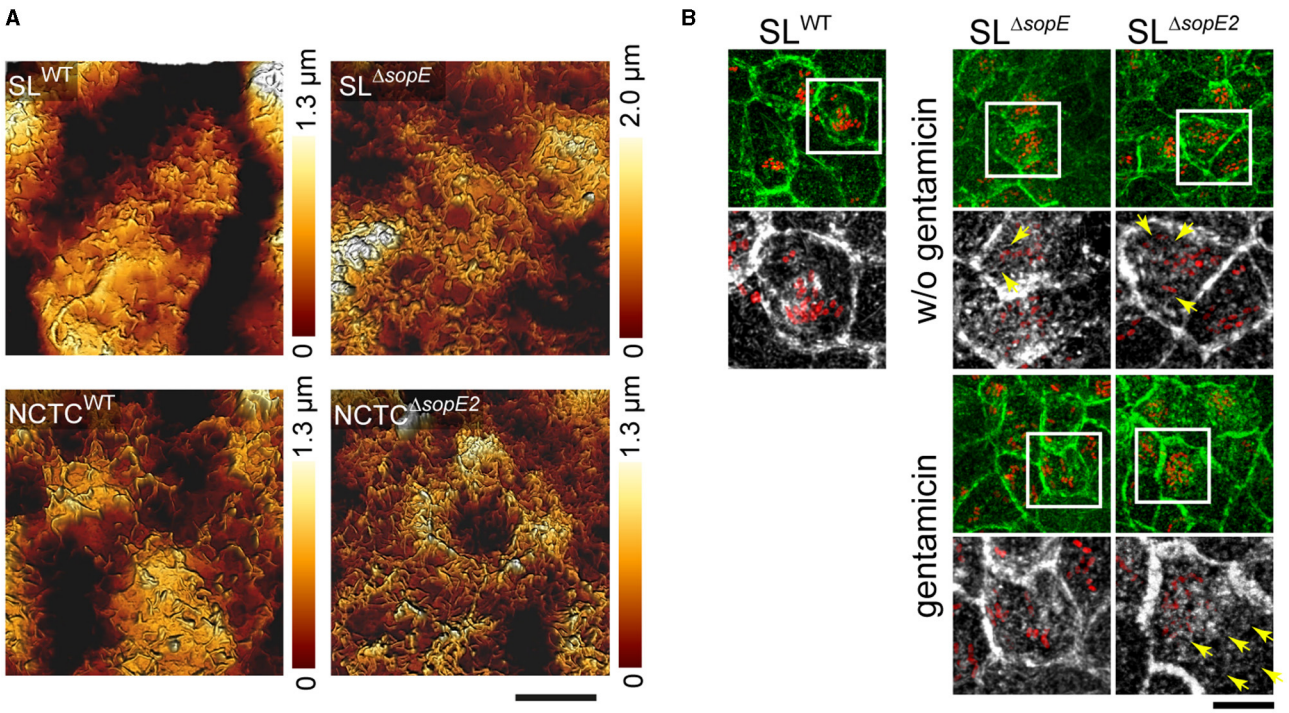

FIGURE 4
Brush border architecture is not restored in PEC infected by STM strains harboring *sopE*. Polarized MDCK cells expressing Lifeact-eGFP were grown as in Figure 3 and were infected with *Salmonella* WT for 25 min. F-actin is shown in green. Non-internalized STM were removed by washing, and cells were incubated for 1 h in media without gentamicin or in a medium containing 100 µg × ml^{-1} gentamicin to kill the remaining extracellular bacteria. Cells were fixed and stained as indicated in Figure 1 and observed by CLSM. **(A)** 3D topology micrographs show the degeneration of the apical side of MDCK cells after internalization of *Salmonella* (cells only treated with gentamicin). **(B)** Formation of RA is induced by SopE. Extracellular STM were removed by washing, and cells were incubated with or without the addition of gentamicin for 1 h. Only cells infected by SL1344$^{\Delta sopE}$ but not treated with gentamicin showed RA. Yellow arrows indicate the formation of RA after internalization of STM at various time points of infection. Scale bars, **(A)** 5 µm, **(B)** 20 µm, and 10 µm for overview and detail, respectively.

RA is still present even after the complete invasion of STM, we investigated if replacing MV with RA alters the apical resorption of MDCK cells. At 1.5 h p.i., gentamicin-treated cells were pulsed for 30 min with FM4-64 FX to label plasma membrane or with fluid tracer dextran-10,000 Alexa568 to follow endocytic uptake. Cells infected by SL^{WT} internalized less dextran than non-infected cells (Figure 7A). Internalized dextran in cells infected by STM SL^{WT} appeared as small accumulations at the apical side of cells and close to clusters of intracellular bacteria. However, no colocalization was observed between STM and the fluorescent tracer (Figure 7A, detail), indicating that the internalized material was not entering the SCV at this time point of infection. Compared to SL^{WT}-infected cells, non-infected cells contained a large number of small-sized vesicles homogenously distributed in the apical region of the cell (Figure 7A). Most of these dextran-positive vesicles colocalized with F-actin, and some were localized at the apical membrane of the cell, indicating recent uptake (Figure 7A, *Z* sections). Such recruitment of actin was not visible in infected cells. Infection by STM SL$^{\Delta sopE}$ resulted in increased dextran uptake compared to non-infected cells. Infection by NCTC^{WT} or NCTC$^{\Delta sopE2}$ did not significantly alter the uptake of dextran, and infected cells presented almost the same number of dextran spots over the inspected area, and uptake was similar to that observed in non-infected cells (mock) (Figure 7B).

In contrast to the reduced dextran internalization, FM4-64 was highly endocytosed in cells infected by STM SL^{WT} compared to non-infected cells (Figures 7C, D). Non-infected cells showed homogenous cytoplasmic membrane labeling by FM4-64 on the apical side (Figure 7C), while in infected cells, FM4-64 signals appeared below the apical membrane and separated from apical F-actin. The FM4-64 signals from infected and mock-infected cells were quantified, indicating that higher levels of intracellular dye in STM SL^{WT}-infected cells were higher than measured for mock-infected cells (Figure 7D).

These results demonstrate that after internalization of STM and apparition of RA, PEC loses the ability to resorb material from the luminal space. This effect is mediated by the translocation of SopE, but not SopE2, since cells infected by strains lacking *sopE2* could resorb apical markers, as shown in Figure 7C. Therefore, SopE dominantly affects the physiological resorption of host cells, likely due to its specific effect on Rac1 (Friebel et al., 2001). Although other strains expressing only SopE2, which acts on Cdc42, could efface MV and induce RA, they failed to abrogate this cellular function in the PEC infection model.

10.3389/fmicb.2024.1329798

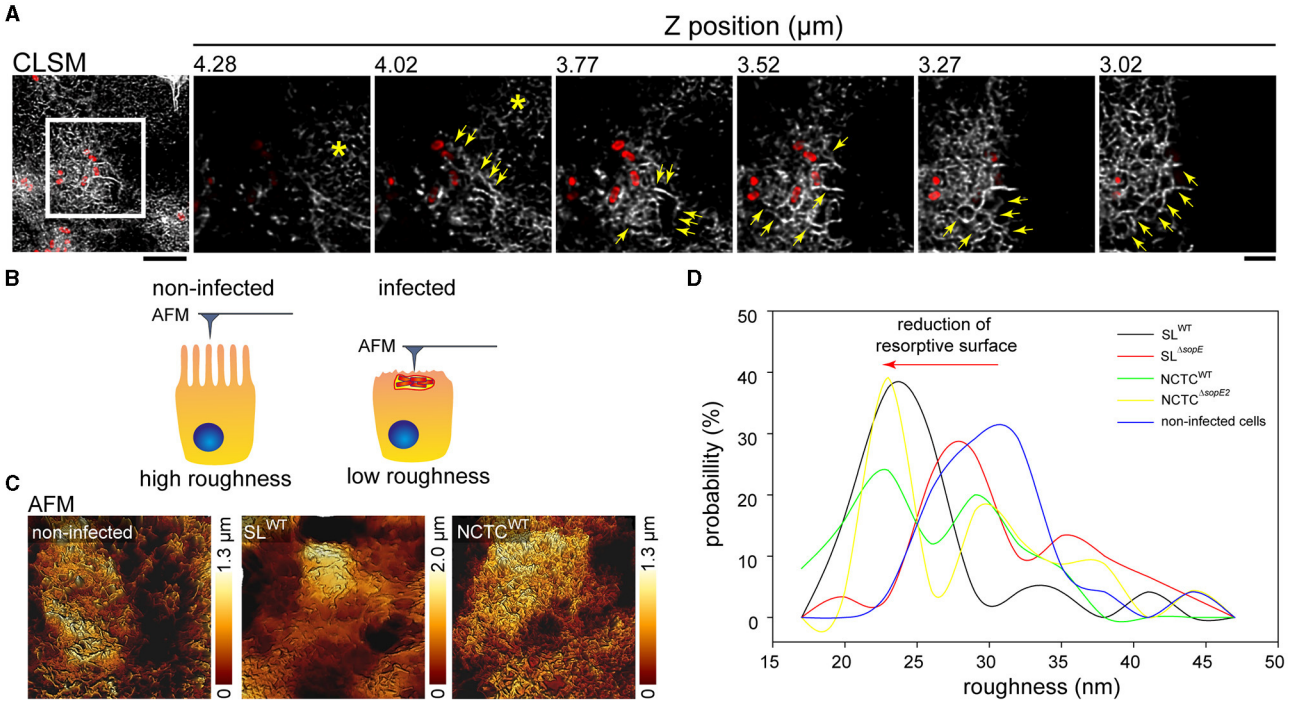

FIGURE 5
Destruction of the brush border by *Salmonella* invasion reduces the apical surface. **(A)** MDCK cells were infected with STM SL^{WT} (red), and F-actin was labeled (gray). Representative CLSM image of a group of cells infected by STM (overview). Detailed images from distinct planes along the *Z*-axes show the organization of RA at the apical side of STM-infected cells (yellow arrows) and the remaining intact MV (asterisk). Scale bar, 10 µm (overview) and 5 µm (detail). **(B)** Model of the roughness measurement by AFM. When cells possess MV on the apical surface, the roughness and deepness are higher than those of cells infected by STM, showing MV effacement with a flatter surface and reduced deepness. **(C)** AFM images of the 3D topology of infected cells without the brush border. Cells were prepared as indicated in Figure 1 for AFM scanning and CLSM. **(D)** Roughness of at least 25 cells was determined by Young's module and presented as the probability of the roughest area in the cell.

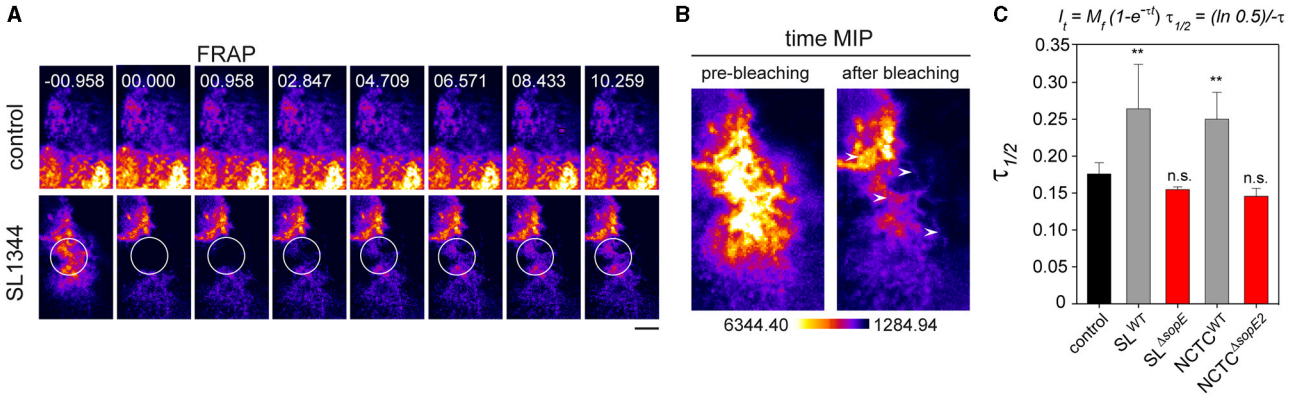

FIGURE 6
Salmonella invasion alters the polymerization of F-actin at the host cell's apical side. PEC were infected at MOI 25 for 25 min and then washed five times with pre-warmed MEM without phenol-red to remove extracellular bacteria. Infected cells in chamber slides were observed by SD microscopy. Areas indicated by circles were photobleached using a laser line 488 nm at 100% transmission for 100 ms. **(A)** Representative images of fluorescence recovery of F-actin after photo-bleaching (FRAP) of STM-infected cells are shown. Non-infected cells without photobleaching served as control. **(B)** Time maximal intensity projections (MIP) of a representative bleached region before and after bleaching. **(C)** The recovery constant (τ) is strongly reduced in cells infected by STM compared to control. Means and standard deviations of at least 25 cells per condition are shown. Quantification and mathematical adjustment were performed as described (Ishikawa-Ankerhold et al., 2012). Scale bar, 2.5 µm. One-way ANOVA was applied for statistical analysis, and results are indicated as not significant (n.s.); $^{**}p < 0.01$.

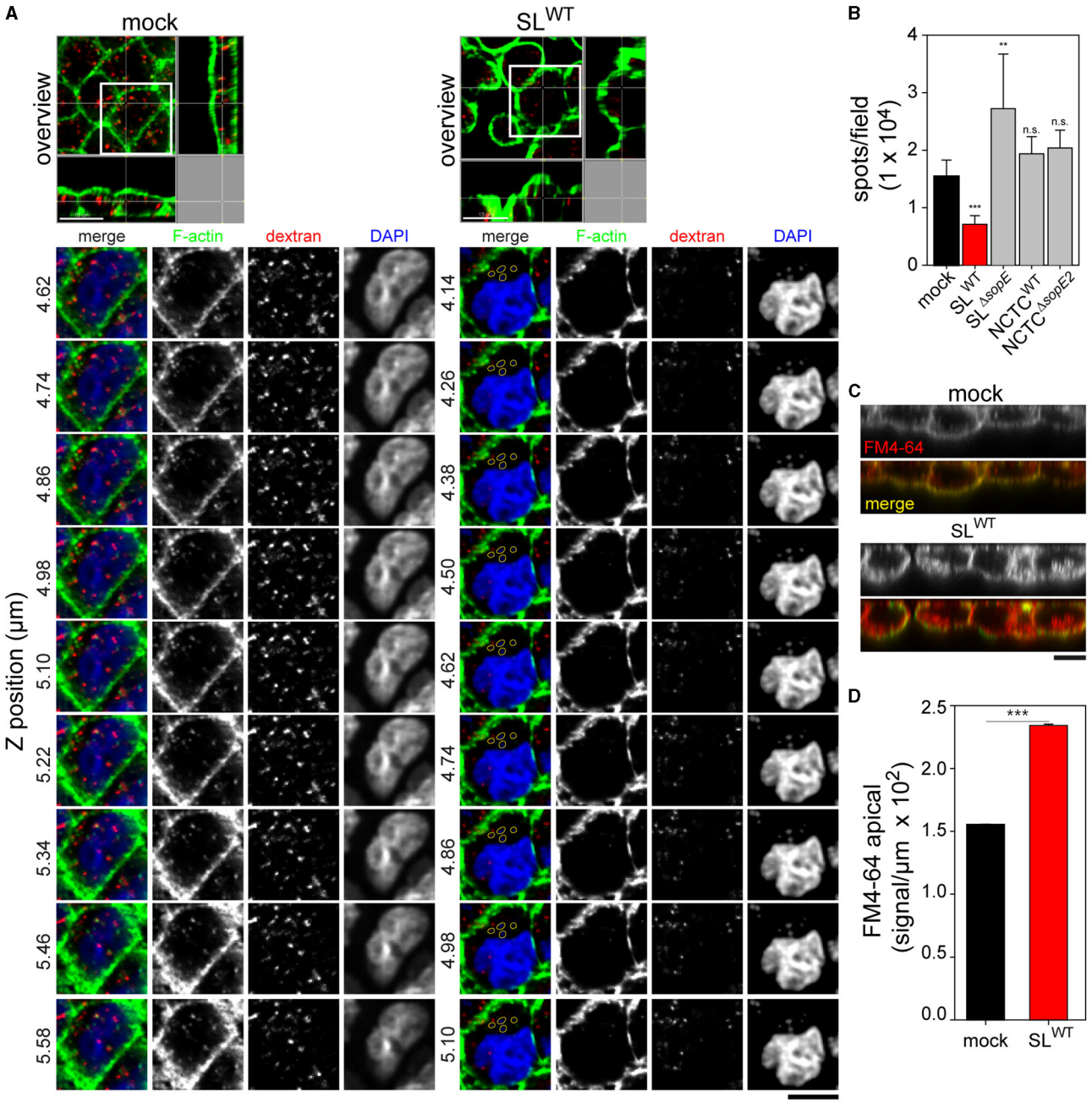

FIGURE 7
Destruction of the brush border by *Salmonella* disrupts the physiologic uptake of the apical side of polarized epithelial cells. PEC were infected, as described in Figure 1. After gentamicin treatment, cells were pulsed with Alexa568-labeled dextran (red) or membrane dye FM4-64FX (red) for 30 min. Cells were further processed as described in Figure 1; actin was labeled by phalloidin (green), and nuclear and bacterial DNA were stained by DAPI (blue). **(A)** Representative orthogonal images show mock-infected cells or cells infected by STM SL^{WT} cells pulsed with dextran Alexa568. Images show lateral views or the *Z*-axes of the cells containing dextran along the cell body. Various *Z* positions are shown. In infected cells, intracellular STM stained by DAPI are outlined yellow. Scale bars, 10 µm. **(B)** Effect of STM infection on endocytosis of dextran Alexa568. Infection of MDCK cells with various STM strains as indicated or mock infection and dextran Alexa568 pulse were performed as above. The numbers of dextran spots were quantified by Imaris as described in Materials and methods section. **(C)** Representative *Z* projections of cells labeled with membrane stain FM4-64 (red). Cells were mock-infected or infected by STM SL^{WT}, and actin (green) was labeled as above. Scale bars, 10 µm. **(D)** Quantification of FM4-64 signal intensities in the apical area of mock-infected or STM SL^{WT}-infected MDCK cells. Scale bars, 10 µm. One-way ANOVA was applied for statistical analysis, and the results are not significant (n.s.); $^{**}p < 0.01$; $^{***}p < 0.001$.

10.3389/fmicb.2024.1329798

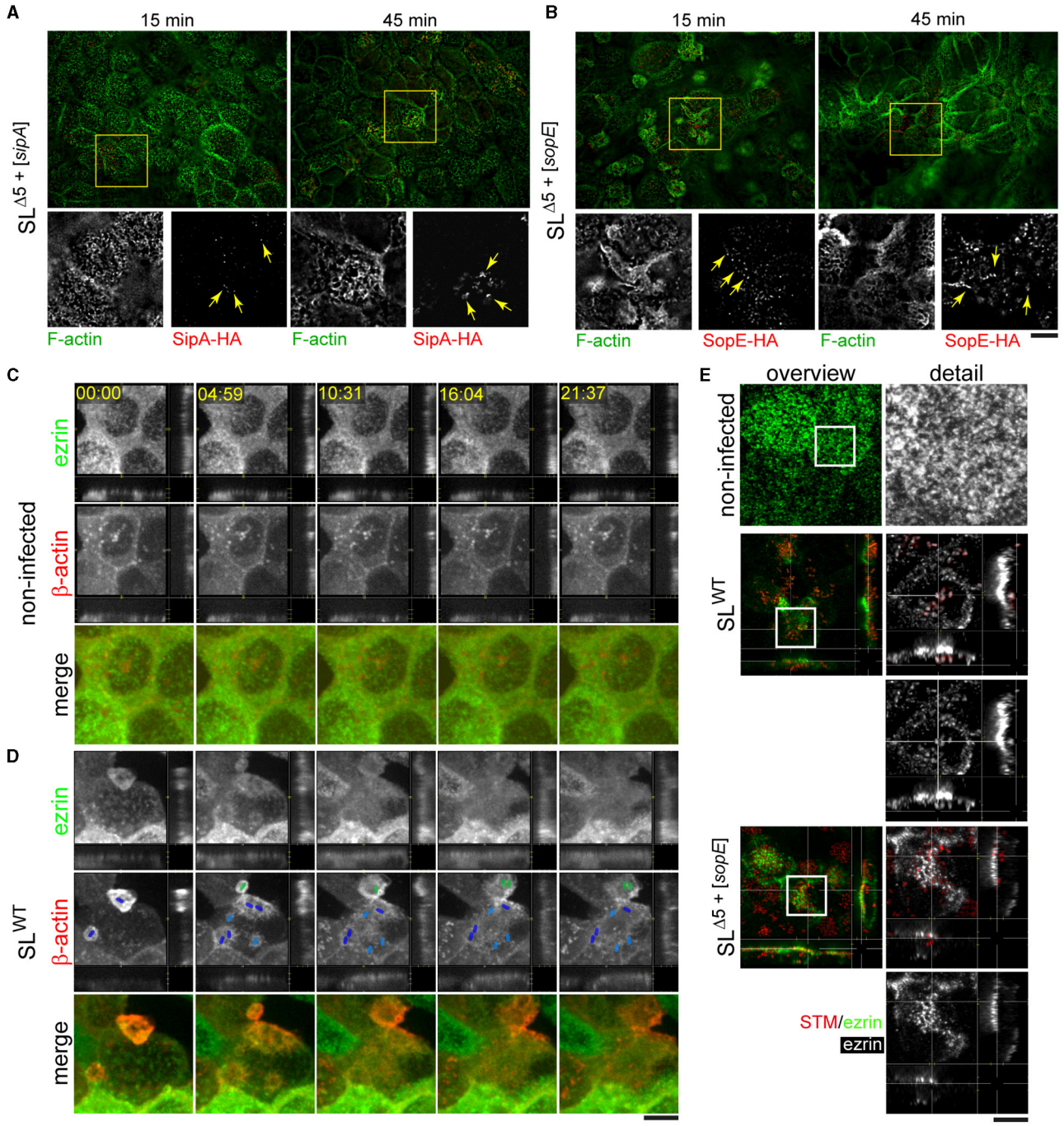

FIGURE 8
STM induces RA by translocation of SopE and SipA and recruits ezrin to the nascent SCV. PEC were infected with STM $SL^{\Delta 5+[sipA::HA]}$ or $SL^{\Delta 5+[sopE::HA]}$ (red) as described in Figure 1B for 15 or 45 min. After fixation and permeabilization, immunostaining for translocated effector proteins with anti-HA antibody (red) was performed, and F-actin was labeled with phalloidin (green) **(A, B)**. Alternatively, infected cells were immunolabeled with anti-ezrin antibody (green), and F-actin was stained by phalloidin (red) **(C, D)**. **(A)** Formation of RA is triggered by SipA only independent of SopE. SipA reorganizes the actin cytoskeleton into RA structures. **(B)** The formation of RA is triggered by SopE only independently of SipA. Both effector proteins strongly localize at the actin filaments at 45 min p.i. Yellow arrows indicated effector proteins SipA **(A)** or SopE **(B)** in the apical portion of MDCK cells. **(C, D)** Ezrin is delocalized after engulfment of STM. MDCK cells transfected with ezrin-eGFP and β-actin-RFP were infected with STM SL^{WT} (not visible, positions indicated by colored rod symbols: dark blue, initial invading STM; light blue, subsequent invading STM; green, STM invading another host cell). See corresponding Supplementary Movie 2 for the time-lapse sequence. **(E)** STM recruits ezrin for the early SCV after the invasion of PEC. MDCK cells were infected with STM SL^{WT} or $SL^{\Delta 5+[sopE]}$. Images are representative of at least three independent experiments. Scale bars, 15 μm and 5 μm **(A, B)** for overview and detail, respectively; 5 μm **(C)**; 20 and 10 μm **(D)** for overview and detail, respectively. Timestamp, min:sec.

Invasion by STM induces the recruitment of ezrin to *Salmonella*-containing vacuoles

Our results demonstrate that only cells highly infected by strains lacking SopE exhibited RA, which diminished after gentamicin treatment. Furthermore, the quantification of the actin polymerization rate was only altered in those cells infected by SL^{WT} or $NCTC^{WT}$ strains. The apical endocytosis of infected cells was altered by the translocation of SopE but not SopE2. These observations indicate that there may be further SPI1-T3SS effector protein functions necessary to cause actin rearrangements in the absence of SopE and SopE2 but are unable to alter apical endocytosis. Our previous work has already demonstrated that SipA can induce actin polymerization by STM strains lacking SopE and SopE2 (Schlumberger and Hardt, 2005; Schlumberger et al., 2007; Felipe-Lopez et al., 2023). Therefore, we used the same reductionist approach to test if SipA induces the formation of RA. We infected cells for 15 or 45 min with STM $SL^{\Delta 5+[sipA]}$ or $SL^{\Delta 5+[sopE]}$, and both effector proteins and F-actin were stained (Figures 8A, B). Micrographs acquired by total internal reflection microscopy (TIRF) indicated that effector proteins were localized in the F-actin-rich apical area of PEC and at 45 min p.i. sufficient amounts of effector protein accumulated to compare the distribution. While SopE was decorating RA structures at larger areas of the apical side of cells (Figure 8B), SipA was highly concentrated in small regions with F-actin (Figure 8A). The distinct distribution was in line with the observed membrane association of SipA close to the SPI1-T3SS translocon and the cytosolic distribution of SopE. The apparent reticular structure was associated with the bacteria residing (not visible) on the apical side of host cells, which continuously translocate SipA, as observed in Figure 8A (detail, 45 min).

Because STM induces massive brush border effacement and diminishes the apical resorption of fluid tracers, we considered that microvillar proteins might be lost after complete MV effacement, which would explain the origin of RA and reduced endocytic uptake. Therefore, we followed the spatial distribution of ezrin after MV effacement. MDCK cells transfected for the expression of ezrin-GFP and β-actin-RFP were infected by STM SL^{WT} (Figure 8C; Supplementary Movie 2) since we observed the most severe phenotypes with this strain. Ezrin clearly localized in MV in non-infected cells or in cells prior to infection. After STM triggered ruffle formation and MV effacement was initiated, ezrin was lost from the MV and recruited to ruffles. However, once STM was completely engulfed, cells did not recover ezrin at the apical membrane. Instead, the signal of ezrin mainly remained in the cytoplasm at the apical side, as images from lateral projections from LCI sequences indicate (Figure 8D). In contrast, non-infected cells showed no changes in the localization of ezrin over the acquisition period (Figure 8C). These results may indicate the recruitment of ezrin to nascent SCV after complete engulfment. To address this hypothesis, MDCK cells were infected for 45 min and stained with antibodies against ezrin. Most ezrin signals were concentrated at nascent SCV harboring STM SL^{WT} (Figure 8E), compared to non-infected cells, which maintained the ezrin at the apical side of the cell. To evaluate whether the recruitment of ezrin is caused by SopE, we used STM $SL^{\Delta 5+[sopE]}$, only translocating SopE, but able to invade PEC and to remodel their actin cytoskeleton (Felipe-Lopez et al., 2023). In cells infected by STM $SL^{\Delta 5+[sopE]}$, ezrin was delocalized from the apical membrane as observed in STM SL^{WT}-infected cells; however, no prominent association with nascent SCV was observed (Figure 8E).

These data demonstrate that SopE mainly controls actin remodeling after complete engulfment by STM. Although SopE-deficient strains could cause MV effacement and induce RA by translocating SipA, these morphological changes were not sufficient to alter the physiological resorption by PEC or to modify actin polymerization to the extent observed in SopE by a single bacterium. The delocalization of ezrin caused by SopE-induced actin rearrangements is an example of the loss of microvillar proteins during the invasion of STM, which might indirectly lead to reduced resorption by PEC.

Discussion

The effacement of MV occurs during infection by various enteric pathogens such as EPEC, *Helicobacter pylori*, or *Citrobacter rodentium*. In contrast to the local destruction of MV by these pathogens, STM invasion causes the complete collapse of MV in PEC, such as enterocytes (Takeuchi, 1967). We previously described that the sole translocation of SopE into host cells caused MV effacement, induced the formation of RA, and mainly mediated the invasion of PEC (Felipe-Lopez et al., 2023). In this study, we additionally found that SopE is a key factor for disturbing resorption by PEC. Yet, strains lacking SopE were still able to efface MV by the accumulation of bacterial cells on the apical side of PEC over prolonged periods of infection. In both cases, the internalization of STM culminated in the appearance of RA on the apical side of PEC. RA remained even after the complete internalization of STM SL^{WT} or $NCTC^{WT}$, but disappeared in cells infected by STM $SL^{\Delta sopE}$ or $NCTC^{\Delta sopE2}$, permitting host cells to partially recover MV after complete STM internalization. Although SopE-deficient strains also efface MV and create RA, their infected cells are still able to endocytose dextran.

Our data demonstrate that reduced invasion due to the absence of SopE can be compensated by prolonged periods of STM exposure that increase the opportunity for multiple STM to interact with host cells and to form bacterial clusters on the PEC apical side (see Figures 1B–F). Our experimental setup is similar to that published by Lorkowski et al. (2014); thus, the accumulation of bacteria is the result of the cooperativity of STM infection, allowing other bacteria to internalize once a "starter" STM cell has triggered membrane ruffles (Misselwitz et al., 2012; Lorkowski et al., 2014). In contrast to STM SL^{WT}, STM $NCTC^{WT}$ did not trigger large ruffles; instead, it formed microcolonies that concluded with the loss of brush border and formation of RA, which completely replaced the brush border architecture.

While all *S. enterica* strains harbor *sopE2*, only a subset additionally possesses *sopE* due to lysogenic conversion through infection by *sopE* phage (Mirold et al., 1999). Previous research showed that several virulence traits of STM are associated with the function of SopE, such as intestinal inflammation due to caspase-1 activation (Muller et al., 2009) and activation of NOD1 signaling (Keestra et al., 2013). By comparing intracellular phenotypes of

STM strains with and without SopE, we recently demonstrated that the presence of SopE leads to increased invasion, damage of the nascent SCV, and escape of STM into host cell cytosol (Röder and Hensel, 2020). Sensing cytosolic STM by the NAIP/NLRC4 inflammasome results in the expulsion of infected PEC into the intestinal lumen (Chong et al., 2021; Fattinger et al., 2021a), and this increases shedding and the further spread of STM. The data reported here add reduced resorption by PEC as a further pathogenic consequence of the presence of SopE in STM strains. Therefore, SopE can be considered as a factor increasing the severity of STM intestinal infections.

MV effacement is caused by bacterial accumulation and RA formation, but capability in endocytosis suggests that a third effector protein is involved in the absence of SopE and SopE2. Indeed, only SipA participated in the formation of RA, as our reductionist approach revealed. We previously demonstrated that SipA, SopE, and SopE2 independently mediate ruffle formation or discrete actin polymerization, leading to the invasion of PEC (Felipe-Lopez et al., 2023). Our observations are supported by results from murine infection models (Zhang et al., 2018; Fattinger et al., 2020). STM can discretely penetrate enterocytes exclusively by the translocation of SipA in the absence of SopE, SopE2, or both SopE and SopE2. These *in vivo* observations support our data showing that RA appears after infection by STM strains only expressing SipA. In our model, the absence of SopE and SopE2 did not alter the endocytosis of PEC and SL$^{\Delta sopE}$, SL$^{\Delta sopEsopE2}$, or NCTC$^{\Delta sopE2}$ still invaded if sufficiently long interaction with host cells was allowed. Contrary to our *in vitro* observations, MV are not effaced *in vivo* by SipA-mediated invasion. These observations would suggest that SipA-mediated invasion of STM may reduce the damage to the intestinal epithelium. Nevertheless, SipA and ezrin mediate the recruitment of neutrophils (Agbor et al., 2011), and inflammation of epithelial tissue is caused by strains expressing only SipA in the ileal loop model (Zhang et al., 2002).

The formation of MV or actin networks is directly proportional to the density of proteins recruited to the apical side of the cell, including bundling, anchoring proteins, and actin (Gov, 2006). Once this group of proteins localizes at the apical side of PEC, actin polymerization and an assembly of bundles originate a protrusion force that first creates actin networks. Further, actin polymerization by treadmilling creates new MV on the apical surface (Gaeta et al., 2021). In contrast, if actin polymerization is disturbed or membrane anchoring fails, then no further bundling proteins are recruited, as we observed with infection of STM.

Hence, in our model, actin polymerization is redirected to ruffle formation by the activity of SipA, SopE, and/or SopE2; the further disorganization of ezrin and depolymerization of actin by villin (Lhocine et al., 2015; Felipe-Lopez et al., 2023) would explain that infected host cells fail to restore their brush border architecture. Instead, the apical surface remains as a reticular structure until the action of virulence proteins ceases, as we observed in those cells treated with gentamicin. Further published evidence supports this model. MV elongation and stabilization depended on the binding and capping functions of EPS8, villin, epsin, and fimbrin (Meenderink et al., 2019; Gaeta et al., 2021). Indeed, PEC of ezrin knockout mice only developed short MV, a disorganized terminal web (Saotome et al., 2004), and showed altered localization of apical transporters (Engevik and Goldenring, 2018). In mice lacking either villin, epsin, fimbrin, or a combination of these three proteins, MV were specifically reduced in amount and developed only short-length structures (Revenu et al., 2012). In yeast, fimbrin contributes to the breaching of F-actin filaments depending on the fimbrin concentration (Laporte et al., 2012). Moreover, the expression of EPS8 also regulates the length of MV in porcine kidney cell lines. Therefore, at low concentrations of fimbrin, disassociation of MV proteins such as ezrin, villin, or ESP8, actin filaments form highly ramified structures as we observed in this study, and supported by our previous work (Felipe-Lopez et al., 2023).

Based on our observations, we propose that loss of ezrin from MV during STM invasion hinders the anchoring of new F-actin filaments (Figure 9). In turn, this would avoid the formation of MV, as previously described (Gloerich et al., 2012; Solaymani-Mohammadi and Singer, 2013; Dhekne et al., 2014; Gaeta et al., 2021). Since actin polymerization required for MV formation is redirected to sites of STM invasion, other bundling proteins may not be properly recruited. Consequently, low concentrations of bundling proteins such as fimbrin (Revenu et al., 2012), ezrin (along with EPS8) (Gaeta et al., 2021), and villin (Meenderink et al., 2019; Felipe-Lopez et al., 2023) may only permit the formation of RA after the complete internalization of *Salmonella* (Figure 9C). The loss of ezrin from the apical side of PEC may be attributed to the degradation of phosphoinositide 4,5 bis-phosphate (PI-4,5P_2) by SopE-activated phospholipase γ (PLC γ) and SopB (Terebiznik et al., 2002; Felipe-Lopez et al., 2023).

MV effacement and formation of RA have further consequences for PEC in this model. Cells infected by SopE-harboring STM lost MV and were deficient in dextran uptake from the luminal side. Previous observations with MDCK cells attributed the altered uptake of fluid tracers to the inhibition of members of the Src kinase pathway (Mettlen et al., 2006). These authors found that after Src kinase activation by decreasing the temperature from 40 to 34°C, cells formed ruffles, which enhanced the uptake of dextran. The uptake of dextran and holo-transferrin was blocked by inhibitors of F-actin formation, phospholipase, and PIP5K, which indicates the participation of active actin polymerization. In our model, the polymerization of actin in infected cells was 50% higher in zones with RA. Despite SopE2 also altering the actin polymerization, endocytosis in cells infected by STM only containing SopE2 was not altered. Therefore, the alteration of actin polymerization by SopE, but not SopE2, and loss of the absorptive surface of PEC are factors affecting the endocytosis of infected cells.

In contrast, we found that the membrane stain FM4-64 was highly adsorbed only in infected cells, where *Salmonella* secretes SopE and forms a macropinocytic cup. The accumulation of FM4-64 was previously associated with the production of phosphatidyl-inositol 3,4,5, tri-phosphate (PI-3,4,5P_3) in macropinocytic cups of macrophages stimulated with M-CSF (Yoshida et al., 2009). PI-3,4,5P_3 is a product of PI3K, a kinase downstream of Rac1. These observations relate to infection by STM expressing SopE; since SopE is a GEF for Rac1, consequently, constant activation of Rac1 via SopE may have further effects on the PI pool at

10.3389/fmicb.2024.1329798

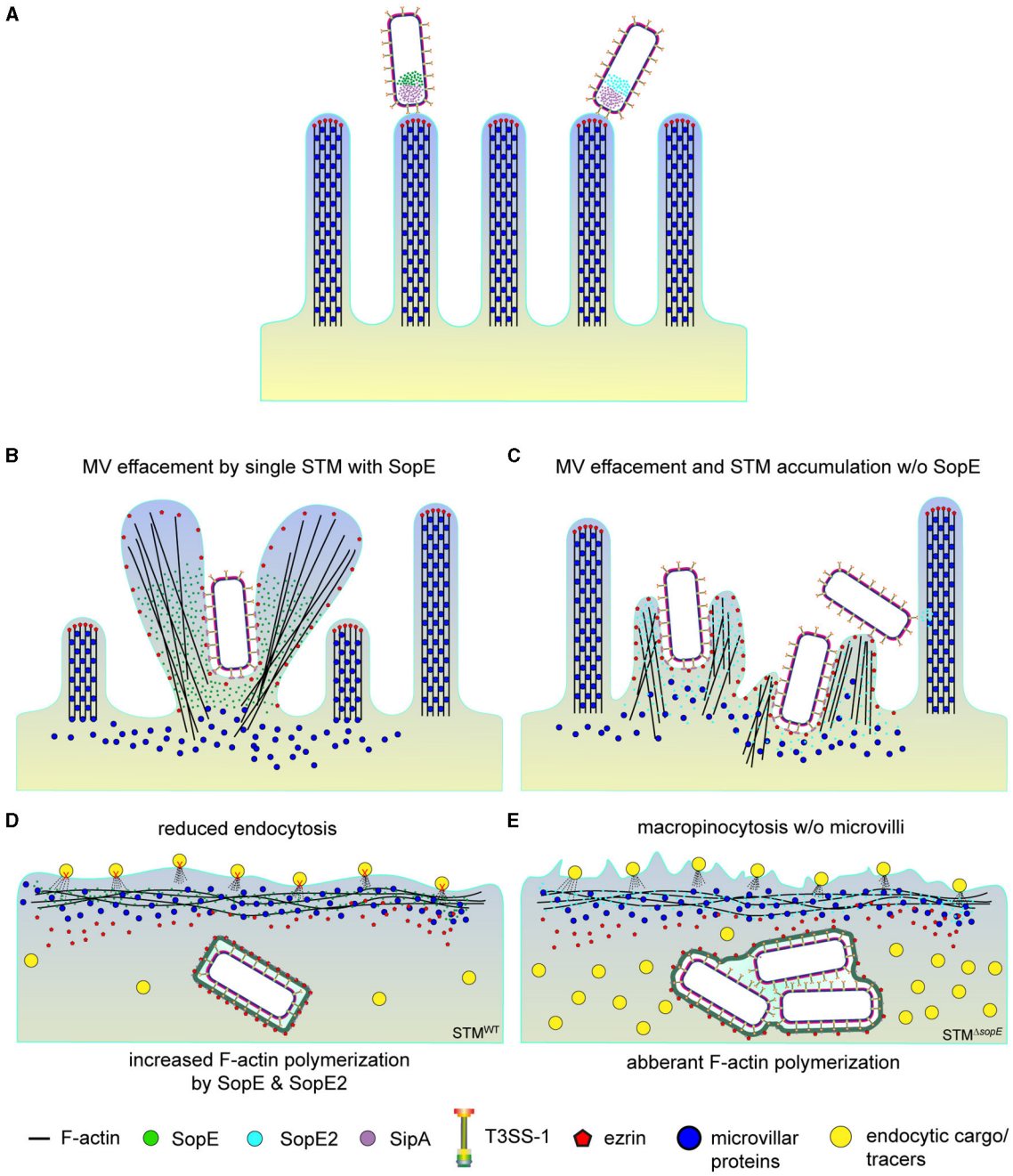

FIGURE 9
Destruction of the brush border by SPI1-T3SS effector SopE abolishes endocytosis of PEC. The model depicts the sequence of events observed during the STM invasion of PEC. **(A)** After adhesion, STM translocate SPI1-T3SS effector proteins into host cells. **(B)** SopE-induced MV effacement also causes delocalization of ezrin and probably other microvillar proteins affected, whereas **(C)** bacterial cells of STM lacking SopE accumulate to cause local actin reorganization and MV effacement. **(D)** Internalization of STM-secreting SopE concludes with RA formation (not displayed), recruitment of ezrin to the nascent SCV, and severe reduction of resorption of luminal content (tracers). Delocalization of ezrin and other microvillar proteins probably prevents recovery of MV but has minor effects on resorption since cells infected by SopE-negative STM **(E)** still endocytose dextran are representative endocytic cargo.

the plasma membrane, which increase during the formation of macropinocytic cups of STM internalization. We speculate that the strong activation of Rac1 by SopE may additionally be the cause of the high recruitment of other proteins, such as Rab5, necessary for the closure of the macropinocytic cups. If so, the amount of Rab5 and other proteins necessary for proper macropinocytosis could be exhausted during STM infection, thus preventing the resorption of luminal content such as dextran. This result also suggests that the selective action of SopE2 on Cdc42 would not affect other proteins necessary for physiological endocytosis.

Similar to our infection model of *Salmonella* in PEC, infection of C2BBe1 cells by EPEC also culminated in a reduction of the

uptake of substrates from the lumen, accompanied by the loss of function of the sodium/D-glucose cotransporter SGLT (Dean et al., 2006). These phenotypes mainly correlated to the infection doses in the experiments and translocation of EPEC effector proteins Map, EspF, Tir, and adhesin Eae. These proteins are necessary to remodel the F-actin in MV since Map binds to the PDZ domain, which interferes with the association of the NHERF transporters to the F-actin cytoskeleton in MV. Its action is enhanced by a cooperative mechanism of the proteins NheI and EspI (Martinez et al., 2010) and the NleH effector protein of EPEC targeting EPS8 to reorganize the apical surface of the host cells to form microcolonies (Lhocine et al., 2015).

Our observations also suggest that effector proteins may not have redundant virulence functions in the host cells but rather cooperatively act to permit a proper internalization of STM into host cells. Another interesting point for further investigation is the reduction of virulence to one or two effector proteins using reduced bacterial infecting doses and long incubation periods for bacterial internalization. Using this setup, we observed no extreme alterations in host cells. Whether this may be sufficient to penetrate enterocytes and disseminate into lymph organs without causing inflammation is still open since SipA triggers neutrophils into the infection area *in vivo* and *in vitro* (Zhang et al., 2002; Agbor et al., 2011). It would be interesting to know whether this inflammation causes erosion of the epithelial layer and confines intestinal infection.

Altogether, our data demonstrate that translocation of SopE and SipA dominantly induces the formation of RA at the apical side of host cells, which is a consequence of the loss of ezrin and probably other microvillar proteins after internalization of *Salmonella*. Furthermore, loss of MV and maintenance of RA via SopE abrogate endocytosis of infected PEC. These physiological alterations of the apical side of PEC and the reduction of the uptake function seem to be a common result of infections by intestinal pathogens. This points out that the organization of the actin and endocytic capacity are highly interdependent processes and are regulated by the same family of proteins in MV, which are directly or indirectly manipulated by bacterial virulence proteins. Further investigations are needed to identify the precise molecular mechanisms behind the alteration of endocytic capacity caused by infection with intestinal pathogens and the physiological consequences.

Materials and methods

Bacterial strains, construction of mutant strains, and plasmids for complementation

Salmonella enterica serovar Typhimurium strain SL1344 (SL^{WT}) and NCTC 12023 ($NCTC^{WT}$) were used as wild-type strains, and their isogenic mutant strains were employed throughout the experiments described in this study (see Table 1). Gene deletion strains were generated by the insertion of an *aph* cassette into specific target genes. Mutations were generated in NCTC12023 by red-mediated recombination (Datsenko and Wanner, 2000) using pKD13 as a template and primers specified in Table 2. If required, mutant alleles were transferred to the SL1344 strain background by P22 transduction as previously described (Felipe-Lopez et al., 2023).

TABLE 1 Bacterial strains used in this study.

Designation	Relevant characteristics	Reference
S. enterica serovar Typhimurium SL1344 strains		
SL1344	wild type, Sm^R	Lab stock
M712	Δ*sipA sopA sopB sopE sopE2*	Ehrbar et al., 2004
M1318	Δ*sopE*	(Hardt Lab)
SB856	Δ*sopE*::*aphT*, Km^R	Hardt et al., 1998
MvP1459	Δ*sopE2*::*aph*, Km^R	Felipe-Lopez et al., 2023
MvP1485	Δ*sopE2*::*aph*, Km^R	This work
S. enterica serovar Typhimurium NCTC 12023 strains		
NCTC12023	Wild type, Nal^S	Lab stock
MvP1412	Δ*sopE2*::*aph*, Km^R	This study

TABLE 2 Oligonucleotides used in this study.

Designation	Sequence 5′-3′
SopE2-Red-Del-For	aaagtgtagctatgcatagttatctaaaaggagaactaccgtgtaggctggagctgcttc
SopE2-Red-Del-Rev	taattcatatggttaatagcactattgtatttactaccacatatgaatatcctccttag
SopE2-Red-Check-For	ctaaaaggagaactaccgtg

Cell lines and culture conditions

All cell lines employed in this study were cultured at 37°C in a humidified atmosphere containing 5% CO_2. For invasion assays and microscopy analyses, MDCK clone Pf was used as a standard cell culture model, kindly provided by the Nephrology department of the University Hospital Erlangen, FAU Erlangen-Nürnberg. Confluent monolayers in 25 cm^2 cell culture flasks were seeded each week in a new 25 cm^2 flask with MEM supplemented with 1 × non-essential amino acids (PAA, Germany), 10% inactivated fetal calf serum (FCS, Sigma, Germany) and 1 × Glutamax (PAA, Germany). Changes in the trans-epithelial electrical resistance (TEER) due to the infection of *Salmonella* were monitored using the cell line Caco-2 BBe1, which is a derivate of Caco-2 cells (ATCC CRL-2102). These cells were cultured in DMEM high glucose without pyruvate (PAA, Germany), containing Glutamax, 10% FCS, and 2.5 $\mu g \times mL^{-1}$ human holo-transferrin (Sigma-Aldrich, Germany). Cells were seeded at 10^5 cells per 12 mm polycarbonate filter insert (0.4 µm pore size, Millipore, Germany). TEER was measured every third day with a platinum electrode and an Ohm meter EVOM (World Precision Instruments, USA). Cells were cultured until a TEER of 500–700 Ω per well was observed, usually 10–15 d. For cultivation, media were supplemented with penicillin/streptomycin (PAA, Germany). The medium was changed every third day.

10.3389/fmicb.2024.1329798

TABLE 3 Plasmids used in this study.

Designation	Relevant characteristics	References
pWSK29	Low copy number, $Carb^R$	Wang and Kushner, 1991
p4040	pWSK29 P_{sicA}::*sipA*::HA	Felipe-Lopez et al., 2023
p4043	pWSK29 P_{sopE}::*sopE*::HA	Felipe-Lopez et al., 2023
p4044	pWSK29 P_{sopE2}::*sopE2*::HA	Felipe-Lopez et al., 2023
pKD4	Vector for *aph* cassette	Datsenko and Wanner, 2000
pKD13	Vector for *aph* cassette	Datsenko and Wanner, 2000
pKD46	λ Red expression	Datsenko and Wanner, 2000
pCP20	FLP expression	Datsenko and Wanner, 2000
p3589	P_{rpsM}::mCherry in pETcoco, Cm^R	This work
pWRG439	P_{rpsM}::mTagRFP in pFPV25.1, $Carb^R$	Roman G. Gerlach

Invasion assays

Five days prior to infection, MDCK cells were seeded at 1 × 10^5 cells per well in 24-well plates (Nunc, Denmark). At least 4 h before infection, the medium was substituted with a medium without antibiotics. Bacterial strains were inoculated in LB and incubated overnight at 37°C with continuous aeration. Cultures were diluted 1:31 in fresh LB and incubated for another 4 h in glass test tubes in a roller drum. Next, the optical density of each culture was measured and adjusted in 1 ml MEM to $OD_{600} = 0.2$ (estimated 3 × 10^8 bacteria × mL^{-1}) to generate a master mix. Cells were infected at multiplicity of infection (MOI) as indicated in subsequent sections, and assays were performed in triplicates for each strain and infection condition. After incubation at indicated periods of time for invasion, cells were washed three times with PBS. Next, fresh medium with gentamicin at 100 μg × mL^{-1} was added for 1 h. Finally, infected cells were washed five times with PBS and lysed with 0.5% deoxycholic acid for 10 min. Lysates were diluted and plated onto Mueller Hinton II agar (BD, Germany) plates with an Eddy Jet spiral platting instrument (IUL Instruments, Barcelona). Plates were incubated at 37°C overnight, and colony-forming units (CFU) were counted. For infection of monolayers on filter inserts, bacterial strains were added at MOI 50, and TEER was recorded every 20 min over a period of 2 h. Finally, cells were washed three times with pre-warmed PBS and fixed with methanol at −20°C overnight.

Immunostaining

For imaging, bacterial strains harbored pWGR435 or pFPV-mCherry for constitutive expression of mTagRFP or mCherry, respectively, under the control of P_{rpsM} (plasmids are listed in Table 3). The same amount of cells as for invasion (see above) were seeded on coverslips and infected in duplicates at MOI 50 with a master mix of the respective STM strain. At various time points after infection, infection was stopped by washing cells with PBS four times. Cells were immediately fixed with pre-warmed 3% PFA in PBS for 1 h at 37°C. After fixation or any subsequent incubation with fluorescent dyes or antibodies, cells were washed three times with PBS at 37°C. Fixed cells were permeabilized by incubation for 15 min at 37°C with 0.5% Triton X-100 (Sigma-Aldrich, Germany) in a blocking solution consisting of 2% BSA (Biomol, Germany) and 2% goat serum (Gibco, Germany) in PBS in a humid chamber. Antibodies were diluted in a blocking solution, and incubations were performed at 37°C in a humid chamber. Rabbit anti-ezrin (Dianova, Germany) was diluted 1:100 and incubated for 1 h. Actin-stain 488-conjugated phalloidin (Cytoskeleton, France) was added at 1:200 dilution and incubated for 45 min at 37°C. Coverslips were then mounted on glass slides with Fluoroprep (Biomerieux, France), sealed with Entellan (Merck, Germany), and kept in the dark at 4°C.

Apical uptake of fluorescent fluid tracers

Fluorescent fluid tracers were deployed to evaluate the uptake at the apical side of MDCK cells after infection and destruction of the brush border. Cells were infected as described for invasion experiments (see above). After 1 h of gentamicin treatment, cells were washed three times with pre-warmed PBS. Next, cells were pulsed with 250 μg × mL^{-1} dextran Alexa-568 10,000 FX, or 50 μg × mL^{-1} of the membrane dye FM4-64FX (Life Technologies, Netherlands). Both fluid tracers were mixed in MEM, 30 mM HEPES, pH 7.4 w/o phenol red, and w/o sodium bicarbonate. Cells were then incubated for 30 min at 37°C at 5% CO_2. Finally, tracers were removed from the cells by washing them three times with pre-warmed PBS. They were then fixed with 3% PFA and further processed for microscopy as described above with additional staining of DNA by adding DAPI at 1:1,000 to Fluoroprep.

Microscopy and live-cell imaging

Images from the fixed samples were acquired with a DMI 6000 SP5 II confocal laser-scanning microscope (Leica Microsystems Wetzlar, Germany). They were acquired with a 100x objective with a numerical aperture of 1.44. The pinhole was adjusted to 1 Airy unit for all acquisitions, and the pixel size of the images was 70.85 × 70.85, with a bit depth of 16 bits. Z-slice thickness was adjusted to 0.12 μm using the Nyquist theorem. The Ar 488 nm laser line was used for Alexa488-conjugated antibodies and eGFP. The HeNe 543 nm laser line was used for the excitation of Alexa568-conjugated antibodies and mCherry or mTagRFP. Images were acquired with Leica Acquisition Software V. 2.3.6. and further processed with Imaris V. 7.6.1 (BitPlane, Switzerland) and FIJI (Max-Planck Institute for Cell Biology, Dresden, Germany).

Live-cell imaging (LCI) was performed using Lifeact-EGFP MDCK cells, which are described before (Felipe-Lopez et al., 2023), and mCherry-, or mTagRFP-expressing *Salmonella* strains. LCI

was performed using a CellObserver microscopy system (Zeiss, Germany) coupled to a Yokogawa spinning disc unit. Images were acquired for 120 min shortly after infection at maximal speed with intervals of 100–200 ms at distances between *Z* planes of 0.30–0.35 µm. LCI was performed with a water immersion objective with a numerical aperture of 1.333. The acquisition was performed with either a cooled CCD camera (CoolSNAP HQ^2, Photometrics) with a chip of 1,040 × 1,392 pixels for high spatial resolution or an EM-CCD camera (Evolve, Photometrics) with a chip of 512 × 512 pixels for high sensitivity and FRAP analysis. The acquisition and processing of the time-lapse images were performed with ZEN 2012. Images from CLSM or SD were deconvolved with Huygens V.4.2 using a theoretical PSF. Bleaching and *Z*-drift were also corrected with Huygens. Further processing and movie export were performed with Imaris 7.6.1.

Quantification of endocytosed fluorescent fluid tracers

Fixed samples of infected MDCK cells fed with dextran Alexa568 10 000 FX were observed by laser confocal-spinning disc microscopy with an EmCCD camera (see above). DAPI-stained structures were excited by a 405 nm laser line; F-actin stained with phalloidin Actin-stain 488 was excited with the laser line 488 nm; finally, dextran-stained samples were excited with a laser line 561. Images were acquired with a 63x oil immersion objective with a refraction index of 1.51 and a numerical aperture of 1.44 through the Z axis with intervals of 0.12 µm between each slice. Images were further deconvolved using Huygens 4.2. for the detection of dextran in all other cells. Then, restored images were visualized in Imaris V.7.6.1. For quantification, dextran spots of the non-infected cells and non-stained cells were set up at a lower threshold for processing the rest of the infected samples. The minor diameter of dextran spots was defined to be ∼ 0.5 µm. Quantification of dextran was then performed using the "Spot" function of Imaris, briefly: a region of interest of 45 × 45 pixels, which represents approximately one cell, was set. Next, the spots with a diameter of ∼0.5 µm were recognized by their maximal intensity signal. The threshold values from the emission spectrum of each sample were then adjusted from 450 to 10,000 voxels from a total emission spectrum of 16,000 voxels. Finally, the whole observation field was processed with these parameters. The average of the total number of spots per field was calculated and plotted as indicated in the Results section.

Images from samples stained with the membrane fluorescent dye FM4-64FX were acquired by confocal laser-scanning microscopy (see below) with the XZY mode. This mode allows the acquisition of a vertical section of the sample w/o *Z*-slices. Therefore, the observation of the distribution of the membrane dye throughout the cytoplasmic membrane was possible. Samples were observed with a 100x-objective with a numerical aperture of 1.44 and a refraction index of 1.51. Image resolution was 1,024 × 1,024 pixels from a field size of 45 × 45 µm with a bit depth of 8 bits. The thickness of each slice in the *Y*-axis was 0.12 µm. FM4-64 or phalloidin Actin-stain 488 were excited by the Ar 488 nm laser line. Images were further processed with FIJI. A profile line was drawn at the apical side of each section. The total signal from the apical side of the section was added, and the average of this signal from several fields was calculated and plotted, as shown in the results section.

Fluorescence recovery after photobleaching in infected MDCK cells

To evaluate the polymerization of F-actin to RA, fluorescence recovery after photobleaching (FRAP) was performed in cells infected by *Salmonella*. MDCK Lifeact-EGFP cells were seeded on treated chamber slides (Ibidi, Germany) at 25,000 cells per well. After 5 days, the medium was substituted with MEM 30 mM HEPES pH 7.4 w/o sodium bicarbonate and phenol red. Then, cells were infected by *Salmonella* at MOI 25 as described for invasion experiments. At 25 min p.i., cells were washed with a pre-warmed MEM medium to avoid alterations of any cellular structures such as MV or RA. Cells were further incubated with MEM as described above and observed by SD microscopy.

Image acquisition was performed at the apical side of the infected cells with a frame rate of 100 ms per frame per channel. The 488 nm and 561 nm laser lines were set to 2 and 5% intensity, respectively. The electrical gain of the EmCCD camera was set to 100 in both channels. Before bleaching, 50 frames were acquired. A bleaching pulse was performed for 500 ms with a 488 nm laser line at transmission of 100% using a pre-established mask of 5 µm. Signal recovery was quantified during 200 frames after the bleaching pulse. Results from the FRAP signal were plotted as relative signals over time in seconds. The recovery constant was calculated from the bleaching point until the next 200 frames by the method described by Ishikawa-Ankerhold et al. (2012). Results were plotted as described above.

Atomic force microscopy

To observe topological changes in cell surface as a consequence of STM-induced cytoskeletal remodeling, AFM measurements were conducted using the NanoWizard II AFM system (JPK Instruments AG, Berlin, Germany). High-resolution surface images were acquired by operating the AFM under ambient conditions in soft contact mode using silicon nitride AFM probes with a nominal force constant of 0.06 N/m (SiNi, Budget Sensors, Wetzlar, Germany). Samples were prepared as described above. For each sample, topographic overview images with a 90 × 90 µm scan area were taken before zoom-ins were generated. All images were polynomially fitted and unsharpened mask filtered using JPK data processing software (JPK Instruments AG). Presented images are 3D projections of the height profiles, tilted 12° in X direction.

Data availability statement

The raw data supporting the conclusions of this article will be made available by the authors, without undue reservation.

Author contributions

AF-L: Conceptualization, Data curation, Investigation, Project administration, Validation, Visualization, Writing – original draft, Writing – review & editing, Formal analysis, Methodology, Resources. NH: Conceptualization, Data curation, Formal analysis, Investigation, Methodology, Resources, Validation, Visualization, Writing – original draft. MH: Conceptualization, Data curation, Investigation, Validation, Visualization, Writing – original draft, Funding acquisition, Project administration, Supervision, Writing – review & editing.

Funding

The author(s) declare financial support was received for the research, authorship, and/or publication of this article. This work was supported by the Deutsche Forschungsgemeinschaft grants P4 and Z within the collaborative research center SFB 944. AF-L was supported by a research fellowship of the German Academic Exchange Service (DAAD/A-0773175). The funders had no role in the design of the study and interpretation of results. Open access publication was supported by the DFG, DEAL project ID: 180879236.

Acknowledgments

We thank the MWK Niedersachsen for the start-up funding of MH.

Conflict of interest

The authors declare that the research was conducted in the absence of any commercial or financial relationships that could be construed as a potential conflict of interest.

The handling editor SH declared a past co-authorship with the author MH.

Publisher's note

Supplementary material

The Supplementary Material for this article can be found online at: https://www.frontiersin.org/articles/10.3389/fmicb.2024.1329798/full#supplementary-material

SUPPLEMENTARY FIGURE 1
Manipulation of the apical side of PEC and F-actin cytoskeleton by STM. Previously reported analyses of the apical side of PEC during STM adhesion and invasion were compiled. **(A)** MDCK cells are infected by STM WT, fixed, and prepared for scanning EM. STM is pseudo-colored red. Modified from Gerlach et al. (2008). **(B)** MDCK cells were infected by STM WT expressing mCherry (red). At indicated time points, p.i. were fixed and labeled for F-actin (white). MV, microvilli; R, membrane ruffle; RA reticular F-actin. Arrowheads indicate RA. Modified from Lorkowski et al. (2014). **(C)** AFM analyses of surface topologies of STM-infected MDCK at indicated time points p.i. modified from Lorkowski et al. (2014). **(D)** Live-cell correlative live-cell scanning electron microscopy of MDCK monolayers expressing Lifeact (green in inserts), infected by STM WT (red in inserts). Arrowhead indicates RA. Modified from Kommnick et al. (2019). **(E)** CLSM and AFM of MDCK Lifeact-GFP cells apical side after infection by STM WT. The arrowhead indicates MV, R, or RA as indicated. Modified from Felipe-Lopez et al. (2023). For full experimental details, see the respective references. Timestamp min:sec. Scale bars, 10 μm (**A**, Left**, B, E**), 1 μm (**A** mid and right, **D**).

SUPPLEMENTARY MOVIE 1
STM destroys the brush border architecture of PEC and induces the formation of reticular F-actin. MDCK Lifeact-eGFP cells (gray) were infected with STM SL^{WT}, $SL^{\Delta sopE}$, $NCTC^{WT}$, or $NCTC^{\Delta sopE2}$. Bacterial strains were expressing mTagRFP or mCherry. Time-lapse series of LCI were recorded for 110 min. Timestamp, h:min:sec.ms. Scale bar, 5 μm. The movie corresponds to Figure 3.

SUPPLEMENTARY MOVIE 2
STM recruits ezrin to the nascent SCV. MDCK cells expressing GFP-ezrin (green) and β-actin-RFP (red) were infected with STM SL^{WT} (not visible), and a time-lapse series of LCI was recorded for 35 min. Timestamp, h:min:sec:ms. Scale bar, 5 μm. The movie corresponds to Figures 8C, D.

References

Agbor, T. A., Demma, Z. C., Mumy, K. L., Bien, J. D., and Mccormick, B. A. (2011). The ERM protein, ezrin, regulates neutrophil transmigration by modulating the apical localization of MRP2 in response to the SipA effector protein during *Salmonella* Typhimurium infection. *Cell. Microbiol.* 13, 2007–2021. doi: 10.1111/j.1462-5822.2011.01693.x

Antonio, P. D., Lasalvia, M., Perna, G., and Capozzi, V. (2012). Scale-independent roughness value of cell membranes studied by means of AFM technique. *Biochim. Biophys. Acta* 1818, 3141–3148. doi: 10.1016/j.bbamem.2012.08.001

Chong, A., Cooper, K. G., Kari, L., Nilsson, O. R., Hillman, C., Fleming, B. A., et al. (2021). Cytosolic replication in epithelial cells fuels intestinal expansion and chronic fecal shedding of *Salmonella* Typhimurium. *Cell Host Microbe* 29, 1177–1185 e1176. doi: 10.1016/j.chom.2021.04.017

Datsenko, K. A., and Wanner, B. L. (2000). One-step inactivation of chromosomal genes in *Escherichia coli* K-12 using PCR products. *Proc. Natl. Acad. Sci. U. S. A.* 97, 6640–6645. doi: 10.1073/pnas.120163297

Dean, P., Maresca, M., Schuller, S., Phillips, A. D., and Kenny, B. (2006). Potent diarrheagenic mechanism mediated by the cooperative action of three enteropathogenic *Escherichia coli*-injected effector proteins. *Proc. Natl. Acad. Sci. U. S. A.* 103, 1876–1881. doi: 10.1073/pnas.0509451103

Delacour, D., Salomon, J., Robine, S., and Louvard, D. (2016). Plasticity of the brush border - the yin and yang of intestinal homeostasis. *Nat. Rev. Gastroenterol. Hepatol.* 13, 161–174. doi: 10.1038/nrgastro.2016.5

Dhekne, H. S., Hsiao, N. H., Roelofs, P., Kumari, M., Slim, C. L., Rings, E. H., et al. (2014). Myosin Vb and rab11a regulate ezrin phosphorylation in enterocytes. *J. Cell Sci.* 127 (Pt 5):1007–1017. doi: 10.1242/jcs.137273

Ehrbar, K., Hapfelmeier, S., Stecher, B., and Hardt, W. D. (2004). InvB is required for type III-dependent secretion of SopA in *Salmonella enterica* serovar Typhimurium. *J. Bacteriol.* 186, 1215–1219. doi: 10.1128/JB.186.4.1215-1219.2004

Engevik, A. C., and Goldenring, J. R. (2018). Trafficking ion transporters to the apical membrane of polarized intestinal enterocytes. *Cold Spring Harb. Perspect. Biol.* 10:a027979. doi: 10.1101/cshperspect.a027979

Fattinger, S. A., Bock, D., Di Martino, M. L., Deuring, S., Samperio Ventayol, P., Ek, V., et al. (2020). *Salmonella* Typhimurium discreet-invasion of the murine gut absorptive epithelium. *PLoS Pathog.* 16:e1008503. doi: 10.1371/journal.ppat.1008503

Fattinger, S. A., Geiser, P., Samperio Ventayol, P., Di Martino, M. L., Furter, M., Felmy, B., et al. (2021a). Epithelium-autonomous NAIP/NLRC4 prevents TNF-driven inflammatory destruction of the gut epithelial barrier in *Salmonella*-infected mice. *Mucosal Immunol.* 14, 615–629. doi: 10.1038/s41385-021-00381-y

Fattinger, S. A., Sellin, M. E., and Hardt, W. D. (2021b). *Salmonella* effector driven invasion of the gut epithelium: breaking in and setting the house on fire. *Curr. Opin. Microbiol.* 64, 9–18. doi: 10.1016/j.mib.2021.08.007

Felipe-Lopez, A., Hansmeier, N., Danzer, C., and Hensel, M. (2023). Manipulation of microvillar proteins during *Salmonella enterica* invasion results in brush border effacement and actin remodeling. *Front. Cell. Infect. Microbiol.* 13:1137062. doi: 10.3389/fcimb.2023.1137062

Finlay, B. B., Gumbiner, B., and Falkow, S. (1988). Penetration of *Salmonella* through a polarized Madin-Darby canine kidney epithelial cell monolayer. *J. Cell Biol.* 107, 221–230. doi: 10.1083/jcb.107.1.221

Frankel, G., Phillips, A. D., Rosenshine, I., Dougan, G., Kaper, J. B., and Knutton, S. (1998). Enteropathogenic and enterohaemorrhagic *Escherichia coli*: more subversive elements. *Mol. Microbiol.* 30, 911–921. doi: 10.1046/j.1365-2958.1998.01144.x

Friebel, A., Ilchmann, H., Aepfelbacher, M., Ehrbar, K., Machleidt, W., and Hardt, W. D. (2001). SopE and SopE2 from *Salmonella typhimurium* activate different sets of RhoGTPases of the host cell. *J. Biol. Chem.* 276, 34035–34040. doi: 10.1074/jbc.M100609200

Gaeta, I. M., Meenderink, L. M., Postema, M. M., Cencer, C. S., and Tyska, M. J. (2021). Direct visualization of epithelial microvilli biogenesis. *Curr. Biol.* 31, 2561–2575 e2566. doi: 10.1016/j.cub.2021.04.012

Galan, J. E. (2021). *Salmonella* Typhimurium and inflammation: a pathogen-centric affair. *Nat. Rev. Microbiol.* 19, 716–725. doi: 10.1038/s41579-021-00561-4

Gerlach, R. G., Claudio, N., Rohde, M., Jäckel, D., Wagner, C., and Hensel, M. (2008). Cooperation of *Salmonella* pathogenicity islands 1 and 4 is required to breach epithelial barriers. *Cell. Microbiol.* 10, 2364–2376. doi: 10.1111/j.1462-5822.2008.01218.x

Ginocchio, C., Pace, J., and Galan, J. E. (1992). Identification and molecular characterization of a *Salmonella typhimurium* gene involved in triggering the internalization of salmonellae into cultured epithelial cells. *Proc. Natl. Acad. Sci. U. S. A.* 89, 5976–5980. doi: 10.1073/pnas.89.13.5976

Gloerich, M., Ten Klooster, J. P., Vliem, M. J., Koorman, T., Zwartkruis, F. J., Clevers, H., et al. (2012). Rap2A links intestinal cell polarity to brush border formation. *Nat. Cell Biol.* 14, 793–801. doi: 10.1038/ncb2537

Gov, N. S. (2006). Dynamics and morphology of microvilli driven by actin polymerization. *Phys. Rev. Lett.* 97:018101. doi: 10.1103/PhysRevLett.97.018101

Hardt, W. D., Urlaub, H., and Galan, J. E. (1998). A substrate of the centisome 63 type III protein secretion system of *Salmonella typhimurium* is encoded by a cryptic bacteriophage. *Proc. Natl. Acad. Sci. U. S. A.* 95, 2574–2579. doi: 10.1073/pnas.95.5.2574

Hölzer, S. U., and Hensel, M. (2012). Divergent roles of *Salmonella* Pathogenicity Island 2 and metabolic traits during interaction of *S. enterica* serovar Typhimurium with host cells. *PLoS ONE* 7:e33220. doi: 10.1371/journal.pone.0033220

Ishikawa-Ankerhold, H. C., Ankerhold, R., and Drummen, G. P. (2012). Advanced fluorescence microscopy techniques - FRAP, FLIP, FLAP, FRET and FLIM. *Molecules* 17, 4047–4132. doi: 10.3390/molecules17044047

Keestra, A. M., Winter, M. G., Auburger, J. J., Frassle, S. P., Xavier, M. N., Winter, S. E., et al. (2013). Manipulation of small Rho GTPases is a pathogen-induced process detected by NOD1. *Nature* 496, 233–237. doi: 10.1038/nature12025

Kommnick, C., Lepper, A., and Hensel, M. (2019). Correlative light and scanning electron microscopy (CLSEM) for analysis of bacterial infection of polarized epithelial cells. *Sci. Rep.* 9:17079. doi: 10.1038/s41598-019-53085-6

Lai, Y., Rosenshine, I., Leong, J. M., and Frankel, G. (2013). Intimate host attachment: enteropathogenic and enterohaemorrhagic *Escherichia coli*. *Cell. Microbiol.* 15, 1796–1808. doi: 10.1111/cmi.12179

Laporte, D., Ojkic, N., Vavylonis, D., and Wu, J. Q. (2012). alpha-Actinin and fimbrin cooperate with myosin II to organize actomyosin bundles during contractile-ring assembly. *Mol. Biol. Cell* 23, 3094–3110. doi: 10.1091/mbc.e12-02-0123

Lhocine, N., Arena, E. T., Bomme, P., Ubelmann, F., Prevost, M. C., Robine, S., et al. (2015). Apical invasion of intestinal epithelial cells by *Salmonella typhimurium* requires villin to remodel the brush border actin cytoskeleton. *Cell Host Microbe* 17, 164–177. doi: 10.1016/j.chom.2014.12.003

Lorkowski, M., Felipe-Lopez, A., Danzer, C. A., Hansmeier, N., and Hensel, M. (2014). *Salmonella enterica* invasion of polarized epithelial cells is a highly cooperative effort. *Infect. Immun.* 82, 2657–2667. doi: 10.1128/IAI.00023-14

Martinez, E., Schroeder, G. N., Berger, C. N., Lee, S. F., Robinson, K. S., Badea, L., et al. (2010). Binding to Na(+) /H(+) exchanger regulatory factor 2 (NHERF2) affects trafficking and function of the enteropathogenic *Escherichia coli* type III secretion system effectors Map, EspI and NleH. *Cell. Microbiol.* 12, 1718–1731. doi: 10.1111/j.1462-5822.2010.01503.x

McConnell, R. E., Higginbotham, J. N., Shifrin, D. A. Jr., Tabb, D. L., Coffey, R. J., and Tyska, M. J. (2009). The enterocyte microvillus is a vesicle-generating organelle. *J. Cell Biol.* 185, 1285–1298. doi: 10.1083/jcb.200902147

McConnell, R. E., and Tyska, M. J. (2007). Myosin-1a powers the sliding of apical membrane along microvillar actin bundles. *J. Cell Biol.* 177, 671–681. doi: 10.1083/jcb.200701144

Meenderink, L. M., Gaeta, I. M., Postema, M. M., Cencer, C. S., Chinowsky, C. R., Krystofiak, E. S., et al. (2019). Actin dynamics drive microvillar motility and clustering during brush border assembly. *Dev. Cell* 50, 545–556 e544. doi: 10.1016/j.devcel.2019.07.008

Mettlen, M., Platek, A., Van Der Smissen, P., Carpentier, S., Amyere, M., Lanzetti, L., et al. (2006). Src triggers circular ruffling and macropinocytosis at the apical surface of polarized MDCK cells. *Traffic* 7, 589–603. doi: 10.1111/j.1600-0854.2006.00412.x

Mirold, S., Rabsch, W., Rohde, M., Stender, S., Tschäpe, H., Rüssmann, H., et al. (1999). Isolation of a temperate bacteriophage encoding the type III effector protein SopE from an epidemic *Salmonella typhimurium* strain. *Proc. Natl. Acad. Sci. U. S. A.* 96, 9845–9850. doi: 10.1073/pnas.96.17.9845

Misselwitz, B., Barrett, N., Kreibich, S., Vonaesch, P., Andritschke, D., Rout, S., et al. (2012). Near surface swimming of *Salmonella* Typhimurium explains target-site selection and cooperative invasion. *PLoS Pathog.* 8:e1002810. doi: 10.1371/journal.ppat.1002810

Muller, A. J., Hoffmann, C., Galle, M., Van Den Broeke, A., Heikenwalder, M., Falter, L., et al. (2009). The *S.* Typhimurium effector SopE induces caspase-1 activation in stromal cells to initiate gut inflammation. *Cell Host Microbe* 6, 125–136. doi: 10.1016/j.chom.2009.07.007

Pedersen, G. A., Jensen, H. H., Schelde, A. B., Toft, C., Pedersen, H. N., Ulrichsen, M., et al. (2017). The basolateral vesicle sorting machinery and basolateral proteins are recruited to the site of enteropathogenic *E. coli* microcolony growth at the apical membrane. *PLoS ONE* 12:e0179122. doi: 10.1371/journal.pone.0179122

Pelaseyed, T., and Bretscher, A. (2018). Regulation of actin-based apical structures on epithelial cells. *J. Cell Sci.* 131:221853. doi: 10.1242/jcs.221853

Revenu, C., Ubelmann, F., Hurbain, I., El-Marjou, F., Dingli, F., Loew, D., et al. (2012). A new role for the architecture of microvillar actin bundles in apical retention of membrane proteins. *Mol. Biol. Cell* 23, 324–336. doi: 10.1091/mbc.e11-09-0765

Röder, J., and Hensel, M. (2020). Presence of SopE and mode of infection result in increased *Salmonella*-containing vacuole damage and cytosolic release during host cell infection by *Salmonella enterica*. *Cell. Microbiol.* 22:e13155. doi: 10.1111/cmi.13155

Saotome, I., Curto, M., and McClatchey, A. I. (2004). Ezrin is essential for epithelial organization and villus morphogenesis in the developing intestine. *Dev. Cell* 6, 855–864. doi: 10.1016/j.devcel.2004.05.007

Schlumberger, M. C., and Hardt, W. D. (2005). Triggered phagocytosis by *Salmonella*: bacterial molecular mimicry of RhoGTPase activation/deactivation. *Curr. Top. Microbiol. Immunol.* 291, 29–42. doi: 10.1007/3-540-27511-8_3

Schlumberger, M. C., Kappeli, R., Wetter, M., Muller, A. J., Misselwitz, B., Dilling, S., et al. (2007). Two newly identified SipA domains (F1, F2) steer effector protein localization and contribute to *Salmonella* host cell manipulation. *Mol. Microbiol.* 65, 741–760. doi: 10.1111/j.1365-2958.2007.05823.x

Segal, E. D., Falkow, S., and Tompkins, L. S. (1996). *Helicobacter pylori* attachment to gastric cells induces cytoskeletal rearrangements and tyrosine phosphorylation of host cell proteins. *Proc. Natl. Acad. Sci. U. S. A.* 93, 1259–1264. doi: 10.1073/pnas.93.3.1259

Sheikh, A., Tumala, B., Vickers, T. J., Martin, J. C., Rosa, B. A., Sabui, S., et al. (2022). Enterotoxigenic *Escherichia coli* heat-labile toxin drives enteropathic changes in small intestinal epithelia. *Nat. Commun.* 13:6886. doi: 10.1038/s41467-022-34687-7

Solaymani-Mohammadi, S., and Singer, S. M. (2013). Regulation of intestinal epithelial cell cytoskeletal remodeling by cellular immunity following gut infection. *Mucosal Immunol.* 6, 369–378. doi: 10.1038/mi.2012.80

Takeuchi, A. (1967). Electron microscope studies of experimental *Salmonella* infection. I. Penetration into the intestinal epithelium by *Salmonella typhimurium*. *Am. J. Pathol.* 50, 109–136.

Tan, S., Noto, J. M., Romero-Gallo, J., Peek, R. M. Jr., and Amieva, M. R. (2011). *Helicobacter pylori* perturbs iron trafficking in the epithelium to grow on the cell surface. *PLoS Pathog.* 7:e1002050. doi: 10.1371/journal.ppat.1002050

Tan, S., Tompkins, L. S., and Amieva, M. R. (2009). *Helicobacter pylori* usurps cell polarity to turn the cell surface into a replicative niche. *PLoS Pathog.* 5:e1000407. doi: 10.1371/journal.ppat.1000407

Teafatiller, T., Subramanya, S. B., Lambrecht, N., and Subramanian, V. S. (2023). *Salmonella* Typhimurium infection reduces the ascorbic acid uptake in the intestine. *Mediators Inflamm.* 2023:2629262. doi: 10.1155/2023/2629262

Terebiznik, M. R., Vieira, O. V., Marcus, S. L., Slade, A., Yip, C. M., Trimble, W. S., et al. (2002). Elimination of host cell PtdIns(4,5)P(2) by bacterial SigD

promotes membrane fission during invasion by *Salmonella*. *Nat. Cell Biol.* 4, 766–773. doi: 10.1038/ncb854

Wang, R. F., and Kushner, S. R. (1991). Construction of versatile low-copy-number vectors for cloning, sequencing and gene expression in *Escherichia coli*. *Gene* 100, 195–199. doi: 10.1016/0378-1119(91)90366-J

Wong, A. R., Pearson, J. S., Bright, M. D., Munera, D., Robinson, K. S., Lee, S. F., et al. (2011). Enteropathogenic and enterohaemorrhagic *Escherichia coli*: even more subversive elements. *Mol. Microbiol.* 80, 1420–1438. doi: 10.1111/j.1365-2958.2011.07661.x

Yoshida, S., Hoppe, A. D., Araki, N., and Swanson, J. A. (2009). Sequential signaling in plasma-membrane domains during macropinosome formation in macrophages. *J. Cell Sci.* 122, 3250–3261. doi: 10.1242/jcs.053207

Zhang, K., Riba, A., Nietschke, M., Torow, N., Repnik, U., Putz, A., et al. (2018). Minimal SPI1-T3SS effector requirement for *Salmonella* enterocyte invasion and intracellular proliferation *in vivo*. *PLoS Pathog.* 14:e1006925. doi: 10.1371/journal.ppat.1006925

Zhang, S., Santos, R. L., Tsolis, R. M., Stender, S., Hardt, W. D., Baumler, A. J., et al. (2002). The *Salmonella enterica* serotype typhimurium effector proteins SipA, SopA, SopB, SopD, and SopE2 act in concert to induce diarrhea in calves. *Infect. Immun.* 70, 3843–3855. doi: 10.1128/IAI.70.7.3843-3855.2002

Frontiers in Microbiology

Explores the habitable world and the potential of microbial life

The largest and most cited microbiology journal which advances our understanding of the role microbes play in addressing global challenges such as healthcare, food security, and climate change.

Discover the latest Research Topics

See more →

Frontiers

Avenue du Tribunal-Fédéral 34
1005 Lausanne, Switzerland
frontiersin.org

Contact us

+41 (0)21 510 17 00
frontiersin.org/about/contact